AIR POLLUTION MODELING

Theories, Computational Methods and Available Software

Paolo Zannetti

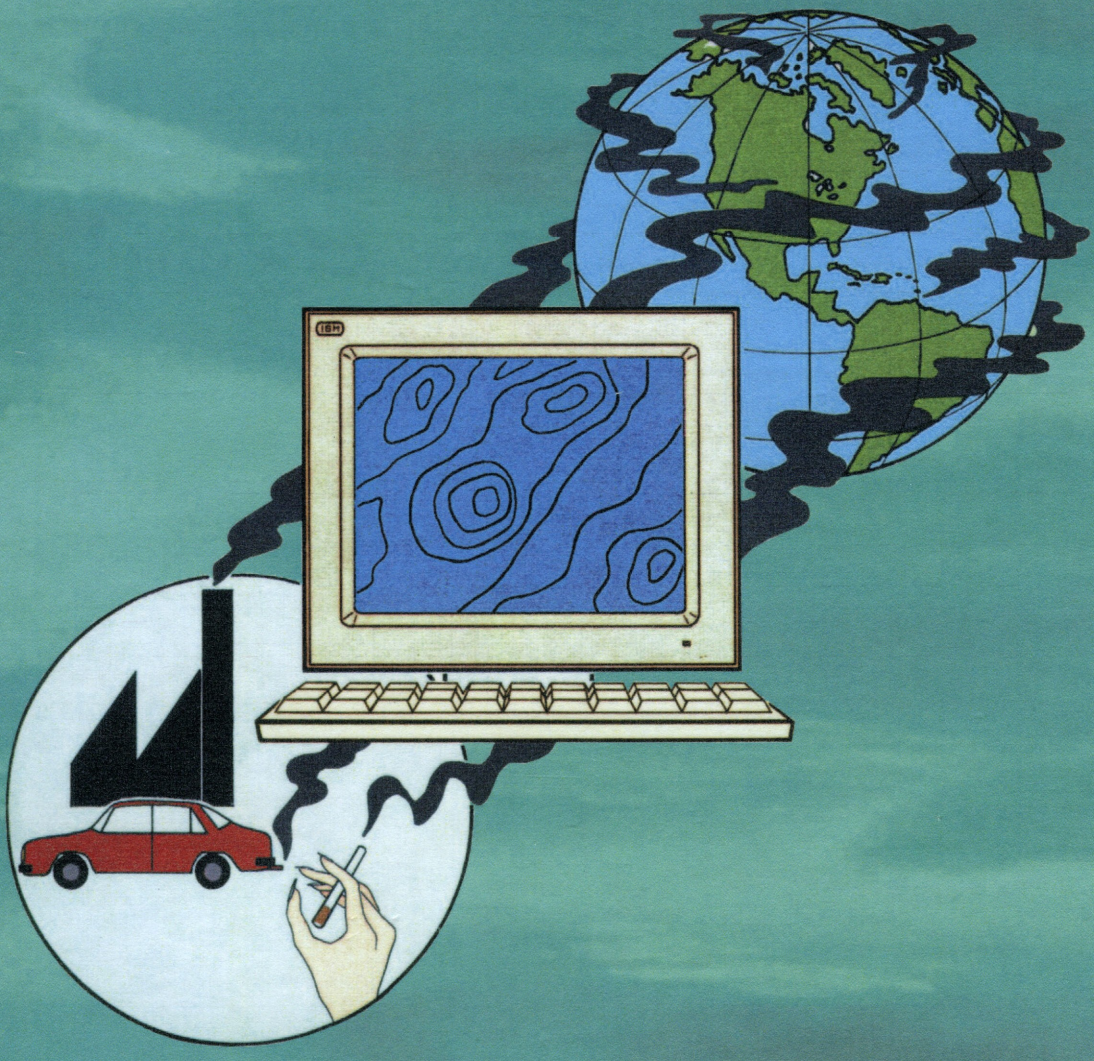

WIT PRESS

AIR POLLUTION MODELING

Theories, Computational Methods and Available Software

Paolo Zannetti*

AeroVironment Inc.
Monrovia, California

Computational Mechanics Publications
Southampton Boston

VAN NOSTRAND REINHOLD
New York

* Currently at IBM Bergen Scientific Centre, Norway

Dr. P. Zannetti
IBM Scientific Centre
Thomohlensgate 55
Bergen High Tech Centre
N-5008 Bergen, Norway

British Library Cataloguing-in-Publication Data
Zannetti, Paolo *1946-*
Air pollution modelling : theories, computational methods and available software
1. Air. Pollution. Mathematical models
I. Title
363.73920113
ISBN 1-85312-100-2

ISBN 1-85312-100-2 Computational Mechanics Publications, Southampton, UK
ISBN 0-945824-84-X Computational Mechanics Publications, Boston, USA
Library of Congress Catalog Card Number 90-62205

Published in the USA by
Van Nostrand Reinhold
115 Fifth Avenue
New York, NY 10003, USA

Distributed in Canada by
Nelson Canada
1120 Birchmont Road
Scarborough
Ontario M1K 5GA, Canada

Library of Congress Catalog Card Number 90-41480
ISBN 0-442-308051

Library of Congress Cataloging in Publication Data
Zannetti, P. (Paolo)
Air pollution modeling : theories, computational methods
and available software / Paolo Zannetti.
p. cm.
Includes bibliographical references and index.
ISBN 0-442-30805-1
1. Air-Pollution-Mathematical models. 2. Atmospheric diffusion-
-Mathematical models. I. Title.
TD 883.1.Z36 1990
628.5'3-dc20

Printed & bound by Antony Rowe Ltd, Eastbourne

Mathematical modeling of air pollution has grown enormously over the last two decades in response to ever-increasing demands to understand and manage air resources. Air Pollution Modeling, the first comprehensive text on this subject, provides both an historical perspective on the evolution of mathematical modeling techniques as well as a carefully-developed survey of contemporary modeling methods. Dr. Zannetti's book fills a long-standing void in this area of environmental science. Air Pollution Modeling will no doubt become a mainstay in the library of air quality scientists, practitioners and managers as well as educators in this field.

Based on a clearly-presented foundation of chemical and physical principles, Air Pollution Modeling introduces relevant historical and recently developed examples of modeling techniques for traditional problems including point source dispersion, plume rise, windfield estimation, and surface deposition. Supplementing these are discussions on a number of contemporary and emergent air quality modeling issues including visibility, dense gas dispersion, indoor air pollution, photochemical oxidants, and global air quality. Complementing the treatment of numerical modeling methods is a chapter on statistical and empirical techniques useful in establishing source-receptor relationships, analysing aerometric data and evaluating the performance of models. Air quality practitioners and students will find the survey on available modeling codes and software to be particularly helpful.
The field of air pollution modeling is expanding rapidly in response to an increasingly complex set of social, political and technological issues. In Air Pollution Modeling, Dr Zanetti has provided an invaluable resource to those in the scientific, educational and public policy communities dealing with these problems.

From a review by: T. W. Tesche PhD

WIT PRESS
Email: witpress@witpress.com
http://www.witpress.com
ISBN: 1853121002

AIR POLLUTION MODELING

Theories, Computational Methods and Available Software

Paolo Zannetti*

AeroVironment Inc.
Monrovia, California

Computational Mechanics Publications
Southampton Boston

VAN NOSTRAND REINHOLD
New York

* Currently at IBM Bergen Scientific Centre, Norway

To those who loved me

Dr. P. Zannetti
IBM Scientific Centre
Thomohlensgate 55
Bergen High Tech Centre
N-5008 Bergen, Norway

British Library Cataloguing-in-Publication Data
Zannetti, Paolo *1946-*
Air pollution modelling : theories, computational methods and available software
1. Air. Pollution. Mathematical models
I. Title
363.73920113
ISBN 1-85312-100-2

ISBN 1-85312-100-2 Computational Mechanics Publications, Southampton, UK
ISBN 0-945824-84-X Computational Mechanics Publications, Boston, USA
Library of Congress Catalog Card Number 90-62205

Published in the USA by
Van Nostrand Reinhold
115 Fifth Avenue
New York, NY 10003, USA

Distributed in Canada by
Nelson Canada
1120 Birchmont Road
Scarborough
Ontario M1K 5GA, Canada

Library of Congress Catalog Card Number 90-41480
ISBN 0-442-308051

Library of Congress Cataloging in Publication Data
Zannetti, P. (Paolo)
Air pollution modeling : theories, computational methods
and available software / Paolo Zannetti.
p. cm.
Includes bibliographical references and index.
ISBN 0-442-30805-1
1. Air-Pollution-Mathematical models. 2. Atmospheric diffusion-
-Mathematical models. I. Título.
TD 883.1.Z36 1990
628.5'3-dc20

Reprinted 1998

Printed & bound by Antony Rowe Ltd, Eastbourne

Preface

Finishing this book is giving me a mixture of relief, satisfaction and frustration. Relief, for the completion of a project that has taken too many of my evenings and weekends and that, in the last several months, has become almost an obsession. Satisfaction, for the optimistic feeling that this book, in spite of its many shortcomings and imbalances, will be of some help to the air pollution scientific community. Frustration, for the impossibility of incorporating newly available material that would require another major review of several key chapters — an effort that is currently beyond my energies but not beyond my desires.

The first *canovaccio* of this book came out in 1980 when I was invited by Computational Mechanics in the United Kingdom to give my first Air Pollution Modeling course. The course material, in the form of transparencies, expanded, year after year, thus providing a growing working basis. In 1985, the ECC Joint Research Center in Ispra, Italy, asked me to prepare a critical survey of mathematical models of atmospheric pollution, transport and deposition. This support gave me the opportunity to prepare a sort of "first draft" of the book, which I expanded in the following years.

The expert reader will notice that this book is uneven. Subjects that I feel comfortable with are discussed extensively, while other subjects are only briefly summarized. I have tried to compensate, with abundant reference citations, for my lack of deep knowledge in some of the technical fields discussed here. Also, I have tried to be fair in the critique of the different modeling techniques, even though some bias is noticeable when, for example, the properties of Lagrangian versus Eulerian models are discussed.

The list of people and organization to thank is endless. I must start with Ivar Tombach who, since 1980, has encouraged me to complete this endeavor and has provided substantial moral and practical support. Then, I want to thank AeroVironment, Inc., the company I have been associated with in the 80's, for having provided an outstanding working environment and continuous, interesting technical challenges. Thoughts of appreciation also go to the IBM Scientific Centers for which I worked in the 70's. I will always be grateful to IBM Italy for getting me involved, in 1971, with air pollution modeling research and for introducing me to a scientific field — environmental modeling — that I have found very satisfactory and rewarding for two decades.

I submitted each chapter of this book to a few reviewers. It is difficult to critique a chapter without reading the entire publication. Nevertheless, their comments and constructive criticism were very useful in finalizing my work. I apologize to some of the reviewers for not being able to incorporate all their suggestions. I hope to do so in the future, if and when a new edition is printed. The reviewers were: Domenico Anfossi, Michel Benaire, Robert Bornstein, Richard Boubel, Gary Briggs, Steven Hanna, Brian Henderson-Sellers, Frans Nieuwstadt, Arnaldo Longhetto, Walter Lyons, Roger Pielke, Chris Pilinis, Brian Sawford, Christian Seigneur, John Seinfeld, Tom Tesche, David Thomson, Tiziano Tirabassi, Paul Urone, Eric Walther, and Robert Yamartino. (A special thanks goes to Tom Tesche who, after reviewing one chapter, found the time to look at the entire manuscript and provided useful general comments.) All reviewers made valuable contributions; errors and omission, however, are only my fault.

This book would never have been published without the efforts and dedication, beyond the line of duty, of Wendy Webb who prepared, using Interleaf© Technical Publishing Software, the camera-ready version of the manuscript. I really owe you a lot W^2! Anita Spiess provided outstanding editorial help. I learned a lot from her editorial changes and her constant struggle for clarity, conciseness and logical sequence.

This book is dedicated to those who loved me. First and foremost, to the memory of my parents, who gave so much and asked for so little.

PAOLO ZANNETTI

Monrovia, California
February, 1990

Contents

1 THE PROBLEM – AIR POLLUTION

1.1 HISTORICAL REMARKS

Ambient air composition over the earth has undergone several changes throughout history. In particular, there is evidence (Chambers, from Stern, 1976) that "the primeval gaseous environment probably contained almost no free oxygen" and that "oxygen in more recent years has accumulated as a result of photosynthetic processes utilized by early nonoxygen-dependent species." Those early living species have either disappeared, as a consequence of these changes, or adapted.

Anthropogenic activities, especially since the 14th century, when coal began to replace wood as the prime source of energy, have provided a clear "perturbation" of the earth's environmental balance. In the atmosphere, these anthropogenic pollutants have often generated locally unhealthful air quality and, sometimes, lethal air pollution concentrations, as during the well-known London episode of December 1952. In addition to short-term episodic effects, atmospheric pollutants are known to generate long-term adverse effects, which are, however, difficult to forecast.

The emergence of petroleum products in this century has characterized a new industrial revolution. In 1945, it was recognized that petroleum products are responsible for a new type of "smog," a photochemical summertime smog, first discovered in the Los Angeles area. Photochemical smog is quite different from the traditional wintertime sulfur smog (the "London" smog) typically generated by the combustion of sulfur-containing fuels, such as coal.

The last decade has been characterized by a growing interest in long-range air pollution transport phenomena and global effects. First in northern Europe and then in eastern North America, it has been shown that large emissions of "primary" pollutants, such as sulfur dioxide (SO_2), undergo chemical transformations in the atmosphere. These transformations generate, hundreds or thousands of kilometers downwind, new chemical species known as "secondary" pollutants, such as the sulfates (SO_4^{2-}). These secondary species are responsible for new adverse affects, such as acidic deposition (or, as commonly and improperly called in the media, acid rain).

Two "global" issues have recently become a major concern: 1) the "greenhouse" effect, which could cause an increase of the earth's average temperature as a consequence of increasing concentrations of carbon dioxide (CO_2), a species that has never been considered a "pollutant" and whose huge emissions have never been controlled; and 2) the possible depletion of the stratospheric ozone layer, a natural protective "blanket" from harmful solar radiation, by certain species emitted by anthropogenic activities. On the subject of global issues, the "nuclear winter" hypothesis should also be mentioned, i.e., the possibility that large fires, following a nuclear war, may inject large amounts of particles into the atmosphere, generating a substantial and prolonged decrease of earth's temperatures.

Other air pollution problems that have recently emerged are (Urone, from Stern, 1986): indoor air pollution, in particular, asbestos; nuclear accidents, especially after the Chernobyl disaster; nonionizing radiation, which seems to cause physiological disfunctions; risk assessment, especially for the characterization and prevention of accidental releases of toxic pollutants (e.g., in the form of heavy gases that have unique dispersion characteristics); and atmospheric visibility and its impairment by air pollutants.

It has often been pointed out that government pollution control action has seldom (or perhaps never) anticipated adverse effects and that only large-scale disasters or environmental deterioration have provided stimuli for effective action and preventive measures. Recent years, however, seem to be characterized by increasing public concern, at least in the western societies, about environmental issues and by the pressure of public opinion on government and industry for major preventive control actions and for the implementation of emergency/accident contingency plans.

1.2 WHAT IS AN AIR POLLUTANT?

Which substances must be considered air pollutants? Or, better, which substances, emitted into the atmosphere, can be considered safe, nonpolluting compounds? The question is certainly not an easy one, since the term "air pollution" can have many definitions.

Williamson (1973) gave a satisfactory clarification of this problem, by elaborating the difference between a "pollutant" and a "contaminant." A contaminant was defined as "anything added to the environment that causes a deviation from the geochemical mean composition." On the other hand, a pollutant, to

be considered such, must be a contaminant responsible for causing some adverse effect on the environment.

Clearly, the distinction between pollutants and contaminants is based on our limited understanding of short-term and long-term adverse effects of each chemical compound. Moreover, this evaluation is complicated by chemical reactions that can transform a contaminant into a pollutant. We can, therefore, say that any contaminant is a potential pollutant and that, in many cases, the two words are synonymous.

An example of the above difference is given by the CO_2 gas that is abundantly emitted into the atmosphere from anthropogenic combustion processes. CO_2 does not present adverse effects to living organisms and was, therefore, considered only a contaminant. Measurements have shown, however, that ambient CO_2 concentrations throughout the world are constantly increasing, which reveals an accumulation in the atmosphere of a considerable fraction of the CO_2 emitted by anthropogenic activities. Since further CO_2 concentration increases are expected to induce an increase in the average temperature of the earth, CO_2 should be considered, in this respect, a pollutant. (See Chapter 13 for further discussion on the CO_2 problem.)

Air pollutants are found in the form of

- gases, e.g., sulfur dioxide (SO_2)
- particulate matter, e.g., fine dust

and are injected into the atmosphere from

- natural sources, e.g., volcanoes, ocean spray, pollen
- anthropogenic sources, e.g., industrial, commercial, agricultural, transportation activities

These "primary" pollutants (i.e., those directly emitted from sources) undergo chemical reactions that result in the subsequent formation of other species, i.e., "secondary" pollutants, in the form of

- gases, e.g., ozone (O_3)
- particulate matter, e.g., sulfates (SO_4^{2-})

One of the most important factors characterizing the atmospheric particulate matter is the size (e.g., the diameter) of the particles. Particles are called

- coarse particles, when their diameter is larger than 2.5 μm

- fine particles (or respirable particulate matter, RPM), when their diameter is less than 2.5 μm; fine particles can also be divided into two modes: the nuclei mode, with diameter below 0.1 μm, and the accumulation mode, with diameter greater than 0.1 μm
- inhalable particles (or inhalable particulate matter, IPM), when their diameter is less than 10 μm

Coarse particles are generally less important, since their large mass causes fast gravitational removal from the ambient air, and are less harmful to the human species, because they are easily removed by the upper respiratory system. Fine particles are more important because of their adverse effects on human health and visibility.

Particles in the atmosphere can also be classified, independently from their size, as

- viable particles (such as pollen, fungi, bacteria, etc.)
- nonviable particles

1.3 POLLUTANT EMISSIONS

1.3.1 Primary Gaseous Pollutants

The primary gaseous emissions of air pollutants are the following (Urone, from Stern, 1976 and 1986)

- sulfur compounds (e.g., SO_2, H_2S)
- nitrogen compounds (e.g., NO, NH_3)
- carbon compounds (e.g., hydrocarbons HC, CO)
- halogen compounds (e.g, fluorides, chlorides, bromides)

1.3.2 Primary Particulate Matter

The primary particles in the atmosphere are

- air ions, with diameters much smaller than 0.1 μm, formed, for example, from solar and cosmic radiation, radioactive material and combustion processes
- Aitken nuclei (i.e., particles smaller than 0.1 μm in diameter) and fine particles between 0.1 and 2.5 μm, formed by natural processes, such as sea spray and forest fires, and by industrial combustion processes

- carbonaceous materials, made up of soot, including elemental carbon and organics
- particles from automotive emissions, mostly lead in the form of oxide, sulfate or bromochloride
- particles containing light metals, such as sodium, magnesium, aluminum, silicon, potassium and calcium
- particles containing heavy metals, such as titanium, vanadium, chromium, manganese, iron, nickel, copper, zinc, arsenic and selenium
- large particles, such as dust and sand transported by wind, particulate matter from industrial activities, or rising dust from off-road transportation
- viable particles, such as pollen, micro-organisms, and insects

Also, since atmospheric particles are hygroscopic in nature, they acquire water to equilibrate to a given humidity.

The sources of particulate matter (Hidy, 1984) are:

- extraterrestrial sources, which only slightly affect concentrations in the planetary boundary layer, but contribute largely to the concentrations of extraterrestrial dust found above 30–40 km height.
- sea salt emissions, generated by the oceans from breaking waves, wind action on the wave crests, or bubbles of foam breaking on the water surface
- suspension of soil dust, from the action of wind or vehicles on loose soil areas
- volcanic eruptions
- forest and brush fires
- anthropogenic emissions, from combustion of fuel and waste, and industrial activities

1.3.3 Radioactive Pollutants

Radioactivity is a primary air pollutant (Eisenbud, from Stern, 1976) from both natural and anthropogenic sources. Natural radioactivity results from the presence of radionuclides, which originate either from radioactive minerals in the earth's crust or from interaction of cosmic radiation with atmospheric gases. Anthropogenic radioactive emissions originate from

- nuclear reactors

- the atomic energy industry (mining, milling, and reactor fuel fabrication)
- nuclear or thermonuclear bomb explosions
- plants reprocessing spent reactor fuel

1.3.4 Secondary Gas Pollutants

Atmospheric chemical reactions (especially the photochemical ones) are responsible for the transformation of primary pollutants into intermediate reaction products (e.g., free radicals) and, finally, into stable end products, the secondary pollutants. The major gaseous secondary pollutants are

- NO_2, formed from primary NO
- O_3, formed via photochemical reactions

A more complete discussion on this subject is presented in Chapter 9.

1.3.5 Secondary Particulate Matter

Atmospheric chemical reactions (especially the photochemical ones) are responsible for the transformation of primary and secondary gaseous pollutants into secondary particles. The main known processes are

- the transformation of SO_2 into sulfates, SO_4^{2-}
- the transformation of NO_2 into nitrates, NO_3^-
- the transformation of organic compounds into organic particles

Secondary particulate matter consists mainly of fine particles (smaller than 2.5 μm), which are in the respirable range and have the potential to adversely affect human health and visibility.

1.3.6 Global SO_x and NO_x Emissions

Sulfur emissions, mainly SO_2, have represented, and still represent, the major and most common air pollution problem throughout the world. SO_2 emissions are responsible for (1) the "London" winter-type smog, (2) several lethal air pollution episodes, and (3) acidic deposition effects associated with sulfate transport and deposition.

The worldwide use of coal and oil as combustion fuels, especially for electric power production, is the major anthropogenic source of SO_2. An initial estimate of worldwide SO_2 emission was given by Robinson (from Strauss, 1972)

as about 133 Tg a^{-1}(*). Cullis and Hirschler (1980) gave a more complete evaluation of the atmospheric sulfur emission budget and cycle. Their results are presented below.

The global atmospheric sulfur cycle is qualitatively described in Figure 1-1. Cullis and Hirschler (1980) provided detailed estimates of the various components of the cycle, as shown in Table 1-1, which gives the total annual natural emissions of atmospheric sulfur (in Tg *S* a^{-1}) and Table 1-2, which presents the anthropogenic emissions of SO_2 from 1965 to 1976 (in Tg SO_2 a^{-1}).

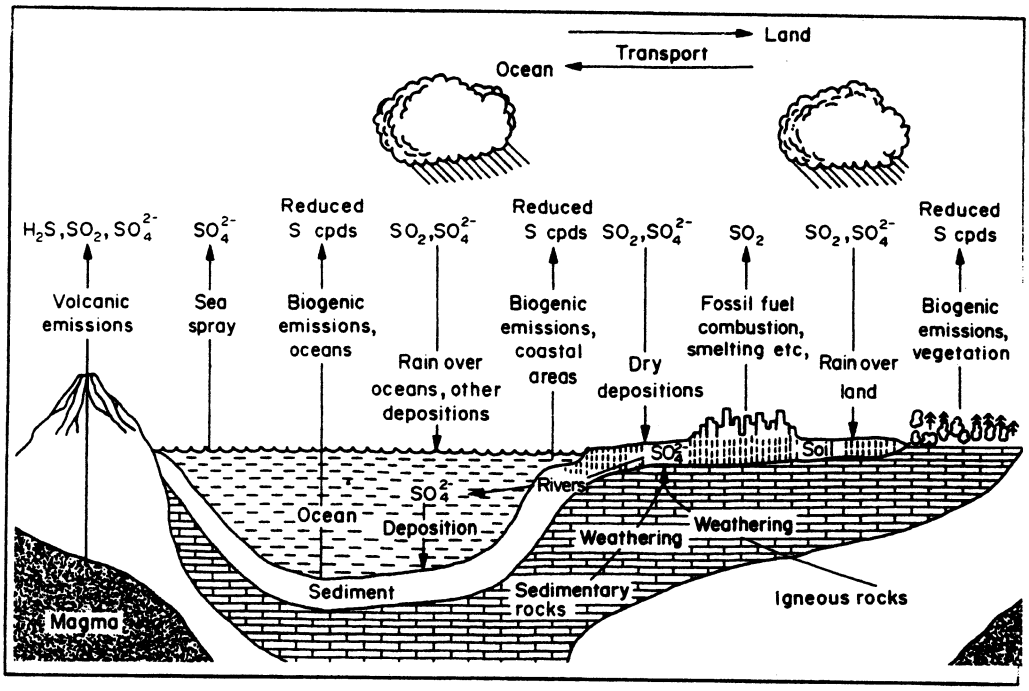

Figure 1-1. The atmospheric sulfur cycle (from Cullis and Hirschler, 1980). [Reprinted with permission from Pergamon Press.]

(*)Tg a^{-1} means 10^{12} grams per year.

Table 1–1. Estimates of natural emissions of atmospheric sulfur (in Tg S a^{-1} = 10^{12} grams per year) (from Cullis and Hirschler, 1980; see this paper for the references mentioned in this table). [Reprinted with permission from Pergamon Press.]

Authors	Removal processes ($Tg\,a^{-1}$)			Emission processes ($Tg\,a^{-1}$)						Net transfer from land to sea ($Tg\,a^{-1}$)†
							Biogenic emissions			
	Total	Precipitation	Dry deposition*	Volcanoes	Sea-spray	Man-made	Sub-total	From sea	From land	
Junge (1963a)	315	140	175		45	40	230	160	70	− 95
Eriksson (1963)	365	200	165		45	40	280	170	110	− 65
Robinson and Robbins (1972)	212	129	83		44	70	98	30	68	+ 64
Kellogg *et al.* (1972)	184	159	25	1	44	50	89	18	71	+ 60
Friend (1973)	217	143	74	2	44	65	106	48	58	+ 33
Bolin and Charlson (1976)	143			3	44	65	31	28	3	− 1
Hallberg (1976)	149			3	44	65	37	34	3	− 7
Granat (1976)	144	106	38	3	44	65	32	27	5	+ 2
Garland (1977)‡	266	112	154		44	70	152	46	106	+ 84
Davey (1978)§	200	123	77	10	44	60	86	26	60	+ 60

*Where subtotals are given only for the combined effects of precipitation and dry deposition, 20% of the sulphur is assumed to be removed by dry deposition, by analogy with nuclear fall-out (Junge, 1963b; Friend, 1973).

†The values are calculated by adding biogenic emissions from land areas to those from volcanoes and due to man and subtracting biogenic emissions from sea and those due to sea-spray.

‡The distribution between land and sea has been calculated on the basis of the percentages used by Robinson and Robbins (1972) in their estimates, from which the data of Garland (1977) originate.

§Somewhat similar estimates are given in an earlier paper by Davey (1973).

Table 1–2. Anthropogenic sulfur emissions (Tg SO_2 a^{-1}) (from Cullis and Hirschler, 1980; see this paper for the references mentioned in this table). [Reprinted with permission from Pergamon Press.]*

	1965		1970		1974		1975		1976	
Coal										
Hard coal	71.4	(47.9)	77.5	(45.0)	81.1	(43.3)	85.5	(45.4)	88.1	(42.5)
Lignite	28.1	(18.9)	30.5	(17.7)	31.6	(16.9)	32.8	(17.4)	33.1	(16.0)
Coal coke	2.4	(1.6)	2.5	(1.5)	2.5	(1.3)	2.5	(1.3)	2.6	(1.2)
Subtotal	102.0	(68.5)	110.4	(64.1)	115.2	(61.5)	120.8	(64.2)	123.8	(59.7)
Petroleum										
Refining	5.7	(3.8)	6.8	(4.0)	5.8	(3.1)	5.5	(2.9)	7.3	(3.5)
Motor spirit	0.3	(0.2)	0.4	(0.2)	0.5	(0.3)	0.5	(0.3)	0.6	(0.3)
Kerosene	0.2	(0.13)	0.1	(0.05)	0.1	(0.04)	0.1	(0.04)	0.1	(0.04)
Jet fuel			0.05	(0.03)	0.1	(0.06)	0.1	(0.06)	0.1	(0.06)
Distillate fuel oil	2.0	(1.3)	2.2	(1.3)	3.0	(1.6)	2.8	(1.5)	3.8	(1.8)
Residual fuel oil	20.3	(13.6)	29.8	(17.3)	37.4	(20.0)	34.3	(18.2)	45.8	(22.1)
Petroleum coke			0.4	(0.2)	0.4	(0.2)	0.5	(0.3)	0.6	(0.3)
Subtotal	28.5	(19.1)	39.6	(23.0)	47.2	(25.2)	43.8	(23.3)	58.3	(28.1)
Non-ferrous ores										
Copper	12.9	(8.7)	15.8	(9.2)	18.4	(9.8)	17.5	(9.3)	18.8	(9.1)
Lead	1.5	(1.0)	1.7	(1.0)	1.6	(0.9)	1.5	(0.8)	1.6	(0.7)
Zinc	1.3	(0.9)	1.2	(0.7)	1.1	(0.6)	1.0	(0.5)	1.0	(0.5)
Subtotal	15.7	(10.5)	18.8	(10.9)	21.1	(11.3)	20.0	(10.6)	21.4	(10.3)
Others										
H_2SO_4	1.6	(1.1)	2.1	(1.2)	2.5	(1.3)	2.4	(1.3)	2.5	(1.2)
Pulp/paper	0.4	(0.2)	0.5	(0.3)	0.5	(0.3)	0.5	(0.3)	0.5	(0.2)
Refuse	0.65	(0.4)	0.65	(0.4)	0.65	(0.3)	0.65	(0.3)	0.65	(0.3)
Sulphur	0.05	(0.04)	0.03	(0.02)	0.05	(0.03)	0.05	(0.03)	0.05	(0.02)
Subtotal	2.7	(1.8)	3.2	(1.9)	3.7	(2.0)	3.6	(1.9)	3.7	(1.8)
Total	148.9†		172.2‡		187.3		188.2		207.2	

*The figures in brackets represent percentages of the total.
†This is a previous value for coal, petroleum and non-ferrous ores (Robinson and Robbins, 1972), to which emissions from other sources have been added.
‡This may be compared with the value of 166 Tg SO_2 predicted for 1970 (Peterson and Junge, 1971).

The main conclusion is that, according to the 1976 estimates, the anthropogenic emissions of sulfur are 104 Tg S a^{-1}, over 40 percent of all atmospheric sulfur emissions, and are expected to exceed the natural emissions before the end of the present century.

A recent reevaluation of SO_x and NO_x emissions (actually, only those from fossil-fuel combustion) is provided by Hameed and Dignon, 1988), who also reveal interesting trends in the geographical variations of these emissions from 1966 to 1980. Through the calculations of two regression models, they provide the annual global emissions of SO_x (in Tg S a^{-1}) that are shown in Figure 1–2. These emissions, however, are approximately half of those estimated

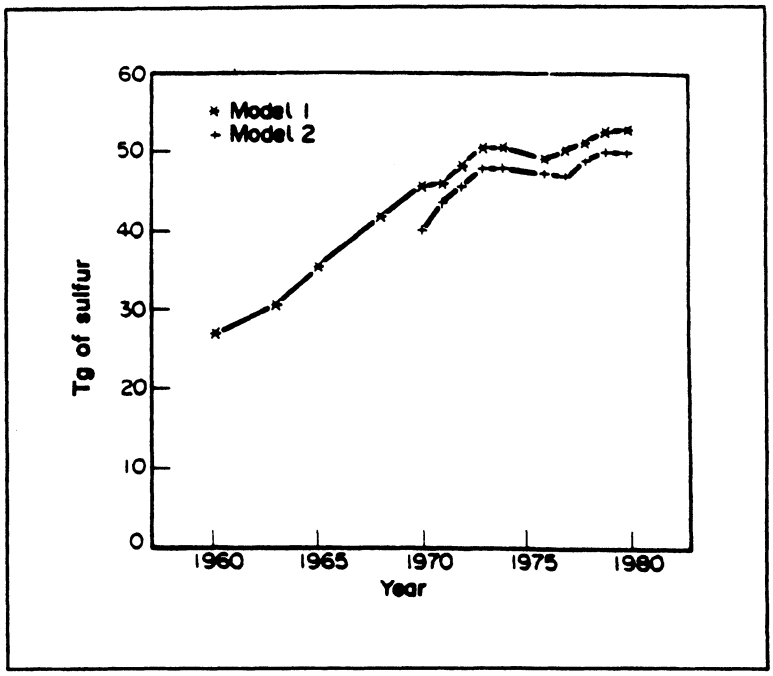

Figure 1–2. Annual global emissions of SO_x from fossil-fuel combustion in Tg of S estimated by Model 1 (upper curve) and Model 2 (lower curve) (from Hameed and Dignon, 1988). [Reprinted with permission from Pergamon Press.]

by Cullis and Hirschler (1980), a fact which evidences the uncertainties in these difficult evaluations.

Hameed and Dignon (1988) also provide trends of NO_x emissions from fossil fuel combustion, which are summarized in Figure 1–3. Their regional analysis also shows that, although the greatest rates of SO_x and NO_x emissions occur in the northern midlatitudes, the greatest increases from 1966 to 1980 have taken place in the tropics, a fact that is having dramatic consequences in the deterioration of urban air quality in third world cities around the world.

1.3.7 Air Pollution Emissions and Air Quality Trends in the United States

Recent studies (e.g., U.S. EPA, 1980, 1985, and 1988) have provided detailed information on air pollution emissions in the United States, which is generally not available for other countries. We summarize here some of the important anthropogenic emission data and trends in the United States (from U.S. EPA, 1988).

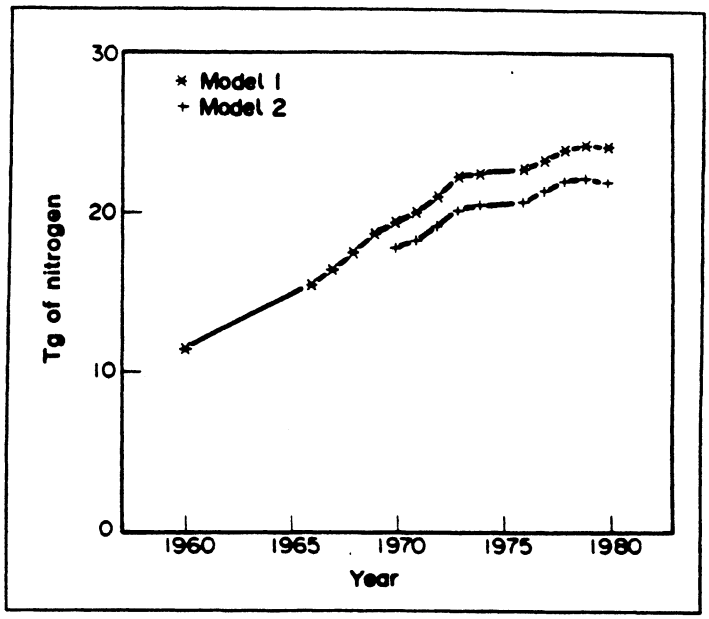

Figure 1-3. Annual global emissions of NO_x from fossil-fuel combustion in Tg of N estimated by Model 1 (upper curve) and Model 2 (lower curve) (from Hameed and Dignon, 1988). [Reprinted with permission from Pergamon Press.]

- **Particulate Matter**

Annual average total suspended particulate (TSP) levels, which have been measured at 1,435 locations, decreased 23 percent between 1977 and 1986, while TSP emissions varied from 9 Tg a^{-1} to 7 Tg a^{-1}. In 1987, the U.S. EPA promulgated new standards for particulate matter using a new indicator, PM_{10} (i.e., inhalable particles with aerodynamic diameters smaller than 10 μm), instead of TSP. This new standard focuses on particles responsible for adverse health effects and, therefore, future U.S. EPA trends will be based on PM_{10} data, collected by PM_{10} monitoring networks being deployed nationally.

- **Sulfur Dioxide, SO_2**

Annual average SO_2 levels measured by 302 continuous monitors decreased 37 percent from 1977 to 1986. Emissions of SO_2 decreased from 27 Tg a^{-1} in 1977 to 21 Tg a^{-1} in 1986. Historic SO_x emission data from 1900 to 1980 can be found in Gschwandtner et al. (1986) and trend analyses of monthly SO_2 emissions are given by Lins (1987).

- **Carbon Monoxide, CO**

The second highest non-overlapping 8-hour average *CO* concentrations measured at 182 sites have shown a decrease of 32 percent between 1977 and 1986. This decrease is due to the implementation of pollution controls for mobile sources. Emissions of *CO* varied from 82 Tg a^{-1} in 1977 to 62 Tg a^{-1} in 1986.

- **Nitrogen Dioxide, NO_2**

Annual average NO_2 concentrations, measured at 111 sites, increased from 1977 to 1979 and then generally decreased through 1986. Measurements in 1986 were 14 percent lower than the 1977 levels. The NO_x emissions have shown a similar trend, remaining in the range of 19–21 Tg a^{-1}. Los Angeles, California, is now the only area in the United States that exceeds the annual air quality standard (53 ppb). Historic NO_x emission data from 1900 to 1980 can be found in Gschwandtner et al. (1986).

- **Ozone, O_3**

The composite average of the second highest daily maximum 1-hour ozone values, recorded at 242 sites, decreased 21 percent from 1977 to 1986, probably due to the combined decrease of NO_x emissions and of volatile organic compound (VOC) emissions, which declined from 24 Tg a^{-1} in 1977 to 19 Tg a^{-1} in 1986.

- **Lead, Pb**

The composite maximum quarterly average of ambient lead concentrations, recorded at 82 urban sites, decreased 87 percent between 1977 and 1986, while lead emissions decreased 94 percent (from $140 \cdot 10^3$ metric tons a^{-1} to $8 \cdot 10^3$ metric tons a^{-1}). This large decrease is mostly due to the reduction of the lead content of leaded gasoline.

1.4 ADVERSE EFFECTS

A vast literature describes the adverse effects of atmospheric pollutants on the environment and on ecology; e.g., Williamson (1973, Chapter 2), Stern (1977a), National Research Council (1983, Chapter 1; for acidic deposition effects), and, especially, Stern (1986). The October 1988 issue of *Atmospheric Environment* was dedicated to human exposure to air pollutants. Adverse effects include the following.

- **Odor**

Ambient atmospheric pollutants can cause disturbing odors, characterized by their quality and intensity. In particular, human beings have a low threshold for sulfur-bearing compounds and these are, therefore, easily detected.

- **Human Health Effects**

Several adverse effects on human health have been identified, especially respiratory effects (bronchitis, pulmonary emphysema and lung cancer). Some pollutants (such as ozone) have possible mutagenic effects, while others have shown carcinogenic effects (see Table 1–3). Pollutants also have synergistic effects, in which, for example, SO_2 damage to the human respiratory system can be greatly enhanced by the presence of fine particles.

- **Materials Damage**

Pollutants damage materials and structures by abrasion, deposition/removal, direct/indirect chemical attack and electrochemical corrosion (Tombach, 1982). Especially in the European countries, air pollution damage to artistic buildings and materials (e.g., marble and statues) is significant. Table 1–4 gives a summary of these effects.

- **Ecological Damage**

Vegetation shows clear damage due to ozone, sulfur dioxide, nitrogen dioxide, fluoride, peroxyacetic nitrate (PAN) and ethylene. Domestic and dairy animals have suffered deleterious effects during several pollution episodes. Livestock damage has been occasioned by fluoride (from heavy chemical industry emissions) and arsenic (e.g., from copper smelters).

- **Meteorological Changes**

On a larger scale, pollutants affect meteorological parameters, as illustrated in Table 1–5. Visibility is impaired by attenuation of solar radiation (urban turbidity), NO_2 absorption of light and particle light scattering. For the latter, small particles, with a size comparable to the wavelength of light (0.40 to 0.70 μm), are the most effective.

- **Effects of Acidic Deposition**

Acidic deposition is a phenomenon in which acidic substances like H_2SO_4, HNO_3, and HCl are brought to earth by dry and wet deposition. This deposition

Table 1–3. Unit risk factors for analysis of inhalation exposure (adapted from the SCAQMD, 1988). These unit risk factors are those developed by the California Department of Health Services for those substances identified as toxic air contaminants by the California Air Resources Board. The unit risk factor is the probability that an individual will contract cancer when exposed, through inhalation, to one $\mu g/m^3$ of a substance over a lifetime (70 years). The weight of evidence classifications are: A, human carcinogen; B, probable human carcinogen (B1, limited human evidence; B2, sufficient animal evidence, but inadequate or no human evidence).

Substance	CAS Number	Unit Risk Factor $(\mu g/m^3)^{-1}$ and Weight of Evidence
Acrylonitrile	107–13–1	6.8×10^{-5} [B1]
Allyl Chloride	107–05–1	5.9×10^{-6} [B2]
Arsenic	7440–38–2	4.3×10^{-3} [A]
Asbestos	1332–21–4	190×10^{-6} per 0.0001 fibers/cm^3 [A]
Benzene	71–43–2	5.3×10^{-5} [A]
Benzidene	92–87–5	6.7×10^{-2} [A]
Benzo(a)Pyrene	50–32–8	1.7×10^{-3} [B2]
Beryllium	7440–41–7	2.4×10^{-3} [B2]
Bis(2–chloroethyl)ether	111–44–4	3.3×10^{-4} [B2]
Bis(chloromethyl)ether	542–88–1	2.7 [A]
1,3–Butadiene	106–99–0	6.7×10^{-5} [B2]
Cadmium	7440–43–9	1.2×10^{-2} [B1]
Carbon tetrachloride	56–23–5	4.2×10^{-5} [B2]
Chlorinated dioxins and dibenzofurans (TCDD equivalent)		38 [B2]
Chlorinated ethanes: 1,2–Dichloroethane (Ethylene dichloride)	107–06–2	2.2×10^{-5} [B2]
Chloroform	67–66–3	2.3×10^{-5} [B2]
Chromium, hexavalent	7440–47–3	1.5×10^{-1} [A]

Table 1–3 (continued)

Substance	CAS Number	Unit Risk Factor $(\mu g/m^3)^{-1}$ and Weight of Evidence
Dichlorobenzidene	91–94–1	4.8×10^{-4} [B2]
2,4–Dinitrotoluene	121–14–2	1.9×10^{-4} [B2]
Diphenylhydrazine	122–66–7	2.2×10^{-4} [B2]
Ethylene dibromide	106–93–4	7.2×10^{-5} [B2]
Ethylene dichloride	107–06–2	2.2×10^{-5} [B2]
Epichlorohydrin	106–89–8	1.2×10^{-6} [B2]
Ethylene oxide	75–21–8	1.0×10^{-4} [B1]
Formaldehyde	50–00–0	1.3×10^{-5} [B1]
Hexachlorobenzene	118–74–1	4.9×10^{-4} [B2]
Hexachlorocyclohexane:		
technical grade	---	5.7×10^{-4} [B2]
alpha isomer	319–84–6	7.6×10^{-4} [B2]
Methylene chloride	75–09–2	4.1×10^{-6} [B2]
Nickel:		
refinery dust	---	2.4×10^{-4} [A]
subsulfide	0120–35–722	4.8×10^{-4} [A]
Nitrosamines:		
Dimethylnitrosamine	62–75–9	1.4×10^{-2} [B2]
Diethylnitrosamine	55–18–5	4.3×10^{-2} [B2]
Dibutylnitrosamine	924–16–3	1.6×10^{-3} [B2]
Phenols:		
2,4,6–Trichlorophenol	88–06–2	5.7×10^{-6} [B2]
Polychlorinated biphenyls	1336–36–3	1.2×10^{-3} [B2]
Trichloroethylene	79–01–6	1.3×10^{-6} [B2]
Vinyl chloride	75–01–4	2.7×10^{-6} [A]

Table 1–4. Air pollution damage to various materials (from Yocum et al. in Stern, 1986). [Reprinted with permission from Academic Press.]

Materials	*Types of damage*	*Principal damaging pollutants*	*Other environmental factors*	*Methods of measurement*	*Mitigation measures*
Metals	Corrosion, tarnishing	Sulfur oxides and other acid gases	Moisture, air, salt, particulate matter	Weight loss after removal of corrosion products, reduced physical strength, change in surface characteristics	Surface plating or coating, replacement with corrosion-resistant material, removal to controlled environment
Building stone	Surface erosion, soiling, black crust formation	Sulfur oxides and other acid gases	Mechanical erosion, particulate matter, moisture, temperature fluctuations, salt, vibration, CO_2, microorganisms	Weight loss of sample, surface reflectivity, measurement of dimensional changes, chemical analysis	Cleaning, impregnation with resins, removal to controlled environment
Ceramics and glass	Surface erosion, surface crust formation	Acid gases, especially fluoride-containing	Moisture	Loss in surface reflectivity and light transmission, change in thickness, chemical analysis	Protective coatings, replacement with more resistant material, removal to controlled environment
Paints and organic coatings	Surface erosion, discoloration, soiling	Sulfur oxides, hydrogen sulfide	Moisture, sunlight, ozone, particulate matter, mechanical erosion, microorganisms	Weight loss of exposed painted panels, surface reflectivity, thickness loss	Repainting, replacement with a more resistant material
Magnetic storage media	Loss of signal, tape failure	Particles	Moisture, abrasion, wear	Signal quality, physical and chemical analysis	Removal to controlled environment, periodic cleaning and recopying

Table 1–4 (continued)

Paper	*Embrittlement discoloration*	*Sulfur oxides*	Moisture, physical wear, acidic materials introduced in manufacture, microoganisms	Decreased folding endurance, pH change, molecular weight measurement, tensile strength	Synthetic coatings, storing in a controlled atmosphere, deacidification, encapsulation, impregnation with organic polymers
Photographic materials	Microblemishes	Sulfur oxides	Particulate matter, moisture	Visual and microscopic examination.	Removal to controlled environment
Textiles	Reduced tensile strength, soiling	Sulfur and nitrogen oxides	Particulate matter, moisture, light, physical wear, washing	Reduced tensile strength, chemical analysis (e.g., molecular weight), surface reflectivity	Replacement, use of substitute materials, impregnation with polymers
Textile dyes	Fading, color change	Nitrogen oxides, ozone	Light, temperature	Reflectance and color value measurements	Replacements, use of substitute materials, removal to controlled environment
Leather	Weakening, powdery surface	Sulfur oxides	Physical wear, residual acids introduced in manufacture	Loss in tensile strength; chemical analysis	Removal to a controlled environment, consolidation with polymers, replacement
Rubber	Cracking	Ozone	Sunlight, physical wear	Loss in elasticity and strength, measurement of crack frequency and depth	Addition of antioxidants to formulation, replacement with more resistant materials

Table 1–5. Approximate minimum concentration thresholds of atmospheric effects due to minor constituents (from Hobbs et al., 1974 as reported by Robinson in Stern, 1977a). [Reprinted with permission from Academic Press.]

Species	*Effect*	*Threshold*	
		Volume per unit volume of air	*kg/km³ of air*
Ice nuclei	Cloud structure and precipitation	10^{-18}	10^{-6}
CCN	Cloud structure and precipitation	10^{-15}	10^{-3}
Aerosols	Visibility and heating rates	10^{-12}	10^{0}
HCl, H_2SO_4	pH of rain	10^{-11}	10^{-2}
Aerosols	pH of rain	10^{-10}	10^{2}
NH_3	pH of rain	10^{-10}	10^{-1}
SO_2	pH of rain	10^{-8}	10^{1}
NO_2	Visibility and heating rates	10^{-7}	10^{2}
O_3	Heating rates	10^{-6}	10^{3}

affects primary receptors (e.g., the surface of soil with no vegetation), secondary receptors (e.g., soil underneath vegetation), and tertiary receptors (e.g., lakes receiving water from runoff from the watershed). Lakes located in both North America and Northern Europe are very sensitive to acid deposition because of their limited buffering capacity. These lakes, when exposed to acid precipitation pass through three stages (Havan, in Stern, 1986), as illustrated in Figure 1–4. The first stage (bicarbonate lakes) is characterized by a steady decrease in the acid–neutralizing (i.e., buffering) capacity. The second stage (transition lakes) begins when the acid–neutralizing capacity is exausted and concentrations of sulfate and metals begin to increase. During the third and final stage (acid lakes), the pH begins to stabilize. By this stage, however, acid–sensitive species have been eliminated. Acidified lakes remain ideal for many recreational activities except fishing.

- **Effects of Carbon Dioxide, CO_2**

On a global scale, there is widespread concern that the increasing anthropogenic CO_2 emissions from combustion processes, and the consequent global increase of CO_2 concentrations, may increase the average temperature of the earth, as illustrated in Table 1–6. Preindustrial (i.e., 1860) CO_2 levels are commonly thought to have been between 270 ppm and 290 ppm. The present levels are about 330 to 340 ppm, with recent growth rates of more than 1 ppm per year.

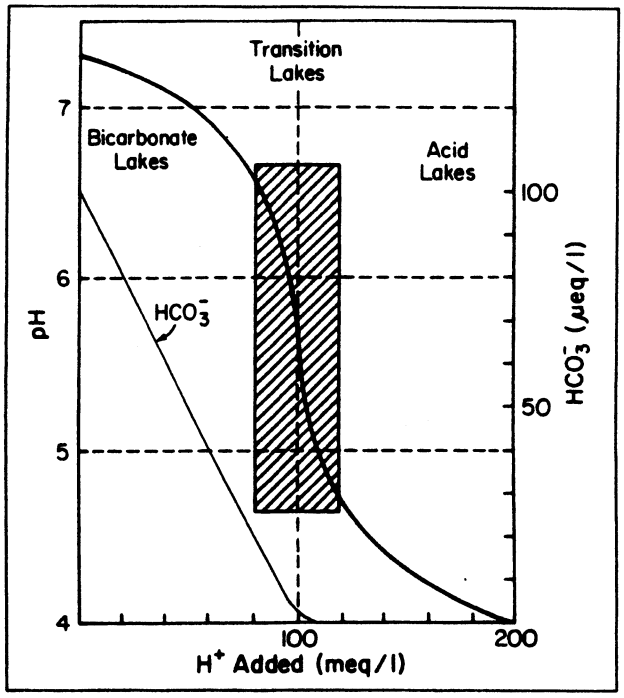

Figure 1–4. Titration curve for a bicarbonate solution with an initial concentration of 100 μEq/liter (from Henriksen, 1980). [Reprinted with permission from Pergamon Press.]

A range analysis for possible future growth of CO_2 ambient concentration is presented in Figure 1–5. (See further discussion on the CO_2 problem in Chapter 13).

- **Effects on Stratospheric Ozone**

Another possibly adverse effect on a global scale is the reduction of stratospheric ozone caused by chlorofluorocarbons, which are stable in the troposphere but are photodissociated in the stratosphere. A reduction of stratospheric ozone would decrease the efficiency of the present protective "blanket" that limits the amount of ultraviolet solar radiation that reaches the earth's surface. (See further discussion on stratospheric ozone in Chapter 13).

1.5 AIR QUALITY LEGISLATION

Several countries in the world have established air pollution laws and regulations and have implemented air quality and/or emission standards. The

Table 1-6. Estimated range of CO_2-induced temperature rise (in °C) (from U.S. EPA, 1980).

Atmospheric CO_2 compared to preindustrial levels	Low Latitude (0°-5°)		Average		High Latitude (80°-90°)	
	O	P	O	P	O	P
2x	0.8	2.4	1.5	2.9	3.6	11
4x	1.9	4.8	2.9	5.8	7.5	18
6x	2.8	6.0	4.1	7.5	9.0	20

O = optimistic; P = pessimistic.

Source: Adapted from Markley, O.W., et al., Socio-political Impacts of Carbon Dioxide Buildup in the Atmosphere Due to Fossil Fuel Combustion, prepared for the U.S. Energy Research and Development Administration, 1977, p. 35.

United States, in particular, has developed a large and complex body of air quality laws directed toward the goals of progressive air quality improvement in those regions characterized by unhealthy concentration levels and environmental preservation in regions with clean air (especially the national parks in the West). Moreover, the U.S. regulations have incorporated the use of several air quality diffusion models as official regulatory tools (e.g., to be used for the authorization of new emissions of air pollutants).

Air quality legislation (or lack of it) has affected the development of air pollution modeling techniques in different countries. In the United States, the air quality regulations, together with the existence of a free market typically oriented toward consulting business activities, have created the proper conditions for the development of "practical" techniques, sometimes very sophisticated ones, but still based on methods that rely upon available data and limited computational resources. In general, U.S. studies have benefited from public and private funding sources and have focused on specific problems with a clear goal-oriented inclination.

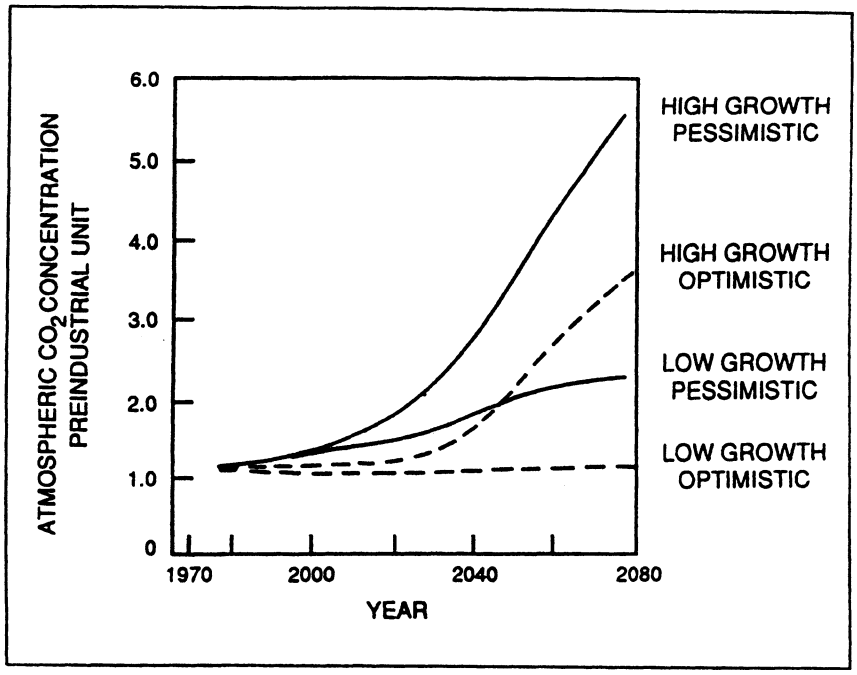

Figure 1–5. Atmospheric carbon dioxide concentrations — range analysis (from U.S. EPA, 1980).

European studies and research activities in this field have been carried out mainly by public organizations, i.e., universities and research centers. However, research centers of private industries have also provided valuable contributions. European research, performed without the pressure of specific legislative goal-oriented objectives, has covered with success interesting and advanced topics. These activities, however, have not yet finalized a set of transferable computer packages like those in the United States.

In long-range transport problems, national legislation is not sufficient and international rules and agreements need to be found. This seems to be a sensitive issue in northeastern North America, where Canada is blaming the United States for a large fraction of their acidic deposition, and in Europe, where many countries are blaming each other for the same issue. The Chernobyl accident has shown everyone that air pollution, unlike people, can freely emigrate from one country to another, and affect even countries like Italy, which many meteorologists believed well-protected by the Alpine mountain chain.

In spite of progress in the last two decades toward economical and political unity in Europe, common environmental legislation is still lacking. The recent common trend of increasing the average height of industrial emissions (especially in power plants) is certainly improving the near-field air quality, but is expanding the effects of long-range transport and acidic deposition all over Europe. As an example of this trend, Figure 1-6 shows that the strong reduction of low- and medium-level SO_2 emissions in the United Kingdom has been associated with almost a doubling of high-level SO_2 emissions during the same period, 1960 to 1980. In the absence of unified legislation, most countries may be tempted in the

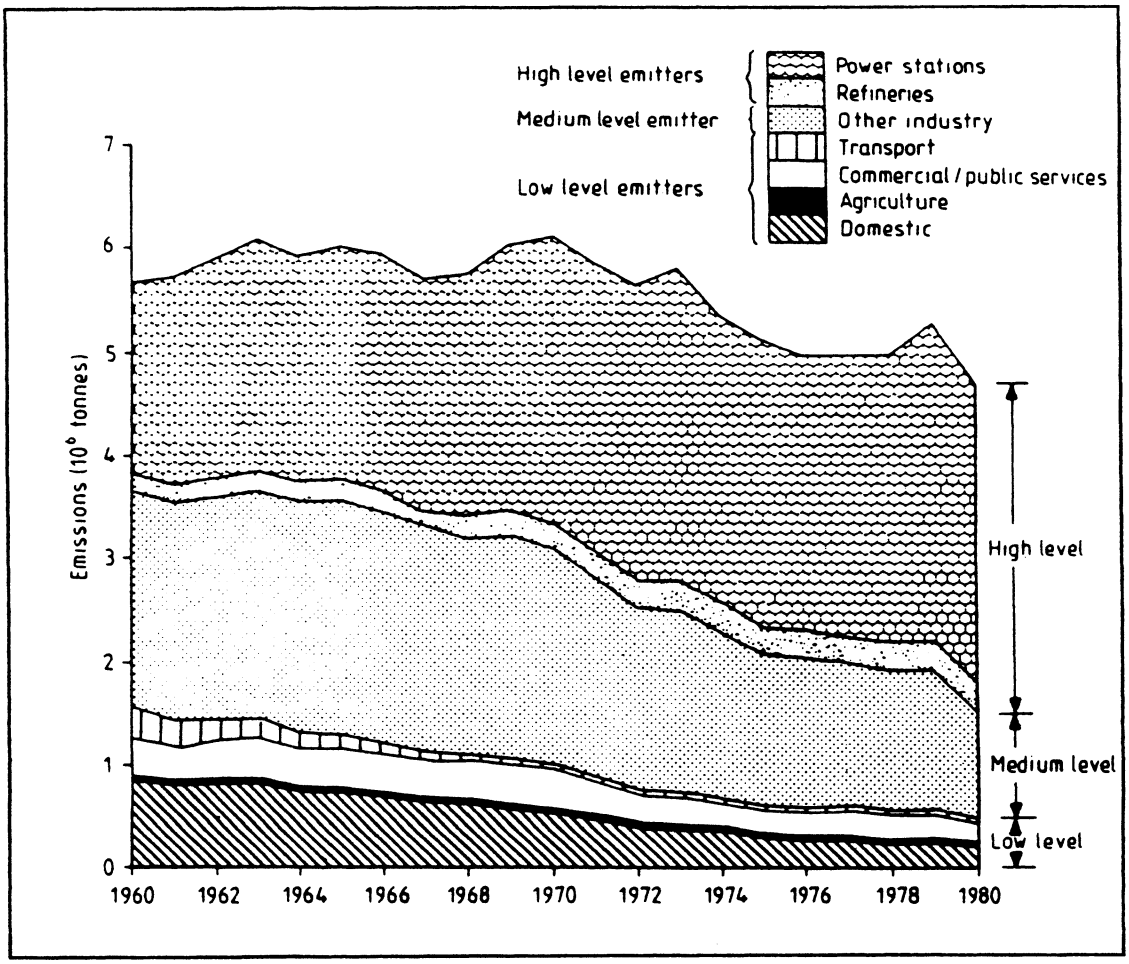

Figure 1-6. Trends in UK sulphur dioxide emissions as a function of height of emission. Data from Warren Spring Laboratory Reports, *as presented by Henderson-Sellers (1984). [Reprinted with permission from IOP Publishing, Ltd.]*

near future to continue increasing emission rates and release heights, thus further increasing their pollution of neighboring nations. Joint European R&D modeling efforts are expected, in the next few years, to provide legislators with suggestions and recommendations for a unified set of European environmental regulations.

Several articles and books have reviewed air quality legislation, especially in the United States. Stern (1977b) presents the national and worldwide air quality management problems and air pollution standards (see, in particular, Heath and Campbell in Stern, 1977b, for air pollution legislation and regulation). Historical review of U.S. air quality laws can be found in Stern (1977c; 1982). Controlled trading, which represents the most recent and, probably, innovative development toward a "free market" approach for air pollution control, is also discussed in U.S. EPA (1981)(*) and Ryan (1981). A review of air pollution legislation and regulation in the European community is provided by O'Riordan (1989).

(*) More information on recent EPA regulations can be obtained from Regulatory Reform Staff, U.S. Environmental Protection Agency PM-223, Washington, D.C. 10460, U.S.A.; telephone (202) 287-0750.

References

Cullis, C.F., and M.M. Hirschler (1980): Atmospheric sulfur: natural and manmade sources. *Atmos. Environ.*, **14**:1263–1278.

Gschwandtner, G., K. Gschwandtner, K. Eldridge, C. Mann, and D. Mobley (1986): Historic emissions of sulfur and nitrogen oxides in the United States from 1900 to 1980. *JAPCA*, **36**(2):139–149.

Hameed, S., and J. Dignon (1988): Changes in the geographical distributions of global emissions of NO_x and SO_x from fossil-fuel combustion between 1966 and 1980. *Atmos. Environ.*, **22**:441–449.

Henderson-Sellers, B. (1984): *Pollution of Our Atmosphere*. Bristol, U.K.: Adam Hilger Ltd., Bristol.

Henriksen, A. (1980): *Water Res.*, **14**:809–813.

Hidy, G.M. (1984): *Aerosols -- An Industrial and Environmental Science*. Orlando, Florida: Academic Press Inc..

Hobbs, P.V., H. Harrison, and E. Robinson (1974). *Science*, **183**:909–915.

Lins, H.F. (1987): Trend analysis of monthly sulfur dioxide emissions in the conterminous United States. *Atmos. Environ.*, **21**(11):2297–2309.

O'Riordan, T. (1989): Air pollution legislation and regulation in the European community: A review essay. *Atmos. Environ.*, **23**(2):293–306.

Ryan, D. (1981): A free enterprise approach to air pollution control. *EPA Journal*, April.

South Coast Air Quality Management District (1988): Proposed Rule 1401. New Source Review of Carcinogenic Air Contaminants. El Monte, California

Stern, A.C., Ed. (1976): *Air Pollution*, 3rd Edition, Volume I. New York: Academic Press.

Stern, A.C., Ed. (1977a): *Air Pollution*, 3rd Edition, Volume II. New York: Academic Press.

Stern, A.C., Ed. (1977b): *Air Pollution*, 3rd Edition, Volume V. New York: Academic Press.

Stern, A.C. (1977c): Prevention of significant deterioration -- A critical review. *JAPCA*, **27**:440.

Stern, A.C. (1982): History of air pollution legislation in the United States. *JAPCA*, **32**:44.

Stern, A.C., Ed. (1986): *Air Pollution*, 3rd Edition, Volume VI. New York: Academic Press.

Strauss, W., Ed. (1972): *Air Pollution Control*. New York: Wiley (Interscience).

Tombach, I. (1982): Measurement of local climatological and air pollution factors affecting stone decay. From *Conservation of Historic Stone Buildings and Monuments*. Washington, D.C.: National Academic Press.

U.S. Environmental Protection Agency (1981): Controlled trading: How to reduce the cost of air pollution control. Booklet prepared by the U.S. EPA Regulatory Reform Staff, Washington, D.C., August.

U.S. Environmental Protection Agency (1980): Environmental outlook 1980. EPA-600/8-80-003.

U.S. Environmental Protection Agency (1985): National air quality and emissions trends report. EPA-450/4-84-029, Research Triangle Park, North Carolina.

U.S. Environmental Protection Agency (1988): National air quality and emission trends report, 1986. EPA-450/4-88-001, Office of Air Quality Planning and Standards, Research Triangle Park, North Carolina.

Williamson, S.J. (1973): *Fundamentals of Air Pollution*. Reading, Massachusetts: Addison-Wesley.

2 THE TOOL - MATHEMATICAL MODELING

Air quality modeling is an essential tool for most air pollution studies. Models can be divided into

- physical models -- small scale, laboratory representations of the phenomena (e.g., wind tunnel, water tank)
- mathematical models -- a set of analytical/numerical algorithms that describe the physical and chemical aspects of the problem

Physical models (Puttock, 1979; Willis and Deardorff, 1981; Mitsumoto and Ueda, 1983; Alessio et al., 1983) have shown interesting results, illuminating mechanisms and providing validation data to developers of mathematical models. Physical models will not be discussed further in this book on mathematical models.

2.1 DETERMINISTIC VERSUS STATISTICAL MODELS

Mathematical models can be

- deterministic models, based on fundamental mathematical descriptions of atmospheric processes, in which effects (i.e., air pollution) are generated by causes (i.e., emissions)
- statistical models, based upon semiempirical statistical relations among available data and measurements

An example of a deterministic model is a diffusion model, in which the output (the concentration field) is computed from mathematical manipulations of specified inputs (emission rates and atmospheric parameters such as dispersion rates). An example of a statistical model is given by the forecast, in a certain region, of the concentration levels in the next few hours, as a statistical function

of (1) the currently available measurements and (2) the past correlation between these measurements and the concentration trends.(*)

Deterministic models are the most important ones for practical applications since, if properly calibrated and used, they provide an unambiguous, deterministic source–receptor relationship. Such a relationship is the goal of any study aiming either at improving ambient air quality or preserving the existing concentration levels from future urban and industrial developments. In other words, only a deterministic model can provide an unambiguous assessment of the fraction of responsibility of each pollutant source to each receptor area, thus allowing the definition and implementation of appropriate emission control strategies.

2.2 WHY AIR QUALITY MODELING?

Air quality models are a unique tool for (Seinfeld, 1975)

- establishing emission control legislation; i.e., determining the maximum allowable emission rates that will meet fixed air quality standards
- evaluating proposed emission control techniques and strategies; i.e., evaluating the impacts of future control
- selecting locations of future sources of pollutants, in order to minimize their environmental impacts
- planning the control of air pollution episodes; i.e., defining immediate intervention strategies, (i.e., warning systems and real–time short–term emission reduction strategies) to avoid severe air pollution episodes in a certain region
- assessing responsibility for existing air pollution levels; i.e., evaluating present source–receptor relationships

Figure 2–1 illustrates the elements of a comprehensive air pollution control strategy in a certain region.

It is important to clarify what air quality modeling is and what it is not. Air quality modeling is an indispensable tool for all the above analyses. It is,

(*) The above distinction is not strict. Some diffusion models, for example, are based on statistical diffusion theories and the performance of a statistical model is always improved when some deterministic information is included in its structure. Mixed deterministic–statistical methods are also available (see Chapter 12).

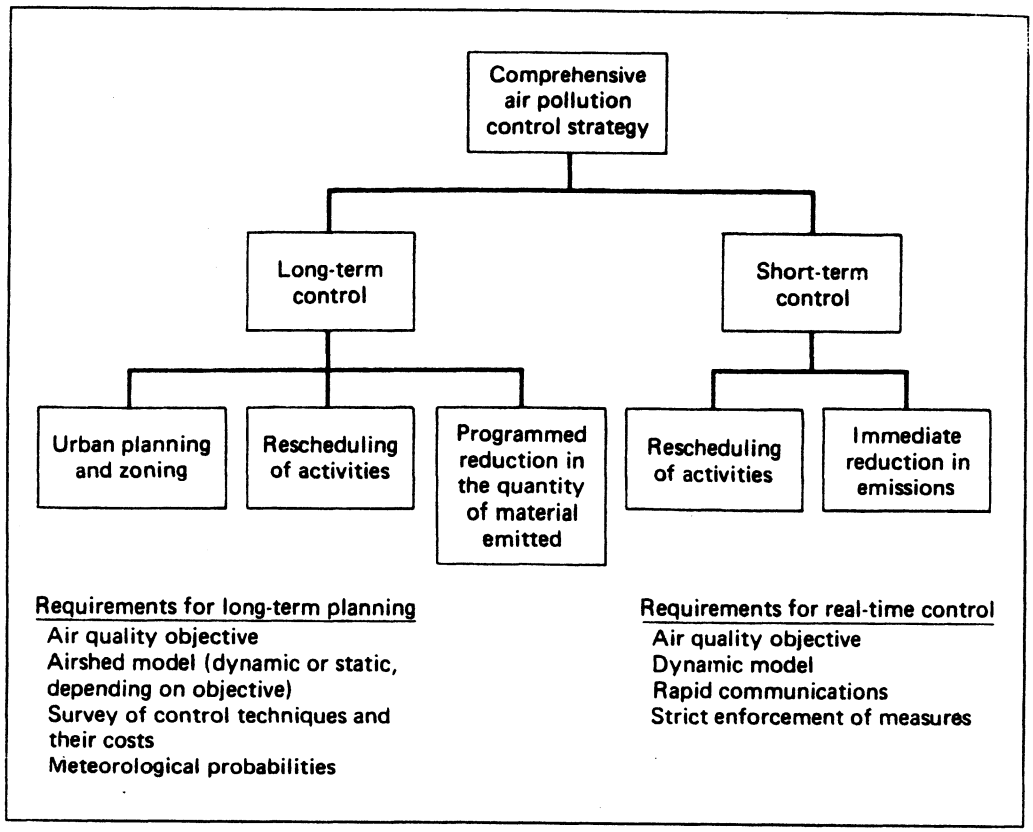

Figure 2–1. Elements of a comprehensive air pollution control strategy for a region (from Seinfeld, 1975). [Reprinted with permission from McGraw–Hill.]

however, only a tool. Modeling, like monitoring, is *not* the solution of the air pollution problem, even though each is sometimes presented as such. Monitoring and modeling studies constitute only a relatively inexpensive activity whose results, in the best case, provide useful information for possible future implementations of much more expensive emission reduction and control strategies.

It is also important to clarify the real role of modeling versus monitoring efforts. It is not unusual to hear qualified scientists making statements such as "Why do we need to model that? Let's measure it; that's all we need," "Models do not work," etc. These statements imply unscientific thinking. Science involves the development of theories (or "models") based on (1) the empirical interpretation of experimental data, (2) the generalization of experimental relationships, or (3) pure speculative thinking subsequently confirmed by experimental results. The advancement of science is not the consequence of monitoring activities, even

though the collection of good, reliable experimental data is often (but not always) a necessary (but not sufficient) condition to it.

The above concepts, which are well-established in most scientific circles, are sometimes alien to the environmental community, where, for example, it is commonly believed that environmental measurements are the "real world." They are not! Monitoring data are indispensable for inferring theories or parameters and calibrating or validating computer simulation packages. Their spatial and temporal resolution, however, is generally insufficient to qualify them as the real world. Only a well-tested and well-calibrated simulation model can be a good representation of the real world, its dynamics and its responses to perturbations. Unfortunately, all over the world, huge investments and efforts are made to collect data that too often remain unused on paper or computer tapes. Too often these monitoring activities are not well coordinated with numerical modelers or not followed by appropriate investment in computer analyses, interpretations and modeling studies that are the logical and indispensable continuation of the initial project.

2.3 MODELING TOPICS

Simulation modeling techniques can be applied to all aspects of the air pollution problem; i.e., (1) to evaluating emission rates, (2) to describing phenomena that take place in the atmosphere, and (3) to quantifying adverse pollutant effects (damage computation) in a certain region. In this book, only the second modeling category will be extensively covered. This will include mathematical models for simulating

- atmospheric transport
- turbulent atmospheric diffusion
- atmospheric chemical and photochemical reactions
- ground deposition

Even with the above limitation, the problem remains formidable. A correct representation of these phenomena and their multimedia (i.e., air–water–land) interactions requires several sets of equations, as illustrated schematically in Figure 2–2. The situation is actually even more complex, because Figure 2–2 does not contain the chemical processes explicitly. Drake (1979) has discussed a complete set of governing equations. Businger (in Nieuwstadt and van Dop, 1982) has given another important survey of equations and concepts in

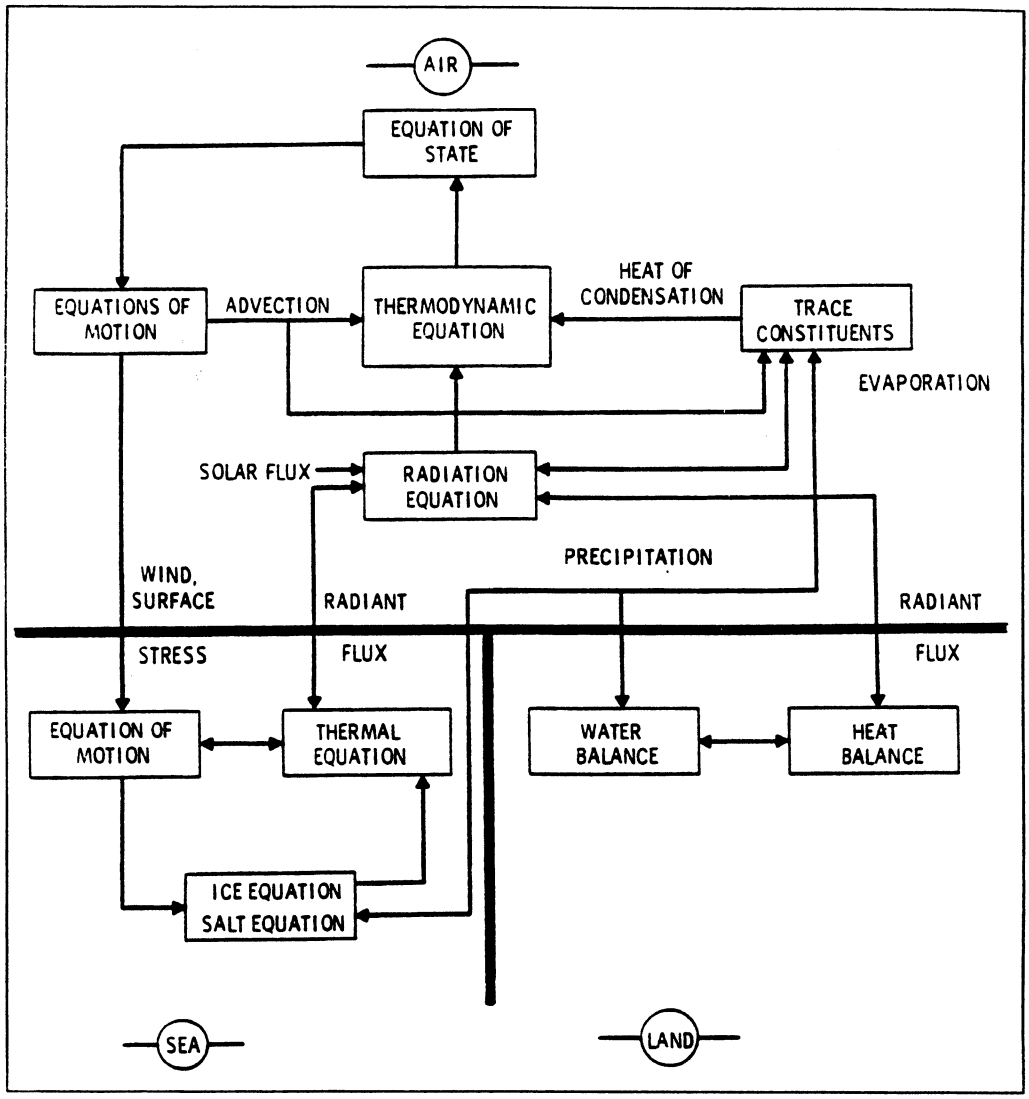

Figure 2–2. Processes comprising weather, climate and the fate of pollutants (from Drake, 1979). [Reprinted with permission from the Electric Power Research Institute.]

atmospheric turbulence and air pollution, while Dutton (1976) and Pielke (1984) have provided full discussion of meteorological equations and modeling. Seinfeld (1986) and Finlayson-Pitts and Pitts (1986) discuss atmospheric chemistry in great detail.

2.4 SOME PRACTICAL CONSIDERATIONS

Practical application of deterministic air quality models requires

- analysis of the problem
- selection of the appropriate model(s)
- application of the selected model(s)

The analysis of the problem requires, as a minimum, the identification of

- the type of pollutant (reactive or nonreactive)
- the averaging time of interest (e.g., instantaneous concentrations, for odor problems; one-hour averages, for short-term cases; or annual averages, for long-term analyses)
- the characteristics of the domain (e.g., simple flat terrain cases or complex orography)
- the computational limitations (e.g., simple assumptions or more complex formulations, depending on the available computational facilities)

Model selection should be performed by taking into account the above factors, as illustrated in Figure 2-3.

Finally, the optimal application of a deterministic model for control strategy analysis should incorporate its calibration and evaluation with local air quality monitoring data, in order to determine its applicability and minimize forecasting errors, as illustrated in Figure 2-4. Only models that have been verified by past data should be used for future forecasting. Calibration and evaluation are, however, difficult in many cases, when sufficient air quality and meteorological data are not available, and impossible in others, when, for example, models are used to simulate the impacts of possible *future* new sources.

Since ideal model application conditions are seldom found, air quality models are often used beyond their theoretical and practical limits of applicability. It is, therefore, not surprising that several model validation studies (e.g., Reynolds et al., 1984a,b; Lewellen and Sykes, 1983; Ruff et al., 1984) have shown unsatisfactory performance, especially when steady-state representations are used to simulate complex, time-dependent atmospheric phenomena.

2.5 MODELING FROM A PHILOSOPHICAL STANDPOINT

Phenomena such as turbulent diffusion can be viewed as stochastic processes; i.e., processes whose dynamics are so complicated that they can only be

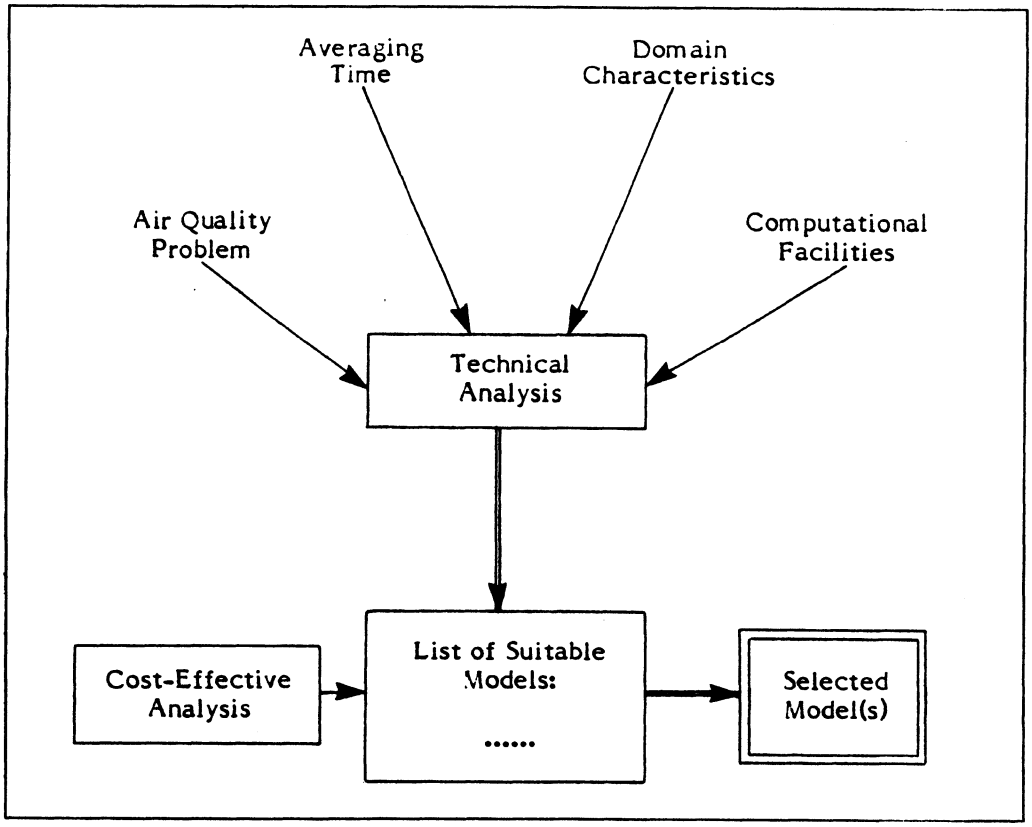

Figure 2–3. Model selection.

treated as if they were affected by random components. Wyngaard (from Nieuwstadt and van Dop, 1982) clarified this point by asking simple questions: "Why is it necessary to *model* them [the equations of motion in the atmospheric boundary layer] before solving them numerically? Why can't we solve them directly on today's large, fast computers?" The answer is provided by his length-scale analysis of the atmospheric turbulent flow, showing that typical boundary layer situations are associated with scales of turbulent motion from 300 m down to 1 mm. Therefore, a numerical grid, for example on a 10 km x 10 km region, would require about 10^{20} grid points to (hopefully) solve all fluctuations. Moreover, initial and time-varying boundary conditions should be exactly specified. This task is clearly impossible at present.

Space- and time-averaging of boundary layer parameters have been considered to provide a valid practical solution, at least for large-scale meteorological phenomena. However, the recent numerical and philosophical analysis of

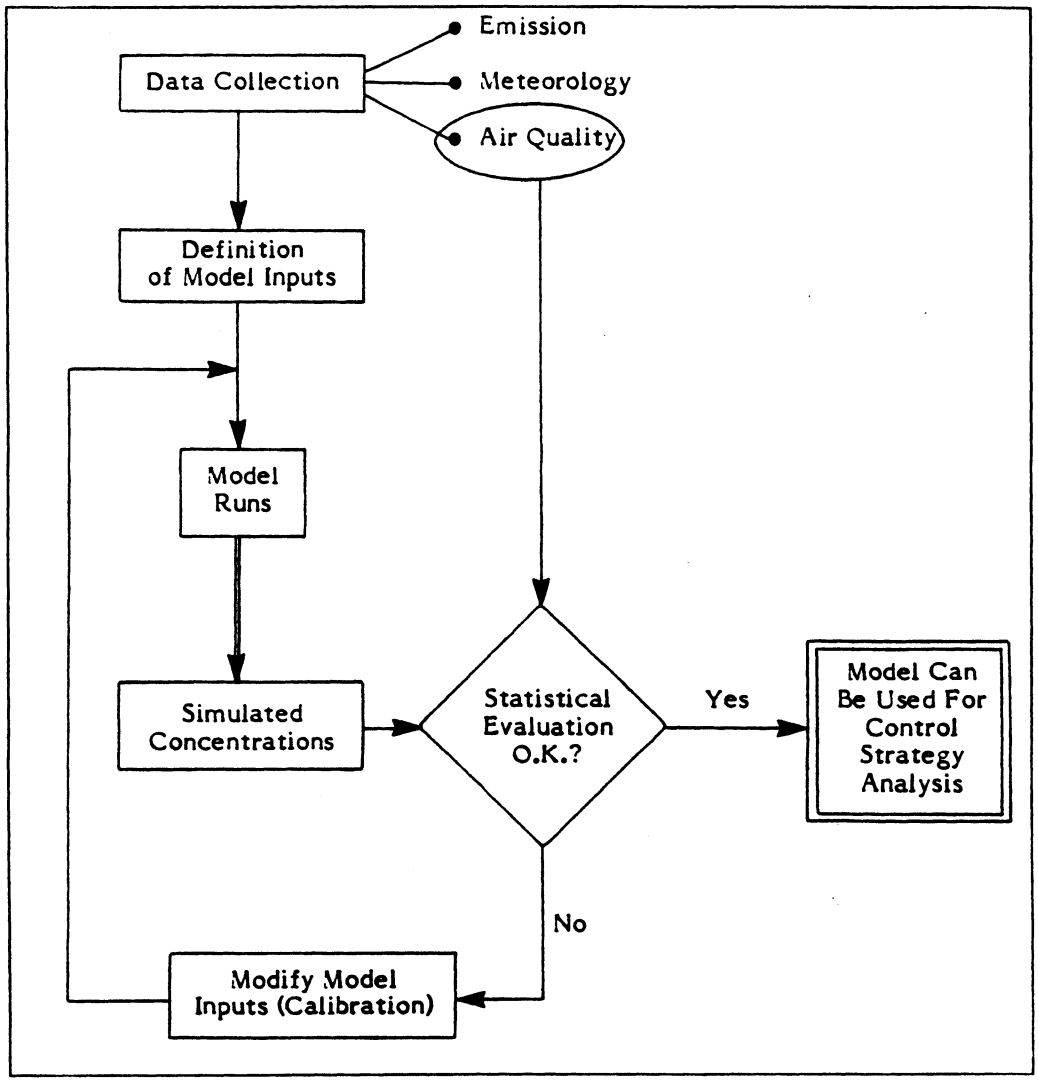

Figure 2–4. Optimal model application.

Lamb (1984) concludes that "due to a combination of our inability to quantify the precise state of the atmosphere and its boundary and to the inherent instability of atmospheric motion, not even large-scale meteorological phenomena can be rendered deterministic." He concludes that even a perfect model, using error-free input data and observations, will provide predicted quantities that still differ from the observed ones. Benarie (1987) provides additional interesting comments on the limits of air pollution modeling. The newly developed theories of chaos (Berge, 1984; Grebogi et al., 1987) seem promising for the understanding of these limits.

2.6 MODEL UNCERTAINTY

Air pollution models vary from simple methods, which possess only a few parameters, to complex ones, characterized by a large number of parameters. As illustrated in Figure 2–5, the larger the number of parameters, the lower the "natural" (or "stochastic") uncertainty associated with the model, and the smaller the errors in the model's representation of the physical reality. Unfortunately, however, the larger the number of input parameters to be specified, the larger the input data error. As indicated in Figure 2–5, there is an optimum number of parameters that minimizes the total model uncertainty. This simple interpretation explains why the performance of complex models is often equal or inferior to that of simpler methodologies. Complex models work well only when their extensive data input requirements are satisfied, which rarely occurs.

Attention must be paid to model evaluation efforts, whose results, because of the considerations above, can be misleading. Complex models can, in fact, because of their high number of parameters, be easily "tuned" or "calibrated" to well fit available measurements. This process does not, however, assure that

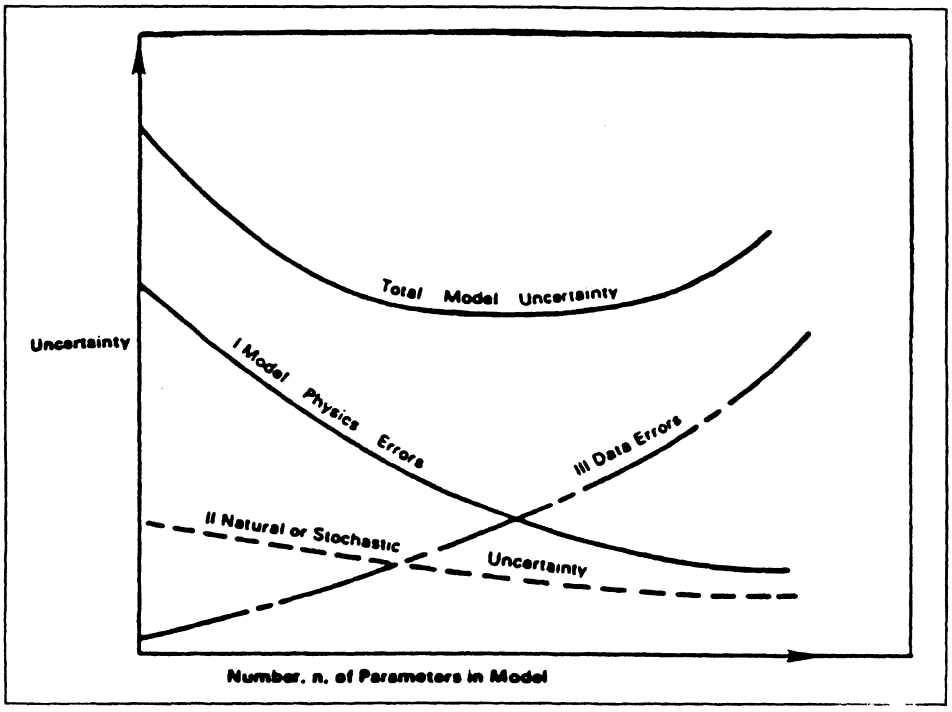

Figure 2–5. Optimal model application (from Hanna, 1989). [Reprinted with permission from Gulf Publishing Co.]

complex models perform better than simpler techniques, when applied on an "independent" data base (i.e., a data base different from the one used for model calibration). In other words, complex models can *fit* the data better than simpler techniques, but this does not necessarily indicate that complex models can *forecast* better than simpler ones.

2.7 SHORT-RANGE AND LONG-RANGE PHENOMENA

A preliminary distinction between the different transport scales of air pollution phenomena can be made as follows:

- near-field phenomena (<1 km from the source); e.g., downwash effects of plume caused by building aerodynamics
- short-range transport (<10 km from the source); e.g., the area in which the maximum ground-level impact of primary pollutants from an elevated source is generally found
- intermediate transport (between 10 km and 100 km); e.g., the area in which chemical reactions become important and must be taken into account
- long-range (or regional or interstate) transport (>100 km); e.g., the area in which large-scale meteorological effects and deposition and transformation rates play key roles.
- global effects; i.e., phenomena affecting the entire earth atmosphere; e.g., CO_2 accumulation

Until fifteen years ago, short-range problems were the major field of investigation, due to the lack of information about long-range atmospheric chemistry and, especially, because of the relatively low height of the emission stacks, so that pollutants were most noticeable only a few kilometers downwind. Moreover, calm, stagnant conditions were generally associated with the air pollution episodes under investigation, thus further restricting the length scale of the problem.

Intermediate and long-range transport processes have received increasing attention in recent years, especially due to the following factors: (1) acidic deposition, (2) visibility degradation, and (3) U.S. environmental legislation, especially the Prevention of Significant Deterioration (PSD) doctrine. Also, the Chernobyl accident has strongly enhanced the interest in long-range studies.

In Europe, where the observed acidification of Scandinavian rivers and lakes was the major starting point for the research in this field, many studies have been performed to derive long-range numerical simulation models that better fit available air quality and meteorological measurements. Among the first studies were the OECD program on Long Range Transport of Air Pollutants (Ottar, 1978) and the Cooperative Program for Monitoring and Evaluation of the Long Range Transmission of Air Pollutants in Europe (EMEP, coordinated by the U.N. Economic Commission for Europe).

Similar interest in long-range dispersion grew also in the United States, primarily inspired by the acid rain problems in the northeastern United States and Canada. Large data bases were collected to study this problem, e.g., the Electric Power Research Institute (EPRI) Sulfate Regional Experiment, SURE (Perhac, 1978; McNaughton, 1980), the U.S. Department of Energy Multistate Atmospheric Power Production Pollution Study (MAP3S) precipitation chemistry network (Dana, 1979), and the Canadian regional study (Whelpdale, from Pack et al., 1978).

As a consequence of this new interest in long-range air pollution problems, the methodologies initially used for studying and simulating short-range phenomena were expanded to simulate long-range cases. Although the two transport situations obey the same physical laws, the following considerations indicate that they require different treatment:

- The time scale of long-range transport is sufficiently large to preclude using stationary homogeneous dispersion conditions. The entire process evolves on a continuous nonstationary basis, where totally different meteorological conditions affect the pollutant dispersion at each time. Consequently, only dynamic nonstationary dispersion models can generally be applied.
- Due to the time scale of long-range transport, factors like deposition and chemistry, which may not need to be taken into account for short-range dispersion, become important.
- Horizontal diffusion can often be neglected when the emission inputs are distributed over a large-scale area, so that the concentration field is initially smoothed out. However, when an Eulerian grid is chosen, the numerical error associated with the advection terms becomes the key factor, especially for point sources. In fact, in spite of the many numerical methods proposed for minimizing numerical error, this remains the major problem for long-range transport, since many advection steps are required to move pollutants

from the emission points to the receptors, and each step contributes to such error. (See Chapter 6 for further discussion on this subject.)

- Vertical diffusion can often be neglected, assuming a homogeneous mixing of pollutants in the entire boundary layer. Elevated plumes during persistent stable conditions cannot always be treated this way, however, as, for example, in the case described by Millan and Chung (1977) where an elevated plume, trapped beneath the subsidence inversion, was detected by a COSPEC remote sensor 400 km from the source. However, even when homogeneous vertical mixing is a reasonable assumption, the problem of understanding the mass flux across a temperature inversion, which often can be significantly higher than expected (Goodman and Miller, 1977), still persists.

- Pollutants transported over a long range often impinge on complex terrain, which generally enhances atmospheric dispersion. However, terrain complexities can sometimes create the opposite effect, where valleys suffer poor ventilation with consequent trapping of pollutants.

One of the major problems in modeling the long-range transport of air pollutants is the determination of the correct trajectory of plumes, since incorrect representations may carry pollutants tens or hundreds of kilometers from the actual point of impact. Pack et al. (1978), in particular, showed that available surface-based meteorological information is generally insufficient for a correct trajectory computation, so that large errors can occur. Moreover, these errors are not random but systematic, depending on the type of advection (cold or warm) and the type of surface (land or sea). They proposed empirical trajectory adjustments to fit existing measurements. Such adjustments require direction changes up to 40 degrees and wind speed changes by up to a factor of two, which indicates the gravity of the problem. Similar results have been obtained by Policastro et al. (1986), which show poor correlation between tracer concentrations and concentrations predicted by eight short-term long-range transport models, with plume trajectory direction errors in the range of 20–45 degrees.

The above results illuminate the importance of gathering detailed, precise wind information, both on the surface and aloft, for proper modeling treatment of regional-scale transport; without precise wind information, even the best dispersion model will fail. Such information can be provided either by interpolation of measurements or by application of numerical meteorological models, as discussed in Chapter 4.

REFERENCES

Alessio, S., L. Briatore, G. Elisei, and A. Longhetto (183): A laboratory model of wake-affected stack's emissions. *Atmos. Environ.*, **17**:1139–1143.

Benarie, M.M. (1987): The limits of air pollution modelling. *Atmos. Environ.*, **21**:(1)1–5.

Berge, P., Y. Pomeau, and C. Vidal (1984): *Order Within Chaos*. New York: John Wiley.

Dana, M.T., Ed. (1979): The MAP3S precipitation chemistry network: Second periodic summary report. PNL 2829, Battelle, Pacific Northwest Laboratory, Richland, Washington.

Drake, R.L. (1979): Mathematical models for atmospheric pollutants. Appendix C: Governing equations for atmospheric trace constituents and solution techniques. Electric Power Research Institute Report EA–1131, Palo Alto, California.

Dutton, J.A. (1976): *The Ceaseless Wind, an Introduction to the Theory of Atmospheric Motion*. New York: McGraw–Hill.

Finlayson–Pitts, B.J., and J.N. Pitts, Jr. (1986): *Atmospheric Chemistry*. New York: John Wiley.

Goodman, J.K., and A. Miller (1977): Mass transport across a temperature inversion. *J. Geographic Res.*, **82**:3463.

Grebogi, C., E. Ott, and J.A. Yorke (1987): Chaos, strange attractors, and fractal basin boundaries in nonlinear dynamics. *Science*, **238**:632–637.

Hanna, S.R. (1989): Plume dispersion and concentration fluctuations in the atmosphere. *Encyclopedia of Environmental Control Technology*. Volume 2, Air Pollution Control. P.N. Cheremisinoff, Editor. Houston, Texas: Gulf Publishing Co.

Lamb, R.G. (1984): Air pollution models as descriptors of cause–effect relationships. *Atmos. Environ.*, **18**(3):591–606.

Lewellen, W.S., and R.I. Sykes (1983): Second-order closure model exercise for the Kincaid power plant plume. EPRI report EA–3079, Electric Power Research Institute, Palo Alto, California.

McNaughton, D.J. (1980): Initial comparison of SURE/MAP3S sulfur oxide observations with long–term regional model predictions. *Atmos. Environ.*, **14**:55–63.

Millan, M., and Y.S. Chung (1977): Detection of a plume 400 km from the source. *Atmos. Environ.*, **11**:939–944.

Mitsumoto, S., and H. Ueda (1983): A laboratory experiment on the dynamics of the land and sea breeze. *J. Atmos. Sci.*, **40**:1228–1240.

Nieuwstadt, F.T., and H. van Dop, Eds. (1982): *Atmospheric Turbulence and Air Pollution Modeling*. Dordrecht, Holland: D. Reidel Publishing Co.

Ottar, B. (1978): An assessment of the OECD study on long–range transport of air pollutants (LRTAP). *Atmos. Environ.*, **12**:445–454.

Pack, D.H., G.J. Ferber, J.L. Heffter, K. Telegradas, J.K. Angell, W.H. Hoecker, and L. Machta (1978): Meteorology of long–range transport. *Atmos. Environ.*, **12**:425–444.

Perhac, R.M. (1978): Sulfate regional experiment in the northeastern U.S.: The SURE program. *Atmos. Environ.*, **12**:641–648.

Pielke, R.A. (1984): *Mesoscale Meteorological Modeling*. Orlando, Florida: Academic Press.

Policastro, A.J., M. Wastag, L. Coke, R.A. Carhart, and W.E. Dunn (1986): Evaluation of short-term long-range transport models; Volume 1, Analysis, procedures and results. U.S. EPA Document EPA-450/4-86-016a.

Puttock, J.S. (1979): Turbulent diffusion from sources near obstacles with separated wakes. Part II. Concentration measurements near a circular cylinder in uniform flow. *Atmos. Environ.*, **13**:15-22.

Reynolds, S.D., R.E. Morris, T.C. Myers, and M.-K. Liu (1984a): Evaluation of three first-order closure models -- Plains site. EPRI Report EA-3078, Electric Power Research Institute, Palo Alto, California.

Reynolds, S.D., C. Seigneur, T.E. Stoeckenius, G.E. Moore, R.G. Johnson, and R.J. Londergan (1984b): Operational validation of Gaussian plume models at a plains site. EPRI Report EA-3076, Electric Power Research Institute, Palo Alto, California.

Ruff, R.E., K.C. Nitz, F.L. Ludwig, C.M. Bhumralkar, J.D. Shannon, C.M. Sheih, I.Y. Lee, R. Kumar, and D.J. McNaughton (1984): Regional air quality model assessment and evaluation. EPRI report EA-3671, Electric Power Research Institute, Palo Alto, California.

Seinfeld, J.H. (1975): *Air Pollution -- Physical and Chemical Fundamentals*. New York: McGraw-Hill.

Seinfeld, J.H. (1986): *Atmospheric Chemistry and Physics of Air Pollution*. New York: John Wiley.

Willis, G.E., and J.W. Deardorff (1981): A laboratory study of dispersion from a source in the middle of the convectively mixed layer. *Atmos. Environ.*, **15**:109-117.

3 AIR POLLUTION METEOROLOGY

Most air pollution phenomena occur in the lower part of the atmosphere called the planetary boundary layer, or PBL. The PBL (which is sometimes called the friction layer) is defined as "the region in which the atmosphere experiences surface effects through vertical exchanges of momentum, heat and moisture" (Panofsky and Dutton, 1984).

The traditional approach is to divide the PBL vertically into various layers, each characterized by different "scaling" parameters. Even in ideal conditions (i.e., a horizontally homogeneous and clear PBL) this vertical differentiation by layers is difficult, especially in the "stable" nighttime boundary layer, where, however, some progress in understanding its structure has been made (Nieuwstadt, 1984). The PBL can be divided into three major sublayers:

- The layer near the ground up to the height of the roughness length z_o, whose typical values are presented in Table 3–1. This layer has traditionally been referred to as a "laminar sublayer." Actually, in this layer molecular viscosity hardly plays a role and turbulent fluxes still occur, except very close to the ground (e.g., 1 mm above the ground) where the motion is primarily laminar. This layer, up to the height z_o, could be called the "roughness layer" and defined as the region above the ground in which turbulence is intermittent or not fully developed. (z_o can also be interpreted as the eddy size at the surface.)

- The surface layer (SL) from z_o to h_s, where h_s varies from about 10 m to 200 m. In this layer, the fluxes of momentum, heat and moisture are assumed to be independent of height and the Coriolis effect is generally negligible.

- The transition (or Ekman) layer (TL) from h_s to z_i, where z_i varies from about 100 m to 2 km. The top of the boundary layer z_i is the "lowest level in the atmosphere at which the ground surface no longer influences the dependent variables through the turbulent transfer of mass" (Pielke, 1984). In special situations, such as during thunderstorms, the boundary layer can extend into the stratosphere (an atmospheric layer between about 10 km and 50 km above the ground). Above z_i, turbulence occurs only in shear

Table 3–1. Roughness length z_o of different types of surface (from McRae et al., 1982; numbers in parentheses refer to references in that publication). [Reprinted with permission from Pergamon Press.]

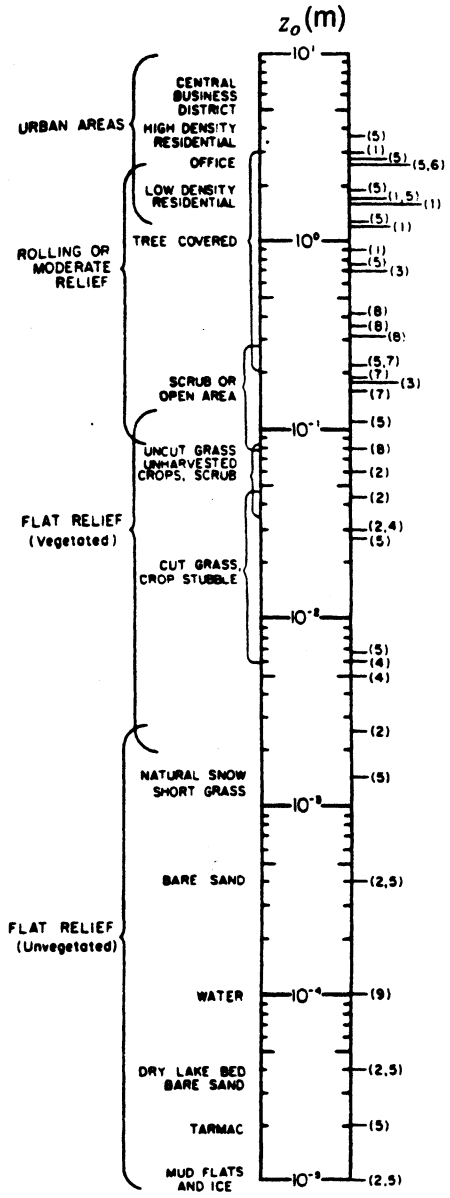

layers (CAT, clear-air turbulence) and inside convective cumulus-type clouds. The altitude z_i is often defined by the height of the lowest temperature inversion, if one exists (Panofsky and Dutton, 1984).

The time-varying meteorological properties of each layer affect the dispersion of pollutants. Between z_o and z_i, turbulent phenomena prevail over molecular phenomena, and the latter become negligible. Below z_o and above z_i, turbulence is not fully developed and therefore molecular motion can play a role in the transfer of mass and energy. Turbulence has strong mixing ability, since its eddies (whose vertical sizes in the atmosphere vary from 1 mm to the size of the PBL) are able to separate nearby parcels of air. As a result, its diffusion rates are several orders of magnitude larger than those of molecular motion.

Among the major meteorological factors that affect air pollution phenomena are

- The horizontal wind (speed and direction), which is generated by the geostrophic wind component, i.e., the pressure gradient wind at the top of the planetary boundary layer (Figure 3-1), and altered by the contribution of terrain frictional forces (Figure 3-2) and the effects of local meteorological winds, such as sea breezes (Figure 3-3), mountain/valley upslope/downslope winds (Figure 3-4) and urban/rural circulations (Figure 3-5)
- The atmospheric stability; i.e., a simple way of categorizing the turbulent status of the atmosphere, which affects the dilution rate of pollutants (Figure 3-6)
- The elevation above the ground
- The strength of the elevated temperature inversion which limits z_i
- The atmospheric vertical motion due to low/high pressure systems (Figure 3-7) or complex terrain effects (hills, mountain ranges, etc.)

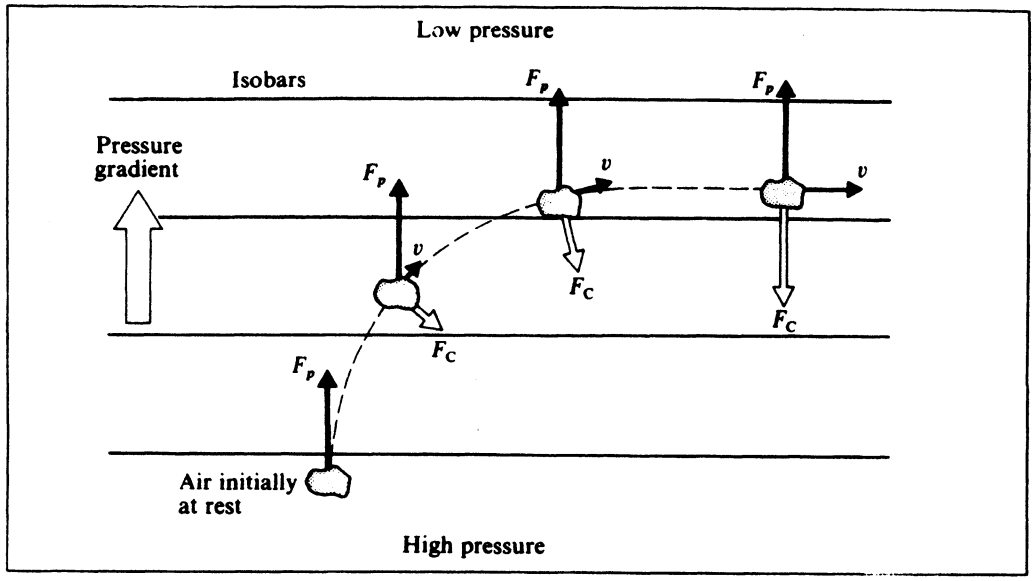

Figure 3–1. Air mass responding to a pressure-gradient force $\mathbf{F_p}$ *is imagined to accelerate initially from rest. Once it gains a velocity* **v**, *the Coriolis force* $\mathbf{F_c}$ *deflects it until a force balance is reached in geostrophic flow (from Williamson, 1973). [Reprinted with permission from Addison–Wesley.]*

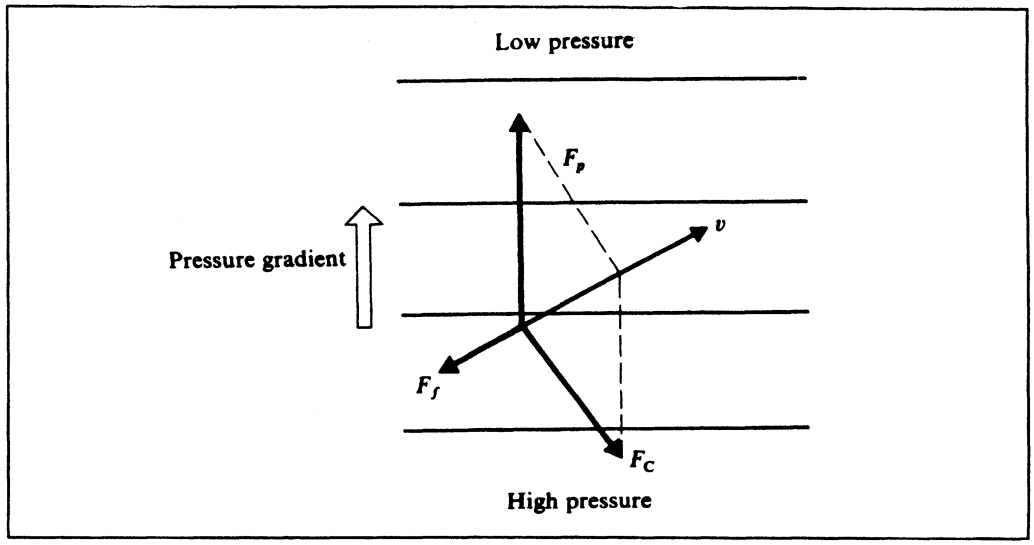

Figure 3–2. Force balance between the pressure gradient force $\mathbf{F_p}$, *the Coriolis force* $\mathbf{F_c}$, *and the frictional force* $\mathbf{F_f}$ *(which must be directed opposite to the wind velocity* **v**) *(from Williamson, 1973). [Reprinted with permission from Addison–Wesley.]*

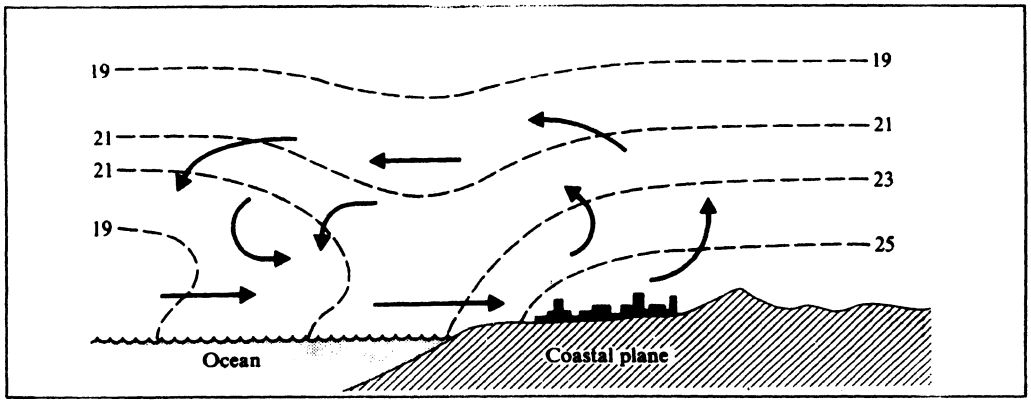

Figure 3–3. *Representative air circulation during a daytime sea breeze. The dashed curves represent contours of uniform temperature (isotherms) and the numbers give their respective temperatures in degrees Celsius (from Williamson, 1973). [Reprinted with permission from Addison–Wesley.]*

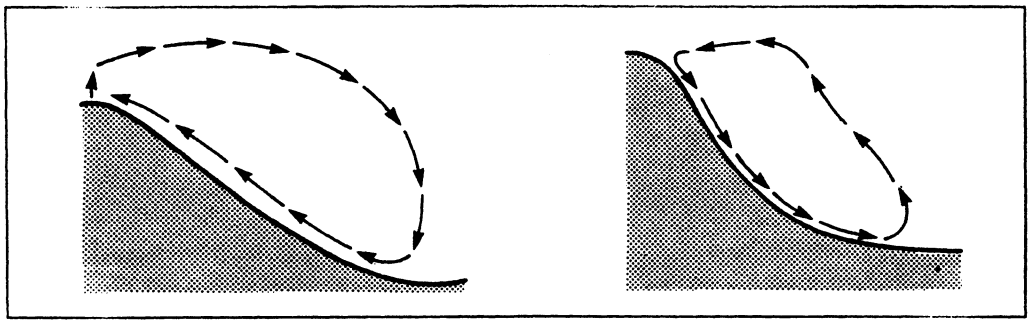

Figure 3–4. *Upslope daytime wind due to greater solar heating on the valley's side than in its center (left), and downslope nighttime wind due to more rapid radiational cooling on the valley's slope than in its center (right). (Adapted from Stern et al., 1984.)[Reprinted with permission from Academic Press.]*

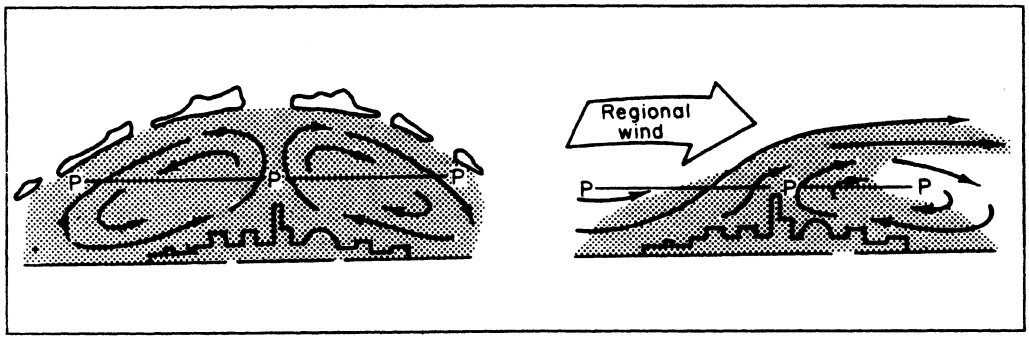

Figure 3–5. *Urban heat island with light regional wind (left) and urban plume with moderate regional wind (right) (from Stern et al., 1984). [Reprinted with permission from Academic Press.]*

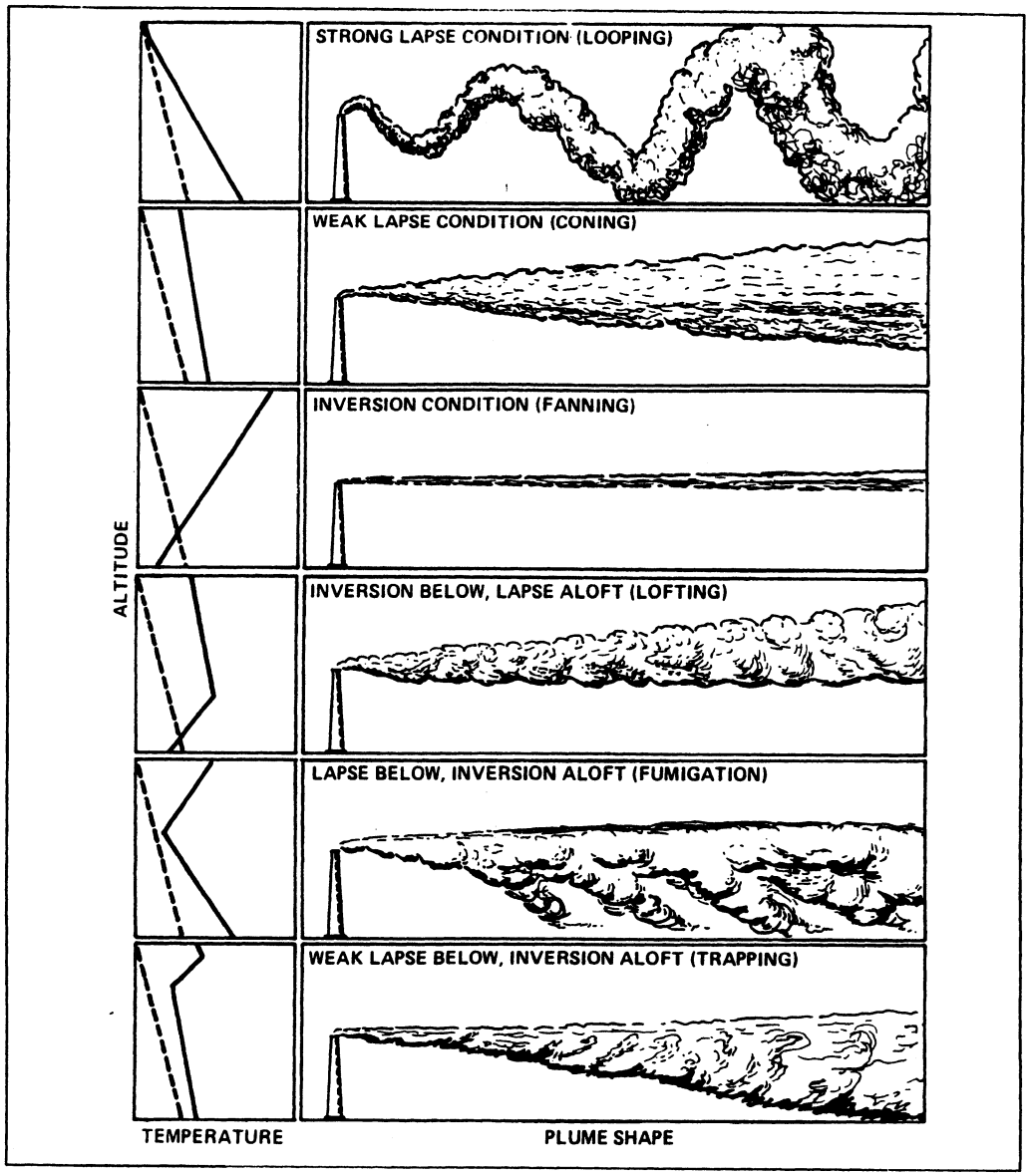

Figure 3–6. Vertical expansion of continuous plumes related to vertical temperature structure. The dashed lines correspond to the dry adiabatic lapse rate for reference (from Stern et al., 1984). [Reprinted with permission from Academic Press.]

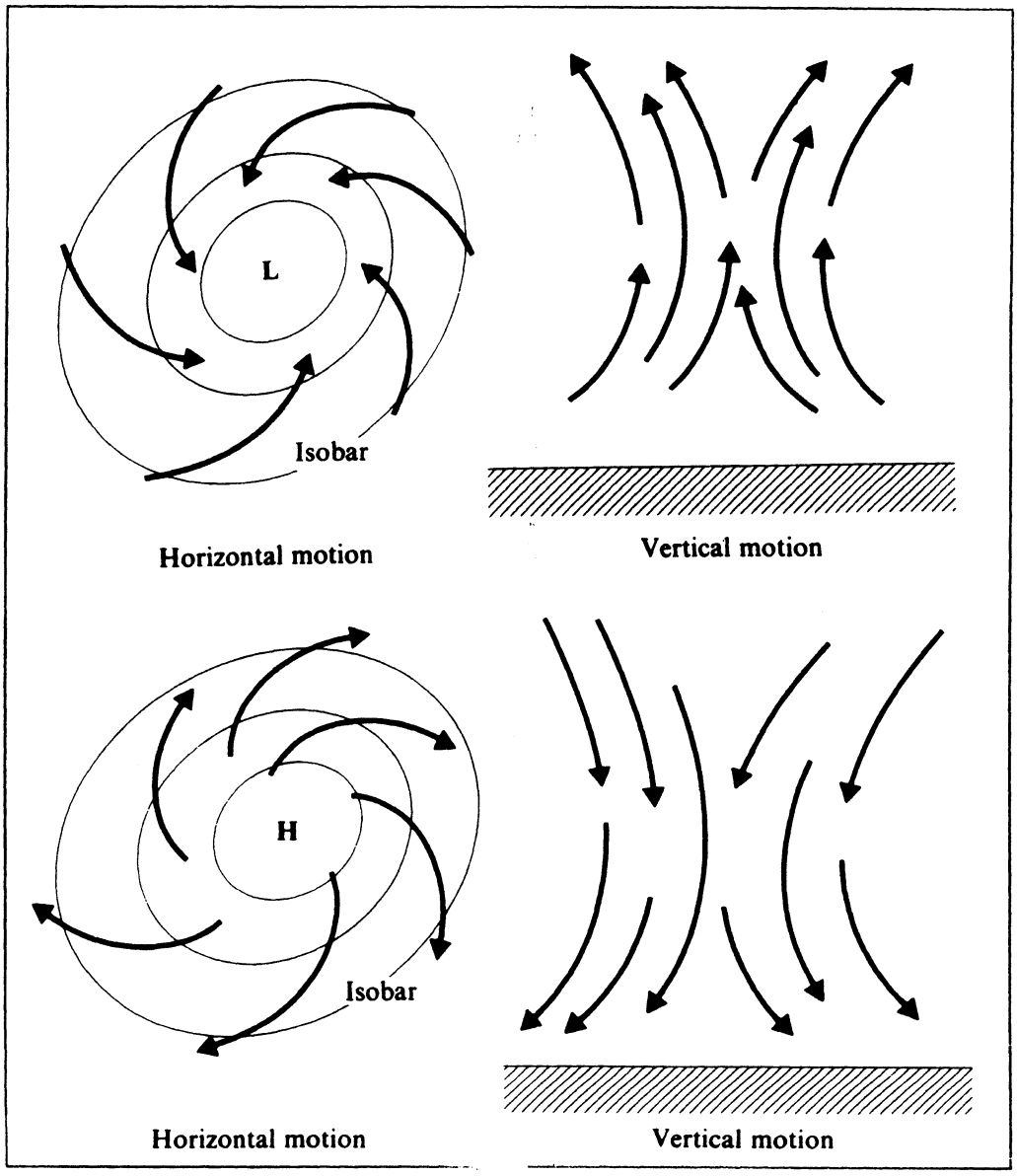

Figure 3–7. *Above: low level counterclockwise spiral of winds, which converge in a cyclone in the Northern Hemisphere; the corresponding vertical motion of the air is depicted at the right. Below: clockwise diverging spiral of winds from an anticyclone in the Northern Hemisphere; the vertically subsiding motion of the air is shown at the right (from Williamson, 1973). [Reprinted with permission from Addison–Wesley.]*

The vertical and, to a lesser extent, horizontal dispersion properties of the PBL are mainly characterized by

- the PBL "stability" conditions (neutral, unstable or stable)
- the PBL's height z_i
- the depth h of the mixed layer (or mixing depth), which is the thickness of the turbulent region next to the ground(*)
- terrain and mesoscale phenomena, with low frequency and directional changes

Atmospheric stability can be characterized by several methods or parameters, such as

- empirical methods (such as the Pasquill scheme presented in Table 3–2 or the Turner method in Table 3–3)
- the flux Richardson number, R_f; i.e., the ratio of the rate of dissipation (or production) of turbulence by buoyancy to the rate of creation of turbulence by shear ($R_f < 0$ for unstable conditions, = 0 for neutral, and > 0 for stable); the absolute value of R_f also indicates the relative importance of convective to mechanical turbulence
- the gradient Richardson number, R_i (related to R_f but easier to measure)
- the Monin–Obukhov length, L ($1/L < 0$ for unstable conditions, $\simeq 0$ for neutral, and > 0 for stable)

3.1 NEUTRAL CONDITIONS

Neutral conditions are characterized by the presence of an isentropic (or adiabatic) vertical temperature profile in the PBL (i.e., $\Delta T/\Delta z \simeq 9.86 \cdot 10^{-3}$ deg/m in dry air, where T is the temperature and z the altitude). They typically occur during daytime–nightime transitions, cloud overcasts, or with strong winds (e.g., greater than 6 m/s at a 10–m elevation, where 10 m is the standard elevation recommended for surface wind monitoring).

(*) In neutral and unstable conditions, $z_i \simeq h$, while in stable conditions, where z_i is the thickness of the ground–based temperature inversion, $h < z_i$, as discussed further below.

Table 3–2. Pasquill dispersion classes: A, very unstable; B, unstable; C, slightly unstable; D, neutral; E, slightly unstable; F, stable; G, very stable (from Dobbins, 1979; adapted from Pasquill, 1974). [Reprinted with permission from John Wiley and Sons.]

Insolation/Cloud Cover		Surface Wind Speed (m/s)				
		<2.0	2 to <3	3 to <5	5 to <6	≥6
Day	Strong Insolation	A	A–B	B	C	C
	Moderate Insolation	A–B	B	B–C	C–D	D
	Slight Insolation	B	C	C	D	D
Day or Night	Overcast	D	D	D	D	D
Night	Thin overcast or ≥0.5 cloud cover	—	E	D	D	D
	≤0.4 cloud cover	—	F	E	D	D

Notes: 1. Strong insolation corresponds to a solar elevation angle of 60° or more above the horizon. Slight insolation corresponds to a solar elevation angle of 15° to 35°.

2. Pollutants emitted under clear nighttime skies with winds less than 2.0 m/s, more recently defined to be class G, may be subject to unsteady meandering which renders the prediction of concentrations at downwind locations unreliable.

Table 3–3. Definition of Turner Classes: 1, very unstable; 2, unstable; 3, slightly unstable; 4, neutral; 5, slightly stable; 6, stable; 7, very stable (from Panofsky and Dutton, 1984). [Reprinted with permission from John Wiley and Sons.]

Wind Speed (knots)	Net Radiation Index						
	4	3	2	1	0	−1	−2
0–1	1	1	2	3	4	6	7
2–3	1	2	2	3	4	6	7
4–5	1	2	3	4	4	5	5
6	2	2	3	4	4	5	6
7	2	2	3	4	4	4	5
8–9	2	3	3	4	4	4	5
10	3	3	4	4	4	4	5
11	3	3	4	4	4	4	4
≥ 12	3	4	4	4	4	4	4

Solar Altitude (a)	Insolation	Insolation Class Number
$60° < a$	Strong	4
$35° < a < 60°$	Moderate	3
$15° < a < 35°$	Weak	2
$a \leq 15°$	Very Weak	1

DEFINITIONS OF NET RADIATION INDEX

1. If the total cloud cover is 10/10 and the ceiling is less than 7000 ft, use net radiation index equal to 0 (whether day or night).
2. For nighttime (between sunset and sunrise):
   (a) If total cloud cover ≤ 4/10, use net radiation index equal to −2.
   (b) If total cloud cover > 4/10, use net radiation index equal to −1.
3. For daytime:
   (a) Determine the insolation class number as a function of solar altitude from Table 6.4.
   (b) If total cloud cover ≤ 5/10, set the net radiation index above equal to the insolation class number.
   (c) If cloud cover > 5/10, modify the insolation class number by the following six steps.
      (1) Ceiling < 7000 ft, subtract 2.
      (2) Ceiling ≥ 7000 ft but < 16,000 ft, subtract 1.
      (3) Total cloud cover equals 10/10, subtract 1. (This will only apply to ceilings ≥ 7000 ft since cases with 10/10 coverage below 7000 ft are considered in item 1 above.)
      (4) If insolation class number has not been modified by steps (1), (2), or (3) above, assume modified class number equal to insolation class number.
      (5) If modified insolation class number is less than 1, let it equal 1.
      (6) Use the net radiation index in Table 6.4 corresponding to the modified insolation class number.

Since urban areas do not become as stable in the lower layers as nonurban areas, stability classes computed as 6 and 7 by this system are called class 5 in urban areas.

In neutral conditions (Panofsky and Dutton, 1984), the PBL's height is estimated (when no measurements of an elevated inversion are available) by

$$z_i \simeq h = const \frac{u_*}{f} \tag{3-1}$$

where *const* = 0.15 to 0.25 and the friction velocity u_* and the Coriolis parameter f are

$$u_* = (-\overline{u' w'})^{1/2} = \sqrt{\tau(0)/\varrho} \tag{3-2}$$

$$f = 2\,\Omega\,\sin\phi \tag{3-3}$$

where u' and w' are the surface wind velocity fluctuations parallel to the mean horizontal wind and vertical, respectively; $\tau(0)$ is the surface stress (also called the downward flux of momentum along the main wind direction); ϱ is the air density; Ω is the earth's rate of rotation ($7.29 \cdot 10^{-5}\ s^{-1}$); and ϕ is the latitude. The surface stress $\tau(0)$ is the ground-level value of the modulus of the horizontal Reynolds stress tensor $\boldsymbol{\tau}$, which, according to the K-theory (in which the flux is assumed to be proportional to the gradient), can be formulated as

$$\boldsymbol{\tau}(z) = K_m \varrho \frac{\partial \mathbf{u}}{\partial z} \tag{3-4}$$

where K_m is the scalar eddy viscosity and $\mathbf{u}$ is the average horizontal wind vector.

Experimental studies show, however, that the actual z_i is often lower than the value predicted by Equation 3-1, since large-scale processes (e.g., air subsidence during high-pressure situation) produce an elevated inversion layer whose bottom elevation represents the actual z_i.

3.2 UNSTABLE CONDITIONS

Unstable conditions are typical in the daytime with positive heat flux at the ground (i.e., sunny conditions). In these conditions, h tends to be about 10 percent higher than the height of the bottom of the lowest elevated inversion, since the lowest part of the inversion layer is often moderately turbulent due to penetrating eddies from below and wind shear effects.

When the height of the lowest elevated inversion is not known, a simple equation for the daily time-variation of $h(t)$ can be derived from the heat energy budget. In fact (Panofsky and Dutton, 1984), it is

$$\gamma_d - \gamma = \frac{\Delta T_o}{h(t)} \tag{3-5}$$

where γ_d is the dry adiabatic lapse rate ($\gamma_d = 9.86\ 10^{-3}$ °C/m), γ is the atmospheric lapse rate (i.e., $\gamma = -\partial T/\partial z$) at sunrise, and ΔT_o is the surface temperature increase between the time t_o (sunrise) and t. Also, conservation of heat energy gives

$$\int_{t_o}^{t} H\,dt = \frac{c_p\,\varrho\,h(t)\,\Delta T_o}{2} \tag{3-6}$$

where H is the surface heat flux, c_p is the specific heat at constant pressure (about 1,000 J deg^{-1} kg^{-1} for dry air), and ϱ is the air density. By combining Equations 3-5 and 3-6, we obtain

$$h(t) = \left(\frac{2 \int_{t_o}^{t} H\,dt}{c_p\,\varrho\,(\gamma_d - \gamma)} \right)^{1/2} \tag{3-7}$$

which can be solved analytically or numerically if $H(t)$ is specified.

In unstable conditions, R_f, R_i and L are negative and $-L$ is the height that separates mainly mechanical turbulence below from mainly convective turbulence above.

3.3 STABLE CONDITIONS

Stable conditions are typically encountered over land during clear nights with weak winds. Under these conditions, a ground-based temperature inversion is present and the temperature increases with height from $z = 0$ to $z = z_i$, the top of the stable PBL. Mechanical turbulence, however, even though strongly attenuated by the downward heat flux H ($H < 0$), creates a mixing layer from $z = 0$ to $z = h$, where h can be much lower than z_i. Monitoring by acoustic sounding techniques is very useful for evaluating h under these conditions. If these measurements are not available, the steady-state asymptotic value h_{eq} of $h(t)$ can be

computed by the formula suggested by Zilitinkevich (see Businger and Arya, 1974).

$$h_{eq} = const \sqrt{\frac{u_*}{f} L} \tag{3-8}$$

with $const \simeq 0.4$ (Garratt, 1982).

Nighttime conditions are frequently characterized by multiple stable layers aloft. This situation is difficult to parameterize, especially because the motion in each layer is almost independent and large wind shear effects are, therefore, encountered. Moreover, real equilibrium conditions are seldom found, which further limits the applicability of Equation 3-8.

3.4 THE STRATIFICATION OF THE PBL

Recent studies have identified new intricacies in the regional differentiation of the PBL, whose vertical structure is more complex than the simple three-layer separation discussed at the beginning of this chapter. Holtslag and Nieuwstadt (1986) provided a detailed discussion on the different scaling regions of the PBL, a discussion which is summarized in Figure 3-8. The main layers shown in Figure 3-8 are discussed further below.

3.4.1 The Surface Layer

The vertical fluxes of heat and momentum in the PBL are typically large at the surface and decrease to zero at z_i. The lower part of the PBL is called the surface layer (or constant-stress layer) and is defined as that layer above the ground in which the vertical variation of the heat and momentum fluxes is negligible (e.g., less than 10 percent). Panofsky and Dutton (1984) suggest that the depth of the surface layer h_s is

$$h_s \simeq h/10 \tag{3-9}$$

which gives $h_s \simeq 100$ m in typical daytime unstable conditions (with $h \simeq 1{,}000$ m) and $h_s \leq 10$ m with typical nighttime stable conditions (where $z_i \simeq 300$ m, but $h \leq 100$ m).

In the surface layer, since τ does not vary with z, the wind direction is constant (see Equation 3-4). Moreover, in the surface layer, the earth's rotation

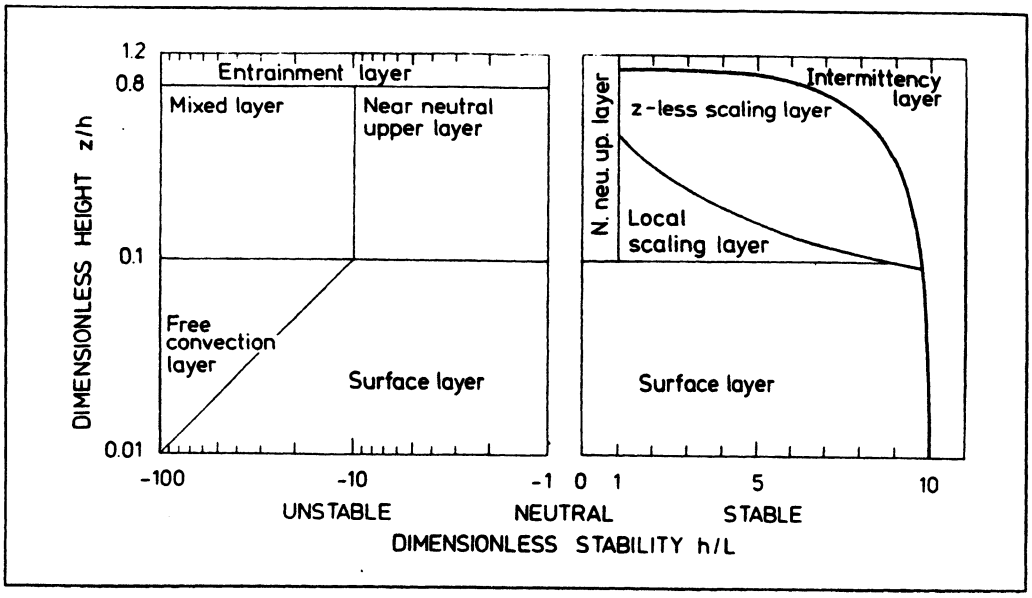

Figure 3–8. The scaling regions of the atmospheric boundary layer, shown as function of the dimensionless height z/h and the stability parameter h/L. When used to determine dispersion regions, the dimensionless height is replaced by z_s/h where z_s is the source height (from Gryning et al., 1987, adapted from Holtslag and Nieuwstadt, 1986). [Reprinted with permission from Pergamon Press.]

effects are assumed to be negligible. Surface layer meteorology and dispersion rates have been satisfactorily explained by the similarity theory, which was first developed by Monin and Obukhov (1954) and which is discussed in Section 3.6. The advantage of this theory is that several atmospheric parameters, when normalized using u_* and L, show a universal behavior that is a function only of z/L.

3.4.2 The Mixed Layer

During unstable conditions, most of the PBL (from $z = -L$ to $z = z_i$) is characterized by dominant convective conditions that require a different scaling from the one provided by the surface layer similarity theory (which is only valid for $z \leq 0.1\ z_i$). This was provided by the mixed-layer scaling introduced by Deardorff (1970), which uses z_i as a length scale (instead of $|L|$), a new velocity

scale w_* instead of u_*, and a third scale, the temperature scale θ_*. They are defined by

$$w_* = \left(\frac{g\,H\,z_i}{c_p\,\varrho\,T_o}\right)^{1/3} \tag{3-10}$$

where g is the acceleration due to gravity (9.806 m s^{-2}), T_o is the surface temperature, and

$$\theta_* = -\frac{H}{c_p\,\varrho\,w_*} \tag{3-11}$$

3.4.3 The Free Convection Layer

During unstable conditions, when z_i is large enough, there is a region in which both surface layer similarity and mixed-layer scaling are valid. This layer, $-L < z < 0.1\ z_i$, when present, is called the free convection layer.

3.4.4 The Stable Layer

A stable atmospheric boundary layer is common over land at night. Under these conditions, h can vary from a few tens of meters with light winds to several hundred meters with strong winds. Caughey et al. (1979) have proposed a stable layer scaling using h as the length scale (as in the mixed layer) and u_* as a velocity scale (as in the similarity theory, since stable layer turbulence is mechanical and not convective).

Theoretical and experimental studies in the stable layer are complicated by the fact that the nighttime boundary layer is usually not in equilibrium, and by the effects of gravity waves (Panofsky and Dutton, 1984). A new "local scaling" approach (Nieuwstadt, 1984) for the stable atmospheric boundary layer, which uses a local (i.e., variable with z) Obukhov length Λ, is discussed in Section 3.7.

3.4.5 The Entrainment Interfacial Layer

Special studies and parameterizations of the entrainment interfacial layer, defined as the layer between approximately 0.8 z_i and 1.2 z_i, have been performed by Deardorff (1972), by Wyngaard et al. (1974) and, more recently and comprehensively, by Wyngaard and LeMone (1980).

3.5 SEMIEMPIRICAL ESTIMATES OF BOUNDARY LAYER PARAMETERS

Meteorological measurements of boundary layer parameters are not often available and, therefore, in most cases, the PBL parameters are not measured directly but inferred from standard meteorological information available for the study region.(*) In this section, semiempirical numerical methods and formulations that allow estimation of PBL parameters are presented.

3.5.1 The PBL Height z_i

The value z_i is determined by the top of the ground-based nighttime inversion (in stable conditions) or the bottom of the first elevated inversion (unstable conditions). In neutral conditions, z_i can be computed by Equation 3–1, unless an elevated inversion is lower than this computed value (in which case z_i is the bottom of the elevated inversion). In unstable conditions, z_i can be computed by Equations 3–6 and 3–7. In stable conditions, z_i can be approximated, at mid-latitudes, by the value $2.4 \cdot 10^3 \, u_*^{3/2}$ (Venkatram, 1980).

3.5.2 The Mixing Height h

In neutral or unstable conditions, the mixing height h is $\simeq z_i$ (or, according to some, 10 percent greater than z_i). In stable conditions, h can be approximated by Equation 3–8.

3.5.3 The Roughness Length z_o

The parameter z_o is generally a function of surface roughness only, even though it may be affected by the wind speed (when the roughness elements bend with the wind) and wind direction (when different terrain features surround the region). It has also been suggested that an "effective" value of z_o should increase with height (Wilczak and Phillips, 1986). The value of z_o can be obtained from tables such as Table 3–1 or computed approximately as

$$z_o = \epsilon/30 \tag{3–12}$$

where ϵ is the average height of the obstacles in the study area.

The roughness length can also be computed from wind profile measurements. In fact, in purely mechanical turbulence (i.e., with strong winds), the

(*) See van Ulden and Holtslag (1985) for an outline of a meteorological preprocessor that is capable of calculating the major PBL parameters that affect atmospheric dispersion from routinely available measurements (and other special measurements, if available).

average wind speed u shows a classical logarithmic wind profile for $z > z_o$, which is given by

$$u(z) = \frac{u_*}{k} \ln\left(\frac{z}{z_o}\right) \tag{3-13}$$

where k is the von Karman constant ($\simeq 0.40$). Equation 3–13 is valid only for uniform terrain. Even in nonuniform terrain, though, Equation 3–13 can be used for representing the average u over large horizontal areas (Panofsky and Dutton, 1984). When the height of the large roughness elements (such as buildings and vegetation) is much smaller than the height of wind observations, Equation 3–13 provides an immediate solution for z_o, using two wind speed measurements u_1 and u_2 at different elevations z_1 and z_2, respectively:

$$\frac{u_2}{u_1} = \frac{\ln\ (z_2/z_o)}{\ln\ (z_1/z_o)} \tag{3-14}$$

When the roughness elements are not small, a displacement length d can be defined (Panofsky and Dutton, 1984), which is typically 70 to 80 percent of the height of the large roughness elements. In this case (see Figure 3–9), the wind profile will be (for $z > d$)

$$u(z) = \frac{u_*}{k} \ln\left(\frac{z-d}{z_o}\right) \tag{3-15}$$

which, again, allows the evaluation of z_o from

$$\frac{u_2}{u_1} = \frac{\ln[(z_2-d)/z_o]}{\ln[(z_1-d)/z_o]} \tag{3-16}$$

3.5.4 The Friction Velocity u_*

During strong winds, the friction velocity u_* can be computed from Equations 3–13 or 3–15 using z_o and a single wind measurement $u_1 = u(z_1)$.

3.5.5 The Surface Stress $\tau(0)$

The surface stress $\tau(0)$ can be estimated by Equation 3–2 using u_*.

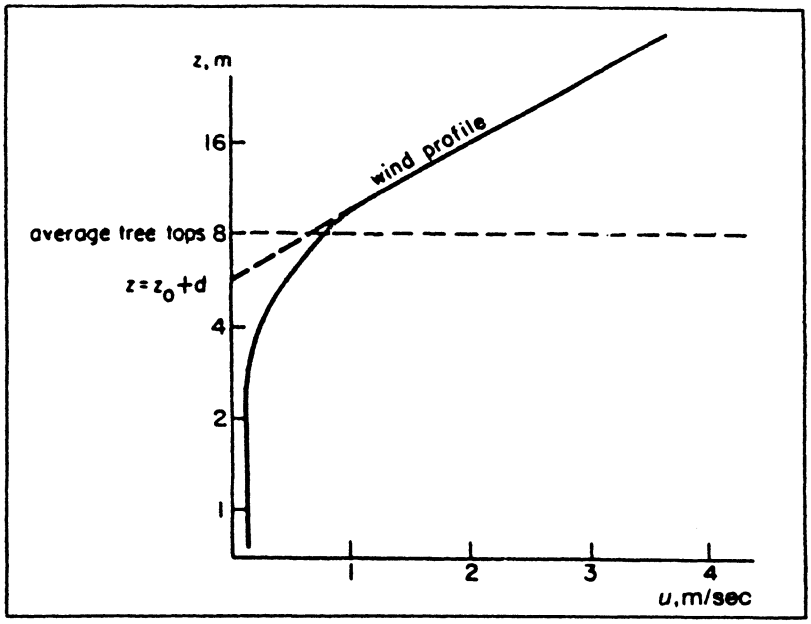

Figure 3–9. Example of wind profile above large roughness elements such as tree (from Panofsky and Dutton, 1984). [Reprinted with permission from John Wiley and Sons.]

3.5.6 K_m in the Neutral Surface Layer

From Equations 3–4 and 3–13, remembering the $\tau(z)$ is constant in t surface layer, the eddy viscosity K_m can be estimated in neutral conditions from single wind measurement by

$$K_m = \frac{k^2 u_1 z_1}{\ln(z_1/z_o)} \qquad (3\text{–}1$$

3.5.7 Monin–Obukhov Length L

The Monin–Obukhov length L is a parameter that characterizes the "s bility" of the surface layer and is calculated from ground-level measurements is computed from

$$L = -\frac{u_*^3 c_p \varrho T}{k g H (1 + 0.07/B)} = -\frac{u_*^3 z_i}{k w_*^3 (1 + 0.07/B)} \simeq -\frac{z_i}{k}\left(\frac{u_*}{w_*}\right)^3 \qquad (3\text{–}1$$

where B is the Bowen ratio (i.e., the ratio of sensible to latent(*) surface heat flux), which can be estimated by

$$B = \frac{\Delta T + 0.01\ \Delta z}{2500\ \Delta q} \tag{3-19}$$

where $\Delta T/\Delta z$ is the temperature vertical gradient and $\Delta q/\Delta z$ is the specific vertical humidity gradient (both at the surface).

L can also be estimated empirically as a function of the Turner class (see Table 3-3) and z_o, as illustrated in Figure 3-10. The empirical curves in Figure 3-10 have been analytically fitted by Liu et al. (1976) and Irwin (1979) using power law functions such as $1/L = a\, z_o^b$. Table 3-4 provides the values of the constants a and b.

Venkatram (1980) has proposed another empirical formulation for L (only for stable nighttime conditions). It is

$$L = 1.1\ 10^3\ u_*^2 \tag{3-20}$$

3.5.8 The Surface Heat Flux H

The surface heat flux H is defined as

$$H = c_p\ \varrho\ \overline{w'T'} \tag{3-21}$$

where w' and T' are the surface values of the fluctuating components of the vertical wind and temperature, respectively. Using the gradient-theory (or K-theory), in which the heat flux is proportional to the temperature gradient, we obtain

$$H(z) = -K_h\, c_p\, \varrho \left(\frac{\partial T}{\partial z} + \gamma_d\right) \tag{3-22}$$

(*) The sensible heat flux is generally proportional to the vertical temperature gradient, while the latent heat flux is the enthalpy flux of water vapor.

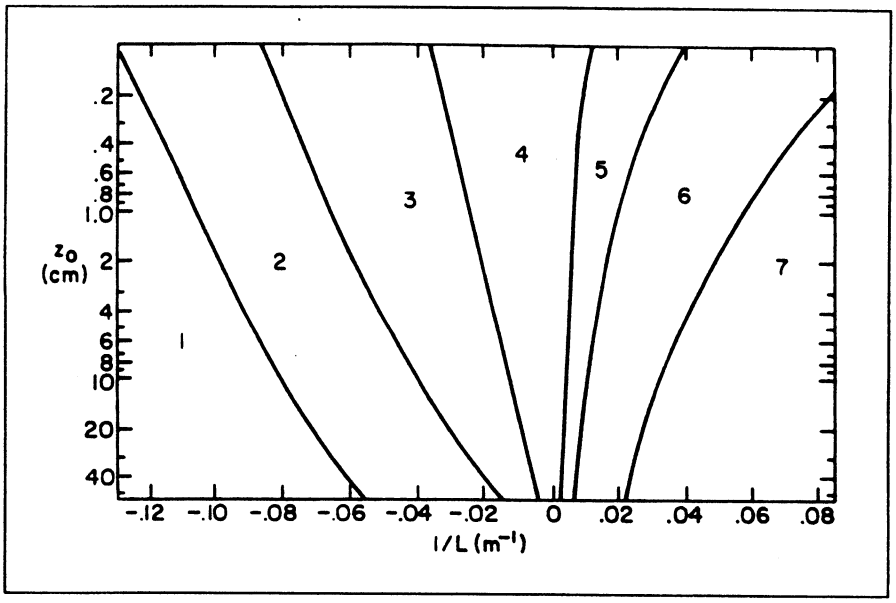

Figure 3–10. Semiempirical relation between L, the Turner class and z_o (from Golder, 1972, as presented by Panofsky and Dutton, 1984). [Reprinted with permission from John Wiley and Sons.]

Table 3–4. Coefficient a, b for the fitting of the curves in Figure 3–10 by $(1/L) = a\, z_o^b$.

Stability Class	*a*	*b*
A	-0.0875	-0.1029
B	-0.03849	-0.1714
C	-0.00807	-0.3049
D	0.	0.
E	0.00807	-0.3049
F	0.03849	-0.1714

which allows an estimate of H at z_o using surface values of ϱ and $\partial T/\partial z$ (K_h is the coefficient of eddy heat conduction). Equation 3–22 can be rewritten as

$$H = -K_h c_p \varrho \left(\frac{\partial \theta}{\partial z}\right)_{z=o} \tag{3–23}$$

using the potential temperature θ defined by

$$\theta(z) = T(z) + \gamma_d z \tag{3–24}$$

3.5.9 The Velocity Scale w_* in the Mixed Layer

The convective velocity scale w_* is computed by

$$w_* = \left(\frac{g H z_i}{c_p \varrho T_0}\right)^{1/3} \tag{3–25}$$

3.5.10 The Temperature Scale θ_* in the Mixed Layer

The temperature scale θ_* is computed by

$$\theta_* = -\frac{H}{c_p \varrho w_*} \tag{3–26}$$

3.5.11 The Richardson Numbers

The Richardson numbers are useful parameters for evaluating atmospheric stability (stable, neutral and unstable conditions correspond to positive, zero and negative Richardson numbers, respectively).

An approximate estimate of the gradient Richardson number R_i can be obtained (Businger, 1966; Pandolfo, 1966) by

$$R_i = z/L \tag{3–27}$$

in unstable conditions and

$$R_i = \frac{z/L}{1 + 5\, z/L} \tag{3-28}$$

in stable conditions.

A quantity easier to measure than R_i, is the bulk Richardson number R_b, given by

$$R_b = \frac{g\, z}{T} \frac{\frac{\partial T}{\partial z} + \gamma_d}{u^2} \tag{3-29}$$

which is related to R_i by

$$R_i = \frac{R_b}{r^2} \tag{3-30}$$

where r is the exponent of the power law

$$u(z) = u_1 \left(\frac{z}{z_1}\right)^r \tag{3-31}$$

that best fits the wind profile. (The level z_1 is arbitrary.) A typical value of r in flat terrain is 1/7, while in rough terrain r can be more than twice this value.

Finally, the relation between the flux Richardson number, R_f, and R_i is

$$R_f = \frac{K_h}{K_m} R_i \tag{3-32}$$

3.5.12 The Variances of Wind Components

In standard meteorological notation (u parallel to the mean wind, v the horizontal crosswind component, and w the vertical component) the horizontal and vertical wind fluctuations are characterized by their "intensities" σ_u, σ_v, σ_w; i.e., the standard deviations of the instantaneous u, v, *and* w values, respectively.

In neutral conditions, it can be assumed that

$$\sigma_u = a\, u_* \tag{3-33}$$

$$\sigma_v = b\, u_* \tag{3-34}$$

$$\sigma_w = c\, u_* \tag{3-35}$$

with the following estimates of the constants in flat terrain (Panofsky and Dutton, 1984)

$$a = 2.39 \pm 0.03 \tag{3-36}$$

$$b = 1.92 \pm 0.05 \tag{3-37}$$

$$c = 1.25 \pm 0.03 \tag{3-38}$$

In rolling terrain, a and b are larger, but c does not seem to change.

In the unstable surface layer, Panofsky et al. (1977a) recommend

$$\sigma_w(z) = 1.25\, u_* \left(1 - 3\frac{z}{L}\right)^{1/3} \tag{3-39}$$

which seems to work in both flat and rolling terrain. For large z in unstable conditions, σ_w becomes independent of u_*. The limit of Equation 3-39 for large z gives

$$\sigma_w(z) = 1.3 \left(\frac{g\, H\, z}{c_p\, \varrho\, T}\right) \tag{3-40}$$

which fits several observations well.

In the entire PBL under unstable conditions, Wilczak and Phillips (1986) obtained

$$\frac{\sigma_w}{w_*} = \left\{1.8\, (z/z_i)^{2/3}\, [1 - 0.91\, (z/z_i)]\right\}^{1/2} \tag{3-41}$$

which fits well both the measurements of Caughey and Palmer (1979) and the laboratory experiments by Deardorff (1974). However, when they compare Equation 3-41 with another set of data (26 days of data collected in the late summers of 1982 and 1983 at the Boulder Atmospheric Observatory, BAO), they obtain σ_w values that are too small (about 20 percent) in magnitude and that can

be fitted, instead, by substituting the constant 2.5 for the constant 1.8 in Equation 3-41.

In the surface layer, Panofsky et al. (1977b) suggest

$$\sigma_u = \sigma_v = u_* \left(12 - 0.5 \frac{z_i}{L}\right)^{1/3} \tag{3-42}$$

for stable and unstable (but not neutral) conditions.

In the entire PBL under unstable conditions, Wilczak and Phillips (1986) suggest

$$\frac{\sigma_u}{w_*} = \frac{\sigma_v}{w_*} = c \left\{ 0.5 \left[2 - (z/z_i)^{1/2}\right] + 0.3 (z/z_i)^{1/2} \right\}^{1/2} \tag{3-43}$$

where c is the surface value ($z = 0$) of σ_u/w_* or σ_v/w_* (a typical value is $c = 0.74$).

3.5.13 Best Fit Estimates of PBL Parameters

Numerical algorithms have been developed that provide best fit estimates of PBL parameters from a limited set of measurements. Similarity theory equations are generally used for these computations.

Nieuwstadt (1978) provided a numerical iterative method that, using average wind $u(z)$ and temperature $\theta(z)$ profiles, minimizes the difference between measurements and theoretical values. This minimization gives a solution for θ_*, u_*, and, therefore, L. The method works better when z_o is known. A second method by Aloysius (1979) is, at least in theory, more powerful, since it allows the evaluation of practically all PBL parameters (L, z_o, u_*, θ_*, H, R_i) using a single profile of either wind or temperature. Both methods have been successfully compared with field measurements.

3.6 SCALING IN THE SURFACE LAYER

The similarity theory (Monin and Obukhov, 1954) allows a valid parameterization of the surface layer. According to this theory (Panofsky and Dutton,

1984), the nondimensional wind shear $\phi_m(z/L)$ is defined by

$$\phi_m(z/L) = \frac{k\,z}{u_*}\,\frac{\partial u}{\partial z} \tag{3-44}$$

where, in neutral conditions,

$$\phi_m = 1 \tag{3-45}$$

in unstable conditions

$$\phi_m = (1 - 16\,z/L)^{-1/4} \tag{3-46}$$

or

$$\phi_m = (1 - 15\,z/L)^{-1/3} \tag{3-47}$$

or

$$\phi_m^4 - 15\,(z/L)\,\phi_m^3 = 1 \tag{3-48}$$

and in stable conditions

$$\phi_m = 1 + 5\,z/L \tag{3-49}$$

The average wind speed u can be obtained by integrating Equation 3-44, a process that does not require the knowledge of the exact form of ϕ_m. It is

$$u(z) = (u_*/k)[\ln(z/z_o) - \psi_m(z/L)] \tag{3-50}$$

where ψ_m is the universal function in the diabatic surface layer wind profile

$$\psi_m(z/L) = \int_{z_o/L}^{z/L} [1 - \phi_m(\zeta)]\frac{d\zeta}{\zeta} \tag{3-51}$$

In neutral conditions

$$\psi_m = 0 \tag{3-52}$$

while, in unstable conditions,

$$\psi_m \simeq \ln\left[\left(\frac{1+x^2}{2}\right)\left(\frac{1+x}{2}\right)^2\right] - 2\,arctg\,x + \pi/2 \qquad (3\text{–}53)$$

with $x = (1 - 16\,z/L)^{1/4}$, and in stable conditions

$$\psi_m = -5\,z/L \qquad (3\text{–}54)$$

In an analogous way, the nondimensional temperature gradient $\phi_h(z/L)$ is defined as

$$\phi_h = \frac{k\,z}{T_*}\,\frac{\partial\theta}{\partial z} \qquad (3\text{–}55)$$

where θ is the potential temperature defined by Equation 3–24 and T_* is the temperature scaling parameter

$$T_* = -\frac{H}{c_p\,\varrho\,u_*} \qquad (3\text{–}56)$$

In neutral conditions

$$\phi_h = 1 \qquad (3\text{–}57)$$

while in unstable conditions

$$\phi_h = (1 - 16\,z/L)^{-1/2} \qquad (3\text{–}58)$$

or

$$\phi_h = 0.74\,(1 - 9\,z/L)^{-1/2} \qquad (3\text{–}59)$$

and in stable conditions

$$\phi_h = 1 + 5\,z/L \qquad (3\text{–}60)$$

or

$$\phi_h = 0.74 + 4.7\,z/L \qquad (3\text{–}61)$$

Again, the integration of Equation 3–55 gives the value of θ at a certain

elevation z, i.e.,

$$\theta(z) - \theta(z_o) = (T_* / k) [\ln(z/z_o) - \psi_h(z/L)] \tag{3-62}$$

where

$$\psi_h(z/L) = \int_{z_o/L}^{z/L} [1 - \phi_h(\zeta)] \frac{d\zeta}{\zeta} \tag{3-63}$$

is the universal function in diabatic surface layer temperature profile.

In neutral conditions

$$\psi_h = 0 \tag{3-64}$$

while in unstable conditions

$$\psi_h \simeq 2 \ln\left[0.5 \left(1 + \sqrt{1 - 16\, z/L}\right)\right] \tag{3-65}$$

and in stable conditions

$$\psi_h = -5\, z/L \tag{3-66}$$

The same concepts apply to other scalars; e.g., the specific humidity q. We just replace $c_p T$ with q and obtain

$$q(z) - q(z_o) = (q_*/k)[\ln(z/z_o) - \psi_q(z/L)] \tag{3-67}$$

where the scaling parameter for the scalar q is

$$q_* = -\frac{Q}{u_* \varrho} \tag{3-68}$$

which is analogous to Equation 3-56, using the vertical flux Q of the scalar q instead of the heat flux H. It is still not clear how to define ψ_q. At present, it seems best to assume $\psi_q = \psi_h$ (Panofsky and Dutton, 1984).

The standard deviation of the vertical wind velocity can be scaled by

$$\sigma_w / u_* = \phi_3(z/L) \tag{3-69}$$

In neutral conditions

$$\phi_3 = const = 1.25 \pm 0.03 \tag{3-70}$$

and in unstable conditions

$$\phi_3 \simeq 1.25\ (1 - 3\ z/L)^{1/3} \tag{3-71}$$

while in stable conditions the large scatter of the data points has not yet allowed a clear interpolation.

The standard deviations of the horizontal wind velocity are scaled by

$$\sigma_u/u_* = \phi_1(z_i/L) \tag{3-72}$$

$$\sigma_v/u_* = \phi_2(z_i/L) \tag{3-73}$$

and are independent of height. In neutral conditions they are constant

$$\phi_1 = 2.39 \pm 0.03 \tag{3-74}$$

$$\phi_2 = 1.92 \pm 0.05 \tag{3-75}$$

while in stable or unstable conditions (Panofsky et al., 1977a) they vary with z_i/L, i.e.,

$$\phi_1 \simeq \phi_2 \simeq (12 - 0.5\ z_i/L)^{1/3} \tag{3-76}$$

The standard deviation of a scalar (e.g., q) is scaled by

$$\sigma_q/q_* = \phi_Q(z/L) \tag{3-77}$$

where ϕ_Q is the normalized σ_q. Again, experimental data in stable conditions present too large a scatter. But in unstable conditions

$$\phi_Q = const\ (z/L)^{-1/3} \tag{3-78}$$

with (Hogstrom and Hogstrom, 1974)

$$const = 1.04 \pm 0.13 \tag{3-79}$$

The above formulations have been successful only in flat terrain cases. Similar scaling approaches have been proposed for other layers in the PBL, but have not yet shown the same success.

3.7 SCALING IN OTHER LAYERS OF THE PBL

Parameterizations of the viscous sublayer near the ground (for $z < z_o$) have been proposed by Zilitinkevich (1970) and Deardorff (1974). Deardorff (1974) has also provided a parameterization of the mixing layer (from h_s to z_i), which seems very realistic when the variation of z_i with time is strongly influenced by surface heating (Pielke and Mahrer, 1975). Accordingly, σ_w can be scaled by

$$\sigma_w/w_* = f(z/z_i) \tag{3-80}$$

where the function f seems to be proportional to $(z/z_i)^{1/3}$.

Internal boundary layers are generated when air advects over heterogeneous surfaces. In these cases, at upper levels, turbulence is characteristic of the original surface, while, at lower levels, it is a function of the new surface. The interface between these two regimes (e.g., stable above and unstable below, or vice versa) is called the internal boundary layer. Deardorff and Peterson (1980) and Deardorff (1981) give a tentative parameterization of such horizontally non-homogeneous boundary layers. Further discussion of internal boundary layer phenomena is provided by Hunt and Simpson (1982).

New insight on the stable atmospheric boundary layer has recently been provided by the "local scaling" approach (Nieuwstadt, 1984), in which a local (i.e., variable with z) Obukhov length Λ is defined as

$$\Lambda(z) = \frac{\tau^{3/2}(z)}{k \frac{g}{T} \overline{w'\theta'}(z)} \tag{3-81}$$

where T is the temperature and w', θ' are the fluctuations of vertical wind velocity and potential temperature (see Section 3.5.8), respectively. The profiles $\tau(z)$, $\overline{w'\theta'}(z)$ and $\Lambda(z)$ can be expressed by the power laws

$$\tau(z)/\tau(0) = (1 - z/h)^{\alpha_1} \tag{3-82}$$

$$\overline{w'\theta'}(z)/\overline{w'\theta'}(0) = (1 - z/h)^{\alpha_2} \tag{3-83}$$

$$\Lambda(z)/L = (1 - z/h)^{\alpha_3} \tag{3-84}$$

where h is the mean mixing height.

The above scheme was not justified theoretically, but seems to provide a convenient approximation, even though it is in contradiction with local scaling

(Holtslag and Nieuwstadt, 1986). In spite of this problem, in horizontally homogeneous and steady conditions, Nieuwstadt (1984) derived $a_1 = 3/2$, $a_2 = 1$ and $a_3 = 5/4$.

Finally, the new "local similarity" theory by Sorbjan (1986 and 1988) must be mentioned. Sorbjan (1986) generalized the Monin–Obukhov (1954) similarity theory to the region above the surface layer and provided universal functions, in agreement with empirical data, for the stable and convective regimes. This extension of the similarity theory, however, is valid only in the lower half of the mixed layer. Sorbjan (1988) presented new hypotheses with new similarity functions that generalize local scaling for the entire mixed layer in convective (i.e., unstable) conditions.

REFERENCES

Aloysius, K.L. (1979): On the determination of boundary-layer parameters using velocity profile as the sole information. *Boundary-Layer Meteor.*, **17**:465–484.

Businger, J.A. (1966): Transfer of heat and momentum in the atmospheric layer. Prog. Artc. Heat Budget and Atmos. Circulation. Rand Corp., Santa Monica, California, pp. 305–332.

Businger, J.A., and S.P. Arya (1974): Heights of the mixed layer in the stable, stratified planetary boundary layer. *Advances in Geophys.*, **18A**:73–92.

Caughey, S.J., and S.G. Palmer (1979): Some aspects of turbulence structure through the depth of the convection boundary layer. *Quart. J. Roy. Meteor. Soc.*, **105**:811–827.

Caughey, S.J., J.C. Wyngaard, and J.C. Kaimal (1979): Turbulence in the evolving stable boundary layer. *J. Atmos. Sci.*, **36**:1041–1052.

Deardorff, J.W. (1970): Convective velocity and temperature scales for the unstable planetary boundary layer. *J. Atmos. Sci.*, **27**:1211–1213.

Deardorff, J.W. (1974): Three-dimensional numerical study of the height and mean structure of a heated planetary boundary layer. *Boundary-Layer Meteor.*, **7**:81–106.

Deardorff, J.W., and E.W. Peterson (1980): The boundary-layer growth equation with Reynolds averaging. *J. Atmos. Sci.*, **37**:1405–1409.

Deardorff, J.W. (1981): Further considerations on the Reynolds average of the kinematic boundary condition. *J. Atmos. Sci.*, **38**:659–661.

Dobbins, R.A. (1979): *Atmospheric Motion and Air Pollution*. New York: John Wiley.

Garratt, J.R. (1982): Observations in the nocturnal boundary layer. *Boundary-Layer Meteor.*, **22**(1):21–48.

Golder, D. (1972): Relations among stability parameters in the surface layer. *Boundary-Layer Meteor.*, **3**:47–58.

Gryning, S.E., A.A. Holtslag, J.S. Irwin, and B. Sivertsen (1987): Applied dispersion modelling based on meteorological scaling parameters. *Atmos. Environ.*, **21**(1):79–89.

Hogstrom, U., and A.S. Hogstrom (1974): Turbulence mechanism at an agricultural site. *Boundary-Layer Meteor.*, **7**:373–389.

Holtslag, A.A., and F.T. Nieuwstadt (1986): Scaling the atmospheric boundary layer. *Boundary-Layer Meteor.*, **36**:201–209.

Hunt, J.C., and J.E. Simpson (1982): Atmospheric boundary layers over nonhomogeneous terrain. In *Engineering Meteorology*, editted by E. Plate, New York: Elsevier, pp. 269–318.

Irwin, J.S. (1979): Estimating plume dispersion: A recommended generalized scheme. Presented at 4th AMS Symposium on Turbulence and Diffusion, Reno, Nevada.

Liu, M.-K., D.R. Durran, P. Mundkur, M. Yocke, and J. James (1976): The chemistry, dispersion, and transport of air pollutants emitted from fossil fuel plants in California: Data analysis and emission impact model. Final report to the Air Resources Board, Contract No. ARB 4-258, Sacramento, California.

McRae, G.J., W.R. Goodin, and J.H. Seinfeld (1982): Mathematical modeling of photochemical air pollution. EQL Report No. 18, Environmental Quality Laboratory, Pasadena, California. Also see: McRae, G.J., W.R. Goodin, and J.H. Seinfeld (1982): Development of a second generation mathematical model for urban air pollution, I. Model formulation. *Atmos. Environ.*, **16**(4):679–696.

Monin, A.S., and A.M. Obukhov (1954): Basic laws of turbulent mixing in the ground layer of the atmosphere. *Trans. Geophys. Inst. Akad.*, Nauk USSR **151**:163–187.

Nieuwstadt, F.T. (1978): The computation of the friction velocity u_* and the temperature scale T_* from temperature and wind velocity profiles by least-squares methods. *Boundary-Layer Meteor.*, **14**:235–246.

Nieuwstadt, F.T. (1984): The turbulent structure of the stable nocturnal boundary layer. *J. Atmos. Sci.*, **41**:2202–2216.

Pandolfo, J.O. (1966): Wind and temperature for constant flux boundary layers in lapse conditions with a variable eddy conductivity to eddy viscosity ratio. *J. Atmos. Sci.*, **23**:495–502.

Panofsky, H.A., H. Tennekes, D.H. Lenscfhow, and J.C. Wyngaard (1977a): The characteristics of turbulent velocity components in the surface layer under convective conditions. *Boundary-Layer Meteor.*, **11**:355–361.

Panofsky, H.A., W. Heck, and M.A. Bender (1977b): The effect of clear-air turbulence on a model of the general circulation of the atmosphere. *Beitr. Phys. Atmos.*, **50**:89–97.

Panofsky, H.A., and J.A. Dutton (1984): *Atmospheric Turbulence*. New York: John Wiley.

Pasquill, F. (1974): *Atmospheric Diffusion*, 2nd Edition. New York: Halsted Press of John Wiley & Sons.

Pielke, R.A., and Y. Mahrer (1975): Technique to represent the heated-planetary boundary layer in mesoscale models with coarse vertical resolution. *J. Atmos. Sci.*, **32**:2288–2308.

Pielke, R.A. (1984): *Mesoscale Meteorological Modeling*. Orlando, Florida: Academic Press.

Sorbjan, Z. (1986): On similarity in the atmospheric boundary layer. *Boundary-Layer Meteor.*, **34**:377–397.

Sorbjan, Z. (1988): Local similarity in the convection boundary layer (CBL). *Boundary-Layer Meteor.*, **45**:237–250.

Stern, A.C., R.W. Boubel, D.B. Turner, and D.L. Fox (1984): *Fundamentals of Air Pollution*. Orlando, Florida: Academic Press.

van Ulden, A.P., and A.A. Holtslag (1985): Estimation of atmospheric boundary layer parameters for diffusion applications. *J. Climate and Appl. Meteor.*, **24**:1196–1207.

Venkatram, A. (1980): Estimating the Monin-Obukhov length in the stable boundary layer for dispersion calculations. *Boundary-Layer Meteor.*, **19**:481–485.

Wilczak, J.M., and M.S. Phillips, (1986): An indirect estimation of convection boundary layer structure for use in pollution dispersion models. *J. Climate and Appl. Meteor.*, **25**:1609–1624.

Williamson, S.J. (1973): *Fundamentals of Air Pollution*. Reading, Massachusetts: Addison-Wesley.

Wyngaard, J.C., O.R. Cote, and K.S. Rao (1974): Modeling the atmospheric boundary layer. *Advances in Geophys.*, **18A**:193–211.

Wyngaard, J.C., and M.A. LeMone (1980): Behavior of the refractive index structure parameter in the entraining convective boundary layer. *J. Atmos. Sci.*, **37**:1573–1585.

Zilitinkevich, S.S. (1970): *Dynamics of the Atmospheric Boundary Layer*. Leningrad: Hydrometerol.

4 METEOROLOGICAL MODELING

Meteorological models are developed for two purposes:

- to understand local, regional, or global meteorological phenomena
- to provide the meteorological input required by air pollution diffusion models

In both cases, the analytical and numerical techniques are similar. In this book, we will focus our attention on the second group of meteorological models; i.e., on those techniques used as a "pre-processor" of available meteorological information in order to prepare the proper input to air quality diffusion models.

Pielke (1984) provides a thorough review of mesoscale (i.e., from a few kilometers to several hundred kilometers) meteorological modeling techniques. His book also presents, in Appendix B, a summary of the organizations active in prognostic numerical mesoscale modeling in 1983 and a list of existing mesoscale models, with a description of their major characteristics. Available diagnostic and prognostic models are discussed by Haney et al. (1989).

Meteorological models can be divided into two categories:

- physical models -- physical small-scale models of atmospheric motion (e.g., wind tunnels)
- mathematical models -- a set of analysis techniques (algebraic and calculus-based) for solving a certain subset of meteorological equations

Mathematical models can be

- analytical models, in which exact analytical solutions are obtained
- numerical models, in which approximate numerical solutions are found using numerical integration techniques

In this book, we will discuss only numerical models, currently the most powerful and promising tools for both meteorological and air quality simulation studies.

Numerical meteorological models can be divided into two groups:

- diagnostic models; i.e., models that are based on available meteorological measurements and contain no time-tendency terms
- prognostic models; i.e., models with full time-dependent equations

Both approaches are discussed below. It must be noted that diagnostic models, even though they include little physics in their calculations, have the important advantage of being able to incorporate information gathered from available measurements. Actually, their performance is strongly dependent upon the density of meteorological measurements in the simulation region: the higher the number of stations, the better the performance of the model. Prognostic models, instead, do incorporate meteorological physics, but cannot use available data to modify their forecasts, even though "nudging" techniques have been proposed (e.g., Hoke and Anthes, 1976) to incorporate observations to a certain extent. One of the major future challenges of meteorological modeling for air quality applications is the proper linkage of diagnostic and prognostic methodologies, to take advantage of the best features of both approaches (e.g., by using the Kalman filtering techniques discussed in Chapter 12).

4.1 DIAGNOSTIC MODELS

Diagnostic models are based on objective analysis of available meteorological data. Their outputs are three-dimensional fields of meteorological parameters derived by appropriate interpolation and extrapolation of available meteorological measurements. They are diagnostic because they cannot be used to forecast the meteorological evolution, but simply provide a best estimate of a steady-state (or quasi steady-state) condition.

They have been used frequently for evaluating mass-consistent flow fields in complex terrain (e.g., Anderson, 1971; Danard, 1977; Dickerson, 1978; Tesche and Yocke, 1978; Sherman, 1978; Liu and Yocke, 1980; Patnack et al., 1983; Mass and Dempsey, 1985). Ludwig and Bird (1980), in particular, developed a mass-consistent method based on principal component analysis that seems quite cost-effective. These mass-consistent flow calculations give satisfactory results (Pielke, 1984) when

- the terrain represents the dominant forcing term

- sufficient meteorological input measurements are available

Figure 4–1 shows an example of diagnostic model output.

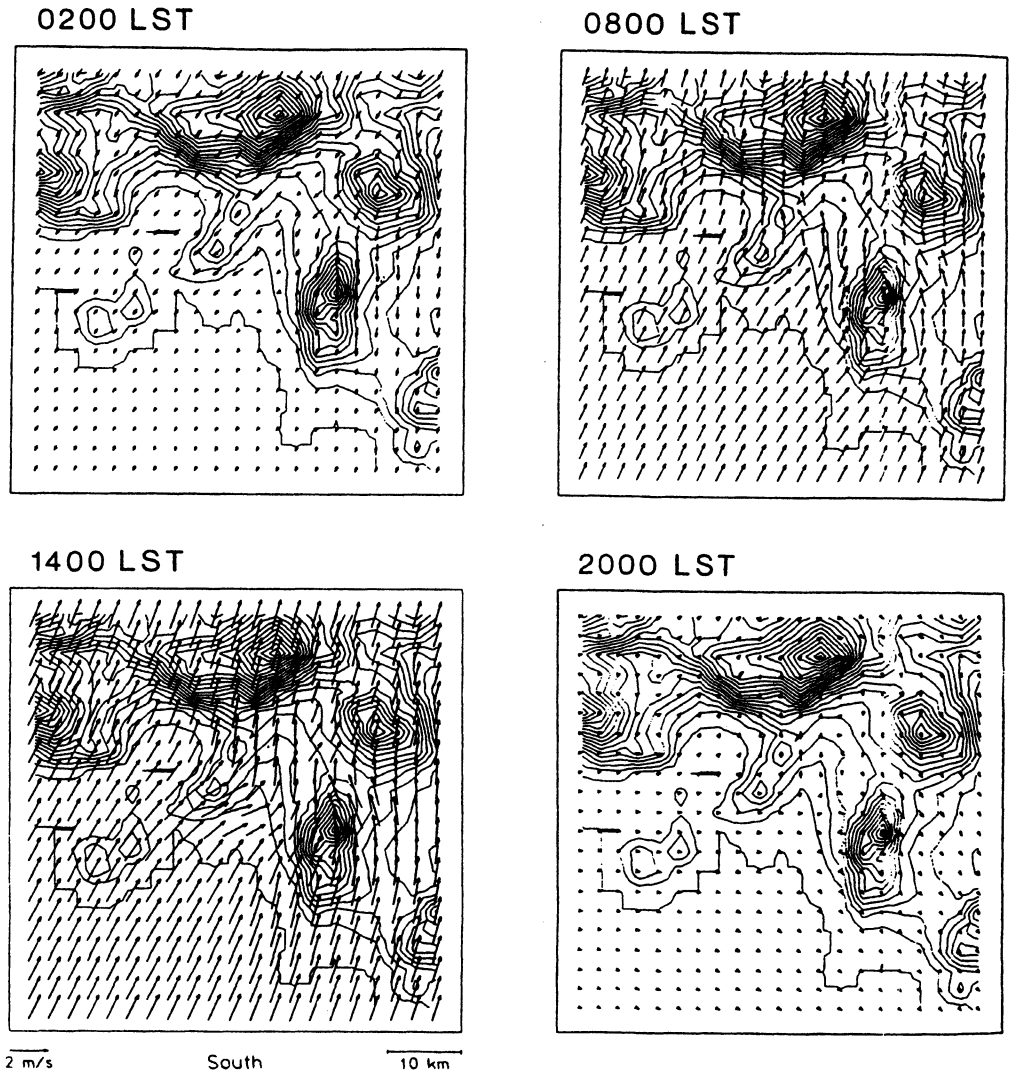

FIGURE 4–1. Reconstructed wind fields in the Athens basin at a height of 10 m AGL for 0200, 0800, 1400 and 2000 LST 26 June 1982 (from Moussiopoulos and Flassak, 1986). [Reprinted with permission from the American Meteorological Society.]

Several diagnostic computer packages are discussed below.

4.1.1 IBMAQ–2

The IBMAQ–2 program (Shir and Shieh, 1974) estimates three–dimensional wind vectors at each point in the computational domain using the following computational steps:

- An initial–guess wind vector is estimated at each grid point from the nearest available observation station.
- These initial values are corrected by recomputing, at each grid point, the wind components as weighted averages of their values at the adjacent grid points. A weighting factor proportional to $1/r^2$ is used, where r is the distance between grid points.
- Each subsequent wind estimate uses the four nearest adjacent grid points.

4.1.2 NEWEST

The NEWEST subroutine of the IMPACT code (Tran and Sklarew, 1979) provides three–dimensional fields of stability and wind. Stability measurements are interpolated using weighting factors proportional to $1/r^4$ and wind measurements are interpolated using weighting factors proportional to $1/r^2$, where the r values are the distances between the grid point at which the interpolation is made and the measurement points. The wind field is then adjusted by a numerical cycle that makes the wind velocity fields mass–consistent. Finally, thermal drainage effects (i.e., daytime upslope and nighttime downslope winds) are included by adding a vertical wind component w_D, where

$$w_D = const \left(\frac{|T_G - T_A|}{T_G} \right)^{1/2} \tag{4–1}$$

in which T_G is the ground temperature on the slope and T_A is the ambient temperature at the same location.

4.1.3 NOABL

The NOABL package (Phillips and Traci, 1978) provides an accurate representation of the terrain by a vertical coordinate transformation in which the lowest coordinate is conformal to the terrain surface. Figure 4–2 illustrates this coordinate transformation, from the (x,z) space to the (x,σ) space.

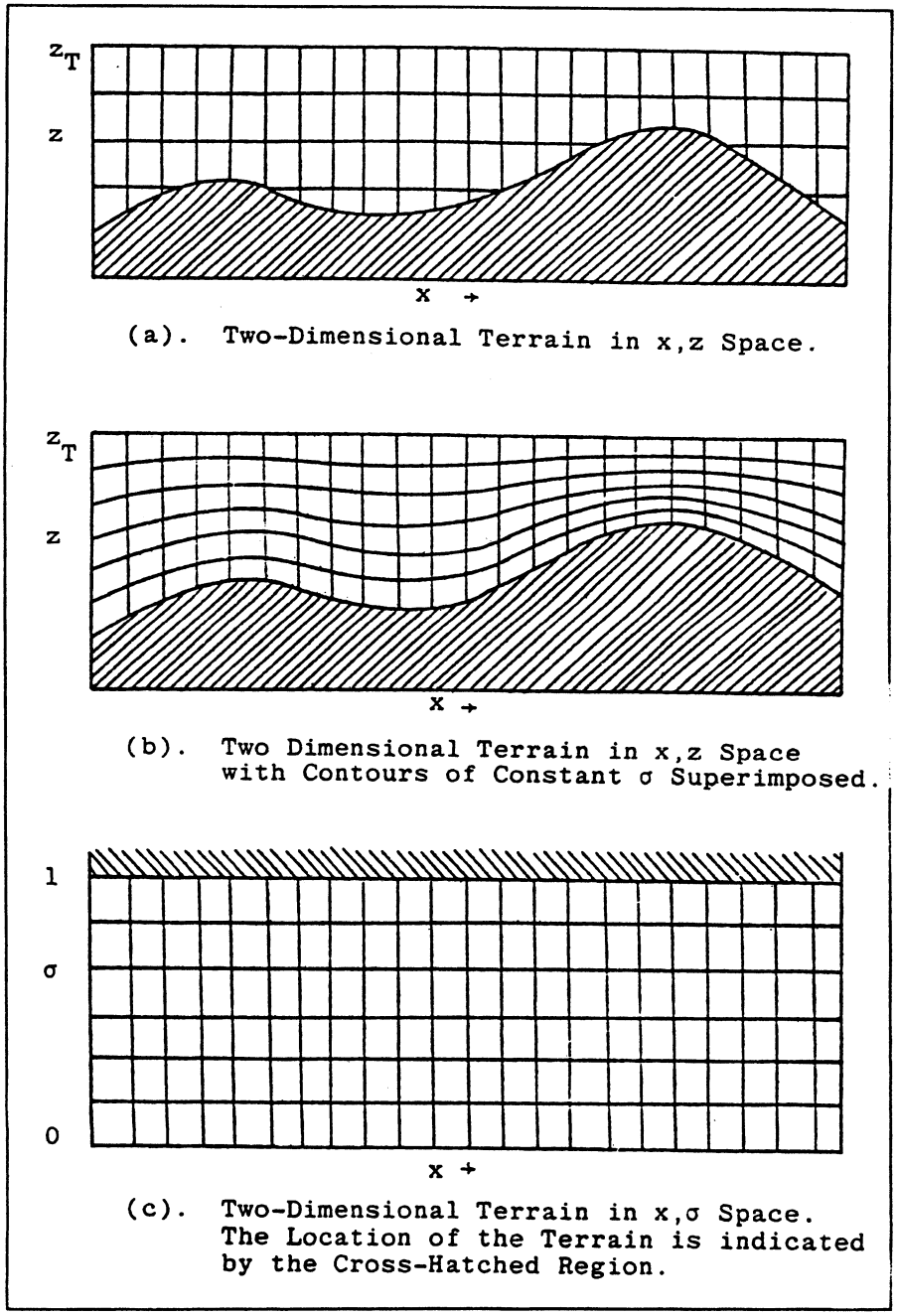

FIGURE 4–2. Terrain coordinate transformation $\sigma = \frac{p - p_t}{p_s - p_t}$ *where p is the pressure,* p_t *is the constant pressure at the top of the domain, and* p_s *is the variable surface pressure (from Phillips and Traci, 1978). [Reprinted with permission from Science Applications, Inc.]*

4.1.4 MASCON

The MASCON model (Dickerson, 1978) is based on variational calculus techniques, which are used to adjust the observed horizontal fluxes so they satisfy the continuity equation (similar to the MATHEW model described below).

4.1.5 MATHEW

The MATHEW model (Sherman, 1978; Rodriguez et al., 1982) produces an average, minimally adjusted three-dimensional wind field, according to the variational analysis formalism described by the integral function

$$E(u,v,w,\lambda) = \int_V [a_1^2 (u-u_o)^2 + a_2^2 (v-v_o)^2 + a_3^2 (w-w_o)^2 + \lambda(\partial u/\partial x + \partial v/\partial y + \partial w/\partial z)]\, dx\, dy\, dz \tag{4-2}$$

where $u(x,y,z)$, $v(x,y,z)$ and $w(x,y,z)$ are the adjusted wind components calculated by the model; $u_o(x,y,z)$, $v_o(x,y,z)$ and $w_o(x,y,x)$ are the wind observations; $\lambda(x,y,z)$ is the Lagrangian multiplier; and a_1, a_2 and a_3 are the Gauss precision moduli (which are related to the observational errors). The above integral is applied throughout the entire computational domain.

The solution u, v, w is found by minimizing E in Equation 4-2; i.e., by a combined minimization of both the difference between observed and adjusted components and the wind divergence. This minimization gives a formula for u, v, w and a differential equation for λ, which can be solved if proper boundary conditions are provided.

4.1.6 Terrain Adjustment With the Poisson Equation

The objective analysis method of Goodin et al. (1980) performs the following numerical steps:

1. The surface wind field is computed by interpolating wind measurements with a weighting factor proportional to $1/r^2$.

2. The wind is adjusted to the terrain by solving the Poisson equation

$$\nabla^2 \phi = \psi(x,y) \tag{4-3}$$

where ϕ is the wind velocity potential and ψ is a forcing function based on the thickness of the PBL and terrain elevation gradients.

3. Upper level winds are interpolated in a terrain-following coordinate system (such as in Figure 4–2), using a weighting factor proportional to $1/r$ and a five-point filter.

4. Iterations are performed until the maximum divergence of the interpolated wind fields is reduced to an acceptable level.

4.1.7 Mass Consistent Wind Generation by Linear Combination of a Limited Number of Solutions

Most of the above wind generation schemes provide solutions that are linear combinations of the input data. A method by Ludwig and Bird (1980) combines the solutions for several linearly independent data sets in an appropriate way to obtain the solution for any arbitrary input. This is performed by principal component analysis, using normalized eigen-vectors.

4.1.8 The ATMOS1 Code

The ATMOS1 model (Davis et al., 1984; King and Bunker, 1984) calculates wind fields with the use of a mass conservation error minimization principle that employs available observations. It provides a three-dimensional wind field using terrain-following coordinates and an expanded vertical grid system that insures resolution near the surface where the drainage flow occurs and where pollutants are normally concentrated.

4.1.9 The Moussiopoulos-Flassak Model

Moussiopoulos and Flassak (1986) developed a mass-consistent model for the calculation of wind velocity fields over complex orography. Velocities are adjusted by solving a three-dimensional elliptic differential equation transformed to a terrain-following coordinate system. One important peculiarity of this model is the full vectorization of its algorithms, which optimizes running time on array processing computers. This model was refined by Moussiopoulos et al. (1988) by improving its numerical algorithms and accounting for atmospheric stability. The model has been applied to reconstruct wind fields, in the basin of Athens, Greece.

4.1.10 The MINERVE Code

MINERVE (Geai, 1987) is a mass-consistent wind field model that reduces the divergence by an iterative procedure that may take into account atmospheric stability. The code was developed by the Electricite' de France.

4.1.11 The Objective Analysis Based on the Cressman Interpolation Method

Fruehauf et al. (1988) developed a computer code for the objective analysis of a two-dimensional field. This code automates the use of a successive corrections method that interpolates data from irregularly spaced points to a regularly spaced grid. The program was implemented in a IBM personal computer and contains isopleth analysis routines for standard meteorological fields such as temperature.

4.1.12 The DWM Code

The DWM code (Douglas and Kessler, 1988) is based on the conservation-of-mass equation. The model incorporates local surface and upper air observations, when available, and provides some information on terrain-generated airflows in regions where local observations are absent. The model is formulated in terrain-following coordinates and uses a two-step procedure to generate a gridded wind field. In Step 1, a domain-mean wind is adjusted for terrain effects, (e.g., lifting and acceleration of the airflow over terrain obstacles, thermodynamically generated slope flows and blocking effects). In Step 2, an objective analysis procedure is applied in which the observations are used within a user-specified radius of influence. This Step 2 procedure consists of interpolation, smoothing, calculation of vertical-velocity field and minimization of the three-dimensional divergence.

4.2 PROGNOSTIC MODELS

Meteorological prognostic models are used to forecast the time evolution of the atmospheric system through the space-time integration of the equations of conservation of mass, heat, motion, water, and if necessary, other substances such as gases and aerosols. The following governing equations have been derived by Pielke (1984):

$$\frac{\partial \varrho}{\partial t} = -(\nabla \cdot \varrho \mathbf{V}) \tag{4-4}$$

$$\frac{\partial \theta}{\partial t} = -\mathbf{V} \cdot \nabla \theta + S_\theta \tag{4-5}$$

$$\frac{\partial \mathbf{V}}{\partial t} = -\mathbf{V} \cdot \nabla \mathbf{V} - (1/\varrho)\, \nabla p - g\, \mathbf{k} - 2\boldsymbol{\Omega} \times \mathbf{V} \tag{4-6}$$

$$\frac{\partial q_n}{\partial t} = -\mathbf{V} \cdot \nabla q_n + S_{q_n}, \; n = 1, 2, 3 \tag{4-7}$$

where

ϱ is the density of the air

$\mathbf{V}$ is the wind vector (u,v,w)

θ is the potential temperature

S_θ represents the sources and sinks of heat (i.e., freezing/melting, condensation/evaporation, deposition/sublimation, exothermic/endothermic chemical reactions, net radiative flux convergence/divergence, dissipation of kinetic energy by molecular motion)

p is the pressure

g is the acceleration of gravity

$\boldsymbol{\Omega}$ is the earth's angular velocity

q_n is the density of the various forms of water (solid, n = 1; liquid, n = 2; and vapor, n = 3)

S_{q_n} is the source–sink term for q_n due to phase change and chemical reactions, where the latter is generally negligible (S_{q_1}: freezing/melting, deposition/sublimation, fallout from above/to below; S_{q_2}: melting/freezing, condensation/evaporation, fallout from above/to below; S_{q_3}: evaporation/condensation, sublimation/deposition)

(The symbol ∇ is the gradient operator, $\nabla\cdot$ is the divergence, $\times$ is the vector cross product, $\mathbf{k}$ is the unit vector along the positive z–axis, and $\cdot$ indicates the scalar product)

Equation 4–4 is the conservation of mass or continuity equation. Equation 4–5 is the conservation of heat derived by assuming the air to behave like an ideal gas and to be in local thermodynamic equilibrium. (It is derived from the first law of thermodynamics and the ideal gas law in a form that includes the contribution of water vapor.) Equation 4–6 is the conservation of motion, according to Newton's second law and contains two external forces, i.e., the pressure

gradient force and the gravity force (which includes, as usual, the earth's centripetal acceleration) and the apparent Coriolis force. Equation 4–6 does not include the internal forces that would be required to take into account the dissipation of momentum by molecular motions. Finally, Equation 4-7 is the conservation of water (solid, liquid and vapor).

Three additional equations -- the definition of potential temperature, the ideal gas law, and the definition of virtual temperature -- complete the above set:

$$\theta = T_v \, (100/p_{mb})^{R_d/c_p} \tag{4–8}$$

$$p = \varrho \, R_d \, T_v \tag{4–9}$$

$$T_v = T \, (1 + 0.61 \, q_3) \tag{4–10}$$

where T_v is the virtual temperature, p_{mb} is the pressure expressed in mb, R_d is the dry gas constant of the atmosphere ($R_d = 287 \, J \, K^{-1} \, kg^{-1}$), and c_p is the specific heat of the air at constant pressure.

The conservation equations, 4–4 through 4–7, together with the latter three equations, 4–8 through 4–10, form a set of 11 simultaneous nonlinear partial differential equations in 11 dependent variables: ϱ, θ, T, T_v, p, V, and q_n. The independent variables are the time t and the spatial coordinates x, y, and z.

To be completed, the above set of equations should include conservation relations for other atmospheric chemical species besides water, e.g., gaseous materials, such as sulfur dioxide, and aerosols, such as sulfates and nitrates. However, the simultaneous solution of both meteorological equations and transport, diffusion, chemical and deposition equations, represent a formidable problem. It is commonly assumed that the concentrations of primary and secondary atmospheric pollutants do not affect the meteorology. Consequently, prognostic meteorological models can be generally applied and can run independently from dispersion models.

Meteorological prognostic modeling aims at finding the solution of the above 11 equations or a subset of them. However, they must be modified and simplified to be solved. For practical applications, these equations are never used in the form shown above. Actual numerical simulations, in fact, require that the 11 variables and the sink–source terms be averaged in space, over grid volumes, and in time, over a computational interval Δt. Grid volume averaging is commonly performed using the Reynolds assumption, in which each variable a is

decomposed into an average term plus a subgrid perturbation (i.e., $a = \overline{a} + a'$), where the average of the subgrid perturbation is assumed to be zero (i.e., $\overline{a'} = 0$). This process, however, creates new additional variables, in the form of average subgrid scale fluxes. This phenomenon is called the "closure" problem.

For example, Reynolds averaging of Equation 4–6 generates new terms, because of the nonzero correlations among the components of $\mathbf{V}'$, the subgrid perturbation of $\mathbf{V}$. And Equation 4–5 generates new cross correlation terms between θ', the subgrid perturbation of θ, and the components of $\mathbf{V}'$. Usually these new variables (or turbulent fluxes) cannot be defined in terms of basic observation principles and, therefore, solutions are found only through semiempirical assumptions. The simplest assumption is the so–called K–theory (or gradient theory), which relates these fluxes to the gradients of the average variables through proportionality terms called eddy coefficients. (Closure and K–theory are discussed in more detail in Chapter 6 in the context of transport and diffusion of an atmospheric pollutant.)

To reduce, modify or simplify the above equation, scale analysis is often used. Scale analysis (the method that determines the relative importance of the individual terms in the conservation relations; Pielke, 1984) is a major tool for identifying and eliminating terms whose contribution can be considered negligible for a certain range of applications. Scale analysis allows, in particular, the definition of the shallow convection form of the continuity equation (or incompressibility assumption)

$$\frac{\partial u}{\partial x} + \frac{\partial v}{\partial y} + \frac{\partial w}{\partial z} = 0 \tag{4–11}$$

the hydrostatic equation (derived from the vertical component of Equation 4–6 for the atmosphere at rest)

$$\frac{\partial p}{\partial z} = -\varrho\, g \tag{4–12}$$

and the evaluation of the geostrophic wind $(u_g,\ v_g)$

$$u_g = \frac{1}{\varrho f}\frac{\partial p}{\partial y} \tag{4–13}$$

$$v_g = \frac{1}{\varrho f}\frac{\partial p}{\partial x} \tag{4–14}$$

which is generally used as a boundary condition at the top of the computational domain.

Further modifications and simplifications of the conservation equations are obtained using averaging techniques and assumptions such as:

- Different parameterizations of the subgrid scale correlation terms, i.e, the turbulence fluxes (a solution to the closure problem)
- The Boussinesq approximations, in which pressure, density and temperature are expressed as the sum of equilibrium values plus a small correction due to atmospheric motion (in practice, the Boussinesq approximations assume that the temporal variations of the density can be neglected, except in the vertical component of Equation 4–6). These approximations lead to considerable simplifications (Seinfeld, 1986), including Equation 4–11.
- A simplified density–weighted mesoscale scalar vorticity, instead of the full vorticity equation in tensor form (Pielke, 1984)

Various sets of simplified equations can be derived from the above scale analyses and averaging processes. Each set, however, must be used with a clear understanding of its physical limitations with respect to the original group of equations 4–4 through 4–10.

Each set of simplified equations represents a group of simultaneous nonlinear partial differential equations. The nonlinearity is given by the presence of products of dependent variables and is one of the major obstacles to obtaining exact (i.e., analytical) solutions.

Linearization techniques, e.g. harmonic (Fourier) analysis, have been used (Pielke, 1984) to derive approximate sets of linear equations, consequently allowing, under certain simplifying assumptions, the identification of their analytical solution. In the past, these methods represented the only possible analysis tools, in spite of their limitations and shortcomings. Today's fast computers allow the evaluation of approximate solutions (i.e., numerical solutions) of a set of nonlinear equations and, therefore, represent the best tool in this field.

Numerical solutions can be computed using the following techniques:

- finite difference schemes
- spectral techniques

- pseudo–spectral methods
- finite elements
- interpolation schemes
- boundary element methods
- particle models

Numerical solutions depend strongly on boundary conditions and initial values; thus, when using numerical methods, special care must be taken to correctly initialize all meteorological variables in the computational domain and to correctly define the time–varying physics at the boundaries.

Several prognostic meteorological models have been developed. Unfortunately, however, most of them are complex research tools whose correct use requires the active involvement of their developers. A comprehensive list of mesoscale numerical models and their characteristics is presented in Appendix B of Pielke (1984). Additional information can be found in reviews of available mesoscale models prepared by Pielke (1988) and Haney et al. (1989).

Among these studies, the development of four advanced meteorological models has been particularly important for air quality applications: 1) the three–dimensional URBMET vorticity–mode model developed by Bornstein et al. (1987); 2) the primitive equation–mode model NMM (Numerical Mesoscale Model) developed by Pielke et al. (1983); 3) the three–dimensional hydrodynamic model HOTMAC (Higher Order Turbulence Model for Atmospheric Circulations) by Yamada (1985) and Yamada and Bunker (1988); and 4) the NCAR/PSU/SUNY model, which is used in the Regional Atmospheric Deposition Model (RADM) (Chang et al., 1987). All four models have been linked with dispersion models: URBMET and the NCAR model have been linked with K–theory grid models, while Pielke's model and HOTMAC are linked with Lagrangian particle simulation codes (see Section 8) (Pielke's model is also linked with the Urban Airshed Model discussed in Section 14.1.1).

4.2.1 The URBMET Model

The URBMET model introduces the stream function and three–dimensional vorticity vector into the equation of conservation of motion 4–6. A few assumptions allow Equation 4–6 to be simplified and applied to the upper portion of the PBL, more precisely the portion above the surface layer. These assumptions are (Bornstein et al., 1985):

- The atmosphere is Boussinesq. In practice, this assumption allows us to ignore temperature-induced density fluctuations in the horizontal terms of Equation 4-6 and produces the incompressible form of the continuity equation.
- The atmosphere is hydrostatic. Consequently, vertical velocities must be computed for conservation of mass.
- Turbulence can be described by eddy coefficients, and horizontal diffusion is characterized by a constant eddy diffusivity.
- Mean thermodynamic and dynamic variables can be defined as the sum of several parts (constant synoptic forcing plus spatial and temporal variations arising only from mesoscale motions).

With the above assumptions, the three components of Equation 4-6 become

$$\frac{\partial u}{\partial t}+\frac{\partial (uu)}{\partial x}+\frac{\partial (vu)}{\partial y}+\frac{\partial (wu)}{\partial z}=-\frac{1}{\varrho_a}\frac{\partial p_M}{\partial x}+f\,(v-v_g) + \frac{\partial}{\partial z}\left(K_{mv}\frac{\partial u}{\partial z}\right)+K_{mh}\left(\frac{\partial^2 u}{\partial x^2}+\frac{\partial^2 u}{\partial y^2}\right) \tag{4-15}$$

$$\frac{\partial v}{\partial t}+\frac{\partial (uv)}{\partial x}+\frac{\partial (vv)}{\partial y}+\frac{\partial (wv)}{\partial z}=-\frac{1}{\varrho_a}\frac{\partial p_M}{\partial y}-f\,(u-u_g) + \frac{\partial}{\partial z}\left(K_{mv}\frac{\partial v}{\partial z}\right)+K_{mh}\left(\frac{\partial^2 v}{\partial x^2}+\frac{\partial^2 v}{\partial y^2}\right) \tag{4-16}$$

$$\frac{\partial u}{\partial x}+\frac{\partial v}{\partial y}+\frac{\partial w}{\partial z}=0 \tag{4-17}$$

where

ϱ_a is the density (constant volume average)

p_M is the mesoscale atmospheric pressure

f is the Coriolis parameter defined by Equation 3-3

u_g, v_g are the geostrophic wind components defined by Equations 4-13 and 4-14

K_{mv} is the vertical momentum eddy transfer coefficient

K_{mh} is the horizontal momentum eddy transfer coefficient

We can relate the velocity $\mathbf{V} = (u,v,w)$ to the stream function vector $\mathbf{\Psi} = (\phi, -\psi, 0)$ by

$$\mathbf{V} = \nabla \times \mathbf{\Psi} \tag{4-18}$$

Consequently, we obtain

$$u = \frac{\partial \psi}{\partial z} \tag{4-19}$$

$$v = \frac{\partial \phi}{\partial z} \tag{4-20}$$

$$w = -\left(\frac{\partial \psi}{\partial x} + \frac{\partial \phi}{\partial y}\right) \tag{4-21}$$

and, by introducing the relative vorticity vector (ξ, η, ζ), we obtain

$$\xi = \frac{\partial v}{\partial z} - \frac{\partial w}{\partial y} \simeq \frac{\partial v}{\partial z} \tag{4-22}$$

$$\eta = \frac{\partial u}{\partial z} - \frac{\partial w}{\partial x} \simeq \frac{\partial u}{\partial z} \tag{4-23}$$

$$\zeta = \frac{\partial v}{\partial x} - \frac{\partial u}{\partial y} \tag{4-24}$$

where the last equalities in Equations 4–22 and 4–23 are valid for a hydrostatic PBL.

Further manipulation allows the derivation of the following vorticity equations for horizontal motion

$$\begin{aligned}\frac{\partial \xi}{\partial t} = &-\frac{\partial (u\xi)}{\partial x} - \frac{\partial (v\xi)}{\partial y} - \frac{\partial (w\xi)}{\partial z} + \xi \frac{\partial u}{\partial x} - \eta\left(f + \frac{\partial v}{\partial x}\right) \\ &+ \frac{g}{\theta_a}\frac{\partial \theta_M}{\partial y} + \frac{\partial^2}{\partial z^2}(K_{mv}\,\xi) + K_{mh}\left(\frac{\partial^2 \xi}{\partial x^2} + \frac{\partial^2 \xi}{\partial y^2}\right)\end{aligned} \tag{4-25}$$

$$\frac{\partial \eta}{\partial t} = -\frac{\partial (u\eta)}{\partial x} - \frac{\partial (v\eta)}{\partial y} - \frac{\partial (w\eta)}{\partial z} + \eta \frac{\partial v}{\partial y} + \xi \left(f - \frac{\partial u}{\partial y} \right)$$
$$+ \frac{g}{\theta_a} + \frac{\partial \theta_M}{\partial x} + \frac{\partial^2}{\partial z^2} (K_{mv}\, \eta) + K_{mh} \left(\frac{\partial^2 \eta}{\partial x^2} + \frac{\partial^2 \eta}{\partial y^2} \right) \qquad (4\text{–}26)$$

With appropriate boundary and initial conditions, Equations 4–19, 4–20, 4–21, 4–22, 4–23, 4–25, and 4–26 are solved in the URBMET model, thus providing the dynamics of V without solving the primitive Equations 4–15, 4–16 and 4–17.

4.2.2 The NMM Model and the ARAMS System

Pielke et al. (1983) developed the NMM model to provide reliable mesoscale meteorological simulations in regions of complex orographies (coastal zones and complex terrain). The model simulates three-dimensional circulations with horizontal grid intervals from 1 km to 10 km. The model, a primitive equation model assuming an incompressible, hydrostatic and noncondensing atmosphere, which has been in widespread use by a number of investigators during the 1980s, performed reasonably well in simulating basic sea breeze circulations and other topographically generated mesoscale flow regimes. Model evaluation has been encouraging (e.g., Segal and Pielke, 1981; and Pielke and Mahrer, 1978).

During 1987–88, a major effort was launched to unify the original "Pielke" model with the nonhydrostatic cloud scale model developed at Colorado State University by Professor William Cotton. The combined Pielke–Cotton model (called ARAMS) greatly expands the range and sophistication of the simulations possible using a mesoscale numerical model.

The Advanced Regional Atmospheric Modeling System (ARAMS) is a generalized, comprehensive and flexible numerical weather prediction system. It is the commercial, tested and documented version of the Colorado State University mesoscale model. The model has evolved over a 15-year period and represents the blending of three different models (two hydrostatic models and a nonhydrostatic cloud model).

ARAMS has the ability to address specific areas of concern by using a two-way interactive nesting scheme between the fine grid and the next coarser grid. The number of grid nests and grid levels in ARAMS is limited only by

computer constraints. This allows maximum resolution in the area of coastlines, sea breeze fronts and steep terrain. The grid nesting allows one to use a large enough grid size to resolve large-scale (synoptic) features while also nesting to a level in which smaller scale forcing (sea breezes, mountain upslope flows, etc.) can be resolved. ARAMS contains options ranging from different initialization schemes to a variety of cloud microphysical parameterizations. Some of the options may be changed between nests. A partial listing of model options includes

- spatial dimension: one-, two-, or three-dimensional
- forecast duration: several hours to five days
- variable horizontal and vertical domains
- multiple nested grids
- horizontal grid sizes: 100 + km to as small as 50 meters
- vertical levels: up to 38
- finite differencing (two schemes)
- turbulent closure (three schemes)
- hydrostatic or nonhydrostatic
- variable coordinate systems: telescoping, interactive, nested
- cloud microphysics (four schemes)
- precipitation parameterization (five schemes)
- radiation schemes (three short wave, two long wave)
- surface temperature (four schemes)
- lateral boundary conditions (three schemes)
- topography: flat or with terrain
- use: uniform or variable
- sea surface temperature: uniform or variable
- upper boundary conditions (five schemes)
- initialization (five schemes)

4.2.3 The HOTMAC Model

The HOTMAC model was originally developed by Yamada (1978 and 1985) and further improved by Yamada and Bunker (1988), who added a "nested grid" capability and improved the simulation of the morning transition by including the effects of shadows produced by the terrain. The unique characteristic of this model is its treatment of turbulence by a second-moment turbulence-closure assumption. The model uses a terrain-following vertical coordinate and

integrates its partial differential equations by using the ADI (alternating direction implicit) method and a time increment that satisfies the Courant–Friedrich–Lewy criteria.

4.2.4 The NCAR/PSU/SUNY Model

The NCAR/PSU/SUNY model (Chang et al., 1987; Seigneur, 1988; Lewellen et al., 1989) is an hydrostatic primitive-equation model that is used to simulate the meteorological fields in the central and eastern United States for acid deposition calculation. The code is capable of simulating cyclogenesis, low-level jets, land–sea breezes, forced airflow over rough terrain, frontal circulation, and mesoscale convective systems.

4.2.5 Non-Hydrostatic Models

The hydrostatic assumption of Equation 4–12 is commonly used in meteorological models. Models that do not use this simplification are called nonhydrostatic and require the solution of the vertical equation of motion and a prognostic or diagnostic equation for pressure. These models demand enormous computational efforts and, therefore, their past and current application has been limited.

Pielke (1984) has shown that, when the hydrostatic assumption is used in meteorological models with terrain-following coordinate systems, the terrain slope must be much less than 45° (e.g., 5°) to assure a correct representation. Also, many studies concluded (Fast and Takle, 1988) that nonhydrostatic effects generally become more important in neutral conditions or when the horizontal length scale is smaller than 1–3 km.

Few nonhydrostatic models are available (e.g., Clark, 1977; Tapp and White, 1976) and require large computational resources. Quasi-nonhydrostatic assumptions can be used, however, to simulate flow over simple terrain features. For example, Fast and Takle (1988) derived a parameterization of the nonhydrostatic pressure and incorporated it into an hydrostatic model. Tests show that this approach is able to reproduce many of the terrain-induced characteristics that the hydrostatic model failed to simulate.

REFERENCES

Anderson, G.E. (1971): Mesoscale influences on wind fields. *J. Appl. Meteor.*, **10**:377–386.

Bornstein, R.D., S. Klotz, R. Street, U. Pechinger, R. Miller (1987): Modeling the polluted coastal urban environment. Vol. 1. The PBL Model. EPRI Report EA–5091, Palo Alto, California.

Chang, J.S., R.A. Brost, I.S. Isaksen, S. Madronich, P. Middleton, W.R. Stockwell, and C.J. Walcek (1987): A three–dimensional Eulerian acid deposition model: Physical concepts and formulation. *J. Geophys. Res.*, **92**:14681–14700.

Clark, T.L. (1977): A small–scale dynamic model using a terrain–following coordinate transformation. *J. Comput. Phys.*, **24**:186–215.

Danard, M. (1977): A simple model for mesoscale effects of topography on surface winds. *Mon. Wea. Rev.*, **105**:572.

Davis, C.G., S.S. Bunker, and J.P. Mutschlecner (1984): Atmospheric transport models for complex terrain. *J. Climate and Appl. Meteor.*, **23**:235–238.

Dickerson, M.H. (1978): MASCON -- A mass–consistent atmospheric flux model for regions with complex terrain. *J. Appl. Meteor.*, **17**:241–253.

Douglas, S.G., and R.C. Kessler (1988): User's guide to the diagnostic wind model (Version 1.0). Systems Applications, Inc., San Rafael, California.

Fast, J.D., and E.S. Takle (1988): Evaluation of an alternative method for numerically modeling nonhydrostatic flows over irregular terrain. *Boundary–Layer Meteor.*, **44**:181–206.

Fruehauf, G., P. Halpern, P. Lester (1988): Objective analysis of a two–dimensional scalar field by successive corrections using a personal computer. *Environ. Software*, **3**(2):72–80.

Geai, P. (1987): Reconstitution tridimensionnelle d'un champ de vent dans un domaine a' topographie complexe a' partir de meusures in situ. EDF, Chatou, France, Final Report DER/HE/34–87.05.

Goodin, W.R., G.J. McRae, and J.H. Seinfeld (1980): An objective analysis technique for constructing three–dimensional urban–scale wind fields. *J. Appl. Meteor.*, **19**:98–108.

Haney, J.L., S.G. Douglas, L.R. Chinkin, D.R. Souten, C.S. Burton, P.T. Roberts (1989): Ozone air quality scoping study for the lower Lake Michigan air quality region. Systems Applications, Inc., Final Report SYSAPP–89/101, San Rafael, California.

Hoke, J.E., and R.A. Anthes (1976): The initialization of numerical models by a dynamic–initialization technique. *Mon. Wea. Rev.*, **104**:1551–1556.

King, D.S., and S.S. Bunker (1984): Application of atmospheric transport models for complex terrain. *J. Climate and Appl. Meteor.*, **23**:239.

Lewellen, W.S., R.I. Sykes, S.F. Parker, D.S. Henn, N.L. Seaman, D.R. Stauffer, and T.T. Warner (1989): A hierarchy of dynamic plume models incorporating uncertainty. Vol. 5: Pennsylvania State University Mesoscale Model (PSU–MM). A.R.A.P. Division of California Research & Technology, Inc., Report EA–6095, Vol. 5, Princeton, New Jersey.

Liu, M.–K., and M.A. Yocke (1980): Siting of wind turbine generators in complex terrain. *J. Energy*, **4**:10–16.

Ludwig, F.L., and G. Byrd (1980): An efficient method for deriving mass-consistent flow fields from wind observations in rough terrain. *Atmos. Environ.*, **14**:585-587.

Mass, C.F., and D.P. Dempsey (1985): A one-level mesoscale model for diagnosing surface winds in mountainous and coastal regions. *Mon. Wea. Rev.*, **110**:1211.

Moussiopoulos, N., and T. Flassak (1986): Two vectorized algorithms for the effective calculation of mass-consistent flow fields. *J. Climate and Appl. Meteor.*, **25**:847-857.

Moussiopoulos, N., T. Flassak, and G. Knittel (1988): A refined diagnostic wind model. *Environ. Software*, 3(2):85-94.

Patnack, P.C., B.E. Freeman, R.M. Traci, and G.T. Phillips (1983): Improved simulations of mesoscale meteorology. Atmospheric Science Laboratory Report ASL CR-83-0127-1. White Sands Missile Range, New Mexico.

Phillips, G.T., and R.M. Traci (1978): A preliminary user guide for the NOABL objective analysis code. Science Applications Inc. Report SAI-78-769-LJ; San Diego, CA. U.S. Department of Energy Report RLO/2440-77-10.

Pielke, R.A., and Y. Mahrer (1978): Verification analysis of the University of Virginia three-dimensional mesoscale model prediction over south Florida for July 1, 1973. *Mon. Wea. Rev.*, **106**:1568-1589.

Pielke, R.A., R.T. McNider, M. Segal, and Y. Mahrer (1983): The use of a mesoscale numerical model for evaluations of pollutant transport and diffusion in coastal regions and over irregular terrain. *Bull. Am. Meteor. Soc.*, **64**:243-249.

Pielke, R.A. (1984): *Mesoscale Meteorological Modeling*. Orlando, Florida: Academic Press.

Pielke, R.A. (1988): Status of mesoscale and subregional models. Vol. 2. Aster, Inc., Research Project RP2434-6, Fort Collins, Colorado.

Rodriguez, D.J., et al. (1982): User's guide to the MATHEW/ADPIC models. UASG 82-16, Lawrence Livermore National Laboratory, University of California Atmospheric and Geophysical Sciences Division, Livermore, California.

Segal, M., and R.A. Pielke (1981): Numerical model simulation of biometeorological heat load conditions—Summer day case study for the Chesapeake Bay area. *J. Appl. Meteor.*, **20**:735-749.

Seigneur, C. (1988): Evaluation of the feasibility of the application of a regional air pollution model to northern California. Second interim report prepared for Pacific Gas and Electric, San Francisco, California.

Seinfeld, J.H. (1986): *Atmospheric Chemistry and Physics of Air Pollution*. New York: John Wiley.

Sherman, C.A. (1978): A mass-consistent model for wind fields over complex terrain. *J. Appl. Meteor.*, 17:312-319.

Shir, C.C., and L.J. Shieh (1974): A generalized urban air pollution model and its application to the study of SO_2 distributions in the St. Louis metropolitan area. *J. Appl. Meteor.*, *13*:185-204.

Tapp, M.C., and P.W. White (1976): A nonhydrostatic mesoscale model. *Quarterly J.Roy. Meteor. Soc.*, **102**:277-296.

Tesche, T.W., and M.A. Yocke (1978): Numerical modeling of wind fields over mountainous regions in California. *Proceedings*, American Meteorological Society Conference on Sierra Nevada Meteorology, South Lake Tahoe, California, June.

Tran, K.T., and R.C. Sklarew (1979): User guide to IMPACT: An integrated model for plumes and atmospheric chemistry in complex terrain. Form & Substance, Inc., Westlake Village, California.

Yamada, T. (1978): A three-dimensional, second-order closure numerical model of mesoscale circulations in the lower atmosphere. Argonne National Laboratory Document ANL/RER-78-1. [Available from National Technical Information Service.]

Yamada, T. (1985): Numerical simulation of the Night 2 data of the 1980 ASCOT experiments in the California Geysers Area. *Arch. for Meteor. , Geophys., and Biolim.*, A34:223-247.

Yamada, T., and S.S. Bunker (1988): Development of a nested grid, second moment turbulence closure model and application to the 1982 ASCOT Brush Creek data simulation. *J. Appl. Meteor.*, 27:562-578.

5 PLUME RISE

In most cases, pollutants injected into ambient air possess a higher temperature than the surrounding air. Most industrial pollutants, moreover, are emitted from smokestacks or chimneys and therefore possess an initial vertical momentum. Both factors (thermal buoyancy and vertical momentum) contribute to increasing the average height of the plume above that of the smokestack. This process terminates when the plume's initial buoyancy is lost by mixing with ambient air.

The physical consequence of the above phenomenon is generally quantified by a single parameter, the plume rise Δh, defined as the vertical displacement of the plume in this initial dispersion phase. Several studies have provided semiempirical formulae for evaluating Δh (e.g., Briggs, 1975); others have provided more complex and comprehensive descriptions of the several physical interactions between the plume and the ambient air (e.g., Golay, 1982).

5.1 SEMIEMPIRICAL Δh FORMULATIONS

A review of the available semiempirical formulations for computing Δh (and its variation with the downwind distance from the source) is presented by Strom (see Stern, 1976) and Hanna et al. (1982). Many equations for Δh have the following form

$$\Delta h(x) = const\ Q_h^a\ x^b\ u^c \qquad (5\text{-}1)$$

where a, b, c are constants, x is the downwind distance, and u is the wind speed at z_s, the source height. Q_h is the heat emission rate of the source and is given by

$$Q_h = Q_m\ c_p\ (T_s - T_a) \qquad (5\text{-}2)$$

where c_p is the specific heat at constant pressure, T_s is the gas exit temperature, T_a is the ambient temperature at z_s, and Q_m is the total mass emission rate given by

$$Q_m = \varrho_s \pi r_s^2 v_s \tag{5-3}$$

where ϱ_s is the density of the total emission, r_s is the exit radius (or the equivalent radius $r_s = \sqrt{A/\pi}$, for a noncircular exit with area A), and v_s is the vertical exit speed.

Among the various schemes, the Briggs (1969) method is one of the most widely known. That method defines the buoyancy flux parameter F_b by

$$F_b = g v_s r_s^2 (T_s - T_a)/T_s \tag{5-4}$$

and the critical downwind distance x^* by

$$x^* = 2.16 F_b^{2/5} z_s^{3/5} \tag{5-5}$$

for $z_s < 305$ m, and

$$x^* = 67 F_b^{2/5} \tag{5-6}$$

for $z_s \geq 305$ m, where z_s is the source height. The critical distance x^* separates the two stages of the plume rise, as discussed below.

For $x \leq x^*$, the plume rise behaves, for all atmospheric stabilities, according to the "2/3 law," i.e., following the formula

$$\Delta h(x) = const\ F_b^{1/3} u^{-1} x^{2/3} \tag{5-7}$$

with *const* between 1.6 and 1.8, with a suggested value of 1.6 (Briggs, 1972). For $x > x^*$, where ambient atmospheric turbulence plays a dominant role, the plume rise formula becomes, for all atmospheric stabilities,

$$\Delta h(x) = 1.6 F_b^{1/3} u^{-1} x^{*2/3} \left[\frac{2}{5} + \frac{16 x}{25 x^*} + \frac{11}{5}\left(\frac{x}{x^*}\right)^2\right]\left(1 + \frac{4 x}{5 x^*}\right)^{-2} \tag{5-8}$$

Subsequently, Briggs (1975) improved the equations for final rise due to turbulence by parameterizing atmospheric turbulence and using appropriate

physical quantities (u_*, w_*, heat flux, and height above the ground). He provided separate formulae for mechanically and convectively induced turbulence. This new formulation was used by Turner (1985) as discussed below.

Other formulations have been proposed by Holland (1953), Brummage (1966), Bringfelt (1969), Fay et al. (1970), Carpenter et al. (1971), and many others.

The above equations are used for buoyant plumes; i.e., when $T_s > T_a$. Jets (i.e., nonbuoyant plumes with $T_s \simeq T_a$) can also be treated by similar equations. For example, according to Briggs (1969), the plume rise of a jet is

$$\Delta h(x) = 2.3\, F_m^{1/3}\, u^{-2/3}\, x^{1/3} \tag{5-9}$$

where the momentum flux parameter F_m is

$$F_m = v_s^2\, r_s^2\, \varrho_s/\varrho \simeq v_s^2\, r_s^2 \tag{5-10}$$

where the last equality in Equation 5–10 is valid for emissions with mass density ϱ_s similar to the air density ϱ. The final rise of a jet in stable conditions is given (Briggs, 1975) by

$$\Delta h = 2.6\, (F_b/u\, s)^{1/3} \tag{5-11}$$

where s is the stability parameter defined below.

In calm conditions (i.e., u less than 1 m s^{-1}), the above formulae cannot be used. In these situations, Briggs (1975) suggests the following equations for the final plume rise in stable conditions:

$$\Delta h = 5.0\, F^{1/4}\, s^{-3/8} \tag{5-12}$$

for buoyant plumes, and

$$\Delta h = 4.0\, F_m^{1/4}\, s^{-1/4} \tag{5-13}$$

for jets, where s is the stability parameter

$$s = \frac{g}{\theta}\frac{\partial\theta}{\partial z} \tag{5-14}$$

and θ is the potential temperature.

Briggs's formulae have been incorporated into most of the U.S. EPA models described in Section 14.1. These formulae represent a reasonable compromise between accuracy and simplicity, even though, according to many (e.g., Henderson–Sellers and Allen, 1985), they may tend to overestimate the plume rise at large distances downwind.

Turner (1985) used the Briggs (1975) formulae and proposed a generalized routine that calculates both plume rise and partial penetration of the plume into the layer above the mixing height. This routine assumes that meteorological data (temperature and wind speed) are available by layers and that the mixing height h and the potential temperature gradient $\partial\theta/\partial z$ above the mixing height are known. The method is based on the following computational steps.

1. Calculation of f, the stack tip downwash correction factor, with the method of Bjorklund and Bowers (1982). The parameter f is computed by first evaluating the Froude number F_r

$$F_r = \frac{v_s^2}{2\,g\,r_s\,(T_b - T_a)/T_a} \tag{5-15}$$

Then, if $F_r < 3$, $f = 1$; otherwise ($F_r \geq 3$) we have the following cases:

- if $v_s \leq u$

$$\Delta h = 0 \tag{5-16}$$

and no further plume rise calculations are required

- if $v_s > 1.5\,u$

$$f = 1 \tag{5-17a}$$

- if $u < v_s \leq 1.5\,u$

$$f = 3(v_s - u)/v_s \tag{5-17b}$$

2. Calculation of the final plume rise Δh by layers. If the plume rise exceeds the top of a layer, computations are repeated for the next layer above

using the residual plume buoyancy. Computations are made using formulae similar to those by Briggs described above.

3. Calculation of the actual final plume rise $\Delta h'$

$$\Delta h' = f \Delta h \tag{5-18}$$

to incorporate stack tip downwash effects when $f < 1$.

4. Incorporation of plume penetration of the mixing height by decreasing the emission rate Q and further adjusting the plume rise. More specifically, the bottom b_p and the top t_p of the plume are computed by

$$b_p = z_s + 0.5\ \Delta h' \tag{5-19}$$

and

$$t_p = z_s + 1.5\ \Delta h' \tag{5-20}$$

If the bottom of the plume is higher than the mixing height (i.e., $b_p \geq h$), Q is set equal to 0, since the plume is assumed to make no contribution inside the mixing layer and to remain trapped in the stable layer above it. Otherwise, if $b_p < h$ and $t_p > h$, only a fraction of the plume has remained inside the mixing layer. In this case, the plume rise is further corrected as

$$\Delta h'' = \frac{h - b_p}{2} - z_s \tag{5-21}$$

and the emission rate Q is substituted with an effective rate of $f'Q$, where

$$f' = \frac{h - b_p}{\Delta h'} \tag{5-22}$$

in order to exclude the fraction $(1 - f')$ of the plume which has perforated the mixing height h.

This plume rise/partial penetration technique provides a computationally simple solution for engineering calculations. However, the problem of correctly modeling partial penetration is still wide open. Turner's plume rise routine described above has been incorporated into the AVACTA II package (Zannetti et al., 1986) as a user option and into the Urban Airshed Model described in Section 14.1.1.

5.2 ADVANCED PLUME RISE MODELS

The semiempirical formulations presented in the previous section have shown, on several occasions, a great degree of uncertainty. Additional methods have been proposed that provide, at least in theory, a better physical representation of the two basic phenomena (see Figure 5–1) related to the plume rise:

1. The vertical increase of the plume centerline.
2. The entrainment of ambient air into the plume and its consequent horizontal and vertical spreading.

Briggs (1975) tabulated the characteristics of 22 "basic" plume rise models and many more have been developed since then. It is hopeless to review them all. Brief considerations of some of them are presented below.

The integral plume rise model of Schatzmann (1979) allows a numerical solution of the equations of the conservation of mass, momentum, concentration and thermal energy. This method seems particularly effective (at least close to the source), since it does not use the common Boussinesq approximation and, therefore, allows the treatment of jet flow with density greatly different from that of ambient air. This model, however, fails to account for the inertia of "effective mass" outside the plume, seems to contain an unrealistic drag term, and shows problems in the mass conservation equation (Briggs, personal communication).

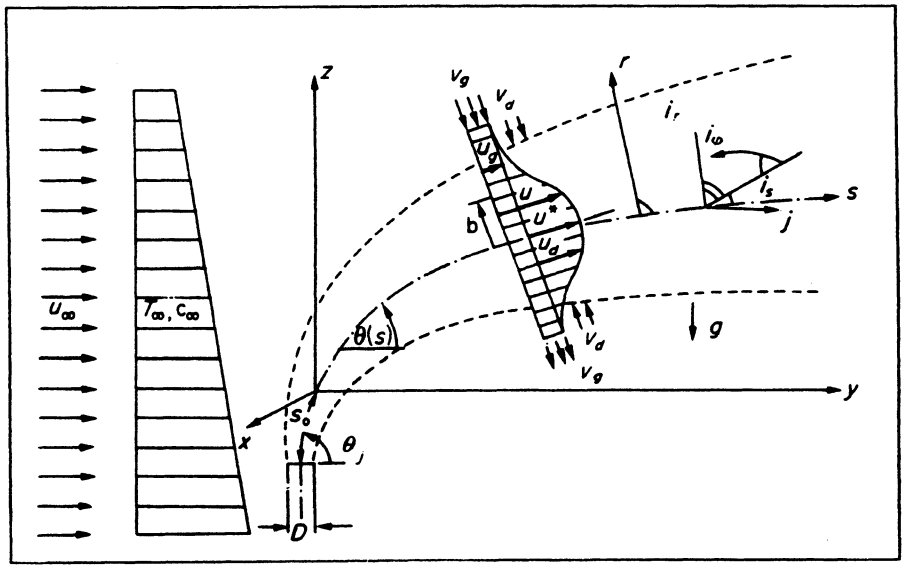

Figure 5–1. Schematic representation of plume rise and entrainment phenomena (from Schatzmann, 1979). [Reprinted with permission from Pergamon Press.]

Golay (1982) has proposed an even more complex approach, a differential entrainment model. It is able to simulate bent-over plumes in complicated vertical atmospheric structures by numerically integrating the conservation equations of mass, momentum, heat, water vapor, liquid water, and the two equations for the turbulent kinetic energy and eddy viscosity in the form presented by Stuhmiller (1974). The major limitation of Golay's approach is the detailed meteorological information that is required; i.e., the vertical profiles of wind speed, virtual potential temperature, relative humidity, turbulence kinetic energy, and turbulent viscosity.

Glendening et al. (1984) have proposed a simpler approach, which numerically integrates the conservation equations, using, however, several simplifying assumptions (the plume is axisymmetric and the three-dimensionality of the plume is ignored).

Henderson-Sellers (1987) has developed a comprehensive model that encompasses both plume rise and pollutant dispersion within a single numerical model formulation. Results are expressed in terms of centerline trajectories, entrainment velocities, rates of spread and ground-level concentrations. The model is also applicable to cases of nonuniform wind and temperature fields as well as to urban terrain. The model has been implemented into an advanced software package (called PRISE) that can run on the IBM PC or compatibles. The code calculates all the phases of the plume (rising, bending over, and [quasi-] equilibrium dispersion) in one continuous formulation.

Probably the most promising technique for the simulation of buoyant plumes in unstable conditions is large eddy simulation (see Section 6.5.2). Nieuwstadt and de Valk (1987) applied such a model to a line source, in which buoyancy was added by increasing the temperature of the source with respect to the ambient temperature. Further work in this direction was performed by van Haren and Nieuwstadt (1989), who obtained reasonable agreement between the output of the large eddy simulation model and the field experiments of Carras and Williams (1984). These large eddy simulation results allow differentiation between the fraction of plume motion caused by convective turbulence and that caused by plume buoyancy. The latter does not seem to obey Briggs' 2/3 law.

Another advanced and computationally-intensive procedure is the Stack Exhaust Model (SEM) developed by Sykes et al. (1989). The SEM model is the most detailed member of a hierarchy of atmospheric models developed for the Electric Power Research Institute (EPRI). This model uses state-of-the-art turbulent simulation techniques in an effort to simulate the initial phase of the plume,

including its buoyant rise and bending-over phase. SEM uses the Reynolds-averaged Navier-Stokes equations, under the assumption of an incompressible, Boussinesq fluid. These equations are solved numerically using second-order finite-difference techniques. The model generally provides steady-state solutions, although it is capable of simulating time-dependent flows.

5.3 SPECIAL CASES

Some special plume rise situations have been investigated and, sometimes, special ad-hoc formulae have been provided. Three cases, in particular, need to be mentioned: the plume rise from multiple sources, the partial perforation of an elevated inversion by a plume, and the plume rise from stacks with scrubbers. These cases are discussed briefly below.

5.3.1 Multiple Sources

Briggs (1975) provided a semiempirical formulation for determining the plume rise from several similar stacks close to each other. Anfossi et al. (1978) and Anfossi (1985) developed and tested a virtual stack concept that allows two or more adjacent sources of different heights and emissions to be merged. In general, interactions among adjacent sources produce an enhancement of their plume rise. Multiple source models are also reviewed by Briggs (1984).

5.3.2 Inversion Partial Penetration

Plume buoyancy is often large enough to allow plumes to perforate, or partially penetrate, an elevated temperature inversion layer (see Figure 5-2). The evaluation of this effect is often critical, especially during daytime conditions when a plume below the inversion is easily diffused toward the ground, while a plume above makes little or no concentration contribution in the PBL. Strom (in Stern, 1976) and Turner (1985) provide simple methods for discriminating between these two cases, as discussed at the end of Section 5.1. Manins (1979) investigates a plume's partial penetration in greater detail suggesting, among other things, that a complete plume penetration is almost impossible since, upon reaching the inversion, there will always be a portion of the plume with insufficient buoyancy for further rise. Similar conclusions have also been shown by semi-quantitative buoyant plume simulations by Lagrangian particle methods (Zannetti and Al-Madani, 1983a and 1983b), which allow a high degree of resolution in the representation of the plume and show a typical behavior, in which

part of the plume is reflected by an elevated inversion, part is trapped inside it and part is able to perforate it, reaching the layer above.

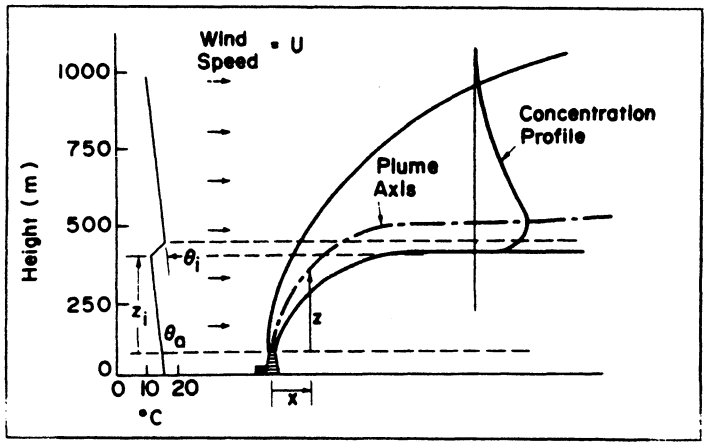

Figure 5–2. Schematic of the interaction of a buoyant plume and an elevated inversion layer (from Manins, 1979). [Reprinted with permission from Permagon Press.]

5.3.3 Stacks with Scrubber

Desulfurization techniques have often been adopted for either the combustibles (e.g., coal cleaning) or the flue gas (scrubbers). The latter technique seems by far the most cost effective for SO_2 emission reduction. Most flue gas desulfurization devices employ a wet scrubbing technique in which a $Ca(OH)_2$ solution is used for partial removal of SO_2.

Plumes from stacks with scrubbers are frequently modeled using the same techniques as the other plumes. Schatzmann and Policastro (1984) reviewed the problem of evaluating Δh for stacks with scrubbers, concluding that "the significant moisture content of the scrubbed plume upon exit leads to important thermodynamic effects during plume rise that are unaccounted for in the usual dry plume rise theories."

Plume rise models for wet plumes (e.g., cooling tower plumes) have been developed by Hanna (1972), Weil (1974) and Wigley and Slawson (1975). Even these formulations, however, are inappropriate for scrubbed plumes, according to Schatzmann and Policastro (1984), because of the simplifications they adopt. Sutherland and Spangler (1980) compared observed plume rise heights for scrubbed and unscrubbed plumes and evaluated the performance of several plume rise formulations. They found that simple plume rise formulae are ques-

tionable even for dry plumes, while moisture effects in scrubbed plumes increase the plume buoyancy and almost compensate for the loss of plume rise due to the temperature decrease induced by the scrubbing system. Plume rise of moist plumes has been reviewed by Briggs (1984).

Schatzmann and Policastro (1984) recommend integral-type models for scrubbed plumes, with the additional requirement of avoiding some common simplifications such as the linearization of the equation of state, first-order approximations in the calculation of the local saturation deficit, and the Boussinesq approximation.

REFERENCES

Anfossi, D., G. Bonino, F. Bossa, and R. Richiardone (1978): Plume rise from multiple sources: A new model. *Atmos. Environ.*, **12**:1821–1826.

Anfossi, D., (1985): Analysis of plume rise data from five TVA steam plants. *J. Climate and Appl. Meteor.*, **24**(11):1225–1236.

Bjorklund, J.R., and J.F. Bowers (1982): User's instruction for the SHORTZ and LONGZ computer programs, Volumes I and II. EPA Document EPA–903/9–82–004A and B, U.S. EPA, Middle Atlantic Region III, Philadelphia, Pennsylvania.

Briggs, G.A. (1969): Plume rise. AEC Crit. Rev. Ser., TID–25075. U.S. At. Energy Comm., Div. Tech. Inform. Ext., Oak Ridge, Tennessee.

Briggs, G.A. (1972): Discussion of chimney plumes in neutral and stable surroundings. *Atmos. Environ.*, **6**:507–510.

Briggs, G.A. (1975): Plume rise predictions. *Lectures on Air Pollution and Environmental Impact Analyses*, Workshop Proceedings, Boston, Massachusetts. September 29 – October 3. pp. 59–111, American Meteorological Society, Boston, Massachusetts.

Briggs, G.A. (1984): Plume rise and buoyancy effects. In *Atmospheric Science and Power Production*, edited by D. Randerson. U.S. Department of Energy Document DOE/ TIC–27601 (DE84005177).

Bringfelt, B. (1969): *Atmos. Environ.*, **3**:609.

Brummage, K.G. (1966): The calculation of atmospheric dispersion from a stack. Stichting CONCAWE, The Hague, The Netherlands.

Calder, K.L. (1949): Eddy diffusion and evaporation in flow over aerodynamically smooth and rough surfaces: A treatment based on laboratory laws of turbulent flow with special reference to conditions in the lower atmosphere. *Q.J. Mech. Math.*, **2**:153.

Carras, J.N., and D.J. Williams (1984): Experimental studies of plume dispersion in convective conditions – 1. *Atmos. Environ.*, **18**:135–144.

Carpenter, S.B., T.L. Montgomery, J.M. Leavitt, W.C. Colbaugh, and F.W. Thomas (1971): *JAPCA*, **21**:491.

Fay, J.A., M. Escudier, and D.P. Hoult (1970): *JAPCA*, **20**:391.

Glendening, J.W., J.A. Businger, and R.J. Farber (1984): Improving plume rise prediction accuracy for stable atmospheres with complex vertical structure. *JAPCA*, **34**:1128–1133.

Golay, M.W. (1982): Numerical modeling of buoyant plumes in a turbulent, stratified atmosphere. *Atmos. Environ.*, **16**:2373–2381.

Hanna, S.R. (1972): Rise and condensation of large cooling tower plumes. *J. Appl. Meteor.*, **11**:793–799.

Hanna, S.R., G.A. Briggs, R.P. Hosker, Jr. (1982): Handbook on atmospheric diffusion. U.S. Department of Energy, Office of Health and Environmental Research Document DOE/ TIC–11223.

Henderson–Sellers, B., and S.E. Allen (1985): Verification of the plume rise/dispersion model USPR: Plume rise for single stack emissions. *Ecological Modelling*, **30**:209–277.

Henderson–Sellers, B., (1987): Modeling of plume rise and dispersion – The University of Salford Model : USPR. *Lecture Notes in Engineering*, edited by C.A. Brebbia and S.A. Orszag. Berlin: Springer–Verlag.

Holland, J.Z. (1953): Meteorology survey of the Oak Ridge area. ORO-99. U.S. At. Energy Comm., Oak Ridge, Tennessee.

Manins, P.C. (1979): Partial penetration of an elevated inversion layer by chimney plumes. *Atmos. Environ.*, **13**:733–741.

Nieuwstadt, F.T., and J.P de Valk (1987): A large-eddy simulation of buoyant and non-buoyant plume dispersion in the atmospheric boundary layer. *Atmos. Environ.*, **21**:2573–2587.

Pasquill, F., and F.B. Smith (1983): *Atmospheric Diffusion, Third Edition*. Chichester, England: Ellis Horwood Ltd.

Schatzmann, M. (1979): An integral model of plume rise. *Atmos. Environ.*, **13**:721–731.

Schatzmann, M., and A.J. Policastro (1984): An advanced integral model for cooling tower plume dispersion. *Atmos. Environ.*, **18**:663–674.

Smith, F.B. (1957): The diffusion of smoke from a continuous elevated point source into a turbulent atmosphere. *J. Fluid Mech.*, **2**:49.

Stern, A.C., Ed. (1976): *Air Pollution*. 3rd Edition, Volume I. New York: Academic Press.

Stuhmiller, J. (1974): Development and validation of a two-variable turbulence model. Science Applications, Inc., Report SAI-74-509-LJ, La Jolla, California.

Sutherland, V.C., and T.C. Spangler (1980): Comparison of calculated and observed plume rise heights for scrubbed and nonscrubbed buoyant plumes. Preprints, Second Joint Conference on Applications of Air Pollution Meteorology, New Orleans, American Meteorological Society, pp. 129–132.

Sykes, R.I., W.S. Lewellen, S.F. Parker, and D.S. Henn (1989): A hierarchy of dynamic plume models incorporating uncertainty. Vol. 2: Stack exhaust model (SEM). A.R.A.P. Division of California Research & Technology, Inc., Final Report EA-6095, Vol. 2, Princeton, New Jersey.

Turner, D.B. (1985): Proposed pragmatic methods for estimating plume rise and plume penetration through atmospheric layers. *Atmos. Environ.*, **19**:1215–1218.

van Haren, L., and F.T. Nieuwstadt (1989): The behavior of passive and buoyant plumes in a convective boundary layer, as simulated with a large-eddy model. *J. Appl. Meteor.*, **28**:818.

Weil, J.C. (1974): The rise of moist, buoyant plumes. *J. Appl. Meteor.*, **13**:435–443.

Wigley, T.M., and P.R. Slawson (1975): The effect of atmospheric conditions on the length of visible cooling tower plumes. *Atmos. Environ.*, **9**:437–445.

Zannetti, P., G. Carboni, R. Lewis, and L. Matamala (1986): AVACTA II – User's Guide. AeroVironment Inc. Document AV-R-86/530.

Zannetti, P., and N. Al-Madani (1983a): Numerical simulations of Lagrangian particle diffusion by Monte-Carlo techniques. VIth World Congress on Air Quality (IUAPPA), Paris, France, May 1983.

Zannetti, P., and N. Al-Madani (1983b): Simulation of transformation, buoyancy and removal processes by Lagrangian particle methods. Fourteenth ITM Meeting on Air Pollution Modeling and Its Application. Copenhagen, Denmark, September 1983.

6 EULERIAN DISPERSION MODELS

Air pollution diffusion can be numerically simulated by several techniques, which are mainly divided into two categories:

1. Eulerian models
2. Lagrangian models

Each of these has advantages and disadvantages in the treatment of atmospheric phenomena. Several authors, and in particular Lamb (from Longhetto, 1980), have investigated the two approaches and their interrelationships in detail, as outlined in Figure 6–1.

The basic difference between the Eulerian and Lagrangian view is illustrated in Figure 6–2, in which the Eulerian reference system is fixed (e.g., with respect to the earth) while the Lagrangian reference system follows the average atmospheric motion.

This section presents the fundamentals of the Eulerian approach and the major Eulerian modeling techniques for atmospheric diffusion. Lagrangian methods are discussed in Chapter 8, while Gaussian dispersion models, which can be seen as both Eulerian and Lagrangian, are presented in Chapter 7. A discussion of the methodologies that have been used to evaluate dispersion models against measurements is presented in Section 12.5.

6.1 THE EULERIAN APPROACH

The Eulerian approach is based (Lamb, from Longhetto, 1980) on the conservation of mass of a single pollutant species of concentration $c(x,y,z,t)$.

$$\frac{\partial c}{\partial t} = -\mathbf{V} \cdot \nabla c + D \nabla^2 c + S \qquad (6\text{–}1)$$

which is similar to Equation 4–7 for the conservation of water, but has the additional (often negligible) molecular diffusion term $D \nabla^2 c$, where D is the molecular diffusivity (about $1.5 \cdot 10^{-5}$ m^2 s^{-1} for air), $\nabla^2 = \partial^2/\partial x^2 + \partial^2/\partial y^2 + \partial^2/\partial z^2$ is the Laplacian operator, and ∇ is the gradient operator.

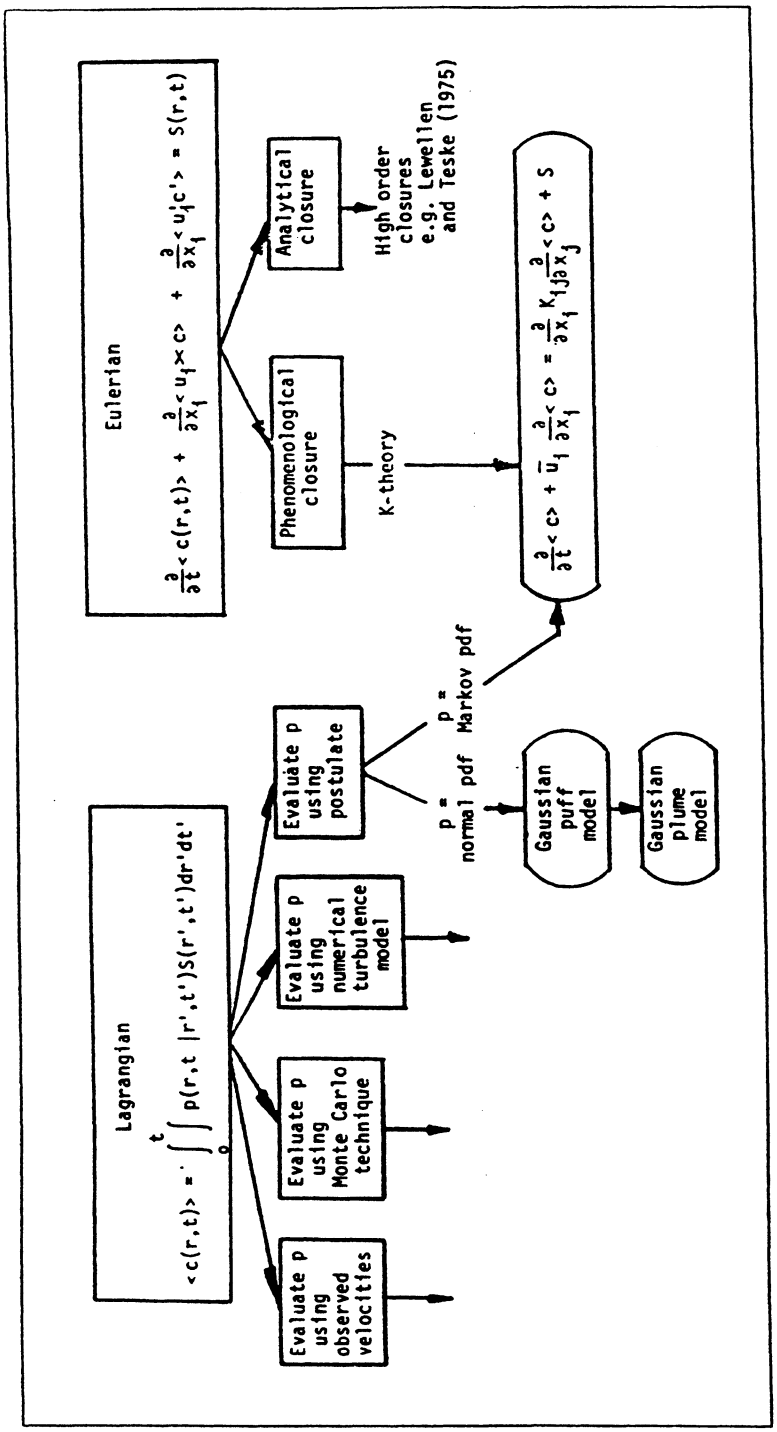

Figure 6–1. Schematic illustration of relationships among the Eulerian and Lagrangian models of turbulent diffusion (from Lamb, in Longhetto, 1980). [Reprinted with permission from Elsevier.]

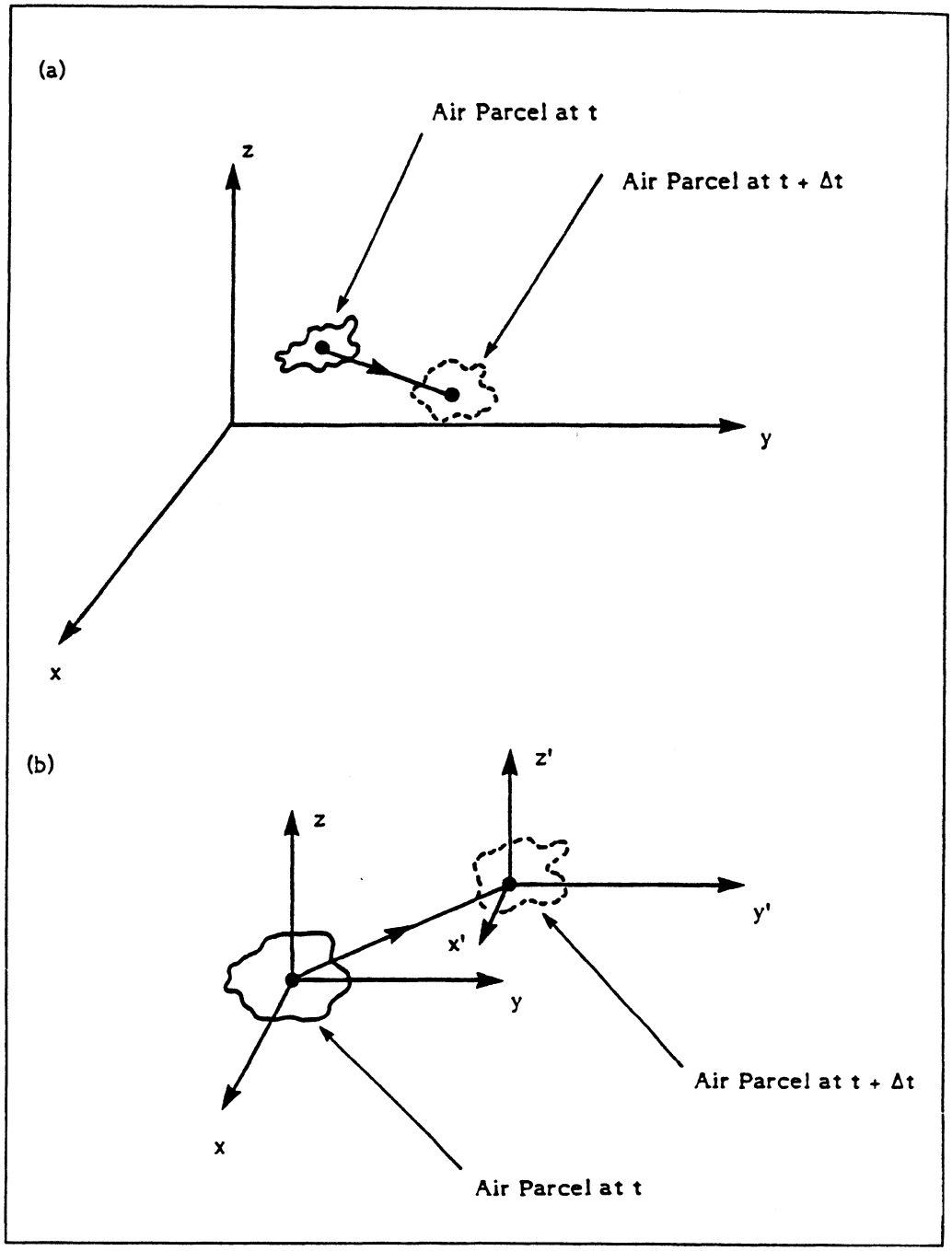

FIGURE 6–2. Eulerian (a) and Lagrangian (b) reference systems for the atmospheric motion.

We assume that the velocity **V** can be represented as the sum of "average" and "fluctuating" components, i.e.

$$\mathbf{V} = \bar{\mathbf{u}} + \mathbf{u}' \tag{6-2}$$

where $\bar{\mathbf{u}}$ represents the portion of the flow that is resolvable using measurements or meteorological models, and $\mathbf{u}'$ is the remaining unresolvable component. We also assume

$$c = \langle c \rangle + c' \tag{6-3}$$

where $\langle\ \rangle$ denotes the ensemble (theoretical) mean, whose meaning is clarified below. Then, substituting Equations 6-2 and 6-3 in 6-1 and taking the ensemble average, we obtain

$$\frac{\partial \langle c \rangle}{\partial t} = - \bar{\mathbf{u}} \cdot \nabla \langle c \rangle - \nabla \cdot \langle c' \mathbf{u}' \rangle + D \nabla^2 \langle c \rangle + \langle S \rangle \tag{6-4}$$

in which, according to the ergodic hypothesis, it is assumed that $\langle \bar{\mathbf{u}} \rangle = \bar{\mathbf{u}}$ and $\langle \mathbf{u}' \rangle = \mathbf{0}$.

Meteorological models have a large unresolved portion $\mathbf{u}'$, which is often of the same order of magnitude as $\bar{\mathbf{u}}$. Therefore, the term $\langle c'\mathbf{u}' \rangle$ is very large and contains most of the turbulent atmospheric diffusion eddies, whose dispersion effects are orders of magnitude larger than the molecular ones. Even with a perfect meteorological model providing detailed information about $\bar{\mathbf{u}}(x,y,z,t)$ (i.e., $\bar{\mathbf{u}} \simeq \mathbf{V}$), the spatial and temporal scales of the smaller turbulent eddies are so small that a correct numerical integration of Equation 6-4 would be practically impossible (it would probably require a grid size of about 1 mm in the entire computational domain; Wyngaard, from Nieuwstadt and van Dop, 1982).

The understanding of $\mathbf{u}'$ as an unresolvable component that can be minimized but never eliminated is the key to understanding the significance of ensemble averaging. Lamb (from Longhetto, 1980) clarifies this point by noting that $\mathbf{u}'$ is a stochastic variable; i.e., there exists an infinite family of functions $\mathbf{u}'$ that satisfy the equation of motion. The situation is described in Figure 6-3, where each possible member $\mathbf{u}'$ of the family generates a different concentration c. The average, at a certain point and time, of all possible concentrations generated by the different $\mathbf{u}'$ gives the "theoretical" ensemble mean $\langle c \rangle$. Naturally, if we could measure $\mathbf{u}'$ and c continuously and everywhere, we could evaluate the exact member of the family that has occurred in reality. Lacking this information, we

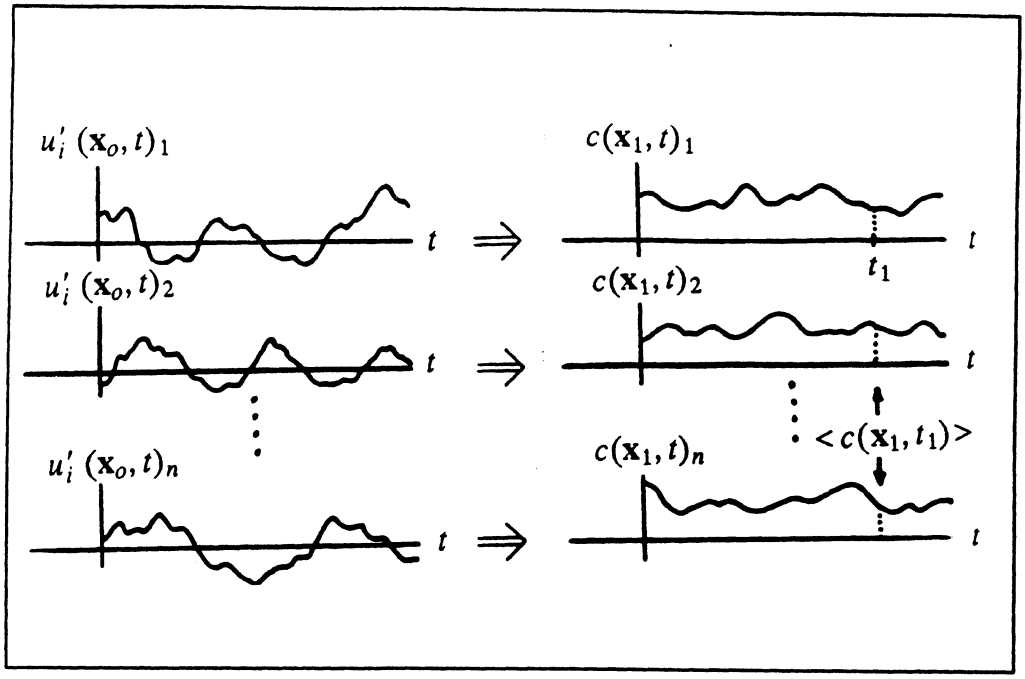

Figure 6–3. The infinite family or ensemble of velocity functions u_i' and the corresponding family of concentration distributions, each portrayed at fixed points $\mathbf{x}_o$ and $\mathbf{x}_1$ as functions of time. The subscript n, n=1,2... , denotes the member or realization of the ensemble. The ensemble mean value <c> at a given time t_1 is formed by averaging $c(\mathbf{x}, t_1)_n$ over the infinite ensemble, as indicated by the vertical dashed line (adapted from Lamb; in Longhetto, 1980).

must assume that all theoretically acceptable $\mathbf{u}'$ are equally possible, thus allowing, in the best possible conditions, the computation of <c> instead of the actual c.

An important conclusion is that the output <c> provided by all Eulerian models is conceptually different from the air quality data gathered from monitoring activities. In fact, monitoring data provide estimates of the actual concentration c (with a certain degree of error associated with the monitoring technique), while model outputs are estimates of <c> (with a certain degree of error because of the input data and the numerical and/or analytical approximations). Therefore, even during ideal conditions (i.e., with no monitoring and modeling errors) model outputs will still differ from concentration measurements. This is often called the intrinsic (unremovable) uncertainty in dispersion modeling.

Another important point can be derived from the analysis of the term $\nabla \cdot \langle c'\mathbf{u}' \rangle$ in Equation 6-4. This term introduces three new unknowns. Therefore, the solution of Equation 6-4 requires a relation between the meteorological input terms or the average terms <c> and these three additional unknowns. The simplest approximation (phenomenological closure) is given by the so-called *K*-theory or gradient-transport theory, in which

$$\langle c' \mathbf{u}' \rangle = -\mathbf{K} \nabla \langle c \rangle \tag{6-5}$$

where **K** is a (3 x 3) turbulent diffusivity tensor whose elements can be estimated from the output of a meteorological model or inferred from meteorological measurements.

Lamb (1973) evaluated the conditions of validity of Equation 6-5. He concluded that *K*-theory is applicable only when $\tau_e/T_c \ll 1$, where τ_e is the maximum time over which an average atmospheric turbulent eddy maintains its integrity and T_c is the time scale of the $\langle c \rangle$ field, i.e., $\partial \langle c \rangle / \partial t \simeq \langle c \rangle / T_c$. Therefore, the *K*-theory is applicable when the changes in the mean concentration field $\langle c \rangle$ have a larger scale than that of turbulent transport, a condition that is commonly violated near strong isolated sources (where T_c is short), especially with large wind direction horizontal meandering or unstable conditions (i.e., large τ_e).

The assumption of Equation 6-5 has, then, a limited applicability and has shown major limitations, especially for the treatment of point sources in unstable conditions. More complex formulations (higher order closure schemes) have been proposed for evaluation $\langle c'\mathbf{u}' \rangle$ and are discussed in Section 6.5.1.

Equation 6-4, with the assumption of Equation 6-5, is generally further simplified by assuming that (1) the tensor **K** is diagonal; (2) the molecular diffusion is negligible; and (3) c represents the concentration of a nonreactive pollutant (i.e., $\langle S \rangle = S$, as discussed below). With these simplifications, Equation 6-4 becomes the "semiempirical equation of atmospheric diffusion,"

$$\frac{\partial \langle c \rangle}{\partial t} = -\bar{\mathbf{u}} \cdot \nabla \langle c \rangle + \nabla \cdot \mathbf{K} \nabla \langle c \rangle + S \tag{6-6}$$

where the elements of **K** are zero, except along its main diagonal (K_{11}, K_{22}, K_{33}). Equation 6-6 can be integrated (analytically or numerically) if the inputs $\bar{\mathbf{u}}$, **K** and S are provided, together with initial and boundary conditions for $\langle c \rangle$.

In the case of a single source in stationary (i.e., $\partial < c > / \partial t = 0$) emission and meteorological conditions, the source term is commonly treated as an upwind boundary condition. For an average wind speed $\bar{u}$(x,y,z) blowing toward the positive x-axis, the following boundary condition applies in the upwind boundary plane (y,z):

$$< c > = \frac{Q}{\bar{u}(0, y_s, z_s + \Delta h)} \delta(z - z_s - \Delta h)\, \delta(y - y_s) \tag{6-7}$$

where Q is the pollutant emission rate, z_s is the physical height of the source located in $(0,y_s)$, Δh is the plume rise, and δ is the Kronecker operator. Using this boundary condition and assuming a steady state, Equation 6–6 becomes simply

$$\bar{\mathbf{u}} \cdot \nabla < c > = \nabla \cdot \mathbf{K} \nabla < c > \tag{6-8}$$

The integration of either Equation 6–6 or Equation 6–8 requires a full specification of boundary conditions. Total reflection conditions are generally assumed at the ground and at the top of the computational domain (which is generally the top of the PBL); i.e.,

$$K_{33} \frac{\partial < c >}{\partial z} = 0 \tag{6-9}$$

which indicates a pollutant flux equal to zero. In order to consider dry deposition phenomena at the ground surface, the following condition is often assumed instead of Equation 6–9 at z = 0 (i.e., at ground level)

$$K_{33} \frac{\partial < c >}{\partial z} = V_d < c > \tag{6-10}$$

which indicates a nonzero pollutant flux, where V_d is the deposition velocity, which is a function of meteorological conditions (e.g., atmospheric stability), pollutant type and surface type. Measured deposition velocities for SO_2 are presented in Figure 6–4, while deposition velocity ranges for several gases are listed in Table 6–1.

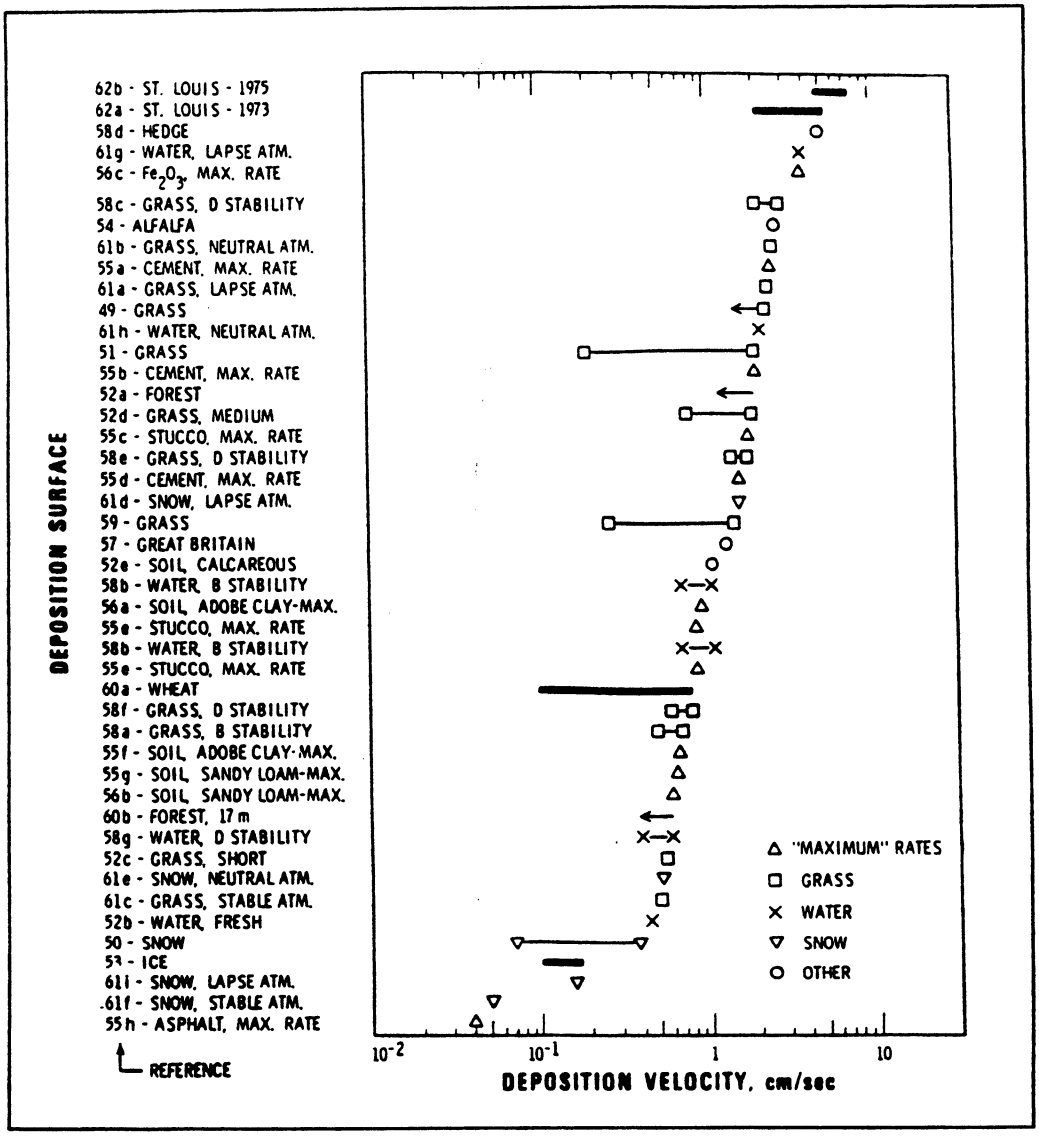

Figure 6–4. *SO_2 deposition velocity summary for different surfaces. From Sehmel (1980); see that paper for references mentioned in the figure. [Reprinted with permission from Academic Press.]*

Table 6–1. Deposition velocity range for gases. From Schmel (1980); see this paper for the references mentioned in the table. [Reprinted with permission from Academic Press.]

Number of references	Depositing gas	Deposition velocity range, cm s^{-1}
14	SO_2	0.04–7.5
20	I_2	0.02–26
2	HF	1.6–3.7
1	ThB	0.08–2.6
1	Fluorides	0.3–2.4
1	Cl_2	1.8–2.1
7	O_3	0.002–2.0
1	NO_2	1.9
2	NO	Minus–0.9
1	PAN	0.8
3	NO_x	Minus–0.5
1	H_2S	0.015–0.38
1	CO_2	0.3
1	$(CH_3)_2S$	0.064–0.28
5	CH_3I	$10^{-4} - 10^{-2}$
1	Kr	2.3×10^{-11} max

On the sides (x,z) and (y,z) of the computational domain, it is generally assumed

$$<c> = 0 \tag{6–11}$$

or

$$<c> = \textit{background value} \tag{6–12}$$

or (Shir and Shieh, 1974)

$$\nabla_h^2 <c> = 0 \tag{6–13}$$

where ∇_h is the horizontal Laplacian operator $\nabla_h^2 = \partial^2/\partial x^2 + \partial^2/\partial y^2$. The latter condition, Equation 6–13, represents a linear extrapolation of the concentration field outside the boundary.

Initial conditions are also required for the interpretation of Equation 6–6, which is time–dependent, and are generally specified by Equations 6–11 or 6–12 throughout the entire computational domain or, in special cases (e.g., Runca, 1977), by a pseudoanalytical plume equation that provides the initial concentration field $<c>$ near the point source(s) and eliminates the difficulties related to the numerical approximation of the S function (i.e., the source term).

If chemical reactions are involved, the assumption $<S> = S$ is no longer valid, and the term $<S>$ must be investigated further. We can say that (using c_m instead of c for the concentrations of all species; where $m = 1, 2, \ldots M$) the source term is

$$S_{c_m} = E_{c_m} + R_{c_m} + P_{c_m} \qquad (6\text{–}14)$$

where $S_{c_m}(x,y,z,t)$ is the total rate of addition (or removal) of the m-th species; $E_{c_m}(x,y,z,t)$ is the direct emission of the m–th species (primary emission); $R_{c_m}(x,y,z,t)$ is the creation/removal term of the m–th species by chemical reactions and is a function of the meteorology (especially ambient temperature and solar radiation) and, in general, of the concentration of all pollutants c_1, $c_2, \ldots c_M$, in (x,y,z) at time t; and $P_{c_m}(x,y,z,t)$ is the removal term for c_m due to precipitation, and is a function of meteorological variables (such as precipitation rate) and the type m of species. Equation 6–14 does not include dry deposition, which is treated as a boundary condition by Equation 6–10.

The ensemble average $<S_{c_m}>$ is a function of $<R_{c_m}>$, which, in general, is a nonlinear function of $c_1, c_2, \ldots c_m$. Thus, the averaging process $<R_{c_m}>$ creates new additional variables of the type $<c_i' c_j'>$, with $i, j = 1, 2, \ldots M$. The most common approximation for avoiding the generation of these new variables is

$$< R_{c_m}(c_1, c_2, \ldots c_M) > \simeq R_{c_m}(<c_1>, <c_2>, \ldots <c_M>) \qquad (6\text{–}15)$$

Again, however, Lamb (1973) showed that the above approximation may be a crude one. His analysis of a simple second-order decay reaction

$$R_{cm} = -\beta\, c_m^2 = -\beta\,(<c_m> + c'_m)^2 \tag{6-16}$$

shows that the approximation of Equation 6-15, i.e.,

$$<R_{cm}> \simeq -\beta <c_m>^2 \tag{6-17}$$

is valid only when

$$\beta <c_{\max}>\ \tau_e << 1 \tag{6-18}$$

Equation 6-18 requires the decay process to be slow (i.e., a small β) compared with turbulent transport time scale. Many photochemical reactions, however, are quite fast and, therefore, do not allow this approximation.

Equations 6-6 or 6-8 can be solved in two ways:

1. by analytical methods, providing exact solutions
2. by numerical methods, providing approximate solutions

These two approaches are discussed below.

6.2 ANALYTICAL SOLUTIONS

Analytical solutions are available for the steady state Equation 6-8 under special, simplifying assumptions. The available formulations have been discussed by Pasquill and Smith (1983), Seinfeld (1986), and Tirabassi et al. (1986). In particular, Roberts (see Calder, 1949) obtained a two-dimensional solution for ground-level sources; Smith (1957) found a solution for elevated sources with $\bar{u}$ and K_z profiles following Schmidt's conjugate law; Rounds (1955) proposed a more general solution, which, however, turned out to be valid only for linear profiles of K_z; finally, Yeh and Huang (1975) and Demuth (1978) obtained a more general analytical solution, which is presented below. This latter solution has been incorporated into an organized computer package, KAPPA-G (Tirabassi et al., 1986), which allows the performance of three-dimensional steady-state simulations using the Gaussian formula for the treatment of horizontal diffusion (as proposed by Huang, 1979).

Remembering that in Equation 6–8 the wind $\bar{u}$ is assumed to blow towards the positive x–axis, we can use the notation

$$K_{11} = K_x \tag{6–20}$$

$$K_{22} = K_y \tag{6–21}$$

$$K_{33} = K_z \tag{6–22}$$

Therefore, Equation 6–8 can be written

$$\bar{u}\frac{\partial}{\partial x}c = \frac{\partial}{\partial z}\left(K_z\frac{\partial}{\partial z}c\right) + \frac{\partial}{\partial y}\left(K_y\frac{\partial}{\partial y}c\right) \tag{6–23}$$

with boundary conditions

$$c = \frac{Q}{\bar{u}(h_e)}\,\delta(z - h_e)\,\delta(y) \qquad \text{at } x = 0 \tag{6–24}$$

and

$$K_z\frac{\partial c}{\partial z} = 0 \qquad \text{at } z = 0,\ h \tag{6–25}$$

where h_e is the final effective height of the emission (i.e., $h_e = z_s + \Delta h$), h is the depth of the mixing layer, $y_s = 0$, and

$$\left|\bar{u}\frac{\partial}{\partial x}c\right| \gg \left|\frac{\partial}{\partial x}\left(K_x\frac{\partial}{\partial x}c\right)\right| \tag{6–26}$$

Equation 6–26 assumes that atmospheric dispersion along the x–axis is negligible in comparison to the transport term.

To integrate Equation 6–23 we define the crosswind integrated concentration

$$\bar{c}(x, z) = \int_{-\infty}^{+\infty} c(x, y, z)dy \tag{6–27}$$

We also make the following assumptions

$$\bar{u}(z) = u_0(z/h_0)^a \tag{6-28}$$

$$K_y(x, z) = \bar{u}(z)\, f(x) \quad (*) \tag{6-29}$$

$$K_z(z) = K_{z0}(z/h_0)^\beta \tag{6-30}$$

and

$$h = +\infty \tag{6-31}$$

where h_0 is the height at which u_0 and K_{z0} are measured (or evaluated) and $f(x)$ is any function of x. Then the solution of Equation 6-23 for ground level concentration ($z = 0$) is (Yeh and Huang, 1975)

$$\bar{c}(x, 0) = \frac{Q}{\lambda^\eta} \frac{1}{\Gamma(\gamma)} \frac{h^{\eta_0}}{u_0^\nu (x\, K_{z0})^\gamma} \exp\left[-\frac{u_0\, h_0^r\, h_e^\lambda}{\lambda^2\, K_{z0}\, x}\right] \tag{6-32}$$

where

$$\lambda = a - \beta + 2 \tag{6-33}$$

$$\nu = (1 - \beta)/\lambda \tag{6-34}$$

$$\gamma = (a + 1)/\lambda \tag{6-35}$$

$$\eta = (a + \beta)/\lambda \tag{6-36}$$

$$r = \beta - a \tag{6-37}$$

and Γ denotes the Gamma function.

With a finite mixing height (i.e., $h < +\infty$) and $h_e < h$ (and with the other assumptions unchanged), the solution of Equation 6-23 is (Demuth, 1978)

$$\bar{c}(x, 0) = \frac{2\, Q\, q\, h_0^a}{h^{a+1}\, u_0} \left\{ \gamma + R^p \sum_{i=1}^{\infty} \left[\frac{J_{\gamma-1}\,(\sigma_{\gamma(i)}\, R^q)\, \sigma_{\gamma(i)}^{\gamma-1}}{\Gamma(\gamma)\, J_{\gamma-1}^2\,(\sigma_{\gamma(i)})\, 2^{\gamma-1}} \right.\right. \cdot \left.\left. \exp\left(-\frac{\sigma_{\gamma(i)}^2\, q^2\, K_{z0}\, x}{h^\lambda\, h_0^r\, u_0}\right)\right]\right\} \tag{6-38}$$

(*) This particular assumption, however, will be used only for deriving Equation 6-44, below.

where

$$R = h_e/h \tag{6-39}$$

$$p = (1 - \beta)/2 \tag{6-40}$$

$$q = \lambda/2 \tag{6-41}$$

In Equation 6-38, J_γ (...) represents the Bessel function of the first kind and order γ, and $\sigma_{\gamma(i)}$ (i=1,2,...) are its roots, i.e., $J_\gamma(\sigma_{\gamma(i)}) = 0$.

The solutions given by Equations 6-32 and 6-38 represent the case when $z = 0$, i.e., the concentration is computed at ground level. If elevated integrated concentrations $\bar{c}(x,z)$ need to be evaluated, the new solution, for $h = +\infty$, is easily obtained from Huang (1979), giving

$$\bar{c}(x,z) = \frac{Q\,(z h_e)^p\, h_0^\beta}{\lambda\, K_{z0}\, x}\, exp\left(-\frac{u_0\, h_0^r\, (z^\lambda + h_e^\lambda)}{\lambda^2\, K_{z0}\, x}\right) I_{-\nu}\left(\frac{2\, u_0\, h_0^r\, (z\, h_e)^q}{\lambda^2\, K_{z0}\, x}\right) \tag{6-42}$$

where $I_{-\nu}$ (...) is the modified Bessel function of the first kind and order $-\nu$.

If $h < +\infty$, the integrated concentration $\bar{c}(x,z)$ is again obtained from Demuth (1978), giving

$$\bar{c}(x,z) = \frac{2\, Q\, q\, h_0^a}{h^{a+1}\, u_0}\left\{\lambda + \left(\frac{z\, R}{h}\right)^p \sum_{i=1}^{\infty}\left[\frac{J_{\gamma-1}(\sigma_{\gamma(i)}\, R^q)\, J_{\gamma-1}(\sigma_{\gamma(i)}(z/h)^q)}{J_{\gamma-1}^2(\sigma_{\gamma(i)})}\right.\right. \cdot \left.\left. exp\left(-\frac{\sigma_{\gamma(i)}^2\, q^2\, K_{z0}\, x}{h^\lambda\, h_0^r\, u_0}\right)\right]\right\} \tag{6-43}$$

Tirabassi et al. (1986) verified, analytically or numerically, that as $z \to 0$, the limit of Equations 6-42 and 6-43 gives Equations 6-32 and 6-38, respectively; and that, as h $\to +\infty$, the limit of Equations 6-38 and 6-43 gives Equations 6-32 and 6-42, respectively.

The above formulae deal with the crosswind integrated concentration $\bar{c}(x,z)$. If we want to calculate the three-dimensional concentration $c(x,y,z)$, horizontal diffusion needs to be included in a way that satisfies Equation 6-29. If we

assume that the plume has a Gaussian concentration distribution in the horizontal with lateral standard deviation $\sigma_y(x)$, we obtain

$$c(x,y,z) = \bar{c}(x,z)\,\frac{1}{\sqrt{2\pi}\,\sigma_y}\,exp\left(-\frac{y^2}{2\,\sigma_y^2}\right) \qquad (6\text{–}44)$$

Equation 6–44, together with any function $\bar{c}(x,z)$ previously derived, can be used for three-dimensional simulations, since the Gaussian assumption for horizontal diffusion gives

$$K_y = \frac{\bar{u}}{2}\,\frac{d\sigma_y^2}{dx} \qquad (6\text{–}45)$$

which satisfies the condition of Equation 6–29.

6.3 NUMERICAL SOLUTIONS

Numerical methods allow the computation of approximate solutions of Equations 6–6 and 6–8 using integration techniques such as

- finite difference methods
- finite element methods
- spectral methods
- boundary element methods
- particle methods

The reader should refer to books on numerical analysis for further discussion of the above numerical techniques.

Finite difference methods (Richtmyer and Morton, 1967) are the oldest technique. Although they possess several disadvantages, they still represent the major and most applied (and best understood) numerical tool for this type of applications. However, finite-difference approximation of the advection term $\bar{\mathbf{u}} \cdot \nabla\langle c\rangle$ always produces a diffusion-type error that artificially increases the

diffusion rates in the simulated concentration output. This numerical phenomenon can be easily understood by analyzing the one-dimensional version of the advection term, i.e.,

$$\frac{\partial c}{\partial t} = - \bar{u} \frac{\partial c}{\partial x} \tag{6-46}$$

With a simple first-order finite-difference scheme, we obtain

$$\frac{c_i^{t+1} - c_i^t}{\Delta t} = \bar{u}_i^t \frac{c_{i+1}^t - c_{i-1}^t}{2\,\Delta x} \tag{6-47}$$

where subscripts indicate spatial discretization (with a grid size Δx) and superscripts indicate time discretization (with interval Δt). The analysis of the truncation terms (Johnson et al., in Stern, 1986) shows that the error ϵ generated by the approximation of using Equation 5–47 instead of Equation 5–46 is

$$\epsilon = \frac{\bar{u}\,\Delta x}{2} (1 - \bar{u}\,\Delta t/\Delta x)\,(\partial^2 c/\partial x^2) \tag{6-48}$$

which is a diffusion-type term, with associated diffusity D_n equal to

$$D_n = \frac{\bar{u}\,\Delta x}{2} (1 - \bar{u}\,\Delta t/\Delta x) \tag{6-49}$$

The term D_n is proportional to the grid size Δx and, especially in regional modeling where grid sizes have typical values of 80 km, generates an artificial diffusion that can easily reach values of the same order of magnitude as (or even greater than) actual atmospheric diffusion, which makes model outputs almost meaningless. Several methods have been proposed to reduce this error (Egan and Mahoney, 1972; Runca and Sardei, 1975; Boris and Book, 1973, who proposed the SHASTA method; Pepper et al., 1979, who used cubic splines and chapeau functions; Zalesak, 1979, who extended the concept of flux corrected transport, FCT, to any number of dimensions; Lamb, 1983, who developed the BIQUINTIC method for his regional scale photochemical model; Orszag, 1971, who first introduced the pseudospectral method; etc.). Numerical evaluations of most of these methods by Chock and Dunker (1983) and Schere (1983) show that a "best" approach cannot be identified for all situations, and that some schemes, like SHASTA, which used to be widely used in photochemical simulation packages, produce unacceptably large amounts of artificial diffusion.

In spite of several shortcomings of K-theory and grid discretization, this approach plays a major role in air pollution simulations, especially when non-linear chemistry is required (as for the evaluation of O_3 impacts). One could argue that the errors introduced by this technique pale in comparison to the assumptions introduced by the Gaussian plume model discussed in Chapter 7.

While analytical solutions require special, simplified functional forms for **K** (i.e., power laws of the altitude z), numerical solutions can accommodate for virtually any function $\mathbf{K}(x,y,z,t)$. Several of these functions have been proposed for evaluating K_H, the horizontal eddy diffusivity (which assumes $K_{11} = K_{22} = K_H$ for any wind direction angle with the x-axis), and K_z the vertical eddy diffusivity.

6.3.1 The Vertical Diffusivity K_z

The vertical diffusivity K_z is generally specified as a function of the altitude z. For example, McRae et al. (1982) use

$$K_z = 2.5\, w_* \, z_i \left[k\frac{s}{z_i}\right]^{4/3} \left[1 - 15\left(\frac{z}{L}\right)\right]^{1/4} \qquad (6\text{–}50)$$

in the unstable surface layer (i.e., $0 \leq z/z_i < 0.05$) and

$$K_z = w_* \, z_i \, f(z/z_i) \qquad (6\text{–}51)$$

in the unstable PBL above the surface layer, where

$$f(z/z_i) = 0.021 + 0.408\left(\frac{z}{z_i}\right) + 1.351\left(\frac{z}{z_i}\right)^2 - 4.096\left(\frac{z}{z_i}\right)^3 + 2.560\left(\frac{z}{z_i}\right)^4 \qquad (6\text{–}52)$$

for $0.05 \leq \frac{z}{z_i} \leq 0.6$,

$$f(z/z_i) = 0.2\, exp\left[6 - 10\left(\frac{z}{z_i}\right)\right] \qquad (6\text{–}53)$$

for $0.6 \leq \frac{z}{z_i} \leq 1.1$, and

$$f(z/z_i) = 0.0013 \qquad (6\text{–}54)$$

for $\frac{z}{z_i} > 1.1$.

Therefore, the eddy diffusivity K_z is $\simeq 0$ for $z \simeq 0$ and $z > z_i$, and has a maximum ($\simeq 0.21\, w_* \, z_i$) when $z/z_i \simeq 0.5$, as shown in Figure 6–5.

In neutral conditions, Shir (1973) adopts

$$K_z = k\, u_* \, z \, exp(-8\, z f / u_*) \tag{6-55}$$

where f is the Coriolis parameter defined by Equation 3-3, while Myrup and Ranzieri (1976) propose,

$$K_z = k\, u_* \, z \tag{6-56}$$

in the surface layer (i.e., $z/z_i < 0.1$), and, above the surface layer,

$$K_z = k\, u_* \, z\, (1.1 - z/z_i) \tag{6-57}$$

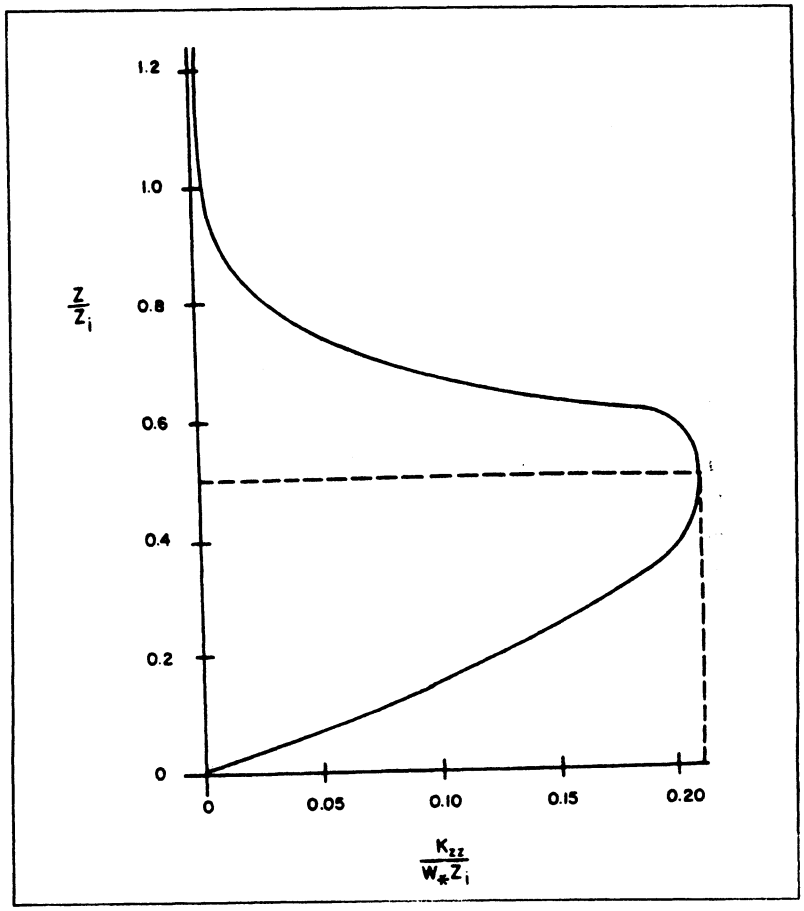

Figure 6-5. Vertical turbulent diffusivity profile under unstable conditions (from McRae et al., 1982). [Reprinted with permission from Academic Press.]

for $0.1 \leq z/z_i \leq 1.1$, and

$$K_z = 0 \tag{6-58}$$

for $z/z_i > 1.1$.

Finally, in stable conditions, Businger and Ayra (1974) propose

$$K_z = \frac{k\, u_* \, z}{0.74 + 4.7(z/L)} \exp\left(-\frac{8 f z}{u_*}\right) \tag{6-59}$$

More discussion about the evaluation of K_z can be found in Seinfeld (1986). It is clear, however, that we do not possess a definite knowledge of K_z above the surface layer and that the application of the K-theory to simulate vertical dispersion during unstable conditions is highly questionable.

6.3.2 The Horizontal Diffusivity K_H

The evaluation of K_H presents several intriguing aspects. It is often (and, perhaps, improperly) assumed that

$$K_H \simeq K_y \tag{6-60}$$

where K_y is the crosswind eddy diffusivity (i.e., with wind blowing along the positive x-axis). If we consider a plume originated at $x = 0$ and carried by the wind along the x-axis, K_y is related, through Equation 6-45, to the standard deviation $\sigma_y(x)$ of the crosswind plume concentration spread. where Equation 6-45 is valid for a travel time t, which is

$$t \gg T_L \tag{6-61}$$

where T_L is the Lagrangian time scale (typically of the order of 100–200 s). The integration of Equation 6-45 gives

$$\sigma_y(x) = \sqrt{2\, K_y\, x/\bar{u}} = \sqrt{2\, K_y\, t} \tag{6-62}$$

which would require σ_y to grow linearly with $x^{0.5}$. But the analysis of data on horizontal dispersion does not confirm Equation 6-63, as illustrated in Figure 6-6. These data show a peculiar property of atmospheric horizontal diffusion, i.e., its accelerating rate. This phenomenon, whose rate can be justified only partially by the theoretical analysis of Taylor (1921), seems to suggest

(Gifford, 1982) that atmospheric diffusion is augmented by the presence of large scale quasihorizontal turbulent wind-field heterogeneities, caused by large-scale surface inhomogeneities of various kinds.

Figure 6-6 clearly shows that the choice of K_y (or K_H) strongly depends upon the travel time t by several orders of magnitude. This creates the paradox that, if we want to estimate K_H in a certain location (x,y,z), for example the center of a grid cell, different values of K_H would be required for the different pollutants coming from different sources, and therefore, having different travel times. An Eulerian grid model cannot really handle this, since, after pollutants are injected into the grid cells, the memory of their different origin is lost. This entire discussion points out a further limitation of K-theory in describing atmospheric diffusion.

Another disturbing aspect of the numerical interpretation of the K-theory equation to simulate horizontal diffusion is that the effective eddy diffusion is the sum of K_H plus the contribution D_n generated by the numerical advection errors (a diffusion term, as explained at the beginning of Section 6.3). In many cases, $D_n > K_H$, which may explain (McRae et al., 1982) why the influence of changes in K_H in the large range 0-500 $m^2 s^{-1}$ is small in the concentration field, as presented by Liu et al. (1976). Due to the numerical error D_n, a K-theory model needs to use nonzero K_H values only during unstable conditions, in which, for example, we can use the formula

$$K_H \simeq 0.1\, w_* \, z_i \simeq 0.1\, z_i^{3/4} \, (-k\, L)^{-1/3} \, u_* \qquad (6\text{-}63)$$

derived from the measurements of Willis and Deardorff (1976).

A final important consideration about K_H derives from the definition of Equation 6-2, in which the wind vector $\mathbf{V}$ is divided into two components, $\overline{\mathbf{u}}$ and $\mathbf{u}'$, where $\overline{\mathbf{u}}$ represents the large portion of the flow that is resolvable using meteorological measurements or models and $\mathbf{u}'$ is the remaining unresolvable component. Clearly, the better the meteorological model or the interpolation of the measurements, the higher the time- and space-resolution of the term $\overline{\mathbf{u}}$ and the smaller the $|\mathbf{u}'|$ values.

This interpretation of Equation 6-2 is very important since that equation is often used to indicate an *intrinsic* property of the atmospheric motion (an average term plus turbulent fluctuation) instead of being interpreted as the sum of a resolvable and unresolvable component. This is a key issue in understanding the turbulent diffusion terms $\langle c'\mathbf{u}' \rangle$ which have been approximated using the

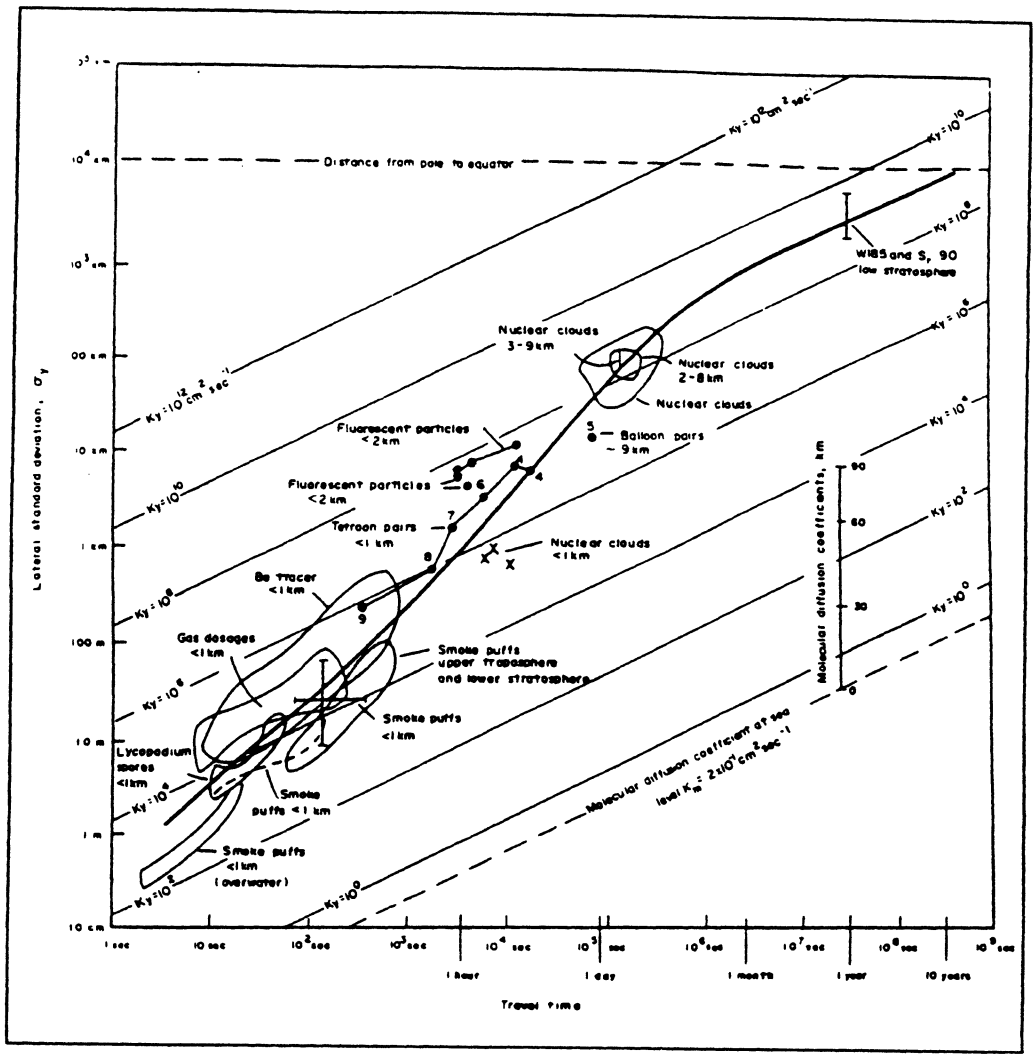

Figure 6–6. Summary of data on horizontal atmospheric diffusion, from Hage and Church (1967), as presented by Gifford (1982). The solid curve illustrates the empirical equation of Hage et al. (1967). [Reprinted with permission from Academic Press.]

K–theory by Equation 6–5, where **K** is a (3 x 3) turbulent diffusivity tensor. From the previous definition of $\mathbf{u}'$, it is clear that the better the meteorological model providing $\bar{\mathbf{u}}$, the lower the $|\langle c'\mathbf{u}'\rangle|$ terms and, consequently, the lower the magnitude of the elements of **K**. In other words, we derive the important (and, to a certain extent, surprising) conclusion that the eddy diffusion coefficients to be used in a diffusion model are a *function of the degree of performance* of the meteorological model used to calculate the meteorological input to the dispersion

model. This is particularly true for horizontal dispersion, since vertical velocity components are generally small in comparison with horizontal transport and, consequently, $\mathbf{u}'$ has a larger horizontal than vertical component.

In order to understand and fully evaluate the consequences of the above considerations, let us discuss a brief example related to long-range transport and horizontal diffusion of a plume from a point source. According to Hanna et al. (1977) and Irwin (1979), for downwind distances x greater than 10 km, the horizontal plume standard deviation σ_y is

$$\sigma_y = 33.3\, \sigma_\theta\, x^{1/2} \tag{6-64}$$

where σ_θ is the standard deviation of the horizontal wind direction expressed in radians. Using Equations 6-62 and 6-64, we obtain

$$K_y = 10^3\, \sigma_\theta^2\, u/2 \simeq K_H \tag{6-65}$$

For typical values of $\sigma_\theta < 0.5$ radians and u < 10 m/s, Equation 6-65 gives K_H values one to two orders of magnitude lower than the bottom of the range of $K_H = 10^4$ to 10^7 m^2 s^{-1} currently used in most long-range models and considered to be the best values to fit actual measurements. This inconsistency can be easily explained using the considerations presented before. In fact, Equations 6-64 and 6-65 implicitly assume that the plume trajectory is known exactly and that σ_y (and K_H) characterize only the plume horizontal growth *and not the uncertainty in plume location*. Actual modeling simulations, however, use or calculate meteorological wind fields, which possess a large degree of uncertainty when used for trajectory computations. Therefore, it is not surprising that actual model calibration tests suggest large values of K_H (10^4 to 10^7 m^2 s^{-1} instead of 10^2 to 10^3 m^2 s^{-1}). This indicates that horizontal diffusion needs to be artificially enhanced for the model to incorporate the uncertainties in the meteorological modeling computation of $\bar{\mathbf{u}}$.

In order to visualize the above considerations, let us consider the simple example in Figure 6-7, in which the contributions of three air pollution sources (S_1, S_2, and S_3) at the receptor R are evaluated through a dispersion model using large K_H values. Even though the model largely overestimates horizontal diffusion, it provides a total concentration value at R (the sum of the three dashed curves) that is quite similar to the measured value (on the solid curve), due to error compensation factors. The model is, in a way, "validated," but its

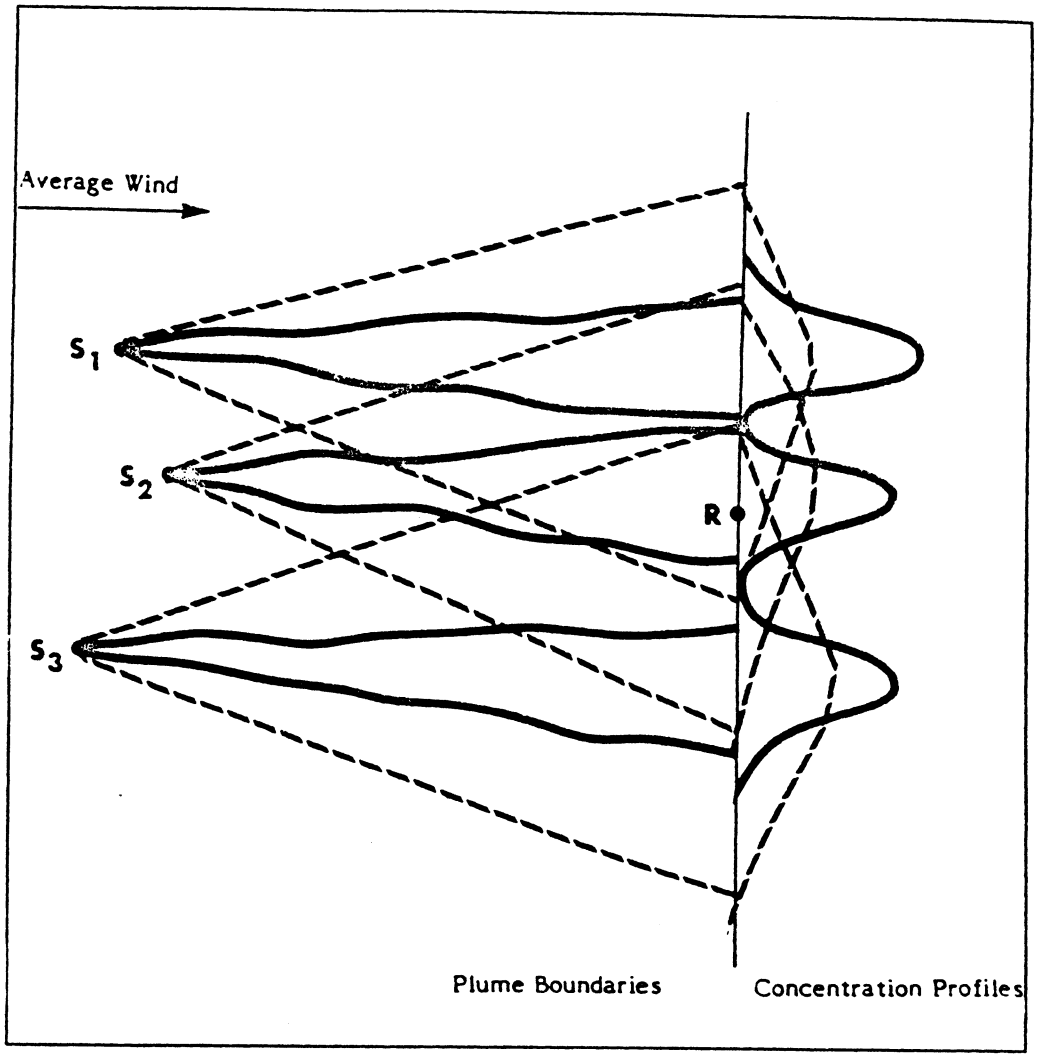

Figure 6–7. An example of the consequence of overestimating horizontal diffusion on the concentration at the receptor R. Solid lines show the actual average plume, while dotted lines show the plume as simulated by the model.

use for evaluating emission reduction strategies will provide incorrect results; specifically, it will suggest useless emission reductions in S_1 and S_3 and insufficient control of S_2.

It is true that regular fluctuations in wind direction cause the solid plumes in Figure 6–7 to sweep around the azimuth in such a way that they all may envelop the receptor R. This variation of the short-term average wind can

sometimes be correctly simulated, for long-term averages, by the dashed plumes, which are computed with an enhanced horizontal diffusion. However, wind direction fluctuations often do not show regular behavior and, therefore, do not support the above approximation. In complex terrain, especially, preferred direction patterns play important roles in determining plume trajectories, and the artificial enhancement of horizontal diffusion for long-term averages may provide incorrect results. Moreover, if nonlinear chemical reactions are used, the formation of secondary pollutants is incorrectly computed when the plume is diffused with artificially high dispersion rates, since the centerline plume concentration is consistently underestimated.

This discussion, which is valid only for the particular location of the receptor R, can, however, be generalized to illuminate a critical problem in most long-range air pollution modeling studies using K-theory grid models. In order to compensate for uncertainties in wind direction information, these models almost always over-estimate horizontal diffusion in a process that smoothes concentration peaks. With "smooth" emission source terms and wind frequency distributions, this assumption is quite acceptable, but, in many cases, this smoothing process creates a loss of deterministic information related to the source-receptor relationship. This loss becomes particularly critical when selective emission reduction strategies are inferred from modeling outputs in order to meet air quality goals at the receptor R.

6.4 BOX MODELS

6.4.1 The Single Box Model

The single box model (Lettau, 1970) is the simplest air pollution model and is based on the mass conservation of pollutant inside an Eulerian box, which generally represents a large area such as a city. The physical concept underlying the box model approach is depicted in Figure 6-8. Mass conservation gives

$$\frac{\partial}{\partial t}(c\, z_i) = Q - c\, z_i \frac{u}{\Delta x} \tag{6-66}$$

which, by integration, gives (Venkatram, 1978)

$$c(t)\, z_i(t) = c(t_o)\, z_i(t_o) \exp(-t/T_f) + Q\, T_f\, (1 - \exp(-t/T_f)) \tag{6-67}$$

If the dynamics of $z_i(t)$ are known, Equation 6–67 allows the computation of $c(t)$. In stationary conditions (i.e., $t = \infty$), c tends to the limit

$$c(\infty) = Q\,T_f/z_i \tag{6–69}$$

which is sometimes a reasonable quasistationary assumption in urban studies.

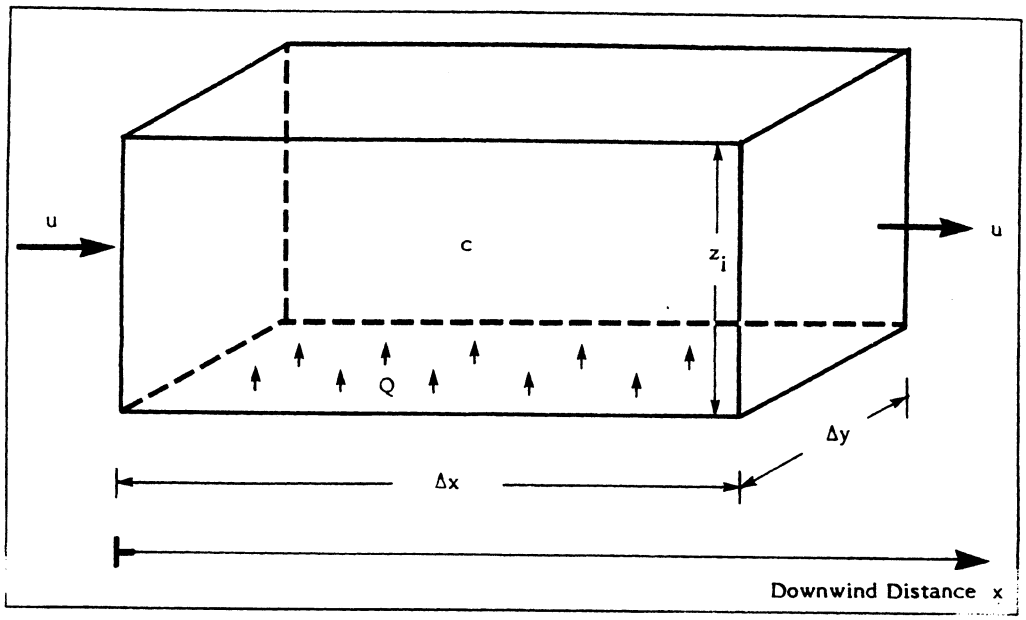

Figure 6–8. The single box model; z_i indicates the time varying mixing height, Δx and Δy are the horizontal dimensions of the box (e.g., the size of the city under investigation), Q is the constant emission for unit of area, c is the time–varying average concentration inside the box, and u is the constant wind speed injecting clean air into the box.

The single box model has frequently been applied for both inert and reactive pollutants; in the latter case, Equation 6–66 has to be modified to incorporate a chemistry module in the mass–balance computations. As a particular example of its application, Meszaros et al. (1978) used a box model for computing the atmospheric sulfur budget over Europe and incorporated both natural/anthropogenic emissions and dry/wet deposition in Equation 6–66. Also, Jensen and Peterson (1979), who used an acoustic sounder for evaluating $z_i(t)$, found good agreement between the single box model output $c(t)$ and urban concentration measurements.

anthropogenic emissions and dry/wet deposition in Equation 6–66. Also, Jensen and Petersen (1979), who used an acoustic sounder for evaluating $z_i(t)$, found good agreement between the single box model output $c(t)$ and urban concentration measurements.

6.4.2 The Slug Model

Venkatram (1978) showed that the box model has a great deal of inertia and cannot properly handle rapid temporal changes in either Q or u. He proposed the slug model as an improvement of the box model, especially during stagnation episodes. The slug model allows the concentration c to vary in the along-wind direction x and in the vertical direction z, but assumes that the concentration does not vary in the crosswind direction y. This allows us to write the mass-conservation equation within the single box in terms of two dimensions (x, z) as

$$\frac{\partial(c\, z_i)}{\partial t} + u\,\frac{\partial(c\, z_i)}{\partial x} = Q \tag{6–70}$$

where x is the downwind distance inside the box. We define the average concentration at x to be $\bar{c}(x)$, where

$$\bar{c}(x)\, z_i(x) = \int_0^{z_i(x)} c(x, z)\, dz \tag{6–71}$$

and $z_i(x)$ is either the mixing height or the vertical size (growing with x) of the "urban plume" generated by the ground level emission Q.

The solution of Equations 6–70 and 6–71 after the emission is shut off (i.e., after Q becomes zero) is

$$\bar{c}(x, t) = (x - u\, t)\,\frac{Q}{z_i(x)} \tag{6–72}$$

for $t \leq x/u$, and

$$\bar{c}(x, t) = 0 \tag{6–73}$$

for $t > x/u$. For $t = T_f$, the above scheme properly gives $\bar{c} = 0$ throughout the entire box, whereas the single box solution of Equation 6–67 is not able to reproduce this complete flushing.

6.4.3 Multi-Box Models

The single box concept has been extended to multi-box simulations (e.g., Ulbrick, 1968; Reiquam, 1970; Gifford and Hanna, 1973). Johnson (in Stern, 1976) describes the multi-box model in its simplest form by the equation

$$\Delta c_{i,j} = [(F_{i-1/2,j} - F_{i+1/2,j}) + (F_{i,j-1/2} - F_{i,j+1/2}) + Q_{ij}\,\Delta t]/V \quad (6\text{–}74)$$

where $\Delta c_{i,j}$ is the variation of the average concentration $c_{i,j}$ in the box i, j during the time interval Δt; i, j are the box horizontal indices; $Q_{i,j}(t)$ is the pollutant emission rate from all sources inside the box; and V is the volume of the box (i.e., $V = \Delta x\ \Delta y\ h$, where h is the height of the box above the ground). F represents the pollutant flux through the sides of the box; i.e.,

$$F_{i\pm1/2,j} = c_{i,j}\,A_{i\pm1/2,j}\,u_{i\pm1/2,j} \quad (6\text{–}75)$$

$$F_{i,j\pm1/2} = c_{i,j}\,A_{i,j\pm1/2}\,u_{i,j\pm1/2} \quad (6\text{–}76)$$

where A is the area of the side of the box, u the wind velocity component perpendicular to A, and the 1/2 term in the indices indicates the side between one cell and the other (e.g., i+1/2 means between i and i+1, and j–1/2 means between j–1 and j).

The two major limitations of this multi-box approach are its neglect of horizontal dispersion and the assumption of instantaneous mixing throughout the box (especially in the vertical). It is, however, computationally fast and, in several cases, may provide satisfactory, cost-effective answers, especially in regions in which detailed meteorological and emission information is not available.

6.5 ADVANCED EULERIAN MODELS

Because of the several shortcomings of the K-theory described in the previous sections, more complex Eulerian formulations for simulating atmospheric diffusion have been proposed. Among them, two have received particular attention: second-order closure modeling (e.g., Lewellen and Teske, 1976) and large eddy simulation techniques (e.g., Nieuwstadt and de Valk, 1987).

6.5.1 Second-Order Closure Modeling

Instead of using the K-theory approximation of Equation 6–5, an exact equation (Donaldson, 1973) can be computed for the second-order correlations

$\langle c'\mathbf{u}'\rangle$. This equation, however, introduces new variables, other than second-order correlations, that leave the system undetermined. A second-order closure model finds a relation between these new variables and the previous ones (i.e., the second-order correlations and the mean flow variables). Using this approach, Lewellen and Teske (1976) obtained a partial differential equation for the turbulent mass flux that has a dual behavior: for the initial plume, characterized by a plume scale that is smaller than the ambient turbulence scale, the equation shows hyperbolic behavior, while, for larger plume scales, the equation shows a smooth transition to parabolic behavior. Only the latter feature can be described well by the K-theory.

The model of Lewellen and Teske (1976) was successfully compared with laboratory simulations (Deardorff and Willis, 1974) of diffusion in convective conditions. The model was able to predict the rise of the maximum concentration from the ground. Comparisons with data collected during tracer experiments, however, were less encouraging (Lewellen and Sykes, 1983) and neither the patterns nor the magnitude of plume concentrations were correctly predicted. Therefore, the practical applicability of higher-order closure models is still questionable, even though some recent results (e.g., Enger, 1986) have shown encouraging features.

Second-order closure techniques have also been used to define new plume and puff methodologies. Sykes et al. (1989a) developed the Second-Order Closure Integrated Plume Model (SCIMP), the model with the lowest resolution in a hierarchy of models developed for EPRI. The model was tested against approximately 500 hours of plume data and seems to perform better than standard U.S. EPA regulatory models (such as MPTER). Sykes et al. (1989b) also developed the Second-Order Closure Integrated Puff model (SCIPUFF), the intermediate resolution member of the hierarchy of models mentioned above. The overall performance results of SCIPUFF were close to those obtained with SCIMP.

6.5.2 Large Eddy Simulation Models

As described by Nieuwstadt and de Valk (1987), a large eddy model such as those developed by Deardorff (1974) and Nieuwstadt et al. (1986), calculates the large-scale turbulent motions by directly solving a set of modified Navier-Stokes equations. These equations are

- a "filtered"(*) momentum equation with extra subgrid terms
- a "filtered" temperature equation with extra subgrid terms
- a Poisson equation for the pressure
- gradient transfer equations for the closure of all the extra terms describing the subgrid motions.
- an equation for the subgrid energy

These equations are solved (typically using finite-difference methods) with grids of about 50 to 100 m and time steps of about 5 s.

Using the output of the Deardorff (1974) model, Lamb (1978) successfully simulated the statistics of nonbuoyant particles in convective conditions. Nieuwstadt and de Valk (1987), instead, used a conservation equation for the contaminant, which is solved concurrently with the large eddy model. This second approach is able to replicate well the laboratory experiments by Willis and Deardorff (1981), who reproduced the behavior of a nonbuoyant contaminant in convective conditions. This good agreement was not recreated using a buoyant plume simulation and comparing it with the experiments of Willis and Deardorff (1983). However, further work by van Haren and Nieuwstadt (1989) shows a reasonable agreement between the output of the large eddy simulation model and the buoyant plume field experiments performed by Carras and Williams (1984).

In conclusion, large eddy simulation models seem promising and represent the approach that is closest to the recreation of the physics of atmospheric diffusion. Their simulation of buoyant plumes, however, needs further study. Also, it is possible that other computational techniques, such as Monte-Carlo Lagrangian particle models (see Chapter 8), will be able to show similar simulation ability at a lower computational cost, by reproducing the main stochastic behavior of atmospheric motion without explicitly solving the Navier-Stokes equations.

(*) By "filtering," we mean the elimination of the small-scale motions that are smaller than the numerical grid.

REFERENCES

Boris, J., and D.L. Book (1973): Flux-corrected transport. I. SHASTA, a fluid transport algorithm that works. *J. Comput. Phys.*, **12**:38–69.

Businger, J.A., and S.P. Ayra (1974): Heights of the mixed layer in the stable, stratified planetary boundary layer. *Adv. Geophys.*, **18A**:73–92.

Calder, K.L. (1949): Eddy diffusion and evaporation in flow over aerodynamically smooth and rough surfaces: A treatment based on laboratory laws of turbulent flow with special reference to conditions in the lower atmosphere. *Quart. J. Mech. Math.*, **2**:153.

Carras, J.N., and D.J. Williams (1984): Experimental studies of plume dispersion in convective conditions – 1. *Atmos. Environ.*, **18**:135–144.

Chock, D.P., and A.M. Dunker (1983): A comparison of numerical methods for solving the advection equation. *Atmos. Environ.*, **17**(1):11–24.

Deardorff, J.W., and G.E. Willis (1974): Physical modeling of diffusion in the mixed layer. *Proceedings*, Symposium on Atmospheric Diffusion Air Pollution sponsored by the American Meteorological Society, Santa Barbara, California, September.

Deardorff, J.W. (1974): Three-dimensional numerical study of the height and mean structure of a heated planetary boundary layer. *Boundary-Layer Meteor.*, **7**:81–106.

Demuth, C. (1978): A contribution to the analytical steady solution of the diffusion equation for line sources. *Atmos. Environ.*, **12**:1255–1258.

Donaldson, C. duP. (1973): Construction of a dynamic model of the production of atmospheric turbulence and the dispersal of atmospheric pollutants. *Proceedings*, Workshop on Micrometeorology sponsored by the American Meteorological Society, Boston, pp. 313–392.

Egan, B.A., and J.R. Mahoney (1972): Numerical modeling of advection and diffusion of urban area source pollutants. *J. Appl. Meteor.*, **11**:312–322.

Enger, L. (1986): A higher order closure model applied to dispersion in a convective PBL. *Atmos. Environ.*, **20**:879–894.

Gifford, F.A., and S.R. Hanna (1973): Modeling urban air pollution. *Atmos. Environ.*, **7**:131–136.

Gifford, F.A. (1982): Horizontal diffusion in the atmosphere: a Lagrangian-dynamical theory. *Atmos. Environ.*, **16**:505–512.

Hage, K.D., P.S. Brown, G. Arnason, S. Lazorick, and M. Levitz (1967): A computer program for the fall and dispersion of particles in the atmosphere. Sandia Corporation Report SC-CR-67-2530, The Travelers Research Center, Inc.

Hage, K.D., and H.W. Church (1967): A computer-programmed model for calculation of fall and dispersion of particles in the atmosphere. *Proceedings*, USAEC Meteor. Info. Meeting, Chalk River Nuclear Labs., 11–14 Sept. 1967, pp. 320–333. Atomic Energy of Canada, Ltd., Report AECL-2787.

Hanna, S.R., et al. (1977): AMS Workshop on Stability Classification Schemes and Sigma Curves — Summary of Recommendations. *J. Climate and Appl. Meteor.*, **58**(12):1305–1309.

Huang, C.H. (1979): A theory of dispersion in turbulent shear flow. Atmos. Environ., **13**:*453–463*.

Irwin, J.S. (1979): Estimating plume dispersion — A recommended generalized scheme. Presented at 4th Symposium on Turbulence and Diffusion, sponsored by the American Meteorological Society, Reno, Nevada.

Jensen, N.O., and E.L. Petersen (1979): The box model and the acoustic sounder, a case study. *Atmos. Environ.*, **13**:717–720.

Lamb, R.G. (1973): Note on application of K-theory to turbulent diffusion problems involving chemical reaction. *Atmos. Environ.*, **7**:235.

Lamb, R.G. (1978): A numerical simulation of dispersion from an elevated point source in the convection layer. *Atmos. Environ.*, **12**:1297–1304.

Lamb, R.G., and D.R. Durran (1978): Eddy diffusivities derived from a numerical model of the convective planetary boundary layer. *Nuovo Cimento*, **1C**:1–17.

Lamb, R.G. (1983): A regional scale (1000 km) model of photochemical air pollution. Part I, Theoretical formulation. U.S. EPA Document EPA–600/3–83–035. Research Triangle Park, North Carolina.

Lettau, H.H. (1970): Physical and meteorological basis for mathematical models of urban diffusion processes. *Proceedings*, Symposium on Multiple-Source Urban Diffusion Models. U.S. EPA Publication No. AP–86.

Lewellen, W.S., and M.E. Teske (1976): Second-order closure modeling of diffusion in the atmospheric boundary layer. *Boundary-Layer Meteor.*, **10**:69–90.

Lewellen, W.S., and R.I. Sykes (1983): Second-order closure model exercise for the Kincaid Power Plant Plume. Electric Power Research Institute Report EA–1616–9, Palo Alto, California.

Liu, M.-K., D.C. Whitney, and P.M. Roth (1976): Effects of atmospheric parameters on the concentration of photochemical air pollutants. *J. Appl. Meteor.*, **15**:829–835.

Longhetto, A., Ed. (1980): *Atmospheric Planetary Boundary Layer Physics*. New York, Elsevier.

McRae, G.J., W.R. Goodin, and J.H. Seinfeld (1982): Mathematical modeling of photochemical air pollution. Environmental Quality Laboratory Report No. 18, Pasadena, California. Also see: McRae, G.J., W.R. Goodin, and J.H. Seinfeld (1982): Development of a second generation mathematical model for urban air pollution. I. Model formulation. *Atmos. Environ.*, **16**(4):679–696.

Meszaros, E., G. Varhelyi, and L. Haszpra (1978): On the atmospheric sulfur budget over Europe. *Atmos. Environ.*, **12**:2273–2277.

Myrup, L.O., and A.J. Ranzieri (1976): A consistent scheme for estimating diffusivities to be used in air quality models. California Department of Transportation Report CA-DOT-TL-7169-3-76-32, Sacramento.

Nieuwstadt, F.T., and H. van Dop, Eds. (1982): *Atmospheric Turbulence and Air Pollution Modeling*. Dordrecht, Holland: Reidel.

Nieuwstadt, F.T., R.A. Brost, and T.L. van Stijn (1986): Decay of convective turbulence, a large eddy simulation. *Proceedings*, 199 Euromech meeting on Direct and Large Eddy Simulation of Turbulence, Munchen, 1985, Braunschweig/Weisbaden, Germany: Friedr. Vieweg & Sohn.

Nieuwstadt, F.T., and J.P. de Valk (1987): A large eddy simulation of buoyant and non-buoyant plume dispersion in the atmospheric boundary layer. *Atmos. Environ.*, **21**(12):2573-2587.

Orszag, S.A. (1971): Numerical simulation of incompressible flows within simple boundaries. I. Galerkin (spectral) representations. *Stud. Appl. Math.*, **50**:293-326.

Pasquill, F., and F.B. Smith (1983): *Atmospheric Diffusion*, Third Edition. New York: Halsted Press, John Wiley and Sons.

Pepper, D.W., C.D. Kern, and P.E. Long, Jr. (1977): Modeling the dispersion of atmospheric pollution using cubic splines and Chapeau functions. *Atmos. Environ.*, **13**:223-237.

Reiquam, H. (1968): *Atmos. Environ.*, **4**:233.

Richtmyer, R.D., and K.W. Morton (1967): *Difference Methods for Initial-Value Problems*. New York: Interscience Publications, John Wiley & Sons.

Rounds, W. (1955): Solutions of the two-dimensional diffusion equation. *Trans. Am. Geophys. Union*, **36**:395.

Runca, E., and F. Sardei (1975): Numerical treatment of the dependent advection and diffusion of air pollutants. *Atmos. Environ.*, **9**:69-80.

Runca, E. (1977): Transport and diffusion of air pollutants from a point source. *Proceedings*, IFIP Working Conference on Modeling and Simulation of Land, Air and Water Resource System, Ghent, The Netherlands.

Schere, K.L. (1983): An evaluation of several numerical advection schemes. *Atmos. Environ.*, **17**:1897-1907.

Sehmel, G. (1980): Particle and gas dry deposition: A review. *Atmos. Environ.*, **14**:983.

Seinfeld, J.H. (1986): *Atmospheric Chemistry and Physics of Air Pollution*. New York: John Wiley & Sons.

Shir, C.C. (1973): A preliminary numerical study of atmospheric turbulent flows in the idealized planetary boundary layer. *J. Atmos. Sci.*, **30**:1327-1339.

Shir, C.C., and L.J. Shieh (1974): A generalized urban air pollution model and its application to the study of SO_2 distributions in the St. Louis metropolitan area. *J. Appl. Meteor.*, **13**:185-204.

Smith, F.B. (1957): The diffusion of smoke from a continuous elevated point source into a turbulent atmosphere. *J. Fluid Mech.*, **2**:49.

Stern, A.C., Ed. (1976): *Air Pollution*. 3rd Edition, Volume I. New York: Academic Press.

Sykes, R.I., W.S. Lewellen, S.F. Parker, and D.S. Henn (1989a): A hierarchy of dynamic plume models incorporating uncertainty. Volume 3: Second-order closure integrated model plume (SCIMP). A.R.A.P. Division of California Research & Technology, Inc., Final Report EA-1616-28, Vol. 3, Princeton, New Jersey.

Sykes, R.I., W.S. Lewellen, S.F. Parker, and D.S. Henn (1989b): A hierarchy of dynamic plume models incorporating uncertainty. Volume 4: Second-order closure integrated puff. A.R.A.P. Division of California Research & Technology, Inc., Final Report EA-6095, Vol. 4, Princeton, New Jersey.

Taylor, G.I. (1921): Diffusion by continuous movements. *Proceedings*, London Math. Soc., **20**: 196-211.

Tirabassi, T., M. Tagliazucca, and P. Zannetti (1986): KAPPA-G, a non-Gaussian plume dispersion model: Description and evaluation against tracer measurements. *JAPCA*, **36**:592-596.

Ulbrick, E.A. (1968): *Socio-Encon. Plan. Sci.*, 1:423.Venkatram, A. (1978): An examination of box models for air quality simulation. *Atmos. Environ.*, **12**:2243-2249.

van Haren, L., and F.T. Nieuwstadt (1989): The behavior of passive and buoyant plumes in a convective boundary layer, as simulated with a large-eddy model. *J. Appl. Meteor.*, **28**:818.

Willis, G.E., and J.W. Deardorff (1976): A laboratory model of diffusion into the convection planetary boundary layer. *Quart. J. Royal Meteor. Soc.*, **102**:427-445.

Willis, G.E., and J.W. Deardorff (1981): A laboratory study of dispersion from a source in the middle of the convectively mixed layer. *Atmos. Environ.*, **15**:109-117.

Willis, G.E., and J.W. Deardorff (1983): On plume rise within a convective boundary layer. *Atmos. Environ.*, **17**:2935-2447.

Yeh, G.T., and C.H. Huang (1975): Three-dimensional air pollutant modeling in the lower atmosphere. *Boundary-Layer Meteor.*, **9**:*381*.

Zalesak, S.T. (1979): Fully multidimensional flux-corrected transport algorithms for fluids. *J. Comput. Phys.*, **31**:335-362.

7 GAUSSIAN MODELS

7.1 THE GAUSSIAN APPROACH

The Gaussian plume model is the most common air pollution model. It is based on a simple formula that describes the three-dimensional concentration field generated by a point source under stationary meteorological and emission conditions. The Gaussian plume model is visualized in Figure 7–1, where, for simplicity, the plume is advected toward the positive x–axis. In a general reference system, the Gaussian plume formula is expressed by

$$c = \frac{Q}{2\pi\sigma_h\sigma_z|\bar{\mathbf{u}}|}\exp\left[-\frac{1}{2}\left(\frac{\Delta_{cw}}{\sigma_h}\right)^2\right]\cdot\exp\left[-\frac{1}{2}\left(\frac{z_s+\Delta h-z_r}{\sigma_z}\right)^2\right] \quad (7\text{–}1)$$

where $c(\mathbf{s},\mathbf{r})$ is the concentration at $\mathbf{r} = (x_r, y_r, z_r)$ due to the emissions at $\mathbf{s} = (x_s, y_s, z_s)$; Q is the emission rate; $\sigma_h(j_h, d)$ and $\sigma_z(j_z, d)$ are the standard deviations (horizontal and vertical) of the plume concentration spatial distribution (often σ_h is referred to as σ_y); j_h and j_z are the horizontal and vertical turbulence states (further discussed below); d is the downwind distance of the receptor from the source, where

$$d = [(\mathbf{r}-\mathbf{s})\cdot\bar{\mathbf{u}}]/|\bar{\mathbf{u}}| \quad (7\text{–}2)$$

$\bar{\mathbf{u}}$ is the average wind velocity vector $(\bar{u}_x, \bar{u}_y, \bar{u}_z)$ at the emission height (it is assumed that $\bar{u}_z \ll (\bar{u}_x^2+\bar{u}_y^2)^{1/2}$); Δ_{cw} is the crosswind distance between the receptor and source (i.e., between the receptor and the plume centerline), where

$$\Delta_{cw} = (|\mathbf{r}-\mathbf{s}|^2 - d^2)^{1/2} \quad (7\text{–}3)$$

and Δh is the emission plume rise, which is a function of emission parameters, meteorology and downwind distance d. Equation 7–1 is applied for $d > 0$; if $d \leq 0$, then $c = 0$.

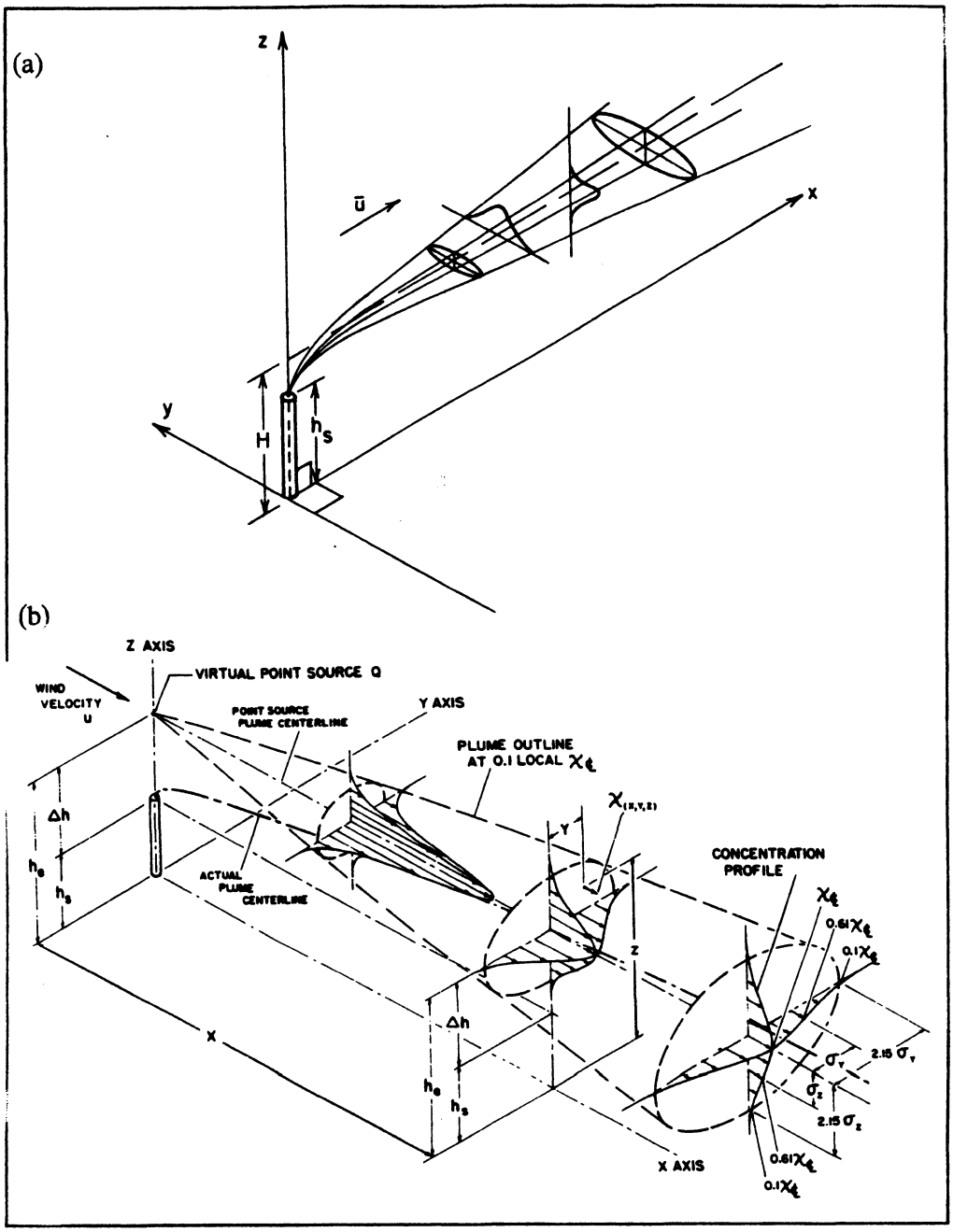

Figure 7–1. The Gaussian plume in a wind-oriented coordinate system (i.e., x along the direction of $\bar{u}$): (a) an elevated source location at (0,0,H) (from Dobbins, 1979). [Reprinted with permission from Academic Press.] (b) three-dimensional concentration profiles (from Strom; in Stern, 1976). [Reprinted with permission from Wiley–Interscience.]

As can easily be seen, Equation 7-1 refers to a stationary state (i.e., c is not a function of time), uses meteorological conditions (wind and turbulence states) that must be considered homogeneous and stationary in the modeled area (i.,e., between s and r), and cannot work in calm conditions where $|\bar{u}| \to 0$. However, the simplicity of the Gaussian approach, its relative ease of use with easily measurable meteorological parameters and, especially, the elevation of this methodology to the quantitative decision-controlling level (U.S. EPA, 1978) have stimulated research aimed at removing some of the limits of the Gaussian theory in treating the complex situations of the real world.

Equation 7-1 is generally written in the form

$$c = \frac{Q}{2\pi\,\sigma_y\,\sigma_z\,\bar{u}} \exp\left[-\frac{1}{2}\left(\frac{y_r}{\sigma_y}\right)^2\right] \exp\left[-\frac{1}{2}\left(\frac{h_e - z_r}{\sigma_z}\right)^2\right] \qquad (7\text{-}4)$$

in which $\bar{u}$ is the average horizontal wind speed, h_e is the effective emission height (i.e., $h_e = z_s + \Delta h$), and σ_y replaces σ_h. Here a wind-oriented coordinate system is also used (as in Figure 7-1). Equation 7-4 can be derived in several ways from different assumptions (see Section 7-10) and can be justified by semiempirical considerations, as Figure 7-2 illustrates, where both the instantaneous and the one-hour average concentration distributions are exemplified. It

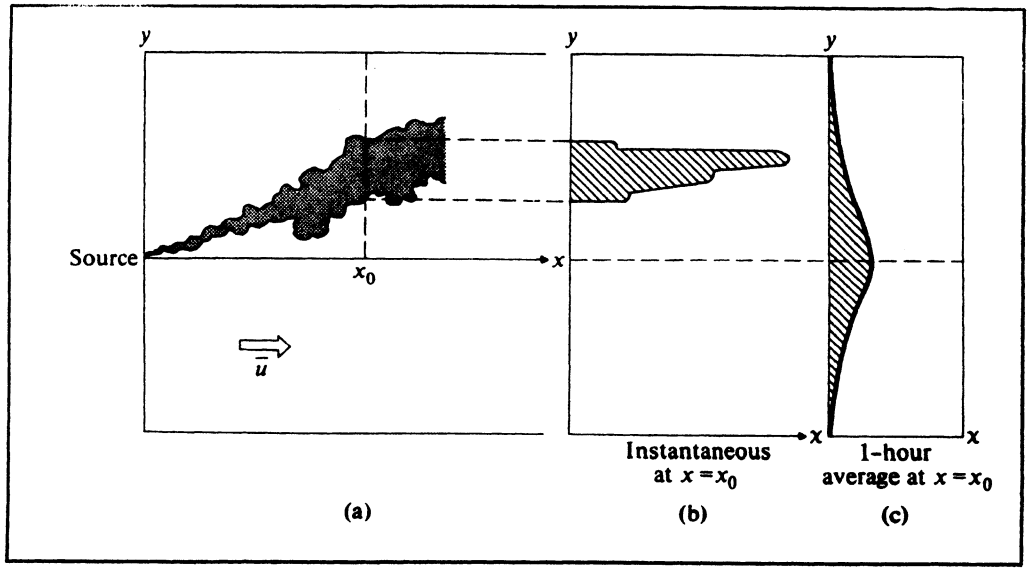

Figure 7-2. *(a) Instantaneous top view of a plume; (b) instantaneous horizontal profile of the plume concentration along a transverse direction at some distance downwind from the source; (c) one-hour average profile for the same downwind distance (from Williamson, 1973). [Reprinted with permission from Addison-Wesley.]*

can be concluded that, even though instantaneous plume concentrations are quite irregular, a sufficiently long averaging time (e.g., one hour) generates, in many cases, bell-shaped concentration distributions that can be well approximated by the Gaussian distribution in both the horizontal and (to a lesser degree) the vertical.

One area of particular emphasis has been the identification, for both simple and complex meteorological or terrain situations, of those parameters that allow Equation 7-4 to give a good estimate of the maximum ground-level concentration. Other applications have used Equation 7-4 in a "climatological" way to provide long-term concentration averages (monthly, seasonally, or annually) at the receptors (e.g., Martin, 1971; Runca et al., 1976). In these climatological applications, each concentration computed by an equation similar to Equation 7-4 is weighted by the frequency of occurrence of its corresponding meteorological condition (see Section 7.6). Other applications have even tried to remove the physical meaning of some of the parameters in Equation 7-4. For example, Melli and Runca (1979) allowed the "wind speed" $\bar{u}$ to change its value as a function of the downwind distance, to produce ground-level concentration values more like those obtained by finite-difference simulations of the same conditions.

In the past, the more complex time-varying applications of simulation modeling techniques have made extensive use of dynamic grid models (mainly, finite-difference simulations following the K-theory approach, as discussed in Chapter 6). However, a growing concern has arisen about some important limitations of such a numerical approach. Specifically, as discussed in Chapter 6, (1) the numerical treatment of the advection terms often produces an unreasonable, artificial diffusion, and (2) K-theory simulation of the growth of a plume from a point source is often fundamentally wrong in turbulent flows. Other well-known limitations are that (3) concentrations are computed as spatial averages in three-dimensional cells (which makes comparison with point measurements difficult and produces an erroneous initial dilution of plumes whose width is smaller than the cell dimensions), and (4) relating the diffusion coefficients K to standard atmospheric measurements is difficult. Also, a numerically correct application of the K-theory requires the grid size to be much less than the plume size, a condition that is difficult to satisfy near the source.

To overcome some of these limitations, modelers have attempted to extend the applicability of the Gaussian method to treat nonstationary, nonhomogeneous conditions. In particular, the segmented plume approach (Chan and Tombach, 1978; Chan, 1979) and the puff approach (Lamb, 1969; Roberts

et al., 1970) were defined to handle pseudosteady-state conditions. Both methods break up the plume into a series of independent elements (segments or puffs) that evolve in time as a function of temporally and spatially varying meteorological conditions. Sections 7.7 through 7.9 will discuss these extensions of the Gaussian approach.

7.2 THE CALCULATION OF σ_y AND σ_z

Concentrations computed by Equation 7–4 depend strongly upon a correct calculation of σ_y and σ_z, which is a major challenge for all Gaussian model applications. We present, in the two subsections below, two general methods for computing σ_y and σ_z. The first method — the preferred one — is based on the calculation of nondimensional functions and makes direct use of turbulence intensity measurements, when available. The second method relies on semiempirical calculations in which the atmosphere is classified into "stability" classes and different σ functions are derived for each class.

7.2.1 The Nondimensional S_y and S_z Functions for the Gaussian Model

Pasquill (1971) suggested the following relationships for plume sigmas, which are consistent with Taylor's statistical theory of diffusion:

$$\sigma_y = \sigma_v \, t \, S_y(t/T_L) \tag{7–5}$$

$$\sigma_z = \sigma_w \, t \, S_z(t/T_L) \tag{7–6}$$

where σ_v and σ_w are the standard deviations of the crosswind and vertical wind vector components (which can be either measured or estimated by the formulae provided in Chapter 3), and S_y and S_z are universal functions of the diffusion (or travel) time t and the Lagrangian time scale T_L. One of the major objectives of current research on Gaussian models is the computation of its nondimensional functions S_y and S_z. In this formulation, it is important to point out that σ_v must include the contribution of the wind direction meandering component.

Draxler (1976) rewrote the above equations as

$$\sigma_y = \sigma_\theta \, x \, S_y(t/T_i) \tag{7–7}$$

$$\sigma_z = \sigma_\phi \, x \, S_z(t/T_i) \tag{7–8}$$

where σ_θ and σ_ϕ are the standard deviations of wind vector azimuth and elevation angles (in radians), x is the downwind distance, and T_i is a normalization factor, proportional to T_L (i.e., $T_L = T_i/1.64$, where T_i is the time required for S_y or S_z to become equal to 0.5; S_y and S_z are always equal to 1 for $t = 0$). Note that $\sigma_\theta = \arctan(\sigma_v/\bar{u})$ and $\sigma_\phi = \arctan(\sigma_w/\bar{u})$, where, for small angles, $\sigma_\theta \simeq \sigma_v/\bar{u}$ and $\sigma_\phi \simeq \sigma_w/\bar{u}$.

Draxler (1976) also analyzed available dispersion data, giving a preliminary evaluation of the specific forms of S_y and S_z and determining T_i. Pasquill (1976) tabulated S_y as a universal function of x only. These tabulated values were then reformulated by Irwin (1979) as

$$S_y(x) = (1 + 0.0308\, x^{0.4548})^{-1} \tag{7-9}$$

for $x \leq 10^4$ m, and

$$S_y(x) = 0.333(10,000/x)^{0.5} \tag{7-10}$$

for $x > 10^4$ m.

The above formulation of S_y is currently accepted as the best way for determining σ_y and has been recommended by the American Meteorological Society Workshop on Stability Classification Schemes and Sigma Curves (Hanna et al., 1977). Phillips and Panofsky (1982), however, suggest a different S_y formulation, which provides a better fit of experimental data for small x and is consistent with inertial-subrange theory, namely

$$S_y = 0.617\left[\frac{T_i}{t} - \frac{(T_i/t)^2}{5.25}\ln\left(1 + 5.25\,\frac{t}{T_i}\right)\right]^{1/2} \tag{7-11}$$

Much investigation is still required to fully evaluate the validity of the above S_y formulations. In particular, the dependence of S_y only upon x is certainly questionable. Incidentally, Lagrangian particle dispersion numerical experiments (e.g., Zannetti and Al-Madani, 1983a,b) have confirmed a behavior of σ_y in agreement with the statistical theory of diffusion and showed a variability of σ_y values, from the same σ_θ input, associated with changes in the autocorrelation structure of the wind direction (that is, a higher time correlation in the wind direction θ is causing, as expected, larger σ_y, even though σ_θ is the same).

The evaluation of S_z is still quite uncertain. Irwin (1979) provided a preliminary universal function S_z and recommended its interim use until more field

data permit the evaluation of a more accurate scheme. In unstable conditions, his S_z function depends upon the depth of the mixing layer h, the diffusion time t, the effective release height h_e, the surface friction velocity u_* and the Monin–Obukov length scale L. Also, Draxler (1976) derived, under neutral and stable conditions,

$$S_z = [1 + 0.9(t/T_o)^{1/2}]^{-1} \tag{7-12}$$

for $z < 50$ m, and

$$S_z = [1 + 0.945(t/T_o)^{0.8}]^{-1} \tag{7-13}$$

for $z \geq 50$ m, in which the characteristic time T_o is $\simeq 50$ s.

Additional considerations on the calculation of S_y and S_z for travel distances less than 10 km in the different layers of the PBL (see Figure 3–8) can be found in Gryning et al. (1987), who, however, propose non-Gaussian vertical concentration profiles in most cases.

It must be pointed out that only the availability of *validated* S_y and S_z functions allows a proper application of Gaussian modeling techniques in a way that makes full use of available meteorological measurements of the standard deviations of the wind vector components. In fact, the simple use of semi-empirical plume sigmas (as discussed below) requires only the evaluation of the stability class (a discrete number) and cannot make use of the exact information on wind fluctuation intensities, when available.

7.2.2 Semiempirical σ Calculations

Several schemes that allow the computation of σ_y and σ_z from the atmospheric stability class and the downwind distance are available. The stability class can be computed using the Pasquill or Turner methods (see Tables 3–2 and 3–3) or from measurements of either σ_θ or σ_w or the vertical temperature gradient $\Delta T/\Delta z$, as Tables 7–1 and 7–2 illustrate. Nighttime conditions are sometimes characterized, especially with low wind speed, by large horizontal dispersion due to wind direction meandering and small vertical dispersion due to the ground-based temperature inversion. Therefore, when stability is evaluated using the standard deviation of the horizontal wind direction fluctuations (see Table 7–2), this stability must be corrected according to Table 7–3 in order to characterize vertical diffusion at nighttime.

Full three-dimensional tracer experiments have shown that horizontal and vertical diffusion rates are often related to different stability categorizations and,

Table 7-1.—Classification of atmospheric stability (data from DeMarrais, 1978; Best et al., 1986; and Hanna, 1989).

Stability classification	Pasquill categories	σ_θ (*) (degrees)	ΔT temperature change with height (°C 10^{-2} m^{-1})	R_i gradient Richardson number at 2 m	$\sigma_w/\bar{u}$
Extremely unstable	A	25.0	< -1.9	-0.9	> 0.15
Moderately unstable	B	20.0	-1.9 to -1.7	-0.5	0.1 - 0.15
Slightly unstable	C	15.0	-1.7 to -1.5	-0.15	
Neutral	D	10.0	-1.5 to -0.5	0	0.05 - 0.1
Slightly stable	E	5.0	-0.5 to 1.5	0.4	
Moderately stable	F	2.5	1.5 to 4.0	0.8	0.0 - 0.05
Extremely unstable	G	1.7	> 4.0		

(*) Standard deviation of horizontal wind direction fluctuation over a period of 15 minutes to 1 hour. The values shown are averages for each stability classification.

Table 7-2. Classification of atmospheric stability[1] (from U.S. EPA, 1986, adapted from Irwin, 1980).

Pasquill stability categories	Standard deviation of the horizontal wind direction fluctuations [2] (degrees)	Standard Deviation of the vertical wind direction fluctuations [2] (degrees)
A	Greater than 22.5°	Greater than 11.5°
B	17.5 to 22.5°	10.0° to 11.5°
C	12.5° to 17.5°	7.8° to 10.0°
D	7.5° to 12.5°	5.0° to 7.8°
E	3.8° to 7.5°	2.4° to 5.0°
F	Less than 3.8°	Less than 2.4°

[1] These criteria are appropriate for steady-state conditions, a measurement height of 10 m, for level terrain, and an aerodynamic surface roughness length of 15 cm. Care should be taken that the wind sensor is responsive enough for use in measuring wind direction fluctuation.

[2] A surface roughness factor of $(z_o/15\ \text{cm})^{0.2}$, where z_o is the average surface roughness in centimeters within a radius of 1-3 km of the source, may be applied to the table values. This factor, while theoretically sound, has not been subjected to rigorous testing and may not improve the estimates in all circumstances.

Table 7–3. Nighttime(*) (vertical) Pasquill stability category based on σ_θ ; i.e., the standard deviation of the horizontal wind direction fluctuations, in degrees (from U.S. EPA, 1986, adapted from Irwin, 1980).

If the σ_θ stability category is	And the wind speed at 10 m is ($m\ s^{-1}$)	Then the Pasquill stability category is
A	< 2.9	F
	2.9 to 3.6	E
	≥ 3.6	D
B	< 2.4	F
	2.4 to 3.0	E
	≥ 3.0	D
C	< 2.4	E
	≥ 2.4	D
D	wind speed not considered	D
E	wind speed not considered	E
F	wind speed not considered	F

(*) Nighttime is considered to be from one hour before sunset to one hour after sunrise.

therefore, a "split-sigma" approach should generally be adopted, in which σ_y and σ_z dynamics are evaluated as functions of "horizontal" and "vertical" stability classes, respectively. Results indicate that σ_θ measurements provide a good estimate of the "horizontal" stability, while vertical temperature gradient data seem appropriate for identifying the "vertical" stability class.

After the computation of the stability class, σ_y and σ_z can be computed at a certain downwind distance x by choosing one of the several available formulae:

1. Pasquill–Gifford sigmas (Gifford, 1961) graphically presented by Turner (1970) and, in an analytical form, by Green et al. (1980), as

$$\sigma_y(x) = \frac{k_1\, x}{[1 + (x/k_2)]^{k_3}} \tag{7–14}$$

$$\sigma_z(x) = \frac{k_4\, x}{[1 + (x/k_2)]^{k_5}} \tag{7–15}$$

where the constants k_1, k_2, k_3, k_4, k_5 are given in Table 7–4.

Table 7–4. Values of the constants in the Equations 7–14 and 7–15.

Stability class	k_1	k_2	k_3	k_4	k_5
A	0.250	927	0.189	0.1020	−1.918
B	0.202	370	0.162	0.0962	−0.101
C	0.134	283	0.134	0.0722	0.102
D	0.0787	707	0.135	0.0475	0.465
E	0.0566	1,070	0.137	0.0335	0.624
F	0.0370	1,170	0.134	0.0220	0.700

The above σ_y, σ_z values were derived (Gifford, 1976) primarily from a diffusion experiment in flat terrain ($z_o \simeq 0.03$ m) in which a nonbuoyant tracer gas was released near the surface and measured (three-minute averages) downwind up to a distance of 800 m from the source. Pasquill–Gifford sigmas are the most used formulation for U.S. EPA regulatory modeling applications.

2. Brookhaven sigmas (Smith, 1968), in which a power law function is assumed for both σ_y and σ_z; i.e.,

$$\sigma = a\,x^b \tag{7–16}$$

Table 7–5 gives the coefficients a and b for each "gustiness" category. Table 7–6 illustrates the relation between the "gustiness" categories and the Pasquill classes. The Brookhaven scheme was derived from elevated releases (108 m) over a rough surface ($z_o \simeq$ 1 m), with concentrations measured up to a few kilometers downwind.

3. Briggs sigmas (Briggs, 1973), in urban and rural versions, provide an interpolation scheme that agrees with Pasquill–Gifford in the downwind range from 100 m to 10 km, except that σ_z values for A and B stability approximate the B_2 and B_1 Brookhaven curves. Table 7–7 gives the Briggs sigmas. The urban Briggs sigmas are also called McElroy–Pooler sigmas, and were derived from several

Table 7–5. Coefficients a and b for Equation 7–16.

Gustiness category	σ_y		σ_z	
	a	*b*	*a*	*b*
B_2	0.40	0.91	0.41	0.91
B_1	0.36	0.86	0.33	0.86
C	0.32	0.78	0.22	0.78
D	0.31	0.71	0.06	0.71

Table 7–6. Relation between the "gustiness" category and the Pasquill class (from Gifford, 1976).

Pasquill class	Gustiness category
A	B_2 (very unstable)
B	B_1 (unstable)
C	B_1 (unstable
D	C (neutral)
E	C/D (neutral/stable)
F	D (stable)

urban dispersion experiments with low-level tracers (McElroy and Pooler, 1968). The U.S. EPA recommends these sigma values as the ones most appropriate for dispersion simulations in urban areas (U.S. EPA, 1984).

Table 7–7. The Briggs (1973) sigma functions for (a) urban and (b) rural conditions (from Panofsky and Dutton, 1984). [Reprinted with permission from Wiley–Interscience.]

(a) Urban Dispersion Parameters (for distances between 100 and 10,000 m)

Pasquill stability	σ_y (m)	σ_z (m)
A–B	$0.32\,x\,(1 + 0.0004\,x)^{-0.5}$	$0.24\,x\,(1 + 0.001\,x)^{0.5}$
C	$0.22\,x\,(1 + 0.0004\,x)^{-0.5}$	$0.20\,x$
D	$0.16\,x\,(1 + 0.0004\,x)^{-0.5}$	$0.14\,x\,(1 + 0.0003\,x)^{-0.5}$
E–F	$0.11\,x\,(1 + 0.0004\,x)^{-0.5}$	$0.08\,x\,(1 + 0.00015\,x)^{-0.5}$

(b) Rural Dispersion Parameters (for distances between 100 and 10,000 m)

Pasquill stability	σ_y (m)	σ_z (m)
A	$0.22\,x\,(1 + 0.0001\,x)^{-0.5}$	$0.20\,x$
B	$0.16\,x\,(1 + 0.0001\,x)^{-0.5}$	$0.12\,x$
C	$0.11\,x\,(1 + 0.0001\,x)^{-0.5}$	$0.08\,x\,(1 + 0.0002\,x)^{-0.5}$
D	$0.08\,x\,(1 + 0.0001\,x)^{-0.5}$	$0.06\,x\,(1 + 0.0015\,x)^{-0.5}$
E	$0.06\,x\,(1 + 0.0001\,x)^{-0.5}$	$0.03\,x\,(1 + 0.0003\,x)^{-1}$
F	$0.04\,x\,(1 + 0.0001\,x)^{-0.5}$	$0.016\,x\,(1 + 0.0003\,x)^{-1}$

Several additional formulations and parameterizations of σ_y and σ_z are available in the literature. See, for example, Briggs (1985) for a review of diffusion parameterizations for the convective (i.e., unstable) PBL.

7.3 REFLECTION TERMS

The basic Gaussian formula is often used with the assumption of total or partial concentration reflection at the surface (see Figure 7–3). Therefore, the last term in Equation 7–4 becomes

$$S(z_r) = \exp\left[-\frac{1}{2}\left(\frac{h_e - z_r}{\sigma_z}\right)^2\right] + r_g \exp\left[-\frac{1}{2}\left(\frac{h_e + z_r}{\sigma_z}\right)^2\right] \quad (7\text{–}17)$$

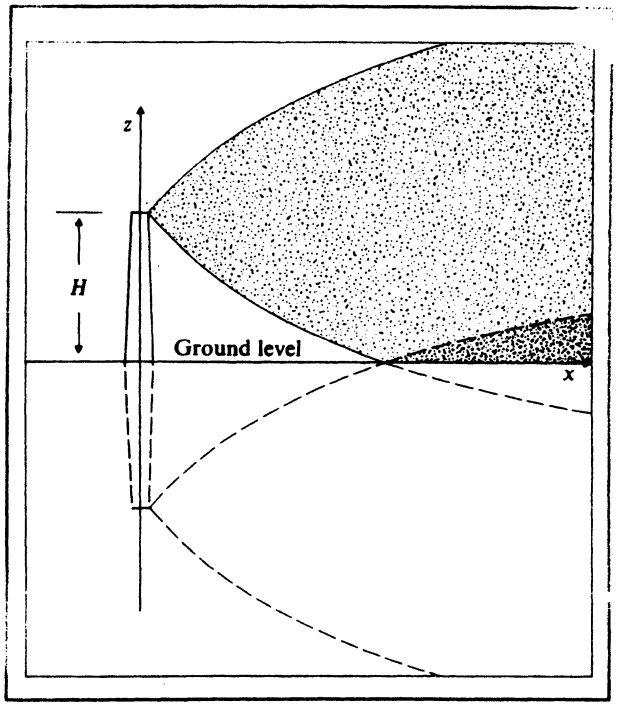

Figure 7–3. Example of ground reflection simulated by the image method; i.e., a vertical source below the ground (from Williamson, 1973). [Reprinted with permission from Addison–Wesley.]

where r_g is the ground reflection coefficient ($r_g = 1$, i.e., total reflection, is generally assumed). For receptors at the ground ($z_r = 0$) with $r_g = 1$, Equation 7–17 becomes

$$S(0) = 2 \exp\left[-\frac{1}{2}\left(\frac{h_e}{\sigma_z}\right)^2\right] \quad (7\text{–}18)$$

which, for ground-level nonbuoyant sources (i.e., $h_e = 0$), gives

$$S(0) = 2 \quad (7\text{–}19)$$

If the plume is emitted within the PBL, it can also be reflected from the top z_i of the PBL, giving

$$S(z_r) = \exp\left[-\frac{1}{2}\left(\frac{h_e - z_r}{\sigma_z}\right)^2\right] + r_g \exp\left[-\frac{1}{2}\left(\frac{h_e + z_r}{\sigma_z}\right)^2\right] + r_i \exp\left[-\frac{1}{2}\left(\frac{2z_i - h_e - z_r}{\sigma_z}\right)^2\right] \tag{7-20}$$

where r_i is the reflection coefficient at z_i ($r_i = 1$, i.e., total reflection, is generally assumed). However, the presence of a second reflecting barrier causes multiple reflections and, therefore, instead of Equation 7–20, it is better to use, for $r_g = r_i = 1$,

$$S(z_r) = \sum_{j=0,\,\pm 1,\,\pm 2,\ldots} \left\{\exp\left[-\frac{1}{2}\left(\frac{z_r + 2\,j\,z_i - h_e}{\sigma_z}\right)^2\right] + \exp\left[-\frac{1}{2}\left(\frac{z_r + 2\,j\,z_i + h_e}{\sigma_z}\right)^2\right]\right\} \tag{7-21}$$

Unfortunately, in some cases, Equation 7–21 converges slowly. To avoid excessive computations, Yamartino (1977) proposed an efficient method for approximating Equation 7–21, in which:

- for $\sigma_z/z_i \leq 0.63$, Equation 7–21 is truncated at $j = 0, \pm 1$
- for $0.63 < \sigma_z/z_i \leq 1.08$, Equation 7–21 is approximated by

$$S(z_r) = \frac{\sqrt{2\,\pi}\,\sigma_z}{z_i}(1 - \beta^2)\,[1 + \beta^2 + 2\,\beta\,\cos(\pi\,z_r/z_i)\,\cos(\pi\,h_e/z_i)] \tag{7-22}$$

where

$$\beta = \exp\left[-\frac{1}{2}\left(\frac{\pi\,\sigma_z}{z_i}\right)^2\right] \tag{7-23}$$

and, for $\sigma_z/z_i > 1.08$, Equation 7–22 is used with $\beta = 0$, giving

$$S(z_r) = \frac{\sqrt{2\pi}\sigma_z}{z_i} \tag{7-24}$$

which, substituted into Equation 7–4, gives the "trapping" equation

$$c = \frac{Q}{\sqrt{2\pi}\sigma_y \bar{u} z_i} \exp\left[-\frac{1}{2}\left(\frac{y_r}{\sigma_y}\right)^2\right] \tag{7-25}$$

Equation 7–25 shows a uniform vertical mixing (between $z = 0$ and $z = z_i$) of the plume, whose concentrations no longer depend upon z.

The above scheme approximates Equation 7–21 with an error < 1.3 percent and is, therefore, quite satisfactory in all applications.

7.4 DEPOSITION/DECAY TERMS

Dry deposition, wet deposition and chemical transformation phenomena are usually taken into account in the Gaussian model by multiplying Equation 7–4 by exponential terms such as

$$\exp\ [-t/T] \tag{7-26}$$

where t is the travel time

$$t = x/\bar{u} \tag{7-27}$$

and T is the corresponding time scale. The relation between the percentage of mass reduction per hour (%/h) and the time scale T in Equation 7–26 is

$$\%/h = 100\ [1 - \exp(-3,600/T)] \tag{7-28a}$$

and, for large T,

$$\%/h \simeq 360,000/T \tag{7-28b}$$

More discussion of atmospheric deposition phenomena is presented in Chapter 10.

7.4.1 Dry Deposition

The time scale of dry deposition, T_d, can be expressed as a function of the deposition velocity V_d (see Equation 6–10), as follows

$$\frac{1}{T_d} = V_d/\Delta_p \tag{7-29}$$

where Δ_p is the vertical thickness of the plume, say

$$\Delta_p \simeq 4\,\sigma_z \tag{7-30}$$

Since dry deposition phenomena occur only after the plume interacts with terrain features, it is often convenient to apply Equation 7–26 only beyond a critical downwind distance x_d, defined as the distance at which $2\,\sigma_z$ is equal to the height of the plume above the ground; i.e.,

$$2\,\sigma_z(x_d) = h_e \tag{7-31}$$

which can be rewritten as

$$x_d = \sigma_z^{-1}(h_e/2) \tag{7-32}$$

where $\sigma_z^{-1}(...)$ is the inverse function of $\sigma_z(x)$.

7.4.2 Wet Deposition

The time scale of the wet deposition, T_w, can be expressed (Draxler and Heffter, 1981) as

$$T_w = \frac{3.6 \cdot 10^6\, P_L}{S_r\, P_R} \tag{7-33}$$

where P_L is the thickness of the precipitation layer (an average climatological value of P_L is 4,000 m), S_r is the scavenging ratio of the pollutant (a typical value for SO_2 is $S_r = 4.2 \cdot 10^5$), and P_R is the precipitation rate in mm/h.

7.4.3 Chemical Transformation

The time scale of the chemical transformation, T_c, is mainly a function of the reactivity of the pollutant. A typical value for SO_2 is T_c = 100,800 s (i.e., 28 hours).

7.5 SPECIAL CASES

Several modifications of the Gaussian equation that have been proposed for simulating special dispersion conditions are discussed in this section.

7.5.1 Line, Area, and Volume Sources

Equation 7-1 or 7-4 can be spatially integrated to simulate the effects of line, area, and volume sources. Analytical integration is often impossible or requires simplifications (especially in the forms of the σ_y and σ_z functions). Therefore, numerical integration is often used for these spatial integrations. Many Gaussian models (see Chapter 14) contain accurate routines for the treatment of line, area, and volume sources.

In several cases, the virtual point source method provides a simple, but satisfactory, treatment of line, area and volume sources, without integration. Using this method, the actual nonpoint source is simulated by an appropriate upwind virtual point source S', as Figure 7-4 illustrates.

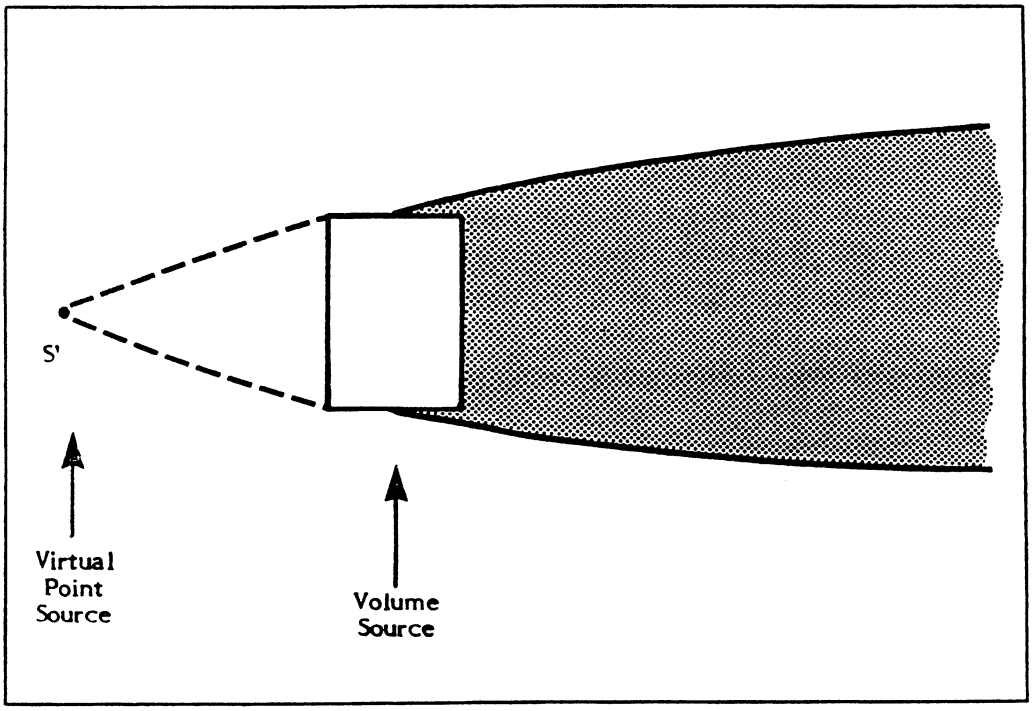

Figure 7-4. The virtual source approach for simulating line, area, and volume sources.

7.5.2 Fumigation

Turner (1970) proposed the following formula to simulate the maximum morning fumigation effects of an elevated plume previously emitted into the stable layer:

$$c(x, 0, z) = \frac{Q}{\sqrt{2\pi}\ \sigma_{yF}\ H_i\ \bar{u}} \tag{7-34}$$

where

$$H_e = h_e + 2\ \sigma_{zs} \tag{7-35}$$

$$\sigma_{yF} \simeq \sigma_{ys} + (h_e/8) \tag{7-36}$$

Equation 7–34 is derived by assuming that the stable plume, characterized by σ_{ys} and σ_{zs}, is suddenly fumigated to the ground. During this fumigation, the plume becomes homogeneously mixed in the vertical, between $z = 0$ and $z = h_e + 2\ \sigma_{zs}$, and expands horizontally following a 15° fumigation trajectory (from H_e to the ground), which causes an increase of σ_y from σ_{ys} to σ_{yF}.

7.5.3 Concentration in the Wake of Building

Several algorithms have been proposed for computing plume downwash effects, which Figure 7–5 outlines. In particular, downwash algorithms have been incorporated into two Gaussian computer codes (see Chapter 14): the Industrial Source Complex Model (ISC; Bowers et al., 1979) and the Buoyant Line and Point (BLP) Source Dispersion Model (Schulman and Scire, 1980). The ISC model was further modified (Schulman and Hanna, 1986) to account for improved understanding of plume rise and downwash around buildings.

A simple estimate of the extra diffusion induced by the buildings can be obtained by increasing the plume sigmas in the following way

$$\sigma_{yw} = (\sigma_y^2 + const\ A/\pi)^{1/2} \tag{7-37}$$

$$\sigma_{zw} = (\sigma_z^2 + const\ A/\pi)^{1/2} \tag{7-38}$$

where σ_y and σ_z are the plume sigmas without the building effects; σ_{yw} and σ_{zw} incorporate the building effects; and A is the area of the building projected onto a vertical plane normal to wind direction.

More discussion of this topic is found in Section 11.3.

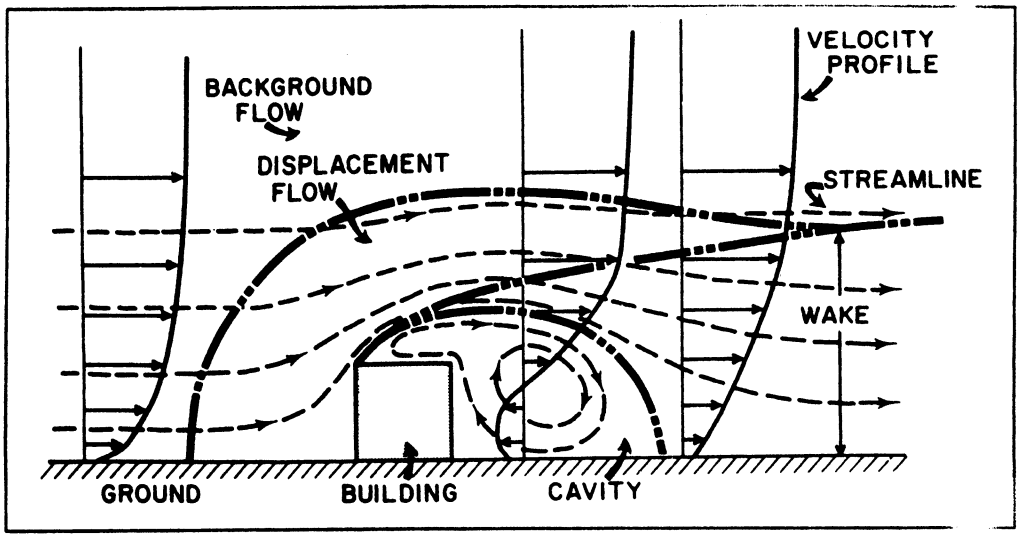

Figure 7–5. Mean flow around a cubical building. The presence of a bluff structure in otherwise open terrain will produce aberrations in the wind flow generally similar to those shown (from Smith, 1968). [Reprinted with permission from the American Society of Mechanical Engineers.]

7.5.4 Plume Trapping Into a Valley

Turner (1970) proposed to treat the plume trapping in a valley in a manner similar to the plume trapping between the ground and z_i ; i.e., similar to the trapping Equation 7–25, but in the horizontal instead of the vertical. With this assumption, in the case of simple uniform flow parallel to the valley axis along x, we obtain for any y,

$$c(x, y, 0) = \left(\frac{2}{\pi}\right)^{1/2} \frac{Q}{W \sigma_z \bar{u}} \exp\left[-\frac{1}{2}\left(\frac{h_e}{\sigma_z}\right)^2\right] \qquad (7\text{–}39)$$

where W is the valley width. Harvey and Hamawi (1986) presented an expanded analytical treatment of plume trapping in a valley.

7.5.5 Tilted Plume

Plumes of large particles having a freefall, i.e., gravitational (settling) velocity V_G can be simulated by the Gaussian tilted plume approach Figure 7–6 illustrates. The plume is tilted downward at an angle whose tangent is $V_G/\bar{u}$, the reflection coefficient at the ground is zero, and most of the plume material is

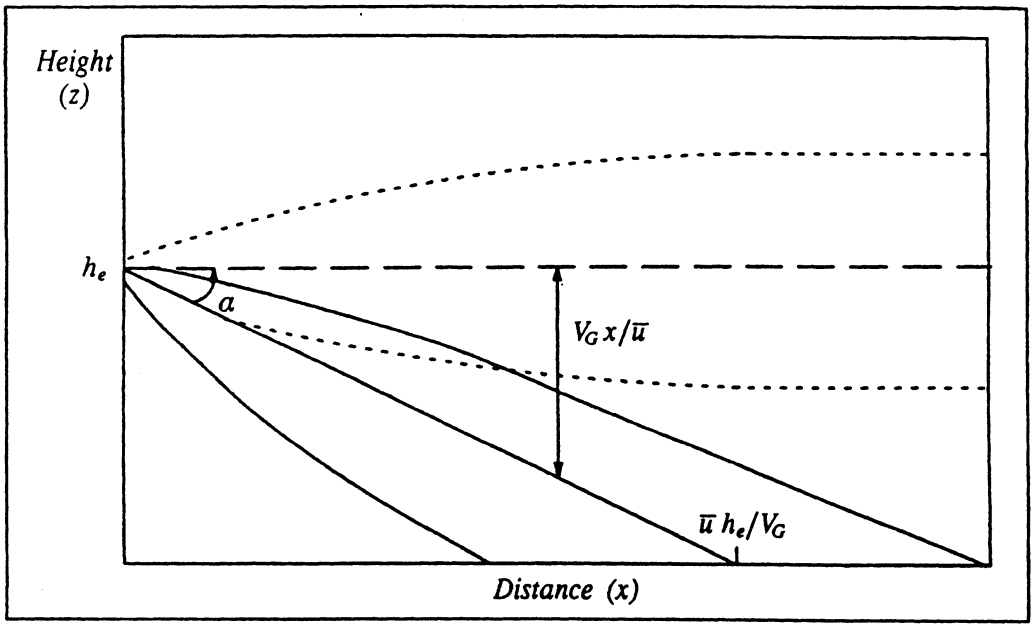

Figure 7–6. Schematic representation of tilted plume treatment of deposition of particles with settling velocity V_G. Solid lines represent the tilted plume, while dotted lines describe the plume shape with $V_G = 0$.

deposited at the ground at a distance of about $\bar{u}\, h_e/V_G$. Section 11.4 provides additional discussion.

7.5.6 Coastal Diffusion and Shoreline Fumigation

Shoreline fumigation is a particularly important problem. As Figure 7–7 illustrates, elevated plumes emitted offshore or near the shoreline initially encounter stable marine dispersion conditions. But when carried inland by the daytime breeze, they eventually penetrate the growing unstable mixing layer inland and are, therefore, fumigated to the ground.

Lyons and Cole (1973) and van Dop et al. (1979) provided the following approximate solution to the fumigation problem. If $z_i(x)$ is the mixing height,

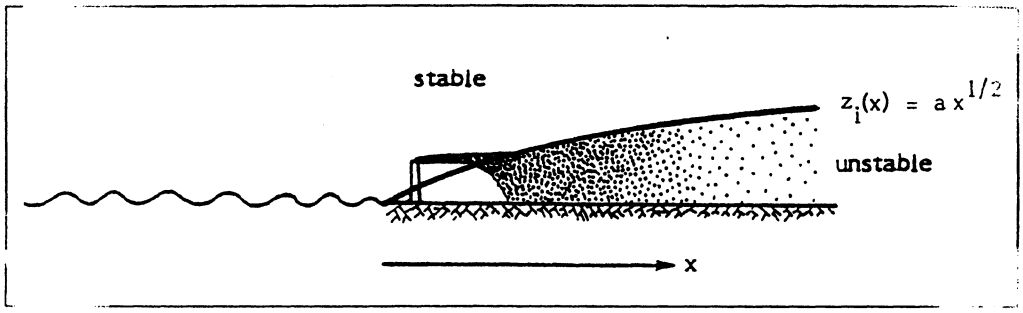

Figure 7–7. Example of plume producing uniform vertical concentration after encountering unstable layer.

expressed as a function of the distance x from the shoreline, the concentration in the fumigation region is

$$c_F(x) = \frac{1}{z_i(x)} \int_{-\infty}^{z_i(x)} c\, dz \tag{7–40}$$

where c is the concentration field generated by the standard Gaussian plume equation with stable sigmas (i.e., σ_{ys}, σ_{zs}). After some simplifying assumptions, we obtain, for small σ_{zs} and $y = 0$,

$$c_F(x) \simeq \frac{Q}{\sqrt{2\,\pi}\ \sigma_{yF}\, u\, z_i(x)} \tag{7–41}$$

where σ_{yF} has been previously defined by Equation 7–36.

A Gaussian code, developed for the U.S. Department of the Interior, simulates the overwater transport and diffusion of pollutants emitted by offshore sources, such as oil platforms. This model (offshore and coastal dispersion, OCD; Hanna et al., 1984) is becoming the official U.S. EPA regulatory tool for these applications.

Section 11.2 presents additional discussion of coastal diffusion phenomena.

7.5.7 Complex Terrain

A few Gaussian computer codes are available for complex terrain simulations. The most recent ones are the rough terrain dispersion model (RTDM; ERT,

1984) and the complex terrain dispersion model (CTDM; Strimaitis et al., 1986), both developed for the U.S. EPA. They incorporate the results of intensive tracer experiment studies in complex terrain.

One of the most important issues in complex terrain modeling by Gaussian formulae is the estimate of the plume centerline height when approaching the terrain height. Three simple assumptions are illustrated in Figure 7–8. Recent, more refined, techniques are presented in Section 11.1.

7.6 THE CLIMATOLOGICAL MODEL

The Gaussian plume equation is often used to simulate the time-varying concentration field by assuming a series of steady-state conditions. In other words, if the hourly emission and meteorological input is known, a steady-state equation (such as Equation 7–4) can be used repeatedly with the assumption that each hour can be represented by a stationary concentration field.

Several air quality applications require the computation of long-term (e.g., annual) concentration averages, thus requiring a large number of hourly

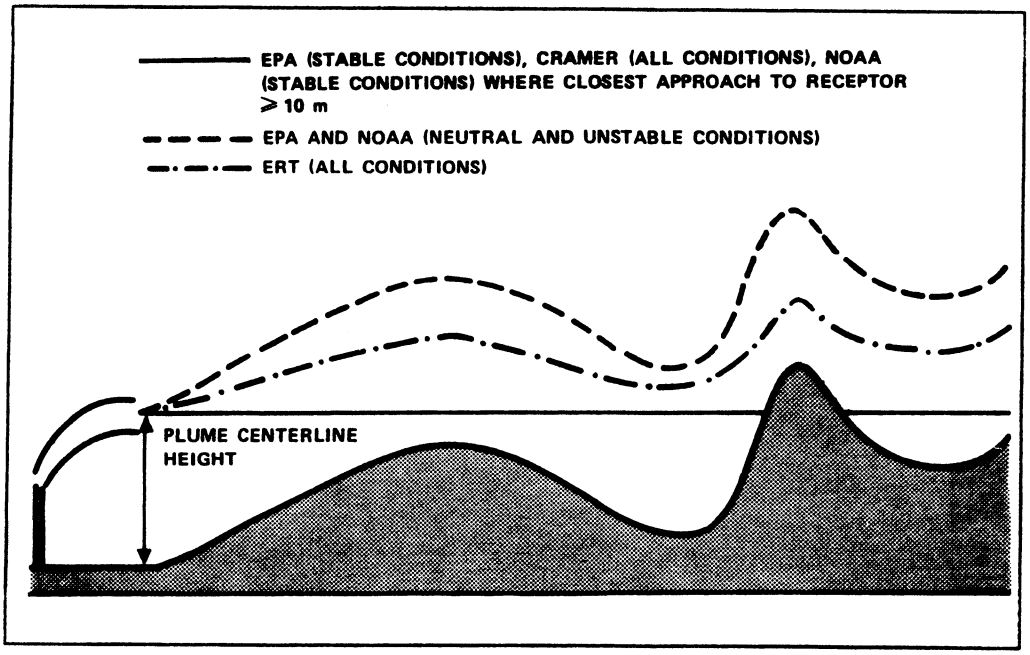

Figure 7–8. Simple assumptions for simulating plume centerline trajectory in complex terrain (from Fabrick et al., 1977). More advanced assumptions are discussed in Section 11.1.

computations (e.g., 8,760 hourly computations for each source–receptor contribution are required to estimate the annual average). Since meteorological and emission conditions are often the same at several different times, many of these hourly computations will provide the same concentration field output. The climatological model takes advantage of this repetition to compute long–term concentration averages without performing an expensive hour–by–hour simulation.

The procedure used is the following. Let us assume that a source can operate in N_i different emission conditions and that the meteorology can be described by N_j meteorological classes. Then the general climatological model equation becomes

$$\bar{c} = \sum_{i=1}^{N_i} \sum_{j=1}^{N_j} f_{ij} Q_i \psi_{ij} / \left(\sum_{i=1}^{N_i} \sum_{j=1}^{N_j} f_{ij} \right) \qquad (7\text{–}42)$$

where $\bar{c}$ is the average concentration in the receptor **r** due to the source in **s** during the period under examination; f_{ij} is the joint frequency of occurrence, during the same period, of the i–th emission condition and the j–th meteorological condition; Q_i is the pollutant emission rate during the i–th emission condition; and $Q_i \psi_{ij}$ is the steady–state equation (e.g., the Gaussian plume equation), which gives the concentration in **r** due to the emission in **s** with the i–th emission and the j–th meteorological scenarios (ψ_{ij} is referred to as the "kernel" of the concentration computation formula). If N_i x N_j is much smaller than the number of hours of the long–term period under investigation, Equation 7–42 is computationally faster than the hour–by–hour simulation and, for most practical cases, almost as accurate. Note that the term ψ_{ij} can be precomputed for all i and j, thus allowing easy recalculations with different emissions Q_i and/or different meteorology f_{ij}.

The climatological model is generally applied with the following further assumptions:

1. The Gaussian plume equation (Equation 7–4) is used for computing the kernel ψ_{ij}.

2. Q is constant (or depends only upon the meteorological condition j).

3. The meteorological condition j is given by the combination of a wind direction class j_1, a wind speed class j_2, and a stability class j_3 [i.e., f_{ij} becomes $f(j_1, j_2, j_3)$].

4. Because of the high frequency of occurrence of wind blowing in each wind direction sector, a uniform crosswind horizontal concentration distribution is assumed within each downwind sector.

5. Receptors are at ground level.

With the above assumptions, Equation 7–42 becomes

$$\bar{c} = \sum_{j_1\, j_2\, j_3} f(j_1,j_2,j_3)\, Q(j_1,j_2,j_3)\, \psi(j_1,j_2,j_3) \Big/ \left(\sum_{j_1\, j_2\, j_3} f(j_1,j_2,j_3) \right) \qquad (7\text{–}43)$$

where $\psi(j_1, j_2, j_3)$ is the uniform crosswind horizontal Gaussian kernel,

$$\psi(j_1,j_2,j_3) = \left(\frac{2}{\pi}\right)^{1/2} \frac{N_{wd}/(2\,\pi\,\Delta_d)}{\sigma_z\,\bar{u}} \exp\left[-\frac{1}{2}\left(\frac{z_s + \Delta h}{\sigma_z}\right)^2\right] \qquad (7\text{–}44)$$

Here N_{wd} is the number of wind direction sectors (i.e., $j_1 = 1, 2, \ldots, N_{wd}$; generally $N_{wd} = 16$); $\Delta_d(\mathbf{s},\mathbf{r},j_1)$ is the horizontal downwind distance between the source and the receptor; $\sigma_z(\Delta_d, j_3)$ is the vertical plume sigma; $\Delta h(j_2, j_3)$ is the plume rise; $\bar{u}(j_2)$ is the wind speed; and z_s is the source height. Equation 7–44 can be precomputed for each j_1, j_2, and j_3, thus providing a fast computational algorithm for $\bar{c}$. Clearly, Equation 7–44 must be applied only when the receptor **r** is downwind of the source **s** for the wind direction class j_2 (where downwind, in this case, means within a sector of $2\pi/N_{wd}$ angle in the horizontal); otherwise, ψ is equal to zero.

If the plume is uniformly mixed in the mixing layer, Equation 7–44 is further simplified as

$$\psi(j_1,j_2,j_3) = \frac{N_{wd}/(2\,\pi\,\Delta_d)}{z_i\,\bar{u}} \qquad (7\text{–}45)$$

where z_i is the mixing height.

Several authors (e.g., Martin, 1971; Calder, 1971; Runca et al., 1976) have used the climatological Gaussian model successfully. These long-term simulations generally provide better results than the short-term ones, due to error cancellation effects.

7.7 THE SEGMENTED PLUME MODEL

The Gaussian steady-state formula described in Equation 7-1 or 7-4 is valid only during transport conditions (e.g., $\bar{u} \geq 1$ m/s) in fairly stationary and homogeneous situations. In order to treat time-varying transport conditions and, especially, changes in wind direction, several authors (e.g., Hales et al., 1977; Benkley and Bass, 1979; Chan et al., 1979) have developed and used segmented Gaussian plume models. In the segmented plume approach, the plume is broken up into independent elements (plume segments or sections) whose initial features and time dynamics are a function of time-varying emission conditions and the local time-varying meteorological conditions encountered by the plume elements along their motion.

The segmented plume features are illustrated in Figure 7-9, which shows a plan view (solid lines) of a segmented plume encountering a progressive change of wind direction along its trajectory. Segments are sections of a Gaussian plume. Each segment, however, generates a concentration field that is

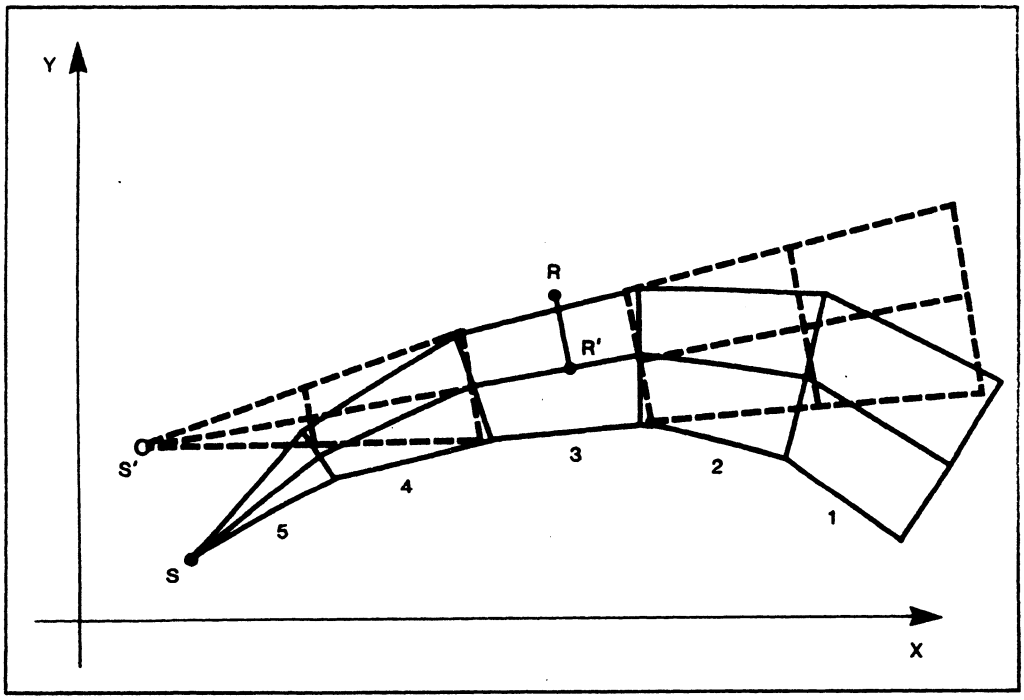

Figure 7-9. Computation of the concentration at the receptor R generated by the segmented plume (solid lines). The computation is performed by evaluating the contribution of the virtual plume (dotted lines) from the virtual source S' passing through the closest segment (number 3) to the receptor R (from Zannetti, 1986). [Reprinted with permission from Pergamon Press.]

still basically computed by Equation 7–1 and that represents the contribution of the entire virtual plume passing through that segment, as Figure 7–9 illustrates. Therefore, only one segment (the closest) affects the concentration computation at each receptor, except that the occurrence of a 180° wind direction change can create a condition where the contribution of two segments (that is, two virtual plumes) should be superimposed at some receptors.

7.8 PUFF MODELS

Puff models (e.g., Lamb, 1969; Roberts et al., 1970) have, like segmented models, been developed to treat nonstationary emissions in nonhomogeneous dispersion conditions. Puff methods, however, have the additional advantage of being able, at least theoretically, to simulate calm or low wind conditions.

The Gaussian puff model assumes that each pollutant emission of duration Δt injects into the atmosphere a mass $\Delta M = Q\Delta t$, where Q is the time-varying emission rate. The center of the puff containing the mass ΔM is advected according to the local time-varying wind vector. If, at time t, the center of a puff is located at $\mathbf{p}(t) = (x_p, y_p, z_p)$, then the concentration due to that puff at the receptor $\mathbf{r} = (x_r, y_r, z_r)$ can be computed using the basic Gaussian puff formula

$$\Delta c = \frac{\Delta M}{(2\pi)^{3/2}\,\sigma_h^2\,\sigma_z}\exp\left[-\frac{1}{2}\left(\frac{x_p - x_r}{\sigma_h}\right)^2\right]\exp\left[-\frac{1}{2}\left(\frac{y_p - y_r}{\sigma_h}\right)^2\right] \cdot \exp\left[-\frac{1}{2}\left(\frac{z_p - z_r}{\sigma_z}\right)^2\right] \tag{7–46}$$

which is often expanded to incorporate reflection and deposition/decay terms. Note that the analytical integration of Equation 7–46 in stationary, homogeneous transport conditions gives the Gaussian plume formula of Equation 7–4.

Equation 7–46 requires the proper evaluation of the horizontal (σ_h) and vertical (σ_z) dynamics of each puff's growth. The total concentration in a receptor at time t is computed by adding the contribution Δc from all existing puffs generated by all sources. Note that the "puff" Equation 7–46 differs from the "plume" Equation 7–4 mainly because an extra horizontal diffusion term has been substituted for the transport term, with the consequent disappearance of the wind speed $\bar{u}$. In other words, in a puff model, the wind speed affects the concentration computation only by controlling the density of puffs in the region (that

is, the lower the wind speed, the closer a puff is to the next one generated by the same source). Therefore, at least in theory, a puff model can handle calm or low-wind conditions, and this approach represents the most advanced and powerful application of the Gaussian formula.

Several studies have discussed the puff modeling approach in detail, improving its application features. In particular, algorithms were proposed and evaluated for incorporating wind shear effects (Sheih, 1978); virtual distance (Ludwig et al., 1977) and virtual age (Zannetti, 1981) computations were defined for correctly evaluating the σ_h and σ_z dynamics of the puff; puff merging (Ludwig et al., 1977) or puff splitting (Zannetti, 1981) were incorporated for performing cost-effective simulations with relatively large Δt (for example, 5 to 10 minutes); and an empirical method was derived (Zannetti, 1981) for evaluating the puff's σ_h and growth during calm or low-wind conditions as a function of currently available σ functions during transport conditions.

The determination of the puff modeling sigmas can be confusing, as discussed by Hanna et al. (1982). There are, in fact, two types of application for puff modeling. The one discussed above uses puffs to simulate the average characteristics (e.g., one-hour average concentrations) of a continuously emitted plume. In this case, it is correct to use the plume sigmas discussed in Section 7.2 to describe the growth of each puff in the plume. But puff (or better, relative diffusion) simulations apply also to the instantaneous or semi-instantaneous sources, defined as those sources where the release time or the sampling time is short compared with the travel time.

Unfortunately, little information is available for the description of the diffusion of a single puff, i.e., for the evaluation of the relative diffusion sigmas, even though it is clear that the plume sigma equations described in Section 7.2 cannot be applied (even though they often are) to relative diffusion calculations.

For relative diffusion, Hanna et al. (1982) recommend the Batchelor's formula

$$\sigma_h^2 = \epsilon t^3 \qquad (7\text{-}47)$$

for puff travel times that are less than 10^4 s, where ϵ is the eddy dissipation rate. They also recommend calculating ϵ locally at first, and then at a height $z = z_i/2$ as σ_z approaches $0.3\ z_i$. The eddy dissipation rate ϵ is given by

$$\epsilon = \frac{u_*^3}{k\,z}\left(\phi_m - \frac{z}{L}\right) \tag{7-48}$$

in the surface layer (ϕ_m was discussed in Section 3.6), while, at heights above the surface layer at midday,

$$\epsilon \simeq 0.5\,H' \tag{7-49}$$

The term H' is the surface buoyancy flux

$$H' = \frac{g}{T}\,\overline{w'T'} = \frac{H\,g}{c_p\,\varrho\,T} \tag{7-50}$$

where H is the surface heat flux defined by Equation 3-21. In neutral conditions, however, $H' = 0$ and, consequently, $\epsilon = 0$. In this case, a better fit of the available data gives, above the surface layer

$$\epsilon = u_*^3/(0.5\,z) \tag{7-51}$$

For travel times greater than 10^4 s, Hanna et al. (1982) suggest

$$\sigma_h = const\ t \tag{7-52}$$

where *const* can be determined by forcing Equation 7-52 to satisfy Equation 7-47 for $t = 10^4$ s, thus giving

$$const = 100\sqrt{\epsilon} \tag{7-53}$$

A similar procedure is proposed for σ_z, except that σ_z is recommended to remain equal to $0.3\ z_i$ for all times after it first reaches this value.

7.9 MIXED SEGMENT-PUFF METHODOLOGY

Zannetti (1986) has recently proposed a new mixed methodology that combines the advantages of both the segment and puff approaches for realistic

and cost-effective simulation of short-term plume dispersion phenomena using the Gaussian formula.

Pollutant dynamics are described by the temporal evolution of plume elements, treated as segments or puffs according to their size. While the segments provide a numerically fast simulation during transport conditions, the puffs allow a proper simulation of calm or low-wind situations.

The methodology is incorporated into a computer package (AVACTA II, Release 3) that gives the user large flexibility in defining the computational domain, the three-dimensional meteorological and emission input, the receptor locations, and in selecting plume rise and sigma fomulae. AVACTA II provides both pollutant concentration fields and dry/wet deposition patterns. The model uses linear chemistry and is applicable to any two-species reaction chain (e.g., SO_2 and SO_4^{2-}), where this approximation is reasonable and an appropriate reaction rate is available.

According to this dynamic segment-puff approach, each plume is described by a series of elements (segments or puffs) whose characteristics are updated at each dispersion time interval Δt (for example, 5 to 10 minutes). Meteorological three-dimensional fields (wind and turbulence status) and emission parameters are allowed to change at each "meteorological" time step Δt_m (typically, 30 to 60 minutes). The dynamics of each element consist of (1) generation at the source; (2) plume rise; (3) transport by advective wind; (4) diffusion by atmospheric turbulence; (5) ground deposition, dry and wet; and (6) chemical transformation, creating secondary pollutant from a fraction of the primary pollutant. The type of element (segment or puff) does not affect its dynamics, but only the computation of the concentration field, which is discussed in Section 7.9.6.

Each element is characterized by the following time-varying parameters (see the example in Figure 7-10) evaluated at its final central point B:

$\mathbf{e} = (x_e, y_e, z_e)$	coordinates of the point B
h_e	elevation of B above the ground (in flat terrain $h_e = z_e$)
M_1, M_2	masses of primary and secondary pollutant
$\sigma_h, \sigma_{z1}, \sigma_{z2}$	standard deviations of the Gaussian concentration distribution; horizontal, vertical below B, and vertical above B, respectively

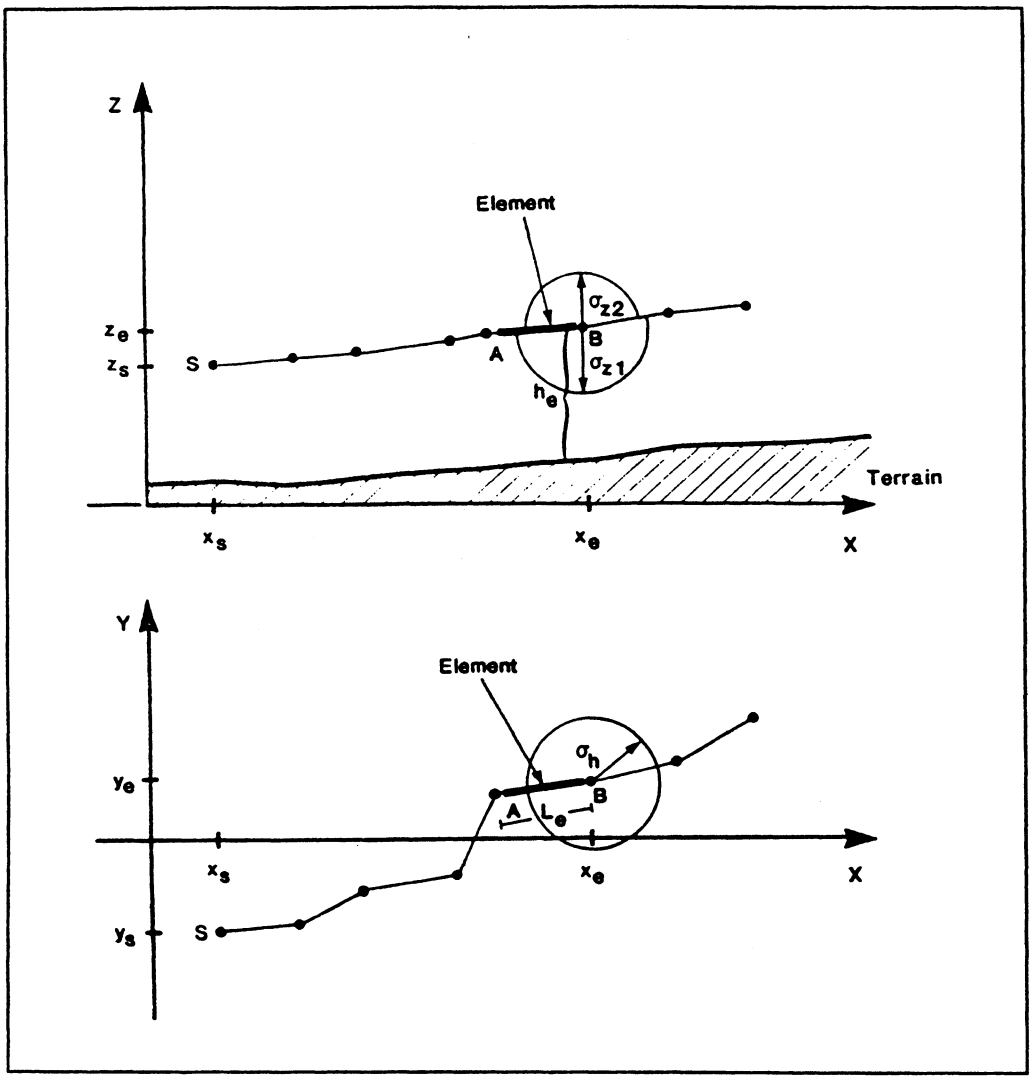

Figure 7–10. Chain of elements from the source S at time t. The time–varying parameters of a selected element in the chain are illustrated (from Zannetti, 1986). [Reprinted with permission from Pergamon Press.]

The characteristics of each element's initial central point A at time t are equal to those, at the same time t, of the final central point of the element successively emitted from the same source.

7.9.1 Generation of Plume Elements

At each time interval Δt, a new element is added to the element "chain" from each source. The parameters defining each new element have the following

initial values: the central final point is set at the source's exit point plus the vertical plume rise Δh; $M_1 = Q_1 \Delta t$, $M_2 = Q_2 \Delta t$, where Q_1 and Q_2 are the current emission rates of primary and secondary pollutants (generally $Q_2 = 0$); and σ_h, σ_{z1}, and σ_{z2} represent the initial sigmas of the plume (for example, 0.369 multiplied by the source exit diameter may be chosen for σ_h, and $\Delta h/3.16$ for σ_{z1} and σ_{z2}).

7.9.2 Transport

At each time interval Δt, the central final point of each existing element is advected according to the current wind vector $\bar{\mathbf{u}} = (u_x, u_y, u_z)$ averaged over the volume covered by the element size (i.e., $\pm 2\sigma$), as follows

$$\mathbf{e}^{(new)} = \mathbf{e}^{(old)} + \bar{\mathbf{u}} \Delta t \tag{7-54}$$

However, if the horizontal transport term

$$u_h = (u_x^2 + u_y^2)^{1/2} \tag{7-55}$$

is less than a critical value $u_{\min}$ (for example, $u_{\min} = 1$ m s^{-1}), u_x and u_y are forced to zero, since it is assumed that such small terms represent more local intermittent effects than actual transport. In this case, however, a large horizontal diffusion may be produced by the large wind direction fluctuations typically encountered during these low wind speed situations.

7.9.3 Diffusion

During each Δt, the element's sigmas are increased based on the virtual distance/age concept (Ludwig et al., 1977; Zannetti, 1981), which operates for either σ_h, σ_{z1}, or σ_{z2}, according to the following scheme.

1. Select the current sigma function $\sigma = \sigma(d)$ for the element (d is the downwind distance) according to the current local meteorology at the element's location; that is, the average atmospheric turbulent status in the volume covered by the element size (atmospheric turbulence status is often represented simply by a "stability class," a discrete number).

2. Evaluate the virtual distance d_v such as

$$\sigma^{(old)} = \sigma(d_v) \tag{7-56}$$

where $\sigma^{(old)}$ is the current sigma value for the element. The computation in Equation 7–56 is straightforward for some sigma formulae (for example, power laws), but requires iterative procedures for others.

3. If $u_h < u_{\min}$ force $u_h = u_{\min}$.

4. Increment sigma by

$$\sigma^{(new)} = \sigma(d_v + u_h \Delta t) \tag{7-57}$$

The above dynamics of the element's sigmas depend upon the choice of the sigma function and the current atmospheric turbulence status at the element's location. A separate turbulence status can be considered for the computation of horizontal (σ_h) and vertical (σ_{z1}, σ_{z2}) increments, if a proper meteorological input is available. For example, the vertical temperature gradient might provide an evaluation of the "vertical" turbulence status, while the horizontal wind direction fluctuation intensity provides a good estimate of the "horizontal" turbulence status. (Without the measurement of the horizontal wind direction fluctuation, the estimate of "horizontal" turbulence status may be quite wrong.) Different values of the vertical turbulence status above and below the element center generate different dynamics for σ_{z1} and σ_{z2}.

7.9.4 Dry and Wet Deposition

Both dry and wet deposition for the primary and secondary pollutants are simulated by first-order reaction schemes and are computed during each Δt by an exponential reduction of the pollutant mass

$$M_i^{(new)} = M_i^{(old)} \exp\left[-P_{i,j}\,\Delta t/360,000\right] \tag{7-58}$$

where i indicates the primary ($i = 1$) or the secondary ($i = 2$) pollutant, j indicates dry ($j = 1$) or wet ($j = 2$) deposition, and $P_{i,j}$ is the corresponding percentage of reduction per hour (% h^{-1}). All mass differences $M_i^{(old)} - M_i^{(new)}$ are deposited and accumulated on the ground.

If the two $P_{i,1}$ for dry deposition are not directly specified as input values, they can be obtained from the deposition velocity values as

$$P_{i,1} = 360,000\ V_i/\Delta z_e \tag{7-59}$$

where V_i are the current deposition velocities at the element's location, and $\Delta z_e = (2\sigma_{z1} + 2\sigma_{z2})$ is the vertical thickness of the element. Equation 7-59 applies only when the plume has reached the ground (that is, $2\sigma_{z1} \geq h_c$), otherwise $P_{i,1} = 0$.

If the two $P_{i,2}$ for wet deposition are not directly specified as input values, they can be obtained (Draxler and Heffter, 1981) from precipitation data as

$$P_{i,2} = S_i\ P_r/(10T_p) \tag{7-60}$$

where S_i are the pollutant scavenging ratios, P_r is the current average precipitation rate at the element's location (mm h^{-1}), and T_p is the thickness (m) of the precipitation layer.

7.9.5 Chemical Transformation

During each Δt, a first-order chemical reaction scheme is adopted, in which the chemical transformation term reduces the mass M_1 of primary pollutant and increases the mass M_2 of secondary pollutant in each element according to

$$M_1^{(new)} = M_1^{(old)} \exp\ (-k\ \Delta t/360,000) \tag{7-61}$$

$$M_2^{(new)} = M_2^{(old)} + (w_2/w_1)\ M_1^{(old)}\ [1 - \exp\ (-k\ \Delta t/360,000)] \tag{7-62}$$

where k is the current chemical transformation factor at the element location expressed as a percentage of reduction per hour (% h^{-1}), and w_i are the pollutant molecular weights ($i = 1, 2$).

7.9.6 Concentration Computation

The plume element dynamics can be computed independently from the type of element (segment or puff). The element type, however, is a key factor in computing the plume concentration field during each Δt. The criterion for

identifying the type of element is the ratio between its length L_e (the horizontal distance between A and B in Figure 7–10) and σ_h. For a segment

$$L_e/\sigma_h > 2 \tag{7–63}$$

and, for a puff,

$$L_e/\sigma_h \leq 2 \tag{7–64}$$

where the center of the puff is located in the middle between A and B. Since σ_h continues to grow with time, all segments will eventually become puffs.

The above algorithm assures that, when segments are transformed into puffs, the distance between two consecutive puffs will not be greater than $2\sigma_h$, which is the condition required (Ludwig et al., 1977) for a series of puffs to provide an almost perfect representation of a continuous plume. In calm or low wind speed conditions, $L_e = 0$ and the elements are generated as puffs directly from the source.

The above scheme allows a realistic and computationally efficient representation of calm, transport and transitional cases. For example, puffs can accumulate for a few hours in the region near the source during calm conditions, and subsequently be advected downwind when the stagnation breaks up. The concentration at each receptor point due to a certain source must account for the contribution of all elements generated from that source; specifically, the sum of the contributions of all existing puffs plus the contribution of the closest segment. This allows a proper dynamic representation of both calm and transport conditions, including the previously mentioned situation in which, due to a 180° change in wind direction, two sections of the same plume may affect the same receptor. In this latter case, in fact, we can generally assume that the elements of the oldest section of the plume may have already become puffs, thus allowing both sections of the plume to contribute to the concentration computation at that receptor.

7.9.6.1 Puff Contribution

The concentration contribution of a single puff at a receptor during each Δt is computed by Equation 7–46, which allows the computation of the primary pollutant concentration c_1 (or the secondary one c_2) from the current values of the puff's variables M_1 (or M_2), σ_h, and σ_{z1} (or σ_{z2} if the receptor is above the center of the puff). These variables are evaluated by interpolation at the center of the puff, that is, the point between its initial and final central points.

7.9.6.2 Segment Contribution

Because of the condition defined in Equation 7–63, each segment has sufficient length L_e to assure that the horizontal "stream-wise" diffusion (that is, diffusion along the length of the segment) can be neglected in comparison with the transport term. This is one of the basic assumptions for Equation 7–4, which is used as the numerical algorithm for computing the concentration field due to a plume segment. This computation requires the identification of the segment closest to the receptor and the use of the segment's variables for computing, with Equation 7–4, the concentration field generated by an equivalent plume passing through the segment, as illustrated in Figure 7–9. The parameters in Equation 7–4 are evaluated in the following way:

1. The segment's variables (M_1, M_2, σ_h, σ_{z1}, σ_{z2}) are interpolated at the point R′ (see Figure 7–9), the closest point to R along the segment centerline.

2. Q is evaluated as a "virtual" current emission rate; i.e.,

$$Q = \left(\frac{M_1}{\Delta t}\right) or \left(\frac{M_2}{\Delta t}\right) \tag{7–65}$$

3. $\bar{u}$ is evaluated as a "virtual" current wind speed; i.e.,

$$\bar{u} = \frac{L_e}{\Delta t} \tag{7–66}$$

(However, $\bar{u}$ is forced to be $\geq u_{\min}$ to avoid unrealistic "convergence" effects.)

4. σ_{z2} is used instead of σ_{z1}, if the receptor R is above the point R'.

Naturally, only the closest segment is used, since its contribution is a surrogate for that of the entire segmented portion of the plume.

7.9.6.3 The Treatment of the Segment–Puff Transition

The concentration computation described in the previous section allows the incorporation of all the advantages of both the puff and the segmented approach. Numerical problems, however, arise when the receptor is close to the point in the plume at which segments grow into puffs (see Zannetti, 1986, for a discussion of how these problems have been eliminated).

7.9.6.4 Splitting of Elements

The breaking of a plume into elements allows the evaluation of their dynamics as a function of the local time-varying meteorological conditions. In particular, during each Δt, the final central point of each element moves from an old to a new position. The horizontal component of this advective displacement is

$$\Delta \mathbf{d}_h = \mathbf{u}_h \, \Delta t \tag{7-67}$$

where $\mathbf{u}_h = (u_x, u_y)$ is the current local horizontal wind vector.

Large values of $|\Delta \mathbf{d}_h|$, due to an increase in wind speed or associated to a change in wind direction, may affect the elements' ability to represent the continuous plume by reducing resolution. The splitting technique, which was originally proposed for puff modeling simulations (Zannetti, 1981), is here incorporated for both puffs and segments and is illustrated in Figure 7-11. This splitting generates, when required, enough fictitious elements along the element's trajectory during Δt to maintain sufficient resolution. The splitting of an element's trajectory is performed to compute its concentration contribution at receptor R when (1) the receptor R is affected by that element, and (2) for puffs, when $|\Delta \mathbf{d}_h| > \sigma_h$ and, for segments, when $|\Delta \mathbf{d}_t| > \sigma_h$, where $\Delta \mathbf{d}_t$ is the component of $\Delta \mathbf{d}_h$ which is perpendicular to the segment's centerline.

In this splitting computation, the masses M_1 and M_2 of the element are equally distributed among the split elements along the trajectory from the old position to the new one.

7.10 DERIVATIONS OF THE GAUSSIAN EQUATIONS

The Gaussian equations can be derived from both Eulerian and Lagrangian considerations and that is the reason Gaussian models are discussed here separately from Eulerian models (Chapter 6) and Lagrangian models (Chapter 8).

There are several ways to derive the steady-state Gaussian plume Equation 7-4. Four methods will be discussed briefly in this section.

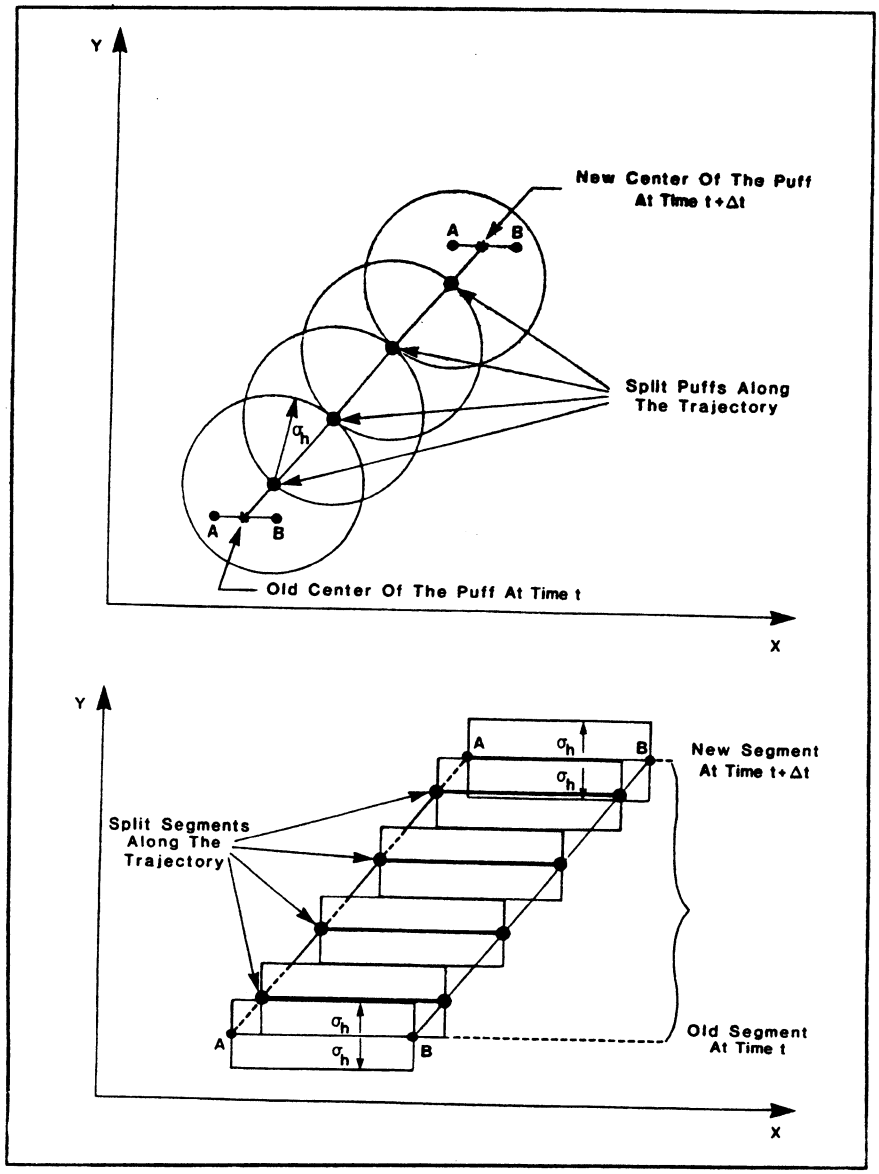

Figure 7–11. Splitting process for a puff (above) and a segment (below). A and B represent the initial and final central points of the element (from Zannetti, 1986). [Reprinted with permission from Pergamon Press.]

7.10.1 Semiempirical Derivation

The straightforward semiempirical derivation is performed by assuming that the plume concentration c, at each downwind distance x, has independent Gaussian distributions both in the horizontal and in the vertical. Therefore,

$$c(x,y,z) = const \frac{1}{\sqrt{2\pi}\sigma_h} \exp\left[-\frac{1}{2}\left(\frac{\Delta_{cw}}{\sigma_h}\right)^2\right] \cdot \frac{1}{\sqrt{2\pi}\sigma_z} \exp\left[-\frac{1}{2}\left(\frac{h_e - z_r}{\sigma_z}\right)^2\right] \tag{7-68}$$

where the symbols are the same as in Section 7.1 but x is used as the downwind distance instead of d.

The mass conservation condition requires all concentration fluxes through each plume cross-sectional plane (y,z) to be the same; i.e., for each x

$$Q = \int_{(y,z)} c(x,y,z)\,\bar{u}\,dydz \tag{7-69}$$

which, with Equation 7–68, gives $const = Q/\bar{u}$, and therefore Equation (7–4).

7.10.2 Gaussian Plume as Superimposition of Gaussian Puffs

A plume can be represented by an infinite series of infinitesimal puffs, where each puff, located in x,y,z, generates the concentration field

$$dc(x,y,z) = \frac{dM}{(2\pi)^{3/2}\sigma_x\sigma_y\sigma_z} \cdot \exp\left\{-\frac{1}{2}\left[\left(\frac{x-x_r}{\sigma_x}\right)^2 + \left(\frac{y-y_r}{\sigma_y}\right)^2 + \left(\frac{z-z_r}{\sigma_z}\right)^2\right]\right\} \tag{7-70}$$

at the receptor (x_r, y_r, z_r), and $dM = Q\,dt = Q\,dx/\bar{u}$ is the mass of the puff. Then, the integration along x of Equation 7–70 gives Equation 7–4, if $\sigma_x = \sigma_y = \sigma_h$.

7.10.3 Analytical Solution of the Steady-State Atmospheric Diffusion Equation 6–8

Several papers provided a derivation of Equation 7–4 by analytical integration of Equation 6–8 under certain simplifying homogeneous conditions

(e.g., Veigele and Head, 1978; Huang, 1979; Melli and Runca, 1979; Lupini and Tirabassi, 1979; Robson, 1983; Seinfeld, 1986). We should not state, however, that the Gaussian Equation 7–4 is a *particular* solution of Equation 6–8. In fact, if Equation 7–4 is derived from Equation 6–8, a condition is imposed on the plume's σ_h and σ_z. In the homogeneous case, this condition is

$$\sigma_h = \sqrt{2\,K_{11}\,x/\bar{u}} = \sqrt{2\,K_{22}\,x/\bar{u}} \tag{7–71}$$

and

$$\sigma_z = \sqrt{2\,K_{33}\,x/\bar{u}} \tag{7–72}$$

Equations 7–71 and 7–72 limit the sigma growth so that it is proportional to $x^{0.5}$, while Gaussian plume simulations benefit from the use of semiempirical σ functions that vary from $\sim x^{0.5}$ to $\sim x^{1.5}$.

Numerical and analytical integrations of Equation 6–8 in *nonhomogeneous* conditions show concentration solutions that are more realistic, in the sense that the plume sigmas are proportional to x^b with $b > 0.5$. Nevertheless, K–theory simulations always present difficulties in reproducing dispersion experiments in unstable conditions. What we want to emphasize here, however, is that the Gaussian equation cannot be considered a particular solution of Equation 6–8, even though its *form* can.

7.10.4 The Gaussian Equations as a Particular Solution of the Lagrangian Equation

All Gaussian plume and puff equations can be seen as a particular solution of the fundamental Lagrangian Equation 8–1, as discussed in the next Chapter.

REFERENCES

Benkley, C.W., and A. Bass (1979): Development of mesoscale air quality simulation models; Volume 3, User's Guide to MESOPUFF (Mesoscale Puff) model. EPA Document 600/7-79-XXX, Research Triangle Park, North Carolina. (See also Scire et al. (1984): User's guide to the MESOPUFF II model and related processor programs. EPA Document 600/8-84-013.)

Best, P.R., M. Kanowski, L. Stumer, and D. Green (1986): Convection dispersion modeling utilizing acoustic sounder information. *Atmos. Res.*, **20**:173.

Bowers, J., J. Bjorklund, and C. Cheney (1979): Industrial source complex (ISC) dispersion model user's guide, Vol. I. Research Triangle Park, North Carolina. EPA Document EPA-450/4-79-030. NTIS Publication PB80-133044.

Briggs, G.A. (1973): Diffusion estimation for small emissions, in environmental research laboratories. Air Resources Atmospheric Turbulence and Diffusion Laboratory 1973 Annual Report. USAEC Report ATDL-106, National Oceanic and Atmospheric Administration, December 1974.

Briggs, G.A. (1985): Analytical parameterization of diffusion: The convective boundary layer. *J.Climate and Appl. Meteor.*, **24**:1167.

Calder, K.L. (1971): *Proceedings,* 2nd Meeting of Expert Panel Air Pollution Modeling, NATO/CCMS Air Pollution, No. 5.

Chan, M.W., and I.H. Tombach (1978): AVACTA -- Air pollution model for complex terrain applications. AeroVironment Inc., Monrovia, California.

Chan, M.W. (1979): A tracer experiment to determine the transport and diffusion of an elevated plume in complex terrain. *Proceedings*, 72nd Annual APCA Meeting, Cincinnati, Ohio, June.

Chan, M.W., S.J. Head, and S. Machiraju (1979): Development and validation of an air pollution model for complex terrain application. Paper presented at NATO/CCMS Air Pollution Pilot Study. Rome, Italy. AeroVironment Technical Paper 9559, Monrovia, California.

DeMarrais, G.A. (1978): Atmospheric stability class determinations on a 481-meter tower in Oklahoma. *Atmos. Environ.*, **12**:1957-1964.

Dobbins, R.A. (1979): *Atmospheric Motion and Air Pollution*. John Wiley & Sons, New York.

Draxler, R.R. (1976): Determination of atmospheric diffusion parameters. *Atmos. Environ.*, **10**:99-105.

Draxler, R.R., and J.L. Heffler (1981): Workbook for estimating the climatology of regional-continental scale atmospheric dispersion and deposition over the United States. NOAA Technical Memorandum ERL ARL-96, Air Resources Laboratories, Silver Spring, Maryland.

Environmental Research and Technology, Inc. (1984): User's guide to the rough terrain diffusion model (RTDM). Environmental Research and Technology Document M2209-585, Concord, Massachusetts.

Fabrick, A., R.C. Sklarew, and J.D. Wilson (1977): *Point Source Modeling*. Form & Substance, Inc., Westlake Village, California.

Gifford, F.A. (1961): Use of routine meteorological observations for estimating the atmospheric dispersion. *Nucl. Safety*, **2**(4):47-57.

Gifford, F.A. (1976): Consequences of effluent release. *Nucl. Safety*, **17**(1):68-86.

Green, A.E., R.P. Singhal, and R. Venkateswar (1980): Analytic extensions of the Gaussian plume model. *JAPCA*, **30**(7):773–776.

Gryning, S.E., A.A. Holtslag, J.S. Irwin, and B. Sivertsen (1987): Applied dispersion modeling based on meteorological scaling parameters. *Atmos. Environ.*, **21**:79–89.

Hales, J.M., D.C. Powell, and T.D. Fox (1977): STRAM -- An air pollution model incorporating non-linear chemistry, variable trajectories, and plume segment diffusion. U.S. EPA Document 450/3-77-012, Research Triangle Park, North Carolina.

Hanna, S.R., et al. (1977): AMS Workshop on Stability Classification Schemes and Sigma Curves -- Summary of Recommendations. *J. Climate and Appl. Meteor.*, **58**(12):1305–1309.

Hanna, S.R., G.A. Briggs, and R.P. Hosker, Jr. (1982): Handbook on atmospheric diffusion. U.S. Department of Energy Document DOE/TIC-11223 (DE82002045), Office of Health and Environmental Research.

Hanna, S.R., L.L. Schulman, R.J. Paine, and J.E. Pleim (1984): Users guide to the offshore and coastal dispersion (OCD) model. Environmental Research and Technology, Concord, Massachusetts. Contract No. 14-08-0001-21138.

Hanna, S.R. (1989): Plume dispersion and concentration fluctuations in the atmosphere. Chapt. 14 *Encyclopedia of Environmental Control Techology*. Vol. 2. P.N. Cheremisinoff, editor. Houston, Texas: Gulf Publishing Company.

Harvey, Jr., R.B., and J.N. Hamawi (1986): A modification of the Gaussian dispersion equation to accommodate restricted lateral dispersion in deep river valleys. *APCA Note-Book*, **36**:171.

Huang, C.H. (1979):A theory of dispersion in turbulent shear flow. *Atmos. Environ.*, **13**:453.

Irwin, J.S. (1979): Estimating plume dispersion -- A recommended generalized scheme. Presented at 4th AMS Symposium on Turbulence and Diffusion, Reno, Nevada.

Irwin, J.S. (1980): Dispersion estimates suggestion #9: Processing of wind data. U.S. EPA Docket Reference No. II-B-33, Research Triangle Park, North Carolina.

Ludwig, F.L., L.S. Gasiorek, and R.E. Ruff (1977): Simplification of a Gaussian puff model for real-time minicomputer use. *Atmos. Environ.* **11**:431–436.

Lupini, R. and T. Tirabassi (1979): Gaussian plume model and advection-diffusion equation: An attempt to connect the two approaches. *Atmos. Environ.*, **13**:1169–1174.

Lyons, W.A., and H.S. Cole (1983): Fumigation and plume trapping on the shores of Lake Michigan during stable onshore flow. *J. Appl. Meteor.*, **12**:494–510.

Lamb, R.G. (1969): An air pollution model of Los Angeles. M.S. thesis, University of California, Los Angeles, 120 pp. (see Lamb, R.G., and M. Neiburger (1971): An interim version of a generalized urban diffusion model. *Atmos. Environ.*, **5**:239–264).

Martin, D.O. (1971): An urban diffusion model for estimating long-term average values of air quality. *JAPCA*, **21**:16–23.

McElroy, J.L., and F. Pooler (1968): St. Louis dispersion study; Volume II, Analysis. National Air Pollution Control Administration, Publication AP-53, 51. U.S. Dept. of Health, Education and Welfare, Arlington, Virginia.

Melli, P., and E. Runca (1979): Gaussian plume model parameters for ground-level and elevated sources derived from the atmospheric diffusion equation in a neutral case. *J. Appl. Meteor.*, **18**:1216–1221.

Pasquill, F. (1971): Atmospheric dispersion of pollution. *J. Roy. Meteor. Soc.*, 97:369–395.

Panofsky, H.A., and J.A. Dutton (1984): *Atmospheric Turbulence*. New York: John Wiley.

Pasquill, F. (1976): Atmospheric dispersion parameters in Gaussian plume modeling; Part 2, Possible requirements for change in the Turner Workbook values. U.S. EPA Document EPA–600/4–76–030b, Washington, D.C.

Phillips, P., and H.A. Panofsky (1982): A reexamination of lateral dispersion from continuous sources. *Atmos. Environ.*, *16*:1851–1859.

Roberts, J.J., E.S. Croke, and A.S. Kennedy (1970): An urban atmospheric dispersion model. *Proceedings*, Symposium on Multiple–Source Urban Diffusion Models. Air Pollution Control Office Publication AP–86, pp. 6.1–6.72.

Robson, R.E. (1983): On the theory of plume trapping by an elevated inversion. *Atmos. Environ.*, **17**:1923–2930.

Runca, E. (1977): Transport and diffusion of air pollutants from a point source. *Proceedings*, IFIP Working Conference on Modeling and Simulation of Land, Air and Water Resource System, Ghent, Belgium.

Schulman, L.L., and J.S. Scire (1980): Development of an air quality dispersion model for aluminum reduction plants. Environmental Research and Technology. Document P–7304A, Concord, Massachusetts.

Schulman, L.L., and S.R. Hanna (1986): Evaluation of downwash modification to the industrial source complex model. *JAPCA*, **36**:256–264.

Seinfeld, J.H. (1986): *Atmospheric Chemistry and Physics of Air Pollution*. New York: John Wiley & Sons.

Sheih, C.M. (1978): A puff pollutant dispersion model with wind shear and dynamic plume rise. *Atmos. Environ.*, **12**:1933–1938.

Smith, M.E. (1968): Recommended guide for the prediction of the dispersion of airborne effluents. 1st edition. American Society of Mechanical Engineers, New York.

Stern, A.C., Ed. (1976): *Air Pollution*. Volume I, 3rd Edition. New York: Academic Press.

Strimaitis, D.G., D.C. DiCristofaro, and T.F. Lavery (1986): The complex terrain dispersion model. EPA Document EPA–600–D–85/220, Atmospheric Sciences Research Laboratory, Research Triangle Park, North Carolina.

Turner, D.B. (1970): Workbook of atmospheric dispersion estimates. EPA, Research Triangle Park, North Carolina. U.S. EPA Ref. AP–26 (NTIS PB 191–482.)

U.S. Environmental Protection Agency (1978): Guideline on air quality models. EPA Document EPA–450/2–78–025. Research Triangle Park, North Carolina.

U.S. Environmental Protection Agency (1986): Guideline on air quality models (Revised). U.S. EPA Document EPA–450/2–78–027R. Research Triangle Park, North Carolina.

van Dop, H., R. Steenkist, and F.T. Nieuwstadt (1979): Revised estimates for continuous shoreline fumigation. *J. Appl. Meteor.*, **18**:133–137.

Veigele, W.J., and J.H. Head (1978): Derivation of the Gaussian plume model. *JAPCA*, **28**:1139–1141.

Williamson, S.J. (1973): *Fundamentals of Air Pollution*. Reading, Massachusetts: Addison–Wesley.

Yamartino, R.J. (1977): A new method for computing pollutant concentrations in the presence of limited vertical mixing. *APCA Note-Book*, **27**(5):467.

Zannetti, P. (1981): An improved puff algorithm for plume dispersion simulation. *J. Applied Meteor.*, **20**(10):1203–1211.

Zannetti, P., and N. Al-Madani (1983a): Numerical simulations of Lagrangian particle diffusion by Monte-Carlo techniques. VIth World Congress on Air Quality (IUAPPA), Paris, May.

Zannetti, P., and N. Al-Madani (1983b): Simulation of transformation, buoyancy and removal processes by Lagrangian particle methods. Fourteenth ITM Meeting on Air Pollution Modeling and Its Application. Copenhagen, Denmark, September.

Zannetti, P. (1986): A new mixed segment–puff approach for dispersion modeling. *Atmos. Environ.*, **20**:1121–1130.

8 LAGRANGIAN DISPERSION MODELS

As introduced in Chapter 6, Lagrangian models provide an alternative method for simulating atmospheric diffusion. They are called Lagrangian because they describe fluid elements that follow the instantaneous flow. The "Lagrangian" term was initially used to distinguish the Lagrangian box models described in Section 8.2 from the Eulerian box models described in Section 6.4. In this case, the difference is manifest, since the Eulerian box does not move, while the Lagrangian box follows the average wind trajectory. The term has, however, been extended to describe all models in which plumes are broken up into "elements," such as segments (see Section 7.7), puffs (see Section 7.8) or fictitious particles (see Section 8.3).

Several efforts have been made to understand and parameterize the relationship between equivalent atmospheric parameters as seen in an Eulerian and a Lagrangian view. Hanna (1979) performed statistical analyses of wind fluctuations and showed that both Lagrangian and Eulerian observations of wind speed fluctuations u' can be simulated by the linear first-order autoregression relationship

$$u'(t+\Delta t) = u'(t)\, R(\Delta t) + u''(t) \qquad (8\text{–}1)$$

where $R(\Delta t)$ is the autocorrelation coefficient at time lag Δt and u'' is a random component. Davis (1982) examined various theories that aim at relating the velocity statistics of Lagrangian particles to the statistics of the Eulerian flow in which they move. Novikov (1969) proposed a connection between Lagrangian and Eulerian probabilities that was then generalized (Novikov, 1986) to fluids with variable density. In spite of the above efforts (and others), uncertainties still persist and a fully acceptable theoretical relationship between Eulerian and Lagrangian variables has not yet been developed (or, if it has, has not been fully tested against experimental data; testing is complicated by the fact that reliable Lagrangian measurements are scarce).

8.1 THE LAGRANGIAN APPROACH

The fundamental Lagrangian equation for atmospheric dispersion of a single pollutant species is

$$< c(\mathbf{r}, t) > = \int_{-\infty}^{t} \int p(\mathbf{r}, t|\mathbf{r}', t')\, S(\mathbf{r}', t')\, d\mathbf{r}'\, dt' \tag{8-2}$$

where the integration in space is performed over the entire atmospheric domain; $<c(\mathbf{r},t)>$ is the ensemble average concentration at $\mathbf{r}$ at time t; $S(\mathbf{r}',t')$ is the source term (mass volume^{-1} time^{-1}); and $p(\mathbf{r},t|\mathbf{r}',t')$ is the probability density function (volume^{-1}) that an air parcel moves from $\mathbf{r}'$ at t' to $\mathbf{r}$ at t, where, for any $\mathbf{r}'$ and $t > t'$,

$$\int p(\mathbf{r}, t|\mathbf{r}', t')\, d\mathbf{r} \leq 1 \tag{8-3}$$

The expression in Equation 8–3 can be less than one when chemical or deposition phenomena are considered; otherwise, mass conservation always requires the value to be equal to one. For a primary pollutant, $S(\mathbf{r}',t')$ is greater than zero only at points $\mathbf{r}'$ where the pollutant is released (e.g., the exit points of stacks). For a secondary pollutant, $S(\mathbf{r}',t')$ can be nonzero virtually anywhere. For both primary and secondary pollutants, however, Equation 8–3, which represents mass conservation, must be satisfied.

Since it is often difficult to evaluate the entire emission "history" $S(\mathbf{r}',t')$ for $-\infty \leq t' \leq t$, Equation 8–2 can be rewritten as the sum of two integral terms

$$\begin{aligned} < c(\mathbf{r}, t) > &= \int p(\mathbf{r}, t|\mathbf{r}', t_o) < c(\mathbf{r}', t_o) > d\mathbf{r}' \\ &+ \int_{t_o}^{t} \int p(\mathbf{r}, t|\mathbf{r}', t')\, S(\mathbf{r}', t')\, d\mathbf{r}'\, dt' \end{aligned} \tag{8-4}$$

in which only the contribution of the sources during $t_o \leq t' \leq t$ needs to be included, since the first integral term accounts for the source contribution before t_o. However, Equation 8–4 requires some estimate of the average concentration $<c>$ at t_o throughout the computational domain.

It must be pointed out that the use of Equation 8–4 instead of Equation 8–2 may be incorrect when the exact fractional impact of a specific source

(or group of sources) needs to be estimated. In fact, when using Equation 8–4, known background concentrations can be used to estimate the term $<c(\mathbf{r}',t_o)>$. But, by so doing, the contribution of a specific source to the concentration $<c(\mathbf{r},t)>$ becomes the sum of two terms: (1) the direct contribution of the second integral of Equation 8–4, and (2) the indirect contribution of the source to the background concentration $<c(\mathbf{r}',t_o)>$. When these two contributions are of the same order of magnitude, as in long-range regional modeling applications, the fractional impact of a specific source becomes difficult to evaluate because, even when the second integral of Equation 8–4 is computed correctly, the contribution of a source to background concentrations is difficult to calculate.

The key parameter in the above equations is the probability density function p, which, for nonreactive pollutants, is a function of only the meteorology (and the type of pollutant when deposition phenomena are considered). Equations 8–2 or 8–4 represent a rigorous description of transport and diffusion processes expressed in a probabilistic notation. The full incorporation of chemical reactions, however, is difficult.

Different assumptions concerning the probability density function p allow the derivation of both Gaussian equations and the K-theory equation, as was illustrated in Figure 6–1. Seinfeld (1975) shows that all Gaussian plume and puff formulas can be derived from the Lagrangian equation (8–2) under the following simplifying assumptions:

1. Turbulence is stationary and homogeneous; i.e.,

$$p(\mathbf{r},\ t|\mathbf{r}',\ t') \ = \ p(\mathbf{r}-\mathbf{r}',\ t-t') \tag{8–5}$$

2. p obeys a multidimensional normal distribution; i.e.,

$$p(\mathbf{r}-\mathbf{r}',\ t-t') \ = \ \frac{1}{(2\,\pi)^{3/2}\,|\mathbf{P}|^{1/2}}\ \exp\,[-\zeta^{T}\mathbf{P}^{-1}\,\zeta/2\ ] \tag{8–6}$$

where each element P_{ij} of the matrix $\mathbf{P}$ is (i and j = 1, 2, or 3)

$$P_{ij} \ = \ <\zeta_i\zeta_j> \tag{8–7}$$

and the "displacements" ζ_i are

$$\zeta_i \ = \ |\mathbf{r}-\mathbf{r}'|_i \ - \ |<\mathbf{r}-\mathbf{r}'>|_i \tag{8–8}$$

in which i indicates the space component (x, y, or z, for i = 1, 2, or 3, respectively).

3. The term $< \mathbf{r} - \mathbf{r}' >$ is the average displacement, which is assumed to be due only to the average (deterministic) wind $\bar{\mathbf{u}}$.

4. $P_{ij} = 0$, for $i \neq j$.

Several types of models can be classified as Lagrangian:

- Lagrangian box, or trajectory, models, which are used for photochemical simulations (see Section 8.2 below)
- Gaussian segmented plume models, which have been discussed in Section 7.7
- Gaussian puff models, which have discussed in Section 7.8
- Particle models (see Section 8.3 below)

8.2 LAGRANGIAN BOX MODELS

Lagrangian box models are similar to the Eulerian box models presented in Section 6.4, with the important difference that a Lagrangian box is a moving box that is advected horizontally according to the local time-varying average wind speed and direction, as illustrated in Figure 8-1 (for a single box) and Figure 8-2 (for a vertical column of boxes, which allows explicit computation of vertical diffusion).

This technique is particularly useful for photochemical simulations (see Chapter 9) and provides average time-varying concentration estimates along the trajectory of the box. The major shortcoming of this technique is the forced assumption of a constant wind speed and direction throughout the PBL, while, in reality, wind shear plays an important role. Another problem of Lagrangian box models is the difficulty in comparing their outputs (i.e., time-varying concentrations along a trajectory) with fixed (Eulerian) air quality monitoring data.

Several Lagrangian box models have been developed for simulating photochemical reactions inside a moving air mass. This development was triggered by the high computational costs of Eulerian photochemical models, in which chemical and photochemical reactions need to be computed in each *fixed* grid cell of the three-dimensional computational domain. Lagrangian box models, instead, perform these calculations on a smaller number of *moving* cells, as outlined in Figures 8-1 and 8-2 for the REM2 model and the DIFKIN model, respectively.

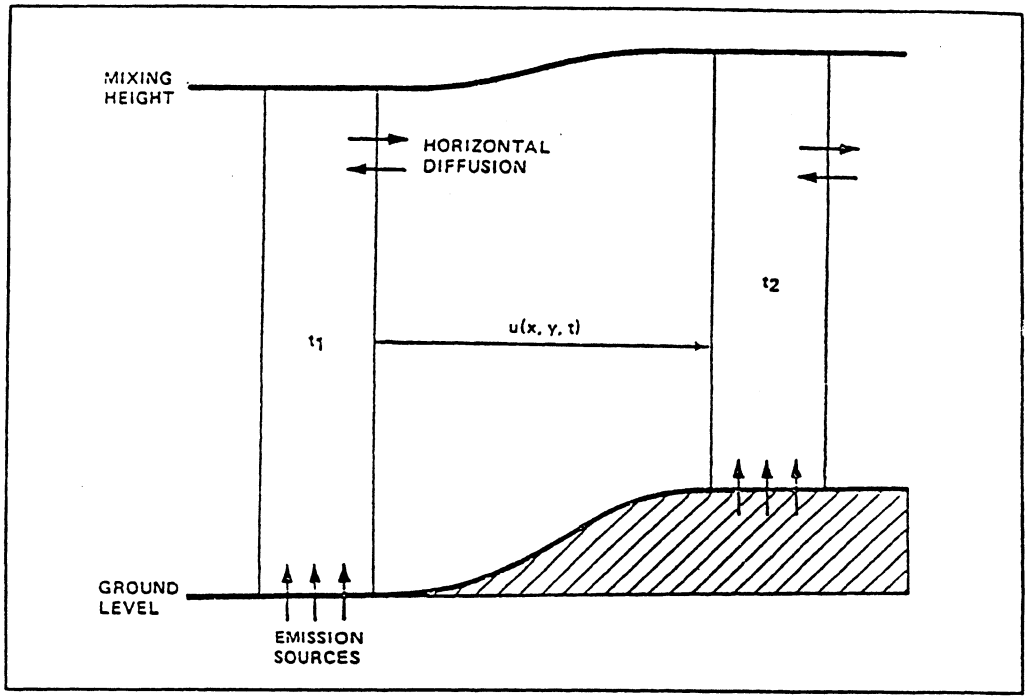

Figure 8–1. Single Lagrangian box dynamics (as in the REM 2 model; Drivas et al., 1977). [Reprinted with permission from the American Meteorological Society.]

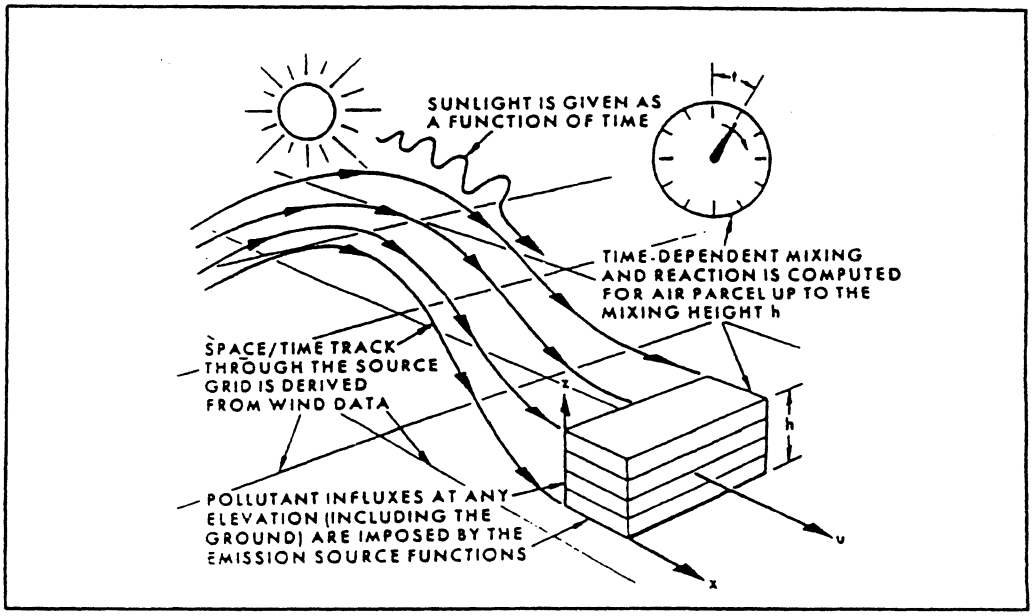

Figure 8–2. Vertical Lagrangian boxes dynamics (as in the DIFKIN model; Martinez et al., 1973).

More recently, two advanced Lagrangian photochemical models have been developed: the TRACE model (Tran, 1981) and the PLMSTAR model (Lurmann et al., 1985). TRACE uses a two-dimensional wall of cells moving along a specified trajectory to simulate the transport of a plume parcel from a source to a receptor. Figure 8-3 shows the moving wall of cells in which TRACE simulates the effects of vertical and horizontal diffusion, emission of primary pollutants from all the source regions entrained by the moving wall, nonlinear photochemical transformations, initial and boundary conditions. The TRACE model solves numerically the following set of coupled, nonlinear, partial differential equations (conservation of mass)

$$\frac{\partial c_i}{\partial t} = \frac{\partial}{\partial y}\left(K_y \frac{\partial c_i}{\partial y}\right) + \frac{\partial}{\partial z}\left(K_z \frac{\partial c_i}{\partial z}\right) + R_i + S_i + D_i \qquad (8\text{-}9)$$

where c_i is the concentration of the i-th species; K_y and K_z are the eddy diffusion coefficients in the crosswind and vertical direction, respectively; R_i is the rate of chemical transformation of the i-th species (creation or removal); S_i is the rate of emission of the i-th species along the trajectory; and D_i is the rate of deposition of the i-th species.

PLMSTAR is a mesoscale Lagrangian photochemical model designed to simulate the behavior of pollutants in chemically reactive plumes interacting with background concentrations. PLMSTAR, like TRACE, considers a moving wall of cells, usually five in the vertical and nine in the horizontal directions. In its movement, the air parcel entrains emissions from other surface or elevated sources. Pollutants within each cell undergo horizontal and turbulent diffusion, chemical reactions and dry deposition.

8.3 PARTICLE MODELS

Particle modeling is the most recent and powerful computational tool for the numerical discretization of a physical system. It has been particularly successful in a wide spectrum of applications (Hockney and Eastwood, 1981), that range from the atomic scale (electron flow in semiconductors, molecular dynamics) to the astronomical scale (galaxy dynamics), with other important applications to plasma and turbulent fluid dynamics. Particle models handle the transport terms, whose correct numerical treatment is very difficult with Eulerian (grid) models, in a straightforward manner. Particles, in fact, have a Lagrangian nature, since they move following the main flow. For this reason, they are often called Lagrangian particles.

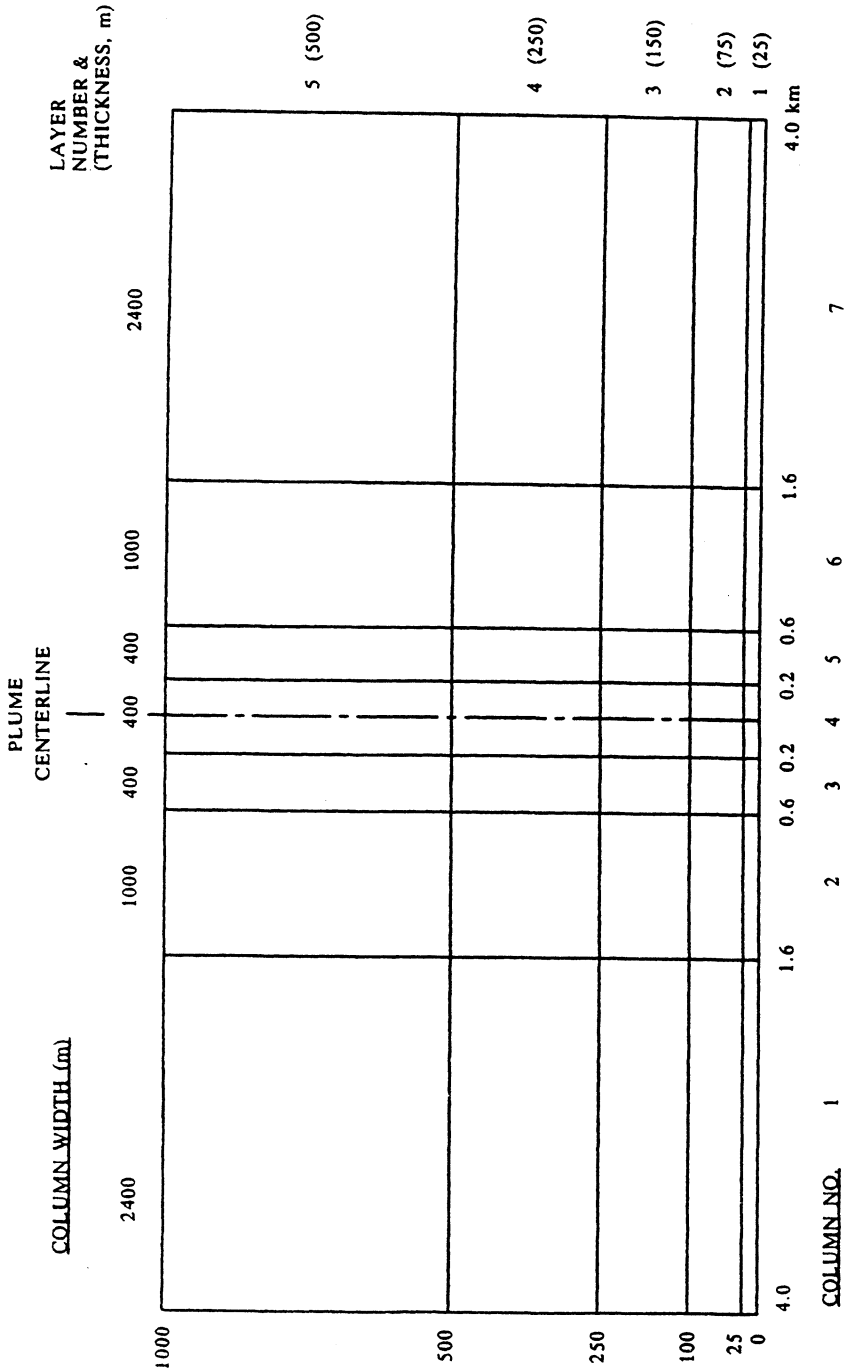

Figure 8–3. Dimensions of moving wall of cells for TRACE model runs (view is upwind). (From Tran, 1981.) [Reprinted with permission from Applied Modeling, Inc.]

Particle models use a certain number of computational (fictitious) particles to simulate the dynamics of a selected parameter (e.g., mass, heat, electrical charge density, etc.). Particle motion can be produced by both deterministic velocities and semirandom pseudovelocities generated using Monte-Carlo techniques. In the latter case, the trajectory of a single particle simply respresents a realization from an infinite set of possible solutions. Important characteristics of the diffusion process can be inferred, however, from the computation of average particle ensemble properties, which are not affected by the randomness of the pseudovelocities if enough particles are used.

Three main types of particle models can be defined (Hockney and Eastwood, 1981):

- particle-particle (PP) models, in which all interaction forces (e.g., gravitational or electric forces) between particles are computed at each time step
- particle-mesh (PM) models, in which forces are computed using a field equation (on a grid) for the potential
- PP-PM or (P^3M) models, a hybrid approach, in which interparticle forces are split into a short-range component (computed using the PP method) and a slowly varying one (represented in a mesh system by the PM method)

Length and time scales (as in all discretization systems) play an important role in particle models. In particular, the relation between the actual physical particles (or elements) and the computer model simulation particles is an important factor for the interpretation of the simulation results. In general, three possible cases can be found (Hockney and Eastwood, 1981):

- a one-to-one correspondence between actual and simulated particles, as, for example, in molecular dynamics simulation
- a description of fluid elements (position, vorticity) as particles, as, for example, in vortex fluid simulations, where the correspondence to physical particles (molecules) is totally lost
- the use of "superparticles;" i.e., simulation particles representing a cloud of physical particles having similar characteristics

Particle models have mostly been applied to simulate (and understand) the spiral structure of the galaxies, to simulate plasma dynamics and the electron flow in semiconductors, and to obtain realistic representations of turbulence in fluid.

In air pollution applications, using Lagrangian particle methods, emitted gaseous material is characterized by a set of computational particles and each particle is "moved" at each time step by pseudovelocities, which take into account the three basic dispersion components: 1) the transport due to the mean fluid velocity; 2) the (seemingly) random turbulent fluctuations of wind components (both horizontal and vertical); and 3) the molecular diffusion (if not negligible). After the pioneering work of Smith (1968) and Hall (1975), Lamb (1978) simulated vertical turbulent phenomena by assigning to each particle a velocity

$$w = w_d + w_s \tag{8-10}$$

where the first term w_d was determined by the Eulerian numerical model of Deardorff (1974) and w_s was a stochastic term describing the effect of subgrid fluctuations not included in the numerical model. (The term w_d was generated every eight seconds on a grid with $\Delta z = 50$ m and, therefore, contained a large fraction of the fluctuating turbulent velocities that, in other models, are simulated by the stochastic terms.) Zannetti (1981, 1984) introduced a scheme for the inclusion of the cross correlation among the velocity fluctuations. Baerentsen and Berkowicz (1984) used two separate equations to describe particle updrafts and downdrafts, under the assumption that the physics of the two phenomena is different.

As illustrated by de Baas et al. (1986), most particle modeling studies of air quality phenomena are numerical solutions of the Langevin stochastic differential equation (Reid, 1979; Gifford, 1982; Sawford, 1984)

$$dw = -(w/T_L)dt + d\mu \tag{8-11}$$

where w is any component of the Lagrangian particle velocity, T_L is its Lagrangian time scale, and $d\mu$ are random velocity increments. The use of this equation, its limitations and possible improvements are described in Section 8.3.5. Several of the concepts introduced above and related to the use of particle modeling in the simulation of atmospheric diffusion will be expanded in the following sections.

8.3.1 Simulation of Atmospheric Diffusion by Particle Models

Equation 8–2 or 8–4 can be solved analytically or numerically. For example, as discussed before, a Gaussian distribution of p, together with other simplifying assumptions, allows the derivation of Gaussian plume and puff equations for $<c>$. More complex functions of p require numerical integrations.

An intuitive solution of Equation 8–2 or 8–4 can be obtained if a set of dynamic atmospheric trajectories of pollutant mass can be generated. Then, for

each trajectory originating from $\mathbf{r}'$ at t', we have $p(\mathbf{r},t|\mathbf{r}',t') = 0$ everywhere, except at the exact location $\mathbf{r} = \mathbf{r}^*$, where the trajectory point is located at t, thus giving $p(\mathbf{r},t|\mathbf{r}',t') = \delta(\mathbf{r}^* - \mathbf{r})$. Therefore, if realistic air parcel trajectories can be computed, the simple calculation of the density of the trajectory points provides an estimate of $<c>$. This is the conceptual basis of a "particle" model for atmospheric dispersion, i.e., a model in which a set of "tracers" (or fictitious computational particles) are used to describe the dynamics of the atmosphere.

Particle models can be used to characterize atmospheric dispersion in two simulation modes: the "single-particle" mode, in which the motion of each particle is independent from the others and, therefore, obeys one-particle statistics; and the "two-particle" mode, used to reproduce *relative* dispersion, e.g., the dispersion properties of a single puff in relation to its center of mass. The second approach has been investigated by several authors (Durbin, 1980; Lamb, 1981; Sawford, 1983; Lee et al., 1985) and, in particular, by Gifford (1982), who used the simple Langevin Equation 8-11 to simulate relative dispersion by constraining the initial particle velocity (see Sawford, 1984, for further discussion of this topic). In the rest of this chapter we will discuss "single-particle" models.

In air pollution applications, simulation particles are moved at each time step by a velocity $\mathbf{u}_e$, which is sometimes called a "pseudovelocity" to emphasize that we do not need to follow precisely each molecule in the atmospheric turbulent flow, but only to define an algorithm for particle displacement computation that gives an accurate density distribution, i.e., an ensemble average. In mathematical notation, if a particle is located in $\mathbf{x}(t_1)$ at time t_1, its position at time t_2 will be

$$\mathbf{x}(t_2) = \mathbf{x}(t_1) + \int_{t_1}^{t_2} \mathbf{u}[\mathbf{x}(t), t]\, dt \tag{8-12}$$

where $\mathbf{u}$ is the "instantaneous" wind vector in each point $\mathbf{x}(t)$ of the particle trajectory between t_1 and t_2.

Atmospheric turbulent properties make $\mathbf{u}$ practically impossible to know, especially due to semirandom components caused by atmospheric turbulent eddies. But the "equivalent" or "effective" wind vector $\mathbf{u}_e$ can be considered

$$\mathbf{u}_e = \int_{t_1}^{t_2} \mathbf{u}[\mathbf{x}(t), t]\, dt/(t_2 - t_1) \tag{8-13}$$

which moves the particle directly from $\mathbf{x}(t_1)$ to $\mathbf{x}(t_2)$ in the interval (t_1, t_2). The problem is then to estimate $\mathbf{u}_e$ from Eulerian measurements of $\mathbf{u}$, keeping in

mind that $\mathbf{u}_e$ must approximate the integral term in Equation 8–13 only on a particle *ensemble* basis. For example, we can define

$$\mathbf{u}_e = \bar{\mathbf{u}} + \mathbf{u}' \tag{8–14}$$

where $\bar{\mathbf{u}}$ is the best estimate of the average Eulerian wind vector (transport) at the particle location, and $\mathbf{u}'$ is a "diffusivity velocity." In other words, $\bar{\mathbf{u}}$ (a smoothly variable term) represents our deterministic understanding of the average transport process, based on Eulerian wind measurement interpolation or provided by a meteorological model, while $\mathbf{u}'$ is an artificial numerical perturbation, which is related to the turbulence intensities and characteristics of those smaller eddies that are not included in the $\bar{\mathbf{u}}$ field.

Since, in Equation 8–14, $\bar{\mathbf{u}}$ is assumed to be known from measurements and/or meteorological model outputs, computing $\mathbf{u}'$ is the key problem of Lagrangian particle modeling. Two fundamental approaches can be followed: the deterministic approach, which represents a numerical procedure for solving the diffusion equation, and the statistical approach, which actually models the randomness of the trajectories of fluid elements. Both approaches are discussed below.

8.3.2 Deterministic Calculation of $\mathbf{u}'$

A typical example of the deterministic approach is given by the particle-in-cell method (Lange, 1978; Rodriguez et al., 1982), in which, after some manipulation of the *K*-theory diffusion equation, the following relation is obtained

$$\mathbf{u}' = \left(-\frac{K}{c}\right)\nabla c \tag{8–15}$$

where K is the eddy diffusion coefficient and c the concentration, computed from particle density. This method generally requires partitioning the computational domain into cells in order to calculate c. It is able to duplicate *K*-theory dispersion, with the important feature of decreasing the numerical advection errors otherwise produced by finite-difference solutions. Using this method, the motion of a single particle will be affected by the time-varying concentration field c, i.e., by the positions of the other particles.

8.3.3 Statistical Calculation of $\mathbf{u}'$

The statistical approach (Monte Carlo–type models) seems more flexible and appealing than the deterministic approach. According to the statistical approach, $\mathbf{u}'$ is a semirandom component computed by manipulating computer-

generated random numbers. To perform this computation, it has generally been assumed that Eulerian measurements of $\mathbf{u}$ can provide statistical information on $\mathbf{u}'$.

If we accept this assumption, we can use, for the diffusivity velocity $\mathbf{u}'$, a statistical generation scheme based on our understanding (and Eulerian measurements) of $\mathbf{u}$. In particular, Hanna (1979) has shown that it is a plausible assumption to describe both Eulerian and Lagrangian wind vector fluctuations by a simple Markov process (autocorrelation process of the first order). If we extend this assumption to $\mathbf{u}'$, we have(*)

$$\mathbf{u}'(t_2) = \mathbf{R}(\Delta t)\, \mathbf{u}'(t_1) + \mathbf{u}''(t_2) \qquad (8\text{–}16)$$

where $\mathbf{R}(\Delta t)$ is a vector containing the autocorrelations with lag $\Delta t = t_2 - t_1$ of the $\mathbf{u}'$ components, and $\mathbf{u}''$ is a purely random vector that will be discussed further below.

Equation 8–16 is the key formula for statistically computing $\mathbf{u}'$. It is a recursive sum of two terms: the first is a function of the "previous" $\mathbf{u}'$ of the same particle, and the second is purely randomly generated. Since Equation 8–16 is computed independently for each particle, two eventually coincident particles at t_1 will have, in general, different displacements, even if their past "history" is exactly the same. Using this approach, the motion of a particle is not affected by the position of the other particles and, therefore, this numerical algorithm is extremely fast, since no interacting forces need to be computed.

To apply Equation 8–16, we need the initial $\mathbf{u}'(t_o)$ for each particle at its generation time t_o (often assumed to be a zero vector or random with variance $\sigma_{u'}^2$) and the dynamic computation of $\mathbf{R}$ and $\mathbf{u}''$. $\mathbf{R}$ can be related to Lagrangian turbulence time scales by

$$\mathbf{R}(\Delta t) = \exp\,[-\Delta t/\mathbf{T}_L] \qquad (8\text{–}17)$$

where $\mathbf{T}_L$ is a vector containing the two horizontal and the one vertical Lagrangian time scales(**). Generally, Lagrangian measurements of $\mathbf{T}_L$ are not available, but empirical relations have been proposed (e.g., Hanna, in Nieuwstadt and van Dop, 1982) to estimate $\mathbf{T}_L$ from Eulerian meteorological measurements (see Section 8.3.6).

(*) In this formula (and the following ones in this chapter), when vectors appear on both sides of an equation, each component of the vector on the left side is computed using only the corresponding component of each vector in the right side (componentwise notation).

(**) Other equations have been proposed instead of Equation 8–17. Note, however, that it is essential that $\mathbf{R}$ is exponential if results are to be independent of Δt (Thomson, personal communication).

Assuming $\mathbf{u}''$ a purely random vector with zero-mean, normally-distributed independent components, we have that $\mathbf{u}''$ is completely characterized by $\sigma_{u''}$; i.e., the standard deviations of its components. By taking the variances of Equation 8-16, we obtain

$$\sigma_{u''} = \sigma_{u'}[1 - \mathbf{R}^2(\Delta t)]^{1/2} \tag{8-18}$$

Equation 8-18 requires the knowledge of $\sigma_{u'}$, the standard deviations of the components $\mathbf{u}'$, which, again, can be approximated by the standard deviations of available Eulerian wind measurements. Therefore, using the standard deviations $\sigma_{u''}$ computed by Equation 8-18, it is easy, with commonly available Monte-Carlo computer programs, to generate each particle's $\mathbf{u}''$ term for use in Equation 8-16.

As discussed in Section 8.3.5, it has been established that the development leading to Equation 8-18 is valid only for stationary, homogeneous and isotropic turbulence. Nevertheless, in situations where meteorological gradients are not too strong, $\mathbf{R}$ and $\sigma_{u'}$ can be considered space and time dependent (but assumed constant between t_1 and t_2 to derive Equation 8-18). Therefore, they can fully incorporate, when available, time-varying three-dimensional meteorological input (Eulerian values) and can simulate, with a high degree of spatial and temporal resolution, extremely complex atmospheric diffusion conditions, which are impossible to treat with other numerical schemes. This approach is grid-free, since, even when the meteorological input $\bar{\mathbf{u}}$, $\mathbf{R}$ and $\sigma_{u'}$ is given at grid points, each particle can move according to meteorological values that can be interpolated exactly at the particle's location. This provides a high degree of resolution, which is controlled only by the number of particles and the length of the time interval Δt, and not by the spatial discretization of the computational domain.

Hanna (in Nieuwstadt and van Dop, 1982) proposed a set of semi-empirical formulae that, from a limited number of meteorological parameters (h, L, w_*, z_o, and u_*) provide the meteorological input at each particle's elevation z required by Equations 8-16 through 8-18. This scheme, in which the subscripts a and c indicate the along-wind and cross-wind horizontal components, respectively, is described below.

- **Unstable Conditions**

In unstable conditions, the horizontal components of $\sigma_{u'}$ are constant, i.e.,

$$\sigma_{u'_a} = \sigma_{u'_c} = u_* (12 + 0.5\, h/|L|)^{1/3} \simeq \sqrt{0.31}\, w_* \tag{8-19}$$

while the vertical component varies with z as follows:

$$\sigma_{u'_z} = 0.96\, w_* \left(\frac{3\,z}{h} - \frac{L}{h}\right)^{1/3} \tag{8-20}$$

for $z \leq 0.03\, h$;

$$\sigma_{u'_z} = w_* \min\left[0.96\left(\frac{3\,z}{h} - \frac{L}{h}\right)^{1/3};\ 0.763\left(\frac{z}{h}\right)^{0.175}\right] \tag{8-21}$$

for $0.03\, h < z < 0.4\, h$;

$$\sigma_{u'_z} = 0.722\, w_* \left(1 - \frac{z}{h}\right)^{0.207} \tag{8-22}$$

for $0.4\, h \leq z < 0.96\, h$; and

$$\sigma_{u'_z} = 0.37\, w_* \tag{8-23}$$

for $0.96\, h < z \leq h$.

The autocorrelations are computed by Equation 8–17, where the two horizontal components of $\mathbf{T}_L$ are constant, i.e.,

$$T_{L_a} = T_{L_c} = 0.15\, \frac{h}{\sigma_{u'_a}} \tag{8-24}$$

and the vertical component varies with z as follows:

$$T_{L_z} = 0.1\, \frac{z}{\sigma_{u'_z}[0.55 + 0.38\,(z - z_o)/L]} \tag{8-25}$$

for $z < 0.1\ h$ and $z - z_o > -L$;

$$T_{L_z} = 0.59 \frac{z}{\sigma_{u'_z}} \tag{8-26}$$

for $z < 0.1\ h$ and $z - z_o < -L$; and

$$T_{L_z} = 0.15 \frac{h}{\sigma_{u'_z}} \left[1 - \exp\left(-\frac{5z}{h}\right)\right] \tag{8-27}$$

for $z > 0.1\ h$.

- **Stable Conditions**

In stable conditions, h represents the top of the mechanically turbulent layer above the ground and can be evaluated by Equation 3–8 or by

$$h = 0.25\ u_* L/f \tag{8-28}$$

The components of $\sigma_{u'}$ vary with z as follows

$$\sigma_{u'_a} = 2.0\ u_* \left(1 - \frac{z}{h}\right) \tag{8-29}$$

$$\sigma_{u'_c} = \sigma_{u'_z} = 1.3\ u_* \left(1 - \frac{z}{h}\right) \tag{8-30}$$

while the autocorrelations are computed by Equation 8–17 with

$$T_{L_a} = 0.15 \frac{h}{\sigma_{u'_a}} \left(\frac{z}{h}\right)^{0.5} \tag{8-31}$$

$$T_{L_c} = 0.07 \frac{h}{\sigma_{u'_c}} \left(\frac{z}{h}\right)^{0.5} \tag{8-32}$$

and

$$T_{L_z} = 0.10 \frac{h}{\sigma_{u'_z}} \left(\frac{z}{h}\right)^{0.8} \tag{8-33}$$

- **Neutral Conditions**

In neutral conditions, the components of $\sigma_{u'}$ are

$$\sigma_{u'_a} = 2.0\, u_* \exp(-3 f z/u_*) \tag{8-34}$$

and

$$\sigma_{u'_c} = \sigma_{u'_z} = 1.3\, u_* \exp(-2 f z/u_*) \tag{8-35}$$

while the autocorrelations are computed again by Equation 8–17 with

$$T_{L_a} = T_{L_c} = T_{L_z} = \frac{0.5\, z/\sigma_{u'_z}}{1 + 15 f z/u_*} \tag{8-36}$$

In addition to the above formulation, it is generally assumed that $\mathbf{u}' = \mathbf{0}$ for $z > h$ and that the particles are totally or partially reflected at the ground and at the top of the PBL -- an operation that also requires a change of sign in the "memory" u'_z of each reflected particle.

8.3.4 The Introduction of the Cross-Correlations

Using Monte-Carlo techniques, it is necessary to simulate realistically the wind fluctuation behavior in a way that is consistent with measured characteristics. Several current models are based on Equation 8–16, which assumes that the components of $\mathbf{u}'$ are statistically independent. This assumption is in disagreement with wind fluctuation measurements, which indicate the existence of non-zero cross-correlation terms. Therefore, Equation 8–16 can be, in many cases, an oversimplification of the atmospheric dispersion processes.

Zannetti (1981), Ley (1982) and Legg (1983) have proposed schemes that include the negative correlation $\overline{u'w'}$ between the "along-wind" component u' and the vertical component w'. For example, Zannetti (1981, 1984) developed the scheme

$$u'_a(t_2) = \phi_1\, u'_a(t_1) + u''_a(t_2) \tag{8-37}$$

$$u'_c(t_2) = \phi_2\, u'_c(t_1) + u''_c(t_2) \tag{8-38}$$

$$u'_z(t_2) = \phi_3\, u'_z(t_1) + \phi_4\, u'_a(t_2) + u''_z(t_2) \tag{8-39}$$

in which the vector $\mathbf{u}'$ is seen in a "flux-coordinate" system where

$$\mathbf{u}' = (u'_a,\ u'_c,\ u'_z) \tag{8-40}$$

and u'_a is the horizontal component along the average wind direction, u'_c is the horizontal cross-wind component, and u'_z is the vertical component. Note that, since the average wind direction varies with space and time, each particle will have, in general, its own time-varying reference system, determined by the horizontal direction of $\bar{\mathbf{u}}$, as defined by Equation 8-14, at the particle's location.

By analytical manipulations of Equations 8-37 through 8-39, the parameters ϕ_1, ϕ_2, ϕ_3, ϕ_4, $\sigma_{u''_a}$, $\sigma_{u''_c}$, and $\sigma_{u''_z}$ are calculated by

$$\phi_1 = r_{u'_a}(\Delta t) \tag{8-41}$$

$$\phi_2 = r_{u'_c}(\Delta t) \tag{8-42}$$

$$\phi_3 = \frac{r_{u'_z}(\Delta t) - \phi_1 r^2_{u'_a u'_z}(0)}{1 - \phi_1^2 r^2_{u'_a u'_z}(0)} \tag{8-43}$$

$$\phi_4 = \frac{r_{u'_a u'_z}(0)\ \sigma_{u'_z}\ [1 - \phi_1 r_{u'_z}(\Delta t)]}{\sigma_{u'_a}\left[1 - \phi_1^2 r^2_{u'_a u'_z}(0)\right]} \tag{8-44}$$

and

$$\sigma^2_{u''_a} = \sigma^2_{u'_a}\ (1 - \phi_1^2) \tag{8-45}$$

$$\sigma^2_{u''_c} = \sigma^2_{u'_c}\ (1 - \phi_2^2) \tag{8-46}$$

$$\sigma^2_{u''_z} = \sigma^2_{u'_z}\ (1 - \phi_3^2) - \phi_4^2\ \sigma^2_{u'_a} - 2\ \phi_1\ \phi_3\ \phi_4\ r_{u'_a u'_z}(0)\ \sigma_{u'_a}\ \sigma_{u'_z} \tag{8-47}$$

where $r_{u'_a}(\Delta t)$, $r_{u'_c}(\Delta t)$, $r_{u'_z}(\Delta t)$ are the autocorrelations, with time lag $\Delta t = t_2 - t_1$, of the components of $\mathbf{u}'$, as defined by Equation 8-40; $r_{u'_a u'_z}(0)$ is the cross-correlation, with no time lag, between u'_a and u'_z; $\sigma_{u''_a}$, $\sigma_{u''_c}$ and $\sigma_{u''_z}$ are the standard deviations of the components of the vector $\mathbf{u}''$

$$\mathbf{u}'' = (u''_a,\ u''_c,\ u''_z) \tag{8-48}$$

where these components are uncorrelated zero-averaged Gaussian noises (i.e., random numbers); and $\sigma_{u'_a}$, $\sigma_{u'_c}$, $\sigma_{u'_z}$ are the standard deviations of the

$\mathbf{u}'$ components. The parameters in Equations 8–41 through 8–47 can vary with space and time, but are assumed constant between t_1 and t_2.

The above method is able to generate a time-varying $\mathbf{u}'$ with any theoretically acceptable degree of auto- and cross-correlations, if the meteorological input is known. The meteorological input $r_{u'_a}(\Delta t)$, $r_{u'_c}(\Delta t)$, $r_{u'_z}(\Delta t)$, $\sigma_{u'_a}$, $\sigma_{u'_c}$, and $\sigma_{u'_z}$ can be obtained using Hanna's scheme presented in the previous section, while the extra term $r_{u'_a u'_z}(0)$ can be estimated at the ground, by analogy with the Eulerian relationship of Equation 3–2, by

$$[r_{u'_a u'_z}(0)]_{z=o} = - \frac{u_*^2}{\sigma_{u'_a} \sigma_{u'_z}} \tag{8–49}$$

Equation 8–49 can be linearly interpolated from $z = 0$ to $z = h$, where $[r_{u'_a u'_z}(0)]_{z=h} = 0$, thus giving, at a generic z below h,

$$[r_{u'_a u'_z}(0)]_z = - \frac{u_*^2}{\sigma_{u'_a} \sigma_{u'_z}} \left(1 - \frac{z}{h}\right) \tag{8–50}$$

If direct measurements of $\sigma_{u'}$ are available, they can be used directly (e.g., by interpolation at different altitudes) instead of using the semiempirical formulae described above. For example, measurements of σ_θ, the standard deviation of the horizontal wind direction, can be used to calculate $\sigma_{u'_c}$, through the relationship

$$\sigma_{u'_c} \simeq \bar{u}\, \sigma_\theta \tag{8–51}$$

where $\bar{u}$ is the average horizontal wind speed and σ_θ is expressed in radians. If measurements of $\mathbf{u}'$ are performed in a fixed orthogonal system x,y,z, i.e.,

$$\mathbf{u}' = (u'_x, u'_y, u'_z) \tag{8–52}$$

then, the standard deviations $\sigma_{u'_x}$ and $\sigma_{u'_y}$ allow the calculation of $\sigma_{u'_a}$ and $\sigma_{u'_c}$ by using (Zannetti, 1984)

$$\sigma_{u'_a} = \frac{\bar{u}_x^2 \sigma_{u'_x}^2 - \bar{u}_y^2 \sigma_{u'_y}^2}{\bar{u}_x^2 - \bar{u}_y^2} \tag{8–53}$$

$$\sigma_{u'_c} = \frac{\bar{u}_x^2 \sigma_{u'_y}^2 - \bar{u}_y^2 \sigma_{u'_x}^2}{\bar{u}_x^2 - \bar{u}_y^2} \tag{8–54}$$

where $\bar{u}_x$ and $\bar{u}_y$ are the horizontal components of the average wind $\bar{u}$ in the fixed coordinate system. Equations 8–53 and 8–54 are derived by assuming that the u'_a and u'_c are not cross–correlated. Also note that these equations are not valid when $|\bar{u}_x| \simeq |\bar{u}_y|$, i.e., when the average wind direction is blowing with an angle of 45 degrees, 135 degrees, 225 degrees, and 315 degrees with respect to the x–axis (in these cases, no alternative equations can be provided; the system orientation simply does not allow discrimination between along–wind and crosswind fluctuations).

Zannetti (1986) expanded the scheme of Equations 8–37 through 8–39 to work in a generic fixed orthogonal system x,y,z, which requires the incorporation of all three cross–correlations among the $\mathbf{u}'$ components. The system becomes

$$u'_x(t_2) = f_1\, u'_x(t_1) + u''_x(t_2) \tag{8–55}$$

$$u'_y(t_2) = f_2\, u'_y(t_1) + f_3\, u'_x(t_2) + u''_y(t_2) \tag{8–56}$$

$$u'_z(t_2) = f_4\, u'_z(t_1) + f_5\, u'_y(t_2) + f_6\, u'_x(t_2) + u''_z(t_2) \tag{8–57}$$

Again, this system is able to generate a time sequence of $\mathbf{u}'$ values with any theoretically acceptable degree of auto– and cross–correlation, if the meteorological input is specified. For Equations 8–55 through 8–57, the meteorological input must include the three cross–correlations $r_{u'_x u'_y}(0)$, $r_{u'_x u'_z}(0)$, and $r_{u'_y u'_z}(0)$. Algebraic manipulations allow the deviation of the parameters f_1, f_2, f_3, f_4, f_5, f_6 and the standard derivations $\sigma_{u''_x}$, $\sigma_{u''_y}$, $\sigma_{u''_z}$ from the meteorological input, as follows. First, analytical manipulation of Equations 8–55 and 8–56 allow the derivation of

$$f_1 = r_{u'_x}(\Delta t) \tag{8–58}$$

$$\sigma^2_{u''_x} = \sigma^2_{u'_x}\,(1 - f_1^2) \tag{8–59}$$

$$f_2 = \frac{r_{u'_y}(\Delta t) - r_{u'_x}(\Delta t)\, r^2_{u'_x u'_y}(0)}{1 - r^2_{u'_x}(\Delta t)\, r^2_{u'_x u'_y}(0)} \tag{8–60}$$

$$f_3 = \frac{r_{u'_x u'_y}(0)\,\sigma_{u'_y}\left[1 - r_{u'_x}(\Delta t)\; r_{u'_y}(\Delta t)\right]}{\sigma_{u'_x}\left[1 - r^2_{u'_x}(\Delta t)\, r^2_{u'_x u'_y}(0)\right]} \tag{8-61}$$

and

$$\sigma^2_{u''_y} = \sigma^2_{u'_y}\,(1-f_2^2) - f_3^2\,\sigma^2_{u'_x} - 2\,f_1 f_2 f_3\, r_{u'_x u'_y}(0)\,\sigma_{u'_x}\,\sigma_{u'_y} \tag{8-62}$$

Then, the terms f_4, f_5 and f_6 are computed by solving the linear system

$$\begin{pmatrix} a_{44} & a_{45} & a_{46} \\ a_{54} & a_{55} & a_{56} \\ a_{64} & a_{65} & a_{66} \end{pmatrix} \begin{pmatrix} f_4 \\ f_5 \\ f_6 \end{pmatrix} = \begin{pmatrix} b_4 \\ b_5 \\ b_6 \end{pmatrix} \tag{8-63}$$

with

$$a_{44} = \sigma_{u'_z} \tag{8-64}$$

$$a_{45} = f_2\, r_{u'_y u'_z}(0)\;\sigma_{u'_y} + f_3 f_1\, r_{u'_x u'_z}(0)\;\sigma_{u'_x} \tag{8-65}$$

$$a_{46} = f_1\, r_{u'_x u'_z}(0)\;\sigma_{u'_x} \tag{8-66}$$

$$a_{54} = f_1\, r_{u'_x u'_z}(0)\;\sigma_{u'_z} \tag{8-67}$$

$$a_{55} = f_1 f_2\, r_{u'_x u'_y}(0)\;\sigma_{u'_y} + f_1 f_3\, r_{u'_x}(\Delta t)\;\sigma_{u'_x} + f_3\,\sigma_{u'_x}\,(1-f_1^2) \tag{8-68}$$

$$a_{56} = f_1\, r_{u'_x}(\Delta t)\;\sigma_{u'_x} + \sigma_{u'_x}\,(1-f_1^2) \tag{8-69}$$

$$a_{64} = f_2\, r_{u'_y u'_z}(0)\;\sigma_{u'_y}\,\sigma_{u'_z} + f_3 f_1\, r_{u'_x u'_z}(0)\;\sigma_{u'_x}\,\sigma_{u'_z} \tag{8-70}$$

$$a_{65} = f_2\, r_{u'_y}(\Delta t)\;\sigma^2_{u'_y} + f_3\, r_{u'_x u'_y}(0)\,\sigma_{u'_x}\,\sigma_{u'_y} + \sigma^2_{u''_y} \tag{8-71}$$

$$a_{66} = f_2 f_1\, r_{u'_x u'_y}(0)\;\sigma_{u'_x}\,\sigma_{u'_y} + f_3\,\sigma^2_{u'_x} \tag{8-72}$$

and

$$b_4 = r_{u'_z}(\Delta t)\ \sigma_{u'_z} \tag{8-73}$$

$$b_5 = r_{u'_x u'_z}(0)\ \sigma_{u'_z} \tag{8-74}$$

$$b_6 = r_{u'_y u'_z}(0)\ \sigma_{u'_y}\ \sigma_{u'_z} \tag{8-75}$$

This system allows a numerical solution of Equation 8-63. (An analytical solution for f_4, f_5, and f_6 could be derived but is too cumbersome.)

Finally, the last term $\sigma_{u''_z}$ is given by

$$\begin{aligned}\sigma^2_{u''_z} &= \sigma^2_{u'_z}\ (1 - f_4^2) - f_5^2\ \sigma^2_{u'_y} - f_6^2 \sigma^2_{u'_x} \\ &- 2 f_4 f_5 \left[f_2\, r_{u'_y u'_z}(0)\ \sigma_{u'_y}\ \sigma_{u'_z} + f_3 f_1\, r_{u'_x u'_z}(0)\ \sigma_{u'_x}\ \sigma_{u'_z}\right] \\ &- 2 f_4 f_6 f_1\, r_{u'_x u'_z}(0)\ \sigma_{u'_x}\ \sigma_{u'_z} - 2 f_5 f_6\, r_{u'_x u'_y}(0)\ \sigma_{u'_x}\ \sigma_{u'_y}\end{aligned} \tag{8-76}$$

It must be pointed out that the methods dealing with the cross-correlations presented above may be inherently inconsistent. At the end of Section 8.3.5, however, we propose a simple mechanism to incorporate these methods into an acceptable theoretical frame.

8.3.5 Simulation of Convective Conditions by Monte-Carlo Particle Models

Some of the most interesting developments of particle modeling have focused on the one-dimensional (i.e., vertical) simulation of convective dispersion conditions, and on the use of the Langevin Equation 8-11 to simulate the Lagrangian vertical velocity w of each particle. As summarized and clarified by de Baas et al. (1986), Equation 8-11 can provide different sets of simulation outputs, depending upon the specification of the random velocity increments $d\mu$.

In homogeneous turbulence, we have

$$\overline{d\mu} = 0 \tag{8-77}$$

$$\overline{(d\mu)^2} = 2\,\overline{u_z^2}\,dt/T_L \tag{8-78}$$

$$\overline{d\mu^3} = 0 \tag{8-79}$$

where u_z is the vertical wind component. Under these limiting conditions and with $dt = t_2 - t_1$, Equation 8–11 becomes equivalent to the vertical component of Equation 8–16. In this case, particle simulations are able to reproduce (e.g., see the simulations of Brusasca et al., 1987, using the MC-LAGPAR model) the theoretical results obtained by Taylor (1921) for homogeneous turbulence as illustrated in Figure 8–4.

Convective conditions in the atmosphere, however, are strongly characterized by nonhomogeneous conditions in which, for example, $\overline{u_z^2}$ varies with the height z. In this situation, if Equation 8–11 is used together with Equation 8–78 and a term $\overline{u_z^2}(z)$ that varies with z, particles have a tendency to be trapped, without any physical justifications, in regions with lower $\overline{u_z^2}$. This accumulation is avoided or minimized by changing Equation 8–77 into

$$\overline{d\mu} = dt\,\partial\overline{u_z^2}/\partial z \tag{8-80}$$

which represents a nonzero mean random forcing (i.e., a drift velocity) proportional to the vertical gradient of $\overline{u_z^2}(z)$. Legg and Raupach (1982) and Ley and Thomson (1983) proposed the use of Equation 8–80 and justified its validity by analyzing the Navier–Stokes equations and concluding that a gradient of $\overline{u_z^2}$ induces a mean pressure force that must be incorporated, through Equation 8–80, into the Langevin Equation 8–11. Similar considerations and results, using the Fokker–Plank equation (which can be seen as the Eulerian equivalent of the Langevin equation), were obtained by Janicke (1981). Other authors (e.g., Wilson et al., 1981, and Sawford, 1985) proposed drift velocity formulations different from Equation 8–80. This second group of formulations, however, seems less appropriate than Equation 8–80, since it contains the instantaneous term u_z' which interferes with the definition of T_L and the correct calculation of the autocorrelation.

A different approach for the treatment of convective conditions by Baerentsen and Berkovicz (1984) and Brusasca et al. (1987) uses two Langevin equations for updrafts and downdrafts, respectively. This allows an explicit, more realistic treatment of the known behavior of air parcel velocities in unstable conditions, in which ascent velocities are stronger than descent velocities, but

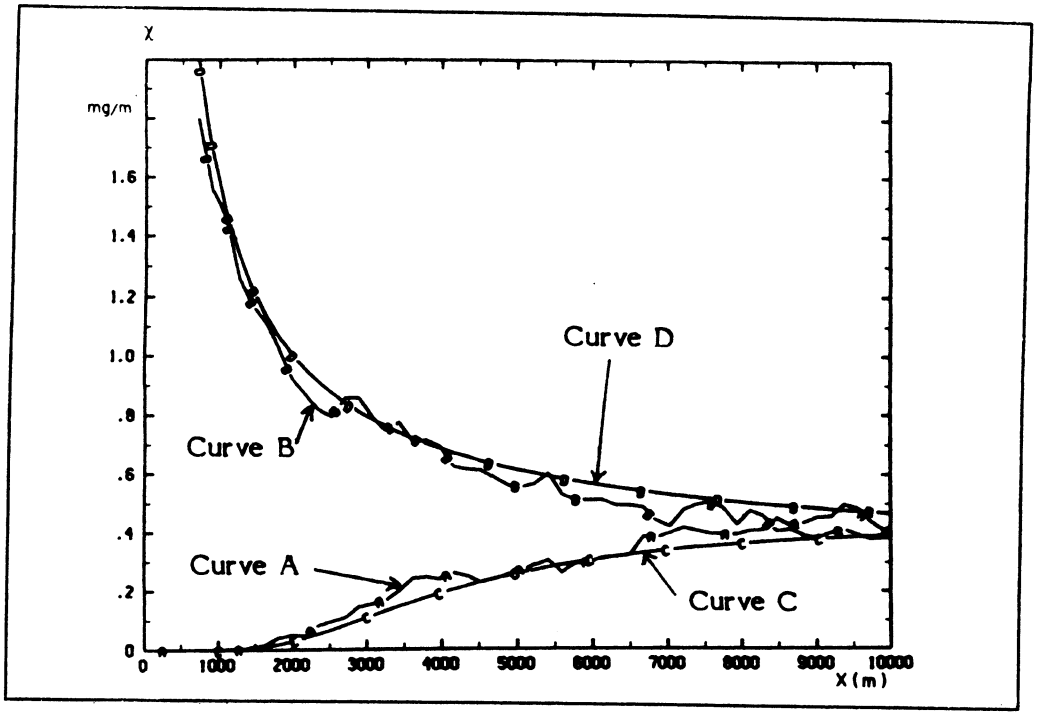

Figure 8–4. Concentration as a function of a downwind distance (from Brusasca et al., 1987). [Reprinted with permission from Computational Mechanics Publications.]

Curve A: *ground–level concentration simulated by MC–LAGPAR*

Curve B: *centerline plume concentration simulated by MC–LAGPAR*

Curve C: *ground–level concentration computed with the analytical solution of Taylor (1921)*

Curve D: *centerline plume concentration computed with the analytical solution of Taylor (1921)*

with shorter duration. For example, Yamamoto et al. (1982) measured average ascent velocities u'_z in the range of 0.5 w_* to 0.6 w_*, while Briggs (1975) proposed 0.4 w_* as a suitable average descent velocity u'_z. Both Baerentsen and Berkowicz (1984) and Brusasca et al. (1987) allow a probabilistic "jumping" of each particle from an updraft to a downdraft, and vice versa, with probabilities that depend upon the time scales of the two phenomena. These methods implicitly assume that updrafts and downdrafts are not included in the average $\overline{u}_z$ terms of Equation 8–14 and do not affect the $\sigma_{u'_z}$ terms (otherwise, updrafts and downdrafts terms would be included twice in the calculations).

The most appealing approach for the treatment of convective conditions is the incorporation of an appropriate term $\overline{(d\mu)^3}$ into the Langevin equation, instead of simply using Equation 8–79. This incorporation has been developed by Thomson (1984) and van Dop et al. (1985) and successfully tested by de Baas et al. (1986). They derived the following expressions for the random forcing function $d\mu$ (instead of Equations 8–77 through 8–79)

$$\overline{d\mu} = \Delta t \left[\partial \overline{u_z^2(z)}/\partial z\right] \tag{8–81}$$

$$\overline{(d\mu)^2} = \Delta t \left[2\, \overline{u_z^2(z)}/T_L + \partial \overline{u_z^3(z)}/\partial z\right] \tag{8–82}$$

$$\overline{(d\mu)^3} = \Delta t \left[3\, \overline{u_z^3(z)}/T_L + \partial \overline{u_z^4(z)}/\partial z - 3\, \overline{u_z^2(z)}\, \partial \overline{u_z^2(z)}/\partial z\right] \tag{8–83}$$

These equations were obtained by Thomson (1984) by imposing the conditions that, for large times, the distribution of particles in the phase space possesses the same distribution as the air.

The use of Equations 8–81 through 8–83 requires the generation of non-Gaussian terms $d\mu$ from a skewed distribution function $P(d\mu)$. Baerentsen and Berkowicz (1984) and de Baas et al. (1986) calculate $P(d\mu)$ by choosing $d\mu$ from two Gaussian distributions $P_1 = N(m_1, \sigma_1)$ and $P_2 = N(m_2, \sigma_2)$ with a chance q and $(1 - q)$, respectively. This allows the derivation of the relationships

$$q\, m_1 + (1-q)\, m_2 = \overline{d\mu} \tag{8–84}$$

$$q\, (m_1^2 + \sigma_1^2) + (1-q)\, (m_2^2 + \sigma_2^2) = \overline{(d\mu)^2} \tag{8–85}$$

and

$$q\, (m_1^3 + 3\, m_1\, \sigma_1^2) + (1-q)\, (m_2^3 + 3\, m_2\, \sigma_2^2) = \overline{(d\mu)^3} \tag{8–86}$$

which can be used with the simplifying assumptions of $m_1^2 = \sigma_1^2$ and $m_2^2 = \sigma_2^2$, since the above equations have two degrees of freedom.

The Langevin Equation 8–11 is approximated by de Baas et al. (1986) in a finite different form, using the explicit, fast and unconditionally stable scheme

$$w(t+\Delta t) = w(t)\, (1 - 0.5\, \Delta t/T_L)\, (1 + 0.5\, \Delta t/T_L)^{-1} + d\mu\, (1 + 0.5\, \Delta t/T_L)^{-1} \tag{8–87}$$

$$z(t+\Delta t) = z(t) + 0.5\, \Delta t\, [w(t+\Delta t) + w(t)] \tag{8–88}$$

where z is the altitude of the particle, w is the Lagrangian vertical velocity of the particle, and the random terms $d\mu$ are computed using Equations 8–81 through 8–83 and numerically generated from the two Gaussian distributions P_1 and P_2, according to Equations 8–84 through 8–86.

Further assumptions are made by de Baas et al. (1986) to simulate convective conditions. Using mixed layer scaling they assume the profile of the second moment to be

$$u_z^2(z)/w_*^2 = 1.54\,(z/z_i)^{2/3}\,\exp(-2\,z/z_i) \tag{8–89}$$

for $z > 0.0025\ z_i$, and

$$\overline{u_z^2} = 0.028\,w_*^2 \tag{8–90}$$

for $z \leq 0.0025\ z_i$. Also, they assume the following profile for the third moment

$$\overline{u_z^3(z)}/w_*^3 = 1.4\,(z/z_i)\,\exp(-2.5\,z/z_i) \tag{8–91}$$

and a constant T_L

$$T_L = c\,z_i/w_* \tag{8–92}$$

with $c = 1$, instead of the common assumption of $c = 0.24 - 0.55$ (Hanna, 1981), which requires some slight adjustments of the profile of $\overline{u_z^3}(z)$ at the top of the PBL, to satisfy the requirement that $\overline{(d\mu)^2} > 0$ at all heights. Finally, they assume the fourth moment to be

$$\overline{u_z^4(z)} = a\left(\overline{u_z^2(z)}\right)^2 \tag{8–93}$$

with $a = 3$, since no measurements of the fourth moment are available. Simulations are performed by generating particles at a source height $z = z_s$ with initial (i.e., $t = 0$) Lagrangian velocities w that obey the relationships

$$\overline{w} = 0 \tag{8–94}$$

$$\overline{w^2} = \overline{u_z^2(z_s)} \tag{8–95}$$

and

$$\overline{w^3} = \overline{u_z^3(z_s)} \tag{8-96}$$

Particles are also reflected at the top ($z = z_i$) and the bottom of the computational domain. All the above assumptions provide particle simulation results that agree well with water tank experiments by Willis and Deardorff (1978, 1981) (see Figure 8–5), wind tunnel experiments of Poreh and Cermak (1984), and field experiments by Briggs (1983).

As noted above, the scheme of Equations 8–81 through 8–83 requires the generation of non-Gaussian terms $d\mu$, a generation that asks for some slight adjustments to force the variance of the random numbers to be positive. Alternatively, the terms $d\mu$ could remain Gaussian and the $(-w/T_L)dt$ term in Equation 8–11 could be modified instead, e.g., by making it nonlinear (Thomson, 1987). This alternative approach avoids the problem met by de Baas et al. (1986) of satisfying the requirement that $\overline{(d\mu)^2} > 0$ at all heights and seems, at least theoretically, a more satisfactory development (Sawford, personal communication).

Schemes such as the one of Equations 8–81 through 9–83 for the solution of Equation 8–11 represent an improvement of the Langevin equation to simulate convective diffusion. However, they complicate the treatment of the cross-correlation terms. These terms, in Section 8.3.4, were discussed under the implicit assumption of using the Langevin Equation 8–11 with the conditions of Equations 8–77 through 8–79, which make it equivalent to Equation 8–16. A simple modification is required to maintain the advantages of both approaches (i.e., the improved Langevin equations for convective simulations and the cross-correlation terms). In fact, either set of Equations 8–37 through 8–39 or 8–55 through 8–57 can be rewritten in the sequence u_z', u_c', u_a' (Equations 8–37 through 8–39) or u_z', u_y', u_x' (Equations 8–55 through 8–57), thus allowing the first equation of either scheme, which does not contain any cross-correlation term, to represent the vertical velocities. By doing so, any complex Langevin equation scheme can be used for u_z' while still maintaining all the cross-correlation terms. (Naturally, however, if equations are rewritten in a different sequence, the derivation of the parameters will change accordingly, even though the general form of the solutions will remain the same.)

8.3.6 Concentration Calculations Using Particle Models

Particle models are a set of algorithms for the generation of realistic trajectories of imaginary, fictitious particles that simulate atmospheric motion. Each particle can be tagged by a mass of pollutant that can be either constant or

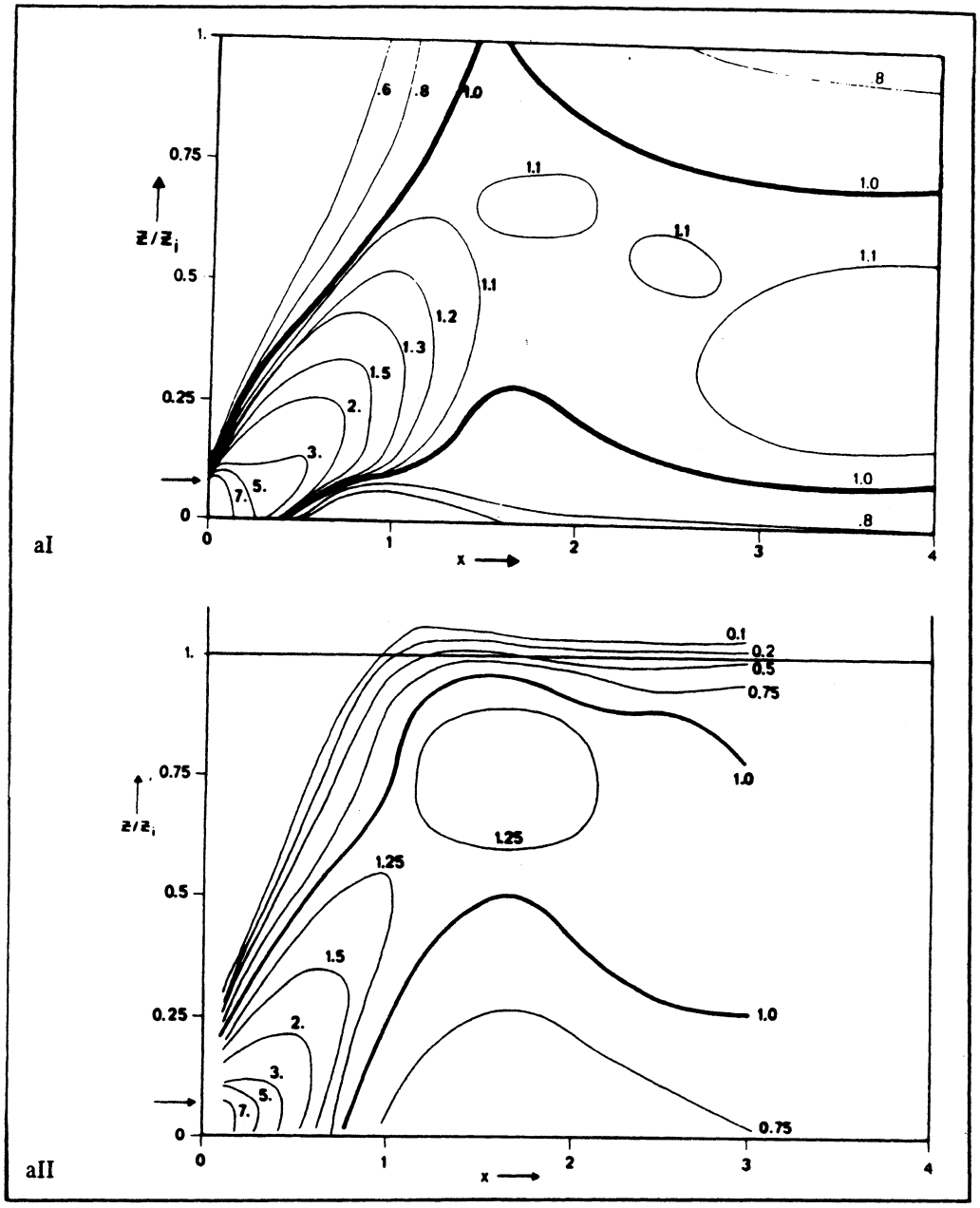

Figure 8–5. Dimensionless concentration contours in the vertical x,z plane. The different plots present the results of the Langevin model (I) and the cross-wind-integrated measurements of Willis and Deardorff (II) for the source heights: (a) $z_s/z_i = 0.067$; (b) $z_s/z_i = 0.24$; (c) $z_s/z_i = 0.49$. Source height is indicated by arrow on ordinate (from de Baas, et al., 1986). [Reprinted with permission from the Royal Meteorological Society.]

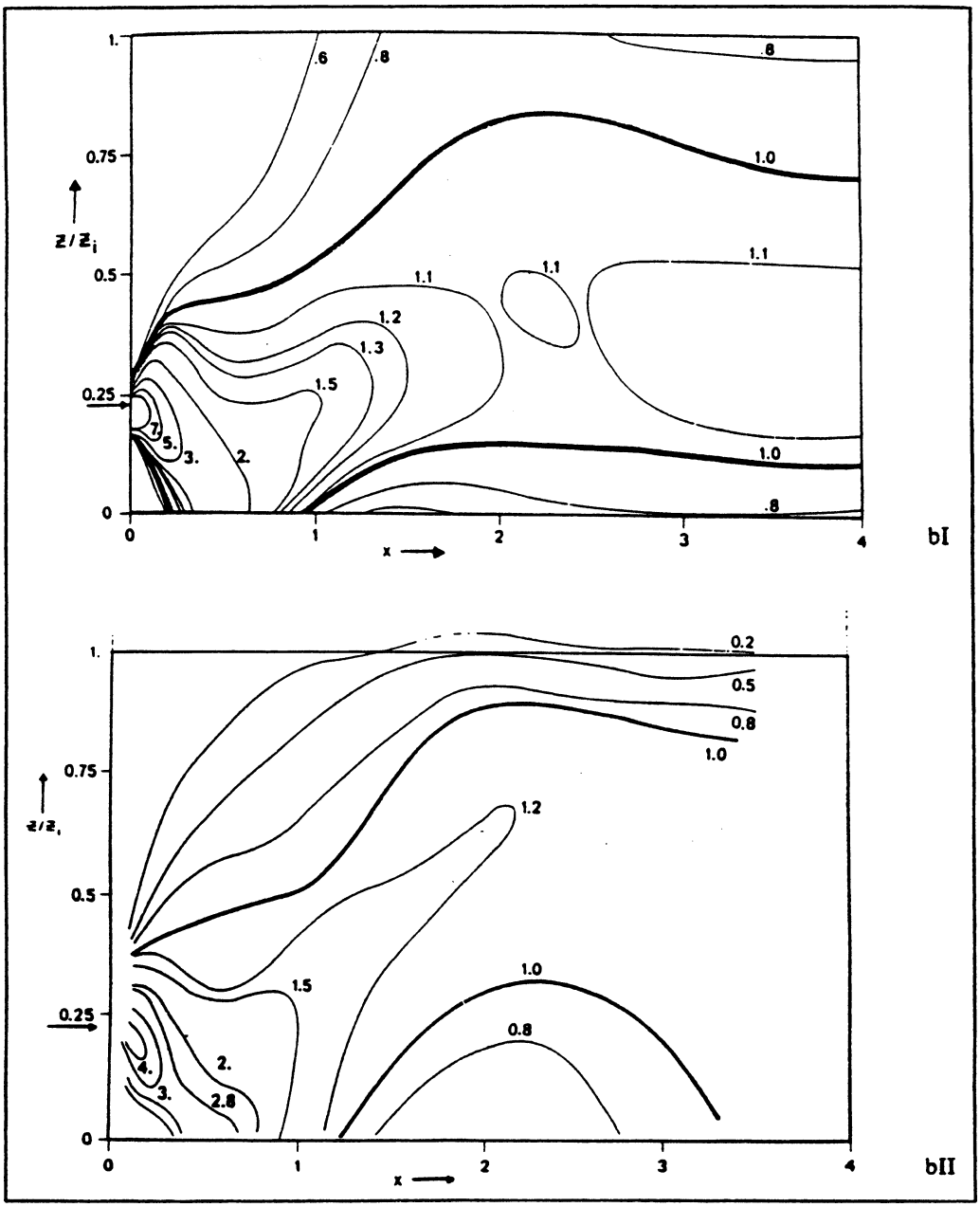

Figure 8–5 (continued).

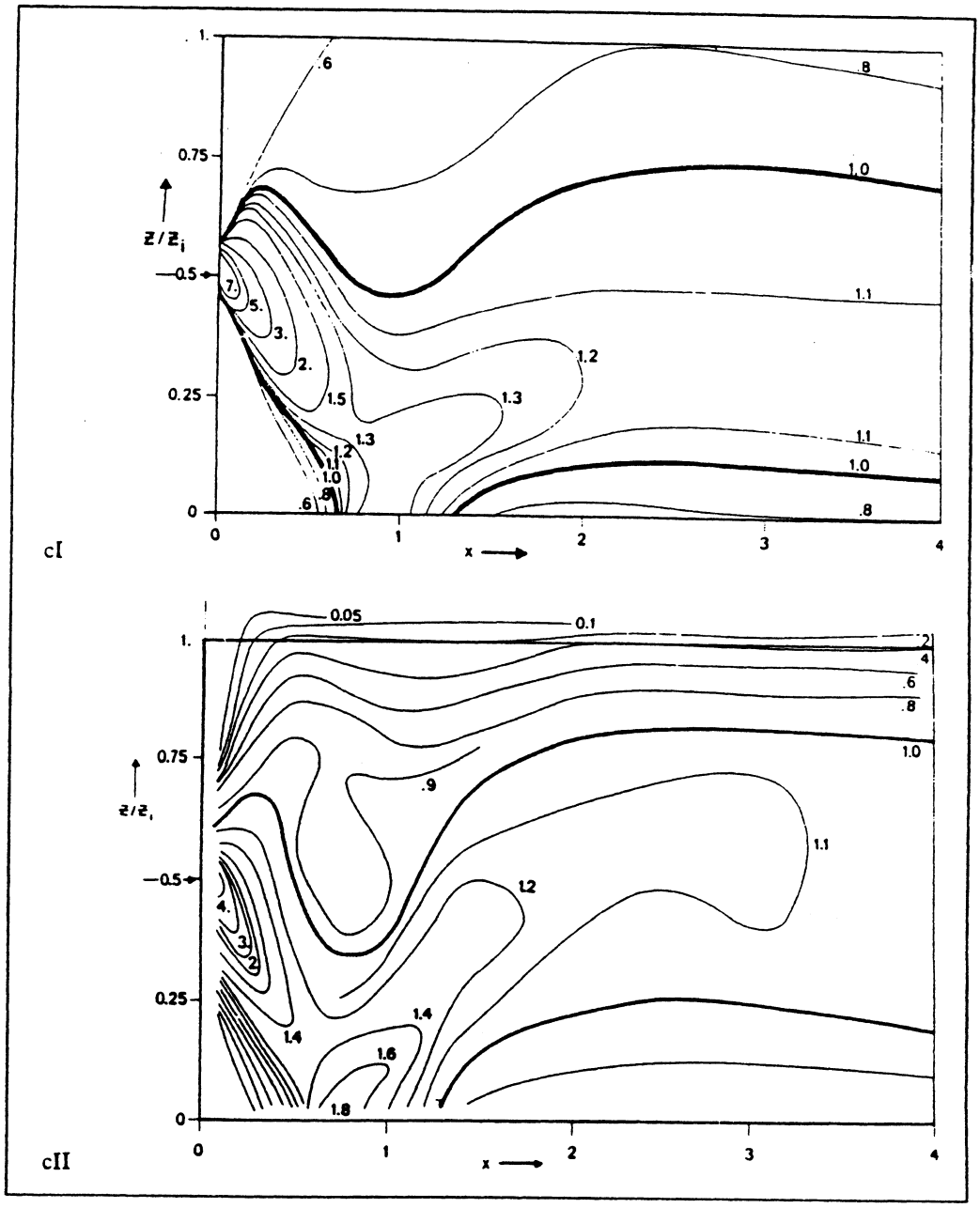

Figure 8–5 (continued).

time-varying to allow loss of mass due to ground deposition and chemical decay phenomena. Therefore, the spatial distribution of particle mass in the computational domain allows the calculation of a three-dimensional mass concentration field, under certain computational assumptions.

For example, the most straightforward assumption is the superimposition, in the computational domain, of a three-dimensional concentration grid. The concentrations are then computed simply by counting the number of particles in each grid cell and accumulating their masses. If concentrations need to be computed only at "receptor" points (e.g., at a ground level), receptor cells can be defined around these points and particles counted only inside those cells. A rigorous concentration calculation, however, should not just add up the particle mass in a given cell at a given time. In fact, the contribution of each particle mass should be weighted by the total time the particle spent inside the cell during each time step (Lamb, 1979b).

One of the great advantages of Monte-Carlo particle models, however, is their "grid-free" characteristics, which allow higher time and space resolution than other simulation techniques. In this respect, grid-free concentration calculations (i.e., calculations that do not require the definition of cells) to maintain this important feature of the model are appealing. "Kernel" methods (Gingold and Monaghan, 1982) allow grid-free concentration calculations that are smooth and efficient. Kernel methods for air quality modeling are discussed by Lorimer (1986). A general form of kernel density estimator is

$$c(\mathbf{r}, t) = \frac{A(\mathbf{r})}{l^3} \sum_{i=1}^{n} m_i \, W(\mathbf{r}_i - \mathbf{r}, l) \tag{8-97}$$

where c is the concentration in $\mathbf{r}$ at time t; l is a time-dependent resolution bandwidth (or smoothing length); m_i is the pollutant mass of each particle i; W is the smoothing kernel, which is a function of l and the distance $\mathbf{r}_i - \mathbf{r}$ of each particle i from the receptor point. $A(\mathbf{r})$ is a correction term for concentration computations at locations $\mathbf{r}$ close to the boundary of the computational domain D, where

$$A(\mathbf{r}) = \frac{l^3}{\int_D W(\mathbf{r}' - \mathbf{r}, l) d\mathbf{r}'} \tag{8-98}$$

which, for an infinite domain D, reduces to $A(\mathbf{r}) = 1$ everywhere.

Several kernel functions W are available in the literature. The most common is the Gaussian kernel, in which

$$\mathbf{d}_i = \mathbf{r}_i - \mathbf{r} \tag{8-99}$$

and

$$W(\mathbf{d}_i, l) = \frac{1}{(2\pi)^{3/2}} \exp\left(-\frac{1}{2}\frac{|\mathbf{d}_i|^2}{l^2}\right) \tag{8-100}$$

The choice of l is critical. This term should not be kept constant, as is done in many applications, but should change in relation to a natural length scale. In general, l should be particle dependent and should be related to the mean interparticle separation around $\mathbf{r}$. Only particles with $|\mathbf{d}_i| < l$ give substantial contribution to c (Lorimer, 1986). If l is too small, the spatial distribution of the concentration c is "jagged" with a series of local maxima at each $\mathbf{r}_i$; if l is too large, c becomes overly smooth.

Using a Gaussian kernel, the particle model becomes very similar to the puff models described in Section 7.8. It is important to note, however, that for a puff model, l is substituted by σ_x, σ_y, and σ_z (i.e., the standard deviations of the spatial concentration distributions of each puff), and these values are related to the physics of atmospheric diffusion, while, in the kernel method, l should be related only to the density of the particles around $\mathbf{r}$. However, Yamada and Bunker (1988) use a kernel density estimator, for their RAPTAD particle model, which makes it, in reality, a puff model, in which each particle i is associated with time-growing σ_{xi}, σ_{yi} and σ_{zi} values that are estimated based on the homogeneous diffusion theory by Taylor (1921).

8.3.7 Particle Simulation of Buoyancy Phenomena

One of the main advantages of Monte-Carlo particle models versus other particle methods (such as the particle-in-cell method described in Section 8.3.2) is the cost-effective ability to move each particle independently from the others. A correct treatment of buoyancy phenomena, however, requires the capability of incorporating, into the particle dynamics, extra velocity terms that simulate plume rise effects and heavy gas phenomena, both functions of local space properties related to the local concentration. Therefore, the motion of each particle affected by buoyancy phenomena depends upon the particle concentration, i.e., the dynamics of neighboring particles.

A simple, analytical approach to account for plume rise phenomena was illustrated by Zannetti and Al-Madani (1983). More comprehensive approaches have been proposed by Cogan (1985) and Gaffen et al. (1987).

8.3.8 Chemistry and Deposition

Since each particle can be tagged by its mass, i.e., the mass of pollutant(s) whose dynamics is represented by that particle, linear chemistry and deposition phenomena can be easily accounted for by properly modifying, in a dynamic way, the mass m_i of each particle. For example, Zannetti and Al-Madani (1983) proposed relationships such as

$$m_i(t + \Delta t) = m_i(t) \exp(-\Delta t/T) \tag{8-101}$$

to account for dry deposition, wet deposition, and linear chemistry transformation, where T is the appropriate time scale of each phenomenon that can vary with time and space. Alternatively, any deposition can be computed using the deposition velocity concept (see Equation 6-10), which requires the calculation of particle mass concentration in the layers just above the ground and a consequent dynamic reduction of the mass m_i of the particle to account for the ground deposition mass flux.

If nonlinear chemistry is required, for example, to simulate atmospheric photochemistry and ozone production, two possible methods can be used. With the first method, a concentration grid can be superimposed on the domain and, at each time step, concentrations can be computed in each grid cell. Then, an Eulerian photochemical model can be used to calculate the effects of chemical reactions from all sources at each time step. If the chemical reactions of a single plume must be simulated, a second method can be used, in which each particle can be considered an expanding box representing a section of the plume that grows with time and entrains background air and, possibly, other emissions along its trajectory. Then, the photochemical module of a Lagrangian box model (see Section 8-2) can be used to calculate the effects of chemical reactions inside each box at each time step. It is clear, however, that nonlinear chemistry by particle models is complex and extremely demanding of computational resources. A proper consideration of nontrivial chemical reactions may well be impossible in a Lagrangian framework. In any case, it would at least require a two-particle approach, since, for a second-order reaction, the reaction rate depends on the reactant covariance, which is a second-order concentration statistics (Sawford, personal communication).

Particle models can also be used to simulate the behavior of actual particulate matter in the atmosphere, whose dynamics is affected by atmospheric

turbulence and gravitational settling velocity V_G, which depends upon the diameter d_p of the aerosol particle. For example, Figure 8–6 shows the velocities with which spherical particles for different particle diameters and densities fall. When these particles hit the ground, permanent deposition can be assumed or, alternatively, probabilistic methods can be used to simulate particle deposition and, when deposited, the possibility of particle resuspension. For example, Zannetti and Al-Madani (1983) use expressions such as

$$q = 1 - \exp(-\Delta t/T) \tag{8-102}$$

to calculate both the deposition probability of a particle that reaches the ground, and the resuspension probability, where T is an appropriate time scale that depends upon meteorology and surface characteristics.

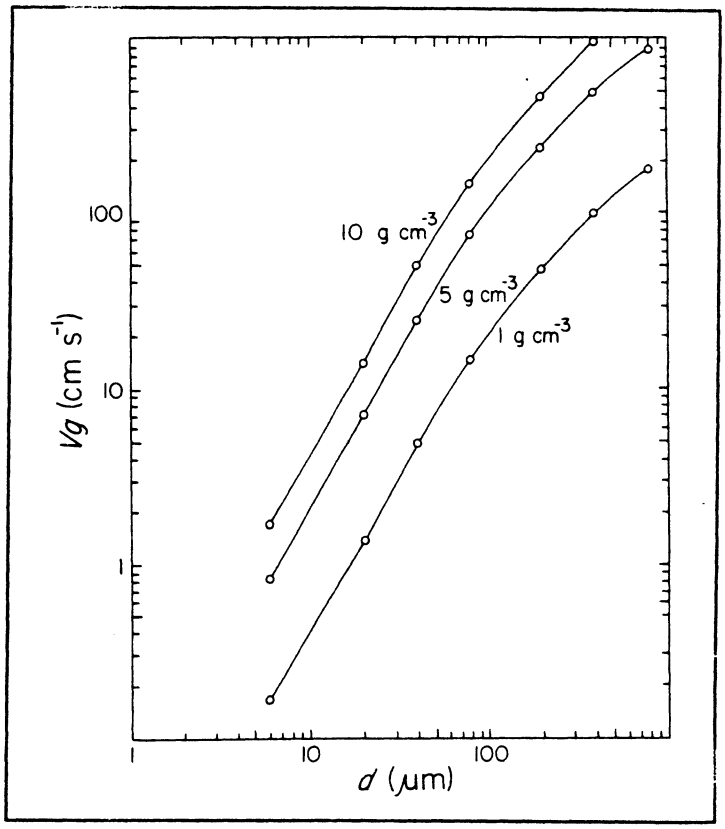

Figure 8–6. Fall velocity of spherical particles as a function of particle diameter and density. (Adapted from Hanna et al., (1982), as presented by Stern et al. (1984)). [Reprinted with permission from Academic Press.]

8.3.9 Advantages and Disadvantages of Particle Models

Dispersion simulation by Lagrangian particles has been called "natural" modeling. These models do not need the input of artificial stability classes, empirical sigma curves, or diffusion coefficients that are practically impossible to measure. Instead, diffusion characteristics are simulated by attributing a certain degree of "fluctuation" to each particle, using, for example, the computer's capability to generate semirandom numbers.

The basic advantages of this approach (e.g., see Lamb et al., 1979a; Lange, 1978) are:

- Compared with grid models, this method avoids the artificial initial diffusion of a point source in the corresponding cell and the advection numerical errors.
- This method is practically free of restricting physical assumptions, since all uncertainties are combined into the correct determination of pseudovelocities.
- Each particle can be tagged with its coordinates, source indicator, mass, activity, species and size, allowing computation of wet and dry deposition, decay, and particle size distribution.
- The meteorological input required can be directly inferred from measured data. The primary information needed is (Lamb et al., 1979a) the variance of wind velocity fluctuations and the Lagrangian autocorrelation function, which can be estimated from Eulerian measurements.

Potentially, this method is superior in both numerical accuracy and physical representativeness. However, much research is still needed to extract, from the scarce available meteorological measurements and our limited theoretical understanding of turbulence processes, the meteorological input required to run this model (i.e., the pseudovelocities to move each particle at each time step).

REFERENCES

Baerentsen, J.H., and R. Berkovicz (1984): Monte Carlo simulation of plume dispersion in the convective boundary layer. *Atmos. Environ.*, **18**:701–712.

Briggs, G.A. (1975): Plume rise predictions, in *Lectures on Air Pollution and Environmental Impact Analyses*. edited by D.A. Augen, Boston: American Meteorological Society.

Briggs, G.A. (1983): Diffusion modeling with convective scaling. AMS specialty conference on Air Quality Modeling of the Urban Boundary Layer, Baltimore.

Brusasca, G., G. Tinarelli, D. Anfossi, P. Zannetti (1987): Particle modeling simulation of atmospheric dispersion using the MC–LAGPAR package. *Envir. Software*, **2**:151–158.

Cogan, J.L. (1985): Monte Carlo simulations of buoyancy dispersion. *Atmos. Environ.*, **19**:867–878.

Davis, R.E. (1982): On relating Eulerian and Lagrangian velocity statistics: Single particles in homogeneous flows. *J. Fluid Mech.*, **114**:1–26.

Deardorff, J.W. (1974): Three–dimensional numerical study of the height and mean structure of a heated boundary layer. *Boundary–Layer Meteor.*, **7**:81–106.

de Baas, A.F., H. van Dop, and F.T. Nieuwstadt (1986): An application of the Langevin equation for inhomogeneous conditions to dispersion in a convection boundary layer. *Quarterly J. Roy. Meteor. Soc.*, **112**:165–180.

Drivas, P.J., M.W. Chan, and L.G. Wayne (1977): Validation of an improved photochemical air quality simulation model. *Proceedings*, AMS joint conference on Applications of Air Pollution Meteorology. Salt Lake City, Utah. November.

Gifford, F.A. (1982): Horizontal diffusion in the atmosphere: Lagrangian–dynamical theory. *Atmos. Environ.*, **16**:505–512.

Durbin, P.A. (1980): A stochastic model of two–particle dispersion and concentration fluctuations in homogeneous turbulence. *J. Fluid Mech.*, **100**:279–302.

Gaffen, D. J., C. Benocci, and D. Olivari (1987): Numerical modeling of buoyancy dominated dispersal using a Lagrangian approach. *Atmos. Environ.*, **21**:1285–1293.

Gingold, R.A., and J.J. Monaghan (1982): Kernel estimates as a basis for general particle methods in hydrodynamics. *J. Computational Phys.*, **46**:429–453.

Hall, C.D. (1975): The simulation of particle motion in the atmosphere by a numerical random–walk model. *Quarterly J. Roy. Meteor. Soc.*, **101**:235–244.

Hanna, S.R. (1979): Some statistics of Lagrangian and Eulerian wind fluctuations. *J. Appl. Meteor.*, **18**:518–525.

Hanna, S.R., G.A. Briggs, and R.P. Hosker, Jr. (1982): *Handbook on Atmospheric Diffusion*, edited by J.S. Smith, Washington, D.C.: Technical Information Center, U.S. Department of Energy.

Hanna, S.R. (1981): Lagrangian and Eulerian time scale relations in the daytime boundary layer. *J. Appl. Meteor.*, **20**:242–249.

Hockney, R.W., and J.W. Eastwood (1981): *Computer Simulation Using Particles*. New York: McGraw–Hill, Inc.

Janicke, L. (1981): Particle simulation of inhomogeneous turbulent diffusion. *Proceedings*, 12th International Technical Meeting of the NATO CCMS. Palo Alto, California: Plenum Press.

Lamb, R.G. (1978): A numerical simulation of dispersion from an elevated point source in the convective planetary boundary layer. *Atmos. Environ.*, **12**:1297–1304.

Lamb, R.G., H. Hogo, and L.E. Reid (1979a): A Lagrangian Monte Carlo model of air pollutant transport, diffusion and removal processes. 4th AMS Symposium on Turbulence, Diffusion and Air Pollution. Reno, Nevada. January.

Lamb, R.G., H. Hogo, and L.E. Reid (1979b): A Lagrangian approach to modeling air pollutant dispersion: Development and testing in the vicinity of a roadway. EPA Research Report EPA-600/4-79-023.

Lamb, R.G. (1981): A scheme for simulating particle pair motions in turbulent fluid. *J. Computational Phys.*, **39**:329–346.

Lange, R. (1978): ADPIC -- A three-dimensional particle-in-cell model for the dispersal of atmospheric pollutants and its comparison to regional tracer studies. *J. Appl. Meteor.*, **17**:320.

Legg, B.J., and M.R. Raupach (1982): Markov chain simulation of particle dispersion in inhomogeneous flows: The mean drift velocity induced by a gradient in Eulerian velocity variance. *Boundary-Layer Meteor.*, **24**:3–13

Legg, B.J. (1983): Turbulent dispersion from an elevated line source: Markov chain simulations of concentration and flux profiles. *Quarterly J. Roy. Meteor. Soc.*, **109**:645–660.

Lee, J.T., G.L. Stone, R.E. Lawson, Jr., and M. Shipman (1985): Monte Carlo simulation of two-particle relative diffusion using Eulerian Statistics. Los Alamos National Laboratory Document LA-UR-85-2008, Los Alamos, New Mexico.

Ley, A.J. (1982): A random walk simulation of two-dimensional turbulent diffusion in the neutral surface layer. *Atmos. Environ.*, **16**:2799–2808.

Ley, A.J., and D.J. Thomson (1983): A random walk model of dispersion in the diabatic surface layer. *Quarterly J. Roy. Meteor. Soc.*, **109**:847–880.

Lorimer, G.S. (1986): The kernel method for air quality modelling; I. Mathematical foundation. *Atmos. Environ.*, **20**:1447–1452.

Lurmann, F.W., D.A. Gooden, and H.M. Collins, Eds. (1985): User's guide to the PLMSTAR air quality simulation model. Environmental Research & Technology, Inc. Document M-2206-100, Newbury Park, California.

Martinez, J.R., R.A. Nordsieck, and M.A. Hirschberg (1973): User's guide to diffusion/kinetics (DIFKIN) code. General Research Corporation Final Report CR-2-273/1, prepared for the U.S. Environmental Protection Agency.

Nieuwstadt, F.T., and H. van Dop, Eds. (1982): *Atmospheric Turbulence and Air Pollution Modeling*. Dordrecht, Holland: D. Reidel.

Novikov, E.A. (1969): *Appl. Math. Mech.*, **33**:887.

Novikov, E.A. (1986): The Lagrangian-Eulerian probability relations and the random force method for nonhomogeneous turbulence. *Phys. of Fluids*, **29**:3907–3909.

Poreh, M., and J.E. Cermak (1984): Wind tunnel simulation of diffusion in a convective boundary layer. *Proceedings*, 29th Oholo Conference on Boundary Layer Structure-Modelling and Application to Air Pollution and Wind Energy. Israel. March.

Reid, J.D. (1979): Markov chain simulations of vertical dispersion in the neutral surface layer for surface and elevated releases. *Boundary-Layer Meteor.*, **16**:3–22.

Rodriguez, D.J., G.D. Greenly, P.M. Gresho, R. Lange, B.S. Lawver, L.A. Lawson, and H. Walker (1982): User's guide to the MATHEW/ADPIC models. Lawrence Livermore National Laboratory Document UASG 82-16, University of California Atmospheric and Geophysical Sciences Division, Livermore, California.

Sawford, B.L. (1983): The effect of Gaussian particle-pair distribution functions in the statistical theory of concentration fluctuations in homogeneous turbulence. *Quarterly J. Roy. Meteor. Soc.*, **109**:339-354.

Sawford, B.L. (1984): The basis for, and some limitations of, the Langevin equation in atmospheric relative dispersion modelling. *Atmos. Environ.*, **11**:2405-2411.

Sawford, B.L. (1985): Lagrangian simulation of concentration mean and fluctuation fields. *J. Clim. Appl. Meteor.*, **24**:1152-1166.

Seinfeld, J.H. (1975): *Air Pollution -- Physical and Chemical Fundamentals*. New York: McGraw-Hill.

Smith, F.B. (1968): Conditioned particle motion in a homogeneous turbulent field. *Atmos. Environ.*, **2**:491-508.

Stern, A.C., R.W. Boubel, D.B. Turner, and D.L. Fox (1984): *Fundamentals of Air Pollution*. Orlando, Florida: Academic Press.

Taylor, G.I. (1921): Diffusion by continuous movements. *Proceedings*, London Math. Soc., **20**: 196-211.

Tran, K. (1981): User's guide for photochemical trajectory model TRACE. Applied Modeling, Inc., Report 81/003. California.

Thomson, D.J. (1984): Random walk modelling of diffusion in inhomogeneous turbulence. *Quarterly J. Roy. Meteor. Soc.*, **110**:1107-1120.

Thomson, D.J. (1987): *J. Fluid Mech.*, **180**:529.

van Dop, H., F.T. Nieuwstadt, and J.C. Hunt (1985): Random walk models for particle displacements in inhomogeneous unsteady turbulent flows. *Phys. of Fluids*, **28**:1639-1653.

Willis, G.E., and J. W. Deardorff (1978): A laboratory study of dispersion from an elevated source within a modeled convective planetary boundary layer. *Atmos. Environ.*, **12**:1305-1311.

Willis, G.E., and J. W. Deardorff (1981): A laboratory study of dispersion from a source in the middle of the convective mixed layer. *Atmos. Environ.*, **15**:109-117.

Wilson, J.D., G. W. Thurtell, and G.E. Kidd (1981): Numerical simulation of particle trajectories in inhomogeneous turbulence; III. Comparison of predictions with experimental data for the atmospheric surface layer. *Boundary-Layer Meteor.*, **12**:423-441.

Yamada, T., and S.S. Bunker (1988): Development of a nested grid, second moment turbulence closure model and application to the 1982 ASCOT Brush Creek data simulation. *J. Appl. Meteor.*, **27**:562-578.

Yamamoto, S., M. Gamo, and Y. Osayuki (1982): Observational study of the fine structure of the convective atmospheric boundary layer. *J. Meteor. Soc. of Japan*, **60**:882-888.

Zannetti, P. (1981): Some aspects of Monte Carlo type modeling of atmospheric turbulent diffusion. *Preprints*, Seventh AMS conference on Probability and Statistics in Atmospheric Sciences. Monterey, California. November, 1978.

Zannetti, P., and N. Al-Madani (1983): Simulation of transformation, buoyancy and removal processes by Lagrangian particle methods. *Proceedings*, 14th international technical meeting on Air Pollution Modeling and its Application. Copenhagen, Denmark. September.

Zannetti, P. (1984): New Monte Carlo scheme for simulating Lagrangian particle diffusion with wind shear effects. *Appl. Math. Modelling*, **8**:188–192.

Zannetti, P. (1986): Monte-Carlo simulation of auto- and cross-correlated turbulent velocity fluctuations (MC-LAGPAR II Model). *Environ. Software*, 1:26–30.

9 ATMOSPHERIC CHEMISTRY

Early air pollution studies dealt with the challenging problem of correctly simulating atmospheric diffusion and, in particular, the maximum ground-level impact of elevated emissions of primary pollutants, such as SO_2. Two major factors, however, focused attention on atmospheric chemistry: 1) photochemical smog, a new, different smog associated with high-temperature "summertime" conditions, and first recognized in the Los Angeles basin in the 1940s; and 2) long-range transport phenomena, clearly identified in the 1970s, that led to the study of multiday transport scenarios of industrial and urban plumes and, consequently, to the simulation of the formation, inside them, of secondary gases and particles.

Atmospheric chemistry deals essentially with four major issues (Seigneur, 1987):

1. Photochemical smog in sunny, urban areas, such as Los Angeles and Mexico City
2. Aerosol chemistry
3. Acidic deposition by dry and wet deposition phenomena (see Section 10)
4. Air toxics

In addition to the above topics, fog chemistry plays an important role, even though understanding of it is limited at the present time.

A correct treatment of atmospheric chemistry requires the solution of chemical kinetic and thermodynamic equations and, when necessary, some treatment of those physical processes (e.g., cloud microphysics, aerosol size, etc.) that affect the evolution of the chemistry of the system. A complete discussion of chemical processes in the atmosphere is beyond the scope of this book. The reader is referred to Seinfeld (1986) and Finlayson-Pitts and Pitts (1986) for a thorough discussion of this subject. In this chapter, we will provide a summary of the major issues related to the understanding and computer simulation of the major atmospheric chemistry phenomena.

9.1 PHOTOCHEMICAL SMOG: NITROGEN OXIDES AND OZONE

Ozone is the major indicator of the presence of urban photochemical smog. Ozone is naturally generated in the stratosphere by a photochemical reaction in which high-energy solar radiation breaks the oxygen molecules, i.e.

$$O_2 + h\nu\ (\lambda < 242\ \text{nm}) \rightarrow 2\,O\cdot \tag{9-1}$$

The oxygen atoms then combine with oxygen molecules to form ozone, i.e.

$$O\cdot + O_2 \rightarrow O_3 \tag{9-2}$$

A small fraction of this stratospheric layer of ozone penetrates the PBL and is responsible for the ambient background concentration of O_3. Stratospheric ozone intrusion into the PBL is also responsible for some natural high concentration values, following large convective thunderstorms.

Anthropogenic generation of O_3 is, again, a photochemical process, in which NO_2, mostly generated from emissions of primary NO from combustion processes, is photochemically dissociated by

$$NO_2 + h\nu\ (\lambda < 430\ \text{nm}) \rightarrow NO + O\cdot \tag{9-3}$$

and the oxygen atom produces ozone via Equation 9-2. This chemical mechanism is the only known process for ozone formation in a polluted atmosphere.

Ozone is scavenged by its reaction with combustion emissions of NO

$$NO + O_3 \rightarrow NO_2 + O_2 \tag{9-4}$$

This reaction is highly effective at night inside the mixing layer because, without solar radiation, the NO_2 cannot be further dissociated by Equation 9-3. Above the mixing layer, however, ozone is not consumed and may, therefore, be fumigated to the ground the following morning, when the nighttime ground-level inversion breaks.

Because of the reaction scheme described above, it is evident that any reaction converting NO to NO_2 (besides Equation 9-4, which actually reduces O_3 concentrations) contributes to ozone formation. NO_2 is formed in combustion exhaust gases by

$$2NO + O_2 \rightarrow 2NO_2 \qquad (9\text{–}5)$$

However, it can be easily seen (e.g., Seinfeld, 1986) that Equation 9–5 is insufficient to account for the O_3 concentrations of a few hundred pbb that are commonly measured during urban photochemical episodes. It has been well established that the NO-to-NO_2 conversion, in a polluted atmosphere, is dominated by the carbon-containing species, as discussed in the next section.

9.2 PHOTOCHEMICAL SMOG: THE ROLE OF THE CARBON-CONTAINING SPECIES

The role of carbon-containing species is essential to understand the NO-to-NO_2 conversion and, consequently, the occurrence of high ozone concentrations.

The simplest carbon-containing species is CO, whose reaction with NO_x is summarized in Table 9–1. This reaction scheme indicates that ozone photolyzes (Reaction 4) to produce an excited $O(^1D)$ oxygen atom, which collides with water (Reaction 6) to produce the two hydroxyl radicals $OH\cdot$, that react with the carbon monoxide (Reaction 7) to produce the hydroperoxyl radical $HO_2\cdot$, a species that is responsible for the oxidation of NO into NO_2 (Reaction 8). Note that the other

Table 9–1. Atmospheric chemistry of CO and NO_x (from Seinfeld, 1986). [Reprinted with permission from John Wiley and Sons.]

Reaction	Rate Constant[a]
1. $NO_2 + h\nu \rightarrow NO + O$	Depends on light intensity
2. $O + O_2 + M \rightarrow O_3 + M$	$6.0 \times 10^{-34}(T/300)^{-2.3}$ cm^6 molecule^{-2} sec^{-1}
3. $O_3 + NO \rightarrow NO_2 + O_2$	$2.2 \times 10^{-12}\exp(-1430/T)$ cm^3 molecule^{-1} sec^{-1}
4. $O_3 + h\nu \rightarrow O(^1D) + O_2$	$0.0028k_1$
5. $O(^1D) + M \rightarrow O + M$	2.9×10^{-11} cm^3 molecule^{-1} sec^{-1}
6. $O(^1D) + H_2O \rightarrow 2OH\cdot$	2.2×10^{-10} cm^3 molecule^{-1} sec^{-1}
7. $CO + OH\cdot \rightarrow CO_2 + HO_2\cdot$	2.2×10^{-13} cm^3 molecule^{-1} sec^{-1}[b]
8. $HO_2\cdot + NO \rightarrow NO_2 + OH\cdot$	$3.7 \times 10^{-12}\exp(240/T)$ cm^3 molecule^{-1} sec^{-1}
9. $OH\cdot + NO_2 \rightarrow HNO_3$	1.1×10^{-11} cm^3 molecule^{-1} sec^{-1}

[a] Baulch et al. (1982).
[b] Atkinson and Lloyd (1984).

radical, $OH\cdot$, is also responsible for the formation of nitric acid HNO_3, through its reaction with NO_2 (Reaction 9).

A similar cycle can be identified for formaldehyde *HCHO*, which is both emitted as primary pollutant and generated as an oxidation product of hydrocarbons. The *HCHO* cycle is presented in Table 9–2. In this cycle, formaldehyde, either by photodissociation (Reaction 4a) or reaction with $OH\cdot$ (Reaction 5), produces the radical $HO_2\cdot$, which oxidizes *NO* into NO_2 (Reaction 6). Figure 9–1 shows how the formation of NO_2 (and, therefore, O_3) is driven by the initial concentration of *HCHO*. Clearly, many other hydrocarbons are involved, but the major features of photochemical smog chemistry are well exemplified by this $NO_x/HCHO$ mechanism.

Other hydrocarbons, besides formaldehyde, include other aldehydes, ketones, paraffins (i.e., alkanes), olefins (i.e., alkenes) and aromatics. Table 9–3 summarizes the typical lifetimes of these hydrocarbons in a polluted atmosphere.

9.3 PHOTOCHEMICAL SMOG: SIMULATION MODELING

Mathematical modeling of photochemical smog requires the numerical simulation of all the chemical reactions that take place between NO_x and

Table 9–2. Atmospheric reaction mechanism involving NO, NO_2 and HCHO (from Seinfeld, 1986). [Reprinted with permission from John Wiley and Sons.]

Reaction	Rate Constant
1. $NO_2 + h\nu \rightarrow NO + O$	Depends on light intensity
2. $O + O_2 + M \rightarrow O_3 + M$	See Table 9–1
3. $O_3 + NO \rightarrow NO_2 + O_2$	See Table 9–1
4. $HCHO + h\nu \rightarrow 2HO_2\cdot + CO$	Depends on light intensity
$\rightarrow H_2 + CO$	Depends on light intensity
5. $HCHO + OH\cdot \rightarrow HO_2\cdot + CO + H_2O$	1.1×10^{-11} cm^3 molecule^{-1} sec^{-1} [a]
6. $HO_2\cdot + NO \rightarrow NO_2 + OH\cdot$	See Table 9–1
7. $OH\cdot + NO_2 \rightarrow HNO_3$	See Table 9–1

[a] Baulch et al. (1982)

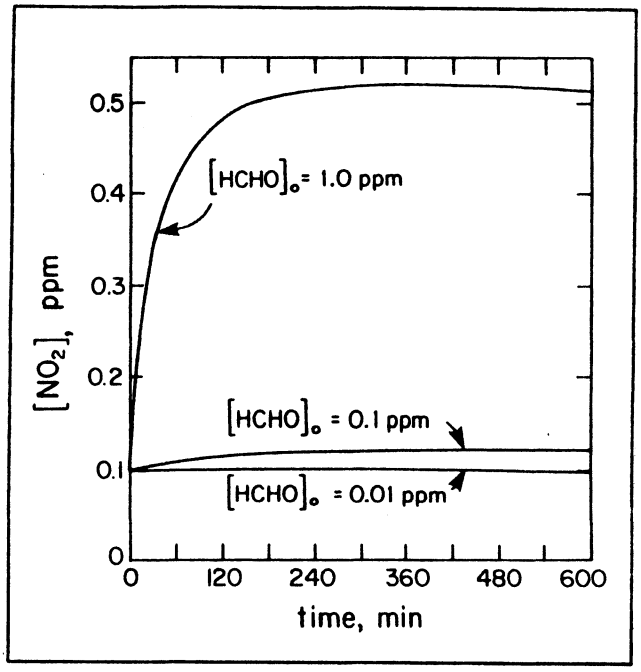

Figure 9–1. Effect of initial concentration of formaldehyde on the dynamics of NO_2 in the photooxidation of a mixture of HCHO, NO, and NO_2 in the air. In the three cases shown, $[NO_2]_0 = 0.1$ ppm and $[NO]_0 = 1.0$ ppm (from Seinfeld, 1986). [Reprinted with permission from John Wiley and Sons.]

carbon-containing compounds, such as paraffins, olefins, aldeydes, ketones and aromatic compounds. An explicit treatment of all these reactions is practically impossible. For example, Kerr and Calvert (1984) developed a chemical kinetic mechanism that includes over 1,000 chemical reactions. Clearly, for most practical purposes, the numerical simulations must use a condensed kinetic mechanism to avoid excessive simulation costs (a portion of an explicit chemical mechanism is presented in Table 9–4).

Three major approaches have been taken (Seigneur, 1987) to develop condensed and computationally affordable kinetic mechanisms for modeling:

1. Surrogate species mechanisms, in which a few hydrocarbons are selected as representative of their respective hydrocarbon class

2. Lumped molecule mechanisms, in which hydrocarbons from the same class are lumped together and a hypothetical species is defined to represent each class (a portion of a lumped mechanism is presented in Table 9–5)

Table 9–3. Photolysis and oxidation lifetime of hydrocarbons in a typical polluted atmosphere[a] (from Seigneur, 1987). [Reprinted with permission from Computational Mechanics Publications.]

Hydrocarbon	Photolysis	O_3 Reaction	OH Reaction	O Reaction	HO_2 Reaction	NO_3 Reaction
Formaldehyde	2 h	--	6 h	--	4 h	8 d
Other Aldehydes	6 h	--	2 to 5 h	--	--	2 to 4 d
Ketones		--	2 h to 10 d	--	--	(b)
Methane	--	--	9 mo	--	--	--
Other Paraffins	--	--	10 min to 9 d	--	--	20 d to 8 mo
Anthropogenic Olefins	--	5 min to 2 d	50 min to 7 h	3 d to 1 y	--	8 s to 3 mo
Natural Olefins	--	1 to 7 h	30 min to 1 h	(b)	--	40 s to 20 min
Alkynes	--	--	7 h to 3 d	--	--	--
Aromatics (nonoxygenated)	--	--	2 h to 2 d	--	--	18 d to 8 mo
Aromatics (oxygenated)	--	--	1 to 2 h	--	--	10 to 30 s

(a) Conditions are for summertime, concentrations of 120 ppb of O_3, 0.2 ppt of OH, 0.002 ppt of O, 40 ppt of HO_2 and 100 ppt of NO_3. Photolysis and reactions with O_3, OH, O and HO_2 are important during daytime, reactions with NO_3 are important at night. Lifetimes which exceed 1 year are not listed. The lifetime is defined as the inverse of the first-order or pseudo-first-order reaction rate parameter. Therefore, it corresponds to the time necessary for the hydrocarbon concentration to decrease to 37 percent of its initial value.
(b) Not available.

3. Carbon-bond mechanism, in which the classification is based on chemical bonds of hydrocarbons and their reactivity (a portion of the carbon-bond mechanism is presented in Table 9–6)

Simulation models based on the above mechanisms are applied, with the major goal of quantifying the complex, nonlinear relationship between the emissions of primary precursors (i.e., NO_x and volatile organic compounds, VOC, often referred to as reactive hydrocarbons, RHC, or nonmethane hydrocarbons, NMHC) and the maximum ground level concentrations of O_3. It is still a major technical and political challenge, in regions like the Los Angeles basin, to assess, in a proper and technically credible way, the most cost-effective reduction of NO_x and VOC emissions that will give a desired decrease in O_3 concentrations

Table 9–4. Portion of an explicit chemical mechanism (from Finlayson–Pitts and Pitts, 1986). [Reprinted with permission from John Wiley and Sons.]

Reaction	Rate Constant[a]
Inorganic Reactions	
(1) $NO_2 + h\nu \rightarrow NO + O(^3P)$	0.35–0.40 min^{-1}
(2) $O(^3P) + O_2 \rightarrow O_3$	2.6×10^1
(3) $O_3 + NO \rightarrow NO_2 + O_2$	2.7×10^1
(4) $O(^3P) + NO_2 \rightarrow NO + O_2$	1.4×10^4
(5) $O_3 + NO_2 \rightarrow NO_3 + O_2$	4.7×10^{-2}
etc.	
Aldehyde Reactions and PAN Formation	
(30) $CH_3CHO + h\nu \xrightarrow{2O_2} CH_3O_2 + HO_2 + CO$	*b*
(31) $CH_3CHO + OH \xrightarrow{O_2} CH_3CO_3 + H_2O$	2.4×10^4
(32) $CH_3O_2 + NO \rightarrow NO_2 + CH_3O$	1.1×10^4
etc.	
α-Dicarbonyl Chemistry	
(43) $CH_3COCHO + OH \xrightarrow{O_2} CH_3COO_2 + CO + H_2O$	2.5×10^4
(44) $CH_3COCHO + h\nu \xrightarrow{2O_2} CH_3COO_2 + HO_2 + CO$	*c*
(45) $CH_3COCHO + h\nu \xrightarrow{2O_2} CH_3O_2 + HO_2 + 2CO$	*c*
etc.	
Toluene Abstraction Pathway	
(48) $C_6H_5CH_3 + OH \xrightarrow{O_2} C_6H_5CH_2O_2 + H_2O$	7.5×10^2
(49) $C_6H_5CH_2O_2 + NO \xrightarrow{O_2} NO_2 + C_6H_5CHO$	9.0×10^3
(50) $C_6H_5CH_2O_2 + NO \rightarrow C_6H_5CH_2ONO_2$	1.0×10^3
etc.	
Toluene Addition Pathway	
(64) $C_6H_5CH_3 + OH \rightarrow C_6H_5(CH_3)OH$	8.7×10^3
(65) $C_6H_5(CH_3)OH + O_2 \rightarrow C_6H_4(CH_3)OH + HO_2$	1.0×10^1
(66) $C_6H_5(CH_3)OH + NO_2 \rightarrow C_6H_4(CH_3)NO_2 + H_2O$	4.4×10^4
etc.	
Conjugated α-Dicarbonyl Chemistry	
(82) $OHCCH{=}CHCHO + OH \xrightarrow{O_2} OHCCH{=}CHC(O)O_2 + H_2O$	4.4×10^4
(83) $OHCCH{=}CHC(O)O_2 + NO \xrightarrow{O_2} OHCCH{=}CHO_2 + NO_2 + CO_2$	1.0×10^4
etc.	

Source: Leone and Seinfeld, 1984.

[a] In units of $ppm^{-1}\ min^{-1}$ unless otherwise stated.

[b] $k_{30} = 8.4 \times 10^{-4}\ k_1$.

[c] $(k_{44} + k_{45}) = 0.019\ k_1$.

Table 9–5. Portion of a lumped chemical submodel used for modeling an urban airshed (from Finlayson–Pitts and Pitts, 1986). An updated version of this mechanism is found in Lurmann et al. (1985). [Reprinted with permission from John Wiley and Sons.]

Reaction	Rate Constant[a]
(1) $NO_2 + h\nu \rightarrow NO + O(^3P)$	0.339 min^{-1}[b]
(2) $O(^3P) + O_2 + M \rightarrow O_3 + M$	$3.9 \times 10^{-6}\, e^{510/T}$
⋮	⋮
(21) $HCHO + h\nu \rightarrow 2HO_2 + CO$	0.00163 min^{-1}
(22) $HCHO + h\nu \rightarrow H_2 + CO$	0.00296 min^{-1}
(23) $HCHO + OH \rightarrow HO_2 + H_2O + CO$	1.9×10^4
(24) $RCHO + h\nu \rightarrow RO_2 + HO_2 + CO$	0.00145
(25) $RCHO + OH \rightarrow RCO_3$	2.6×10^4
(26) $C_2H_4 + OH \rightarrow RO_2$	1.2×10^4
(27) $C_2H_4 + O \rightarrow RO_2 + HO_2$	1.2×10^3
(28) $OLE + OH \rightarrow RO_2$	8.9×10^4
(29) $OLE + O \rightarrow RO_2 + RCO_3$	2.2×10^4
(30) $OLE + O_3 \rightarrow (a_1)RCHO + (a_2)HCHO + (a_3)HO_2 + (a_4)RO_2 + (a_5)OH + (a_6)RO$	0.136
(31) $ALK + OH \rightarrow RO_2$	4.7×10^3
(32) $ALK + O \rightarrow RO_2 + OH$	99.8
(33) $ARO + OH \rightarrow RO_2 + RCHO$	1.6×10^4
(16) $RO_2 + NO \rightarrow RO + NO_2$	1.2×10^4
(18) $NO_2 + OH \rightarrow HNO_3$	1.5×10^4
(42) $RCO_3 + NO_2 \rightarrow PAN$	2.07×10^3
(43) $PAN \rightarrow RCO_3 + NO_2$	$4.77 \times 10^{16}\, e^{-12516/T}$
(44) $NO_2 + NO_3 \rightarrow N_2O_5$	$2.19 \times 10^2\, e^{861/T}$
(46) $N_2O_5 + H_2O \rightarrow 2HNO_3$	1.5×10^{-5}
⋮	⋮
(52) $2RO_2 \rightarrow 2RO$	196

Source: McRae et al., 1982a,b.

[a] In units of ppm^{-1} min^{-1} unless otherwise stated.

[b] Average of daylight hours.

to meet the local air quality standards. These are the type of multibillion dollar air quality control questions that can properly be answered only through the application of the most advanced photochemical models.

Several Lagrangian and Eulerian models contain numerical routines for the treatment of multispecies chemical reactions. A description of the practical implementation of a photochemical reaction mechanism (i.e., a numerical

simulation scheme) in an Eulerian grid model is described by McRae et al. (1982b) and briefly summarized below. Also, particularly important is the "Atkinson–Carter" gas-phase photochemical mechanism, which has been implemented into a flexible, easy-to-update software system (Carter, 1988). This mechanism can run in its most complete version, can be extended to include new representations, can be refined by the choice of parameters, and, finally, can be condensed for practical use in airshed models. Appropriate software tools make the above operations much easier to perform than with other mechanisms.

Table 9–6. A portion of the carbon bond mechanism (from Finlayson–Pitts and Pitts, 1986). An updated version of this mechanism can be found in Gery et al. (1987). [Reprinted with permission from John Wiley and Sons.]

Reaction	Rate Constant ($ppm^{-1}\ min^{-1}$)
$NO_2 + h\nu \rightarrow NO + O$	k_1[a]
$O + O_2 (+ M) \rightarrow O_3 (+ M)$	2.08×10^{-5}
$O_3 + NO \rightarrow NO_2 + O_2$	25.2
$O + NO_2 \rightarrow NO + O_2$	1.34×10^{4}
$O_3 + NO_2 \rightarrow NO_3 + O_2$	5×10^{-2}
$NO_3 + NO \rightarrow NO_2 + NO_2$	2.5×10^{4}
$NO_3 + NO_2 + H_2O \rightarrow 2HNO_3$	2.0×10^{-3}
$HNO_2 + h\nu \rightarrow NO + OH$	$0.19\ k_1$
$NO_2 + OH \rightarrow HNO_3$	1.4×10^{4}
$NO + OH \rightarrow HNO_2$	1.4×10^{4}
$CO + OH \xrightarrow{O_2} CO_2 + HO_2$	4.5×10^{2}
$OLE + OH \xrightarrow{O_2} CAR + CH_3O_2$	3.8×10^{4}
$PAR + OH \xrightarrow{O_2} CH_3O_2 + H_2O$	1.3×10^{3}
$ARO + OH \xrightarrow{O_2} CAR + CH_3O_2$	8×10^{3}
$OLE + O \xrightarrow{2O_2} HC(O)O_2 + CH_3O_2$	5.3×10^{3}
$PAR + O \xrightarrow{O_2} CH_3O_2 + OH$	20
$ARO + O \xrightarrow{2O_2} HC(O)O_2 + CH_3O_2$	37
$ARO + NO_3 \rightarrow$ products (aerosol)	1.0×10^{2}
$OLE + O_3 \xrightarrow{O_2} \alpha[HC(O)O_2] + HCHO + OH$	1.5×10^{-2}
$CAR + OH \xrightarrow{O_2} HC(O)O_2 + H_2O$	1.0×10^{4}
$CAR + h\nu \xrightarrow{2O_2} \alpha HC(O)O_2 + \alpha HO_2 + (1 - \alpha)CO$	$6.0 \times 10^{-3}\ k_1$

Source: Whitten and Hogo, 1977; Whitten et al., 1980.
[a]Varies with light intensity.

9.3.1 A Numerical Simulation Scheme

Using the approximation of Equation 6–15, chemical reactions are represented by the terms R_{c_m}, $m = 1, 2 \ldots M$. If we assume a homogeneous, isothermal, isobaric system with M single-phase species ($m = 1, 2, \ldots M$), which simultaneously participate in N elementary reaction steps ($n = 1, 2, \ldots N$), then, formally, the reaction set can be written in terms of linear combinations

$$\sum_{m=1}^{M} r_{nm}\, c_m \rightarrow \sum_{m=1}^{M} p_{nm}\, c_m \; ; \; n = 1, 2, \ldots N \tag{9–6}$$

This equation extends over all M species, to allow for the possibility that a given species can participate in a reaction as both a product and a reactant.

Equation 9–6 can be written in a compact matrix notation

$$\mathbf{Rc} \rightarrow \mathbf{Pc} \tag{9–7}$$

where $\mathbf{c}$ is the concentration $\mathbf{c} = [c_1, c_2, \ldots c_m]^T$, and $\mathbf{R}$ and $\mathbf{P}$ are the reactant and product stoichiometric matrices, respectively, which contain the $N \times M$ elements r_{nm} and p_{nm}. If the rates f_n of the N individual reactions are given, then the kinetics of the reaction set is described by the following set of ordinary differential equations

$$d\mathbf{c}/dt = \mathbf{S}^T \mathbf{F} \tag{9–8}$$

where $\mathbf{S}$ is the stoichiometric matrix

$$\mathbf{S} = \mathbf{P} - \mathbf{R} \tag{9–9}$$

and $\mathbf{F} = [f_1, f_2, \ldots f_N]^T$. Equation 9–8 can be numerically integrated if appropriate initial conditions are provided.

The determination of $\mathbf{F}$ is still a major area of experimental and theoretical investigation. For diluted chemical systems, a common approximation is the so-called "mass action law," in which f_n can be expressed as a product of the concentration c_m of the species involved in the n-th reaction, i.e.,

$$f_n = k_n \prod_{m=1}^{M} c_m^{r_{nm}} \tag{9–10}$$

where k_n is a temperature-dependent rate constant given by

$$k_n(T) = A_n \exp(-B_n/T) \tag{9-11}$$

Due to the large number of hydrocarbons, many chemical mechanisms use the "lumped" approach, in which hydrocarbon chemistry is given by

$$HC_j + X_y \xrightarrow{\overline{k}_j^{(y)}} \text{products} \tag{9-12}$$

which involves a reaction between the molecule X_y (typically atomic oxygen O, hydroxyl radical OH, or ozone O_3) and the j-th hydrocarbon class. It is assumed that all hydrocarbons are divided into reactivity classes, such as olefins, aromatics, alkanes and aldehydes. The computation of the "lumped" rate constants $\overline{k}_j^{(y)}$ is given by

$$\overline{k}_j^{(y)} = \frac{\sum_{p=1}^{p_j} k_p^{(y)} n_p}{\sum_{p=1}^{p_j} n_p} \tag{9-13}$$

where n_p is the number of moles of the generic species p in the hydrocarbon class j, and $k_p^{(y)}$ is the rate constant for the reaction rate between the species p and X_y.

Some key reactions in the photochemical models involve the photolysis of such species as nitrogen dioxide NO_2, formaldehyde $HCHO$, and nitrous acid $HONO$. For a typical species A, the photodissociation step can be written as

$$A + h\nu \xrightarrow{k} \text{products} \tag{9-14}$$

with the forward reaction rate

$$R = -dc_A/dt = k\, c_A \tag{9-15}$$

where c_A is the concentration of the species A.

The photolysis rate constant k, at the spatial location $\mathbf{x}$ and time t, of any pollutant present in the atmosphere in small concentrations is given by the numerical integration of

$$k = \int_0^\infty \sigma\,[\lambda,\ T(\mathbf{x})]\ \phi\,[\lambda,\ T(\mathbf{x})]\ I\,[\lambda,\ t,\ \mathbf{x}]\ d\lambda \qquad (9\text{-}16)$$

where $\sigma\,[\lambda, T(\mathbf{x})]$ is the wavelength (λ) dependent absorption cross section (cm^2) for the species at temperature $T(\mathbf{x})$; $\phi\,[\lambda, T(\mathbf{x})]$ is the quantum yield for the reaction; and I is the actinic irradiance (photons/cm^2-sec). The numerical evaluation of Equation 9-16 requires data for the species absorption cross sections and quantum yields as a function of λ and the local zenith angle.

9.3.2 Eulerian and Lagrangian Implementations

Photochemical schemes, such as those presented above, are able to calculate the dynamics of all photochemical species in each computational cell at each time step. In Eulerian photochemical models (e.g., McRae et al., 1982b, Tesche et al., 1984, and Carmichael et at., 1986) the K-theory is used to simulate atmospheric diffusion and a three-dimensional grid is superimposed to cover the entire computational domain. (Efforts were also made to embed one or more reactive plume models into K-theory grid models, as in the Plume-Airshed Reactive-Interactive System (PARIS) developed by Seigneur et al., 1983.) In the Lagrangian photochemical models (e.g., API, 1985; Lurmann et al., 1985), which were discussed in Section 8.2, columns or walls of cells are advected according to the main wind, in a way that allows the incorporation of the emissions encountered along their trajectory. Lagrangian models also use K-theory to calculate vertical and (when available) horizontal diffusion.

The main advantage of Lagrangian models versus Eulerian ones is computational speed, which can be one to two orders of magnitude faster because of the smaller number of grid cells used in Lagrangian models versus Eulerian models(*). Lagrangian models, however, provide concentration outputs along trajectories and, therefore, their outputs are difficult to compare with concentration measurements at fixed locations. Examples of simulations by photochemical Eulerian models are presented in Figures 9-2 and 9-3. It should be noted that the only photochemical model currently recommended (i.e., with a "preferred" status) by the U.S. EPA is the Urban Airshed Model (UAM), an Eulerian K-theory grid model that employs a simplified version of the Carbon-Bond II Mechanism (Ames et al., 1985a and 1985b). The UAM model is discussed in Section 14.1.1.

(*)The new generation of micro- and mini-computers, however, has sharply decreased computer costs. Today, an Eulerian photochemical model can perform a three-day simulation of a large air basin (such as Los Angeles) on a workstation in less than 16 CPU hours (Tesche, personal communication).

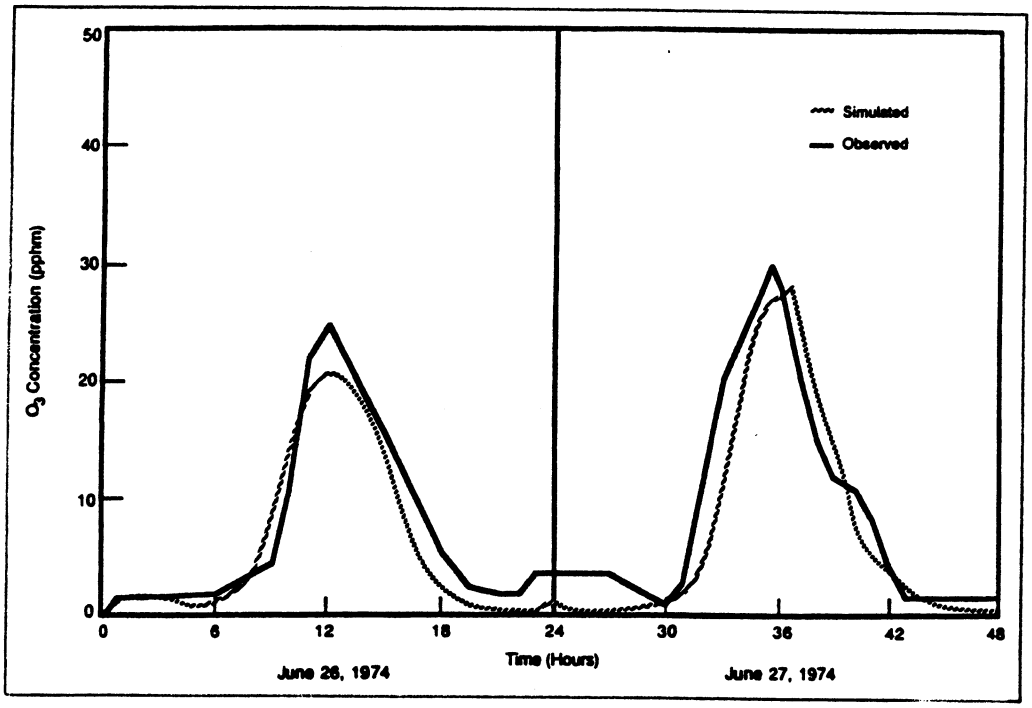

Figure 9–2. Simulation of the ozone concentration at the Pasadena monitoring station in the Los Angeles metropolitan area (from Seigneur, 1987). [Reprinted with permission from Computational Mechanics Publications.]

9.3.3 The EKMA Technique

A proper elaboration of the outputs of Lagrangian photochemical models allows the use of a simple method, the so-called EKMA (Empirical Kinetic Modeling Approach) technique (Dodge, 1977) to evaluate the importance of both NMHC and NO_x (and their ratio) in formulating O_3 control strategies. An example of EKMA isopleths is presented in Figure 9–4, in which point A illustrates a city that is characterized by an NMHC/NO_x ratio of 8:1 and a "design" value (defined as the second highest hourly O_3 measured concentration) of O_3 of 0.28 ppm. The isopleths allow the definition of different strategies to meet a certain ozone air quality standard. For example, if no change in ambient NO_x is expected and the future goal for the design value of ozone is 0.12 ppm, then the control strategy requires a progress from point A to point B in Figure 9–4, i.e., a reduction of NMHC by approximately 67 percent.

As seen in the example above, the EKMA method establishes, graphically, a relationship between the concentrations of ozone "precursors" (NO_x and NMHC) and the design value of ozone. Note the nonlinearities in Figure 9–4:

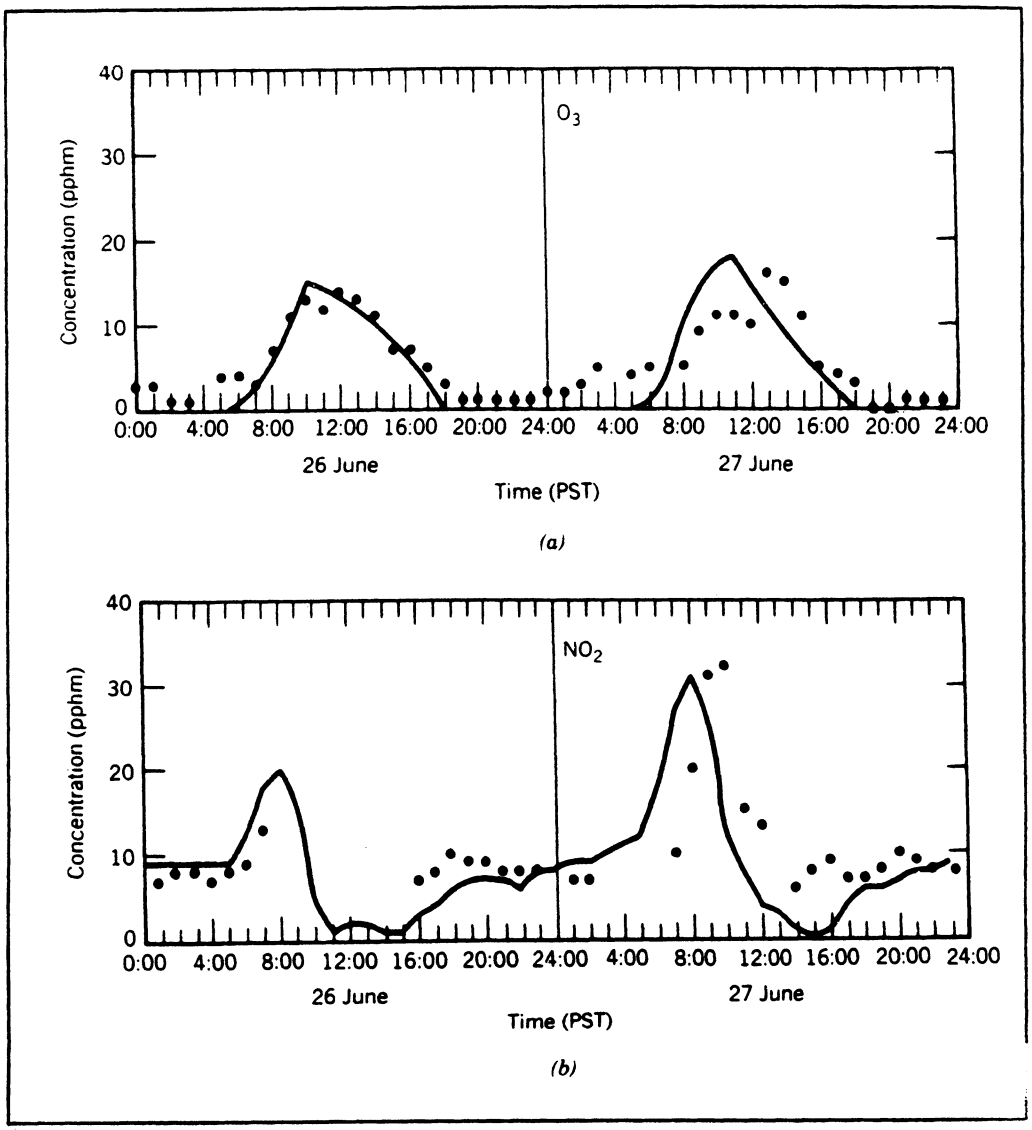

Figure 9–3. Observed (●) and model predicted (—) concentrations of (a) O_3 and (b) NO_2 in downtown Los Angeles, June 26 and 27, 1974 (from McRae and Seinfeld, 1983, as presented by Finlayson–Pitts and Pitts, 1986). [Reprinted with permission from John Wiley and Sons.]

depending on the position of A, different emission reductions of NMHC and/or NO_x can cause both decrease and *increase* of O_3. For example, for high NMHC/NO_x ratios, O_3 does not vary with NHMC controls, while for low NMHC/NO_x ratios, NO_x controls can actually *increase* O_3.

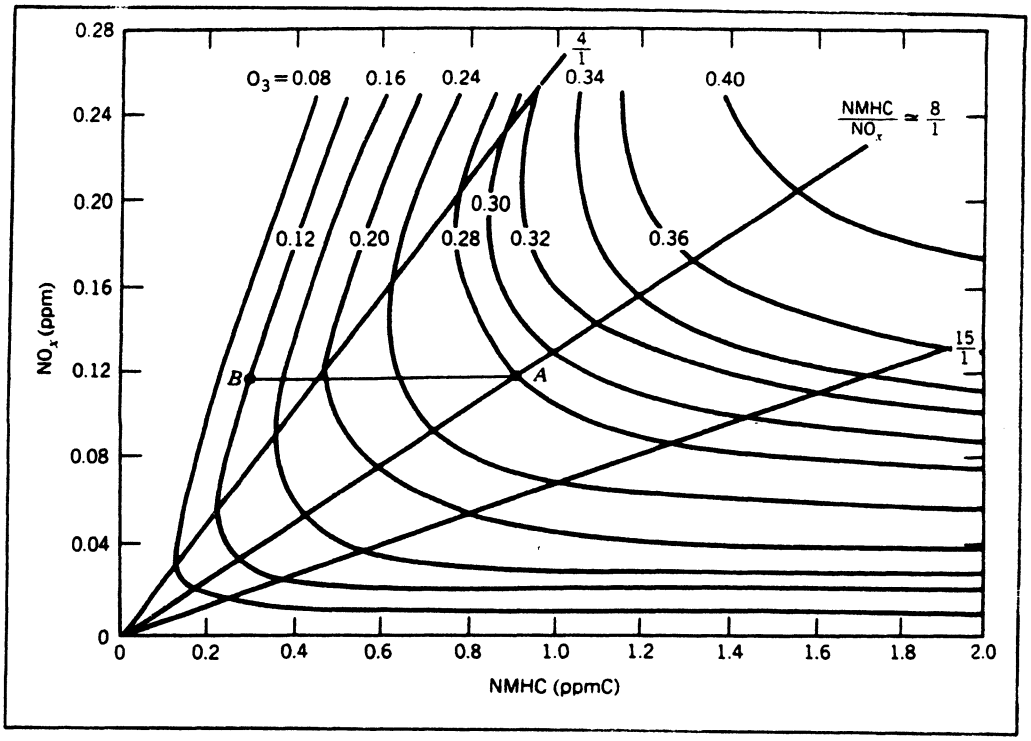

Figure 9–4. Ozone isopleths used in the EKMA approach (from Dodge, 1977, as presented by Finlayson–Pitts and Pitts, 1986). [Reprinted with permission from John Wiley and Sons.]

EKMA isopleths should be used with caution, since they represent an oversimplified empirical description of complex nonlinear phenomena. The generic isopleths in Figure 9–4 are based on a series of chemical, meteorological, geographical, background and emission assumptions. A computer program, the OZIPM–2 package (Gipson, 1984) allows the generation of city–specific isopleths, under conditions defined by the user.

9.4 AEROSOL CHEMISTRY

A detailed discussion of aerosol chemistry is clearly beyond the scope of this book. Therefore, in this section, we briefly discuss the major problems related to aerosol formation and dynamics. We also present a few recent modeling mechanisms.

Atmospheric aerosols consist of primary aerosol (i.e., directly emitted into the atmosphere; e.g., fugitive dust) and secondary aerosol, which is formed in the atmosphere through chemical reactions (e.g., sulfates). Typically (Seigneur, 1987), secondary aerosol range in size from about 0.01 μm to 2 μm, while primary aerosols are associated with larger sizes of about 1μm to 100 μm.

Aerosols play an important role in many air pollution studies. Small particles can be inhaled and cause adverse effects to the human pulmonary system. Also, particulate matter in the range of 0.1 to 1 μm is the most efficient at scattering light and, therefore, secondary aerosols are often the major cause of anthropogenic impairment of atmospheric visibility. Finally, sulfate and nitrate aerosols are the major cause of acidic deposition.

The formation of secondary particulate matter is due to several mechanisms (Finlayson-Pitts and Pitts, 1986):

1. reaction of gases to form low-vapor-pressure products, which combine to form new particles or condense on preexisting particles
2. reaction of gases on the surfaces of existing particles to form condensed products
3. chemical reactions within the aerosol itself

These mechanisms are illustrated in Figure 9-5.

The complex chemistry of secondary aerosols involves three phases (Seigneur, 1987):

1. the gas phase, where condensable species are chemically formed
2. the aerosol aqueous phase, where chemical reactions can take place
3. the aerosol solid phase, which may deliquence into aqueous phase, and vice versa.

A comprehensive discussion of gas-phase and aqueous-phase atmospheric chemistry is presented in Seinfeld (1986).

9.4.1 The SO_2 - to - SO_4^{2-} Formation

Secondary sulfates represent, in most cases, the major problem in aerosol acid precipitation and visibility studies. The formation of sulfates SO_4^{2-} from primary emissions of SO_2 follows the pattern described below (Seinfeld, 1986).

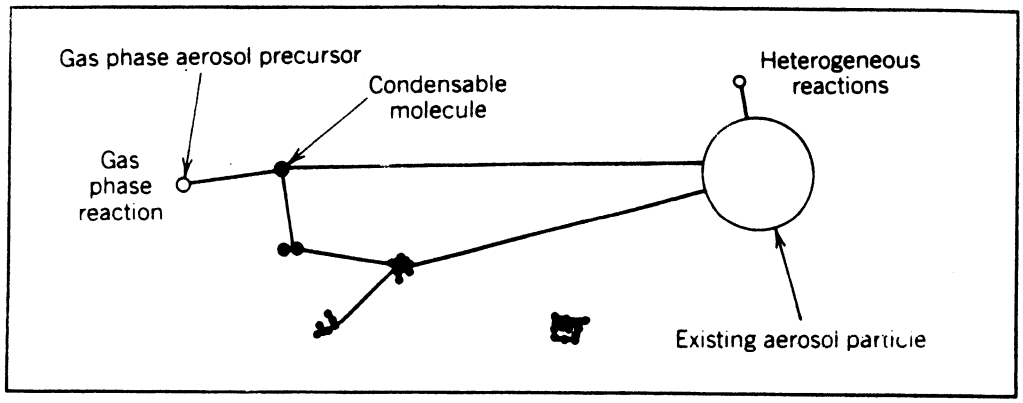

Figure 9–5. *A schematic diagram showing aerosol formation by different chemical mechanisms. Condensable molecules formed by chemical reactions involving gas-phase precursors can combine with other condensable molecules or molecular clusters to form new particles, or condense on preexisting aerosol causing them to grow. Alternatively, aerosol precursor gases can react to form a secondary aerosol on the surface of, or within, existing aerosol particles (from McMurry and Wilson, 1982, as presented by Finlayson–Pitts and Pitts, 1986). [Reprinted with permission from John Wiley and Sons.]*

Sulfur dioxide has a tendency to react with oxygen in air, thus giving

$$2SO_2 + O_2 \rightarrow 2SO_3 \qquad (9\text{–}17)$$

In a moist atmosphere, SO_3 reacts with water vapor to form sulfuric acid

$$SO_3 + H_2O \rightarrow H_2SO_4\ (aq) \qquad (9\text{–}18)$$

The above reactions, though thermodynamically favorable, are in general very slow and, therefore, are not important under most atmospheric conditions. When liquid-phase catalytic reactions of SO_2 are not important, gas reactions are mostly

$$OH\cdot + SO_2 \rightarrow HOSO_2\cdot \qquad (9\text{–}19)$$

which is probably followed by

$$HOSO_2\cdot + O_2 \rightarrow HO_2\cdot + SO_3 \tag{9-20}$$

$$SO_3 + H_2O \rightarrow H_2SO_4 \tag{9-21}$$

The reactions above describe the gas-phase oxidation of SO_2. An important role however, is often played by SO_2 oxidation inside fog or cloud droplets, which follows other reaction pathways.

Once H_2SO_4 is produced, it will rapidly acquire water vapor and nucleate to form small particles or condense on existing particles. If enough ammonia (NH_3) gas is present in the atmosphere, it will neutralize the acidic H_2SO_4, thus creating ammonium sulfate $(NH_4)_2SO_4$, the preferred form of sulfate, in condensed or particulate form. Otherwise, ammonium bisulfate NH_4HSO_4 or letovicite $(NH_4)_3\,H(SO_4)_2$ will be produced.

Experimental studies have shown that the complex homogeneous (i.e., gas-phase) SO_2-to-SO_4^{2-} conversion is strongly dependent upon ambient concentration values of the free radical $OH\cdot$; this allows the definition and use of semiempirical formulas for SO_2 oxidation, such as (SAI, 1984)

$$-\frac{1}{[SO_2]}\,\frac{d[SO_2]}{dt} = k_{22}\,[OH] \tag{9-22}$$

where the brackets indicate concentrations and $k_{22} \simeq 2.0\ 10^3\ \text{ppm}^{-1}\ \text{min}^{-1}$. The free radical $OH\cdot$ is active at extremely low concentrations through reaction cycles in which $OH\cdot$ is produced and consumed. $OH\cdot$ is produced by photochemical reactions such as

$$HONO + h\nu\ (\lambda < 400\ \text{nm}) \rightarrow OH\cdot + NO \tag{9-23}$$

$$O_3 + h\nu\ (\lambda < 319\ \text{nm}) \rightarrow O_2 + O\cdot \tag{9-24}$$

$$O\cdot + H_2O \rightarrow 2\,OH\cdot \tag{9-25}$$

$$H_2O_2 + h\nu \rightarrow 2\,OH\cdot \tag{9-26}$$

$$NO + HO_2\cdot \rightarrow NO_2 + OH\cdot \qquad (9\text{–}27)$$

etc.

and is terminated at dark by recombination of peroxyl radicals

$$HO_2\cdot + HO_2\cdot \rightarrow H_2O_2 + O_2 \qquad (9\text{–}28)$$

9.4.2 The NO – to – NO_3^- Formation

The formation of atmospheric nitrates is often as important as sulfate formation. We have seen in the previous sections that the primary emissions of NO can be oxidized into NO_2, which forms nitric acid through several mechanisms, such as

$$OH\cdot + NO_2 \rightarrow HNO_3 \qquad (9\text{–}29)$$

and

$$NO_2 + O_3 \rightarrow NO_3 + O_2 \qquad (9\text{–}30)$$

$$NO_3 + HO_2\cdot \rightarrow HNO_3 + O_2 \qquad (9\text{–}31)$$

Then, if NH_3 is present, HNO_3 will generate ammonium nitrate (NH_4NO_3) in condensed or particulate form.

As done before for the SO_2 – to – SO_4^{2-} reaction, NO_2 – to – NO_3^- conversion can be parameterized (SAI, 1984) as a simple function of $OH\cdot$ concentration by

$$-\frac{1}{[NO_2]}\frac{d[NO_2]}{dt} = k_{32}[OH] \qquad (9\text{–}32)$$

where $k_{32} \simeq 1.4\ 10^4\ \text{ppm}^{-1}\ \text{min}^{-1}$.

9.4.3 Aerosol Models

The simulation of the dynamics of multicomponent atmospheric aerosols is a formidable problem that includes (Pilinis et al., 1987) new particle formation by homogeneous heteromolecular nucleation, gas–to–particle conversion, coagulation and dry deposition. A spatially–uniform, dynamic multicomponent aerosol

can be characterized by its size-distribution distribution function, whose dynamic behavior is governed by the "general dynamic equation" (Gelbard and Seinfeld, 1979; Seinfeld, 1986). The sectional approximation of this equation uses, instead of a continuous size distribution for each aerosol species, a series of step functions (Warren and Seinfeld, 1985), as follows

$$\frac{\partial c_{ij}}{\partial t} + \nabla \cdot (\bar{\mathbf{u}}\, c_{ij}) = \nabla \cdot (\mathbf{K}\, \nabla c_{ij}) + \left[\frac{\partial c_{ij}}{\partial t}\right]_{\text{cond./evapor.}} + \left[\frac{\partial c_{ij}}{\partial t}\right]_{\text{coag.}} + \left[\frac{\partial c_{ij}}{\partial t}\right]_{\text{sources/sinks}} \tag{9-33}$$

where c_{ij} is the mass concentration of species i in the j-th size section, $\bar{\mathbf{u}}$ is the average wind field, and $\mathbf{K}$ is the diffusivity tensor. (This equation follows the K-theory described in Chapter 6.)

Equation 9-33 is a general dynamic equation. It can be approximated in three different ways: 1) solving the continuous size distribution numerically; 2) using a step-function approximation and solving numerically (the preferred approach); or, 3) using log-normal distributions and solving numerically. Seigneur et al. (1986) performed a comparative review of these three approaches.

An idealized schematic of the composition of atmospheric aerosols is presented in Figure 9-6. An aerosol model must be able to account for both inorganic and organic constituents. For inorganic aerosols, three models have been developed (Pilinis et al., 1987) to determine the thermodynamic equilibrium of the sulfate-nitrate-chloride-sodium-ammomium-water system, where the following components are possible

- gas phase : NH_3, HCl, HNO_3, H_2O
- liquid phase : H_2O, NH_4^+, SO_4^{2-}, NO_3^-, H^+, Na^+, Cl^-, HSO_4^-, H_2SO_4
- solid phase : Na_2SO_4, $NaHSO_4$, $NaCl$, $NaNO_3$, NH_4Cl, NH_4NO_3, $(NH_4)_2SO_4$, NH_4HSO_4, $(NH_4)_3\,H(SO_4)_2$

These three models account for the rates of transfer of each species between the gas and aerosol phases and, given the sulfate, the HNO_3 and NH_3 concentrations, as well as temperature and relative humidity, are able to determine the equilibrium phase of the system by minimizing the total Gibbs free energy.

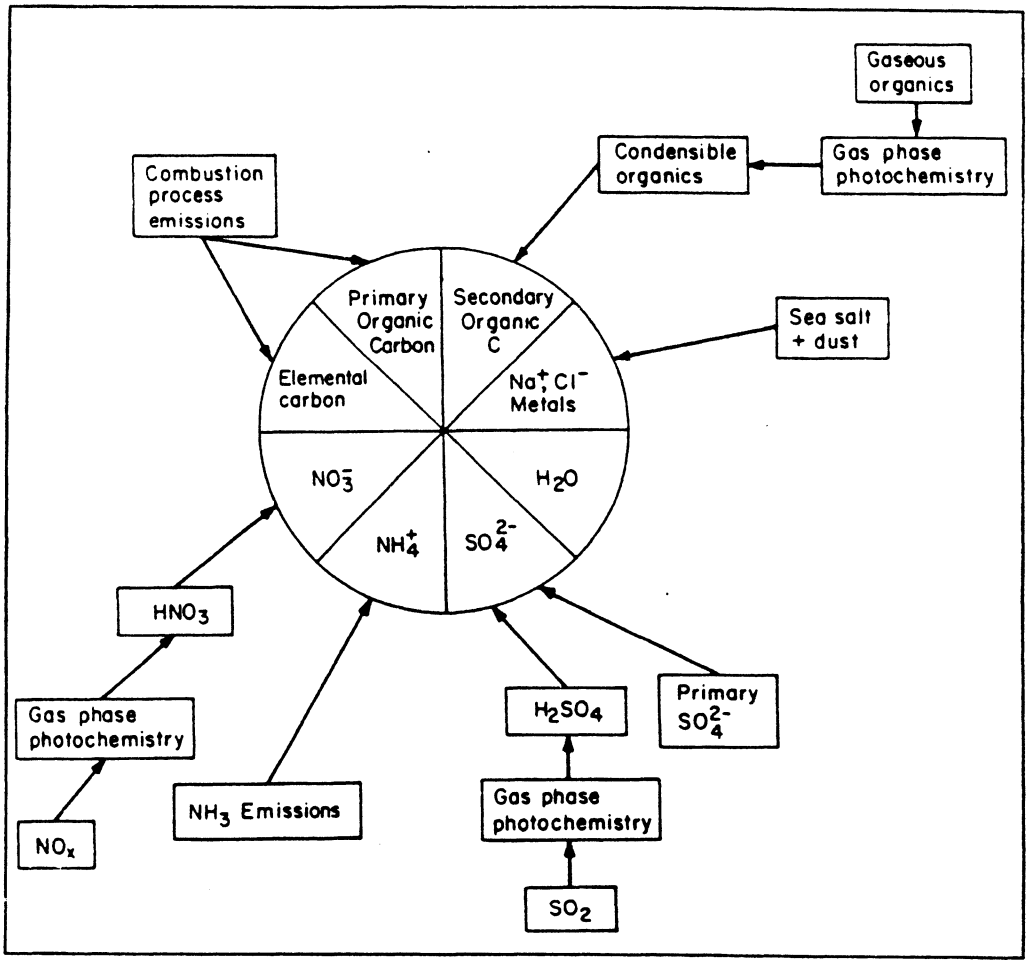

Figure 9–6. Idealized schematic of the composition of atmospheric aerosols. The principal sources and particle formation mechanisms are indicated (from Pilinis and Seinfeld, 1988). [Reprinted with permission from Pergamon Press.]

Organic particulate matter is made of both primary and secondary organic compounds. Primary aerosols result from condensation of various organic species that are the product of gas-phase photooxidation of primary hydrocarbons. The simulation of secondary organic species is difficult and, in spite of several experimental studies, many reaction pathways and physical properties of various condensable species are not well understood.

The Eulerian gas-aerosol model developed by Pilinis and Seinfeld (1988) was applied to simulate air quality in the South Coast Air Basin of California, on a day (30 August 1982) for which 4-h average concentrations data for sulfate,

nitrate, ammonium, chloride, sodium, calcium and magnesium were available. The model, which may require the solution of as many as 224,730 ordinary differential equations, used about 8 CPU hours of a CRAY X-MP for a one-day simulation. Model outputs are encouraging, showing predictions of aerosol concentrations generally within the uncertainty of the measurements. This model, which has provided the first three-dimensional predictions of the concentrations and size distributions of inorganic and organic aerosols in an urban region, shows that water plays an important role (it is more than 50 percent of the aerosol mass at humidities above 80 percent). The major inorganic aerosol species were secondary (sulfates and nitrates), while primary organics were the major organic aerosol species.

The complex photochemical aerosol models discussed above can be used only for episodic situations. Other techniques should be used for long-term simulations. For example, Tesche and McNally (1989) developed the Annual Average Urban Airshed Model (3AM) — a software structure designed to use routine emissions, meteorological and air quality data to predict hourly ozone concentrations over the period of a month or a year (plans for including secondary PM_{10} aerosols and air toxics have also been designed by the authors).

9.5 AIR TOXICS

One of the most important developments in air quality studies and regulation is the growing awareness of the toxicity of airborne chemical species. Specific legislation has identified and classified suspected carcinogenic and mutagens. The assessment of the population risk of exposure to these substances has become a key technical and regulatory issue, at least in the United States.

Air toxics can undergo different chemical reactions and their reactivities are know to vary greatly. Chemical reactions may decrease, with time, the concentrations of certain toxic pollutants. Unfortunately, the opposite is also true, and chemicai reactions can, sometimes, transform a contaminant into an air toxic species.

Seigneur (1987) illustrates the range of chemical behavior of air toxics by discussing the chemistry of four species: chromium (Cr), benzo(a)pyrene (BaP), benzene (C_6H_6) and formaldehyde ($HCHO$).

Chromium, which is emitted as particulate matter, exists in the atmosphere in two stable oxidation states: Cr (III) and Cr (VI). The latter is suspected

to be a carcinogenic compound, while, for the former, no evidence of carcinogenicity is available at the present time. The assessment and quantification of the chemistry patterns *Cr* (III) ⇔ *Cr* (VI) are, therefore, extremely important to assess the potential toxicity of chromium emissions.

The carcinogenicity of benzo(a)pyrene (*BaP*) is well recognized. Its half-life in the atmosphere is highly variable, depending upon its exposure to different species, such as NO_2 and O_3. *BaP* half-life can vary from 35 minutes to several hours, with results much different exposure effects.

Benzene chemistry is relatively simple, since it reacts primarily with $OH\cdot$ and has a lifetime of 15 to 150 hours. Due to the complexity of the urban photochemistry, however, $OH\cdot$ concentrations are often highly uncertain and do not allow precise estimates of benzene reactivity.

Formaldehyde has been shown to be carcinogenic to rats, even though there is no evidence of carcinogenicity in humans. This substance plays a key role both in photochemical smog formation (see Table 9-2) and as an indoor pollutant. It is a good example of toxic pollutants that are also very reactive in the atmosphere.

The four examples above indicate the importance of understanding and correctly simulating the chemistry of air toxic substances. Reliable simulations, tested against the limited data available, can then be used to calculate the population exposure to air toxics and the expected consequences of this exposure (e.g., in terms of risk factors of cancer induction and noncarcinogenic effects, both chronic and acute).

REFERENCES

Ames, J., T.C. Myers, L.E. Reid, D.C. Whitney, S.H. Golding, S.R. Hayes, and S.D. Reynolds (1985a): SAI Airshed Model Operations Manual. Vol. I: User's Manual. U.S. EPA Publication EPA-600/8-85-007a. U.S. Environmental Protection Agency, Research Triangle Park, North Carolina. (NTIS No. PB 85-191567)

Ames, J., S.R. Hayes, T.C. Myers, and D.C. Whitney (1985b): SAI Airshed Model Operations Manuals. Vol. II: Systems Manual. EPA Publication EPA-600/8-85-007b. U.S. Environmental Agency, Research Triangle Park, North Carolina.

Applied Modeling, Inc. (1985): User's guide to the photochemical trajectory model trace. API, Woodland Hills, California.

Atkinson, R., and A.C. Lloyd (1984): Evaluation of kinetic and mechanism data for modeling of photochemical smog. *J. Phys. Chem. Ref. Data*, **13**:315-444.

Baulch, D.L., R.A. Cox, P.J. Crutzen, R.F. Hampson, Jr., F.A. Kerr, J. Troe, and R.P. Watson (1982): Evaluated kinetic and photochemical data for atmospheric chemistry, Supplement 1. CODATA Task Group on Chemical Kinetics, *J. Phys. Chem. Ref. Data*, **11**:327-496.

Carmichael, G.R., L.K. Peters, and T. Kitada (1986): A second generation model for regional-scale transport/chemistry/deposition. *Atmos. Environ.*, **20**:173-188.

Carter, W.P. (1988): Documentation of a gas phase photochemical mechanism for use in airshed modeling, Appendix B. Contract No. A5-122-32. University of California, Statewide Air Pollution Research Center, Riverside, California.

Dodge, M.C. (1977): Combined use of modeling techniques and smog chamber data to derive ozone-precursor relationships. *Proceedings*, International Conference on Photochemical Oxidant Pollution and Its Control, Vol. II, edited by B. Dimitriades, U.S. Environmental Protection Agency Document EPA-600/3-77-001b, pp. 881-889.

Finlayson-Pitts, B.J., and J.N. Pitts, Jr. (1986): *Atmospheric Chemistry: Fundamental and Experimental Techniques*. New York: John Wiley.

Gelbard, F., and J.H. Seinfeld (1979): The general dynamic equation for aerosols—theory and application to aerosol formation and growth. *J. Colloid Interface Sci.*, **69**:363-382.

Gery, M.W., G.Z. Whitten, and J.P. Killus (1987): Development and testing of the CBM-IV for urban and regional testing. U.S. EPA Contract 68-02-4136. Systems Applications, Inc., San Rafael, California.

Gipson, G.L. (1984): User's manual for OZIPM-2: Ozone isopleth plotting with optional mechanisms/Version 2. U.S. Environmental Protection Agency Document EPA-450/4-84-024, Office of Air Quality Planning and Standards, Monitoring and Data Analysis Division, Research Triangle Park, North Carolina.

Kerr, J.A., and J.G. Calvert (1984): Chemical transformations modules for Eulerian acid deposition models, I. The gas-phase chemistry. U.S. Environmental Protection Agency, Research Triangle Park, North Carolina.

Leone, J.A., and J.H. Seinfeld (1984): Updated chemical mechanism for atmospheric photooxidation of toulene. *Int. J. Chem. Kinetics*, **16**:159.

Lurmann, F.W., D.A. Godden, and H.M. Collins (1985): User's guide to the PLMSTAR air quality simulation model. Environmental Research & Technology Document M-2206-100, Newbury Park, California.

McRae, G.J., W.R. Goodin, and J.H. Seinfeld (1982a): Mathematical modeling of photochemical air pollution. Final Report to the California Air Resources Board, Contracts A5-046-87 and A7-187-30.

McRae, G.J., W.R. Goodin, and J.H. Seinfeld (1982b): Development of a second-generation mathematical model for urban air pollution; I. Model formulation. *Atmos. Environ.*, **16**:679.

McRae, G.J., and J.H. Seinfeld (1983): Development of a second generation mathematical model for urban air pollution; II. Evaluation of model problems. *Atmos. Environ.*, **17**:501.

Pilinis, C., J.H. Seinfeld, and C. Seigneur (1987): Mathematical modeling of the dynamics of multicomponent atmospheric aerosols. *Atmos. Environ.*, **21**:943-955.

Pilinis, C., and J.H. Seinfeld (1988): Development and evaluation of an Eulerian photochemical gas-aerosol model. *Atmos. Environ.*, **22**:1985-2001.

Seigneur, C., T.W. Tesche, P.M. Roth, M.-K. Liu (1983): On the treatment of point source emissions in urban air quality modeling. *Atmos. Environ.*, **17**(9):1655-1676.

Seigneur, C., A.B. Hudischewskyj, J.H. Seinfeld, K.T. Whitby, E.R. Whitby, J.R. Brock, and H.M. Barnes (1986): Simulation of aerosol dynamics: A comparative review of mathematical models. *Aerosol Sci. and Tech.*, **5**:205-222.

Seigneur, C. (1987): Computer simulation of air pollution chemistry. *Environ. Software*, **2**:116.

Seinfeld, J.H. (1986): *Atmospheric Chemistry and Physics of Air Pollution*. New York: John Wiley.

Systems Applications, Inc. (1984): Visibility and other air quality benefits of sulfur dioxide emission controls in the eastern United States: Volume I. Systems Applications draft report SYSAPP-84/165, San Rafael, California.

Tesche, T.W., C. Seigneur, W.R. Oliver, and J.L. Haney (1984): Modeling ozone control strategies in Los Angeles. *J. Environ. Eng.*, **110**:208-225.

Tesche, T.W., and D.E. McNalley (1989): A three-dimensional photochemical-aerosol model for episodic and long-term simulation: Formulation and initial application in the Los Angeles Basin. Presented at the annual meeting of the American Chemical Society, Miami Beach, Florida, September.

Warren, D.R., and J.H. Seinfeld (1985): Simulation of aerosol size-distribution evolution in systems with simultaneous nucleation, condensation and coagulation. *Aerosol Sci. & Technol.*, **4**:31-43.

Whitten, G.Z., and H. Hogo (1977): Mathematical modeling of simulated photochemical smog. U.S. Environment Agency Report EPA-600/3-77-011. Research Triangle Park, North Carolina.

Whitten, G.Z., H. Hogo, and J.P. Killus (1980): The carbon-bond mechanism: A condensed kinetic mechanism for photochemical smog. *Environ. Sci. & Technol.*, **14**:690.

10 DRY AND WET DEPOSITION

Deposition phenomena are the way in which the atmosphere cleans itself. The process is efficient as only a few gases (most notably CO_2) show signs of global increase in spite of the large emission of pollutants from both natural and anthropogenic sources. There are two types of deposition mechanisms: dry deposition, i.e., the uptake at the earth's surface (soil, water, or vegetation), and wet deposition, i.e., absorption into droplets followed by droplet precipitation (e.g., by rain) or impaction on the earth's surface (e.g., fog droplets).

This section describes and discusses deposition phenomena and their mathematical treatment (see also Yamartino, in Houghton, 1985). Recently, deposition processes have received much attention. The development of long-range transport (LRT) studies and experiments has required a better understanding of these phenomena, whose importance is proportional to the length scale of the investigation -- the larger the space and time scales, the better deposition phenomena need to be understood and simulated, in order to predict correctly concentration impacts. Moreover, acidic deposition has become an important environmental issue (e.g., see the review by Schwartz, 1989, for a general discussion of acid deposition phenomena), which has required a correct representation of deposition phenomena, not just to forecast *concentration* impacts, but to assess *deposition* rates and their adverse effects.

The deposition modules of air quality models possess large uncertainties and much work seems still to be required to provide an accurate parameterization of the complex deposition phenomena. Performance evaluation studies of deposition modules have been performed by several authors (e.g., Doran et al., 1984; Doran and Horst, 1985).

10.1 DRY DEPOSITION

Dry deposition is commonly measured by the deposition velocity V_d, which was defined by Equation 6-10 as the ratio between the pollutant deposition flux F (g m^{-2} s^{-1}) and the pollutant concentration c (g m^{-3}), i.e.,

$$V_d = F/c \qquad (10\text{-}1)$$

V_d is not a real velocity but an "effective" one. (It has been called a velocity mostly because of its units.) In fact, as discussed below, only large particles possess a deposition velocity dominated by gravitational effects and, therefore, interpretable as an actual velocity.

As far as gases are concerned, dry deposition is strongly affected by their chemical interactions with the surface. See, for example, Figure 6–4, where SO_2 deposition velocities for different surfaces are presented.

For particles, deposition velocities have been computed from wind tunnel experiments, as for example shown in Figure 10–1. As discussed by Nicholson (1988a), for very small particles (i.e., with a diameter less than 0.1 μm), Brownian motion allows rapid movements across the viscous air layers just above

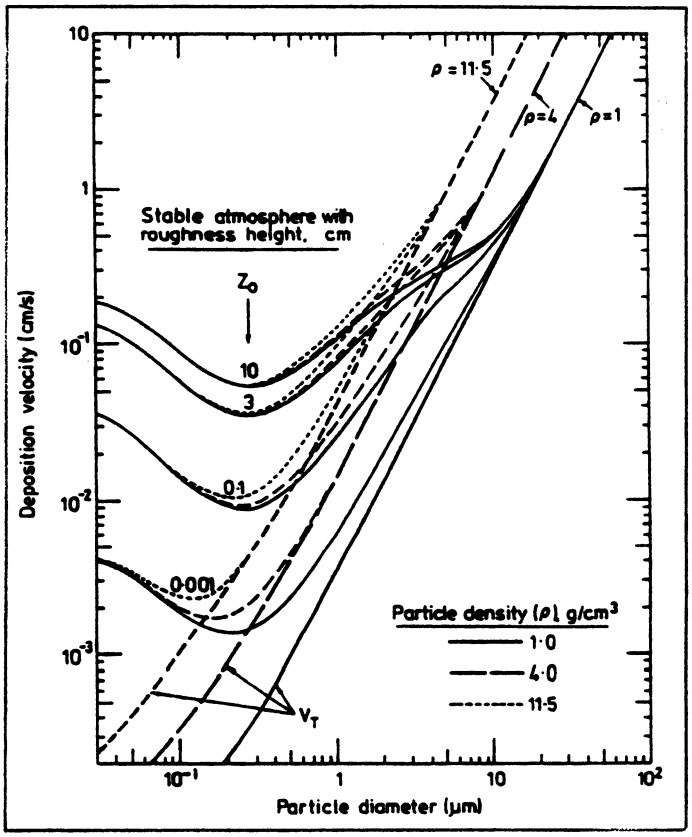

Figure 10–1. Extrapolations from correlations of wind-tunnel measured deposition velocities for z = 1 m, densities of 1, 4 and 11.5 g cm^{-3}. V_T represents terminal settling velocity (from Sehmel, 1980, as presented by Nicholson, 1988a). [Reprinted with permission from Permagon Press.]

the surface, while the motion of large particles (i.e., with a diameter greater than 1 μm) is dominated by sedimentation (gravitational) effects, as shown in Figure 10–1 where the "terminal" velocity V_T (or gravitational settling velocity V_G) increases with particle size. Intermediate size particles are strongly affected by impaction and interception phenomena, which are difficult to quantify correctly. In particular, particles in the size range 0.1 to 1 μm have low predicted deposition velocities due to the relative weakness of Brownian motion and gravitational settling effects, even though field measurements indicate high deposition rates. Surface roughness, as illustrated in Figure 10–1 seems to play an important role in a stable atmosphere, as it significantly influences the near–surface turbulence and, in turn, the rate of pollutant transfer to the surface.

A literature review of dry deposition velocities of oxides of sulfur and nitrogen, based on long–range transport modeling studies in North America, is provided by Voldner et al. (1986).

Dry deposition phenomena are often parameterized using Equation 10–1, which requires the knowledge of the deposition velocity V_d for both primary and secondary pollutants, a velocity whose evaluation (as illustrated in Figure 6–4 for the SO_2) is uncertain. The theory of gaseous and particle dry deposition is complex: it is governed both by transfer in the gas phase and by sorption at the surface, which is generally assumed to be an irreversible process.

Following the description of Garland (1978), when the concentration $c(0)$ at the surface is not too high, the rate of sorption is expected to be proportional to $c(0)$. In this case, the concentration flux at the surface is

$$F = \frac{c(0)}{r_s} \tag{10–2}$$

where r_s is the surface resistance s (m^{-1}) which, in ideal conditions, depends only on the affinity of the surface for the particular pollutant under examination. The flux can be related to a vertical dispersion coefficient K_z; i.e.,

$$F = K_z(z)\frac{\partial c}{\partial z} \tag{10–3}$$

which, by integration, gives

$$F = \frac{c(z) - c(0)}{r_g(z)} \tag{10–4}$$

where

$$r_g(z) = \int_0^z \frac{dz'}{K_z(z')} \tag{10-5}$$

is the gas-phase resistance.

From Equations 10-2 and 10-4, we obtain

$$F = \frac{c(z)}{r_s + r_g(z)} \tag{10-6}$$

indicating that the total resistance $r(z)$ to deposition is simply the additive sum of the resistances sequentially encountered by the pollutant in its journey to its final sink. This total resistance

$$r(z) = r_s + r_g(z) \tag{10-7}$$

can then be expressed in terms of deposition velocity by

$$V_d(z) = \frac{1}{r(z)} = \frac{F}{c(z)} \tag{10-8}$$

The surface resistance r_s is a function of the physical and chemical properties of the surface and the pollutant and is difficult to evaluate. The gas-phase resistance is easier to evaluate in a turbulent flow, where eddy diffusion dominates and the transport characteristics are expected to be the same for all gases, vapors and small particles (e.g., not greater than a few μm). Similarity theory considerations allow, for example, the estimates presented in Table 10-1, in which r_g is computed as a function of surface type, z_o, wind speed, L, u_*, and elevation.

Most long-range transport models use the above formulation, together with some empirical evaluation of V_d either as a constant or as a function of surface type and hour of the day. LRT models are sensitive to dry deposition computations (Doran, 1979; Smith, 1981), and the reliability of their outputs is affected by the lack of direct evaluation and verification studies of dry deposition phenomena.

Several LRT models, however, do not use Equation 10-7 in a direct way, but decrease the pollutant mass by a certain fraction df during the time dt, where

$$df = \frac{V_d}{\Delta z_e}\, dt \tag{10-9}$$

Surface and z_0 (m)	Wind speed at 100 m ($m\,s^{-1}$)	Monin–Obukhov length, L^* (m)	u_* ($m\,s^{-1}$)	$r_g(1)$ ($s\,cm^{-1}$)	$r_g(100)$ ($s\,cm^{-1}$)
Grass	3	∞	0.13	1.25	2.1
(0.01)		−11	0.18	0.89	1.21
	10	∞	0.45	0.41	0.67
		−215	0.49	0.38	0.57
		+630	0.41	0.44	0.77
Cereal crop	3	∞	0.18	0.87	1.5
(0.1)		−27	0.25	0.66	0.93
	10	∞	0.59	0.32	0.50
		−480	0.64	0.30	0.45
		+1700	0.57	0.33	0.54
				$r_g(5)$	
Forest	3	∞	0.27	0.26	0.54
(1.0)		−85	0.36	0.20	0.43
	10	∞	0.89	0.11	0.24
		−1500	0.93	0.10	0.22
		+6100	0.88	0.11	0.24

* Unstable conditions (L negative) assume a heat flux of 50 W m^{-2} and stable conditions (L positive) assume a downward heat flux of 10 W m^{-2}. $L = \infty$ when conditions are neutral. In stable conditions at the lower wind speed, the surface is isolated from the 100 m level, preventing diffusion from this height and making resistances from 1 m unpredictable.

Table 10–1. Examples of calculated values of the gas-phase resistance (from Garland, 1978). [Reprinted with permission from Pergamon Press.]

and Δz_e is the vertical thickness of the plume. The fractional reduction can then be integrated and dynamically computed at each time step Δt by the exponential mass reduction

$$M^{(new)} = M^{(old)} \exp\left(-\frac{\Delta t}{T_d}\right) \tag{10-10}$$

where $M^{(old)}$ and $M^{(new)}$ are the old and new masses, respectively, of the plume element under consideration, and $T_d = \Delta z_e / V_d$ is the time scale of the dry deposition process.

Zannetti and Al-Madani (1983) proposed a probabilistic approach for a parameterization of dry deposition, resuspension and permanent absorption phenomena using Lagrangian particle methods (discussed in Section 8.3). According to this method, if a plume is represented by the dynamics of, say, n_p active particles, at the end of each time step Δt, all active particle locations need to be tested to single out those particles (say n_b) that, because of semirandom fluctuations, have been moved below terrain. Some of these n_b particles will be

reflected and the rest will be deposited on the ground. If T_d is the time scale of this partial deposition process, each of the n_b particles below the terrain has a probability

$$p_d = 1 - \exp\left(\frac{-\Delta t}{T_d}\right) \tag{10-11}$$

of being deposited. Therefore, $p_d n_b$ randomly selected particles (among the previously identified n_b) will be deposited, and the rest of them ($n_b - p_d n_b$) will be reflected.

Particles deposited on the ground can be resuspended back to the computational domain or permanently absorbed by the ground. If n_d is the current number of deposited particles and T_s is the time scale of the resuspension process, each of these n_d particles has a probability

$$p_s = 1 - \exp\left(\frac{-\Delta t}{T_s}\right) \tag{10-12}$$

of being resuspended. Therefore, at each time step, $p_s n_d$ particles will be resuspended; but if a particle remains deposited on the ground for longer than a critical value T_{dmax}, the particle will be permanently absorbed.

T_d, T_s, and T_{dmax} are functions of the meteorology (especially the surface wind speed) and of the characteristics of both the pollutant and the ground surface. The proper inference of these values is a challenging task.

Alternatively, the same probabilistic method described by Equations 10–11 and 10–12 can be used in a way in which, instead of deleting randomly selected particles from a certain group, an appropriate reduction of mass is applied to all particles of the group. For example, in applying Equation 10–11, instead of deleting $p_d n_b$ randomly selected particles from the previously identified group of n_b particles, a reduction of the mass M of each of the n_b particles can be applied, such as

$$M^{(new)} = (1 - p_d)\, M^{(old)} \tag{10-13}$$

and all particles will be reflected. This second way of applying the probabilistic approach for deposition simulations may be easier to handle computationally, even though it requires the attribution of a time-varying mass to each particle.

Dry deposition of small particles has been reviewed recently by Nicholson (1988). Also, Noll and Fang (1989) have proposed a dry deposition model for coarse particles, while Nicholson (1988b) has reviewed particle resuspension phenomena.

- **A More Refined Simulation of Dry Deposition**

A few new models, e.g., CALGRID (Yamartino et al., 1989), incorporate more refined mechanisms for simulating dry deposition of gases and particles, such as those suggested by Sehmel (1980) and Hicks (1982). New parameterizations have also been proposed by Wesely (1989). The mechanisms of the CALGRID model are summarized below.

Deposition velocity, as anticipated in Equation 10–8, is expressed as the inverse of a sum of "resistances" in three sequential layers:

1. The surface layer, i.e., the layer in which atmospheric fluxes are constant (typically 20 m above the ground). In this layer, pollutant transfer is characterized by atmospheric turbulence properties.
2. The deposition layer, i.e., a thin layer just above the surface characterized by intermittent turbulence. In this layer, gases are affected by molecular diffusion and particles by Brownian diffusion and inertial impaction.
3. The vegetation layer, which is a major sink for many pollutants, a pathway that, in CALGRID, includes deposition directly to the ground or water surface.

For gases, we have

$$V_d = (r_a + r_d + r_c)^{-1} \tag{10–14}$$

where r_a is the atmospheric resistance through the surface layer, r_d is the deposition layer resistance, and r_c is the canopy/vegetation resistance. All resistances are in units of s m^{-1}.

The atmospheric resistance r_a can be derived (Wesely and Hicks, 1977) by

$$r_a = \frac{1}{k\, u_*} [\ln(z_s/z_o) - \psi_c] \tag{10–15}$$

where z_s is the reference height (m), z_o is the roughness length (m), k is the von Karman constant ($\simeq 0.4$), u_* is the friction velocity (m s^{-1}), and ψ_c is a stability correction term needed to take into account the effects of buoyancy-induced changes in flux-gradient relationships. It is generally assumed that the pollutant transfer is similar to that for heat and, therefore, $\psi_c = \psi_h$, where ψ_h was discussed in Section 3.6.

The deposition layer resistance can be parameterized as a function of the Schmidt number S_c, i.e.,

$$r_d = d_1 \frac{S_c^{d_2}}{k\, u_*} \tag{10-16}$$

where

$$S_c = \nu/D \tag{10-17}$$

ν is the kinematic viscosity of the air (m^2 s^{-1}), D is the molecular diffusivity of the pollutant (m^2 s^{-1}), and d_1, d_2 are empirical parameters ($d_1 \simeq 1.6 - 16.7$, and $d_2 = 0.4 - 0.8$, with a suggested choice of $d_1 = 5$, $d_2 = 0.66$).

The canopy resistance r_c accounts for the main pathways for uptake/reaction of the pollutant in the vegetation surface and can be computed by

$$r_c = [LAI/r_f + LAI/r_{cut} + 1/r_g]^{-1} \tag{10-18}$$

where LAI is the leaf area index (i.e., the ratio of leaf surface area divided by ground surface area), r_f is the internal foliage resistance, r_{cut} is the cuticle resistance, and r_g is the ground or water surface resistance. Moreover, the internal foliage resistance is due to two components

$$r_f = r_s + r_m \tag{10-19}$$

where r_s is the resistance for transport through the stomatal pore and r_m is the resistance to dissolution or reaction of the pollutant in the mesophyll cells.

Values for r_s and r_m are discussed by O'Dell et al. (1977). The resistance r_{cut} is parameterized by Pleim et al. (1984). The ground resistance is discussed by Pleim et al. (1984), while liquid phase resistance is parameterized by Slinn et al. (1978).

Dry deposition of particulate matter differs from that of gases. In fact, for particles, the resistance in the vegetation layer (r_c) is practically zero, since

particles that penetrate the deposition layer stick to the surface. Also, particles are affected by the gravitational settling V_g and this represents an alternative pathway to turbulent exchange for reaching the ground. Therefore, for particles, the deposition velocity involves resistances "in parallel" and is given as

$$V_d = (r_a + r_d + r_a r_d V_g)^{-1} + V_g \tag{10-20}$$

in which r_a is computed by Equation 10–15, and the deposition layer resistance is

$$r_d = (S_c^{-2/3} + 10^{-3/S_t})^{-1} u_*^{-1} \tag{10-21}$$

where S_c is the Schmidt number given by Equation 10–17 (where D, in this case dealing with particles, is the Brownian diffusivity of the pollutant in air instead of the molecular diffusivity), and S_t is the Stokes number

$$S_t = \frac{V_g u_*^2}{g \nu} \tag{10-22}$$

The gravitational settling V_g is a function of the particle size, shape and density (e.g., see Figure 8–6). For particles that can be approximated by spheres, the Stokes equation gives

$$V_g = [d_p^2 g (\varrho_p - \varrho_a) C]/(18 \mu) \tag{10-23}$$

where d_p is the particle diameter (m), ϱ_p is the particle density ($g\ m^{-3}$), ϱ_a is density of the air ($g\ m^{-3}$) and C is the Cunningham correction factor for small particles

$$C = 1 + (2\lambda/d_p)\,[a_1 + a_2 \exp(-a_3 d_p/\lambda)] \tag{10-24}$$

where λ is the mean free path of air molecules ($\lambda = 6.53\ 10^{-6}$ cm) and a_1, a_2, a_3 are constants (= 1.257, 0.40, 0.55).

10.2 WET DEPOSITION

Extensive discussion of wet deposition phenomena can be found in Seinfeld (1986), Finlayson-Pitts and Pitts (1986), and Hales (1986). Only a brief outline will be given here.

Wet deposition is caused by both precipitation scavenging and surface deposition of fog and cloud droplets. Unlike dry deposition, a phenomenon that

occurs in the lower layers of the PBL, precipitation scavenging affects all volume elements aloft inside the precipitation layer. Following Seinfeld (1986), the wet flux of a pollutant to the surface is

$$W_g = \int_o^\infty \Lambda(z,t)\, c(x,y,z,t)\, dz \tag{10–25}$$

for gases and

$$W_p = \int_o^\infty \Lambda(d_p;z,t)\, c(d_p;x,y,z,t)\, dz \tag{10–26}$$

for particles, where Λ is the washout coefficient and c the concentration expressed, for particles, as a function of the particle diameter d_p. It must be noted that Λ varies spatially and temporally. Techniques are available (e.g., Scott, 1982) for calculating Λ as a function of storm type and precipitation amounts, information that can be inferred from NWS observations.

The knowledge of the wet flux W (W_g or W_p) allows the definition of the wet deposition velocity

$$V_w = \frac{W}{c(x,y,0,t)} \simeq \overline{\Lambda} H \tag{10–27}$$

where the last equality assumes that the pollutant is uniformly distributed between $z = 0$ and $z = H$. The wet deposition velocity V_w can be computed by

$$V_w = w_r\, p_o \tag{10–28}$$

where w_r is the species-specific washout ratio (i.e., the concentration of material in surface-level precipitation divided by the concentration of material in surface-level air) and p_o is the precipitation intensity (m s^{-1}). For example, if $w_r = 10^6$ and $p_o = 2.8\ 10^{-7}$ m s^{-1} (i.e., corresponding to a typical light rainfall of 1 mm h^{-1}), then $V_w = 28$ cm s^{-1}, which gives, for $H = 1000$ m, $\overline{\Lambda} = 2.8\ 10^{-4}$ s^{-1}.

The estimate of w_r from available acid rain chemistry data collected in the monitoring networks allows, under certain conditions, a direct evaluation of wet deposition of pollutants (Slinn et al., 1978; Baker et al., 1983; Davies, 1983; Bilonick and Nichols, 1983). (See also Wisniewski and Kinsman, 1982, for an overview of acid precipitation monitoring activities in North America.) In fact, after the washout (or scavenging) coefficients $\overline{\Lambda}$ are evaluated, wet deposition can be dynamically computed by decreasing the mass of the plume elements according to Equation 10–10, where the time scale T_d is replaced by

$$T_w = 1/\overline{\Lambda} \tag{10-29}$$

the time scale of the wet deposition process.

Seinfeld (1986) provides a detailed mathematical discussion of precipitation scavenging of particles, and the calculation of collision efficiencies and scavenging rates, and precipitation of gases, for both irreversibly soluble gases (such as nitric acid, HNO_3) and reversibly soluble gases. Also, a generalized multidimensional model for precipitation scavenging and atmospheric chemistry has been presented by Hales (1989).

In addition to precipitation phenomena, wet deposition is also caused by surface impaction of polluted droplets of fog or cloud. These phenomena, whose parameterization is still poorly understood, are outlined in Figure 10–2.

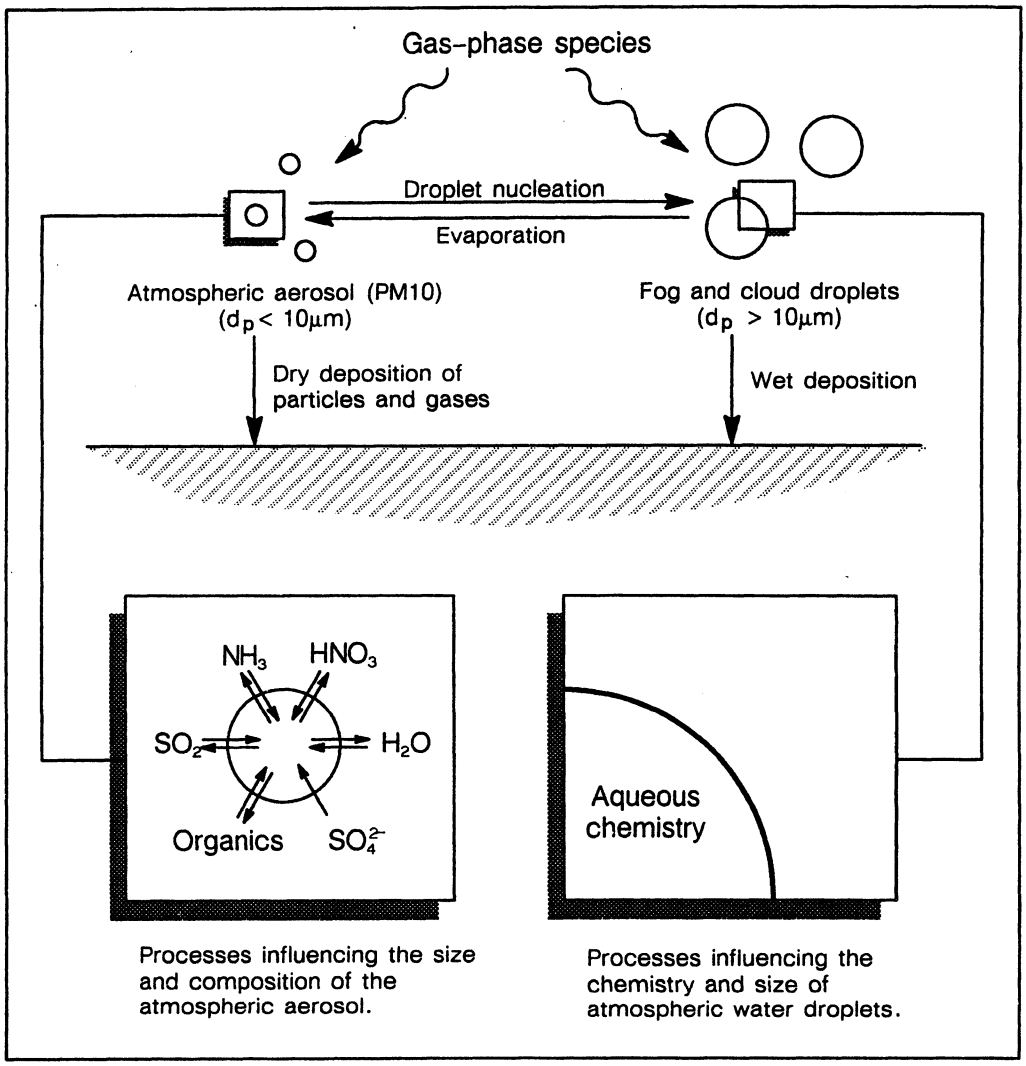

Figure 10–2. Flow chart of atmospheric processes leading to airborne and deposited acidity (from Seinfeld, personal communication).

REFERENCES

Baker, M.S., D. Caniparoli, and H. Harrison (1981): An analysis of the first year of MAP3S rain chemistry measurements. *Atmos. Environ.*, **15**:43–55.

Bilonick, R.A., and D.G. Nichols (1983): Temporal variations in acid precipitation over New York State -- What the 1965–1979 USGS data reveal. *Atmos. Environ.*, **17**:1063–1072.

Davies, T.D. (1983): Sulphur dioxide precipitation scavenging. *Atmos. Environ.*, **17**:797–805.

Doran, J.C. (1979): Sensitivity of particle deposition to changes in deposition velocity. *Atmos. Environ.*, **13**:1269–1273.

Doran, J.C., et al. (1984): Field validation of exposure assessment models. Vol. I, Data. U.S. EPA Document EPA-600/3-84-092a. Office of Research and Development, Research Triangle Park, North Carolina. Also NTIS PB85-107209, Springfield, Virginia.

Doran, J.C., and T.W. Horst (1985): An evaluation of Gaussian plume-depletion models with dual-tracer field measurements. *Atmos. Environ.*, **19**:939–951.

Finlayson-Pitts, B.J., and J.N. Pitts, Jr. (1986): *Atmospheric Chemistry*. New York: John Wiley.

Garland, J.A. (1978): Dry and wet removal of sulphur from the atmosphere. *Atmos. Environ.*, **12**:349–362.

Hales, J.M. (1986): The mathematical characterization of precipitation scavenging and precipitation chemistry. In *The Handbook of Environmental Chemistry*, Vol. 4, Part A, edited by O. Hutzinger. Heidelberg: Springer-Verlag.

Hales, J.M. (1989): A generalized multidimensional model for precipitation scavenging and atmospheric chemistry. *Atmos. Environ.*, **23**(9):2017–2031.

Hicks, B.B. (1982): In *Critical Assessment Document on Acid Deposition* (Chapter VII – Dry Deposition). ATDL Contributory File 81/24. Atmospheric Turbulence and Diffusion Laboratory, NOAA, Oak Ridge, Tennessee.

Houghton, D.D., Ed. (1985): *Handbook of Applied Meteorology*. New York: Wiley-Interscience.

Nicholson, K.W. (1988a): The dry deposition of small particles: A review of experimental measurements. *Atmos. Environ.*, **22**(12):2653–2666.

Nicholson, K.W. (1988b): A review of particle resuspension. *Atmos. Environ.*, **22**(12):2639–2651.

Noll, K.E., and K.Y. Fang (1989): Development of a dry deposition model for atmospheric coarse particles. *Atmos. Environ.*, **23**(3):585–594.

O'Dell, R.A., M. Taheri, and R.L. Kabel (1977): A model for uptake of pollutants by vegetation. *JAPCA*, **27**:1104–1109.

Pleim, J.E., A. Venkatram, and R.J. Yamartino (1984): *The Dry Deposition Model, Vol. 4. ADOM/TADAP Model Development Program*. Ontario Ministry of the Environment, Rexdale, Ontario, Canada.

Schwartz, S.E. (1989): Acid deposition: Unraveling a regional phenomenon. *Science*, **243**:753–763.

Scott, B.C. (1982): Theoretical estimates for scavenging coefficient for soluble aerosol as function of precipitation type, rate, and altitude. *Atmos. Environ.*, **16**:1735–1762.

Sehmel, G.A. (1980): Particle and gas dry deposition: A review. *Atmos. Environ.*, 14:983–1011.

Seinfeld, J.H. (1986): *Atmospheric Chemistry and Physics of Air Pollution*. New York: John Wiley.

Slinn, W.G., L. Hasse, B.B. Hicks, A.W. Hogan, D. Lal, P.S. Liss, K.O. Munnich, G.A. Sehmel, and O. Vittori (1978): Some aspects of the transfer of atmospheric trace constituents past the air–sea interface. *Atmos. Environ.*, 12:2055–2087.

Smith, F.B. (1981): The significance of wet and dry synoptic regions on long– range transport of pollution and its deposition. *Atmos. Environ.*, 15:863–873.

Voldner, E.C., L.A. Barrie, and A. Sirois (1986): A literature review of dry deposition of oxides of sulphur and nitrogen with emphasis on long–range transport modelling in North America. *Atmos. Environ.*, 20(11):2101–2123.

Wesely, M.L., and B.B. Hicks (1977): Some factors that affect the deposition rates of sulfur dioxide and similar gases on vegetation. *JAPCA*, 27:1110–1116.

Wesely, M.L. (1989): Parameterization of surface resistances to gaseous dry deposition in regional–scale numerical models. *Atmos. Environ.*, 6:1293–1304.

Wisniewski, J., and J.D. Kinsman (1982): An overview of acid rain monitoring activities in North America. *J. Climate and Appl. Meteor. Soc.*, 63:598–618.

Yamartino, R.J., J.S. Scire, S.R. Hanna, G.R. Carmichael, Y.S. Chang (1989): CALGRID: A mesoscale photochemical grid model. Sigma Research Corp. Report A049–1. Prepared for the California Air Resources Board, Sacramento, California.

Zannetti, P., and N. Al–Madani (1983): Simulation of transformation, buoyancy and removal processes by Lagrangian particle methods. Fourteenth ITM Meeting on Air Pollution Modeling and Its Application. Copenhagen, Denmark, September 1983.

11 SPECIAL APPLICATIONS OF AIR POLLUTION MODELS

This chapter presents some discussion of special applications of air pollution models:

- complex (rough) terrain problems
- coastal diffusion
- diffusion around buildings
- gravitational settling
- heavy gas dispersion
- cooling tower plumes
- source emission modeling of accidental spills
- indoor air pollution
- regulatory modeling

11.1 COMPLEX (ROUGH) TERRAIN

Dispersion in complex terrain is still poorly understood, even though recent dispersion experiments and studies, such as the U.S. EPA Complex Terrain Model Development Project, have allowed important parameterizations of simplified cases (e.g., dispersion near an isolated small hill and possible plume impact on it). The three major problems in complex terrain applications are

1. The correct evaluation of the trajectory of plume centerline and, in particular, its possible impact upon the elevated terrain.
2. The computation of the enhancement of plume dispersion (both in the horizontal and the vertical) caused by the extra turbulence induced by the complexity of the terrain features.
3. The determination of possible effects caused by streamlines dividing around the terrain obstacles.

An overview of complex terrain modeling is given by Egan (1984), Egan and Schiermeier (1986), and Venkatram (Venkatram and Wyngaard, 1988).

Many studies (Sacre, 1979; Mason and Sykes, 1979; Hunt et al., 1979; Britter et al., 1981; Taylor and Walmsley, 1981; Jenkins et al., 1981; Ryan and Lamb, 1984) have focused on the "small hill" case. Snyder (1985) has reviewed pollutant transport and diffusion in stable, stratified flow. A report on air flow and dispersion in rough terrain has also been provided by Hunt et al. (1984).

In the simplified case of plume dispersion near a small hill, Hunt et al. (1979) demonstrated experimentally the existence of a critical height H_c

$$H_c = H_h (1 - Fr) \tag{11-1}$$

where H_h is the hill height and Fr is the Froude number. Equation 11-1 is derived under the simplifying assumptions of strongly stable atmosphere, constant density gradient and uniform velocity profile, and gives an estimate of H_c, which is the height that separates the streamlines that can pass over the crest of the hill and those that cannot. The Froude number is defined as

$$Fr = \frac{u}{N H_h} \tag{11-2}$$

where u is the characteristic wind speed, N is the Brunt-Vaisala frequency

$$N = \left(-\frac{g}{\varrho} \frac{\partial \varrho}{\partial z} \right)^{1/2} \tag{11-3}$$

ϱ is the density of the air and g is the gravity acceleration. Strongly stable conditions occur for $0 < Fr < 1$, which is the case when Equation 11-1 applies.

Egan (1984) describes how the Gaussian plume model in Equation 7-1 can be used to treat the two extremes of flow behaviors defined by whether streamlines are above or below H_c. For dispersion below H_c (i.e., the "wrap" component), the flow is restricted to travel in horizontal planes toward or around the sides of the hill, as shown in Figure 11-1 and in Region I of Figure 11-2. Concentrations on the "impact" side of the hill, i.e., its upwind face, are given by

$$c(d, z_r) = \frac{P(\theta_d)}{d} c_0(d, z_r) = \frac{Q P(\theta_d)}{\sqrt{2\pi}\, \sigma_z(d)\, u\, d} \cdot \left(\exp\left[-0.5 \left(\frac{z_r - h_e}{\sigma_z} \right)^2 \right] + \exp\left[-0.5 \left(\frac{z_r + h_e}{\sigma_z} \right)^2 \right] \right) \tag{11-4}$$

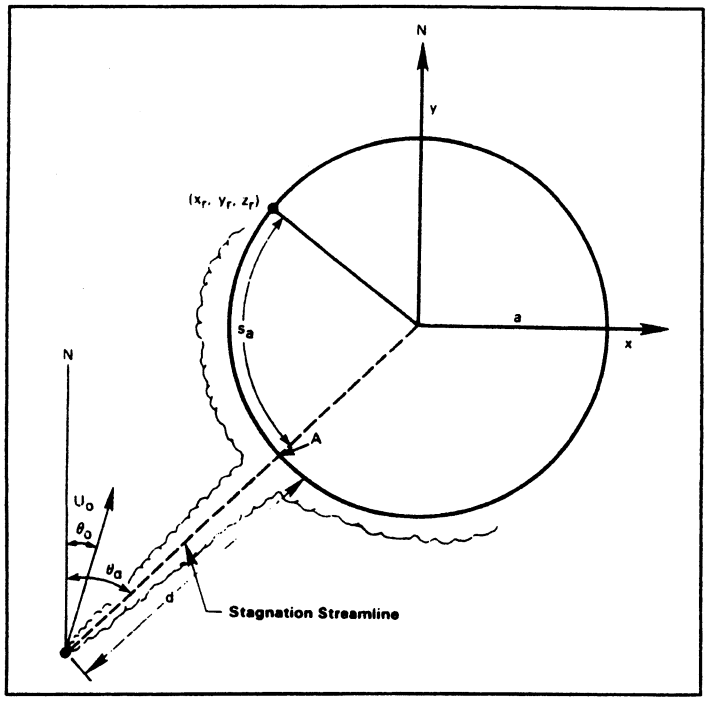

Figure 11–1. Plume dispersion in the region of horizontal flow (from Egan, 1984). [Reprinted with permission from D. Reidel.]

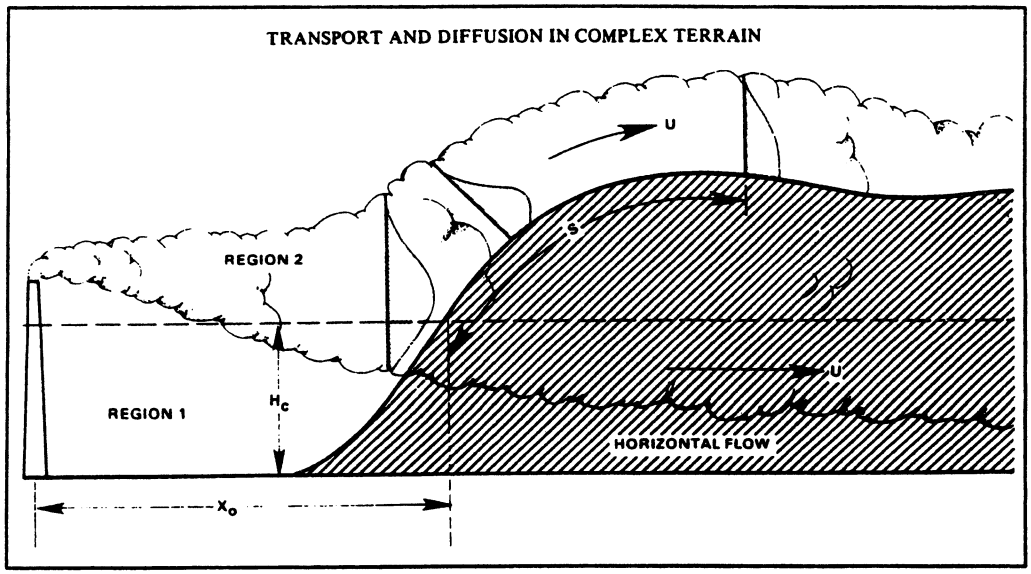

Figure 11–2. Dispersion and flow regions for stratified flow around hills (from Egan, 1984). [Reprinted with permission from D. Reidel.]

where Q is the emission rate, d is the distance from the source to the hillside receptor, z_r is the receptor elevation (above the base of the hill), u is the wind speed, σ_z is the vertical standard deviation of the plume concentration distribution at distance d, h_e is the effective plume height (above the base of the hill), and $P(\theta_d)$ is the probability density function of wind direction θ over an hour averaging time. If $P(\theta_d)$ is Gaussian, we have

$$P(\theta) = \frac{1}{\sqrt{2\pi}} \exp\left[-0.5\left(\frac{\theta-\bar{\theta}}{\sigma_\theta}\right)^2\right] \tag{11-5}$$

where $\bar{\theta}$ is the mean wind direction and σ_θ is the standard deviation of θ in the hour. In Equation 11-4, ground reflection is relative to the base of the hill (i.e, $z = 0$) and not to the hill surface.

For receptors around the side of the hill, the horizontal distance s of the source to a receptor is

$$s = d + s_a \tag{11-6}$$

as illustrated in Figure 11-1. In this case, the plume is reflected by the hill and the concentration at the receptor is computed by treating the vertical distribution of plume material below H_c as a source distribution and integrating the response function (or Green's function) from the hill base to H_c. This integration gives

$$c(s, z_r) = \frac{P(\theta_d)}{s} \int_0^{H_c} \frac{c_o(d, z)}{\sqrt{2\pi}\,\sigma_z'} \cdot \left(\exp\left[-0.5\left(\frac{z_r - z}{\sigma_z'}\right)^2\right] + \exp\left[-0.5\left(\frac{z_r + z}{\sigma_z'}\right)^2\right]\right) dz \tag{11-7}$$

where $c_o(d, z)$ is given by Equation 11-4, and

$$(\sigma_z')^2 = \sigma_z^2(s) - \sigma_z^2(d) \tag{11-8}$$

The portion of the plume above H_c is treated by the "lift" algorithm, in which plume material, as shown in Region 2 of Figure 11-2, is assumed to travel up and over the hill, the horizontal dispersion is enhanced, and the material is fully reflected from the hill surface. In this region, concentrations are computed by integrating the response function from H_c to infinity, i.e.,

$$c(s, \theta_d, z_p) = \frac{2\,P(\theta_d)}{s} \int_{H_c}^{\infty} \frac{c_o(s, z)}{\sqrt{2\pi}\ \sigma_z'} \cdot \exp\left[-0.5\left(\frac{z - H_c}{\sigma_z'}\right)^2\right] dz \quad (11\text{–}9)$$

where z_p denotes the elevation of the ground surface (above the base of the hill), and c_o, σ_z' and s were previously defined.

In this case, instead of Equation 11–8, σ_z' can be defined in a way to enhance vertical dispersion through a terrain factor τ, i.e.,

$$(\sigma_z')^2 = \frac{\sigma_z^2(s)}{\tau^2} - \sigma_z^2(d) \quad (11\text{–}10)$$

where

$$\tau = PPC \quad (11\text{–}11)$$

for $z_p \geq h_e$, and

$$\tau = 1 - (1 - PPC)\,\frac{z_p - H_c}{h_e - H_c} \quad (11\text{–}12)$$

for $z_p \leq h_e$, where PPC is the plume path coefficient, which is about 0.4–0.5 (Hanna et al., 1984).

The U.S. EPA has presently only five models that can be used where the height of the terrain exceeds the height of the emission stack: VALLEY, COMPLEX I, COMPLEX II, RTDM, and CTDM. Only the latter, however, incorporates the equations presented above. Much R&D activity is in progress to improve both theoretical and actual performance of dispersion models in complex terrain. In particular, the U.S. EPA has sponsored model development efforts for stable plume impaction on high terrain (Lavery et al., 1982), and the U.S. DOE has sponsored the Atmospheric Sciences in Complex Terrain program (ASCOT), in which tracer experiments in very rugged terrain have been performed with the objective of understanding the wind transport pattern near the surface (Dickerson and Gudiksen, 1980). Moreover, important results are expected in future from the third experiment in the EPRI Plume Model Validation and Development (PMV&D) program that took place in 1985.

11.2 COASTAL DIFFUSION

The literature contains reports of many studies in which the air pollution dispersion near the shoreline of a large body of water is simulated with advanced

numerical techniques in order to take into account the hydrodynamics of the breeze effect and the consequent dispersion (Bornstein and Runca, 1977; Dieterle and Tingle, 1979; Dobosy, 1977; Pielke et al., 1983; Pielke et al., 1988; Lyons et al., 1987; and Segal et al., 1988). Unfortunately, application of such methodologies requires depth of technical expertise in the selection of modeling parameters and the interpretation of results, and extensive computer time and storage (even though prototypes of real-time mesoscale modeling systems can run today on the new generation of minisupercomputers integrated with graphics workstations). Therefore, these methods cannot currently be considered practical for routine applications. However, they do provide realistic numerical simulations that should be considered in the development of simpler techniques. Summary articles on mesoscale transport in coastal zones are provided in Lyons (1975), Lyons et al. (1983), Kaleel et al. (1983), and Moran et al. (1986).

A simple Gaussian model application in these circumstances has often given interesting results in spite of the complexity of the problem (e.g., Runca et al., 1976). Therefore, many studies have been developed for extending and improving the Gaussian formula to simulate coastal dispersion conditions. The work of Lyons and Cole (1973; further developed by van Dop et al., 1979), postulates a stable Gaussian plume advected over an unstable mainland surface, as depicted in Figure 11-3. This can be simulated by a fumigation formula in which concentration is vertically homogeneous and varies only with the distance from the shoreline (see Section 7.5.6). Because of recirculating flows, however, straight-line Gaussian models may fail catastrophically. Also, the coastal environment has very high levels of shear that are difficult to describe with plume models and require high-resolution methods (e.g., a combination of a mesoscale numerical model and a Lagrangian particle model; Lyons et al., 1988).

As discussed by Stunder and SethuRaman (1986), plume dispersion modules in coastal regions need to include calculations of the following parameters:

1. the Thermal Internal Boundary Layer (TIBL) height, i.e., the variation of h with the distance inland from the shoreline
2. the dispersion rates inside the convective, unstable TIBL and in the stable air above the TIBL
3. partial penetration of the TIBL by the plume
4. overwater dispersion rates (if the plume is emitted offshore)

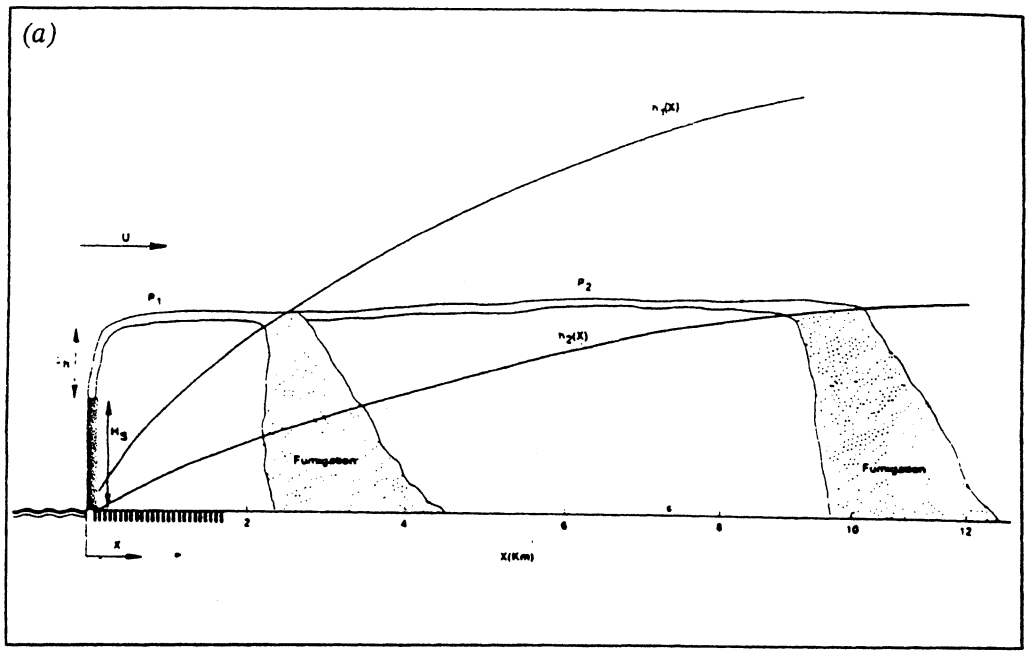

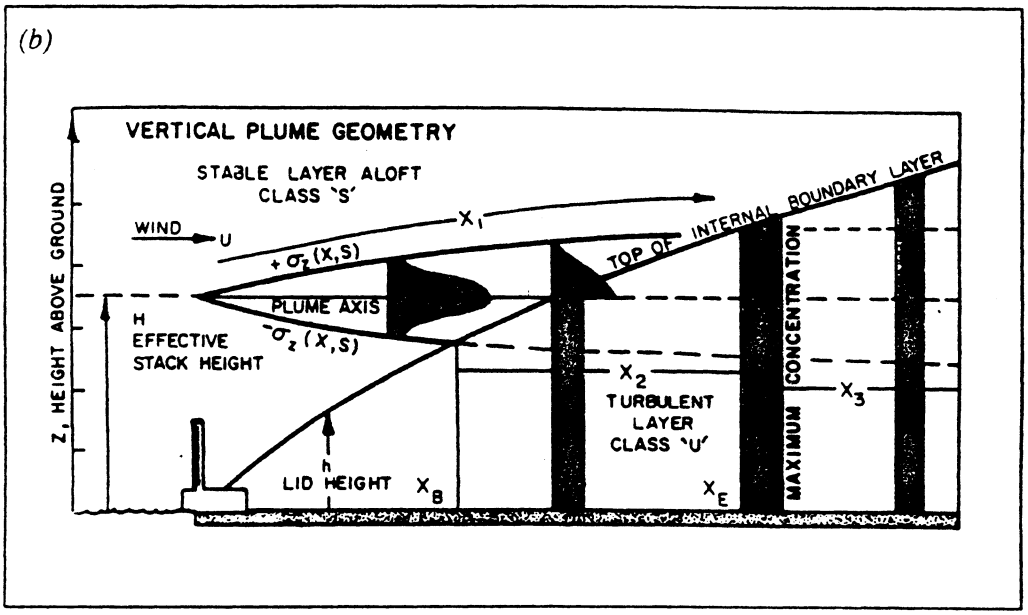

Figure 11–3. *(a) Typical dispersion pattern in coastal areas. (b) Plume geometry of Lyons and Cole (1973 model). $\sigma_z(x, s)$represents vertical dispersion coefficients. X_B, X_E represents the beginning and end points of fumigation. (From Stunder and SethuRaman, 1986.) [Reprinted with permission from Pergamon Press.]*

11.2.1 The TIBL Height

Weisman (1976) proposed the following equation for the TIBL height $h(x)$

$$h(x) = \left(\frac{2 H_o x}{\varrho c_p \frac{\partial \theta}{\partial z} u(10)} \right)^{1/2} \qquad (11\text{–}13)$$

where x is the downwind distance from the shoreline (m), H_o is the overland heat flux ($w\ m^{-2}$), ϱ is the density of the air ($1.2\ 10^3\ g\ m^{-3}$), c_p is the specific heat at constant pressure ($0.24\ cal\ g^{-1}\ K^{-1}$), $\partial\theta/\partial z$ is the overwater potential temperature gradient and $u(10)$ is the wind speed at 10 m above the ground.

Equation 11–13 was successfully tested against field studies by Stunder and SethuRaman (1986). More extended calculations of $h(x)$ are provided by Lyons et al. (1981) and Stunder and SethuRaman (1985).

11.2.2 Dispersion Rates (Plume Sigmas) Inside and Above the TIBL

Inside the TIBL, the dispersion of a plume can be described by the σ_y, σ_z formulas discussed in Chapter 7 for unstable conditions. Above the TIBL, plume sigmas for stable atmospheric conditions are often suggested. It must be noted, however, that little or no turbulence can be found above h and that, therefore, even the most stable σ_y, σ_z formulas can overestimate the plume spread above the TIBL. On the other side, however, if wind shear is strong above the TIBL, horizontal diffusion will be larger than suggested by the stable σ_y formulae.

11.2.3 Plume Partial Penetration

Since $h(x)$, defined by Equation 11–13, increases with the distance x from the shoreline, an elevated plume will progressively penetrate the TIBL, as illustrated in Figure 11–3. If the vertical concentration distribution of the plume is Gaussian with standard deviation $\sigma_z(x)$, the fraction of the plume that has penetrated the TIBL at x is (Stunder and SethuRaman, 1986)

$$\int_{-\infty}^{P} (2\pi)^{-1/2} \exp\left(-\frac{P^2}{2}\right) dP \qquad (11\text{–}14)$$

where

$$P = \frac{h(x) - h_e}{\sigma_z(x)} \qquad (11\text{–}15)$$

11.2.4 Overwater Dispersion Rates

Several dispersion experiments have recently provided new information on plume dispersion rates over water. This has allowed new, more realistic parameterizations of the phenomenon.

Hanna et al. (1985) developed the Offshore and Coastal Dispersion (OCD) model, in which the overwater plume is described by the Gaussian equation, whose σ_y and σ_z are computed as follows. The total σ_y is calculated by adding the contributions from turbulence, σ_{yt}, buoyant plume enhancement, σ_{yb}, wind direction shear, σ_{ys}, and structural downwash, σ_{yo}, i.e.,

$$\sigma_y^2 = \sigma_{yt}^2 + \sigma_{yb}^2 + \sigma_{ys}^2 + \sigma_{yo}^2 \tag{11-16}$$

Similarly, the total σ_z is computed by

$$\sigma_z^2 = \sigma_{zt}^2 + \sigma_{zb}^2 + \sigma_{zo}^2 \tag{11-17}$$

since wind direction shear does not affect σ_z.

According to Pasquill (1976)

$$\sigma_{yb}^2 = \sigma_{zb}^2 = (\Delta h)^2/10 \tag{11-18}$$

and

$$\sigma_{ys}^2 = 0.03\,(\Delta WD)^2\,x^2 \tag{11-19}$$

where ΔWD is the wind direction shear in radians.

The turbulence contributions are

$$\sigma_{yt} = i_y\ x\ S_y(x) \tag{11-20}$$

$$\sigma_{zt} = i_z\ x\ S_z(x) \tag{11-21}$$

where

$$i_y = \sigma_v/u\ (\simeq \sigma_\theta \text{ for small angles}) \tag{11-22}$$

$$i_z = \sigma_w/u\ (\simeq \sigma_\phi \text{ for small angles}) \tag{11-23}$$

are the turbulence intensities.

For overwater dispersion, Hanna et al. (1985) propose the following interpretation of the Briggs' (1973) formulation:

$$S_y(x) = (1 + 0.0001\,x)^{-1/2} \tag{11-24}$$

for $x \leq 10^4$ m (S_y is kept constant for $x > 10^4$ m) and

$S_z(x)$	Overwater Stability	
1	A and B	(11-25a)
$(1 + 0.0002\,x)^{-1/2}$	C	(11-25b)
$(1 + 0.0015\,x)^{-1/2}$	D	(11-25c)
$(1 + 0.0003\,x)^{-1}$	E and F	(11-25d)

Overwater stability is computed from the Monin-Obukov length L (defined using the virtual temperature) and the roughness length z_o, using the method of Golder (1972) illustrated in Figure 3-10. An additional stability class is added (Class G) when $\partial\theta/\partial z \geq 5°C\ 10^{-2}\ m^{-1}$, a value found only when warm air is advected over cold water.

If σ_θ is not measured, an approximate formula (Hanna, 1983), which agrees with boundary layer theory and recent field observations, gives

$$i_y \simeq 0.5/u \tag{11-26}$$

for $u < 10\ m\ s^{-1}$.

The above parameterization is the most applicable, at the present time, since it has been fully implemented into a common-domain computer package — the OCD model. Other studies, however, have provided similar parameterizations, e.g., Dabberdt (1986), who analyzed ten atmospheric tracer experiments, which provided 62 hours of dispersion data. He used these data to evaluate four dispersion parameterization schemes:

1. the Pasquill-Gifford-Turner method (Turner, 1970)
2. the Pasquill (1976) method
3. the Draxler (1976)-Irwin (1979) method
4. the Briggs (1976) method

He found the second and third scheme to provide a good estimate of σ_y, while all methods give a poor estimate of σ_z.

An additional parameterization of plume dispersion over water is also provided by Skupniewicz and Schacher (1986).

11.3 DIFFUSION AROUND BUILDINGS

Several studies have tried to evaluate the dispersion behavior around buildings (see Figure 7–5) and a few of them have proposed empirical algorithms to simulate these peculiar effects. One of the commonest techniques is based on the studies of Huber and Snyder (1976) and Huber (1977) and has been incorporated into the U.S. EPA Industrial Source Complex model (ISC; Bowers et al., 1979). This technique is based on the results of tunnel experiments with a building crosswind dimension double that of the building height, and with atmospheric stability from C (slightly unstable) to D (neutral).

The first step in this wake–effect evaluation method (Bowers et al., 1979) is to calculate the plume rise due to momentum alone. If the plume height, given by the sum of the stack height and the momentum rise at a downwind distance of two building heights, is greater than either 2.5 building heights (2.5 h_b) or the sum of the building height and 1.5 times the building width ($h_b + 1.5\, h_w$), the plume is assumed to be unaffected by the building wake. Otherwise, the plume is assumed to be affected by the building wake.

The effects of building wakes are accounted for by modifying only σ_z, for plumes from stacks with plume height to building height ratios greater than 1.2 (but less than 2.5), and by modifying both σ_y and σ_z, for plume height to building height ratios less than or equal to 1.2. The plume height used for computing the plume height to stack height ratio is the same plume height used to determine whether the plume is affected by the building wake. The procedure defines buildings as squat ($h_w \geq h_b$) or tall ($h_w < h_b$). The building width h_w is approximated by the diameter of a circle with an area equal to the horizontal area of the building. Then, a general procedure is defined below for modifying σ_z and σ_y at distances greater than 3 h_b, for squat buildings, or 3 h_w, for tall buildings.

The modified σ_z equation for a squat building is given by

$$\sigma_z' = 0.7\, h_b + 0.067\, (x - 3\, h_b) \qquad (11\text{–}27)$$

for $3\, h_b < x < 10\, h_b$, and

$$\sigma_z' = \sigma_z(x + x_z) \tag{11-28}$$

for $x \geq 10\ h_b$, where h_b is the building height, x is the downwind distance, σ_z is the value of a selected sigma function, and x_z is defined below. For a tall building, Huber (1977) suggests that the width scale h_w replace h_b in Equations 11-27 and 11-28. The modified σ_z equation for a tall building is then given by

$$\sigma_z' = 0.7\ h_w + 0.067\ (x - 3\ h_w) \tag{11-29}$$

for $3\ h_w < x < 10\ h_w$ or

$$\sigma_z' = \sigma_z(x + x_z) \tag{11-30}$$

for $x \geq 10\ h_w$.

The vertical virtual distance x_z is added to the actual downwind distance x at downwind distances beyond $10\ h_b$ (squat buildings) or $10\ h_w$ (tall buildings), in order to account for the enhanced initial plume growth caused by the building wake. Thus, x_z for a squat building is

$$x_z = \left(\frac{1.2\ h_b}{a}\right)^{1/b} - 0.01\ h_b \tag{11-31}$$

where the constants a and b are dependent upon atmospheric stability. Similarly, the vertical virtual distance for tall buildings is given by

$$x_z = \left(\frac{1.2\ h_w}{a}\right)^{1/b} - 0.01\ h_w \tag{11-32}$$

Similar equations are also provided by Bowers et al. (1979) for the computation of the modified (i.e., enhanced) σ_y' for both squat and tall buildings.

The air flow in the building cavity (see Figure 7-5) is highly variable and generally recirculating, and the procedure defined in this section is not appropriate for estimating concentrations within such cavities. In this case, the downwash procedure found in Budney (1977) may be used to obtain a worst-case estimate.

Other schemes, in addition to those presented above, are available for computing atmospheric downwash. A comparative study of four different

schemes has been performed by Starheim and Knudson (1981). Modifications of the downwash algorithms presented in this section have also been proposed by Shulman and Hanna (1986).

11.4 GRAVITATIONAL SETTLING

Gravitational settling is the major factor affecting the dry deposition of large particles (say, with diameter greater than 10 μm), such as wind-raised dust. The settling velocity is a function of shape, density and size of the particle and, for small particles, is negligible when compared with turbulent vertical velocities. However, small particles may form larger particles by aggregation and then be effectively removed by gravitational settling. Figure 11-4 presents typical values of the settling velocity V_G as a function of particle diameter and density. These values were computed using Stokes' law for particles with diameters up to 60 μm, i.e.,

$$V_G = \frac{d^2 g \, \varrho_p}{18\mu} \tag{11-33}$$

where d is the diameter of the particle, g is the gravity acceleration, ϱ_p is the particle density and μ is the dynamic viscosity of the air ($= 1.8\ 10^{-4}\ g\ s^{-1}\ cm^{-1}$). For larger particles, Stokes' law is modified according to Van der Hoven (1968).

The behavior of a "titled" plume, i.e., a plume of particles affected by gravitational settling V_G, is presented in Figure 7-6.

11.5 HEAVY GAS DISPERSION

The production, transportation and storage of large quantities of heavy gases represent a serious danger to the public. Heavy gas clouds constitute a severe environmental hazard. A cloud of methane, propane or butane may be flammable if its mean volume concentration is higher than about 1 percent (Eidsvik, 1980); a cloud of chlorine may be poisonous at concentrations of about 10^{-5} percent! A typical scenario is given by the spill of liquified natural gas (LNG) (Zeman, 1982). After the liquid spills, heat is transferred to the liquid layer from the underlying surface (soil or water) and the liquid boils off. The released vapor has a temperature of 113°K and a specific gravity of about 1.65. After building up to a certain depth, it starts to spread under the forces of gravity. As the cold vapor comes into contact with a warm surface, strong turbulent convection is triggered. After the gravity current exhausts its excess potential

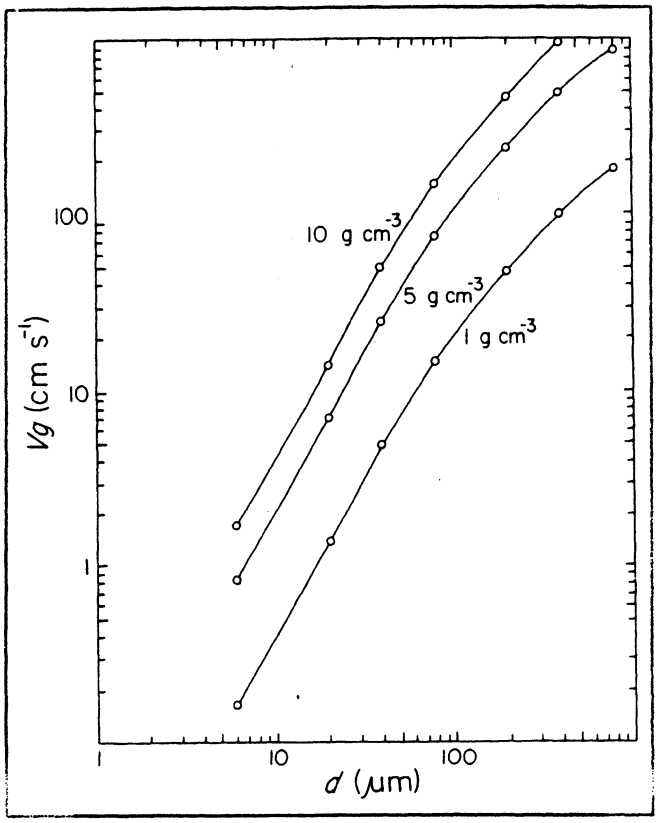

Figure 11–4. Fall velocity of spherical particles as a function of particle diameter and density. Source: Adapted from Hanna et al. (1982) as presented by Stern et al. (1984). [Reprinted with permission from Academic Press.]

energy through mixing, heating and spreading, the diluted vapor cloud will behave like a passive contaminant subject to atmospheric dispersion.

Some modeling techniques have been proposed and tested for the simulation of heavy gas dispersion. In the simple model proposed by Eidsvik (1980), the horizontal dimension of the cloud is assumed to increase due to the gravity fall of the cloud, and the cold cloud is heated from below and from air entrainment. The model predicts accurately some experimental data on heavy gas dispersion.

Zeman (1982) investigated gravity currents and developed a simple one-layer model that simulates the formation of the gravity flow by boiling the spilled liquified gas, the three-dimensional gravity flow in the presence of wind, and the convective heating and its contribution to the entrainment of ambient air. He also

identified the scaling laws of the above phenomena, which are shown to agree with the model predictions.

An interesting comparison of the performance of three dense gas dispersion models is presented by Ermak et al. (1981). In this study, the predictions from three vapor dispersion models for cold dense gas releases are compared with the results from several 40 m^3 LNG spill experiments conducted at China Lake, California, in 1980. The models vary considerably in the degree to which they approximate important physical phenomena and include restricting assumptions. The simplest model (GD), a modified Gaussian plume model, predicted a vapor cloud that was always too high and too narrow by a factor of 1.5 to 3. The second model (SLAB), a layer-averaged conservation equation model with one independent spatial variable (downwind distance), generally predicted the maximum distance to the lower flammability limit (LFL) and cloud width quite well. SLAB assumes the vertical concentration distribution is nearly uniform, so that the vertical concentration gradient $\partial c/\partial z$ is essentially zero from the ground up through most of the cloud and then very steep at the top of the cloud. This was generally not the case in these experiments, especially in the high wind speed tests, where the vertical concentration gradient was found to be more gradual throughout the cloud. The last model (FEM3) is a fully three-dimensional conservation equation model, which predicted the concentration distribution in time and space rather well. A particular achievement of this model was the prediction of a bifurcated cloud structure observed in one experiment conducted with a low ambient wind speed. Both the SLAB and FEM3 models accurately predicted the length of time required for the cloud to disperse to a level below the LFL, even in the low wind speed test, where the vapor cloud lingered over the source region for a considerable length of time after the LNG spill was terminated.

Modeling reviews of heavy gas dispersion in the atmosphere are provided by McNaughton and Berkowitz (in Hartwig, 1980), Havens (1985), and Krogstad and Jacobsen (1989). Fay and Zemba (1985) propose an algorithm for treating initially compact dense gas clouds, i.e., clouds whose initial shapes have nearly equal vertical and horizontal dimensions. In particular, they model the initial spreading motion of the cloud with a constant global entrainment rate obtained from experimental values. Turbulence is then added to this initial entrainment. Fay and Zemba (1986) also propose a quasi-one-dimensional flow model of an isothermal dense gas plume (integral model). The interactions of a heavier-than-air gas near a two-dimensional obstacle have been studied and modeled by Sutton et al. (1986), who added streamline curvature and buoyancy corrections to the basic turbulence formulation. A review of recent field tests and mathematical

modeling of atmospheric dispersion of large spills of denser-than-air gases is provided by Koopman et al. (1989).

11.6 COOLING TOWER PLUMES

Cooling towers conserve water and prevent the discharge of heated water to streams, lakes and estuaries. A brief review of cooling tower plumes and drift deposition phenomena can be found in the handbook by Hanna et al. (1982).

In a cooling tower, hot water from the industrial process drips over wooden or plastic barriers and evaporates into the air that passes through the tower. As a result, about 540 calories of heat are lost for each gram of water evaporated. Cooling towers can be tall (e.g., 150 m tall and 30 m in radius) natural-draft towers, in which vertical motions are induced by density differences, or short (e.g., 20 m tall and 5 m in radius) mechanical-draft towers, in which vertical motions are forced by large fans. Vertical velocities of about 5 m s^{-1} are observed in natural draft towers and about 10 m s^{-1} in mechanical draft towers. Temperature and moisture differences between the plume and the environment are about the same in both types of towers, about 20°C and 0.03 g/g, respectively. The plume is saturated when it leaves the tower, and liquid water concentrations are about 0.001 g/g.

Heat and moisture fluxes from cooling towers at large power plants can cause fog or cloud formation and can, at times, induce additional precipitation. Another potential problem is drift deposition, in which circulating cooling water with drop sizes ranging from 50 to 1,000 μm is carried out of the tower and may be deposited on nearby structures and vegetation. These drops generally contain salts, fungicides, and pesticides, which may harm the surfaces they strike. A comprehensive review of atmospheric effects of cooling tower plumes is given by Hanna (1981).

A schematic illustration of a cooling tower plume is presented in Figure 11-5, while the outlines of a cooling tower vapor plume and a drift drop plume are illustrated in Figure 11-6.

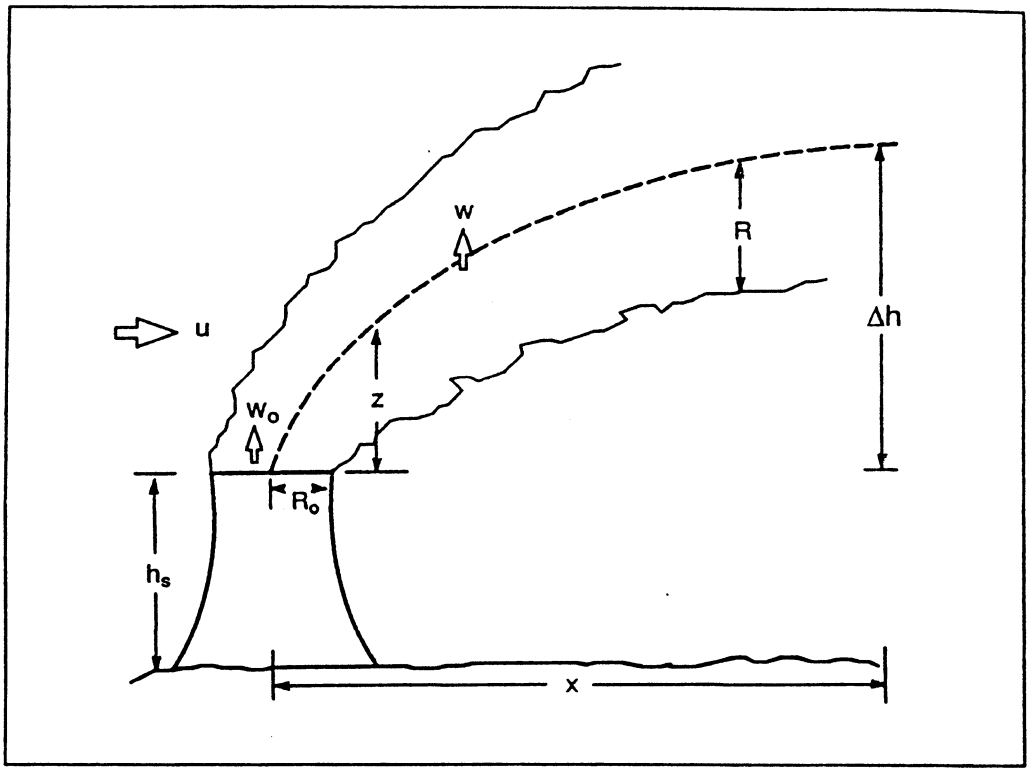

Figure 11–5. Cooling tower plume (adapted from Hanna et al., 1982).

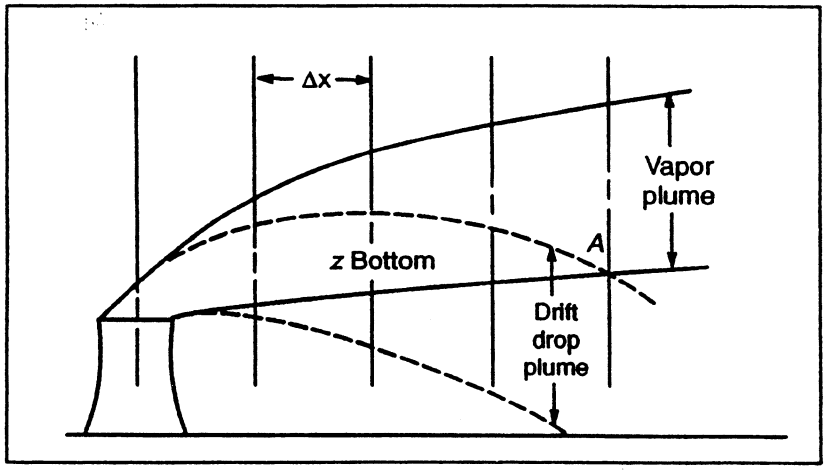

Figure 11–6. Outline of a cooling tower vapor plume and a drift drop plume (for drops in a narrow size range). By point A, all drift drops in this size range have dropped out of the plume (adapted from Hanna et al., 1982).

Several mathematical models are available to simulate the peculiar characteristics of cooling-tower plume dispersion. The fundamental nondimensional parameters that govern the dispersion of natural-draft cooling tower (NDCT) plumes are (Carhart et al., 1982)

- the initial densimetric Froude number F_o, where

$$F_o = W_o \left(g \frac{\varrho_o - \varrho_a}{\varrho_a} \right)^{-1/2} \tag{11-34}$$

- the velocity ratio

$$U_o / W_o \tag{11-35}$$

- the local ambient stability s', where

$$s' = \left(\frac{d}{4\, U_o} \right)^2 \frac{g}{T_a} \frac{d\theta_a}{dz} \tag{11-36}$$

- and the ambient moisture deficit

$$V^* = q_o - q_a \tag{11-37}$$

where W_o is the top exit velocity, U_o is the wind speed at the tower top, d is the tower exit diameter, θ_a is the ambient potential temperature, ϱ_o and ϱ_a are, respectively, the tower exit density and ambient density at the tower top (including moisture effects), and q_o, q_a are the exit plume and ambient specific humidities, respectively.

Carhart et al. (1982) provide an evaluation of the theory and actual performance of 16 models commonly used for the prediction of plume rise from natural draft cooling towers. The best models can predict visible plume rise within a factor of two and visible plume length within a factor of 2.5, but only for 50 percent of the cases tested.

Finally, a new, calibrated, advanced integral model for plume rise from single natural draft cooling towers has been proposed by Schatzmann and Policastro (1984). This model is based on the integration of three-dimensional conservation equations and includes a treatment of plume thermodynamics and tower downwash effects.

11.7 SOURCE EMISSION MODELING OF ACCIDENTAL SPILLS

The most important parameter in the simulation of accidental spills of hazardous materials is the "source term," i.e., the quantitative evaluation of the dimension, rate and duration of the spill. Source emission models are summarized in Chapter 4 of Hanna and Drivas (1987), who describe the physical and chemical principles that are appropriate for the various types of spill scenarios and provide formulae for the simulation of

- gas jet releases, generated from a small puncture in a pressurized pure gas pipeline or in the vapor space of a pressurized gas storage tank (as illustrated in Figure 11–7)
- liquid jet releases
- two-phase jet releases
- flashing processes
- liquid pool evaporation (single and multicomponent)

Table 11–1 lists some available source emission models (see Table 14–1 for additional information on these models).

11.8 INDOOR AIR POLLUTION

It is evident that the air people breathe inside buildings (at home or at work) and while traveling (by car, bus, subway, airplane, etc.) is quite different from the air outdoors. Traditional pollutants, such as SO_2 and CO, can infiltrate into buildings from outside. The real problem with indoor air quality, however, is the indoor emission of pollutants and their accumulation due to poor ventilation and air exchange.

The major indoor air pollution problems are (U.S. EPA, 1988):

- Radon, a naturally occurring gas resulting from the radioactive decay of radium, found in many types of rocks and soils. Radon enters buildings through cracks in the foundations.
- Environmental tobacco smoke, i.e., smoke that nonsmokers are exposed to from smokers. It contains inorganic gases, heavy metals, particulates, VOCs, and products of incomplete burning. Major progress has been made in North America in reducing or eliminating tobacco smoke in many indoor environments. Unfortunately,

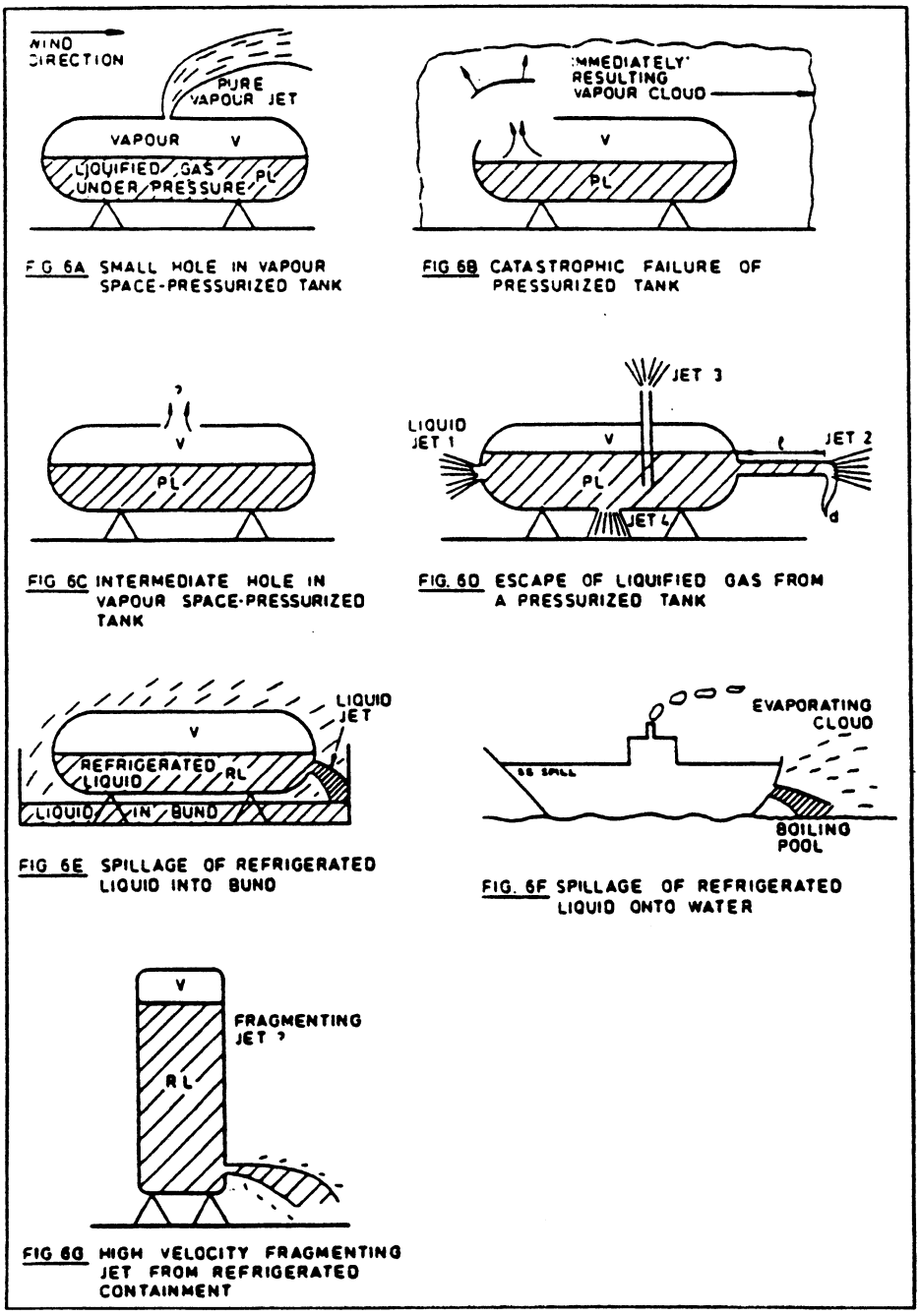

Figure 11–7. Illustration of some conceivable release mechanisms, from Fryer and Kaiser (1979), as presented by Hanna and Drivas (1987). In most cases, the jet could be two phase (vapor plus entrained liquid aerosol). [Reprinted with permission from the American Institute of Chemical Engineers.]

Table 11–1. List of some available source emission models. More details are given in Table 14–1 (from Hanna and Drivas, 1987; see this publication for the references listed below). [Reprinted with permission from the American Institute of Chemical Engineers.]

- Evaporation Models:
  - Ille and Springer (1978)
  - Army (Whitacre et al., 1986)
  - Shell SPILLS (Fleischer, 1980)
  - USAF ESL (Clewell, 1983)
  - Air Weather Service (AWS, 1978)
  - Illinois EPA (Kelty, 1984)
  - Stiver and Mackay (1982)
  - Monsanto (Wu and Schroy, 1979)
  - Shaw and Briscoe (1978)
- Jet Models:
  - Wilson (1979)
- Jet and Evaporation Models:
  - CHARM (Eltgroth et al., 1983)
  - Ontario MOE (MOE, 1983)
  - AIRTOX (Paine et al., 1986)
  - Kunkel (1983, 1985)
  - DENZ (Fryer and Kaiser, 1979)
  - COBRA (Alp, 1985)

the rest of the world lags behind in the progress toward a civilized respect for nonsmokers' rights.

- Asbestos fibers, used in a variety of building materials for insulation, fireproofing, wallboard, ceiling tiles, floor tiles, etc.
- Formaldehyde, used in furniture, foam insulation, and pressed wood products.
- Other VOCs, such as perchlorethylene emitted by dry-cleaned clothes, and paints and cleaning compounds.
- Biological pollutants, originating from heating, ventilation, air conditioning systems and humidifiers, when improperly cleaned and maintained.

- Pesticides, such as termiticides and wood preservatives.

Clearly, since most people spend a large majority of their time indoors (at least in the industrialized countries), indoor air quality may affect human health more than outdoor air quality. Therefore, the common practice of relating measurements of outdoor pollutants to human exposure can be fundamentally wrong in most circumstances.

Direct measurements of indoor air quality are, naturally, the best way to evaluate the existence and the gravity of indoor air pollution. In some cases, however, indoor air quality modeling may provide useful complementary information. A general mathematical model of indoor dynamics of gases and aerosols was presented by Nazaroff and Cass (1986, 1989) and is summarized below.

The building is represented by a set of interconnected chambers, where, in each chamber, pollutants are well mixed. Within each chamber i, the rate of change of concentration C_{ijk}, for each component k and (for aerosols) each section j, is given by the equation

$$\frac{dC_{ijk}}{dt} = S_{ijk} - L_{ijk}C_{ijk} \qquad (11\text{–}38)$$

where S_{ijk} is the source term, which includes direct emission, avective transport from other chambers and outside, and (for aerosols) coagulation of mass from smaller particles into the section j; L_{ijk} is the sum of all sinks, including loss to the surfaces, removal by ventilation and filtration, and (for aerosols) loss to a larger size due to coagulation.

Equation 11–38 provides a solution of $C_{ijk}(t)$ if the input parameters, S_{ijk} and L_{ijk}, and the initial conditions $C_{ijk}(0)$ are provided. The input parameters, of course, vary with time.

11.9 REGULATORY MODELING

In the U.S., laws and regulations have been formalized into a series of procedures dealing with air quality permitting requirements that affect the operations of existing industrial facilities and the design of new ones. As a consequence of the Clean Air Act and its amendments, the use of selected air pollution models has been formalized in order to achieve the goal of definite answers (yes or no) for the permitting process.

This regulatory application of air pollution models has the main advantage of being performed under the same set of procedures for all applicants, aiming at the objective evaluation of the air quality impact generated by their proposed pollutant-emitting modifications or new facilities. Clear, objective rules are a prerequisite of fairness, which is accomplished through a set of procedures developed by the U.S. Environmental Protection Agency (EPA) (each state, however, may have its own set of additional local regulations to comply with). Generalized rules may, sometimes, however, be in contrast with best scientific judgment, which, in a complex field such as atmospheric dispersion, would require flexibility and subjective interpretation. As a consequence, regulatory application of dispersion models may, sometimes, use bad science or, often, push scientific methodologies beyond the limits of their applicability.

Historical reviews of U.S. air quality laws are presented by Stern (1977; 1982). A useful summary of practical requirements is contained in the handbook prepared by ERT (1985).

The most important regulatory process is the process of evaluating an application for a federal "permit to construct," i.e., a New Source Review (NSR). This review is required for new plants that could emit 100 tons per year of any pollutant or for modifications to major existing plants that will cause increases greater than defined minimum values. These "De Minimis" amounts are presented in Table 11-2.

An NSR process varies depending on the location of the new source. Areas where the National Ambient Air Quality Standards (NAAQS) for all criteria(*) pollutants are met are designated "attainment" and are subject to the Prevention of Significant Deterioration (PSD) doctrine. If one or more pollutants do not meet the NAAQS standards, the area is designated as "nonattainment" (NA) for those pollutants.

For PSD areas, maximum "increments" of SO_2 and Total Suspended Particles (TSP) have been established. Therefore, a PSD review will use appropriate techniques (i.e., dispersion models) to evaluate whether the proposed emission will consume a "tolerable" part of the allowable increment. The size of these increments depends on the classification of the area. In Class I areas, i.e., regions that require the highest degree of protection, such as national parks and wilderness areas, the increments are small, while Class II and Class III areas have larger increments to allow some industrial development. No Class III areas have been designated yet, however.

(*) A criteria pollutant is a pollutant for which an NAAQS exists.

Table 11–2. De Minimis emission rates (from ERT, 1985). [Reprinted with permission from ENSR.]

Pollutant	Emission Rates (tons per year)
Carbon monoxide	100
Nitrogen oxides	40
Sulfur dioxide	40
Particulate matter	25
Ozone	40 tpy of volatile organic compounds
Lead	0.6
Asbestos	0.007
Beryllium	0.0004
Mercury	0.1
Vinyl chloride	1
Fluorides	3
Sulfuric acid mist	7
Hydrogen sulfide (H_2S)	10
Total reduced sulfur (including H_2S)	10
Reduced sulfur compounds (including H_2S)	10

For NA areas, no further air quality deterioration is allowed. Consequently, "offsets" need to be found. In other words, other existing emissions in the area need to be eliminated or reduced by control technology, in order to obtain a permit for the new source.

The entire NSR process is outlined in Figure 11–8. Mathematical modeling plays an important role in both PSD and NA areas. In the former, modeling simulations verify that the new source impacts are below the allowable fraction of the increment level for that pollutant in that region. In the latter, modeling simulations confirm the net improvement in air quality achieved by adding the new source and subtracting the offsets in the region. Models can also be used to clarify monitoring needs and select both meteorological and air quality

monitoring sites. Modeling guidelines are available (U.S. EPA, 1984) to help in the proper regulatory use of these numerical techniques. Specific regulatory models are discussed in Chapter 14.

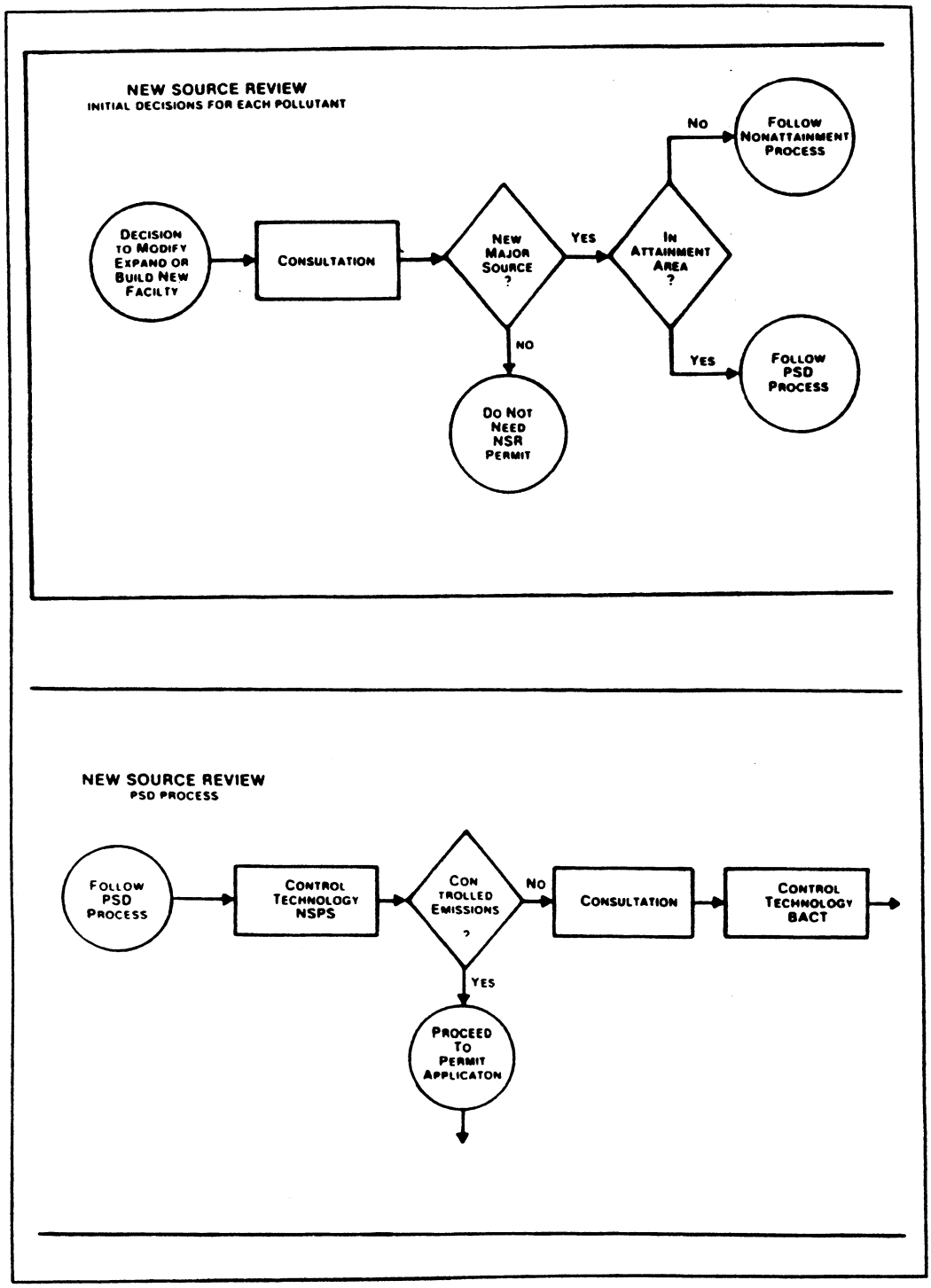

Figure 11–8. New source review (from ERT, 1985). [Reprinted with permission from ENSR.]

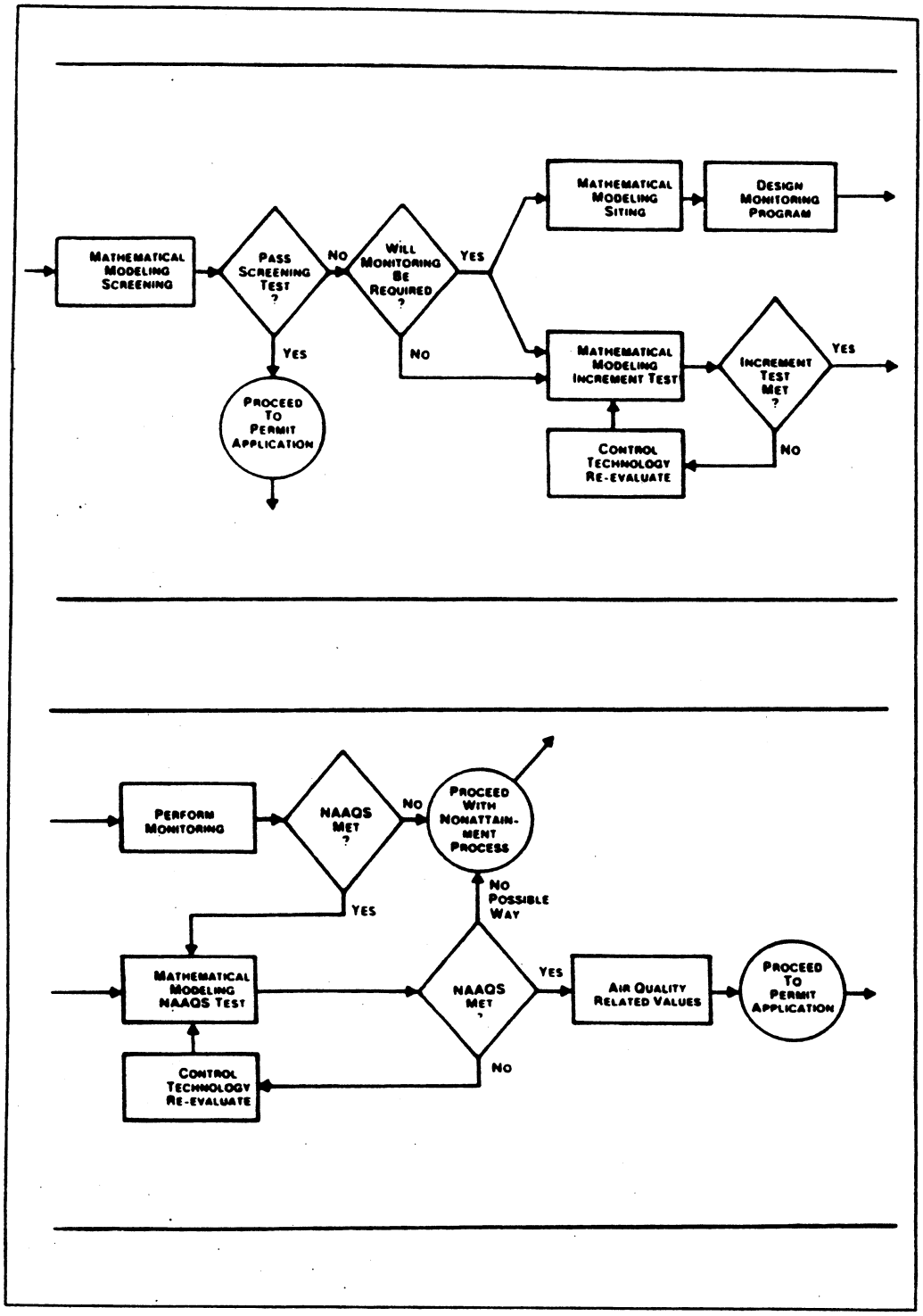

Figure 11–8. New source review (continued)

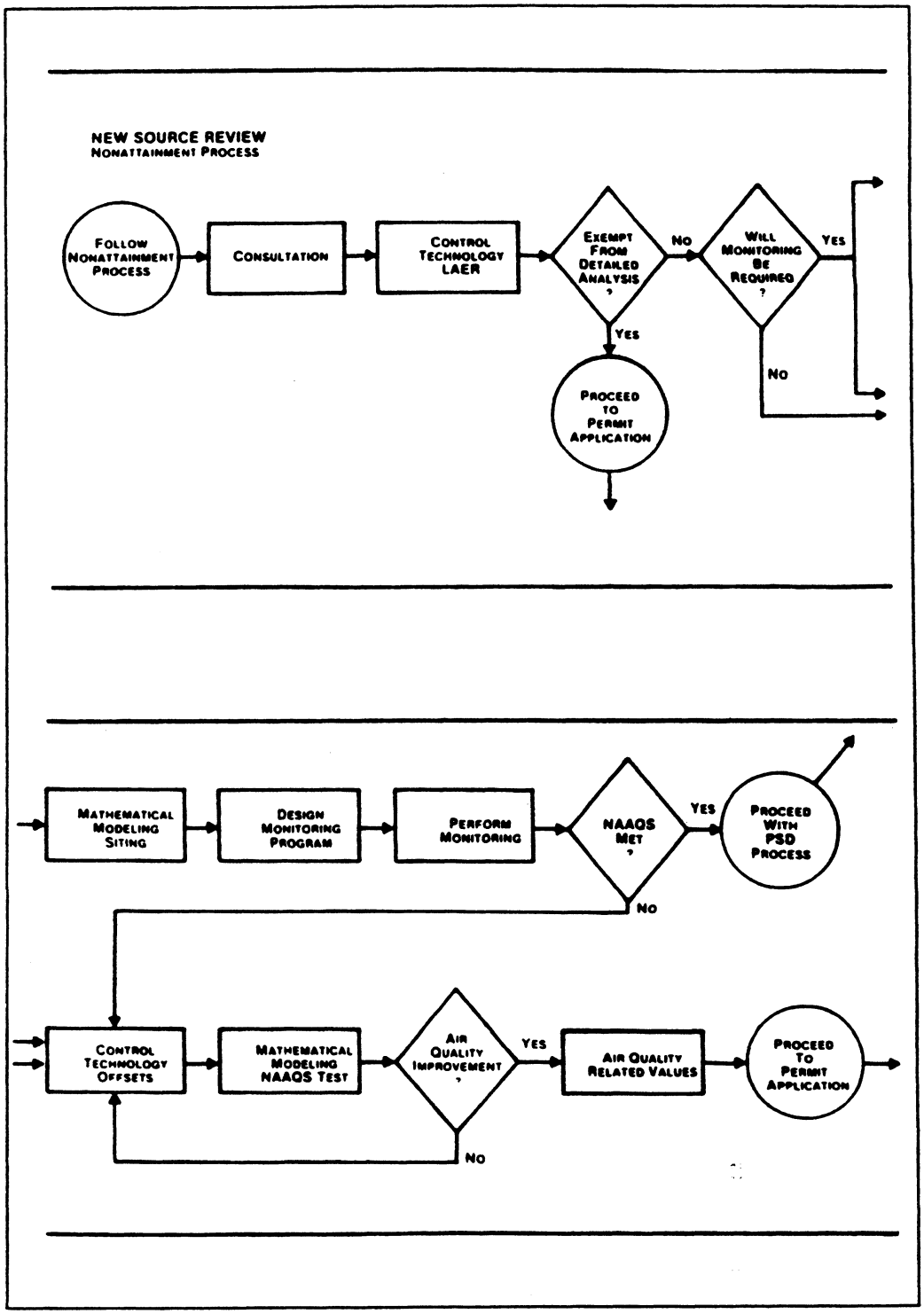

Figure 11–8. New source review (continued)

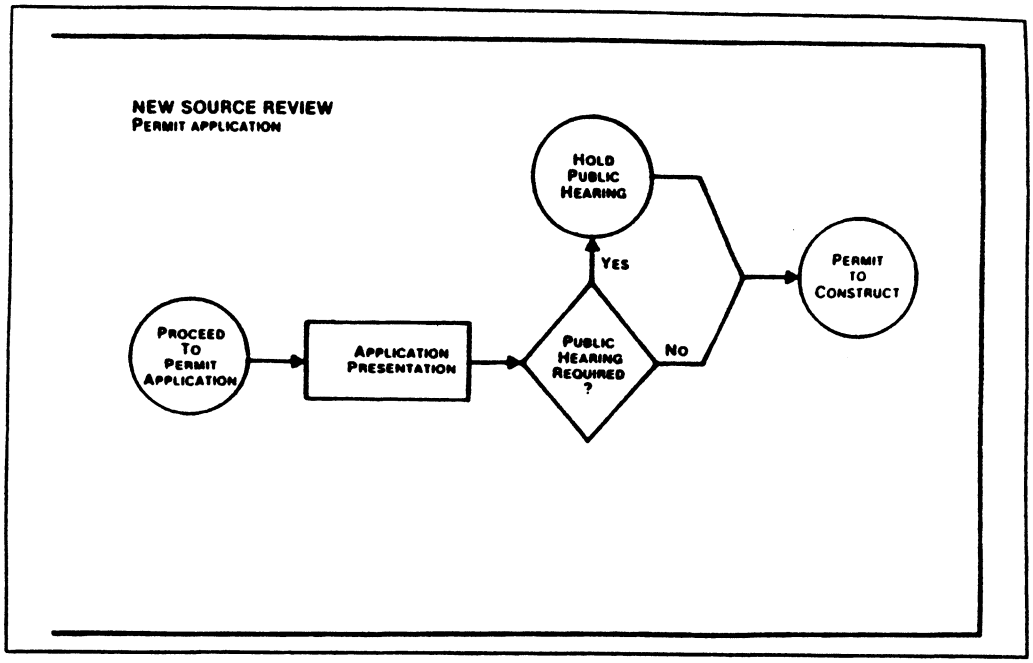

Figure 11–8. New source review (continued)

REFERENCES

Bornstein, R.D., and E. Runca (1977): Preliminary investigations of SO_2 patterns in Venice, Italy using linked PBL and K-models, including removal processes. Paper presented at the AMS joint converence on Applications of Air Pollution Meteorology, Salt Lake City, Utah, November.

Bowers, J.F., J. Bjorklund, and C. Cheney (1979): Industrial source complex (ISC) dispersion model user's guide, Vol. I. U.S. Environmental Protection Agency Document EPA-450/4-79-030, Research Triangle Park, North Carolina.

Briggs, G.A. (1973): Diffusion estimates for small emissions. ATDL Cont. 79, ATDL, NOAA, Oak Ridge, Tennessee.

Briggs, G.A. (1976): Diffusion estimation for small emissions. 1973 Annual Report, USAEC Report ATDL-106, Environmental Research Laboratories, Air Resources Turbulence and Diffusion Division, NOAA, Oak Ridge, Tennessee.

Britter, R.E., J.C. Hunt, and K.J. Richards (1981): Air flow over a two-dimensional hill: Studies of velocity speed-up, roughness effects and turbulence. *Quarterly J. Roy. Meteor. Soc.*, **107**:91-110.

Budney, L.J. (1977): Guidelines for air quality maintenance planning and analysis, Volume 10 (revised): Procedures for evaluating air quality impact of new stationary sources. U.S. Environmental Protection Agency Report EPA-450/4-77-001, Research Triangle Park, North Carolina.

Carhart, R.A., A.J. Policastro, and S. Ziemer (1982): Evaluation of mathematical models for natural-draft cooling-tower plume dispersion. *Atmos. Environ.*, **16**:67-83.

Dabberdt, W.F. (1986): Overwater atmospheric diffusion: Measurements and parameterization. *J. Climate and Appl. Meteor.*, **25**:1160-1171.

Dieterle, D.A., and A.G. Tingle (1979): A numerical study of mesoscale transport of air pollutants in sea-breeze circulations. Paper presented at the Fourth AMS Symposium on Turbulence, Diffusion and Air Pollution, Reno, Nevada, January.

Dobosy, R. (1977): Dispersion of atmospheric of atmospheric pollutants in flow over the shoreline of a large body of water. *J. Appl. Meteor.*, **18**:117-132.

Draxler, R.R. (1976): Determination of atmospheric diffusion parameters. *Atmos. Environ.*, **10**:99-105.

Egan, B.A. (1984): Transport and diffusion in complex terrain (review). *Boundary-Layer Meteor.*, **30**:3-28.

Egan, B.A., and F.A. Schiermeier (1986): Dispersion in complex terrain: A summary of the AMS Workshop held in Keystone, Colorado, 17-20 May 1983. *Bull. Amer. Meteor. Soc.*, **67**:1240-1247.

Eidsvik, K.J. (1980): A model for heavy gas dispersion in the atmosphere. *Atmos. Environ.*, **14**:769-777.

Environmental Research and Technology, Inc. (1985): *ERT Handbook: Requirements for industrial facilities under the Clean Air Act: Dispersion modeling of toxic materials*. Acton, Massachusetts.

Ermak, D.L., S.T. Chan, D.L. Morgan, and L.K. Morris (1981): A comparison of dense gas dispersion model simulations with Burro series LNG spill test results. Paper UCRL-86713, preprint *J. Hazardous Materials*, Lawrence Livermore National Laboratory, Livermore, California.

Fay, J.A., and S.G. Zemba (1985): Dispersion of initially compact dense gas clouds. *Atmos. Environ.*, **19**:1257–1261.

Fay, J.A., and S.G. Zemba (1986): Integral model of dense gas plume dispersion. *Atmos. Environ.*, **20**:1347–1354.

Fryer, L.S., and G.D. Kaiser (1979): DENZ — A computer program for the calculation of the dispersion of dense toxic or explosive gases in the atmosphere. SRD R 152 UKAEA, Culcheth, UK.

Golder, D. (1972): Relations among stability parameters in the surface layer. *Boundary-Layer Meteor.*, **3**:47–58.

Hanna, S.R. (1981): Atmospheric effects of energy production. In *Atmospheric Science and Power Production*, edited by Darryl Randerson. U.S. Department of Energy Report DOE/TIC-27601.

Hanna, S.R., G.A. Briggs, R.P Hosker, Jr. (1982): *Handbook on Atmospheric Diffusion*. U.S. Department of Energy Document DOE/TIC-11223 (DE82002045).

Hanna, S.R. (1983): Lateral turbulence intensity and plume meandering during stable conditions. *J. Climatol. Appl. Meteor.*, **22**:1424.

Hanna, S.R., B.A. Egan, C.J. Vaudo, and A.J. Currei (1984): A complex terrain dispersion model for regulatory applications at the Westvaco Luke Mill. *Atmos. Environ.*, **18**:685–699.

Hanna, S.R., L.L. Schulman, R.J. Paine, J.E. Pleim, and M. Baer (1985): Development and evaluation of the offshore and coastal dispersion model. *JAPCA*, **35**:1039–1047.

Hanna, S.R., and P.J. Drivas (1987): *Guidelines for Use of Vapor Cloud Dispersion Models*, New York: Center for Chemical Process Safety, American Society of Chemical Engineers.

Hartwig, S., Ed. (1980): *Heavy Gas and Risk Assessment*. Dordrecht, Holland: Reidel.

Havens, J.A. (1985): The atmospheric dispersion of heavy gases: An update. *Proceedings*, Assessment and Control of Major Hazards, Institution of Chemical Engineers Symposium Series No. 93.

Huber, A.H., and W.H. Snyder (1976): Building wake effects on short stack effluents. Preprint volume for the Third AMS Symposium on Atmospheric Diffusion and Air Quality, Boston, Massachusetts.

Huber, A.H. (1977): Incorporating building/terrain wake effects on stack effluents. Preprint volume for the AMS Joint Conference on Applications of Air Pollution Meteorology, Boston, Massachusetts.

Hunt, J.C., J.S. Puttock, and W.H. Snyder (1979): Turbulent diffusion from a point source in stratified and neutral flows around a three-dimensional hill, Part I. Diffusion equation analysis. *Atmos. Environ.*, 13:1227–1239.

Hunt, J.C.R., D.P. Lalas, and D.N. Asimakopoulos (1984): Air flow and dispersion in rough terrain: A report on Euromech 173. *J. Fluid Mech.*, 142:201–216.

Irwin, J.S. (1979): Scheme for estimating dispersion as a function of release height. U.S. Environmental Polution Agency Document EPA-600/4-79-062, Research Triangle Park, North Carolina.

Jenkins, G.J., P.J. Mason, W.H. Moores, and R.I. Sykes (1981): Measurements of the flow structure around Ailsa Craig, a steep, three-dimensional, isolated hill. *Quarterly J. Roy. Meteor. Soc.*, 107:833–851.

Kaleel, R.J., D.L. Shearer, and B.L. MacRae (1983): Atmospheric transport and diffusion mechanisms in coastal circulation systems. U.S. Nuclear Regulatory Commission Document NUREG/CR-3250, Washington, D.C.

Koopman, R.P., D.L. Ermak, and S.T. Chan (1989): A review of recent field tests and mathematical modeling of atmospheric dispersion of large spills of denser-than-air gases. *Atmos. Environ.*, 4:731–745.

Krogstad, P.A. and O. Jacobsen (1989): Dispersion of heavy gases. *Encyclopedia of Environmental Control Technology, Vol. 2, Air Pollution Control*, edited by P.N. Cheremisinoff. Houston, Texas: Gulf Publishing Co.

Lavery, T.F., A. Bass, B. Greene, R.V. Hatcher, A. Venkatram, and B.A. Egan (1982): The cinder cone butte dispersion experiments. *Preprints*, Third AMS Joint Conference in Applications of Air Pollution Meteorology, Boston, Massachusetts.

Lyons, W.A., and H.S. Cole (1973): Fumigation and plume trapping on the shores of Lake Michigan during stable onshore flow. *J. Appl. Meteor.*, 12:494–510.

Lyons, W.A. (1975): Turbulent diffusion and pollutant transport in shoreline environments. In *Lectures on Air Pollution and Environmental Impact Analysis*, edited by D. Haugen. Boston: American Meteorological Society.

Lyons, W.A., E.R. Sawdey, J.A. Schuh, R.H. Calby, and C.S. Keen (1981): An updated and expanded coastal fumigation model. *Proceedings*, 74th Annual APCA Meeting. Philadelphia, Pennsylvania.

Lyons, W.A., C.S. Keen, and J.A. Schuh (1983): Modeling mesoscale diffusion and transport processes for releases within coastal zones during land/sea breezes. U.S. Nuclear Regulatory Commission Document NUREG/CR-3542. University of Minnesota, Dept. of Mechanical Engineering.

Lyons, W.A., J.A. Schuh, D.A. Moon, R.A. Pielke, W. Cotton, and R.W. Arritt (1987): Short range forecasting of sea breeze generated thunderstorms at the Kennedy Space Center: A real-time experiment using a primitive equation mesoscale numerical model. *Proceedings*, American Meteorological Society Symposium on Mesoscale Analysis and Forecasting. Vancouver, Canada.

Lyons, W.A., R.A. Pielke, D.A. Moon, J.A. Schuh, and C.S. Keen (1988): Dispersion of toxic gases in complex sea/land breezes: A new technique using a mesoscale numerical model and a Lagrangian particle model. *Proceedings*, JANNAF Environmental Protection Subcommittee, U.S. Naval Postgraduate School. Monterey, California.

McNaughton, D.J., and C.M. Berkowitz (1980): Overview of U.S. research activities in the dispersion of dense gases. In *Heavy Gas and Risk Assessment*, edited by S. Hartwig, Dordrecht, Holland: Reidel, pp. 15–54.

Mason, P.J., and R.I. Sykes (1979): Flow over an isolated hill of moderate slope. *Quarterly J. Roy. Meteor. Soc.*, **105**:383–395.

Moran, M.D., R.W. Arritt, M. Segal, and R.A. Pielke (1986): Modification of regional-scale pollutant dispersion by terrain-forced mesoscale circulations. *Proceedings*, 2nd Int'l. Conf. on Meteorology of Acidic Deposition. Albany, New York.

Nazaroff, W.M., and G.R. Cass (1986): *Environ. Sci. Technol.*, **20**:924–934.

Nazaroff, W.M., and G.R. Cass (1989): Mathematical modeling of indoor aerosol dynamics. *Environ. Sci. Technol.*, **23**:157–166.

Pasquill, F. (1976): Atmospheric dispersion parameters in Gaussian plume modeling, Part II. Possible requirements for change in the Turner workbook values. U.S. Environmental Polution Agency Report EPA-600/4-760306, Research Triangle Park, North Carolina.

Pielke, R.A., R.T. McNider, M. Segal, and Y. Mahrer (1983): The use of a mesoscale numerical model for evaluations of pollutant transport and diffusion in coastal regions and over regular terrain. *J. Climate and Appl. Meteor.*, **64**:243–249.

Pielke, R.A., M. Segal, and R. W. Arritt (1988): Numerical modeling of the effect of local source emissions on air quality in and around Shenandoah National Park. Prepared for the National Park Service, Dept. of the Interior, NPS Grant No. NA81RAH00001, Amendment 17, Item 15.

Runca, E., P. Melli, and P. Zannetti (1976): Computation of long-term average SO_2 concentration in the Venetian area. *Appl. Math. Modeling*, 1:9–15.

Ryan, W., and B. Lamb (1984): Determination of dividing streamline heights and Froude numbers for predicting plume transport in complex terrain. *JAPCA*, **31**:152–155.

Sacre, C. (1979): An experimental study of the airflow over a hill in the atmospheric boundary layer. *Boundary-Layer Meteor.*, **17**:381–401.

Schatzmann, M., and A.J. Policastro (1984): An advanced integral model for cooling tower plume dispersion. *Atmos. Environ.*, **18**:663–674.

Segal, M., R.A. Pielke, R.W. Arritt, M.D. Moran, C.H. Yu, and D. Henderson (1988): Application of a mesoscale atmospheric dispersion modeling system to the estimation of SO_2 concentrations from major elevated sources in Southern Florida. *Atmos. Environ.*, **22**:1319–1334.

Shulman, L.L., and S.R. Hanna (1986): Evaluation of downwash modifications to the industrial source complex model. *JAPCA*, **36**:258–264.

Skupniewicz, C.E., and G.E. Schacher (1986): Parameterization of plume dispersion over water. *Atmos. Environ.*, **20**:1333–1340.

Snyder, W.H. (1985): Fluid modeling of pollutant transport and diffusion in stably stratified flows over complex terrain. *Ann. Rev. Fluid Mech.*, **17**:239–266.

Starheim, F.J., and M.E. Knudsen (1987): Atmospheric downwash: A comparative study. *Proceedings*, APCA specialty conference on Dispersion Modeling from Complex Sources, April.

Stern, A.C. (1976): *Air Pollution*, Third Edition, Volume 1. New York: Academic Press.

Stern, A.C. (1977): Prevention of significant deterioration -- A critical review. *JAPCA*, **27**:440.

Stern, A.C. (1982): History of air pollution legislation in the United States. *JAPCA*, **32**:44.

Stern, A.C., R.W. Boubel, D.B. Turner, and D.L. Fox (1984): *Fundamentals of Air Pollution*, Second Edition, Orlando, Florida: Academic Press.

Stunder, M., and S. SethuRaman (1985): A comparative evaluation of the coastal internal boundary-layer height equations. *Boundary-Layer Meteor.*, **32**:177–204.

Stunder, M., and S. SethuRaman (1986): A statistical evaluation and comparison of coastal point source dispersion models. *Atmos. Environ.*, **20**:301–315.

Sutton, S.B., H. Brandt, and B.R. White (1986): Atmospheric dispersion of a heavier-than-air gas near a two-dimensional obstacle. *Boundary-Layer Meteor.*, **35**:125–153.

Taylor, P.A., and J.L Walmsley (1981): Estimates of wind-speed perturbation in boundary-layer flow over isolated low hills -- A challenge. *Boundary-Layer Meteor.*, **20**:253–257.

Turner, D.B. (1970): *Workbook of Atmospheric Dispersion Estimates*, U.S. Public Health Service Publication.

U.S. Environmental Protection Agency (1984): Guidelines on air quality models. Draft report EPA-450/2-78-027, Research Triangle Park, North Carolina.

U.S. Environmental Protection Agency (1988): Environmental progress and challenges: EPA's update. Document EPA-230-07-88-033, Office of Policy Planning and Evaluation, Washington, D.C.

van der Hoven, I. (1968): Deposition of particles and gases. In *Meteorology and Atomic Energy 1968*, edited by D. Slade, U.S. Atomic Energy Commission NTIS Report TID-24190, Oak Ridge, Tennessee.

van Dop, H., R. Steenkist, and F.T. Nieuwstadt (1979): Revised estimates for continuous shoreline fumigation. *J. Appl. Meteor.*, **18**:133–137.

Venkatram, A., and J.C. Wyngaard, Eds. (1988): *Lectures on Air Pollution Modeling*, Boston, Massachusetts: American Meteorological Society.

Weisman, B. (1976): On the criteria for the occurrence of fumigation inland from a large lake – A reply. *Atmos. Environ.*, **12**:172–173.

Zeman, O. (1982): The dynamics and modeling of heavier-than-air, cold gas releases. *Atmos. Environ.*, **16**:741–751.

12 STATISTICAL METHODS

Statistical methods are frequently used in air pollution studies. Several types of statistical models, methods and analyses will be discussed in this chapter.

The fundamental aspects of atmospheric diffusion are based on statistical theories (Taylor, 1921), as confirmed by the recent, promising development of Lagrangian Monte–Carlo techniques for pollutant dispersion simulations. These methods have been discussed in Chapter 8. Moreover, the newly developed theories of chaos (Berge et al., 1984; Grebogi et al., 1987), also based on stochastic methods, seem promising for the treatment of turbulence in fluid flows. These statistical aspects of chaos theory will not, however, be discussed further here.

In this chapter, we will address the following topics: 1) frequency distribution of air quality measurements and the characterization of extreme values, a subject that is important for regulatory purposes; 2) time series analysis, in the time and the frequency domain; 3) the joint application of deterministic and statistical techniques (e.g., by using Kalman filters); 4) receptor modeling techniques; 5) the statistical methodologies that can be used to evaluate the performance of air quality dispersion models; 6) interpolation and graphic techniques, such as Kriging, pattern recognition, cluster analysis, and fractal analysis; and 7) optimization methods.

A general distinction between statistical and deterministic approaches is that air pollution deterministic models initiate their calculations at the pollution sources and aim at the establishment of cause–effect relationships, while statistical models are characterized by their direct use of air quality measurements to infer semiempirical relationships. Statistical models are useful in situations such as real–time short–term forecasting, where the information available from measured concentration trends is generally more relevant than that obtained from deterministic analyses.

The reader can find some general information about basic statistical methods for air pollution data in Gilbert (1987). Statistical analysis with missing data — a problem often encountered in environmental applications — is discussed by Little and Rubin (1987). References and more specific applications are discussed in the sections below.

12.1 FREQUENCY DISTRIBUTION

As noted by Seinfeld (1986), "air pollution concentrations are inherent random variables because of their dependence on the fluctuations of meteorolo cal and emission variables." A random variable is characterized by two ma factors: its probability density function and its autocorrelation structure. Tl probability density function *pdf(c)* gives the probability *pdf(c)dc* that the conce tration c, of a certain species at a particular location during a certain time perio is between c and $c+dc$. The autocorrelation function quantifies the "serial" beha ior of the "time series" of concentrations, i.e., the relationship between the co centration value at t, and those at previous times, for a certain species at particular location. Nonstationary phenomena strongly complicate these statis cal characterizations. Often, if not always, concentration measurements posse highly nonstationary features. Under these conditions, both *pdf* and autocorrel tion vary with season and even the hour of the day (Zannetti et al., 1978).

The autocorrelation structure of concentration values plays a key role understanding the variation with time of concentration. For example, high pos tive autocorrelation means that peak concentration values tend to be followed l high values and that clean periods tend to be followed by low pollution periods a behavior that is typically measured in air pollution studies. The evaluation the *pdf*, however, has received more attention in air pollution statistical studi because its determination is useful in regulatory applications based on the co cept of air quality "standards," i.e., ambient concentration values that should n be exceeded. In other words, the knowledge, from direct measurements or oth techniques, of the *pdf* allows the calculation of the exact number of violations (expected violations) of a specified air quality standard, as illustrated in Fi ure 12–1), where the integral of *pdf(c)dc*, from the air quality standard value to infinity, gives the probability of exceedance of c_s.

Therefore, it is important to calculate or estimate the *pdf*. This operatic requires two steps: 1) the evaluation of *the form* of the *pdf* (e.g., a log–norm *pdf*) and 2) the evaluation of the parameters of this chosen form. Several fr quency distribution functions have been proposed and used to fit air quali measurements. Georgopoulos and Seinfeld (1982), Tsukatami and Shigemits (1980), and Marani et al. (1986) discuss and summarize several of them, inclu ing the following distributions:

- Log–normal
- Weibull
- Gamma

- Three-parameter log-normal
- Three-parameter Weibull
- Three-parameter beta
- Four-parameter beta
- Pearson

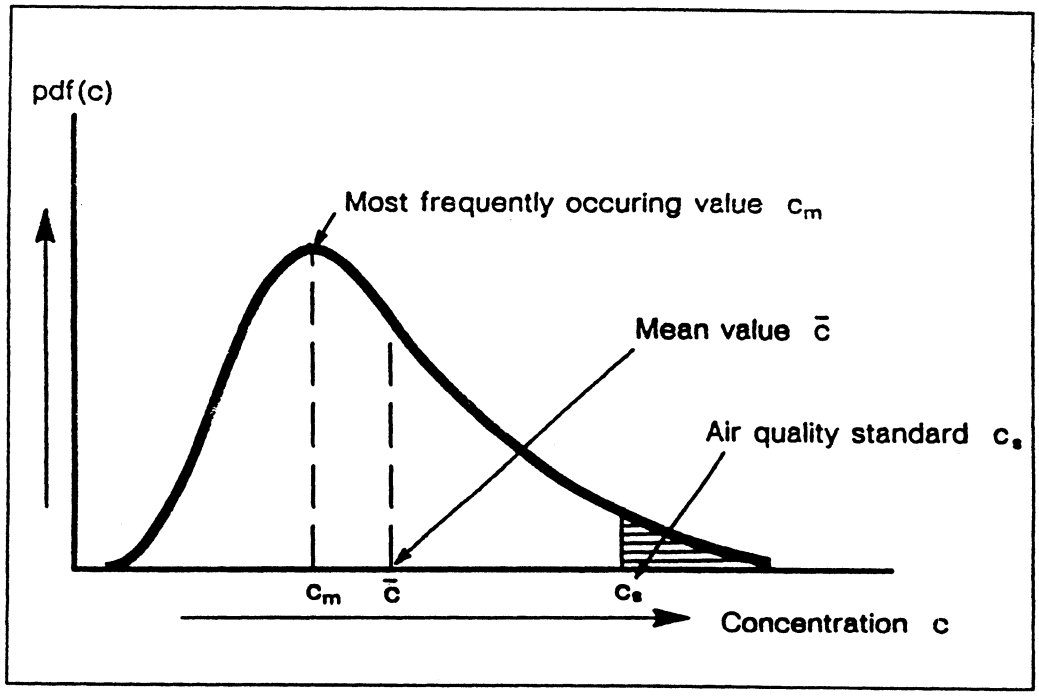

Figure 12–1. Example of application of the pdf to calculate the probability of exceedance of air quality standard c_s.

The most common distribution is the log-normal distribution, which is represented by

$$pdf(c) = \frac{1}{(2\pi)^{1/2}\, c\, \ln \sigma_g} \exp\left[-\frac{(\ln c - \ln \bar{c}_g)}{2 \ln^2 \sigma_g)}\right] \qquad (12\text{–}1)$$

where $\bar{c}_g$ is the geometric mean and σ_g is the geometric standard deviation of c. According to this distribution, the logarithms of the concentrations have a normal (i.e., Gaussian) distribution $N(\ln \bar{c}, \ln \sigma_g)$. Even though heuristic justifications have been provided for explaining the occurrence of log-normal distributions (Cats and Holtslag, 1980; Kahn, 1973), no *a priori* reason seems to exist for preferring one distribution above the others (Seinfeld, 1986).

The log-normal distribution has been studied by several authors, including Larsen (1971), whose pioneering work identified the following relations, sometimes referred to as Larsen's laws:

1. Pollutant concentrations are lognormally distributed for all averaging times

2. Median concentrations (50th percentile) are proportional to the averaging time raised to an exponent

3. Maximum concentrations are approximately inversely proportional to the averaging time raised to an exponent

An example of SO_2 concentration measurements mostly in agreement with the above laws is presented in Figure 12-2. Other data sets, however, may show less agreement (especially secondary pollutants, such as NO_2 and O_3).

Frequency distributions are mostly used to assess the probability of occurrence of *high* concentration values (e.g., exceedances). Therefore, it is most important that these distributions be accurate at their right tail than elsewhere. It is well known, however, that statistics of extreme values are the most affected by uncertainties, even though *ad hoc* methods have been proposed to handle extreme values (e.g., Roberts, 1979; Williams, 1984; Drufuca and Giuliano, 1978; Horowitz and Barakat, 1979; Chock and Sluchak, 1986; and Surman et al., 1987). It is unfortunate, from a statistical point of view, that U.S. air quality standards were chosen as values that can be exceeded only once a year. This choice has put the standards at the very end of the frequency distribution tail, where little confidence can be given to either measurements or theoretical estimates. Alternative choices of standards, i.e., the 95th percentile, would have been more "stable" and less questionable. Some countries are moving toward this alternative. For example, Italy introduced, in 1983, new SO_2 standards based on the 50th and 98th percentiles of the SO_2 daily average concentrations, instead of the previous 30-minute and daily not-to-be-exceeded standards.

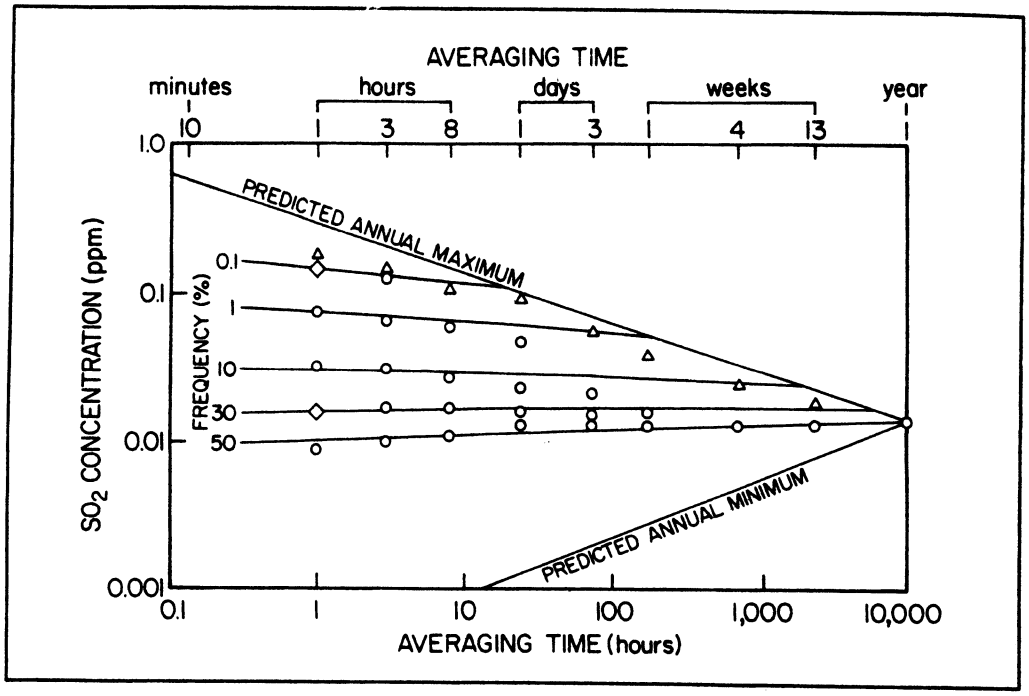

Figure 12–2. Sulfur dioxide concentration versus averaging time and frequency for 1980 at the United States National Aerometric Data Bank (NADB) Site 264280007 HO1, 8227 S. Broadway, St. Louis, Missouri. Source: Chart courtesy of Dr. Ralph Larsen, United States Environmental Protection Agency, Research Triangle Park, North Carolina (from Stern et. al., 1984). [Reprinted with permission from Academic Press.]

12.2 TIME SERIES ANALYSIS

Time series analysis methods aim at the analysis of data arranged in a time sequence, either in the time domain (e.g., Box–Jenkins methods) or in the frequency domain (e.g., spectral analysis). They include the following methods:

- Box–Jenkins approach
- Spectral analysis
- Regression analysis
- Trend analysis
- Principal components analysis

These statistical modeling approaches can be used in a "black box" mode when, for example, time series of concentrations are analyzed without any other

information, just to evaluate their intrinsic variations and without attempting any physical explanation. Or, they can be used in a "gray box" mode, in which other parameters, for example meteorological and emission terms, are included, in an effort to incorporate, within a statistical frame, deterministic relations.

These methods can be used either in a "batch" or a "real-time" mode. Batch simulations perform statistical analyses of past measurements, in an effort to establish empirical relationships. Real-time applications (e.g., Bacci et al., 1981; Finzi and Tebaldi, 1982) require the availability of on-line data and provide forecasts that can be used by decision-makers for real-time intervention strategies, in a effort to mitigate possible incoming concentration episodes.

The Box-Jenkins methodology (Box and Jenkins, 1970; new edition, 1976) is considered the most cost-effective approach for time-series analysis and has been frequently applied to evaluate meteorological and air quality measurement patterns. This theory has been described and summarized in several books and articles and will not be discussed here. The general form of the Box-Jenkins equation to describe a time series is

$$\phi_p(B)\ \Phi_P(B^s)\ \nabla^d\ \nabla_s^D\ z_t\ =\ \theta_q(B)\ \Theta_Q(B^s)\ a_t \qquad (12\text{-}2)$$

where ϕ_p is the autoregressive operation of order p, Φ_p is the seasonal autoregressive operation of order P with seasonality s, B is the backward operator, ∇ is the difference operator, ∇_s is the seasonal difference operator, z_t is the time series, θ_q is the moving average operator of order q, Θ_Q is the seasonal moving average operator of order Q and a_t is a Gaussian white noise. In general, however, simple forms of Equation 12-2 (with only three to four terms) are sufficient to well characterize z_t. Figure 12-3 shows an example of Box-Jenkins forecasting.

Important simulations and results, using the Box-Jenkins theory, have been provided by Chock et al. (1975); by Simpson and Layton (1983) for the forecasting of ozone peaks; by Tiao el al., (1975), who modified the Box-Jenkins approach for treating the effects of intervention strategies during the period in which the time series has been collected; by Roy and Pellerin (1982) for the evaluation of long-term trends and intervention analysis; by Zinsmeister and Redman (1980) for aerosol data; and by Murray and Farber (1982) for evaluating and historical visibility data base.

Spectral analysis techniques (Jenkins and Watts, 1968) allow the identification of cycles in meteorological and air quality time-series measurements. In particular, two studies (Tilley and McBean, 1973; Trivikrama et al., 1976) first

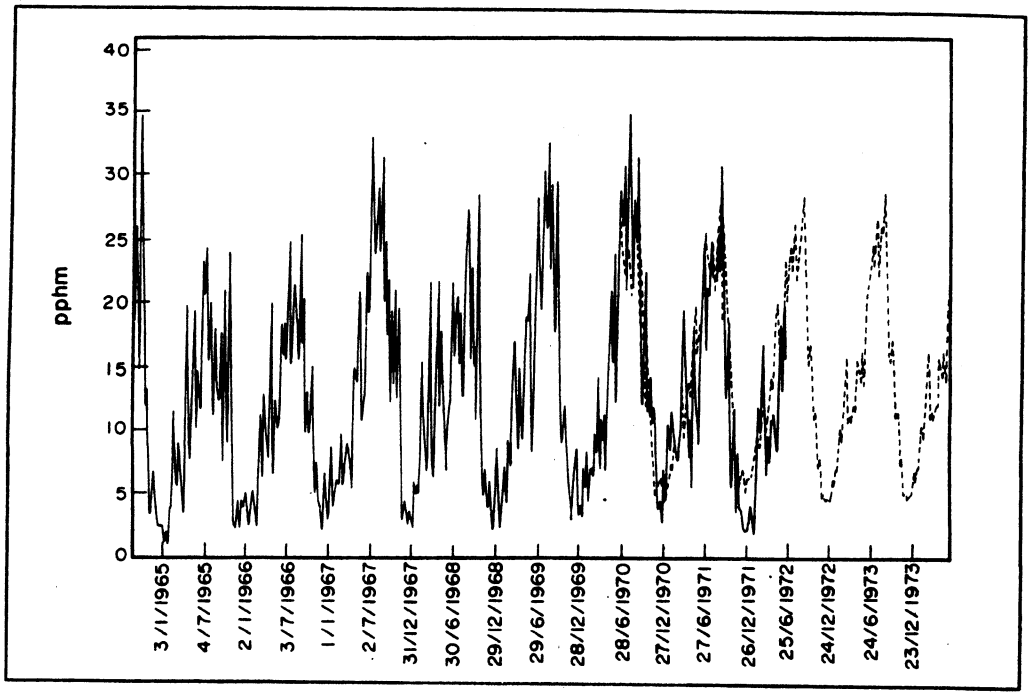

Figure 12–3. Univariate time series analysis of oxidant concentrations. The solid line indicates actual data and the dashed line forecasted data (from Chock et al., 1975). [Reprinted with permission from Pergamon Press.]

showed the existence of the following main oscillations of SO_2 and wind speed data: semidiurnal, diurnal, and three- to three-and-a-half-day period. Semidiurnal cycles have been ascribed to local phenomena (like the sea breeze), while the longest period seems to be caused by synoptic weather variations, which have a period close to three-and-a-half days in the study area (northeastern United States). Figure 12–4 shows an example of spectral analysis of SO_2, wind speed, temperature and pressure .

Regression analyses are a particular type of multiple time-series analysis, in which, for example, meteorological measurements are statistically related to air quality concentrations. Examples of multiple linear regression studies are presented in Figure 12–5, where visibility reduction is interpreted as a function of pollutant concentrations and meteorological conditions, and Figure 12–6, where oxidant concentrations are predicted as a multiple linear regression of the logarithm of the solar radiation intensity, wind speed and dry bulb temperature.

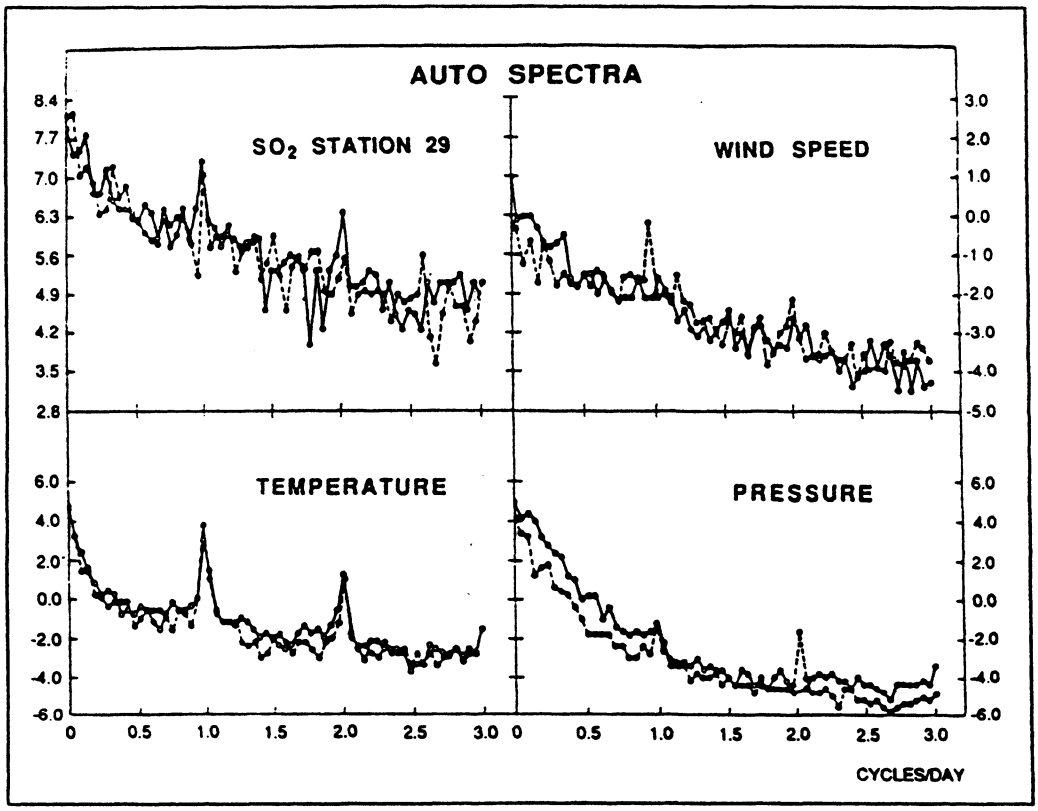

Figure 12–4. Logarithm of the power autospectra of SO_2 and meteorological hourly data (wind speed, temperature and pressure) during a six-month summer period (dots) and a six-month winter period (circles) (from Zannetti, et al., 1978a). [Reprinted with permission from Pergamon Press.]

Trend and seasonal variations are also assessed by multiple regression models, e.g., as performed by Buishand et al. (1988). Principal components have also been used to calculate pollutant distributions and predictions (Petersen, 1970; Henry and Hidy, 1979; Lin, 1982).

Time series methods can be applied in two modes: a "fitting" mode and a "forecasting" mode. In the forecasting mode, the model parameters (e.g., the regression coefficients) are estimated from one set of measurements and, subsequently, the time series model is applied, with these estimated parameters, to another set of measurements to calculate the forecasting performance. In the fitting mode, the same set of measurements is used for both parameter estimation and model performance evaluation. Clearly, only the forecasting mode

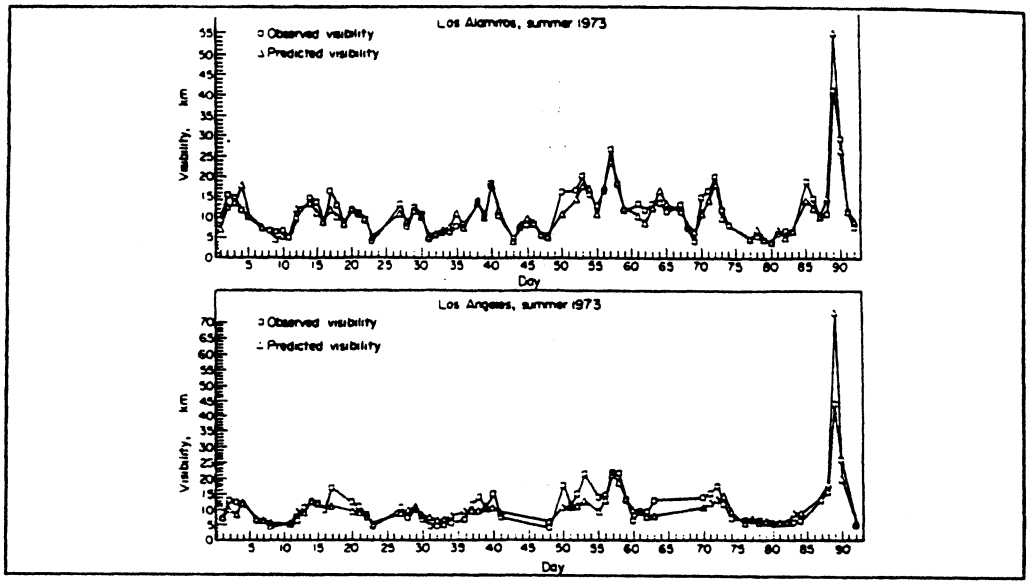

Figure 12–5. *Observed and predicted values for visibility (visual range in km) at Los Alamitos and Los Angeles, Summer 1973 (from Barone et al., 1978). [Reprinted with permission from Pergamon Press.]*

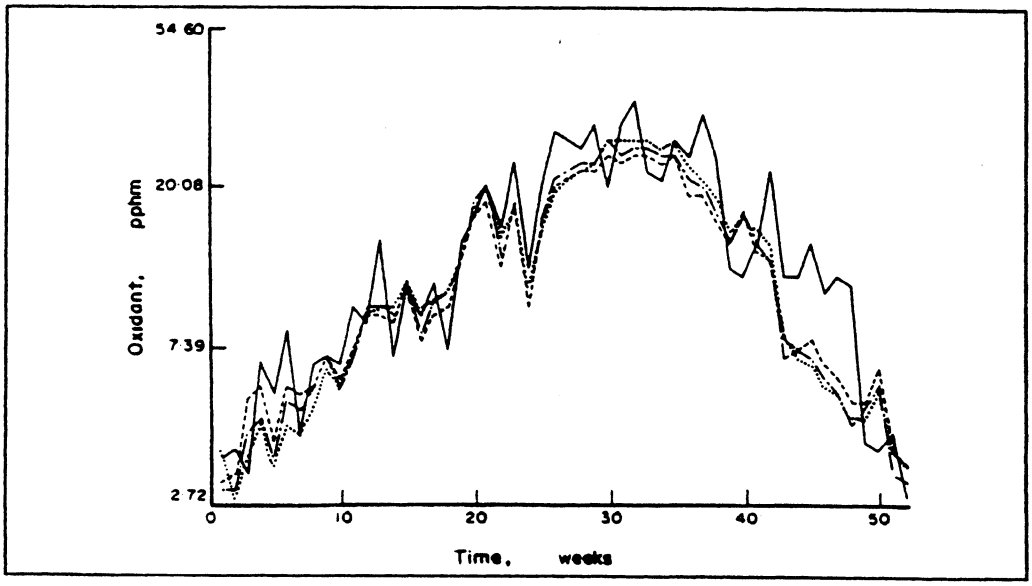

Figure 12–6. *Predicted and actual oxidant levels (in log scale) for 1970. —— actual values; —— Aitken's model; –•–•– OLS model; ••••• lagged model (long term prediction) (from Chock et al., 1975). [Reprinted with permission from Pergamon Press.]*

provides an unambiguous evaluation of model performance, while the fitting mode overestimates the model's forecasting ability.

A useful combination of fitting and forecasting can be obtained by applying time series models in an "adaptive" mode, in which, at each time t, the model parameters are re-estimated using the measurements of a "learning" period of duration T (i.e., from $t-T$ to t). In this way, if the duration T is appropriate, the model's performance can be maximized. Figure 12–7 shows an example of the adaptive technique using two simple models (AR(1) and AR(1)CS). Note that both models have an optimum T which gives a forecasting performance that exceeds even that of the fitting model.

12.3 MIXED DETERMINISTIC STATISTICAL MODELS (KALMAN FILTERS)

Semiempirical methods and real-time filters, especially the Kalman filters, have been frequently used for updating the forecasting capabilities of a predictor (generally a *deterministic* predictor) based upon the availability of real-time measurements of the system variables. (A common application of the Kalman filter is in navigation space guidance and orbit determination, where computations are dynamically changed according to real-time measurements of the flying object's position and velocity.) The Kalman filter technique and its application to air pollution problems are discussed below.

12.3.1 Introduction to Kalman Filters

The principle of least squares estimation originated at the beginning of the 19th century, but only a century and a half later, starting with the pioneering work of Wiener (1949), a substantial innovation allowed its "recursive" application, as explained below.

Let us consider, following the discussion by Young (1974), the linear regression problem

$$y = \mathbf{x}^T \mathbf{a} \tag{12–3}$$

in which a variable y is related to n other linearly independent variables $\mathbf{x} = [x_1, x_2, \ldots, x_n]^T$, through the unknown coefficients $\mathbf{a} = [a_1, a_2, \ldots, a_n]^T$. Then, if we have k observations of y and $\mathbf{x}$, we can obtain an estimate $\mathbf{a}'_k$ of $\mathbf{a}$ by using the least squares method, as follows

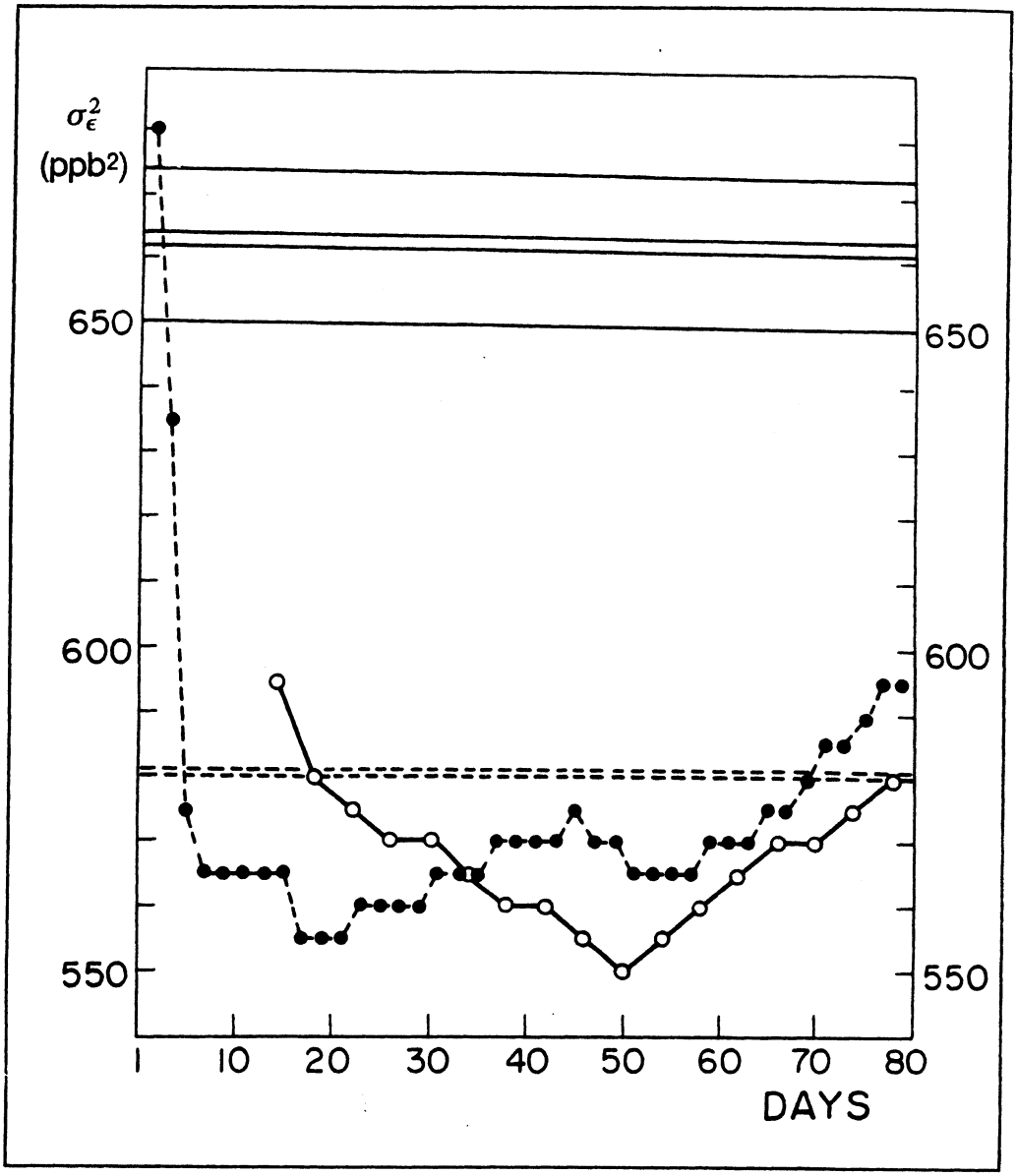

Figure 12–7. *Values of σ_ϵ^2, the forecasting error variance, for the AR(1) (dots) and AR(1)CS (circles) adaptive models applied to hourly SO_2 data (one–year analysis). The error variance is plotted against the length T of the learning period. The horizontal lines show comparable σ_ϵ^2 values of nonadaptive models for fitting (dashed lines) and forecasting (solid lines) cases. (Forecasting was obtained by using the parameters estimated during the same season one year before) (from Zannetti, 1978). [Reprinted with permission from the Air Pollution Control Association.]*

$$\mathbf{a}'_k = \left[\sum_{i=1}^{k} \mathbf{x}_i \mathbf{x}_i^T\right]^{-1} \sum_{i=1}^{k} \mathbf{x}_i y_i \qquad (12\text{–}4)$$

But if the number k is increasing, i.e., if new observations of y and $\mathbf{x}$ are progressively gathered, the updating of the estimate $\mathbf{a}'_k$ requires a repeated application of Equation 12–4. To avoid this expensive calculation, Plackett (1950) rewrote Equation 12–4 in a "recursive" form in which $\mathbf{a}'_k$ is a linear sum of the estimate obtained after k–1 observations (i.e., $\mathbf{a}'_{k-1}$), plus a correction term based on the newly–received information y_k and $\mathbf{x}_k$. This recursive form provides results mathematically identical to Equation 12–4.

The next step was provided by Kalman (1960), who expanded the work of Wiener (1949) and solved the general problem of estimating a set of parameters $\mathbf{a}_k$ in which:

- $\mathbf{a}_k$ represents, in a more general form, the "state" of a dynamic system
- parametric invariance (i.e., $\mathbf{a}_k = \mathbf{a}_{k-1}$, for all k) is not assumed any more
- the parameters $\mathbf{a}_k$ vary according to the general stochastic evolution scheme ("state equation" or "message model")

$$\mathbf{a}_k = \mathbf{F}(k, k-1)\mathbf{a}_{k-1} + \mathbf{G}(k, k-1)\mathbf{w}_k \qquad (12\text{–}5)$$

  where $\mathbf{F}(k, k\text{–}1)$ is an $n \times n$ transition matrix, $\mathbf{G}(k, k\text{–}1)$ is an $n \times m$ input matrix, and $\mathbf{w}_k$ is an $m \times 1$ vector of independent random variables with zero mean and covariance matrix $\mathbf{Q}$.

- "noisy" measurements $\mathbf{y}_k = [y_1, y_2, \ldots, y_p]_k^T$ are available that are linearly related to $\mathbf{a}_k$ by the "observation equation" or "observation model"

$$\mathbf{y}_k = \mathbf{H}_k \mathbf{a}_k + \mathbf{v}_k \qquad (12\text{–}6)$$

  where $\mathbf{H}_k$ is a $p \times n$ coefficient matrix and $\mathbf{v}_k$ is the measurement error assumed to be a $p \times 1$ vector of independent random variables with zero mean and covariance matrix $\mathbf{R}$

Then, the equations of the Kalman filtering method allow a recursive computation of

- the estimates $\mathbf{a}'_{k+j}$ (j = 1, 2, ...) of $\mathbf{a}_{k+j}$ by considering only the effect of the most recent observation $\mathbf{y}_k$ instead of resolving at

each time the entire problem by the classical least squares regression technique

- the estimate of the covariance matrix of the forecasting error $\mathbf{a}_{k+j} - \mathbf{a}'_{k+j}$ and, therefore, an important indication of the accuracy of the estimates $\mathbf{a}'_{k+j}$ and information on their convergence

In the Kalman filter outlined above, the state vector $\mathbf{a}_k$ can be any numerical description of the state of a dynamic system, e.g., the location of a space ship, concentrations of pollutants in the atmosphere, or a velocity field representing groundwater dynamics. Then, the transition matrix $\mathbf{F}$ contains our (imperfect) deterministic representation of the phenomenon (e.g., a set of physical equations reduced into a linear matrix form(*)), and $\mathbf{y}_k$ are the limited measurements available. Then the Kalman filter, as outlined below, provides a method for forecasting the evolution of $\mathbf{a}_k$, which takes into account both the "deterministic" component $\mathbf{F}$ (predictor) and the continuous, on-line information (corrector) provided by the measurements $\mathbf{y}_k$.

Starting from Equations 12-5 and 12-6, it is possible to develop (Jazwinski, 1970; Sage and Melsa, 1971) an unbiased linear minimum-error-variance algorithm (Kalman filter) to estimate the state of a linear time-varying dynamic system driven by white noise of zero mean and known variance. Under the further assumptions that $\mathbf{v}$, $\mathbf{w}$, and $\mathbf{a}$ are mutually uncorrelated, the relevant formulae, where $\mathbf{a}(t_2|t_1)$ is the estimate at time t_1 of $\mathbf{a}(t_2)$, are (**)

- predicted state

$$\mathbf{a}(t+1|t) = \mathbf{F}(t+1,t)\,\mathbf{a}(t|t) \tag{12-7}$$

- predicted error covariance matrix

$$\mathbf{V}_{\tilde{\mathbf{a}}}(t+1|t) = \mathbf{F}(t+1,t)\,\mathbf{V}_{\tilde{\mathbf{a}}}(t|t)\,\mathbf{F}^T(t+1,t) + \mathbf{G}(t)\,\mathbf{V}_{\mathbf{w}}(t+1)\,\mathbf{G}^T(t) \tag{12-8}$$

- filter gain matrix

$$\begin{aligned}\mathbf{K}(t+1) = {} & \mathbf{V}_{\tilde{\mathbf{a}}}(t+1|t)\,\mathbf{H}^T(t+1) \\ & [\mathbf{H}(t+1)\,\mathbf{V}_{\tilde{\mathbf{a}}}(t+1|t)\,\mathbf{H}^T(t+1) + \mathbf{V}_{\mathbf{v}}(t+1)]^{-1}\end{aligned} \tag{12-9}$$

(*) Nonlinear Kalman filters are also available, but will not be discussed here.

(**) In the formulae below, time is explicitly indicated by t, instead of using the subscript k as in the notation of the previous equations.

- filtered state after processing the observation $\mathbf{y}(t+1)$

$$\mathbf{a}(t+1|t+1) = \mathbf{a}(t+1|t) + \mathbf{K}(t+1)\,[\mathbf{y}(t+1) - \mathbf{H}(t+1)\,\mathbf{a}(t+1|t)] \quad (12\text{–}10)$$

- new error covariance matrix

$$\mathbf{V}_{\tilde{\mathbf{a}}}(t+1|t+1) = [\mathbf{I} - \mathbf{K}(t+1)\,\mathbf{H}(t+1)]\,\mathbf{V}_{\tilde{\mathbf{a}}}(t+1|t) \quad (12\text{–}11)$$

where $\mathbf{V}_{\tilde{\mathbf{a}}}(t_2|t_1)$ is the covariance of the error $\tilde{\mathbf{a}} = \mathbf{a}(t_2) - \mathbf{a}(t_2|t_1)$ and $\mathbf{I}$ is the identity matrix. See Zannetti and Switzer (1979a) for a rewriting of the above methodology in a computer-oriented recursive form referred to a forecast performed from 1 to p time steps ahead.

12.3.2 Applications of Kalman Filters to Air Quality Problems

Kalman filters have been used in air pollution problems to obtain more accurate predicted values in episode forecasting and control. This can be done by considering $\mathbf{a}_k = \mathbf{a}(t)$ as the vector of concentrations of a pollutant at the grid points of a grid dispersion model (Bankoff and Hanzevack, 1975; Melli et al., 1981) or at the pollutant monitoring points (Sawaragi et al., 1976) of the study area. The state vector $\mathbf{a}(t)$ might also be extended to include some additional adaptive parameters (Bankoff and Hanzevack, 1975), but we will not discuss this extension here. Then the transition matrix $\mathbf{F}$ becomes either the matrix of the spatial discretization (K-model) of the transport and diffusion equation (Bankoff and Hanzevack, 1975; Melli et al., 1981) (including time-dependent emission and meteorological inputs) or a multiple regression matrix (Sawaragi et al., 1976). Model inaccuracies and emissions and meteorology input errors are included in the system noise process $\mathbf{w}(t)$.

A hybrid (*) air quality application of the Kalman filter was developed by Zannetti and Switzer (1979a) who limited the dimension of the state vector $\mathbf{a}$ to the number of air quality monitoring stations, but incorporated the contribution of the meteorology by having the transition matrix $\mathbf{F}$ depend upon the time-varying meteorological conditions. They evaluated the coefficients of $\mathbf{F}$ in an "adaptive" manner, i.e., using a first-order Markov chain on a learning time period of given fixed length close to the forecasting time (see previous discussion at the end of Section 12.2 for a description of the "adaptive" forecasting technique).

(*) This approach is a hybrid one since the matrix $\mathbf{F}$ is not computed using a set of deterministic equations, but is calculated using statistical methods, in which a different matrix $\mathbf{F}$ is estimated for each meteorological class.

An important problem arises in the application of the Kalman filter to air pollution problems. In fact, it is necessary to avoid the high dimensionality of the resulting Kalman filter equations. For example, when **F** is the time-evolution transition matrix of the *K*-model, a simple spatial grid of 20 × 20 × 10 points produces Kalman filter matrices of dimension 4000 × 4000. Methods have been developed to simplify this problem. In particular, either the Green function can be used to reduce the equation of the *K*-model to a difference equation of relatively small dimension (Hino, 1974), or a discrete form of Chandrasekar-type equations (*) can be applied for the same goal (Desalu et al., 1974). Alternatively, the region can be partitioned into subregions (Bankoff and Hanzevack, 1975; Melli et al., 1981) and, if the subvectors of the subregions are not coupled (or are weakly coupled), the filter algorithm can be applied separately to each of the subvectors, thus reducing the size of the matrices that must be manipulated. Finally, a multiple linear regression model can be used (Sawaragi et al., 1976) for **F**, thus reducing the dimension of the filter to the number of monitoring stations in the area. However, this loses the "physical" information of the diffusion phenomenon.

An example of use of Kalman filters to forecast air pollution episodes is shown in Figure 12-8. Note that the forecasting performance of the method decreases when, instead of using the actual meteorological data, meteorological forecasts are used.

12.4 RECEPTOR MODELS

Receptor models are the dream of the air pollution experimentalist. A dream that, till now, has been only partially fulfilled. The basic concept of the receptor modeling approach is the apportionment of the contribution of each source, or group of sources, to the measured concentrations without reconstructing the dispersion pattern of the pollutants. In other words, while dispersion models compute the contribution of a source to a receptor as the product of the emission rate by a dispersion factor, receptor models start with *observed* ambient aerosol concentrations at a receptor and seek to apportion the observed concentrations among several source types (e.g., industrial, transportation, soil, etc.), based on the known chemical compositions (i.e., the chemical fractions) of source and receptor materials.

(*) This alternative method completely bypasses direct calculation of the covariance matrices, while still retaining the properties of the Kalman filter.

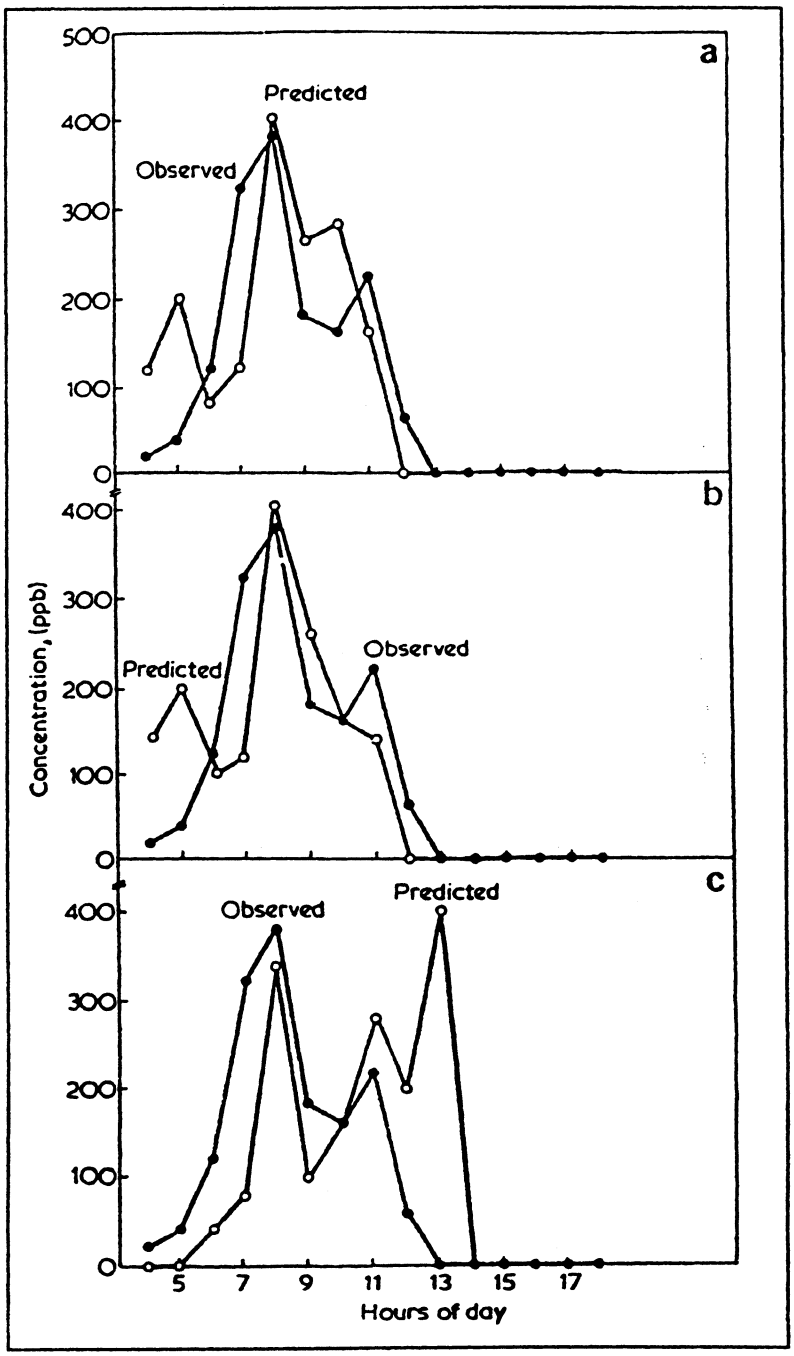

Figure 12–8. *Kalman predictions of a four hour–ahead episode with different meteorological inputs: (a) meteorology is forecast, (b) true meteorological values are used, (c) meteorology is persistent. From Fronza et al. (1979). [Reprinted with permission from Butterworth Scientific.]*

In mathematical notation, the concentration c_{ik} of the species i in the k–th sample at a certain monitoring station can be written as

$$c_{ik} = \sum_{j=1}^{p} a_{ij} D_{jk} E_{jk} \qquad (12\text{–}12)$$

where p sources (or groups of sources) are assumed to contribute to c_{ik}, a_{ij} is the fractional amount of the component i in the emission from the j–th source, D_{jk} is the atmospheric dispersion term and E_{jk} is the emission rate (i.e., $D_{jk} E_{jk} = S_{jk}$ is the total contribution of the source j to the k–th sample in the receptor). Dispersion models assume a_{ij}, D_{jk} and E_{jk} to be known (or obtainable from emission and meteorological data) and estimate the output c_{ik}. For receptor models, the concentrations c_{ik} and source "profiles" a_{ij} are measured instead, and the D_{jk} E_{jk} products are computed as a model result.

Receptor models can be classified into four categories (Henry et al., 1984):

- chemical mass balance (CMB)
- multivariate models
- microscopic models
- source–receptor hybrids

The first two categories are discussed below.

12.4.1 Chemical Mass Balance (CMB)

Chemical mass balance (CMB) models are based on a sample of n chemical properties of both source and receptor, thus giving n equations

$$c_i = \sum_{j=1}^{p} a_{ij} S_j, \; i = 1, 2, \ldots n \qquad (12\text{–}13)$$

Then, if $p \leq n$, the source contributions S_j can be computed by solving the overdetermined linear system (12–13).

Henry et al., (1984) identify five methods of calculating S_j:

1. the tracer property method, which simply assumes that each source j possesses a unique species i which is common to no other source

2. the linear programming method
3. the ordinary least-squares method, which estimates S_j by minimizing the sum of squares of the differences between the measured c_i values and those calculated by Equation 12-3 weighted by the analytical uncertainty of the c_i measurement
4. the effective variance least-square method, which includes the consideration of the errors in the a_{ij} terms and provides more reliable confidence intervals for the outputs S_j
5. the ridge regression, which is one approach useful in handling the "multicollinearity" problem; i.e., the case when two or more sources have similar chemical composition (in this case the least-squares solutions are mathematically unstable)

12.4.2 Multivariate Models

Multivariate models are used to solve Equation 12-12 in which multiple sampling data (k = 1, 2, ...) are considered. The objective of the multivariate models is to use the c_{ik} measurements for predicting

- the number p of sources affecting the monitoring station
- which a_{ij} is associated with which S_j
- when possible, both a_{ij} and S_{jk}

Multivariate methods include (Henry et al., 1984)

- factor analysis based on eigenvector analysis of the cross-product data matrix. (Caution should be used in applying this technique. As pointed out by Henry (1987), current factor analysis receptor models are "biased" in the statistical sense and, in inexperienced hands, can give large errors in source apportionment.)
- target transformation factor analysis, for extracting maximum information about the number and nature of sources with no or very limited *a priori* information other than the elemental composition data (see also Hopke, 1988)
- multiple linear regression, a linear least-squares fitting process that requires a tracer element to be determined for each source j (or each source category)
- extended Q-mode factor analysis, which is a CMB-type model (single sample) that uses multivariate methods to deconvolve the receptor composition into a sum of source compositions

All the above receptor modeling techniques are still under theoretical and empirical development. Review papers are provided by Watson (1984), Henry et al., (1984), and Gordon (1988). Receptor models are becoming a major analysis tool and are much applied, especially for aerosol mass apportionment computations (e.g., see the article of Scheff el al., 1984, for the Chicago area, and the article of Chow et al., 1985, for Portage, Wisconsin). Receptor models seem extremely powerful and promising tools for analyses intended to complement but not to substitute for the information provided by dispersion modeling techniques. Actually, mixed dispersion–receptor modeling methodologies (e.g., Chow et al., 1985) seem to be the most promising. The need for this mixed approach is well indicated by the schematic illustration presented in Figure 12–9. Much investigation, however, is still required to assess the degree of reliability of receptor techniques and, especially, their sensitivity to input data errors.

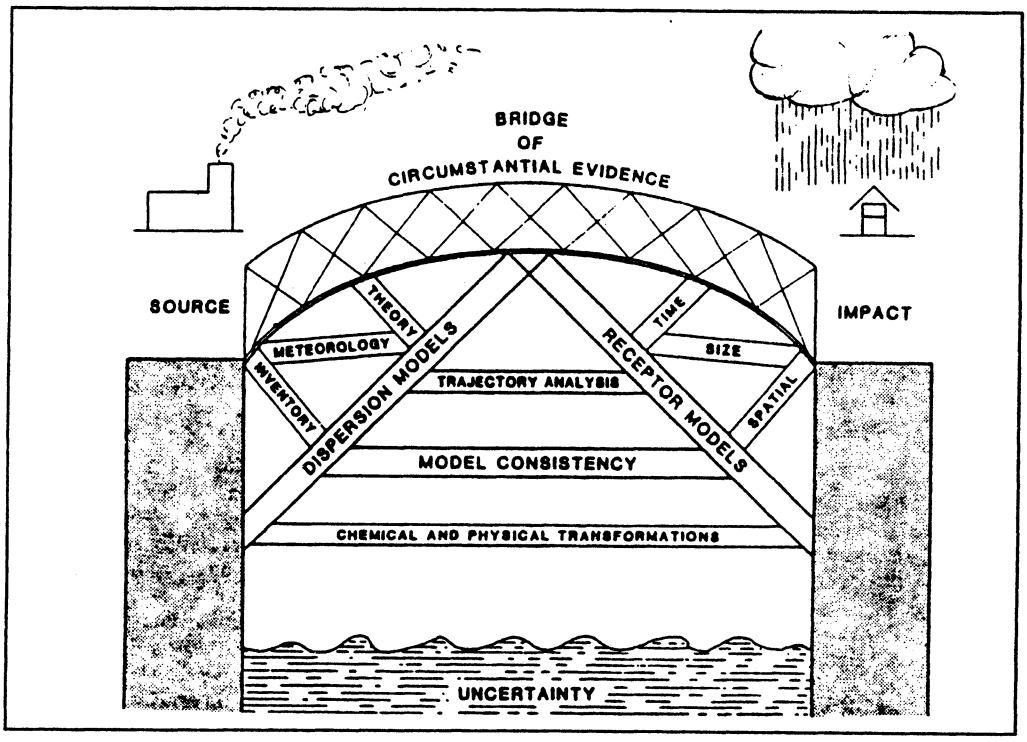

Figure 12–9. Schematic illustration of the need to use many different independent approaches to establish a strong bridge of circumstantial evidence quantitatively linking a source to its impact (from Cooper, 1983). [Reprinted with permission from Pollution Atmospherique.]

12.4.3 Receptor Models for Secondary Particulate Matter

The receptor modeling techniques presented above can simulate only primary particulate matter. Modifications have been recently proposed (Malm et al., 1989) to include adjustments that allow the simulation of secondary particulate matter (primarily sulfates) and deposition phenomena. In mathematical notation, we can rewrite Equation 12–12 as

$$c_{irt} = \Sigma_j a_{ijt} E_{jt} D_{jrt} a_{ijrt} \qquad (12\text{–}14)$$

where c_{irt} is the concentration of the species i in the sample at the receptor r during the time interval t, a_{ijt} is the fraction of emission of the species i from the source j, E_{jt} is the total emission from source j, D_{jrt} is the dispersion factor from the source j to the receptor r, and a_{ijrt} is the adjustment for gain or loss of the species i traveling from the source j to the receptor r.

With this approach, sulfur can be traced by a receptor model by including its emission as SO_2 and the transformation of some SO_2 to SO_4^{2-}. For example, for sulfur as SO_2, the term a can be defined as

$$a_{ijrt} = (1 - f_d)\,(1 - f_c) \qquad (12\text{–}15)$$

where f_d is the mass fraction of SO_2 that is deposited and f_c is the mass fraction of SO_2 that is chemically converted to SO_4^{2-}, both before reaching the receptor r. For sulfur as SO_4^{2-}, we have instead

$$a_{ijrt} = (1 - f_d')\, f_c \qquad (12\text{–}16)$$

where f_d' is the mass fraction of total sulfur that is deposited before reaching the receptor r and f_c is the same as above.

It is evident that a correct determination of f_d, f_d' and f_c requires correct assumptions on deposition and chemical transformation along the air parcel trajectory and, therefore, the application of some sort of deterministic method. The practical application of this technique, therefore, requires a hybrid approach, in which dispersion models still need to be applied to provide the input f_d, f_d' and f_c required by the receptor model.

12.5 PERFORMANCE EVALUATION OF DISPERSION MODELS

The performance of both Lagrangian and Eulerian dispersion models can be estimated by comparing their predictions against field measurements. Tracer

experiments are particularly helpful in evaluating the capability of these models to properly simulate transport and diffusion. Comparison between model outputs and measurements are performed using both qualitative data analysis techniques and quantitative statistical methods.

Initially (say, till a decade ago), this comparison was simple. The outputs of dispersion models were plotted against measurements and simple parameters such as the correlation coefficient were computed. High correlation values (a rare result) indicated that the model was good, low correlation (the most common case) that the model was poor. It is now clear that the problem is not so simple.

First of all, there are measurement errors, a fact that often seems forgotten in the common belief that monitoring data are "the real world." More importantly, even error-free measurements possess space and time limitations that prevent their use beyond their "representativeness" regions around the monitoring point. These representativeness regions are often very small and the comparison of measurements with grid-averaged model outputs is inappropriate. Second, certain statistical parameters, such as the correlation coefficient, can provide misleading results (e.g., Zannetti and Switzer, 1979b). Third, it has been shown that models possess intrinsic uncertainties (e.g., Venkatram, 1988a) that cannot be removed and that their outputs are "ensemble" averages, while measurements are just "realizations" (Lamb, from Longhetto, 1980). Fourth, and most important, models rely upon emission and meteorological inputs. Often the errors in the determination of these inputs fully justify the disagreements between predictions and observations (e.g., Irwin et al., 1987). In other words, the old computer law "garbage in, garbage out" can happen here, too.

In the last decade, several methods for systematic statistical evaluation of air quality model performance have been proposed (e.g., see the survey by Bornstein and Anderson, 1979, and the methodologies proposed by Venkatram, 1982 and 1983). But the most innovative results came from two workshops organized by the American Meteorological Society. These workshops provided specific guidelines on the use of statistical tools in air quality applications; a summary of their recommendations is provided in two papers by Fox (1981 and 1984).

The most interesting comments and recommendations from the above workshops were

- the concern about the absolute, rather than statistical nature of U.S. air quality standards

- the possibility of computing statistics between measured and computed data, even when these data are not coupled in time and/or in space
- the identification of reducible errors and inherent uncertainties
- the recommendations to decision makers to educate themselves and accept the challenge of decision making with quantified uncertainty

The second point was and is the most controversial. What this means is that apples *can* be compared with oranges, for certain purposes. In fact, a model forecast of the maximum concentration impact c_A at location A at time t_1 can be compared with the measurement of maximum concentration impact c_B at location B at a time t_2, and if the two values are close, we are allowed to conclude that, for practical applications, the model can be considered a "good predictor" of the maximum impact. Scientifically speaking, this is not true; if A is distant from B and t_1 is much different from t_2, the model clearly does not work properly and the similarity between c_A and c_B is only accidental. Scientifically speaking, models should not just predict well, but they should do it for the *right* reason. But for practical regulatory applications, the criterion of "decoupling" concentration data in space and time should not be seen as a complete scientific aberration.

The decoupling in space has some acceptable justifications. As illustrated in Figure 12–10, sometimes plume models work well, but their performance can be spoiled by small (and quite common) errors in the measurement or the estimate of the wind direction. The decoupling in time, however, is hard to swallow.

Several recent studies have continued to investigate the problem of statistically evaluating the performance of air quality models. Interesting new methods were proposed at the DOE Model Validation Workshop, October 23–26, 1984, Charleston, South Carolina, and by Alcamo and Bartnicki (1987) and Hanna (1988). Major operational evaluations of air quality models have been sponsored by EPRI (e.g., Reynolds et al., 1984; Ruff et al., 1984; Moore et al., 1985; and Reynolds et al., 1985).

Some agreements on performance evaluation seem to be well accepted today. Terminology, at least, is more clear. Model *calibration* is the adjustment of empirical model constants, within their physical bounds, to optimize agreement with observations. If properly done, calibration is important and acceptable and should not be referred to as "fudging" or "massaging" results. Model *validity* is the "theoretical" ability of the model, with error-free model inputs. Therefore, a model can be validated against a theory or another model, but not against

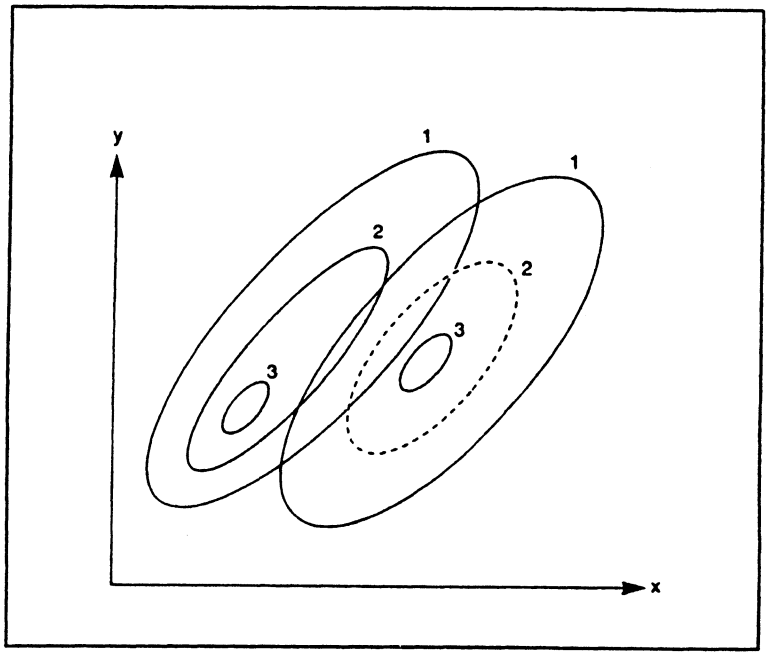

Figure 12–10. Illustration of displacement of observed and predicted ground-level concentration patterns. Isopleths represent points with the same concentration. The point-by-point correlation is poor, but the patterns are clearly similar (from Hanna, 1988). [Reprinted with permission from the Air Pollution Control Association.]

measurements. Model *evaluation* is the quantification of the performance of the model in real cases with real data. Model *verification* is the successful validation and/or evaluation of the model.

For practical applications, several statistical parameters can be used to evaluate pairs of predicted/observed concentrations. Among them

- The bias, i.e., the average difference of predicted minus observed values
- The gross error, i.e., the average of the absolute differences
- The variance of the differences
- The correlation coefficient between predicted and observed values
- The regression line, which ideally should have slope one and intercept zero

- The normalized fractional bias *FB* (Irwin and Smith, 1984) where

$$FB = 2(\bar{c}_p - \bar{c}_o)/(\bar{c}_p - \bar{c}_o) \quad (12\text{–}17)$$

  and $\bar{c}_p$, $\bar{c}_o$ are the predicted and observed average concentrations, respectively. *FB* varies between –2 and 2 with an optimum value of zero

- The normalized mean square error *NMSE* (Hanna and Heinold, 1985), where

$$NMSE = \overline{(c_p - c_o)^2}/(\bar{c}_p\, \bar{c}_o) \quad (12\text{–}18)$$

  where c_p and c_o are the single concentration values

- Skill scores (e.g., Murphy, 1988)
- Frequency distribution analysis of the differences
- Autocorrelation and spectral analysis of the differences. Often, repetitive or physically meaningful patterns in the differences can be identified and removed, thus improving the practical performance of the model (e.g., a daily cycle in the average difference may indicate emission input errors and can be empirically removed to maximize model performance)

Often data are insufficient for reliable statistical analysis. In this case, resampling procedures, such as "bootstrap" and "jackknife" techniques can be used to generate new "synthetic" data sets from the original data using an empirical set of rules (e.g., Heidam, 1987; Hanna, 1987). Finally, we must emphasize the powerful use of graphical methods for performance evaluation. In many cases, qualitative observations of multiple time plots, isopleths, cumulative frequency distributions, may say more than a thousand skill scores.

12.6 INTERPOLATION METHODS AND GRAPHIC TECHNIQUES

Several techniques that can be labeled as interpolation methods and graphic techniques will be discussed in this section. They are:

- Kriging
- pattern recognition
- cluster analysis
- fractals

12.6.1 Kriging

The Kriging technique was originally developed by Matheron (1971). It is an interpolation technique that possesses three major advantages with respect to other interpolation methods (Venkatram, 1988b):

1. its interpolations are made with weights that do not depend upon data values
2. it provides an estimate of the interpolation error
3. it is an exact interpolation since the interpolation at any observation point is the observation itself

In mathematical notation, observations $z(\mathbf{x}_j)$ of the variable z at locations $\mathbf{x}_j$ allow a Kriging interpolation of $z(\mathbf{x})$ at any point $\mathbf{x}$. Simple Kriging is done by assuming that

$$z(\mathbf{x}) = m + \epsilon(\mathbf{x}) \tag{12-19}$$

where m is a fixed component and ϵ is a stochastic component. Then, the Kriging estimate z'_k of $z(\mathbf{x}_k)$ at a generic point $\mathbf{x}_k$ is assumed to be a linear combination of the observations $z_j = z(\mathbf{x}_j)$, i.e.,

$$z'_k = \sum_j \lambda_j z_j \tag{12-20}$$

where the λ_j are independent of z_j and are calculated by variational calculus, imposing the condition that the ensemble average variance of z'_k be a minimum. This condition allows the calculation of the λ_j terms and the Lagrangian multiplier μ.

The variance of the interpolation error is computed by

$$< (z'_k - z_k)^2 > = \sum_j \lambda_j \gamma_{jk} + \mu \tag{12-21}$$

where the brackets < > indicate ensemble averaging and the semi-variogram γ_{jk} is defined by

$$\gamma_{jk} = < (z_j - z_k)^2 > /2 \tag{12-22}$$

and quantifies the effects of the stochastic term ϵ on the difference between $z(\mathbf{x}_j)$ and $z(\mathbf{x}_k)$. The term γ_{jk} cannot be calculated from observations and its correct determination is the major challenge in the application of the Kriging

technique. Kriging is good only if the assumed model for γ_{jk}, i.e., for the spatial relationships among measurements, is good. Barnes (1980) provides a few choices for γ_{jk}. A common, simplifying assumption is often made by assuming that γ_{jk} depends only upon the distance $|\mathbf{x}_j - \mathbf{x}_k|$.

The Kriging technique has recently been applied to environmental problems. Venkatram (1988b) used it with annual averages of sulfur wet deposition in the eastern United States, and Eynon (1988) applied Kriging to perform a statistical analysis of chemical measurements in about 10,000 precipitation samples collected during the period 1979 through 1983 in the eastern United States. Results seem encouraging, even though Fedorov (1989) claimed that other estimators, such as the generalized least squares (GLS) and the moving least squares (MLS) can successfully compete with the Kriging technique.

An example of Kriging is given in Figures 12–11 through 12–13. Figure 12–11 shows locations and values of annual wet deposition sulfur measured in 1980 in the eastern United States. Figure 12–12 illustrates the simple Kriging applied to these data, while Figure 12–13 shows a more realistic interpolation in which the pattern is estimated by a simple statistical long range model. Clearly, interpolation features improve when some deterministic information is added.

12.6.2 Pattern Recognition

Pattern recognition techniques have been applied to a large number of fields. These techniques can categorize sets of observations, by graphical methods, and perform forecasting. The theory of pattern recognition is found in Nilsson (1965), Arkadev and Braverman (1967), Fu (1968; 1974) and Fukanaga (1976).

Pattern recognition methods have been applied in atmospheric studies for air pollution control (Tauber, 1978), to characterize local sources (Edgerton and Holdren, 1987), and to automatically compute the mixing height from LIDAR measurements (Endlich et al., 1979).

12.6.3 Cluster Analysis

Methods of hierarchical cluster analysis are frequently applied in many research fields. A clear and detailed introduction to cluster analysis is given by Romesburg (1984). This method covers a variety of techniques that can be used to find out which objects in a set are similar. Cluster analysis is useful for classification purposes, even though it is used for several other purposes. Cluster analysis techniques have been applied, for example, to identify sources of

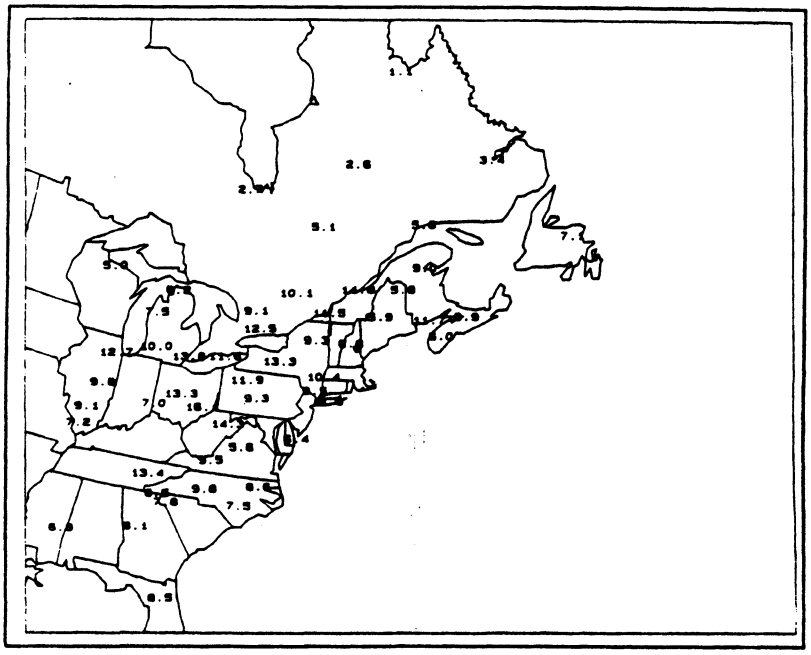

Figure 12–11. Locations and values of annual wet deposition of sulfur measured during 1980. Units are kg ha^{-1} (from Venkatram, 1988). [Reprinted with permission from Pergamon Press.]

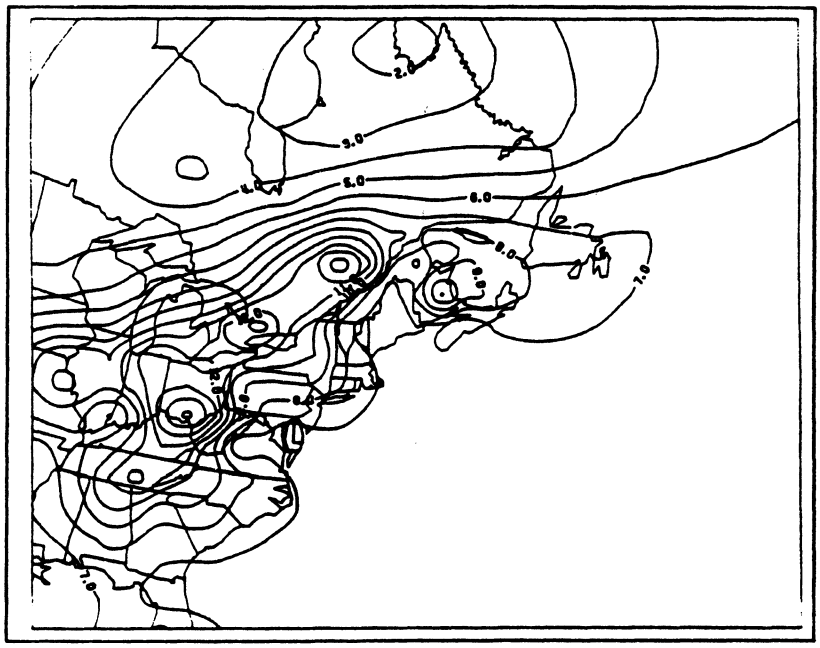

Figure 12–12. Pattern of annual sulfur wet deposition derived by applying simple Kriging to observations shown in Figure 12–11 (from Venkatram, 1988). [Reprinted with permission from Pergamon Press.]

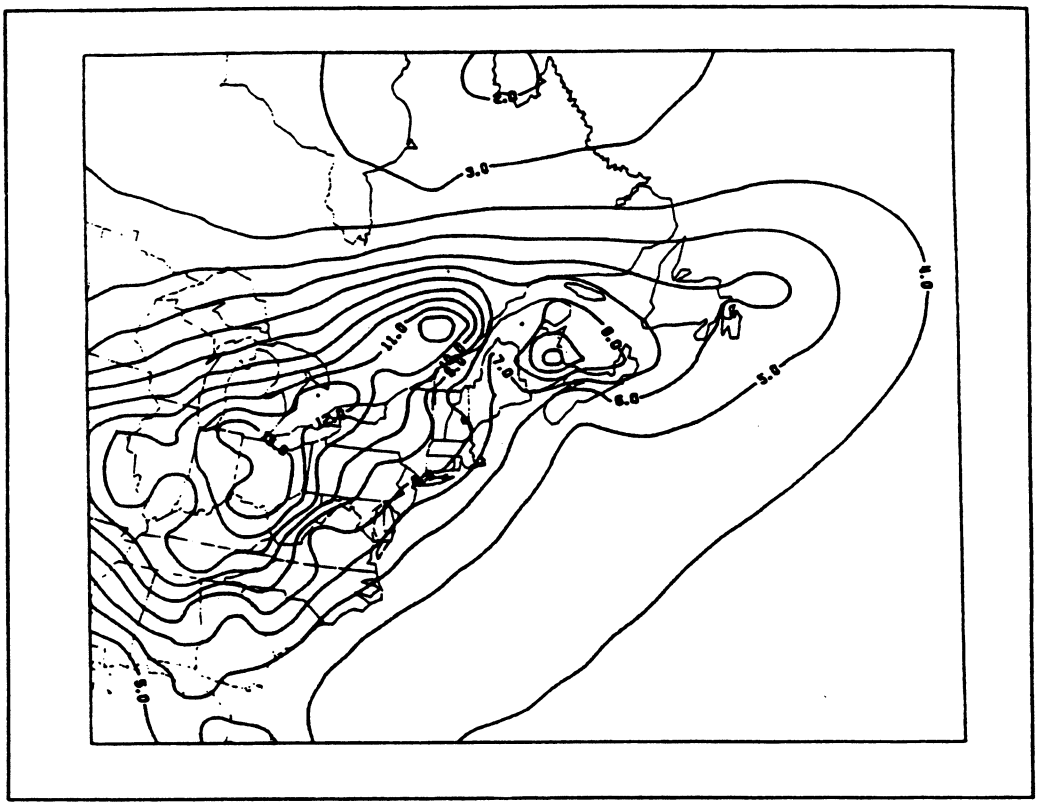

Figure 12–13. Same as Figure 12–12, except that pattern is estimated from statistical long–range transport model (from Venkatram, 1988). [Reprinted with permission from Pergamon Press.]

particulate matter (Gomez and Martin, 1987) and to perform source apportionment of atmospheric aerosols (Van Borm and Adams, 1988).

12.6.4 Fractals

Fractals are geometric shapes with roughness characteristics that are qualitatively similar at all scales. Techniques based on the fractals concept were introduced by Mandelbrot (1975) and have become very popular. In fact, many lines and surfaces in nature are well depicted by fractals, which, therefore, allow the production of synthetic, but realistic looking, landscapes. Fractals are useful for qualitative reproduction of natural phenomena, such as turbulent motion, and for image compression techniques. Their most interesting application is probably in conjunction with chaos theories, which were briefly discussed at the beginning of this chapter.

In atmospheric studies, fractals allow the depiction of turbulent eddies, the reproduction of the similarity theory, and the numerical simulation of de-

tailed and complex characteristics of fluid flows. An overview of the application of fractals to atmospheric sciences is presented by Ludwig (1989).

12.7 OPTIMIZATION METHODS

Optimization needs are often present in air quality studies. For example, emission reductions should always be optimized, to allow the most effective reductions within the allowable budgets. The most common application of optimization methods occurs in the design of a monitoring network, where nonlinear programming techniques are used to determine the number and disposition of ambient air quality stations. This determination can be done under different constraints (e.g., a primary purpose of a network might be the assessment of maximum ground-level concentration impact for compliance with air quality standards). A vast literature exists in this field. Examples of applications are given by Seinfeld (1972), Noll et al. (1977), Nakamori and Sawaragi (1984), Liu et al. (1986), and Langstaff et al., (1987).

REFERENCES

Alcamo, J., and J. Bartnicki (1987): A framework for error analysis of a long-range transport model with emphasis on parameter uncertainty. *Atmos. Environ.*, **21**(10):2121–2131.

Arkadev, A.G., and E.M. Braverman (1967): *Teaching Computers to Recognize Patterns.* London: Academic Press.

Bacci, P., P. Bolzern, and G. Fronza (1981): A stochastic predictor of air pollution based on short-term meteorological forecasts. *J. Appl. Meteor.*, **20**(2):121–129.

Bankoff, S.G., and E.L. Hanzevack (1975): The adaptive filtering transport model for prediction and control of pollutant concentration in an urban airshed. *Atmos. Environ.*, **18**:701–712.

Barnes, M.G. (1980): The use of Kriging for estimating the spatial distribution of radionuclides and other spatial phenomena. Tran-Stat, Battelle Memorial Institute, Pacific Northwest Laboratories., Richland, Washington.

Barone, J.B., T.A. Cahill, R.A. Eldred, R.G. Flocchini, D.J. Shadoan, and T.M. Dietz (1978): A multivariate statistical analysis of visibility degradation at four California cities. *Atmos. Environ.*, **12**:2213–2221.

Berge, P., Y. Pomeau, and C. Vidal (1984): *Order Within Chaos.* New York: John Wiley.

Bornstein, R.D., and S.F. Anderson (1979): A survey of statistical techniques used in validation studies of air pollution prediction models. Technical Report No. 23, Stanford University, Stanford, California.

Box, G.E., and G.M. Jenkins (1976): *Time Series Analysis, Forecasting and Control.* San Francisco: Holden-Day.

Buishand, T.A., G.T. Kempen, A.J. Frantzen, H.F. Reijnders, and A.J. van den Eshof (1988): Trend and seasonal variations of precipitation chemistry data in the Netherlands. *Atmos. Environ.*, **22**(2):339–348.

Cats, G.J., and A.A. Holtslag (1980): Prediction of air pollution frequency distribution. Part I: The lognormal model. *Atmos. Environ.*, **14**:255–258.

Chock, D.P., and P.S. Sluchak (1986): Estimating extreme values of air quality data using different fitted distributions. *Atmos. Environ.*, **20**(5):989–993.

Chock, D.P., T.R. Terrel, and S.B. Levitt (1975): Time-series analysis of Riverside, California air quality data. *Atmos. Environ.*, **9**:978–989.

Chow, J.C., P.W. Severance, and J.D. Spengler (1985): A composite application of source and receptor models to fine particle concentrations in Portage, Wisconsin. *Proceedings,* 78th Annual APCA Meeting. Detroit, Michigan, June.

Cooper, J.A. (1983): Receptor model approach to source apportionment of acid rain precursors. *Proceedings,* VIth World Congress on Air Quality, Paris, France, May 16–20, pp. 223–229.

Desalu, A.A., L.A. Gould, and F.C. Schweppe (1974): Dynamic estimation of air pollution. *IEEE Transactions on Automatic Control AC-19,* pp. 904–910.

Drufuca, G., and M. Giugliano (1978): Relationship between maximum SO_2 concentration, averaging time and average concentration in an urban area. *Atmos. Environ.*, **12**:1901–1905.

Edgerton, S.A., and M.W. Holdren (1987): Use of pattern recognition techniques to characterize local sources of toxic organics in the atmosphere. *Environ. Sci. Technol.*, **21**(11):1102–1107.

Endlich, R.M., F.L. Ludwig, and E.E. Uthe (1979): An automatic method for determining the mixing depth from LIDAR observations. *Atmos. Environ.*, **13**:1051–1056.

Eynon, B.P. (1988): Statistical analysis of precipitation chemistry measurements over the eastern United States. Part II: Kriging analysis of regional patterns and trends. *J. Appl. Meteor.*, **27**:1334–1343.

Fedorov, V.V. (1989): Kriging and other estimators of spatial field characteristics (with special reference to environmental studies). *Atmos. Environ.*, **23**(1):175–184.

Finzi, G., and G. Tebaldi (1982): A mathematical model for air pollution forecast and alarm in an urban area. *Atmos. Environ.*, **16**(9):2055–2059.

Fox, D.C. (1981): Judging air quality model performance. *J. Climate and Appl. Meteor.*, **62**:599–609.

Fox, D.C. (1984): Uncertainty in air quality modeling. *J. Climate and Appl. Meteor.*, **65**:27–36.

Fronza, G., A. Spirito, and A. Tonielli (1979): Real-time forecast of air pollution episodes in the Venetian region. Part 2: The Kalman predictor. *Appl. Math. Model.*, **3**:409–415

Fu, K.S. (1968): *Sequential Methods in Pattern Recognition.* New York: Academic Press.

Fu, K.S. (1974): *Syntactic Methods in Pattern Recognition.* New York: Academic Press.

Fukunaga, K. (1972): *Introduction to Statistical Pattern Recognition.* New York: Academic Press.

Georgopoulos, P.G., and J.H Seinfeld (1982): Statistical distributions of air pollutant concentrations. *Environ. Sci. & Technol.*, **16**:401A–415A.

Gilbert, R.O. (1987): *Statistical Methods for Environmental Pollution Monitoring.* New York: Van Nostrand Reinhold.

Gomez, M.L., and M.C. Martin (1987): Applications of cluster analysis to identify sources for airborne particles. *Atmos. Environ.*, **21**(7):1521–1527.

Gordon, G.E. (1988): Receptor models. *Environ. Sci. & Tech.*, **22**(10):1132.

Grebogi, C., E. Ott, and J.A. Yorke (1987): Chaos, strange attractors, and fractal basin boundaries in nonlinear dynamics. *Science*, **238**:632–637.

Hanna, S.R., and D.W. Heinold (1985): Development and application of a simple method for evaluating air quality models. American Petroleum Institute Publication 4409, Washington, D.C.

Hanna, S.R. (1988): Air quality model evaluation and uncertainty. *JAPCA*, **38**:406–412.

Hanna, S.R. (1989): Confidence limits for air quality model evaluations, as estimated by bootstrap and jackknife resampling methods. *Atmos. Environ.*, **23**(6):1385–1389.

Heidam, N.Z. (1987): Bootstrap estimates of factor model variability. *Atmos. Environ.*, **21**(5):1203–1217.

Henry, R.C. (1987): Current factor analysis receptor models are ill-posed. *Atmos. Environ.*, **21**(8):1815–1820.

Henry, R.C., and G.M. Hidy (1979): Multivariate analysis of particulate sulfate and other air quality variables by principal components. Part I: Annual data from Los Angeles and New York. *Atmos. Environ.*, **13**:1581–1596.

Henry, R.C., C.W. Lewis, P.K. Hopke, and H.I. Williamson (1984): Review of receptor model fundamentals. *Atmos. Environ.*, **18**:1507–1515.

Hino, M. (1974): Prediction of atmospheric pollution by Kalman filtering. *Proceedings*, Symposium on Modeling for Prediction and Control of Air Pollution.

Hopke, P.K. (1988): Target transformation factor analysis as an aerosol mass apportionment method: A review and sensitivity study. *Atmos. Environ.*, **22**(9):1777–1792.

Horowitz, J., and S. Barakat (1979): Statistical analysis of the maximum concentration of an air pollutant: Effects of autocorrelation and non-stationarity. *Atmos. Environ.*, **13**:811–818.

Irwin, J.S., and M.E. Smith (1984): Potentially useful additions to the rural model performance evaluation. *J. Climate and Appl. Meteor.*, **65**:559.

Irwin, J.S., S.T. Rao, W.B. Peterson, and D.B. Turner (1987): Relating error bounds for maximum concentration estimates to diffusion meteorology uncertainty. *Atmos. Environ.*, **21**(9):1927–1937.

Jazwinski, A.H. (1970): *Stochastic Processes and Filtering Theory*. New York: Academic Press.

Jenkins, G.M., and D.G. Watts (1968): *Spectral Analysis and Its Applications*. San Francisco: Holden-Day.

Kahn, H.D. (1973): Distribution of Air Pollutants. *JAPCA*, **23**:973.

Kalman, R.E. (1960): A new approach to linear filtering and prediction problems. *J. Basic Eng.*, pp. 35–108

Langstaff, J.E., C. Seigneur, M.-K. Liu, J.V. Behar, and J.L. McElroy (1987): Design of an optimum air monitoring network for exposure assessments. *Atmos. Environ.*, **21**(6):1393–1410.

Larsen, R.I. (1971): EPA Publication No. AP-89, Research Triangle Park, North Carolina.

Little, R.J., and D.B. Rubin (1987): *Statistical Analysis with Missing Data*. New York: John Wiley.

Lin, G.Y., (1982): Oxidant prediction by discriminant analysis in the south coast air basin of California. *Atmos. Environ.*, **16**(1):135–143.

Longhetto, A., Ed. (1980): *Atmospheric Planetary Boundary Layer Physics*. New York: Elsevier.

Liu, M.–K., J. Arvin, R.I. Pollack, J.V. Behar, and J.L. McElroy (1986): Methodology for designing air quality monitoring networks. I: Theoretical aspects. *Environ. Monitoring and Assessment*, **6**:1–11.

Ludwig, F.L. (1989): Atmospheric fractals — A review. *Environ. Software*, **4**(1):9–16.

Malm, W., K. Gebhart, D.A. Latimer, T.A. Cahill, R. Eldred, R.A. Pielke, R. Stocker, J.G. Watson (1989): Winter Haze Intensive Tracer Experiment. National Park Service draft final report, December.

Mandelbrot, B.B. (1975): On the geometry of homogeneous turbulence with stress on the fractal dimension of the iso–surfaces of scalars. *J. Fluid Mech.*, **72**:401–416.

Marani, A., 1. Lavagnini, C. Buttazzoni (1986): Statistical study of air pollutant concentrations via generalized gamma distributions. *JAPCA*, **36**:1250–1254.

Matheron, G. (1971): The theory of regionalized variables and its applications. Ecole des Mines de Paris, Fontainbleau No. 5.

Melli, P., P. Bolzern, G. Fronza, and A. Spirito (1981): Real–time control of sulphur dioxide emissions from an industrial area. *Atmos. Environ.*, **15**: 653–666.

Moore, G.E., M.–K. Liu, and R.J. Londergan (1985): Diagnostic validation of Gaussian and first–order closure plume models at a moderately complex terrain site. Systems Applications, Inc., Final Report EA–3760, San Rafael, California.

Murphy, A.H. (1988): Skill scores based on the mean square error and their relationships to the correlation coefficient. *J. Climate and Appl. Meteor.*, **116**:2417–2424.

Murray, L.C., and R.J. Farber (1982): Time series analysis of an historical visibility data base. *Atmos. Environ.*, **16**:2299–2308.

Nakamori, Y., and Y. Sawaragi (1984): Interactive design of urban level air quality monitoring network. *Atmos. Environ.*, **18**(4):793–799.

Nilsson, N.J. (1965): *Learning Machines*. McGraw–Hill.

Noll, K.E., T.L. Miller, J.E. Norco, and R.K. Raufer (1977): An objective air monitoring site selection methodology for large point sources. *Atmos. Environ.*, **11**:1051–1059.

Petersen, J.T. (1970): Distribution of sulfur dioxide over metropolitan St. Louis, as described by empirical eigenvectors, and its relation to meteorological parameters. *Atmos. Environ.*, **4**:501–518.

Plackett, R.L. (1950): *Biometrika*, **37**:149.

Reynolds, S.D., C. Seigneur, T.E. Stoeckenius, G.E. Moore, R.G. Johnson, and R.J. Londergan (1984): Operational validation of Gaussian plume models at a plains site. Systems Applications, Inc., Final Report EA–3076, San Rafael, California.

Reynolds, S.D., T.C. Myers, J.E. Langstaff, M.-K. Liu, G.E. Moore, and R.E. Morris(1985): Operational validation of Gaussian and first-order closure plume models at a moderately complex terrain site. Systems Applications, Inc., Final Report EA-3759, San Rafael, California.

Romesburg, H.C. (1984): *Cluster Analysis for Researchers*. Belmont, California: Lifetime Learning Publications.

Roberts, E.M. (1979): Review of statistics of extreme values with applications to air quality data. Part I: Review. *JAPCA*, **29**(6):632–637.

Roberts, E.M. (1979): Review of statistics of extreme values with applications to air quality data. Part II: Applications. *JAPCA*, **29**(7):733–740.

Roy, R., and I. Pellerin (1982): On long term air quality trends and intervention analysis. *Atmos. Environ.*, **16**:161–169.

Ruff, R.E., K.C. Nitz, F.L. Ludwig, C.M. Bhumralkar, J.D. Shannon, C.M. Sheih, I.Y. Lee, R. Kumar, and D.J. McNaughton (1984): Regional air quality model assessment and evaluation. SRI International Final Report EA-3671, Menlo Park, California.

Sage, A.P., and I.L. Melsa (1971): *Estimation Theory with Applications to Communications and Control*. New York: McGraw-Hill.

Sawaragi, Y., T. Soeda, T. Yoshimura, S. Oh, Y. Chujo, and H. Ishihara (1976): The predictions of air pollution levels by nonphysical models based on Kalman filtering method. *J. Dynamic Sys., Measurement and Control*, **98**(12):375–386.

Scheff, P.A., R.A. Wadden, and R.I. Allen (1984): Development and validation of a chemical element mass balance for Chicago. *Environ. Sci. Technol.*, **18**:923–931.

Seinfeld, J.H. (1972): Optimal location of pollutant monitoring stations in an airshed. *Atmos. Environ.*, **6**:847–858.

Seinfeld, J.H. (1986): *Atmospheric Chemistry and Physics of Air Pollution*. New York: John Wiley.

Simpson, R.W., and A.P. Layton (1983): Forecasting peak ozone levels. *Atmos. Environ.*, **17**:1649–1654.

Surman, P.G., J. Bodero, and R.W. Simpson (1987): The prediction of the numbers of violations of standards and the frequency of air pollution episodes using extreme value theory. *Atmos. Environ.*, **21**(8):1843–1848.

Tauber, S. (1978): Pattern recognition methods in air pollution control. *Atmos. Environ.*, **12**:2377–2382.

Tiao, G.C., G.E. Box, and W.J. Hamming (1975): Analysis of Los Angeles photochemical smog data: A statistical overview. *JAPCA*, **25**:260–268.

Tilley, T., and G.A. McBean (1973): An application of spectrum analysis to synoptic-pollution data. *Atmos. Environ.*, **7**:793–801.

Trivikrama, S.R., P.I. Samson, and A.R. Pedadda (1976): Spectral analysis approach to the dynamics of air pollutants. *Atmos. Environ.*, **10**:375–379.

Tsukatami, T., and K. Shigemitsu (1980): *Atmos. Environ.*, **14**:245.

Van Borm, W.A., and F.C. Adams (1988): Cluster analysis of electron microprobe analysis data of individual particles for source apportionment of air particulate matter. *Atmos. Environ.*, **22**(10):2297–2307.

Venkatram, A. (1982): A framework for evaluating air quality models. *Boundary-Layer Meteor.*, **24**:371–385.

Venkatram, A. (1983): Uncertainty in predictions from air quality models. *Boundary-Layer Meteor.*, **27**:185–196.

Venkatram, A. (1988a): Inherent uncertainty in air quality modeling. *Atmos. Environ.*, **22**(6):1221–1227.

Venkatram, A. (1988b): On the use of Kriging in the spatial analysis of acid precipitation data. *Atmos. Environ.*, **22**(9):1963–1979.

Watson, J.G. (1984): Overview of receptor model principles. *JAPCA*, **34**:619–623.

Wiener, N. (1949): *The Extrapolation, Interpolation and Smoothing of Stationary Time Series.* New York: John Wiley.

Williams, P.C. (1984): Data handling, simultaneity, and rare events. *JAPCA*, **34**:945–951.

Young, P. (1974): Recursive approaches to time series analysis. In *The Inst. of Mathematics and its Application*, pp. 209–224.

Zannetti, P. (1978): Short-term real-time control of air pollution episodes in Venice. *Proceedings*, 71st Annual APCA Meeting, Houston, Texas, June.

Zannetti, P., G. Finzi, G. Fronza, and S. Rinaldi (1978): Time series analysis of Venice air quality data. IFAC Symposium on Environmental Systems, Planning, Design, and Control, August 1–5, 1977, Kyoto, Japan.

Zannetti, P., and P. Switzer (1979a): The Kalman filtering method and its application to air pollution episode forecasting. Paper presented at the APCA Specialty Conference on Quality Assurance in Air Pollution Measurement, New Orleans, Louisiana, March.

Zannetti, P., and P. Switzer (1979b): Some problems of validation and testing of numerical air pollution models. *Proceedings*, Fourth Amer. Meteor. Soc. Symp. on Turbulence, Diffusion, and Air Pollution, Reno, Nevada. January, pp. 405–410.

Zinsmeister, A.R., and T.C. Redman (1980): A time series analysis of aerosol composition measurements. *Atmos. Environ.*, **14**:201–215.

13 MODELING OF ADVERSE AIR QUALITY EFFECTS

Often the real goal of an air pollution study is not only to evaluate the concentration field of atmospheric pollutants, but also to quantify their adverse effects. In other words, often one needs to quantify a relation

$$E = f(\mathbf{c}) \tag{13-1}$$

where E represents a quantitative description of an adverse effect (e.g., the reduction in atmospheric visual range) and the vector $\mathbf{c}$ represents the ambient pollutant concentrations. The relation f can vary from a simple semiempirical formulation, based on empirical data, to a complex simulation mechanism of the adverse effects. As an example of a simple relation, long-term ambient concentrations of carcinogenic pollutants measured in a certain region R can be empirically related to the number of extra cancers that they are expected to generate in the next (say) 30 years, in the population P living in the region R. As an example of a complex relation, mathematical models of the human body's respiratory system can be used to assess the short-term and long-term effects of a predefined pattern of exposure to toxic pollutants.

Adverse effects of atmospheric pollutants have been studied by several authors. A full volume (Volume II, Stern, 1977) of the Stern air pollution series is dedicated to this topic. More recently, Volume VI (Stern, 1986), which is a supplement of Stern (1977), integrates Volume II with additional discussion of 1) physical and economic systems, 2) vegetation, 3) acidic deposition on aquatic ecosystems, and 4) human health.

Adverse effects can be divided into

1. short-term and long-term ecological damage to
   - human health (e.g., see Lipfert (1985) for a discussion of a possible connection between mortality and air pollution)
   - animals
   - plants (e.g., see the critical review by McLaughlin (1985) on the effects on air pollution of forests)

2. damage to human "welfare," such as
   - atmospheric visibility impairment
   - odors (e.g., see Poostchi et al. (1986) for a comparison of models used for the determination of odor thresholds)
   - undesired changes in local weather
3. economical damages to
   - materials
   - structures
   - real estate values
   - artistic heritage (e.g., see Tombach (1982) for a discussion of climatological and air pollution factors affecting stone decay)
4. global effects due to
   - CO_2 accumulation
   - stratospheric ozone depletion
   - nuclear winter scenarios

In this chapter, we will discuss the use of mathematical models in some of the above fields, particularly

1. atmospheric visibility
2. CO_2 accumulation and the "greenhouse" effect
3. depletion of stratospheric ozone
4. nuclear winter scenarios

13.1 VISIBILITY IMPAIRMENT

Visibility impairment and its modeling is a significant issue in the U.S., where visibility has been recognized as an important aesthetic value to be preserved, especially in high scenery regions such as the national parks.

Two major topics have been addressed by visibility modeling techniques:

1. plume visibility, models of which simulate the visual effects of a single plume

2. regional haze, models of which address the visibility impairment (mainly a reduction of visual range) caused by large air masses containing high concentrations of fine particles.

13.1.1 Plume Visibility

The objective of a plume visibility model is the evaluation of a plume's impact on human vision in a certain region. This is achieved by a series of simulation modules, as illustrated in Figure 13–1, in which, starting from the plume's emission data, results regarding the plume's appearance are obtained.

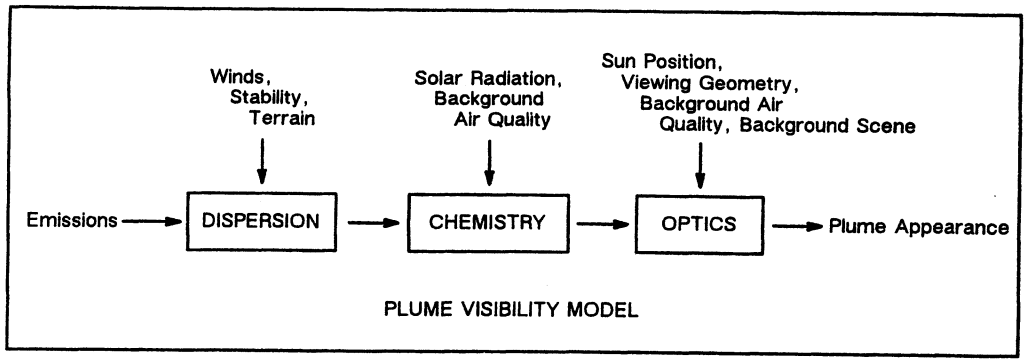

Figure 13–1. The organization of modules in a plume visibility model (from White, 1984). [Reprinted with permission from the American Petroleum Institute.]

Figure 13–2 is a more detailed description of the computational modules of a plume visibility model. The main simulation processes are

1. plume dispersion by atmospheric turbulence
2. plume chemistry, in which NO is converted to NO_2 and SO_2, NO_2 and organic gases are oxidized into SO_4^{2-}, NO_3^- and organic particles, respectively
3. particle growth
4. atmospheric optics
5. human perceptual effects of visibility impairment

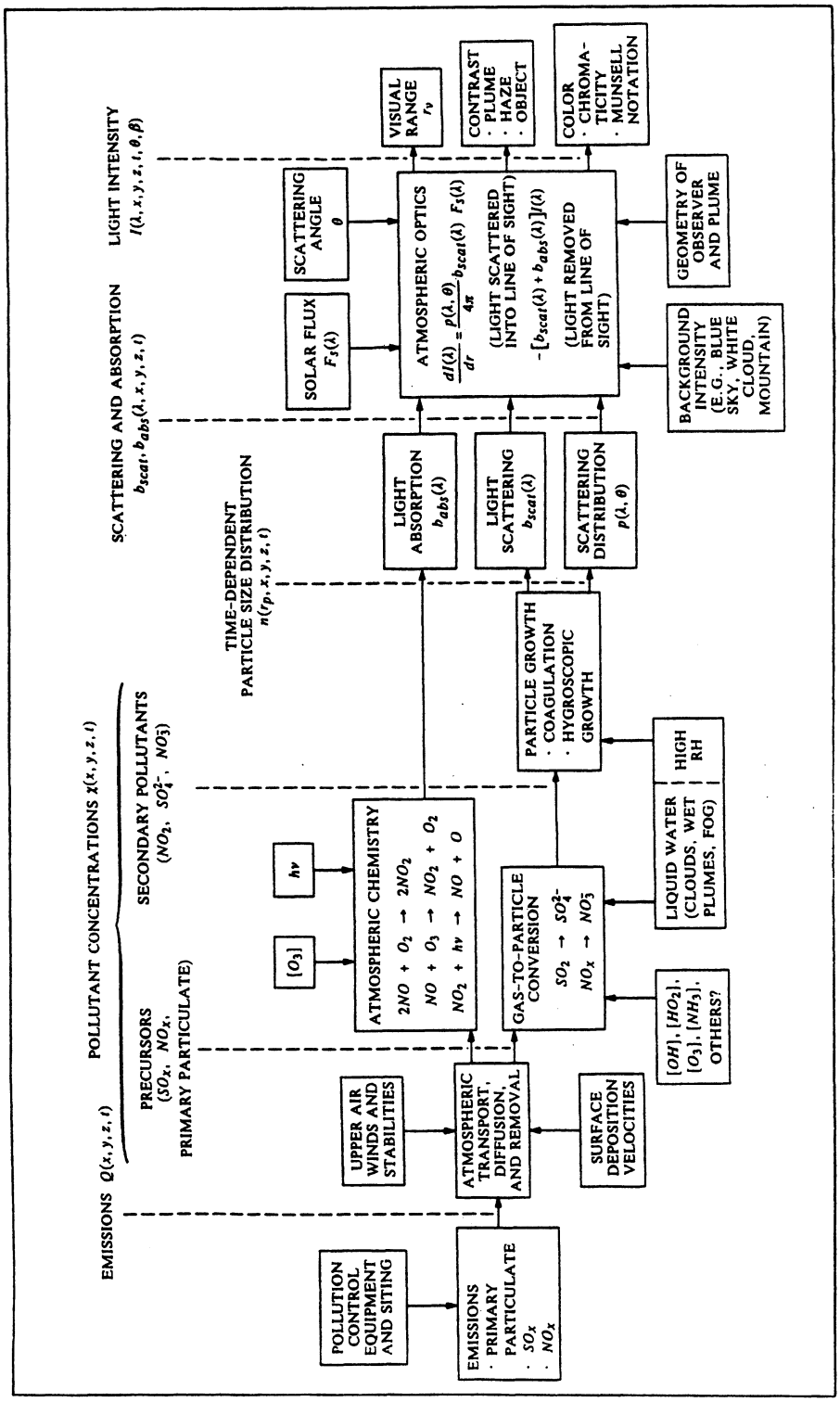

Figure 13–2. Schematic logic flow diagram of the visibility models (from Latimer et al., 1980). [Reprinted with permission from the American Meteorological Society.]

Four visibility packages, among others, are available for plume visibility simulations (White, 1984):

1. the ERT Visibility Model, Version 3 (Drivas et al., 1981)
2. the Los Alamos Visibility Model (Williams et al., 1980 and 1981)
3. the PHOENIX model (Eltgroth and Hobbs, 1979)
4. the PLUVUE Model (Latimer and Samuelsen, 1978; Latimer et al., 1980(*)

An intercomparison study (White, 1984) tested the performance of these four models against field data collected by the VISTTA measurement program. The U.S. EPA and the Salt River Project (SRP) cosponsored the VISTTA project to collect suitable data near the SRP's Navajo Generation Station in northern Arizona in order to evaluate plume visibility models. According to White (1984), "none of the models is successful in predicting observed variation in plume dispersion or concentration parameters," and "much of the observed variability appears due to short-term fluctuations in source emissions and atmospheric transport." The interesting conclusion of this preliminary intercomparison study points out that future model development should focus on improving the parameterization of plume dispersion which, in the available models, appears to be the major component presently limiting model performance.

13.1.2 Regional Haze

Plume visibility impairment is not the only aspect of the air quality–visibility issue. Especially in the eastern U.S., visibility is impaired by regional haze much more than by single plumes. Regional haze is due to both natural causes (e.g., high relative humidity) and the presence of fine particulate matter (particles ≤ 2.5 μm in aerodynamic diameter).

One of the basic assumptions of current (e.g., Latimer and Hogo, 1987) regional haze studies is that the visual range r_v can be computed using the Koschmieder relationship

$$r_v = K/b_t \qquad (13\text{–}2)$$

where K is the Koschmieder constant, initially estimated as 3.9, but re-evaluated as 3.0 for air quality applications (Tombach and Allard, 1983). The parameter b_t

(*) A revision of the PLUVUE model, called PLUVUE II, is currently available (Latimer and Ireson, 1988).

is the total light extinction coefficient, which is assumed to be an additive function of each atmospheric contributor to light scattering and absorption. In many cases, it is assumed that

$$b_t = b_s + b_{ns} \tag{13-3}$$

where b_s is the fraction of b_t due to the sulfates and b_{ns} combines the contribution of all other components (nitrates, organics, NO_2, etc.). The fraction b_s can be related to the average SO_4^{2-} concentration by

$$b_s = const\ c_{SO_4}\ f(RH) \tag{13-4}$$

where c_{SO_4} is the sulfate concentration and $f(RH)$ is a function of the relative humidity RH (e.g., as in SAI, 1984).

One of the major issues in regional haze modeling is the evaluation of the visual range improvements associated with SO_2 emission reductions (e.g., a 50 percent SO_2 emission reduction has often been proposed in the eastern United States). Several authors have addressed this problem in both episodic summertime studies (Ferman et al., 1981; Stevens et al., 1984; Weiss et al., 1982) and annual average calculations (Latimer and Hogo, 1987; Zannetti et al., 1988). Such quantifications, however, are difficult to perform for several reasons: 1) the large uncertainties that even advanced models possess in simulating long-range transport, diffusion, chemistry and deposition of atmospheric sulfur; 2) the difficulty in quantifying the roles that other components, such as non-sulfate-containing fine particles, coarse particles and gases, play in visibility impairment; and 3) the scarcity of suitable field data, since most measurement studies are conducted during episodic conditions, while annual average assessments require input data that represent other conditions as well as episodic.

The effect of SO_2 emission reduction on visual range is complicated by four major factors that cause nonlinear behavior; they are discussed below:

1. Atmospheric light extinction is caused by the concentration of fine particles and other airborne components. SO_2 emission controls will largely affect only the fraction of light extinction that is due to fine particles. (Actually, SO_2 controls will also affect sulfate-containing coarse particles, but, in general, with negligible associated visibility improvements.)

2. The fine particle aerosol is composed of sulfate-containing particles and of particles containing other species (but no sulfates).

SO_2 emission controls will affect only the fraction of the fine particles that contains sulfates. (Actually, SO_2 controls may increase the concentration of nonsulfate particles such as nitrate and chloride; see Pilinis (1989).)

3. Fine sulfur-containing particles are a fraction of the total concentration of sulfur in the atmosphere in both gaseous and particulate form. They are produced mostly by SO_2-to-SO_4^{2-} chemical transformations that appear to be nonlinear. Therefore, although SO_2 emission controls will decrease proportionately the total ambient sulfur along the trajectories of plumes from controlled regions, the fine sulfates may decrease to a lesser extent because of the nonlinear chemistry.

4. Total ambient sulfur in one geographical area is due to both local emissions and sulfur transported from other regions. SO_2 emission controls will affect only the fraction of sulfur that is transported from the regions affected by the control scenario.

Because of these four factors, the percent of visibility improvement (e.g., the percentage improvement of visual range) is expected to be much less than the percent reduction of SO_2 emissions.

Another complication is caused by the role of water adsorbed by both sulfate and nonsulfate particles. This adsorbed water affects visibility by increasing the mass of fine particles and, consequently, the atmospheric light extinction. However, the water mass is generally unknown, since fine particles are measured at a low relative humidity RH_o (e.g., $RH_o \simeq 0.4$), where most of the water is removed from the particles collected on the ambient sampling filters.

Since fine particle concentrations (F) are the sum of sulfate (SO_4)(*) and nonsulfate (NS) species, a simple mechanism for evaluating the role of adsorbed water (Cass, 1979; Tang et al., 1981; Appel et al., 1985) is given by

$$F^{(w)} = K_s\, SO_4 + K_{ns}\, NS \qquad (13\text{-}5)$$

(*) Here we use SO_4 instead of SO_4^{2-} to indicate that the entire sulfate particle (i.e., NH_4HSO_4 or $(NH_4)_2SO_4$, not just the anion SO_4^{2-}, must be accounted for in computing the fine particle concentration. This distinction is important since most aerosol measurements provide the sulfate SO_4^{2-} concentration only.

where $F^{(w)}$ is the concentration of fine particles including adsorbed water. K_s (a term greater than one) represents a suitable "amplification" of the SO_4 concentration to allow for the adsorbed water and, in a similar way, K_{ns} represents the increase for the concentration NS of nonsulfate particles, where

$$K_s = \left(\frac{1 - RH_o}{1 - RH}\right)^{\beta_s} \tag{13-6}$$

and

$$K_{ns} = \left[h_{ns}\left(\frac{1 - RH_o}{1 - RH}\right)^{\beta_{ns}} + (1 - h_{ns})\right] \tag{13-7}$$

In the formulas above, RH is the ambient relative humidity, h_{ns} is the fraction of NS that is hygroscopic, and β_s, β_{ns} are exponents that need to be evaluated ($\beta = 1$ or 2 have often been chosen). More complex modeling techniques can be used to calculate more precise values of K_s and K_{ns}. For example, Pilinis and Seinfeld (1987) developed and tested a computer code that performs a chemical equilibrium calculation in the sulfate, nitrate, chloride, sodium, ammonium and water system. This code successfully predicted the concentrations of various aerosol species at Long Beach, California. Its application, however, requires detailed air quality and meteorological information that is often unavailable on a regional and annual average basis. Hence, semiempirical relations such as Equations 13–6 and 13–7 must, at least at the present time, be used.

13.2 CO_2 ACCUMULATION AND THE "GREENHOUSE" EFFECT

More carbon dioxide (CO_2) is emitted by anthropogenic processes than any other substance. CO_2 does not show adverse effects to the earth ecology. Several studies, however, point out that CO_2 strongly adsorbs electromagnetic radiation at a wavelength of about 15 μm, which corresponds to the maximum intensity of the earth radiation (the atmosphere and the CO_2 are transparent to the sun's radiation, which heats the earth's surface, but about 30 percent of the sun's radiation is reflected into space). Therefore, an increase of CO_2 in the global atmosphere can trigger a general increase of the earth's temperature, an effect that has been called the "greenhouse" effect.

CO_2 measurements indeed show a constant accumulation pattern. Current CO_2 concentrations (above 340 ppm) tend to increase by 1 ppm per year (see Figure 13-3). With the continuous industrial and urban development expected in the next decades, CO_2 concentrations could easily reach, in the next century, values two to three times the current ones (i.e., between 600 and 1,000 ppm).

Several models forecast the meteorological consequences of these possible CO_2 increases. Manabe and Wetherald (1975) predict that a CO_2 concentration of 600 ppm should increase the average temperature of the earth of about 2-3°C with maxima of about 7-10°C at high latitudes. The consequent (Mercer, 1978) melting of the polar glaciers would cause a 5 m increase of the mean sea level. Coastal cities and large sections of Holland and Florida would be covered by

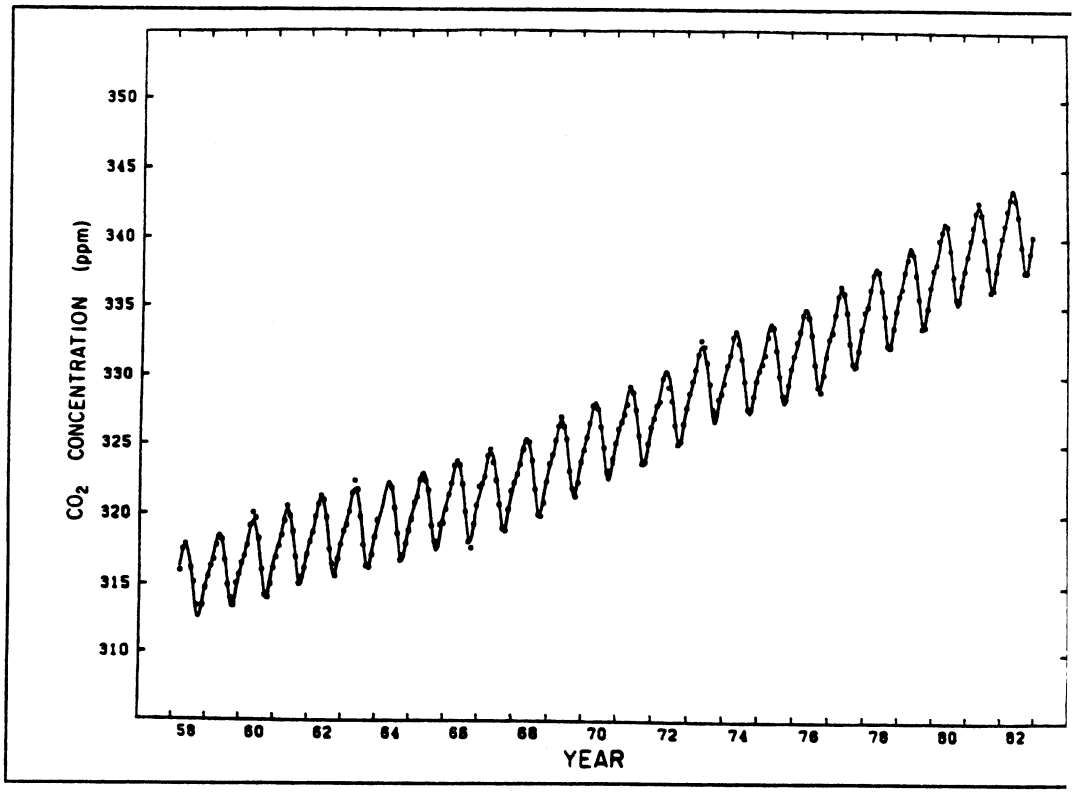

Figure 13-3. Concentrations of atmospheric CO_2 at Mauna Loa Observatory, Hawai pressed as a mole fraction in parts per million of dry air. The dots monthly averages. Selected data have been adjusted to the center of each m The curve represents the fit simultaneously to an exponential function, a function and a linearly increasing seasonal cycle (from Bacastow et al., 1 [Reprinted with permission from the American Geophysical Union.]

water. The above simulations have been confirmed by other studies (Schneider, 1975; Manabe and Wetherald, 1980).

The temperature measurements on the earth, however, have not shown the same systematic increase as the CO_2 concentration, even though worldwide high temperatures in 1988 could be a first measureable sign of the greenhouse effect. On the contrary, the earth's average temperature, after a constant slow increase between 1880 and 1940, decreased in the following 40 years by more than half a degree. These latter data can be interpreted in several ways:

1. CO_2 increase is not, due to "feedback" effects (Newell and Dopplick, 1979), really affecting the earth's temperature.

2. The earth's temperature is mainly controlled by variations in the solar radiation (e.g., the Gleissberg cycle, of about 90 years, in the solar activity; Agee, 1980).

3. Increasing concentrations of anthropogenic particles in the atmosphere are increasing the albedo (i.e., the fraction of solar radiation directly reflected by the atmosphere into the space), thus reducing the fraction of the incoming solar radiation that heats the earth's surface.

4. The effects of the CO_2 increase are not yet noticeable.

CO_2 is not the only trace gas that can cause the greenhouse effect. Other trace gases contribute, as shown in Table 13–1, which illustrates trace gas concentrations and trends (observed trends and projected mid–21st century values). Hansen et al. (1988) used a three-dimensional climate model to simulate the combined global climate effects of time-dependent variations of trace atmospheric gases (CO_2, CH_4, N_2O, CFCs) and aerosols. Among their several conclusions is that the greenhouse effect should be clearly identifiable (i.e., measureable) in the 1990s and that temperature changes will be sufficiently large to have major impacts, especially in the frequency of occurrence of extreme events.

Additional discussion of the CO_2 problem can be found in articles by Idso (1984) and Hileman (1984). Overviews of research activities in this field are discussed by Riches et al. (1985) and Lal and Jain (1989). It must be pointed out that trace gas accumulation is just one of many factors affecting global scale climate. Figure 13–4 illustrates a reconstruction of the mean global temperature in the last 150,000 years. We are currently in the middle of an interglacial period, which should be followed by a natural cooling, unless CO_2 accumulation induces a "superinter-glacial" period.

Table 13-1. Trace gas concentrations and trends: observed and projected. The concentrations are from Dickinson and Cicerone (1986); the decadal trends for 1975 to 1985, showing the percentage of increase in concentrations, are from Rasmussen and Khalil (1986). (From Ramanathan, 1988). [Reprinted with permission from the American Association for the Advancement of Science.]

Gas	Concentrations		Observed trends for 1975–1985 (%)	Mid-21st century
	Pre-1850	1985		
CO_2	275 ppmv	345 ppmv	4.6	400–600 ppmv
CH_4	0.7 ppmv	1.7 ppmv	11.0	2.1–4 ppmv
N_2O	0.285 ppmv	0.304 ppmv	3.5	0.35–0.45 ppmv
CFC-11	0	0.22 ppbv	103.0	0.7–3.0 ppbv
CFC-12	0	0.38 ppbv	101.0	2.0–4.8 ppbv
Tropospheric O_3 * (below 12 km)		10–100 ppbv		
CH_3CCl_3	0	0.13 ppbv	155.0	
CCl_4	0	0.12 ppbv	24.0	

*Values (below 9 km) for before 1850 are 0 to 25% less than present-day; values (below 12 km) predicted for mid-21st century are 15 to 50% higher.

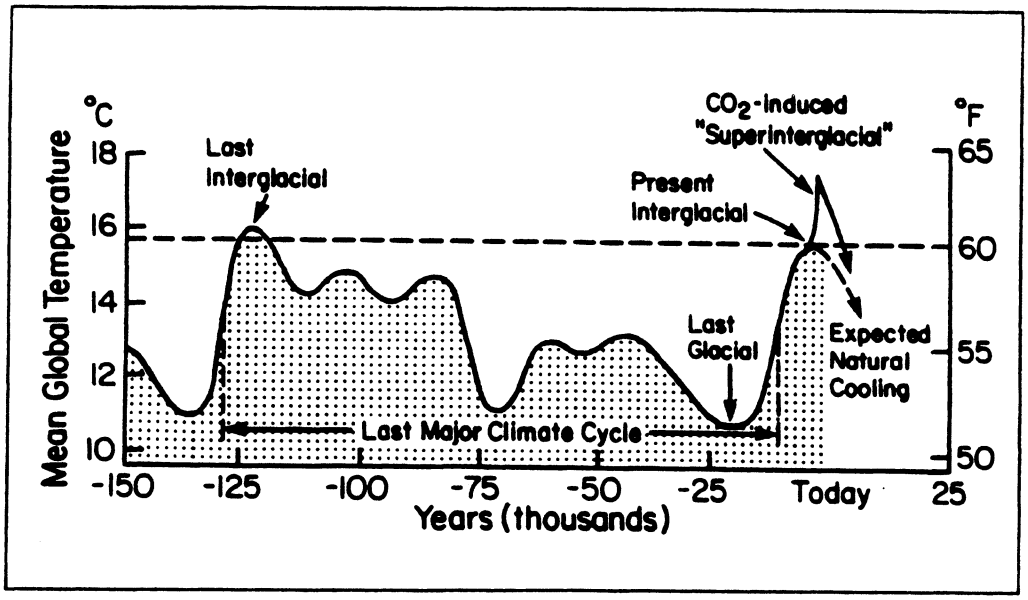

Figure 13-4. Potential effect of carbon dioxide on global climate (from Urone, in Stern, 1986). [Reprinted with permission from Academic Press.]

13.3 STRATOSPHERIC OZONE

The lower stratosphere (i.e., between an altitude of 10 and 20 km) contains an ozone layer that absorbs an appreciable part of the ultraviolet (UV) energy of the solar radiation. Without this ozone layer, the sea-level component of light that directly causes sunburn (erythema), a narrow spectral range centered at 0.297 μm, would increase its intensity, causing, among other things, an increase in the incidence of skin cancer.

Combustion products from high altitude aircraft and missiles constitute a threat to the ozone shield. In particular, *NO* emissions (Dobbins, 1979) enter the cycle

$$NO + O_3 \rightarrow NO_2 + O_2 \qquad (13\text{–}8)$$

$$NO_2 + O \rightarrow NO + O_2 \qquad (13\text{–}9)$$

and consume ozone and the oxygen free radicals in a "catalytic" sequence (i.e., without *NO* destruction). Another catalytic sequence is generated by the hydroxyl *OH*, which is also a product of combustion.

Another chemical threat to stratospheric ozone is posed by compounds that are emitted from human activities at the earth's surface, but that may diffuse to the stratosphere due to their extended lifetime. For example, halocarbons, such as CFC-11 ($CFCl_3$) and CFC-12 (CF_2Cl_2), undergo photolitic decomposition in the stratosphere because of the ultraviolet intensity. This generates atomic chlorine *Cl*, which enters the cycle (Dobbins, 1979)

$$Cl + O_3 \rightarrow ClO + O_2 \qquad (13\text{–}10)$$

$$ClO + O \rightarrow Cl + O_2 \qquad (13\text{–}11)$$

and consumes both O_3 and O in a catalytic sequence (*Cl* is not consumed).

Recent observations of global ozone concentrations have revealed the following aspects of the phenomenon (Tung and Yang, 1988):

1. The year-to-year decline of the October ozone minimum over Antarctica is associated with a decline of the midlatitude ozone maximum.
2. These declines appear to be associated with a cooling of the lower stratosphere in middle and high latitudes.

3. The interannual October mean column ozone changes over Antarctica appear to follow a quasibiennial oscillation. This variation is in phase with the tropical oscillation of the east–west wind.

4. The seasonal spring deepening of the minimum column ozone appears to be associated with an intensification of the surrounding maximum in midlatitudes.

5. There is spatial correlation between total ozone patterns and temperature distributions in the lower stratosphere.

6. In November, the Antarctic ozone hole is filled in.

Initial modeling simulation (NAS Report, 1979) indicated an expected decrease of stratospheric ozone by −1.5 percent (±1.1 percent) during the period 1970–1978. However, this decrease was not confirmed by ozone measurements during the same period (Reinsel et al., 1981).

More recent data have shown alarming results. For example (Bornstein, 1986a), the British Antarctic Survey measured 0.32 cm of ozone above their station in Antarctica in 1957, 0.32 cm in 1970, 0.30 cm in 1980, 0.24 cm in 1980 and only 0.20 cm in 1984. These data, among others, seem to indicate a deepening of the Antarctic ozone hole, a phenomenon that many theories suggest can be related to the release of the chlorine in fluorocarbons.

Recent results from the Ozone Trend Panel(*) (Kerr, 1988) indicate that, after a large reanalysis of the ozone measurements collected in the last 17 years, the stratospheric ozone is indeed decreasing, sometimes even faster than previously predicted. This decrease, which is shown in Figure 13–5, indicates a year–round effect. These new data and data elaboration strongly indicate anthropogenic chlorine as primarily responsible and raise questions about the sufficiency of the proposed production controls (50 percent) on chlorofluorocarbons (CFCs).

Tung and Yang (1988) have made comprehensive modeling simulations of changes in Antarctic and global ozone. Their simulations have been successful in reproducing the quasibiennial signal in the year-to-year variations. They conclude that atmospheric dynamics is an important component of the phenomenon, even through not the sole cause of the Antarctic ozone hole, since ozone depletion seems more severe than can be accounted for by pure advection phenomena.

(*) A creation of NASA in colloboration with the National Oceanic and Atmospheric Administration, the Federal Aviation Administration, the World Meteorological Organization, and the United Nations Environment Program.

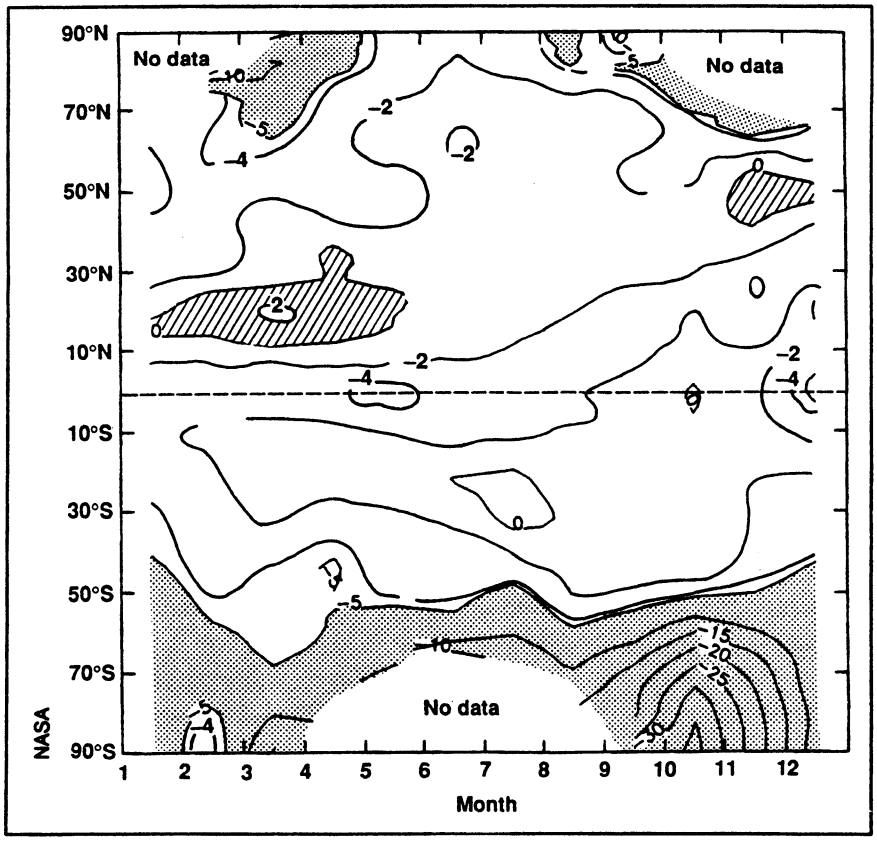

Figure 13–5. The decrease of stratospheric ozone. This is a plot of the percent change in total ozone from 1979–80 to 1986–87 as determined by the satellite-borne Total Ozone Mapper Spectrometer. The tendency toward larger losses at higher, colder latitudes and colder seasons is apparent. The Antarctic ozone hole is in the lower right (from Kerr, 1988). [Reprinted with permission from the American Association for the Advancement of Science.]

13.4 NUCLEAR WINTER

The meteorological effects of a major nuclear exchange have been a subject of debate in the last few years. Crutzen and Birk (1982) first recognized that large fires following a nuclear war may inject large amounts of particles into the atmosphere, whose absorption of the sunlight could generate a substantial and prolonged decrease of earth's temperatures, i.e., a nuclear winter. This suggestion was elaborated by Turco et al. (1983) in what is known as the TTAPS study

(from the initials of the authors). Their conclusion, using a one-dimensional model, was dramatic: a decrease of 30–40°C in land surface temperatures.

More recent simulations using two- and three-dimensional models have provided contradictory results. For example, Malone et al. (1986), using a three-dimensional global model, simulated 1) localized injection of smoke, 2) wind transport, 3) sunlight absorption, and 4) precipitation removal. They found an even longer-lasting "nuclear winter," due to higher residence time than that normally assumed for the troposphere. However, in contrast with the TTAPS study, Penner et al. (1986), using a two- and three-dimensional model, concluded that little smoke is expected to be injected into the stratosphere, even for very intense fires. They also pointed out that, for intense fires, significant amounts of water vapor are condensed, raising the possibility of early scavenging of smoke particles by precipitation.

Mitchell and Slingo (1988) improved the calculations of the climatic effects of nuclear war by including two important phenomena that were not treated by previous studies: 1) the diurnal cycle of insolation and 2) surface and boundary layer parameterizations, including a four-layer soil model. The results did not change much, since the errors caused by neglecting the two phenomena above were approximately equal and opposite.

It can be concluded (Mitchell and Slingo, 1988; Bornstein, 1986b) that the greatest uncertainty in the "nuclear winter" theory is in the amount of smoke and dust that would be injected into the atmosphere and the parameterization of the deposition phenomena. A typical emission scenario is 180 Tg (million metric tons) of soot. With this emission, virtually all models agree that the sunlight will be blocked. The disagreement is about how cold it would get and for how long. Reviews of the atmospheric effects of a nuclear war are presented by Colbeck and Harrison (1986) and Colbeck (1989).

REFERENCES

Agee, E. (1980): Present climatic cooling and a proposed causative mechanism. *J. Climate and Appl. Meteor.*, **61**:1356–1367.

Appel, B.R., Y. Tokiwa, J. Hsu, E.L. Kothny, and E. Hahn (1985): Visibility as related to atmospheric aerosol constituents. *Atmos. Environ.*, **19**(9):1525–1534

Bacastow, R.B., C.D. Keeling, and T.P. Whorf (1985): Seasonal amplitude increase in atmospheric CO_2 concentration at Mauna Loa, Hawaii, 1959–1982. *J. Geophys. Res.*, **90**:10,529–10,540.

Bornstein, R.D. (1986a): Interview of Brian Toon. *Environ. Software*, **1**(3):189.

Bornstein, R.D. (1986b): Interview of Alan Robock. *Environ. Software*, **1**(2):132.

Cass, G.R. (1979): On the relationship between sulfate in air quality and visibility with examples in Los Angeles. *Atmos. Environ.*, **13**:1069–1084.

Colbeck, I., and R.M. Harrison (1986): The atmospheric effects of nuclear war — A review. *Atmos. Environ.*, **20**(9):1673–1681.

Colbeck, I. (1989): Atmospheric effects of nuclear war. *Encyclopedia of Environmental Control Technology. Vol. 2, Air Pollution Control,* edited by P.W. Cheremisinoff. Houston, Texas: Gulf Publishing.

Crutzen, P.J., and J.W. Birks (1982): The atmosphere after nuclear war: Twilight at noon. *Ambio*, **11**:114–125.

Dickinson, R.E., and R.J. Cicerone (1986): *Nature*, **319**:109.

Dobbins, R.A. (1979): *Atmospheric Motion and Air Pollution*. New York: John Wiley & Sons.

Drivas, P.J., A. Bass, and D.W. Heinold (1984): A plume blight visibility model for regulatory use. *Atmos. Environ.*, **15**:2179–2184.

Eltgroth, M.W., and P.V. Hobbs (1979): Evolution of particles in the plumes of coal-fired power plants, II. A numerical model and comparison with field measurements. *Atmos. Environ.*, **13**:953–976.

Ferman, M.A., G.T. Wolff and N.A. Kelly (1981): The nature and sources of haze in the Shenandoah Valley/Blue Ridge Mountain Area. *JAPCA*, **31**:1074–1081.

Hansen, J., I. Fung, A. Lacis, D. Rind, S. Lebedeff, R. Ruedy, G. Russell, and P. Stone (1988): Global climate changes as forecast by Goddard Institute for Space Studies three-dimensional model. *J. Geophys. Res.*, **93**:9341–9364.

Hileman, B. (1984): Recent reports on the greenhouse effect. *Environ. Sci. & Technol.*, **18**:45A–46A.

Idso, S.B. (1984): A review of recent reports dealing with the greenhouse effect of atmospheric carbon dioxide. *JAPCA*, **34**:553–555.

Kerr, R.A. (1988): Stratospheric ozone is decreasing. *Res. News, Science*, **239**:1489–1491.

Lal, M., and A.K. Jain (1989): Increasing anthropogenic constituents in the atmosphere and associated climatic changes. *Encyclopedia of Environmental Control Technology. Vol. 2, Air Pollution Control,* edited by P.W. Cheremisinoff. Houston Texas: Gulf Publishing.

Latimer, D.A., and G.S. Samuelsen (1978): Visual impact of plumes from power plants: A theoretical model. *Atmos. Environ.*, **12**:1455–1465.

Latimer, D.A., R.W. Bergstrom, C.D. Johnson, and J.P. Killus (1980): Visibility modeling. Paper presented at the American Meteorological Society/Air Pollution Control Association 2nd Joint Conference on Applications of Air Pollution Meteorology, New Orleans, Louisiana, March.

Latimer, D.A., and H. Hogo (1987): The relationship between SO_2 emissions and regional visibility in the eastern United States. *Proceedings,* APCA Specialty Conference "Visibility Protection: Research and Policy Aspects." Grand Teton National Park, Wyoming, September 1986.

Latimer, D.A., and R.G. Ireson (1988): Workbook for plume visual impact screening and analysis. Systems Applications, Inc., Report SYSAPP–88/121, prepared for the National Park Service and the U.S. Environmental Protection Agency.

Lipfert, F.W. (1985): *Environ. Sci. & Technol.*, **19**(9):764–770.

Malone, R.C., L.H. Auer, G.A. Glatzmaier, M.C. Wood, O.B. Toon (1986): Nuclear winter: Three–dimensional simulations including interactive transport, scavenging and solar heating of smoke. *J. Geophys. Res.*, **91**:1039–1053.

Manabe, S., and R.T. Wetherald (1975): The effects of doubling CO_2 concentration on the climate of a general circulation model. *J. Atmos. Sci.*, **32**:3–15.

Manabe, S., and R.T. Wetherald (1980): On the distribution of climate change resulting from an increase in CO_2 content of the atmosphere. *J. Atmos. Sci.*, **37**:99–118.

McLaughlin, S.B. (1985): Effects of air polution on forests: A critical review. *JAPCA*, **35**(5): 512–534.

Mercer, J.H. (1978): West Antarctic ice sheet and CO_2 greenhouse effect: A threat of disaster. *Nature*, **271**:321–325.

Mitchell, J.F., and A. Slingo (1988): Climatic effects of nuclear war: The role of atmospheric stability and ground heat fluxes. *J. Geophys. Res.*, **93**:7037–7045.

NAS (National Academy of Sciences) (1979): Stratospheric ozone depletion by halocarbons: Chemistry and transport. National Reseach Council, Washington, D.C.

Newell, R.E., and T.G. Dopplick (1979): Questions concerning the possible influence of anthropogenic CO_2 on atmospheric temperature. *J. Appl. Meteor.*, **18**:822–825.

Penner, J.E., L.C. Haselman, Jr., and L.L. Edwards (1986): Smoke–plume distributions about large–scale fires: Implications for simulations of "nuclear war." *J. Climate and Appl. Meteor.*, **25**:1434–1444.

Pilinis, C., and J.H. Seinfeld (1987): Continued development of a general equilibrium model for inorganic multicomponent atmospheric aerosols. *Atmos. Environ.*, **21**:2453–2466.

Pilinis, C. (1989): Numerical simulation of visibility degradation due to particulate matter: Model development and evaluation. *J. Geophys. Res.*, **94**(D7):9937–9946.

Poostchi, E., A.W. Gnyp, and C.C. St. Pierre (1986): Comparison of models used for the determination of odor thresholds. *Atmos. Environ.*, **20**(12):2459–2464.

Ramanathan, V. (1988): A greenhouse theory of climate change: A test by an inadvertent global experiment. *Science*, **240**:293

Rasmussen, R.A., and M.A. Khalil (1986): *Science*, **232**:1623.

Reinsel, G., G.C. Tiao, M.N. Wang, R. Lewis, and D. Nychka (1981): Statistical analysis of stratospheric ozone data for the detection of trends. *Atmos. Environ.*, **15**:1569–1577.

Riches, M.R., and F.A. Koomanoff (1985): Overview of the Department of Energy carbon dioxide research program. *J. Climate and Appl. Meteor*, **66**:152–158.

Schneider, S.H. (1975): On the carbon dioxide–climate confusion. *J. Atmos. Sci.*, **32**:2060–2066.

Stern, A.C., Ed. (1977): *Air Pollution*, 3rd Edition, Volume II. New York: Academic Press.

Stern, A.C., Ed. (1986): *Air Pollution*, 3rd Edition, Volume VI. New York: Academic Press.

Stevens, R.K., T.G. Dzubay, C.W. Lewis, and R.W. Shaw (1984): Source apportionment methods applied to the determination of the origin of ambient aerosols that affect visibility in forested areas. *Atmos. Environ.*, **18**:261–272.

Systems Applications, Inc. (1984): Visibility and other air quality benefits of sulfur dioxide emission controls in the Eastern United States, Vol. I. SAI Draft Report SYSAPP–84–165, San Rafael, California.

Tang, I.N., W.T. Wong, and H.R. Munkelwitz (1981): The relative importance of atmospheric sulfates and nitrates in visibility reduction. *Atmos. Environ.*, **15**(12):2463–2471.

Tombach, I. (1982): Measurement of local climatological and air pollution factors affecting stone decay. From *Conservation of Historic Stone Buildings and Monuments*. National Academic Press, Washington, DC.

Tombach, I., and D. Allard (1983): Visibility measurement techniques intercomparison in the Eastern United States. AeroVironment Report AV–FR–83/509, Monrovia, California.

Tung, K.K, and H. Yang (1988): Dynamical component of seasonal and year-to-year changes in Antarctic and global ozone. *J. Geophys. Res.*, **93**:12,537–12,559.

Turco, R., O.B. Toon, T. Ackerman, J.B. Pollack, and C. Sagan (1983): Nuclear winter: Global consequences of multiple nuclear explosions. *Science*, **222**:1283–1292.

Weiss, R.W., T.V. Larson, and A.P. Waggoner (1982): In situ rapid-response measurement of $H_2SO_4/(NH_4)_2SO_4$ aerosols in rural Virginia. *Environ. Sci. & Technol.*, **16**:525–532.

White, W.H. (1984): An intercomparison of plume visibility models with VISTTA observations at the Navajo Generating Station. American Petroleum Institute final report, Washington, D.C.

Williams, M.D., E. Treiman, and M. Wecksung (1980): Plume blight visibility modeling with a simulated photograph technique. *JAPCA*, **30**:131–134

Williams, M.D., L.Y. Chan, and R. Lewis (1981): Validation and sensitivity of a simulated-photograph technique for visibility modeling. *Atmos. Environ.*, **15**:2151–2170.

Zannetti, P., I. Tombach, and S. Cvencek (1988): Semiempirical analysis of the visibility improvements from SO_2 emission controls in the eastern United States. *Proceedings*, 81st APCA Annual Meeting. Dallas, Texas. June 19–24.

14 AVAILABLE COMPUTER PACKAGES

Many computer programs have been developed for meteorological and air quality simulations. Some of them, generally the simplest, are well documented and relatively easy to use. Most of them, however, require users with good technical skills and, often, the supervision of the developers of the codes.

Readers that desire to be informed about air pollution and meteorological software are encouraged to use, among others, the following sources of information.

- New software, for air pollution and hazardous waste problems, is reviewed each month in the *Journal of the Air Pollution Control Association*, (now the *Journal of the Air and Waste Management Association*, P.O. Box 2861, Pittsburgh, Pennsylvania 15230, USA).
- The European Association for the Science of Air Pollution (EURASAP) prints a monthly newsletter dealing with conferences, air pollution modeling and other topics. The newsletter is edited by Prof. P.J.H. Builtjes, MT-TNO, P.O. Box 342, 7300 AH Apeldoorn, The Netherlands.
- A monthly *Environmental Software* report is published by Donley Technology, P.O. Box 335, Garrisonville, Virginia 22463, USA. It presents a summary of software tools in environmental studies, especially for U.S. regulatory applications. The same group has published the *1989 Environmental Software Directory.*
- The California Air Resources Board publishes the *Modeling Center News*, dealing mostly with air pollution issues in California (contact Terry McGuire, Chief, Technical Support Division, Air Resources Board, P.O. Box 2815, Sacramento, California 95812, USA.
- New software is presented in the quarterly journal *Environmental Software* (published by Computational Mechanics Publications, Ashurst Lodge, Ashurst, Southampton SO4 2AA, UK.
- An annual environmental software review is presented in the January issue of the *Pollution Engineering* journal (1935 Shermer Road, Northbrook, Illinois 60062, USA).

Selected meteorological and air quality packages are discussed in the sections below. The reader is also referred to Appendix B, Part 2, and Appendix C of Roth et al. (1988) for a comprehensive compendium of air quality models.

14.1 U.S. EPA MODELS AND UNAMAP(*)

In the last fifteen years in the United States, air quality models have been systematically used as official decision-making tools for State Implementation Plan (SIP) revisions for existing sources and new source reviews, including those activities related to Prevention of Significant Deterioration (PSD). The U.S. Environmental Protection Agency (U.S. EPA) has periodically provided guidelines and recommendations to identify for all interested parties, those techniques and data bases it considers acceptable (U.S. EPA, 1978, 1984, 1986, and 1987).

Many of the models the U.S. EPA recommends are available as part of UNAMAP (Version 6) (see Turner et al., 1989), and can be obtained from the U.S. EPA's Support Center for Regulatory Air Models Bulletin Board System (SCRAM-BBS) by dialing in on the Bulletin Board number (919) 541-5742. Alternatively, the models can be obtained on a 9-track magnetic tape from

Computer Products
National Technical Information Service
U.S. Department of Commerce
Springfield, VA 22161
Phone: (703) 487-4650

The U.S. EPA divides the air quality models into four generic classes:

1. Gaussian
2. numerical
3. statistical or empirical
4. physical

Gaussian models, which are the most widely used, are recommended for estimating the impact of nonreactive pollutants. Numerical models (i.e., grid models or box models) are suggested for urban applications involving reactive pollutants (e.g., photochemical smog). Other models can be used for particular applications. Moreover, the models are categorized by two levels of sophistication:

(*) The text in this section is taken from the U.S. EPA (1986 and 1987).

- Screening techniques (or screening models). These are relatively simple estimation techniques that provide *conservative* estimates of air quality impacts. They can, in several cases, eliminate from further consideration those sources that clearly do not contribute to ambient concentrations.
- Refined models. These provide a more detailed treatment of physical and chemical processes, require more detailed and precise input data, have higher computational costs, and provide (at least theoretically) a more accurate estimate of the source impact and the effectiveness of different control strategies.

The U.S. EPA also divides the air quality models recommended in its guideline into "preferred" and "alternative" models. Preferred models are those that EPA either found to perform better than others in a given category, or chose on the basis of other factors such as fast use, public familiarity, cost or resource requirements, and availability. These preferred models can be used for regulation applications without a formal demonstration of applicability, as long as they are used as indicated by the U.S. EPA (1986 and 1987). Alternative models can be used when (1) a demonstration can be made that the model produces concentration estimates equivalent to the estimates obtained using a preferred model; (2) a statistical performance evaluation has been conducted using measured air quality data and the results of that evaluation indicate the alternative model performs better for the application than a comparable preferred model; (3) there is no preferred model for the specific application but a refined model is needed to satisfy regulatory requirements.

The U.S. EPA constantly solicits new refined models that are based on sounder scientific principles and that are more reliable in estimating pollutant concentrations. Models that are submitted in accordance with the EPA's requirements will be evaluated as submitted. These requirements are

- The model must be computerized and functioning in a common FORTRAN language suitable for use on a variety of computer systems.
- The model must be documented in a user's guide that identifies the mathematics of the model, data requirements and program operating characteristics at a level of detail comparable to that available for currently recommended models, e.g., the Single Source (CRSTER) Model.

- The model must be accompanied by a complete test data set, including input parameters and output results. The test data must be included in the user's guide as well as provided in computer-readable form.
- The model must be useful to typical users, e.g., state air pollution control agencies, for specific air quality control problems. Such users should be able to operate the computer program(s) from available documentation.
- The model documentation must include a comparison with air quality data or with other well-established analytical techniques.
- The developer must be willing to make the model available to users at reasonable cost or make it available for public access through the SCRAM-BBS or the National Technical Information Service; the model cannot be proprietary.

14.1.1 The EPA's Preferred Models

The U.S. EPA preferred air quality models are (U.S. EPA, 1986 and 1987)

- Buoyant Line and Point Source Dispersion Model (BLP)
- CALINE 3
- Climatological Dispersion Model (CDM 2.0)
- Gaussian-Plume Multiple Source Air Quality Algorithm (RAM)
- Industrial Source Complex Model (ISC)
- Multiple Point Gaussian Dispersion Algorithm with Terrain Adjustment (MPTER)
- Single Source Model (CRSTER)
- Urban Airshed Model (UAM)
- Offshore and Coastal Dispersion Model (OCD)

A brief description of each of the above models is presented below.

- **Buoyant Line and Point Source Dispersion Model (BLP)**

Reference: Schulman, L.L., and J.S. Scire (1980): *Buoyant Line and Point Source (BLP) Dispersion Model User's Guide*. Document P-7304B. Environmental Research and Technology, Inc., Concord, Massachusetts. (NTIS PB81-164642)

Availability: This model is available as part of UNAMAP (Version 6).

Abstract: BLP is a Gaussian plume dispersion model designed to handle unique modeling problems associated with aluminum reduction plants and other industrial sources where plume rise and downwash effects from stationary line sources are important.

Recommendations for Regulatory Use: The BLP model is appropriate for the following applications:

- aluminum reduction plants that contain buoyant, elevated line sources
- rural area
- transport distances less than 50 kilometers
- simple terrain
- one-hour to one-year averaging times.

- **CALINE 3**

Reference: Benson, P.E. (1979): *CALINE 3 – A Versatile Dispersion Model for Predicting Air Pollutant Levels Near Highways and Arterial Streets.* Interim report FHWA/CA/TL-79/23. Federal Highway Administration, Washington, D.C. (NTIS PB80-220841)

Availability: The CALINE 3 model computer tape is available from NTIS as PB80-220833. The model is also available from the California Department of Transportation (manual free of charge and approximately $50 for the computer tape). Requests should be directed to

Mr. Marlin Beckwith
Chief, Office of Computer Systems
California Department of Transportation
1120 N. Street
Sacramento, CA 95814

Abstract: CALINE 3 can be used to estimate the concentrations of nonreactive pollutants from highway traffic. This steady-state Gaussian model can be applied to determine air pollution concentrations at receptor locations downwind of "at-grade," "fill," "bridge," and "cut section" highways located in relatively uncomplicated

terrain. The model is applicable for any wind direction, highway orientation, and receptor location. The model has adjustments for averaging time and surface roughness and can handle up to 20 links and 20 receptors. It also contains an algorithm for deposition and settling velocity so that particulate concentrations can be predicted.

Recommendations for Regulatory Use: CALINE 3 is appropriate for the following applications:

- highway (line) sources
- urban or rural areas
- simple terrain
- transport distances less than 50 kilometers
- one hour to 24 hours averaging times

- **Climatological Dispersion Model (CDM 2.0)**

References: Irwin, J.S., T. Chico, and J. Catalano (1985): *CDM 2.0 – Climatological Dispersion Model – User's Guide*. U.S. Environmental Protection Agency, Research Triangle Park, North Carolina. (NTIS PB86-136546)

Availability: This model is available as part of UNAMAP (Version 6).

Abstract: CDM is a climatological steady-state Gaussian plume model for determining long-term (seasonal or annual) arithmetic average pollutant concentrations at any ground-level receptor in an urban area.

Recommendations for Regulatory Use: CDM is appropriate for the following applications:

- point and area sources
- urban areas
- flat terrain
- transport distances less than 50 kilometers
- long-term averages over one month to one year or longer

- **Gaussian-Plume Multiple Source Air Quality Algorithm (RAM)**

References: Turner, D.B., and J.H. Novak (1978): *User's guide for RAM*. Publication EPA-600/8-78-016 Vols. A and B. U.S. Environmental Protection Agency, Research Triangle Park, North Carolina. (NTIS PB294791 and PB294792).

Catalano, J.A., D. B. Turner, and H. Novak (1987): *User's Guide for RAM, Second Edition*. U.S. Environmental Protection Agency, Research Triangle Park, North Carolina. (Distributed as part of UNAMAP, Version 6, documentation.)

Availability: This model is available as part of UNAMAP (Version 6).

Abstract: RAM is a steady-state Gaussian plume model for estimating concentrations of relatively stable pollutants, for averaging times from an hour to a day, from point and area sources in a rural or urban setting. Level terrain is assumed. Calculations are performed for each hour.

Recommendations for Regulatory Use: RAM is appropriate for the following applications:

- point and area sources
- urban areas
- flat terrain
- transport distances less than 50 kilometers
- one-hour to one-year averaging times

- **Industrial Source Complex Model (ISC)**

Reference: Environmental Protection Agency (1986): *Industrial Source Complex (Isc) Dispersion Model User's Guide*, Second Edition, Volumes 1 and 2. Publications EPA-450/4-86-005a, and -005b. U.S. Environmental Protection Agency, Research Triangle Park, North Carolina. (NTIS PB86-234259 and PB86-234267)

Environmental Protection Agency (1987): *Industrial Source Complex (ISC) Dispersion Model. Addendum to the User's Guide*. U.S. Environmental Protection Agency, Research Triangle Park, North Carolina.

Availability: This model is available as part of UNAMAP (Version 6).

Abstract: This ISC model is a steady-state Gaussian plume model that can be used to assess pollutant concentrations from a wide variety of sources associated with an industrial source complex. This model can account for the following: settling and dry deposition of particulates; downwash; area, line and volume sources; plume rise as a function of downwind distance; separation of point sources; and limited terrain adjustment. It operates in both long-term and short-term modes.

Recommendations for Regulatory Use: ISC is appropriate for the following applications:

- industrial source complexes
- rural or urban areas
- flat or rolling terrain
- transport distances less than 50 kilometers
- one-hour to annual averaging times

- **Multiple point Gaussian Dispersion Algorithm with Terrain Adjustment (MPTER)**

Reference: Pierce, T.D., and D.B. Turner (1980): *User's Guide for MPTER*. Publication EPA-600/8-80-016. U.S. Environmental Protection Agency, Research Triangle Park, North Carolina. (NTIS PB80-197361)

Chico, T., and J.A. Catalano (1986): *Addendum to the User's Guide for MPTER*. U.S. Environmental Protection Agency, Research Triangle Park, North Carolina 27711. (Distributed as part of UNAMAP, Version 6, documentation.)

Availability: This model is available as part of UNAMAP (Version 6).

Abstract: MPTER is a multiple point source algorithm. This algorithm is useful for estimating air quality concentrations of relatively non-reactive pollutants. Hourly estimates are made using the Gaussian steady-state model.

Recommendations for Regulatory Use: MPTER is appropriate for the following applications:

- point sources
- rural or urban areas
- flat or rolling terrain (no terrain above stack height)
- transport distances less than 50 kilometers
- one-hour to one-year averaging times

- **Single Source (CRSTER) Model**

Reference: Environmental Protection Agency (1977): *User's Manual for Single Source (CRSTER) Model.* Publication EPA-450/2-77-013. U.S. Environmental Protection Agency, Research Triangle Park, North Carolina. (NTIS PB271360)

Catalano, J.A. (1986): *Single Source (CRSTER) Model. Addendum to the User's Manual.* U.S. Environmental Protection Agency, Research Triangle Park, North Carolina 27711. (Distributed as part of UNAMAP, Version 6, documentation.)

Availability: This model is available as part of UNAMAP (Version 6).

Abstract: CRSTER is a steady-state, Gaussian dispersion model designed to calculate concentrations from point sources at a single location in either a rural or urban setting. Highest and highest second-highest concentrations are calculated at each receptor for 1-hour, 3-hour, 24-hour, and annual averaging times.

Recommendations for Regulatory Use: CRSTER is appropriate for the following applications:

- single point sources
- rural or urban areas
- flat or rolling terrain (no terrain above stack height)

- **Urban Airshed Model (UAM)**

References: Ames, J., T.C. Myers, L.E. Reid, D.C. Whitney, S.H. Golding, S.R. Hayes, and S.D. Reynolds (1985): *SAI Airshed Model Operations Manuals. Volume I, User's Manual.* Publication EPA-600/8-85-007a. U.S. Environmental Protection Agency, Research Triangle Park, North Carolina. (NTIS PB85-191567)

Ames, J.S., R. Hayes, T.C. Myers, and D.C. Whitney (1985): *SAI Airshed Model Operations Manuals. Volume II, Systems Manual.* Publication EPA-600/8-85-007b. U.S. Environmental Protection Agency, Research Triangle Park, North Carolina. (NTIS PB85-191575)

Environmental Protection Agency, 1980. *Guideline for Applying the Airshed Model to Urban Areas.* Publication EPA 450/4-80-020. U.S. Environmental Protection Agency, Research Triangle Park, North Carolina. (NTIS PB81-200529)

Availability: The computer code is available on magnetic tape from

Computer Products
National Technical Information Service
U.S. Department of Commerce
Springfield, VA 22161
Telephone: (703) 487-4650

Abstract: UAM is an urban-scale, three-dimensional, grid-type, numerical simulation model. The model incorporates a condensed photochemical kinetics mechanism for urban atmospheres. The UAM is designed for computing ozone (O_3) concentrations under short-term, episodic conditions lasting one or two days resulting from emissions of oxides of nitrogen (NO_x) and volatile organic compounds (VOC). The model treats urban VOC emissions as their carbon-bond surrogates.

Recommendations for Regulatory Use: UAM is appropriate for the following applications

- single urban areas having significant ozone attainment problems in the absence of interurban emission transport
- one-hour averaging times

- **Offshore and Coastal Dispersion Model (OCD)**

Reference: Hanna, S.R., L.L. Schulman, R.J. Paine and J.E. Pleim (1984): *The Offshore and Coastal Dispersion (OCD) Model User's Guide, Revised*. OCS Study MMS 84-0069. Environmental Research and Technology, Inc., Concord, Massachusetts (NTIS PB86-159803)

Availability: The above user's guide is available for $40.95 from NTIS. The computer tape is available from NTIS as PB85-246106 at a cost of $800. Technical contact is

Minerals Management Service
ATTN: Mitchell Baer
12203 Sunrise Valley Drive, Mail Stop 644
Reston, VA 22091

Abstract: OCD is a straight-line Gaussian model developed to determine the impact of offshore emissions from point sources on the air quality of coastal regions. OCD incorporates overwater plume transport and dispersion as well as changes that occur as the plume crosses the shoreline. Hourly meteorological data are needed from both offshore and onshore locations. These include water surface temperature, overwater air temperature, and relative humidity.

Some of the key features include platform building downwash, partial plume penetration into elevated inversions, direct use of turbulence intensities for plume dispersion, interaction with the overland internal boundary layer, and continuous shoreline fumigation.

Recommendations for Regulatory Use: The Minerals Management Service has recommended OCD for emissions located on the outer continental shelf (Federal Register 50, 12248, 28 March 1985). OCD is applicable for overwater sources where onshore receptors are below the lowest source height. Where onshore receptors are above the lowest source height, offshore plume transport and dispersion may be modeled on a case-by-case basis in consultation with the U.S. EPA regional office.

14.1.2 The EPA's Alternative Models

The U.S. EPA's list of alternative air quality models is presented below:

- Air Quality Display Model (AQDM)
- Air Resources Regional Pollution Assessment (ARRPA) Model
- APRAC-3
- AVACTA II
- COMPTER
- ERT Air Quality Model (ERTAQ)
- ERT Visibility Model
- HIWAY-2
- Integrated Model for Plumes and Atmospheric Chemistry in Complex Terrain (IMPACT)
- LONGZ
- Maryland Power Plant Siting Program Model (PPSP)
- Mesoscale Puff Model (MESOPUFF II)
- Mesoscale Transport Diffusion and Deposition Model for Industrial Sources (MTDDIS)
- Models 3141 and 4141
- MULTIMAX
- Multiple Point Source Diffusion Model (MPSDM)
- Multi-Source Model (SCSTER)
- Pacific Gas and Electric Plume 5 Model
- PLMSTAR Air Quality Simulation Model
- Plume Visibility Model (PLUVUE II)
- Point, Area, Line Source Algorithm (PAL)
- Random Walk Advection and Dispersion Model (RADM)
- Reactive Plume Model (RPM-II)
- Regional Transport Model (RTM-II)
- SHORTZ
- Simple Line-Source Model (GMLINE)

- Texas Climatological Model (TCM)
- Texas Episodic Model (TEM)

A brief description of each of these models is presented below.

- **Air Quality Display Model (AQDM)**

Reference: TRW Systems Group (1969): *Air Quality Display Model*. Prepared for National Air Pollution Control Administration, DHEW, U.S. Public Health Service, Washington, D.C. (NTIS PB189194)

Availability: The above user's guide is available from NTIS at a cost of $16.95. This model is available at no cost in the form of a punched card deck from

Library Services
MD-35
U.S. Environmental Protection Agency
Research Triangle Park, North Carolina 27711
ATTN: Ann Ingram

Abstract: AQDM is a climatological steady-state Gaussian plume model that estimates annual arithmetic average sulfur dioxide and particulate concentrations at ground level in urban areas. A statistical model based on Larsen (1971) is used to transform the average concentration data from a limited number of receptors into expected geometric mean and maximum concentration values for several different averaging times.

- **Air Resources Regional Pollution Assessment (ARRPA) Model**

Reference: Mueller, S.F., R.J. Valente, T.L. Crawford, A.L. Sparks, and L.L. Gautney, Jr. (1983): *Description of the Air Resources Regional Pollution Assessment (ARRPA) Model*. Document TVA/ONR/AQB-83/14. Tennessee Valley Authority, Muscle Shoals, Alabama.

Availability: The computer code and sample input for this model on magnetic tape and a copy of the user's guide are available from

Computer Services Development Branch
Office of Natural Resources and Economic Development
Tennessee Valley Authority
OSWHA
Muscle Shoals, AL 35660
Telephone: (205) 386-2985

A hard copy of the model output corresponding to the sample input is also available. The cost of copying model information to a buyer-supplied 2400-ft, high density tape is estimated to be about $100. The user's guide is free of charge.

Abstract: The ARRPA model is a medium/long-range segmented-plume model. It is designed to compute air concentrations and surface dry mass deposition of sulfur dioxide and sulfate. A unique feature of the model is its use of prognostic meteorological output from the National Weather Service's Boundary Layer Model (BLM). Boundary-layer conditions are computed by the BLM on a grid with a spatial resolution of 80 km, and are archived in intervals of three hours. BLM output used by this model includes three-dimensional wind field components and potential temperature at ten height levels from the surface through 2000 m above the surface.

- **APRAC-3**

Reference: Simmon, P.B., R.M. Patterson, F.L. Ludwig, and L.B. Jones (1981): *The APRAC-3/Mobile 1 Emissions and Diffusion Modeling Package*. Publication EPA 909-9-81-002. U.S. Environmental Protection Agency, Region IX, San Francisco, California. (NTIS PB82-103763)

Availability: This model is available as part of UNAMAP (Version 6).

Abstract: APRAC-3 computes hourly average carbon monoxide concentrations for any urban location. The model calculates contributions from dispersion on various scales: extraurban, from freeway, arterial, and feeder street sources; and local, from dispersion within a street canyon. It requires an extensive traffic inventory for the city of interest. APRAC-3, as it exists on UNAMAP (Version 6), has been updated with Mobile 2 emission factors.

- **AVACTA II**

Reference: Zannetti, P., G. Carboni, and R. Lewis (1985): *AVACTA II User's Guide (Release 3)*. Technical Report AV-OM-85/520, AeroVironment Inc., Monrovia, California.

Availability: A magnetic tape copy of the FORTRAN coding and the user's guide are available at a cost of $2,500 (nonprofit organization) or $3,500 (other organizations) from

AeroVironment Inc.
825 Myrtle Avenue
Monrovia, CA 91016
Telephone: (818) 357-9983

Abstract: The AVACTA II model is a Gaussian model in which atmospheric dispersion phenomena are described by the evolution of plume elements, either segments or puffs. The model can be applied for short-time (e.g., one-day) simulations in both transport and calm conditions.

The user is given flexibility in defining the computational domain, the three-dimensional meteorological and emission input, the receptor locations, the plume-rise formulas, the sigma formulas, etc. Without explicit user's specifications, standard default values are assumed.

AVACTA II provides both concentration fields on the user-specified receptor points, and dry/wet deposition patterns throughout the domain. The model is particularly oriented to the simulation of the dynamics and transformation of sulfur species (SO_2 and SO_4), but can handle virtually any pair of primary-secondary pollutants.

- **COMPTER**

Reference: State of Alabama (1980): *COMPTER Model User's Guide*. Alabama Department of Environmental Management, Air Division, Montgomery, Alabama.

Availability: This model is available to users for tape and reproduction charges. If a tape is sent, the reproduction is free. Send tape and desired format and specifications to

Mr. Richard E. Grusnick
Chief, Air Division
Alabama Department of Environmental Management
1751 Federal Drive
Montgomery, AL 36109

Abstract: COMPTER is based on the Gaussian steady-state technique applicable to both urban and rural areas. The model does the following: (a) determines maximum 24-hour, 3-hour, 1-hour and variable-hour concentrations for both block and running averages; (b) considers elevated terrain with the standard plume-chopping technique or stability dependent plume path trajectory; (c) uses annual hourly meteorological data in the CRSTER preprocessor format; (d) uses Pasquill-Gifford stability curves; (e) allows for stability class substitution in the stable categories. Typical model use is for rural areas with moderate to low terrain features.

- **ERT Air Quality Model (ERTAQ)**

Reference: Environmental Research & Technology, Inc. (1980): *ERTAQ User's Guide*. Document M-0186-001E. Environmental Research & Technology, Inc., Concord, Massachusetts.

Availability: The above report and a computer tape are available from

Computer Products
National Technical Information Service
U.S. Department of Commerce
5825 Port Royal Road
Springfield, Virginia 22161
Telephone: (703) 487-4650

Abstract: ERTAQ is a multiple point, line and area source dispersion model that uses the univariate Gaussian formula with multiple reflections.

With the fugitive dust option, entrainment of particulates from ground-level sources and subsequent deposition are accountable. The model offers an urban/rural option and calculates long-term or worst-case concentrations due to arbitrarily located sources for arbitrarily located receptors above or at ground level. Background

concentrations and calibration factors at each receptor can be user specified. Unique flexibility is afforded by postprocessing storage and manipulation capability.

- **ERT Visibility Model**

Reference: Drivas, P.J., M. Savithri, and D.W. Heinold (1980): *ERT Visibility Model, Version 3, Technical Description and User's Guide*. Document M2020-001. Environmental Research & Technology, Inc., Concord, Massachusetts.

Availability: The above report and a computer tape are available from:

Computer Products
National Technical Information Service
U.S. Department of Commerce
5825 Port Royal Road
Springfield, VA 22161
Telephone: (703) 487-4650

Abstract: The ERT visibility model is a Gaussian dispersion model designed to estimate visibility impairment for arbitrary lines of sight due to isolated point source emissions by simulating gas-to-particle conversion, dry deposition, NO-to-NO_2 conversion, and linear radiative transfer.

- **HIWAY-2**

Reference: Petersen, W.B. (1980): *User's Guide for HIWAY-2*. Publication EPA-600/8-80-018. U.S. Environmental Protection Agency, ESRL, Research Triangle Park, North Carolina. (NTIS PB80-227-556)

Availability: This model is available as part of UNAMAP (Version 6).

Abstract: HIWAY-2 can be used to estimate the concentrations of nonreactive pollutants from highway traffic. This steady-state Gaussian model can be applied to determine air pollution concentrations at receptor locations downwind of "at-grade" and "cut-section" highways located in relatively uncomplicated terrain. The model is applicable for any wind direction, highway orientation, and receptor location. The model was developed for situations where hori-

zontal wind flow dominates. The model cannot consider complex terrain or large obstructions to the flow such as buildings or large trees.

- **Integrated Model for Plumes and Atmospheric Chemistry in Complex Terrain (IMPACT)**

Reference: Fabrick, A.J., and P.J. Haas (1980): *User Guide to IMPACT: An Integrated Model for Plumes and Atmospheric Chemistry in Complex Terrain*. Document DCN 80-241-403-01. Radian Corporation, 8501 Mo-Pac Blvd., Austin, Texas.

Availability: A magnetic tape containing the IMPACT model, a set of test data, and a copy of the IMPACT user's guide are available for a cost of $500 from

Howard Balentine
Senior Meteorologist
Radian Corporation
Post Office Box 9948
Austin, TX 78766

Abstract: IMPACT is an Eulerian, three-dimensional, finite-difference grid model designed to calculate the impact of pollutants, either inert or reactive, in simple or complex terrain, emitted from either point or area sources. It automatically treats single or multiple point or area sources, the effects of vertical temperature stratifications on the wind and diffusion fields, shear flows caused by the atmospheric boundary layer or by terrain effects, and chemical transformations.

- **LONGZ**

Reference: Bjorklund, J.R., and J.F. Bowers (1982): *User's Instructions for the SHORTZ and LONGZ Computer Programs,* Volumes I and II. Publication EPA 903/9-82-004. U.S. Environmental Protection Agency, Region III, Philadelphia, Pennsylvania.

Availability: The model is available as part of UNAMAP (Version 6).

Abstract: LONGZ uses the steady-state univariate Gaussian plume formulation for both urban and rural areas in flat or complex terrain to

calculate long-term (seasonal and/or annual) ground-level ambient air concentrations attributable to emissions from up to 14,000 arbitrarily placed sources (stacks, buildings and area sources). The output consists of the total concentration at each receptor due to emissions from each user-specified source or group of sources, including all sources. An option that considers losses due to deposition (see the description of SHORTZ) is deemed inappropriate by the authors for complex terrain, and is not discussed here.

- **Maryland Power Plant Siting Program (PPSP) Model**

References: Brower R. (1982): *The Maryland Power Plant Siting Program (PPSP) Air Quality Model User's Guide*. Ref. No. PPSP-MP-38. Prepared for Maryland Department of Natural Resources, by Environmental Center, Martine Marietta Corporation, Baltimore, Maryland. (NTIS PB82-238387)

Weil, J.C., and R.P. Brower (1982): *The Maryland PPSP Dispersion Model for Tall Stacks*. Ref. No. PPSP-MP-36. Prepared for Maryland Department of Natural Resources, by Environmental Center, Martine Marietta Corporation, Baltimore, Maryland. (NTIS PB82-219155)

Availability: Two reports referenced above are available from NTIS. The model code and test data are available on magnetic tape for a cost of $210 from

Power Plant Siting Program
Department of Natural Resources
Tawes State Office Building
Annapolis, MD 21401
ATTN: Dr. Michael Hirshfield

Abstract: PPSP is a Gaussian dispersion model applicable to tall stacks in either rural or urban areas, but in terrain that is essentially flat (on a scale large compared to the ground roughness elements). The PPSP model follows the same general formulation and computer coding as CRSTER, also a Gaussian model, but differs in four major ways. The differences are in the scientific formulation of specific ingredients or "sub-models" to the Gaussian model and are based on recent theoretical improvements as well as sup-

porting experimental data. The differences are the following: (1) stability during daytime is based on convective scaling instead of the Turner criteria; (2) Briggs's dispersion curves for elevated sources are used; (3) Briggs's plume-rise formulas for convective conditions are included; and (4) plume penetration of elevated stable layers is given by Briggs' (1984) model.

- **Mesoscale Puff Model (MESOPUFF II)**

Reference: Scire, J.S., F.W. Lurmann, A. Bass, and S.R. Hanna (1984): *User's Guide to the Mesopuff II Model and Related Processor Programs*. Publication EPA 600/8-84-013. U.S. Environmental Protection Agency, Research Triangle Park, North Carolina. (NTIS PB84-181775)

Availability: This model is available as part of UNAMAP (Version 6).

Abstract: MESOPUFF II is a short-term, regional-scale puff model designed to calculate concentrations of up to five pollutant species (SO_2, SO_4, NO_x, HNO_3, NO_3). Transport, puff growth, chemical transformation, and wet and dry deposition are accounted for in the model.

- **Mesoscale Transport Diffusion and Deposition Model for Industrial Sources (MTDDIS)**

Reference: Wang, I.T., and T.L. Waldron (1980): *User's Guide for MTDDIS Mesoscale Transport, Diffusion, and Deposition Model for Industrial Sources*. EMSC6062.1UR(R2). Combustion Engineering, Newbury Park, California.

Availability: a magnetic tape copy of the FORTRAN coding and the user's guide are available for a cost of $100 from

Dr. I.T. Wang
Combustion Engineering
Environmental Monitoring and Services, Inc.
2421 West Hillcrest Drive
Newbury Park, CA 19320

Abstract: MTDDIS is a variable-trajectory Gaussian puff model applicable to long-range transport of point source emissions over level or

rolling terrain. It can be used to determine 3-hour maximum and 24-hour average concentrations of relatively nonreactive pollutants from up to ten separate stacks.

- **Models 3141 and 4141**

Reference: Enviroplan, Inc. (1981): *User's Manual for Enviroplan's Model 3141 and Model 4141*. Enviroplan, Inc., West Orange, New Jersey.

Availability: A magnetic tape copy of the FORTRAN coding and the user's guide are available for a cost of $1,900 from

Environplan, Inc.
59 Main Street
West Orange, NJ 07052

Abstract: Models 3141 and 4141 are modifications of CRSTER (UNAMAP VERSION 3) and are applicable to complex terrain, particularly where receptor elevation equals or exceeds the stack-top elevation. The model uses intermediate ground displacement procedures and dispersion enhancements developed from an aerial tracer study and ground-level concentrations measured for a power plant located in complex terrain.

- **MULTIMAX**

Reference: Moser, J.H. (1979): *Multimax: An Air Dispersion Modeling Program for Multiple Sources, Receptors, and Concentration Averages*. Shell Development Company, Westhollow Research Center, P.O. Box 1380, Houston, Texas. (NTIS PB80-170178)

Availability: The above report is available from NTIS ($16.95 for paper copy; $5.95 on microfiche). The access number for the computer tape for MULTIMAX is PB80-170160, and the cost is $370.00. Requests should be sent to

Computer Products
National Technical Information Service
U.S. Department of Commerce
5825 Port Royal Road
Springfield, VA 22161
Telephone: (703) 487-4650

Abstract: MULTIMAX is a Gaussian plume model applicable to both urban and rural areas. It can be used to calculate highest and second-highest concentrations for each of several averaging times due to up to 100 sources arbitrarily located.

- **Multiple Point Source Diffusion Model (MPSDM)**

Reference: Environmental Research & Technology, Inc. (1984): *User's guide to MPSDM.* Document PB881585. Environmental Research & Technology, Inc., Concord, Massachusetts.

Availability: The above report and a computer tape are available from

Computer Products
National Technical Information Service
U.S. Department of Commerce
5825 Port Royal Road
Springfield, VA 22161
Telephone: (703) 487-5650

Abstract: MPSDM is a steady-state Gaussian dispersion model designed to calculate, in sequential mode or in "case-by-case" mode, concentrations of nonreactive pollutants resulting from single or multiple source emissions. The MPSDM model may be used for sources located in flat or complex terrain, in a univariate (σ_z) or bivariate (σ_y, σ_z) mode. Sufficient flexibility is allowed in the specification of model parameters to enable the MPSDM user to duplicate results that would be obtained from many other Gaussian point-source models. A number of features are incorporated to facilitate site-specific model validation studies.

- **Multi-Source (SCSTER) Model**

Reference: Malik, M.H., and B. Baldwin (1980): *Program Documentation for Multi-Source (SCSTER) Model.* Program documentation EN7408SS. Southern Company Services, Inc., Technical Engineering Systems, 64 Perimeter Center East, Atlanta, Georgia.

Availability: The SCSTER model and user's manual are available at no charge to a limited number of persons through Southern Company Services. A magnetic tape must be provided by those desiring the model. Requests should be directed to

Mr. Bryan Baldwin
Research Program Supervisor
Air Quality Program
Southern Company Services
P.O. Box 2625
Birmingham, AL 35202

Abstract: SCSTER is a modified version of the EPA CRSTER model. The primary distinctions of SCSTER are its ability to consider multiple sources that are not necessarily collocated, its enhanced receptor specifications, its variable plume height terrain adjustment procedures and plume distortion from directional wind shear.

- **Pacific Gas and Electric PLUME5 Model**

Reference: Pacific Gas and Electric (1981): *User's Manual for Pacific Gas and Electric PLUME5 Model.* San Francisco, California.

Availability: The user's manual will be supplied for cost of reproduction. An IBM version of the model can be obtained on a user-supplied tape free of charge from

Mr. Robert N. Swanson
Pacific Gas and Electric Company
245 Market Street, RM 451
San Francisco, CA 94106

Abstract: PLUME5 is a steady-state Gaussian plume model applicable to both rural and urban areas in uneven terrain. Pollutant concentrations at 500 receptors from up to 10 sources with up to 15 stacks each can be calculated using up to 5 meteorological inputs. The model in its "basic" mode is similar to CRSTER and MPTER. Several options are available that allow better simulation of atmospheric conditions and improved model outputs. These options allow plume rise into or through a stable layer and crosswind spread of the plume by wind directional shear with height, initial

plume expansion, mean (advective) wind speed, terrain considerations, and chemical transformation of pollutants.

Differences between PLUME5 and CRSTER are in the following areas: stability class determination, hourly mixing height schemes, hourly stable layer data, randomization of wind direction, extent of data set required for preprocessing meteorological data inputs.

- **PLMSTAR Air Quality Simulation Model**

Reference: Lurmann, F.W., D.A. Godden, and H. Collins (1985): *User's Guide to the PLMSTAR Air Quality Simulation Model.* ERT Document M-2206-100, Environmental Research & Technology, Inc., Newbury Park, California.

Availability: The above report and a computer tape are available from

Computer Products
National Technical Information Service
U.S. Department of Commerce
5825 Port Royal Road
Springfield, VA 22161
Telephone: (703) 487-4650

Abstract: PLMSTAR is a mesoscale Lagrangian photochemical model designed to predict atmospheric concentrations of O_3, NO_x, HNO_3 PAN, SO_2, SO_4 from reactive hydrocarbons, NO_x and SO_x emissions. It is intended to simulate the behavior of pollutants in chemically reactive plumes resulting from major point source emissions. The model's Lagrangian air parcel is subdivided into a five-layer/nine-column domain of computational cells. The approach allows for realistic simulation of the combined effects of atmospheric chemical reactions and pollutant dispersion in the horizontal and vertical directions. Other key features of the model include the ability to generate trajectories at any level of a three-dimensional, divergence-free wind field; the ability to calculate and use the time- and space-varying surface deposition of pollutants; an up-to-date $O_3/RHC/NO_x/SO_x$ chemical mechanism that uses eight classes of reactive hydrocarbons; the ability to handle both point and area source emissions simultaneously; and the

ability to simulate overwater conditions and land/water transitions.

- **Plume Visibility Model (PLUVUE II)**

Reference: Seigneur, C., C.D. Johnson, D.A. Latimer, R.W. Bergstrom, and H. Hogo (1984): *User's Manual for the Plume Visibility Model (PLUVUE II)*. Publication EPA-600/8-84-005. U.S. Environmental Protection Agency, Research Triangle Park, North Carolina. (NTIS PB84-158302)

Availability: This model is available as part of UNAMAP (Version 6).

Abstract: The Plume Visibility Model (PLUVUE II) is a computerized model used for estimating visual range reduction and atmospheric discoloration caused by plumes resulting from the emissions of particles, nitrogen oxides and sulfur oxides from a single emission source. PLUVUE II predicts the transport, dispersion, chemical reactions, optical effects and surface deposition of point or area source emissions. Addenda to the user's manual were prepared in February 1985 to allow the execution of PLUVUE II and test cases on the UNIVAC computer. The addenda are included in the UNAMAP (Version 6) documentation.

- **Point, Area, Line Source Algorithm (PAL-DS)**

Reference: Petersen, W.B. (1978): *User's Guide for PAL — A Gaussian-Plume Algorithm for Point, Area, and Line Sources*. Publication EPA-600/4-78-013. Office of Research and Development, Research Triangle Park, North Carolina. (NTIS PB281306)

Rao, K.S., and H.F. Snodgrass (1982): *PAL-DS Model: The PAL Model Including Deposition and Sedimentation*. Publication EPA-600/8-82-023. Office of Research and Development, Research Triangle Park, North Carolina. (NTIS PB83-117739)

Availability: This model is available as part of UNAMAP (Version 6).

Abstract: PAL-DS is an acronym for this point, area, and line source algorithm and is a method of estimating short-term dispersion using Gaussian plume steady-state assumptions. The algorithm can be used to estimate concentrations of nonreactive pollutants at

99 receptors for averaging times of 1 to 24 hours, for a limited number of point, area, and line sources (99 of each type). This algorithm is not intended for application to entire urban areas but to assess the impact on air quality, on scales of tens to hundreds of meters, of portions of urban areas such as shopping centers, large parking areas, and airports. Level terrain is assumed. The Gaussian point source equation estimates concentrations from point sources after determining the effective height of emission and the upwind and crosswind distance of the source from the receptor. Numerical integration of the Gaussian point source equation is used to determine concentrations from the four types of line sources. Subroutines are included that estimate concentrations for multiple lane line and curved path sources, special line sources (line sources with endpoints at different heights above ground), and special curved path sources. Integration over the area source, which includes edge effects from the source region, is done by considering finite line sources perpendicular to the wind at intervals upwind from the receptor. The crosswind integration is done analytically; integration upwind is done numerically by successive approximations. The PAL–DS model uses Gaussian plume-type diffusion–deposition algorithms based on analytical solutions of a gradient-transfer model. The PAL–DS model can treat deposition of both gaseous and suspended particulate pollutants in the plume since gravitational settling and dry deposition of the particles are explicitly accounted for. The analytical diffusion–deposition expressions in the PAL–DS model, in the limit when pollutant settling and deposition velocities are zero, reduce to the usual Gaussian plume diffusion algorithms.

- **Random–walk Advection and Dispersion Model (RADM)**

References: Austin, D.I., A.W. Bealer, and W.R. Goodin (1981): *Random–Walk Advection and Dispersion Model (RADM), User's Manual.* Dames & Moore, Los Angeles, California.

Runchal, A.K., W.R. Goodin, A.W. Bealer, D.I. Austin (1981): *Technical Description of the Random–Walk Advection and Dispersion Model (RADM).* Dames & Moore, Los Angeles, California.

Availability: A magnetic tape of the computer code and the user's manual are available for a cost of $440.00 from

Mr. C. James Olsten
Dames & Moore
445 South Figueroa Street
Suite 3500
Los Angeles, CA 90071–1665

Abstract: RADM is a Lagrangian dispersion model that uses the random-walk method to simulate atmospheric dispersion. The technical procedure involves tracking tracer particles having a given mass through advection by the mean wind and diffusion by the random motions of atmospheric turbulence. Turbulent movement is calculated by determining the probability distribution of particle movement for a user-defined time step. A random number between 0 and 1 is then computed to determine the distance of particle movement according to the probability distribution. A large number of particles is used to statistically represent the distribution of pollutant mass. Concentrations are calculated by summing the mass in a volume around the receptor of interest and dividing the total mass by the volume. Concentrations can be calculated for any averaging time. RADM is applicable to point and area sources.

- **Reactive Plume Model (RPM–II)**

Reference: D. Stewart, M. Yocke, and M.–K. Liu (1981): *Reactive plume model – RPM–II, User's guide*. Publication EPA–600/8–81–021. U.S. Environmental Protection Agency, ESRL, Research Triangle Park, North Carolina. (NTIS PB82–230723)

Availability: The above report is available from NTIS ($16.95 for paper copy; $5.95 on microfiche). The access number for the computer tape is PB83–154898, and the cost is $460.00. Requests should be sent to

Computer Products
National Technical Information Service
U.S. Department of Commerce
Springfield, VA 22161
Telephone: (703) 487–4650

Abstract: The Reactive Plume Model, RPM–II, is a computer model for estimating short–term concentrations of primary and secondary pollutants resulting from point or area source emissions. The model is capable of simulating the complex interaction of plume dispersion and nonlinear photochemistry. Two main features of the model are (1) the horizontal resolution within the plume, which offers a more realistic treatment of the entrainment process, and (2) its flexibility with regard to choices of chemical kinetic mechanisms.

- **Regional Transport Model (RTM–II)**

Reference: Morris, R.E., D.A. Stewart, and M.–K. Liu (1982): *Revised User's Guide to the Regional Transport Model – Version II.* Publication SYSAPP–83/022. Systems Applications Inc., San Rafael, California.

Availability: The computer code is available on magnetic tape for a cost of $100 (which includes the user's manual) from

Systems Applications, Inc.
101 Lucas Valley Road
San Rafael, CA 94903

Abstract: The Regional Transport Model (RTM–II) is a computer–based air quality grid model whose primary use is estimating the distribution of air pollution from multiple point sources and area sources at large distances (on the scale of several hundred to a thousand kilometers). RTM–II offers significant advantages over other long–range transport models because it is a quasi–three–dimensional hybrid (grid plus Lagrangian puff) approach to the solution of the advection–diffusion equation. Furthermore, its formulation allows the treatment of spatially and temporarily varying wind, mixing depths, diffusivity, and transformation rate fields. It is also capable of treating spatially varying surface depletion processes. While the modeling concept is capable of predicting concentration distributions of many pollutant species (e.g., NO_x, CO, TSP, etc.), the most notable applications of the model to date focus on the long–range transport and transformation of SO_2 and sulfates.

- **SHORTZ**

Reference: Bjorklund, J.R., and J.F. Bowers (1982): *User's Instructions for the SHORTZ and LONGZ Computer Programs,* Volumes I and II. Publication EPA-903/9-82-0004a and b, U.S. Environmental Protection Agency, Region III, Philadelphia, PA.

Availability: This model is available as part of UNAMAP (Version 6).

Abstract: SHORTZ uses the steady-state bivariate Gaussian plume formulation for both urban and rural areas in flat or complex terrain to calculate ground-level ambient air concentrations. It can calculate 1-hour, 2-hour, 3-hour, etc., average concentrations due to emissions from stacks, buildings and area sources for up to 300 arbitrarily placed sources. The output consists of the total concentration at each receptor due to emissions from each user-specified source or group of sources, including all sources. If the option for gravitational settling is invoked, analysis cannot be accomplished in complex terrain without violating mass continuity.

- **Simple Line-Source Model (GMLINE)**

Reference: Chock, D.P. (1980): *User's Guide for the Simple Line-Source Model for Vehicle Exhaust Dispersion Near a Road.* Environmental Science Department, General Motors Research Laboratories, Warren, Michigan.

Availability: Copies of the above reference are available without charge from

Dr. D.P. Chock
Environmental Science Department
General Motors Research Laboratories
General Motors Technical Center
Warren, MI 48090

The user's guide contains the short algorithm of the model.

Abstract: GMLINE is a simple steady-state Gaussian plume model that can be used to determine hourly (or half-hourly) averages of exhaust concentrations within 100m from a roadway on relatively flat terrain. The model allows for plume rise due to the heated exhaust, which can be important when the crossroad wind is low. It also

uses a new set of vertical dispersion parameters that reflects the influence of traffic-induced turbulence.

- **Texas Climatological Model (TCM-2)**

Reference: Staff of the Texas Air Control Board (1980): *User's Guide to the Texas Climatological Model (TCM)*. Texas Air Control Board, Permits Section, 6330 Highway 290 East, Austin, Texas.

Availability: The TCM-2 model is available from the Texas Air Control Board at the following cost:

User's manual only	$20.00
User's manual and model (magnetic tape)	$80.00

Requests should be directed to

Data Processing Division
Texas Air Control Board
6330 Highway 290 East
Austin, TX 78723

Abstract: TCM is a climatological steady-state Gaussian plume model for determining long-term (seasonal or annual arithmetic) average pollutant concentrations of nonreactive pollutants.

- **Texas Episodic Model (TEM-8)**

Reference: Staff of the Texas Air Control Board (1979): *User's Guide to the Texas Episodic Model*. Texas Air Control Board, Permits Section, 6330 Highway 290 East, Austin, TX.

Availability: The TEM-8 model is available from the Texas Air Control Board at the following costs:

User's manual only	$20.00
User's manual and model (magnetic tape)	$80.00

Requests should be directed to

Data Processing Division
Texas Air Control Board
6330 Highway 290 East
Austin, TX 78723

Abstract: TEM is a short-term, steady-state Gaussian plume model for determining short-term concentrations of nonreactive pollutants.

14.2 OTHER MODELS

Many other models are available for air quality applications. Some are listed below in alphabetical order.

- ACID, a receptor-oriented backward trajectory model for long-range transport and deposition (Samson et al., 1982)
- ADEPT, a decision framework software to aid in the analysis of policy alternatives for acidic deposition (EPRI, 1989)
- ADPIC, a particle-in-cell model (Lange, 1978)
- Air Quality Model Performance Assessment Package (Bencala and Seinfeld, 1979)
- ARAMS, the Advanced Regional Atmospheric Modeling System, a generalized, comprehensive and flexible numerical weather prediction system (Colorado State University)
- ATMOS1, a diagnostic wind model for wind simulations in complex terrain (Davis et al., 1984; King and Bunker, 1984)
- CALGRID, a new three-dimensional Eulerian photochemical model with advanced mechanisms for dry and wet deposition (Yamartino et al., 1989)
- COMPLEX I and II, Gaussian dispersion models for complex terrain applications (Gulfreund et al., 1983)
- CTDM, a complex terrain dispersion model (Strimaitis, 1986)
- DIFKIN, a Lagrangian multi-box photochemical model (Martinez et al., 1973)
- DWM, a diagnostic wind model capable of generating three-dimensional wind fields in complex terrain from limited observations (Douglas and Kessler, 1988)

- EKMA, Empirical Kinetic Modeling Approach, for simple simulations of the effects of O_3 control strategies (Dodge, 1977)
- ENAMAP-2, a source-oriented Lagrangian model for long-range transport and deposition (Nitz et al., 1983)
- FEM3, a full three-dimensional model for heavy gas dispersion (Ermak et al., 1981)
- GD, a simple Gaussian model for heavy gas dispersion (Ermak et al., 1981)
- HOTMAC, a three-dimensional hydrodynamic model for simulating higher order turbulence for atmospheric circulation (Yamada, 1985)
- IBMAQ-2, a model for meteorological and dispersion simulations (Shir and Shieh, 1976)
- KAPPA-G, a non-Gaussian steady-state dispersion model (Tirabassi et al., 1986)
- Los Alamos Visibility Model, for visibility impairment computations (Williams et al., 1980 and 1981)
- MASCON, a mass-consistent atmospheric flux model for meteorological simulations in complex terrain (Dickerson, 1978)
- MATHEW, an objective meteorological model (Sherman, 1978)
- MC-LAGPAR II, a Monte-Carlo Lagrangian particle model (Zannetti et al., 1988)(*)
- MINERVE, a mass-consistent wind field model for diagnostic simulations (Geai, 1987)
- MPRM, a general purpose computer processor for organizing available meteorological data into a format suitable for use by air quality dispersion models (available from SCRAM BBS)
- NCAR/PSU/SUNY, a mesoscale meteorological model for regional simulations (Chang et al., 1987)
- NMM, a primitive equation-mode numerical mesoscale model (Pielke et al., 1983)
- NOABL, an objective meteorological model (Phillips and Traci, 1978)

(*) An improved version of this code, MC-LAGPAR III, is available. This code also comes as a Macintosh II version, with fully interactive graphics and user-friendly interface.

- OZIPM-2, a program that generates city-specific isopleths to be used in the EKMA methodology (Gipson, 1984)
- PARIS, Plume-Airshed Reactive-Interactive System, an urban air quality model that is capable of providing a detailed treatment of large point source emissions by embedding one or more reactive plume models into the UAM model (the UAM model is described in Section 14.1.1) (Seigneur et al., 1983)
- PHOENIX, a model for visibility impairment computations (Eltgroth and Hobbs, 1979)
- PRISE, a comprehensive model for plume rise and pollution dispersion (Henderson-Sellers, 1987)
- PTPLU, a model for estimating the location of the maximum short-term concentration (Pierce et al., 1982)
- RAPTAP, a Lagrangian particle model for Monte Carlo dispersion simulation (Yamada and Bunker, 1988)
- RDV 2.0, a relief valve discharge screening model (available from SCRAM BBS)
- REM II, a Lagrangian single-box photochemical model (Drivas et al., 1977)
- RIVAD, a plume-segment Lagrangian model for regional transport and deposition simulation (SAI, 1984)
- RTDM, a sequential Gaussian plume model designed to estimate ground-level concentrations in rough terrain (Paine and Egan, 1987)
- SCIMP, Second-Order Closure Integrated Plume Model, a plume methodology using second-order closure techniques (Sykes et al., 1989b)
- SCIPUFF, Second-Order Integrated Puff Model, a puff methodology using second-order closure techniques (Sykes et al., 1989c)
- SCREEN, a PC-compatible companion to the revised screening procedures developed by the U.S. EPA to estimate air quality impact of stationary sources (U.S. EPA, 1988a)
- SEM, Stack Exhaust Model, for advanced simulations of the initial phase of the plume, including its buoyant rise and bending-over phase (Sykes et al., 1989a)
- SLAB, a layer-averaged conservation equation model for heavy gas dispersion (Ermak et al., 1981)

- SMOG, a photochemical model for ozone simulations (Allen and Munger, 1981)
- TRACE, a Lagrangian box photochemical model (Tran, 1981)
- URBMET (3D version), a prognostic meteorological model (Bornstein et al., 1985)
- VALLEY, a steady-state Gaussian model (Burt, 1980) in which plume height is adjusted according to terrain elevation for stable cases (available from SCRAM BBS)
- VISCREEN, to predict the visual impact of a plume (U.S. EPA, 1988b)
- 3AM, the Annual Average Urban Airshed Model structure, which uses routine emissions, meteorological and air quality data to provide hourly ozone concentrations over long periods of time (e.g., one year) (Tesche and McNally, 1989). The methodology includes a plan for incorporating secondary PM_{10} aerosols and air toxics.
- 3D, a second-order closure mesoscale model (Yamada, 1978)

14.3 VAPOR CLOUD DISPERSION MODELS

Hanna and Drivas (1987) provide guidelines for use of vapor cloud dispersion models and review the available software for simulating source emissions (e.g., tank rupture, pipe break, venting of runaway reaction), and transport/diffusion phenomena of buoyant, nonbuoyant and dense gases. This review was based on literature investigation and the analysis of questionnaires sent to modelers.

Table 14–1 presents the models for which a questionnaire was completed, while Table 14–2 summarizes the results from model questionnaires.

Table 14–1. Models for which questionnaire was completed. Addresses and references are listed (from Hanna and Drivas, 1987; see this publication for the references mentioned in this table). [Reprinted with permission from the American Institute of Chemical Engineers.]

Model	Address	Scientific Validity	Evaluation
AVACTA II	P. Zannetti, Aerovironment, 825 Myrtle Ave., Monrovia, CA 91016	Zannetti et al. 1986	
CARE	G. Verholek, ESC, 200 Tech. Center Dr., Knoxville, TN 37912	Verholek 1986	
CHARM	H. Balentine, Radian, P.O. Box 9948, Austin, TX 78766	Eltgorth and Smith 1983	Balentine and Eltgorth 1985, McNaughton et al. 1986
COBRA III	E. Alp, CSC, 2 Tippett Rd., Downsview, Ont., Canada M3H2V2	Alp 1985, Oliverio et al. 1986	
CRUNCH	A. Byrne, SRD, Wigshaw L., Culceth, England WA34NE	Jagger 1983	
DEGADIS	J. Havens, Un. Arkansas, Dept. Ch. Eng., Fayetteville, AR 72701	Havens and Spicer 1985	Spicer and Havens 1986
DENZ	Same as CRUNCH	Fryer and Kaiser 1979	
D2DC	Commander, USA, CRDC, Aberdeen Proving Ground, MD 21010-5423	Whitacre et al. 1986	
EAHAP	J. Cornwell, EAI, P.O. Box 1508, Norman, OK 73069		
Eidsvik	Y. Gotoas, NIAR, P.B. 64, N-2001 Lillestrom, Norway	Eidsvik 1981	Gotaas 1985
Emissions	J. Schroy, Monsanto, 800 N. Lindbergh Blvd., St. Louis, MO 63167	Wu and Schroy 1979	
EPIDIS	J. Woodward, FSE, 200 Woodport Road, Sparta, NJ 07971		
FEM3	S. Chan, LLNL, P.O. Box 808, Livermore, CA 94550	Chan 1983	Ermak et al. 1982, 1985
GASP	Same as CRUNCH	Webber 1986, Brighton 1985	
HASTE	A. Puri, ERT, 696 Virginia Road, Concord, MA 01742	Paine et al. 1986	Heinold et al 1986, McNaughton et al 1986
HEAVYPUFF	N. Jensen, Riso N.L., DK-4000 Roskilde, Denmark		
HEGADAS	M. Pikaar, Shell, Postbus 162, 2501 AN the Hague, Holland	Colenbrander 1980; Colenbrander and Puttock 1983	Puttock et al 1982
INPUFF2.0	W. Petersen, EPA, RTP, NC	Petersen and Lavdas 1986	
MIDAS	K. Woodard, Pickard Lowe & Garrick, 1615 M Street, Wash., DC 20036		
ModSys	Same as COBRA III		
PLUMEPATH	Same as HEGADAS	Ooms 1972, Ooms et al. 1974	
RIMPUFF	T. Mikkelsen, Riso, N.L., DK-4000 Roskilde, Denmark		
SAFE	P. Ross, AOSTRA, 10010-106 St., Edmonton, Alberta T5J 3L8		
SAFEMODS	P. Raj, TMS, 99 S. Bedford Street, Burlington, MA 01803-5128	Raj 1981, 1985, 1986	
SAFER	G. Gelinas, Safer, 5700 Corsa Avenue, Westlake Village, CA 91362		
SAFETI	R. Cox, Technica, 7/12 Tavistock Sq., London WC1H9LT	Ale and Whitehouse 1986	
SLAB	D. Ermak, LLNL, P.O. Box 808, Livermore, CA 94550	Ermak et al. 1982	Ermak and Chan 1985
SPILLS	J. Moser, Shell, P.O. Box 1380, Houston, TX 77001	Fleischer 1980	Kunkel 1983
SRI PUFF	F. Ludwig, SRI International, Menlo Park, CA 94025		
TELJET	Same as SAFETI		
TRAUMA	Same as CRUNCH	Wheatley 1986	
VAPID	Same as HEAVYPUFF	Jensen 1983	
WHAZAN	Same as SAFETI	Kayes 1985	

Table 14–2. Results from model questionnaires (most answers are given as Y = Yes or N = No) as of December 1986 (from Hanna and Drivas, 1987). [Reprinted with permission from the American Institute of Chemical Engineers.]

Question	AVACTA II	CARE	CHARM	COBRA III	CRUNCH	DEGADIS	DENZ	D2DC	EAHAP	Eidsvik	Emissions	EPIDIS	FEM3	GASP	HASTE
Operating Information															
Form of model: H=Hardware; S=Software	S	H;S	H;S	S	S	S	S	S	S	H;S	S	S	S	S	H;S
Main use: R=Research; A=Applied	R;A	A	A	A	R;A	R;A	R;A	A	R	R;A	A	A	R	R;A	A
Operate in interactive mode?	N	Y	Y	N	Y	Y	N	Y	Y	Y	N	Y	N	N	Y
Support system?		Y	Y		N	Y	N	Y	Y	N	N			N	Y
Number sold or given away?	2	15	80		>10	>10	>10	40	5		0				6
Link to emergency system?		Y	Y		N	N	N	N	N	N	N			N	Y
Input Data															
Accept real time weather data?	N	Y	Y	N	N	N	N	N	N	N	N	N	N	N	Y
Method of data entry: H=Hand; F=data file memory; D=disk or tape	F	H;F;D	H;F;D	H;F	F	H;F	F	H	H	H	H;F	H;F;D	F	H;F	H;F
Source Emissions Model?	N	Y	Y	Y	N	N	N	Y	Y	N	Y	Y	Y	Y	Y
Evaporation of Spilled Liquids?		Y	Y	Y				Y	Y		Y	Y	Y	Y	Y
Flashing		Y	Y	Y				N	Y		Y	Y	N	N	Y
Multicomponents		N	N	N				N	Y		Y	N	N	N	N
Entrainment as aerosols?		Y	Y	Y				N	N		N	Y	N	N	Y
Heat transfer, substrate to cloud?		Y	N	Y				N	Y		Y	Y	Y	Y	Y
Number of substrates (W=Water; S=Soil)		W;S		W;S					W;S		W;S	W;S	W;S	W;S	W;S
Mass transfer in liquid phase?		Y	N	N				N	Y		Y	Y	N	Y	Y
Evaporation of aerosols		N	Y	Y				N	N		N	Y	N	N	Y
Gas flux from container rupture?		N	Y	Y				N	Y		N	Y	N	N	Y
Condens. of moisture in vapor cloud?		N	Y	Y				N	Y		N	Y	Y	N	N
Wind influence on evaporation?		Y	Y	N				Y	Y		Y	Y	N	N	Y
Number of chemicals hardwired (I=input by user)		50,I	83	5,I				17	21		I	10,I	I	I	I
Transport and Dispersion Model?	Y	Y	Y	Y	Y	Y	Y	Y	Y	Y	N	Y	Y	N	Y
Releases treated: I=Instantaneous; C=Continuous; V=Variable	I;C;V	C;V	I;C;V	V	C	I;C;V	I	I;C;V	I;C;V	I;C		V	I;C		I;C;V
Dense cloud?	N	Y	Y	Y	Y	Y	Y	N	Y	Y		Y	Y		Y
Jet?	Y	N	Y	N	N	N	N	Y	Y	N		N	N		N
Neutral cloud?	Y	Y	Y	N	Y	Y	Y	Y	Y	N		Y	Y		Y
Buoyant cloud?	Y	N	Y	N	N	N	N	Y	Y	N		N	N		Y
Surface roughness?	Y	Y	N	Y	Y	Y	Y	Y	Y	Y		Y	Y		Y
Complex terrain handled?	Y	Y	N	N	N	N	N	N	N	N		N	Y		N
U variations in time and space?	Y	Y	N	N	N	N	N	N	N	N		N	Y		N
Indoor concentrations?	N	N	N	N	N	N	N	N	N	N		N	N		N
Building wake effects?	N	Y	Y	N	N	N	N	N	N	N		N	Y		Y
Advection/Dispersion Model: B=Box or Slab; G=Gaussian; K=K/numerical	G	G	G	B	B;G	K	B;G	G	B;G	B;G		K	K		B;G
Along-wind dispersion?	Y	Y	Y	Y	N	Y	Y	N	Y	Y		Y	Y		Y
Vertical wind shear?	N	Y	N	Y	Y	Y	Y	N	Y			Y	Y		Y
Chemical reactions in plume?	Y	Y	Y	N	N	Y	N	N	N	N		N	N		N
Dry or wet deposition?	Y	Y	N	N	N	N	N	D	N	N		N	N		N
Concentration fluctuations?	N	N	N	N	N	N	N	N	N	N		Y	N		N
Number of chemicals (I=input)	I	50,I	83	5,I		5		17	21			10,I	I		I
Output															
Averaging time (minutes) (I=input)		15	1-10	3		10						0			
Distance limits (km)								20	100			70	10		
Evaluation?	Y	N	Y	Y	Y	Y	Y	N	Y	Y	Y	Y	Y	N	N
How are data presented T=Table; G=Graph		T;G	T;G		T	T	T;G	T;G	T;G	T	T;G	T;G	T;G	T;G	T;G

Table 14–2 (continued)

	HEAVYPUFF	HEGADAS	INPUFF2.0	MIDAS	ModSys	PLUME PATH	RIMPUFF	SAFEMODS	SAFER/TRACE	SLAB	SPILLS	SRI PUFF	TRAUMA	VAPID
Operating Information														
Form of model: H=Hardware; S=Software	S	S	S	S;H	S	S	S	S;H	S;H	S	S	S	S	S
Main use: R=Research; A=Applied	R	R;A	A	R;A	A	R;A	A	R;A	A	R;A	A	R	A	R
Operate in interactive mode?	N	N	N	Y	N	N	Y	Y	Y	N	Y	Y	N	N
Support system?	N	N	Y	Y	N	N	Y		Y			N	N	
Number sold or given away?		1	120	20		>10	3		75		>100			
Link to emergency system?		N	N	Y	N	N			Y				N	
Input Data														
Accept real time weather data?	N	N	N	Y	N	N	Y	Y	Y	N	N	N	N	N
Method of data entry: H=Hand; F=data file memory; D=disk or tape	H;F;D	F	D	H;F;D	H;F	F	F	H;F;D	H;F;D	F	H	H;F;D	F	H;F;D
Source Emissions Model?	N	Y	N	Y	Y	N	Y	Y	Y	Y	Y	N	Y	Y
Evaporation of Spilled Liquids?		Y		Y	N			Y	Y	Y	Y		N	Y
Flashing		N		Y	N			Y	Y	N	Y		Y	Y
Multicomponents		N		Y	Y		Y	Y	Y	N	N		N	
Entrainment as aerosols?		N		N	N			Y	Y	N	N		N	
Heat transfer, substrate to cloud?		Y		Y	N			Y	Y	Y	Y		N	
Number of substrates (W=Water; S=Soil)		W;S		W;S				W;S	W;S		S			
Mass transfer in liquid phase		N		Y	N			Y	Y	N	Y		Y	
Evaporation of aerosols		N		N	N			Y	Y	N	N		Y	
Gas flux from container rupture?		N		Y	Y		Y	Y	Y	N	Y		T	
Condens. of moisture in vapor cloud?		Y		N	N			Y	Y	N	N		Y	
Wind influence on evaporation?		N		Y	N			Y	Y	N	Y		N	Y
Number of chemicals hardwired (I=input by user)		I		I	2		25	I	I	1	34+		I	
Transport and Dispersion Model?	Y	Y	Y	Y	Y	Y	Y	Y	Y	Y	Y	Y	Y	Y
Releases treated: I=Instantaneous; C=Continuous; V=Variable	I	C;V	C;V	V	V	C	I;C;V	I;C;V	I;C;V	C	C,V	V	C	V
Dense cloud?	Y	Y	N	Y	Y	Y		Y	Y	Y	N	N	N	Y
Jet?	Y	N	N	Y	Y	Y	N	Y	Y	N	N	N	N	N
Neutral cloud?	Y	N	Y	Y	Y	Y	Y	Y	Y	Y	Y	Y	Y	Y
Buoyant cloud?	Y	N	Y	Y	Y	Y	Y	Y	N	N	N	N	N	N
Surface roughness?	Y	Y	N	Y	Y	N	Y	Y	Y	Y	N	N	N	Y
Complex terrain handled?	N	N	N	Y	N	N	Y	Y	Y	N	N	N	N	N
U variations in time and space?	N	N	Y	Y	N	N	Y	Y	Y	N	N	Y	N	N
Indoor Concentrations?	N	N	N	Y	N	N	N	Y	N	N	N	N	N	N
Building wake effects?	N	N	N	Y	N	N	N	N	N	N	N	N	N	N
Advection/Dispersion Model: B=Box or Slab; G=Gaussian; K=K/numerical	B	B;G	G	B;G;K	G;K	G	G	B;G	B;G	B	G	G	B	B
Along-wind dispersion?	Y	Y	N	Y	Y	N	Y	Y	Y	N	N	Y	N	N
Vertical wind shear?	Y	Y	N	Y	Y	N	Y	Y	N	N	Y	N	N	Y
Chemical reactions in plume?	N	N	N	N	Y	N	N	Y	Y	N	N	N	Y	N
Dry or wet deposition?	N	N	Y	Y	N	N	Y	Y	N	N	N	N	Y	D
Concentration fluctuations?	N	N	N	N	Y	N	Y	Y	N	N	N	N	N	N
Number of chemicals (1=Input)	4	I		I	2	I	25	900	I	1	34+		1	1
Output														
Averaging time (minutes)(I=input)		I	3,60			0		0.5,1		I	10	60		10
Distance limits (km)			100	10		1	20	5			10			10
Evaluation?	N	Y	Y	Y	Y		Y	Y	Y	Y	Y		N	N
How are data presented T=Table; G=Graph	T;G	T	T	T;G	T;G	T	T;G	T;G	T;G	T;G	T,G		T	T;G

Table 14–2 (continued)

	SAFE	SAFETI	TSCJET	WHAZAN
Operating Information				
Form of model: H=Hardware; S=Software	S	S	S	S
Main use: R=Research; A=Applied	A	A	A	A
Operate in interactive mode?	Y	Y	Y	Y
Support system?	Y	Y	Y	Y
Number sold or given away?	1	7	6	60
Link to emergency system?	N	N	N	N
Input Data				
Accept real time weather data?	Y	N	N	N
Method of data entry: N=Hand; F=data file memory; D=disk or tape	N;F;D	N;F;D	N;F	N
Source Emissions Model?	N	Y	Y	Y
Evaporation of Spilled Liquids?		Y	N	Y
Flashing		Y	Y	Y
Multicomponents		N	N	N
Entrainment as aerosols?		Y	Y	Y
Heat transfer, substrate to cloud?		Y	N	Y
Number of substrates (N=Water; S=Soil)		S		S
Mass transfer in liquid phase		Y	N	Y
Evaporation of aerosols		Y	Y	Y
Gas flux from container rupture?		Y	Y	Y
Condens. of moisture in vapor cloud?		Y	Y	Y
Wind influence on evaporation?		N	N	Y
Number of chemicals hardwired (I=input by user)		60,I	62,I	20,I
Transport and Dispersion Model?	Y	Y	Y	Y
Releases treated: I=Instantaneous; C=Continuous; V=Variable	C;V	I;C;V	C	I;C;V
Dense cloud?	N	Y	Y	Y
Jet?	Y	Y	Y	Y
Neutral cloud?	Y	Y	Y	Y
Buoyant cloud?	Y	Y	Y	Y
Surface roughness?	Y	Y	Y	Y
Complex terrain handled?	N	N	N	N
U variations in time and space?	Y	N	N	N
Indoor Concentrations?	N	N	N	N
Building wake effects?	N	N	N	N
Advection/Dispersion Model: B=Box or Slab; G=Gaussian; K=K/numerical	G;K	B;G		B;G
Along-wind dispersion?	Y	N	N	N
Vertical wind shear?	Y	N	N	N
Chemical reactions in plume?	Y	N	N	N
Dry or wet deposition?	Y	Y	N	N
Concentration fluctuations?	Y	N	N	N
Number of chemicals (I=Input)	I	60,I	62,I	20,I
Output				
Averaging time (minutes)(I=input)	60	10	10	10
Distance limits (km)	50	20		
Evaluation?	N	N	Y	N
How are data presented T=Table; G=Graph	T;G	T,G	T,G	T,G

14.4 COMPUTER SYSTEMS FOR CHEMICAL EMERGENCY PLANNING

The U.S. EPA (1989) has identified the computer systems applicable to Title III of the Superfund Amendments and Reauthorization Act of 1986, i.e., those packages that are suitable for local planning and for assistance in emergency response planning (e.g., hazard identification, vulnerability analysis through modeling of the releases, risk analysis, regulatory requirements, etc.).

This preliminary list of computer applications and systems is presented to Table 14–3.

Table 14–3. Preliminary list of computer applications and and systems of potential use under SARA Title III (from U.S. EPA, 1989). Two asterisks indicate an apparent high degree of usefulness. All systems require an IBM–compatible microcomputer, unless otherwise specified.

ACRONYM/ABBREVIATION	SYSTEM NAME	VENDOR	CONTACT ADDRESS/PHONE	PURPOSE/DESCRIPTION/REQUIREMENTS
ACAPP	Aqueous Chemical and Physical Properties	P.S. Lowell & Co., Inc.	8868 Research Blvd Suite 309 Austin, TX 78758 (512) 454-4797	Predicts properties and computes chemical and solid-liquid phase equilibrium for aqueous mixtures. Up to 20 composition data sets may be handled in memory at once. Requires 512K memory.
ACT		Techdata	6615 la Mora Houston, TX 77083 (713) 498-0797	Designs activated sludge systems. Also provides data data for flow modeling and permits.
ADPM	Automated Defense Priority Model Development	Roy F. Weston, Inc.	Judith Hushon 955 L'Enfant Plaza, SW 6th Floor Washington, DC 20024 (202) 646-6800	System considers surface water and groundwater pathways of exposure in evaluating the potential for adverse effects. Air and soil pathways will be added as will numerous built-in error checking routines.
AIRDAS	Air Quality and Meteorological Monitoring Data Acquisition System	Enviroplan, Inc.	Michael Abrams 59 Main St. West Orange, NJ 07052 (201) 325-1544	Collects, processes, displays, and reports air quality and meteorological data. Requires Data General Corp. MicroECLIPSE processor.
AMINE-1		TECS Software, Inc.	P.O. Box 720730 Houston, TX 77272 (713) 561-6143	Performs preliminary design of MEA, DEA, and MDEA plants through mass and energy balance calculations for all major equipment involved.
ANASOFT		Anafaze, Inc.	Mike Jacobs 1041 17th Ave. Santa Cruz, CA 95062 (408) 479-0415	Records results of environmental monitoring data: flows, pH, pollution levels, waste disposal areas and control of pollution.
APE	Air Pollution Emissions	Jerome R. Barta	Jerome R. Barta 1513 White Post Cedar Park, TX 78613 (512) 258-1812 (Call after 4 PM)	Tracks air pollution emissions. Screen formats for data input and output in Basic. User can customize using Basic.

Table 14–3 (continued)

ACRONYM/ABBREVIATION	SYSTEM NAME	VENDOR	ADDRESS/PHONE	PURPOSE/DESCRIPTION/REQUIREMENTS
ARCHIE	Automated Resource for Chemical Hazard Incident Evaluation	Department of Transportation	Stacy Gerard ARCHIE Support (DHM-15/Room 8104) U.S. Department of Transportation 400 7th Street, S.W. Washington, D.C. 20590 (202) 366-4900	Program created for DOT, EPA, and FEMA to aid emergency preparedness personnel in assessing the sequence and nature of events that may follow an accident. ARCHIE incorporates several estimation methods that may be used to assess the vapor discharge, fire, and explosion impacts associated with episodic discharges of hazardous materials.
ASPER	Activated Sludge Performance Evaluation Routines	Cochrane Associates, Inc.	Jay J. Fink 236 Huntington Ave. Boston, MA 02115 (617) 247-0444	Evaluates the performance of each unit of a wastewater treatment plant based on hydraulic loadings, solid flux loadings, food/microorganism ratios, sludge age, settleability, and related parameters.
BASIS	Text Information Management System (TIMS)	Information Dimensions	655 Metro Place South Suite 500 Dublin, OH 43017 (614) 761-7300	Provides access to textual and numeric data in its databases for information retrieval and reporting needs. Features word proximity and phrase searching; thesaurus and index.
Batchmaster Plus		Pacific Micro Software Engineering	35 59th Place Long Beach, CA 90803 (213) 434-0011	MSDS, HMIS labeling modules.
BEE - SARA		Bowman Environmental Engineering	P.O. Box 29072 Dallas, TX 75229 (214) 241-1895	Dispersion modeling software including EPA dispersion models, data entry programs, vulnerability zones, meteorological data processing programs, and puff-type programs for modeling gas releases. Uses more than 20 models.
BEESTAR, CRSMET, STAR WROSE		Bowman Environmental Engineering	P.O. Box 29072 Dallas, TX 75229 (214) 241-1895	Meteorological data processing. Prepares data in a suitable format for input in models.
BeSafe	BeSafe Hazardous Substance Information and Tracking Module	Azimuth Technologies, Inc.	P.O. Box 5787 Pasadena, CA 91117 (818) 405-0300	Information management system designed to aid in the creation of MSDSs. Includes packages containing hazardous materials data for compliance with "Right to Know" legislation.

Table 14–3 (continued)

ACRONYM/ABBREVIATION	SYSTEM NAME	VENDOR	ADDRESS/PHONE	PURPOSE/DESCRIPTION/REQUIREMENTS
BLUE SKY		Kelon Corporation	P.O. Box 64577 Tucson, AZ 85716 (602) 299-5636	An integrated package that creates air pollution permits, calculates and reports on emission inventory information and individual air pollution incidents.
BREEZE AIR		Trinity Consultants, Inc.	12801 N Central Expwy Suite 1200 Dallas, TX 75243 (214) 661-8100	Air pollution dispersion models derived from the UNAMAP6 stationary source models and other specialized dispersion models. Uses more than 20 models. Requires 512K memory and 132 column printer.
BREEZE HAZ		Trinity Consultants, Inc.	12801 N Central Expwy Suite 1200 Dallas, TX 75243 (214) 661-8100	Models toxic gas releases. Two models available: SHELL SPILLS and TRPUF (based on EPA PUFF). Graphical output. Requires 512K memory and 132 column printer.
CALS/EWDS	Computer Automated Laboratory System/ Environmental Waste Database System	Beckman Instruments Inc.	Lab. Automation Operations 160 Hopper Ave. Waldwick, NJ 07463 (201) 444-8900	CALS combines sample tracking facilities with a database for management and documentation of information in the environmental waste monitoring laboratory. EWDBS provides a reporting format that prints data on the NPDES form.
**CAMEO II	Computer-Aided Management of Emergency Operations, Version 1.02	U.S. Department of Commerce - NOAA/U.S. Environmental Protection Agency - Office of Solid Waste and Emergency	Mark Miller NOAA HazMat Resp. Branch 7600 Sand Point Wy NE Seattle, WA 98115 (206) 526-6317 John Laumer National Safety Council 444 N. Michigan Ave. Chicago, IL 60611 (312) 527 4800 x5606	Emergency planning and response information including the following: chemical information, response information, air modeling, mapping, response resources inventory, facility information, route information, population information, emergency recordkeeping, MSDS information, Section 304 release reports, information request records, facility reports, and planning introduction and assistance. Requires Apple computer equipment.
CAMEO	Computer-Aided Management of Emergency Operations, IBM Version	U.S. Department of Commerce - NOAA/U.S. Environmental Protection Agency - Office of Solid Waste and Emergency	Mark Miller NOAA HazMat Resp. Branch 7600 Sand Point Wy NE Seattle, WA 98115 (206) 526-6317	Database of chemical data and response information.

Table 14–3 (continued)

ACRONYM/ABBREVIATION	SYSTEM NAME	VENDOR	ADDRESS/PHONE	PURPOSE/DESCRIPTION/REQUIREMENTS
CARE	Computerized Airborne Release Evaluation	Environmental Systems Corporation	Ron Webb 200 Tech Center Dr. Knoxville, TN 37912 (615) 688-7900	Uses mathematical models to assess gas cloud movements. Uses gas detectors and weather sensors to alert user of release, and provides plume dispersion, effects, and response information.
CASH/TRACK		Livingston Enterprises	2855 Kifer Road Santa Clara, CA 95051 (408) 986-8866	Full inventory chemical tracking system designed to extract Tier I and Tier II information for assistance in reporting.
CEMDAS	Continuous Emission Monitoring Data Acquisition System	Enviroplan, Inc.	Ron Zowan 59 Main Street West Orange, NJ 07052 (201) 325-1544	Data acquisition system for continuous emission monitoring of ambient air or stack emissions. Also provides reports.
CENS	Computerized Emergency Notification System	Advanced Systems Laboratories, Inc.	7137 West Main St. Lima, NY 14485 (716) 624-3276	Can be used with CERS or CMSDS. Determines if incident requires emergency notification based on quantity of release. Telephone roster included. Requires 640K memory and hard disk.
**CERS	Computerized Emergency Response Series	Advanced Systems Laboratories, Inc.	7137 West Main St. Lima, NY 14485 (716) 624-3276	Determines response procedures for incidents based on data from CMSDS and CHIMS. Includes firefighting information, personal protective equipment, emergency first aid procedures, spill and containment procedures, waste disposal procedures, and physical and health hazards. Requires 640K memory and hard disk.
CHARM	Complex Hazardous Air Release Model	Radian Corp.	Lou Fowler 8501 Mo-Pac Blvd. Attn: CHARM P.O. Box 9948 Austin, TX 78766 (512) 454-4797	Primarily models chemical releases to the air. Includes a chemical database and map editor and is capable of mapping concentration isopleths. Allows real-time meteorological data input.
CHART/PC		Engineering Applications Specialists, Inc.	5610 Medical Circle Suite 31 Madison, WI 5371 (608) 273-0065	Computerized psychometric chart. User provides two independent properties of moist air and program calculates the remaining properties.

Table 14–3 (continued)

ACRONYM/ABBREVIATION	SYSTEM NAME	VENDOR	ADDRESS/PHONE	PURPOSE/DESCRIPTION/REQUIREMENTS
CHCS	Computerized Hazard Compliance Series	Advanced Systems Laboratories, Inc.	7137 West Main St. Lima, NY 14485 (716) 624-3276	Provides compliance information including lists of hazardous substances under SARA, OSHA, and CERCLA, Tier I reports, Tier II reports, emergency and release reporting. Requires 640K memory and hard disk.
CHCS Compliance Engine		Advanced Systems Laboratories, Inc.	7137 West Main St. Lima, NY 14485 (716) 624-3276	Assists with SARA Title III compliance. User inputs information and system provides compliance status and tasks required for compliance.
CHEM MASTER Version 2.1		ITS Technologies	Angela Loundes 9 East Stow Road Marlton, NJ 08053 (609) 983-7300 (800) 727-2487	Aids in SARA Title III compliance and chemical inventory tracking. Database of over 3,800 regulated chemicals. Has capability of tracking and reporting for multiple facilities. Prints in-house warning labels, prepares Section 311 reports and facsimiles of Tier I and Tier II reports.
CHEM MULTI BASE		CHEM Multi BASE, Inc.	P.O. Box 350 Mahomet, IL 61853 (217) 586-4131	Database of 16,000 chemicals with synonyms and trade names. Government numbers and information are cross referenced with MSDSs for all DOT regulated chemicals. Includes tracking and inventory system.
CHEMASYST		ICF Incorporated	June Bolstridge 9300 Lee Highway Fairfax, VA 22031-1207 (703) 934-3208 (800) 283-2243	Manages data needed to comply with SARA Title III and OSHA HSC Regulations. Provides text, guidance materials, instructions, and interpretations of the requirements; forms for reporting; databases of physical and chemical properties of some regulated chemicals; lists of chemicals that require reporting; Section 313 chemical references/sources/ citations; and an approved list of synonyms. Stores calculations of estimated releases and prints information onto submittable EPA forms.
CHEMCALC 1, Separations Calculations		Gulf Publishing Company, Book Division	P.O. Box 2608 Houston, TX 77252 (713) 520-4444	Programs for use with multi-component mixtures to determine the conditions and compositions at the dew point and at the bubble point.

Table 14–3 (continued)

ACRONYM/ABBREVIATION	SYSTEM NAME	VENDOR	ADDRESS/PHONE	PURPOSE/DESCRIPTION/REQUIREMENTS
CHEMCALC 7	Chemical Compound Databank	Gulf Publishing Company, Book Division	P.O. Box 2608 Houston, TX 77252 (713) 520-4444	Contains the physical properties of 500 compounds. Estimates properties at temperature or pressure within a specified range. Includes OSHA toxicity data, DOT notations, and directory of manufacturers for each compound. Requires 2 disk drives.
CHEMCALC 11, AMSIM	Amine Gas Treating Plant Simulator	Gulf Publishing Company, Book Division	P.O. Box 2608 Houston, TX 77252 (713) 520-4444	Models processes for absorption and stripping of H_2S and CO_2 in a gas stream. For hydrocarbon gases, also calculates hydrocarbons absorbed and stripped.
CHEMMASTER		Envirogenics, Inc.	136 W. Franklin Ave. Pennington, NJ 08534 (609) 737-3233	Chemical inventory system for Tier I/II information. Includes capacity to inventory quantity and location information. Contains database of 3100 hazardous chemicals.
CHEMEST	Chemical Property Estimation System	Camp, Dresser, & McKee, Inc.	Dr. Warren Lyman 1 Center Plaza Boston, MA 02108 (617) 742-5151 x5711	Designed to predict environmentally important properties of organic chemicals. Requires DEC VAX and IBM PC.
CHEMLINE	Chemical Dictionary Online	National Library of Medicine	8600 Rockville Pike Bethesda, MD 20894 (301) 496-1131	Online chemical dictionary with over 500,000 records on chemical substances found in the TOXLINE, TOXBACK65, TOXBACK74, RTECS, MEDLINE, and TDB databases, as well as the EPA TSCA Inventory. Search capability by synonyms, CAS Registry Numbers, and by classes of compounds. Prime time connect cost is $54 per hour.
CHEM-PLY		Environmental Communications Consultants, Inc.	1759 Sharwood Place Crofton, MD 21114 (301) 858-0332 (301) 793-0622	Provides brief regulatory information for RCRA, OSHA, and SARA compliance; also full text. Access to a 2,700 chemical data base with hazard information, precautions, and health effects. Menu-driven software.
CHEMTOX DATABASE		Resource Consultants	P.O. Box 1848 Brentwood, TN 37024 (615) 373-5040	Information on 3,500 chemical substances that are hazardous and of economic importance. Data include chemical names, CAS and DOT numbers, properties, exposure limits, EPA waste information, and spill response information. Quarterly updates. Requires 320K memory and 10Meg hard disk.

Table 14–3 (continued)

ACRONYM/ABBREVIATION	SYSTEM NAME	VENDOR	ADDRESS/PHONE	PURPOSE/DESCRIPTION/REQUIREMENTS
CHEMTREC	Chemicals in Transportation Emergency Center	Chemical Manufacturers Association (CMA)	2501 M Street, NW Washington, DC 20037 (202) 887-1255 (800) 424-9300	Available during a transportation-related emergency to provide hazard warning and assistance to response personnel. Modem allows direct access to HIT, the CMA's response information database.
CHIMS	Computerized Hazardous Inventory Management System	Advanced Systems Laboratories, Inc.	7137 West Main St. Lima, NY 14485 (716) 624-3276	Calculates and prints Tier I and Tier II inventory reports. Also assists with inventory and chemical storage information required for Toxic Chemical Release Reports. Requires 640K memory and hard disk.
**CHIP	Community Hazmat Information Platform	Material Safety Data Systems, Inc.	2674 E. Main St. Suite C-107 Ventura, CA 93003-2899 (805) 648-6800	Contains four modules that store and retrieve information: Administrative Information module for administrative information for local government; Emergency Response module for emergency response information for local government; Hazmat Handler Information module for handler information; and Hazmat Information module which contains hazardous material data for local government and handlers.
CHIT	Chemical Hazard Identification and Training	Marcom Marketing Group, Ltd.	P.O. Box 9557 4 Denny Road Wilmington, DE 19809 (800) 654-CHIT	Hazardous chemical information storage and retrieval for facilities. Modules for: MSDS, right-to-know requests, spill procedures, training, and labeling.
CHRIS	Chemical Hazard Response Information System	Chemical Information Systems, Inc.	Fein-Marquart 7215 York Rd Baltimore, MD 21212 (800) CIS-USER	Provides chemical information to assist response to emergencies involving spills of hazardous materials. Contains chemical, physical, and biological data, and specific response-oriented information (e.g., countermeasures). Developed by the U.S. Coast Guard.

Table 14–3 (continued)

ACRONYM/ABBREVIATION	SYSTEM NAME	VENDOR	ADDRESS/PHONE	PURPOSE/DESCRIPTION/REQUIREMENTS
CHRIS and CHRIS PLUS	Chemical Hazard Records and Inventory Software	Random House	Linda Goldfarb Jane Rathbun 201 East 50th Street New York, NY 10022 (800) 733-3000	Primarily recordkeeping system for individual facilities. Includes information on chemicals and manufacturers and records of accidents and training. Chris Plus adds capability of storing and printing MSDS information and assists with the preparation of Tier I and Tier II reports and right-to-know requests. Both systems contain database of 600 toxic substances and synonyms.
CIS	Chemical Information Service	Fein-Marquart Associates, Inc.	7215 York Road Baltimore, MD 21212 (800) CIS-USER	Collection of databases providing information that includes chemical properties, basic effects, and response techniques. $300 annual subscription fee; $20 - $95 per computer connect hour.
CMSDS	Computerized MSDS System	Advanced Systems Laboratory, Inc.	7137 West Main St. Lima, NY 14485 (716) 624-3276	Software manages and tracks MSDS database information by chemical ID, supplier, synonyms, components, registry numbers, completion status, uses, and hazard classes. Subscription updating. Requires 640K memory and hard disk.
COMPLIANCE MANAGER		OSHA-SOFT Corporation	Peter Bragdon P.O. Box 894 Concord, NH 03301 (603) 672-7230	Facility-specific information system that manages information on the following modules: MSDS MANAGER, TRAINING MANAGER and INVENTORY MANAGER.
COPE		Metcalf & Eddy, Inc.	10 Harvard Mill Sq. Wakefield, MA 01880 (617) 246-5200	COPE has 9 modules: PM scheduler, corrective maintenance, equipment history, equipment reference listing, spare parts entry, database integrity verification, and training.
CORKES		Roy F. Weston, Inc.	Judith Hushon 955 L'Enfant Plaza, SW Washington, DC 20024 (202) 646-6800	Provides facility-specific information for emergency situations.
CoVOCalc		Dawn Graphics Company	19 Edgehill Road Winchester, MA 01890 (617) 721-0456	Spreadsheet template that calculates expected VOC emissions from use of paints, inks, and coatings. Prints out EPA data forms.

Table 14–3 (continued)

ACRONYM/ABBREVIATION	SYSTEM NAME	VENDOR	ADDRESS/PHONE	PURPOSE/DESCRIPTION/REQUIREMENTS
CSIN	Chemical Substance Information Network	U.S. EPA/Office of Pesticides and Toxic Substances	Mr. Dalton Tidwell/ Dr. Sidney Siegal OPTS Chemical Coordination Staff (TS-777) 401 M Street, SW Washington, DC 20460	Complex switching network that provides user access to over 400 individual databases. Necessary to obtain user codes for various vender databases.
CTCRRS	Computerized Toxic Chemical Release Reporting System	Advanced Systems Laboratories, Inc.	7137 West Main St. Lima, NY 14485 (716) 624-3276	Assists with completion of EPA Form R using CMSDS and CHIMS information. Also tracks reporting requirements and emission and waste treatment. Requires 640K memory and hard disk.
CYCLONE		TECS Software, Inc.	P.O. Box 720730 Houston, TX 77272 (713) 561-6143	Does the following calculations for a gas or air cyclone: sizing, pressure drop, and fractional and overall efficiency.
DATASTREAM		Datastream Systems, Inc.	1200 Woodruff Road Suite C-40 Greenville, SC 29607 (803) 297-6775	System designed for industrial and municipal wastewater treatment facility data management, including key process parameters and plant evaluation.
DIALOG		DIALOG Information Services	3460 Hillview Ave. Palo Alto, CA 94304 (415) 858-3785	Reference system containing information from all areas of science, technology, and medicine. $10 - $285 per computer connect hour.
DIPPR	Design Institute for Physical Property Data	National Bureau of Standards		Data compilation of pure compound properties.
ECMS	Environmental Compliance Monitoring System	Versar Environmental Systems	9200 Rumsey Road Columbia, MD 21045-1934 (301) 964-9200	Facility-specific system including modules for air emissions, calendar, facility and agency processes, groundwater, hazardous waste, incident response, permit tracking, solid (non-hazardous) waste, work orders, and wastewater.

Table 14–3 (continued)

ACRONYM/ABBREVIATION	SYSTEM NAME	VENDOR	ADDRESS/PHONE	PURPOSE/DESCRIPTION/REQUIREMENTS
ECOTRAC	Environmental Data Management System	HAZOX Corporation	Daniel Fullerton 12600 W. Colfax Ave. Suite C420 Lakewood, CO 80215 (303) 237-1065	Provides manifest tracking, permit tracking, source inventory, environmental events, TSCA required data management, waste disposal costs, and groundwater monitoring.
**EIS/C	Emergency Information System/Chemical	Research Alternatives, Inc.	Maxine Orens Suite 3 966 Hungerford Dr. Rockville, MD 20850 (301) 424-2803	Primarily an emergency planning and response system. Records chemical, facility, transportation, vulnerable population, and other planning and response information. Presents information on maps. Prepares Tier I and II reports. Stores MSDS information.
EMERGENCY CALL SYSTEM		Weith Computer Products and Services	802 Brittany Suite 101 Bowling Green, OH 43402 (419) 352-8659	Automatically calls emergency response personnel based on incident specific information.
EMERGENCY RESPONSE COMPUTER PROGRAM		Ontario Ministry of Environment	Air Resources Branch 880 Bay Street 4th floor Toronto, Ontario M5S 1Z8	Release modeling system. Contains database of chemicals and characteristics which may be modified by user. User selects chemical, weather conditions and type of release for simple or heavy gas modeling. Output is numeric for times and distances with graphic capabilities.
ENFLEX DATA 313		ERM Computer Services, Inc.	Terry Percel 855 Springdale Dr. Exton, PA 19341 (800) 365-2146 (800) 544-3118	Calculates releases by four principle methods to the following media: water, POTW, Underground Injection, Stack or Point Air, Fugitive, Land, Waste Offsite, and other processes in the facility. Also performs a mass balance function around each process; prints Form R and submits to EPA; provides for unlimited comments; and stores unused calculations.
ENFLEX INFO		ERM Computer Services, Inc.	Terry Percell 855 Springdale Dr. Exton, PA 19341 (800) 365-2146 (800) 544-3118	Provides access to the full text of current federal and state environmental regulations. Includes NJ and PA regulations. Provided on a subscription basis, and furnished on CD-ROM compact laser disc.

Table 14–3 (continued)

ACRONYM/ABBREVIATION	SYSTEM NAME	VENDOR	ADDRESS/PHONE	PURPOSE/DESCRIPTION/REQUIREMENTS
EnviroBase III	Environmental Data Management System	Enviro Base Systems	Michael H. Freeland 2 Inverness Drive East Suite 101 Englewood, CO 80112 (303) 790-8396	Organizes, analyzes, and generates reports of laboratory analytic data associated with groundwater, soils and surface sampling and testing programs. Written and compiled in Clipper, an extension of dBase III. Requires DOS 3.0 or greater with at least 410K of free RAM, and a hard disk with at least 1.5 megabytes of free storage space.
EnviroLab III	Laboratory Data Management System (LDMS)	Enviro Base Systems	Richard L. Sayrs, Jr. 2 Inverness Drive East Suite 101 Englewood, CA 80112 (303) 790-8396	Organizes analytical laboratory paperwork: sample log-in and tracking to final analysis reporting and invoicing, operates on single-CPU or local area network of IBM PC/XT/AT/80386 or compatible.
ENVIRONMENTAL AIDE		Odessa Engineering	P.O. Box 26537 Austin, TX 78755 (512) 251-5543	Screen oriented, menu driven program that facilitates data editing, data analysis and preparation of reports for stack emissions.
ETIS	Environmental Technical Information System	U.S. Army	Ron Webster Construction Engineering Research Laboratory P.O. Box 4005 Champaign, IL 61820	Computerized information retrieval system that aids the Army and other government agencies in preparing environmental impact statements.
FIESTA	Field Slug Test Analyzer	Roy F. Weston, Inc.	Judith Hushon 955 L'Enfant Plaza, SW 6th Floor Washington, DC 20024 (202) 646-8600	Uses raw data from field tests to compute hydraulic conductivity; computed value is evaluated by the expert system for its correctness with regard to these considerations: site-specific geological characteristics, validity of test procedures, accuracy of the raw data, and the computational method. System is written in Arity-Prolog on a PC.
FINANCIAL ANALYSIS OF WASTE MANAGEMENT ALTERNATIVES		General Electric Company Corporate Environmental Programs	Mr. Richard MacLean 3135 Easton Turnpike Fairfield, CT 06431 (203) 373-3077	System calculates the long-term costs, including liability, associated with environmental control technologies. Requires printer with capability of printing 240 columns of width

Table 14–3 (continued)

ACRONYM/ABBREVIATION	SYSTEM NAME	VENDOR	ADDRESS/PHONE	PURPOSE/DESCRIPTION/REQUIREMENTS
FINDEX		HAZOX Corporation	Daniel Fullerton P.O. Box 637 Chadds Ford, PA 19317 (215) 388-2030 (800) 558-6942	Indexing and retrieval software for searching MSDS files.
FLAREHDR and FLARESTK		TECS Software, Inc.	P.O. Box 720730 Houston, TX 77272 (713) 561-6143	Two programs, one of which determines header size based on maximum allowable relief velocity along the header and the other program calculates flare tip diameter and stack height.
FLOW GEMINI	Environmental Information Management System and Occupational Health Information System	Flow General, Inc.	Dr. Wanda Rappaport 7655 Old Springhouse Rd McLean, VA 22102 (703) 893-5900	Generates reports, schedules, and reminders; summary, detail, and status; and inventory, inspection and monitoring for permits, air and water monitoring, waste, PCBs and problems and events. Generates MSDSs, and aids in waste tracking and environmental audits. Requires DEC VAX or IBM mini or mainframe.
FRES	First Responders Expert System	Roy F. Weston, Inc.	Judith Hushon 955 L'Enfant Plaza, SW Washington, DC 20024 (202) 646-6800	Provides pollutant toxicity information and optimal response strategy.
GASPROPS		Software Systems Corporation	P.O. Box 202017 Austin, TX 78720 (512) 451-8634	Computes thermodynamic properties of air, argon, carbon monoxide, carbon dioxide, hydrogen, nitrogen, oxygen, water vapor, and products of combustion for hydrocarbons. Computes all properties from any two independent properties.
GEMS	Graphical Exposure Modeling System	U.S. EPA	Cathy Turner Pat Harrigan Office of Toxic Subst. TS-798 Washington, DC 20460 (202) 382-3929 (202) 382-3397	On-line system. Provides support for exposure assessments of toxic substances. Includes chemical property estimation techniques, statistical analysis, multi-media modeling, and graphics display (including models).

Table 14–3 (continued)

ACRONYM/ABBREVIATION	SYSTEM NAME	VENDOR	ADDRESS/PHONE	PURPOSE/DESCRIPTION/REQUIREMENTS
GLIDE	Geographically Locate Inventoried Dangers Easily		Jerome Barta 1513 White Post Cedar Park, TX 78613 (512) 258-1812 (call after 4 PM)	Provides capability to inventory and retrieve information on stored hazardous chemicals and their proximity to central areas.
GROUNDWATER/DMS	Groundwater Data Management System	CSW Data Systems	One Overlocker Road Poughkeepsie, NY 12603 (914) 454-0090	A data management package which tracks the data associated with a groundwater monitoring network. The system quantifies and identifies all forms of data, reports, analyses, corporate and government standards. Requires 4.6 megs of hard disk space; 640K RAM, 80286 (80386) processor and a DOS version of 3.30 or higher.
HAZARD		North American Software, Inc.	George Stephens P.O. Box 3309 Tustin, CA 92680 (714) 830-6248	Database system that is designed to aid in producing both the EPA Manifest and Drum Labels. Includes DOT information for verification.
HAZARDLINE		Occupational Health Services, Inc.	John Fee Suite 2407 450 7th Avenue New York, NY 10123 (800) 445-6737 (212) 967-1100	Online information on hazardous substances. Includes: response information and medical effects data with unique search capabilities. Cost is $120 per hour (1983).
Hazardous Incident Data Base		U.S. EPA	Pacita Tibay Woodbridge Ave. Edison, NJ 08837 (201) 321-6632	Search and retrieval system designed to direct the user to documented first-spill incidents. No charge.
Hazardous Material Document and Package Verification System		Bureau of Dangerous Goods, Ltd.	Russell Bowen Front & Erickson Sts Essington, PA 19029 (215) 521-0900	Prepares shipper's declaration and identifies marking, labeling, and other packaging requirements.
**HazKNOW Know-IT-ALL		HazMat Control Systems, Inc.	Carolyn Husemoller 3409 Lakewood Blvd Suite 2C Long Beach, CA 90808 (213) 429-9055	Stores hazmat information; generates documents and reports; MSDS document management.

Table 14–3 (continued)

ACRONYM/ABBREVIATION	SYSTEM NAME	VENDOR	ADDRESS/PHONE	PURPOSE/DESCRIPTION/REQUIREMENTS
HAZM	Hazardous Waste Manager	Z Micro Systems	P.O. Box 6634 San Pedro, CA 90734 (213) 831-4888	Records and prints waste disposal manifests on official forms and outputs reports by waste category, transporter, and disposal site. Also records MSDSs. Requires 256K memory.
**HAZMIN	The Hazardous Material Information Network	Logical Technology, Inc.	Vicky Demoss P.O. Box 3655 Peoria, IL 61614 (309) 677-3303	System manages hazardous materials: includes storage, inventory, compliance, and training. MSDS based emergency response data storage and retrieval. Assists with Tier I/II reports. Extensive search capabilities. Requires VAX. PC version scheduled for release in early 1988.
HAZOX LABEL PROGRAM		HAZOX Corporation	Kathleen Goddard P.O. Box 637 Chadds Ford, PA 19317 (215) 388-2030 (800) 558-6942	Prepares labels for containers. User may copy information from MSDSs or other text files. May be used in conjunction with TOXIC ALERT.
HAZOX EMPLOYEE TRAINING LEDGER		HAZOX Corporation	Kathleen Goddard P.O. Box 637 Chadds Ford, PA 19317 (215) 388-2030 (800) 558-6942	Employee recordkeeping system. Tracks worker training, job location, and job assignments, as well as employee courses and qualifications. May be used in conjunction with TOXIC ALERT.
HAZ/TRAK		HAWKWA Group, Inc.	Russ Hannula P.O. Box 321 Mundelein, IL 60060 (312) 949-8488	Computerizes MSDSs in OSHA-174 format. Also tracks material use and storage. Requires 448K memory and 2 disk drives.
HAZWASTE		HazMat Control Systems, Inc.	Carolyn Husemoller 3409 Lakewood Blvd Suite 2C Long Beach, CA 90808 (213) 429-9055	Hazardous waste data management and reporting system. Prepares hazardous waste manifests. Requires 10 Meg hard disk and 132 column printer.
HMIS	Hazardous Materials	Defense Logistics Agency Information System	Rhonda Herns Rockville, MD (301) 468-8858	DoD system that stores MSDS information, quantity and manufacturer, and National Stock numbers. On-line Database and microfiche. Cost: $30 - $40 per hour. For DoD facilities only.

Table 14–3 (continued)

ACRONYM/ABBREVIATION	SYSTEM NAME	VENDOR	ADDRESS/PHONE	PURPOSE/DESCRIPTION/REQUIREMENTS
HMMS	Hazardous Materials Management System	Caelus	Larry Williams Caelus Inc. 1100 Paulsen Center W. 421 Riverside Spokane, WA 99201 (509) 624-8794 or Craig Van Velzer Wang Laboratories, Inc. N1000 Argonne Rd Suite 100 Spokane, WA 99212 (509) 922-2136	Integrates both Wang supplied and Caelus supplied software into a system for managing data and reporting requirements. Includes: aliases, trade and industry standard names and IDs; components of mixtures and compounds; plant sites, annual usage, and storage locations; hazardous properties and medical precautions; approved treatment or remedies; MSDSs; references; protective equipment and requirements; approved suppliers and/or manufacturers; agencies; reporting forms. Can run stand-alone on any Wang VS computer.
HWCS	Hazardous Waste Computer System	National Safety Council	P.O. Box 11933 Chicago, IL 60611 (800) 621-7619 (312) 527-4800	Tracks waste from collection to treatment. Database of 2,600 common chemicals which provides the EPA number for each chemical, DOT classification for hazardous waste transport, and permit information. Templates for all required forms, labels, and notices.
HYCARB		Software Systems Corporation	Donna Schmidt P.O. Box 26065 Austin, TX 78755-0065 (512) 451-8634	Computes the thermodynamic and transport properties of 78 common petroleum and chemical industry hydrocarbons.
IEMIS	Integrated Emergency Management Information	Federal Emergency Management Agency	Dr. Bob Jaske 500 C Street SW Room 627 Washington, DC 20472 (202) 646-2865	FEMA's database system for emergency response information for governments. For use in planning, training, and eventually real-time operational decision-making for all types of emergencies. Includes plume dispersion modeling. A wide variety of access options are available.
INFO (EHIS)	Emergency/Hazmat Information System	Emergency Automation Inc.	Gary Hill 1401 Wilson Blvd. Suite 720 Arlington, VA 22209 (703) 522-4550	An incident information management tool for hazardous materials emergency responders.

Table 14–3 (continued)

ACRONYM/ABBREVIATION	SYSTEM NAME	VENDOR	ADDRESS/PHONE	PURPOSE/DESCRIPTION/REQUIREMENTS
INHEC1		Roy F. Weston, Inc.	Judith Hushon 955 L'Enfant Plaza, SW Washington, DC 20024 (202) 646-6800	INHEC1 is a front-end to the HEC-1 model developed by Hydrologic Engineering Center. Assists in modeling a watershed and creating the inputs to HEC-1 for hydrologic simulations. INHEC1 contains information about the requirements and limitations of HEC-1 and rainfall-runoff processes.
INVENTORY MANAGER		OSHA-SOFT Corporation	Peter Bragdon P.O. Box 668 Amherst, NH 03031 (603) 672-7230	Tracks hazardous materials in workplace and inventory for purchasing. Includes manufacturer listings.
IRIS	Integrated Risk Information System	DIALCOM, Inc.	Mike McLaughlin 600 Maryland Ave, SW Washington, DC 20024 (202) 488-0550	On-line database containing chemical files that present summaries of hazard and dose-response assessments for carcinogenic and/or noncarcinogenic effects and contain information on Office of Drinking Water Health Advisories, EPA regulations and guidelines (e.g., Clean Air Act regulations and Drinking Water Criteria) acute toxicity, and physical/chemical properties.
ISCST	Industrial Source Complex Short Term	Trinity Consultants, Inc.	Shirley Lake 12801 N. Central Expwy Suite 1200 Dallas, TX 75243 (214) 661-8100	Software for dispersion modeling; uses Gaussian plume model. The system calculates concentration or deposition values for inputed time periods. May be used in conjunction with "Breeze Air."
LABSYS	Laboratory Selection Expert System	Roy F. Weston, Inc.	Judith Hushon 955 L'Enfant Plaza SW 6th Floor Washington, DC 20024 (202) 646-6800	Assists in identifying appropriate analytical laboratories to evaluate environmental samples (e.g., soil, water, sludge, waste, air) for characterizing hazards at a site. The system factors type of sample, suspected pollutants, user's needs for on-site evaluation, and laboratories' locations, capabilities, and qualifications.
**MANGUARD		ManGuard Systems, Inc.	Craig Rylee 25972 Novi Road Suite 203 Novi, MI 48050 (313) 349-3830	Twelve Modules addressing environmental activities monitored by EPA, RCRA, OSHA, CERCLA, and DOT regulations. Includes SARA reporting module containing MSDS and production information, SARA reporting assistance, tracking capabilities.

Table 14–3 (continued)

ACRONYM/ABBREVIATION	SYSTEM NAME	VENDOR	ADDRESS/PHONE	PURPOSE/DESCRIPTION/REQUIREMENTS
MEDLARS	Medical Literature Analysis Retrieval System	National Library of Medicine	Carolyn Tilley MEDLARS Management Section 8600 Rockville Pike Bethesda, MD 20894 (301) 496-6193	Collection of databases containing toxicological research information and literature citations.
MESOCHEM	Chemical Atmospheric and Hazard Assessment System	Impell Corporation	Becky Cropper 300 Tristate Internat'l Suite 400 Lincolnshire, IL 60069 (312) 940-2090	Software for atmospheric dispersion and chemical exposure assessment. A plume dispersion model.
MESOREM Jr.		Impell Corporation	Becky Cropper 300 Tristate Internat'l Suite 400 Lincolnshire, IL 60069 (312) 940-2090	Atmospheric release analysis system that includes back calculations of source release rates from field readings, terrain modeling, meteorological conditions modeling of multipoint dose and deposition exposures. Also provides ingestion exposure reports for atmospheric effluent pathways.
METROHEALTH		Lamb & Associates, Inc.	Tommy Roach P.O. Box 638 Lumberton, NC 28359 (919) 739-3181	Multi-user safety and health package. Records data on personnel and MSDS information. Assists with medical reports and OSHA forms.
METROSOFT		Metrosonics	Rob Brauch P.O. Box 23075 Rochester, NY 14692 (716) 334-7300	Industrial hygiene information record system. Utilizes hand held monitoring system to record exposure data on computer.
microCHRIS		The HazMat Software Co./ AIA Corporation	Rod Nenner 134 Middle Neck Rd Suite 210 Great Neck, NY 11021 (516) 829-5858 (800) 284-6737	Coast Guard CHRIS system. Includes chemical designations, observable characteristics, health hazards, responses to discharges, fire hazards, chemical reactivity, water pollution, shipping information, hazard assessment codes, hazard classifications, and physical and chemical properties. Requires 640K memory and 10Meg hard disk.

Table 14–3 (continued)

ACRONYM/ABBREVIATION	SYSTEM NAME	VENDOR	ADDRESS/PHONE	PURPOSE/DESCRIPTION/REQUIREMENTS
microOHM/TADS		The HazMat Software Co./ AIA Corporation	Rod Nenner 134 Middle Neck Rd Suite 210 Great Neck, NY 11021 (516) 829-5858 (800) 284-6737	Microcomputer version of EPA's Oil and Hazardous Materials Technical Assistance Database. Contains emergency response, physical and chemical properties, and hazards of 1400 compounds. Requires 640K memory and 10Meg hard disk.
MIDAS	Meteorological Information and Dispersion Assessment System	Pickard, Lowe and Garrick, Inc.	Mark Abrams 1615 M Street, NW Suite 730 Washington, DC 20036 (202) 659-1122	Calculates impact of gaseous releases under routine or accident conditions.
MSDS ALERT		HAZOX Corporation	Kathleen Goddard P.O. Box 637 Chadds Ford, PA 19317 (800) 558-6942 (215) 388-2030	MSDS database.
MSDS Engine Software		GENIUM Publishing Corporation	1145 Catalyn St. Schenectady, NY 12303-1836 (518) 377-8854	Collection of MSDSs. Has capability to create additional MSDSs and search by name and CAS#.
MSDS-MAN	MSDS-MAN	Spumifer American, Inc.	Pete Dyke P.O. Box 3267 St. Augustine, FL 32085 (904) 824-0603	Data base manager for MSDSs.
MSDS MANAGER		OSHA-Soft Corporation	Peter Bragdon P.O. Box 668 Amherst, NH 03031 (603) 672-7230	Software containing MSDS information in OSHA format. Stores and prints MSDSs; assists with training of employees.
MSDS-PC		J.J. Keller & Associates, Inc.	145 W. Wisconsin Ave. P.O. Box 368 Neenah, WI 54957-0368 (800) 558-5011	User created chemical information database. Includes trade name, manufacturer, ingredients, CAS Number, and plant location. Requires 256K memory.

Table 14–3 (continued)

ACRONYM/ABBREVIATION	SYSTEM NAME	VENDOR	ADDRESS/PHONE	PURPOSE/DESCRIPTION/REQUIREMENTS
MSDSPLUS		Robert E.J. Thomas & Associates, Inc.	Dr. Robert J. Thomas Woodsboro, Md. 21798 (301) 695-5603	MSDS recording and tracking system. Used to maintain employee and inventory records. System also has ability to track location and first and last date that a chemical was used or stored at a facility.
MSDSFILE		HazMat Control Systems, Inc.	Carolyn Husemoller 3409 Lakewood Blvd Suite 2C Long Beach, CA 90808 (213) 429-9055	Prepares, prints, and stores MSDSs. Creates reports. Requires 10Meg hard disk.
OASIS	Operator Assisted Sewer Information System	Public Works Software, Inc.	Jerry Cadwell Harbor Plaza P.O. Box 580 Port Hueneme, CA 93401 (805) 488-7324	Database for management of sanitary and storm wastewater collection systems. Maintains field operations data including safety history, engineering data, inspection records, and work orders. Requires 640K memory and hard disk.
OPERATOR 10		Macola Incorporated	Don Knaur P.O. Box 485 Marion, OH 43301-0485 (614) 382-5999 (800) 468-0834	Assists in the management of wastewater treatment plants using four programs: Process Evaluation for generating process equations; Inventory/Maintenance for work order generation and printouts, preventive maintenance, and inventory tracking; Industrial Pollutant Monitoring for record-keeping and report generation; and Process Monitoring/Reporting for process reports and other reports. Each requires 512K memory and 10Meg hard disk.
ORBIT		Pergamon	Orbit Action Desk Infoline, Inc. 8000 Westpark Dr. McLean, VA 22102 (703) 442-0900	Database of information from all areas of science, technology, and medicine, as well as business, current affairs, and humanities. $30 - $160 per computer connect hour.
OSHA-SOFT CFR		OSHA-SOFT Corporation	Peter Bragdon P.O. Box 668 Amherst, NH 03031 (603) 672-7230	Text of 29 CFR(OSHA) and 40 CFR(EPA) regulations on disk. Requires 512K memory and hard disk.

Table 14–3 (continued)

ACRONYM/ABBREVIATION	SYSTEM NAME	VENDOR	ADDRESS/PHONE	PURPOSE/DESCRIPTION/REQUIREMENTS
PART B OUTLINE		Weith Computer Products & Services	Roger Weiter 802 Brittany Suite 101 Bowling Green, OH 43402-1511 (419) 352-8659	Assists user with writing Part B application. Cites regulations by number.
PART B PERMITTING			Gerald Rich 17719 Brim Road Bowling Green, OH 43402 (419) 352-7085 (after 5:30 p.m.)	Permit application assistance for hazardous waste facilities on diskettes.
PCB HAZARD		U.S. Construction Engineering Research Laboratory	Attn: Bernie Donahue P.O. Box 4005 Champaign, IL 61820-1305 (217) 373-6733	Provides guidance on the repair and disposal of transformers containing 50 ppm or more of PCB's.
POSSEE	Plant Organizational Software System for Emissions from Equipment	Chemical Manufacturers Association (CMA)	Deborah Stine 2501 M Street, NW Washington, DC 20037 (202) 887-1176	Supports the organization, entry, and analysis of plant data and field measurements of fugitive emissions. A menu-driven system.
PRETRE		Cochrane Associates, Inc.	Jay J. Fink 236 Huntington Ave. Boston, MA 02115 (617) 247-0444	Information management system for wastewater treatment facilities. Assists with monitoring compliance, tracking construction projects, producing reports, and generating letters.
PRETREATMENT		Spica Systems	4921 Seminary Road Suite 1502 Alexandria, VA 22311 (703) 671-5874	Series of programs for implementing EPA's categorical pretreatment standards. Contains data forms for identifying and collecting information needed for Applicability, production, special conditions, and flow.
PSYCHRO		Software Systems Corporation	P.O. Box 202017 Austin, TX 78720 (512) 451-8634	Computes properties of air-water vapor mixtures for HVAC, combustion, aerodynamic, and meteorological applications. Any two independent properties may be inputed by user.

Table 14–3 (continued)

ACRONYM/ABBREVIATION	SYSTEM NAME	VENDOR	ADDRESS/PHONE	PURPOSE/DESCRIPTION/REQUIREMENTS
PTPLU-2		Trinity Consultants, Inc.	Shirley Lake 12801 N. Central Expwy Suite 1200 Dallas, TX 75080 (214) 661-8100	Dispersion modeling software based upon EPA's UNAMAP. System is upgraded version of PTMAX; it is a screening model that can be applied to single sources.
Quantum Software		Quantum Software Solutions, Inc.	Laurie Breck P.O. Box 640 Ann Arbor, MI 48107-0640 (313) 761-2175	Series of compliance assistance modules including: Worker Right to Know, Asbestos Compliance Tracking, Community Right to Know, Firefighter Right to Know, assistance with report generation and Underground Tank Inventory.
Rainbo MSDS-PRO, SARA, and SAFETY		Pro Am Safety	Zoltan Toth P.O. Box 750 Gibsonia, PA 15044 (412) 443-0410	Database management system for MSDS information. Modules include SARA, for assistance in creating reports for Title III, and SAFETY for accident and incident record-keeping.
Regulation Scanning System		Data Regs. Inc.	Robert McCardy 243 West Main St. Kutztown, PA 19530 (215) 683-5098	Hazardous materials transportation regulations on disk. System displays text of regulations by chemical name or number. Also searches by keyword. Updates to regulations are provided on a monthly basis.
RESREC	Disposal Alternatives Planning and Resource Recovery Systems	Roy F. Weston, Inc.	Judith Hushon 955 L'Enfant Plaza, SW Washington, DC 20024 (202) 646-6800	Assists in planning disposal systems for community waste. The model accepts appropriate inputs describing the community's situation and constraints, performs cost analyses for various scenarios to account for uncertainties in the input, and provides the system with heuristic indicators which describe the results. Interprets the results and provides advice on planning scenarios to be used as guidelines for making a study of appropriate alternative scenarios.
RODA	Records and Operations Management	Metcalf & Eddy, Inc.	Eric Burman 529 Main Street Charlestown, MA 02129 (617) 241-8850	Data management system for wastewater treatment operators.

Table 14–3 (continued)

ACRONYM/ABBREVIATION	SYSTEM NAME	VENDOR	ADDRESS/PHONE	PURPOSE/DESCRIPTION/REQUIREMENTS
RTECS	Registry of Toxic Effects of Chemicals	National Library of Medicine, Specialized Information Services	Genne Gosloth 8600 Rockville Pike Building 38A Bethesda, MD 20894 (301) 496-1131	On-line database containing records for more than 50,000 potentially toxic chemicals. Source for basic acute and chronic toxicity information. Prime-time cost is about $5 per hour.
SAFECHEM II	Management System	SAFEWARE, INC.	4677 Old Ironsides Dr. Santa Clara, CA 95054 (408) 727-2436	Hazardous chemical management system implemented on a proprietary database package.
SAFER	System Approach for Emergency Response	SAFER Emergency Systems, Inc.	Darlene Davis Dave Dillehay 756 Lakefield Road Westlake Village, CA 91361 (818) 707-2777	Facility spill response, tracking of releases, materials inventory, and training.
SAM	Laboratory Information Management System	Radian Corporation	Mike McAnally P.O. Box 9948 8501 Mo-Pac Blvd Austin, TX 78766 (512) 454-4797	Laboratory tracking, scheduling, reporting, and statistical analysis.
**SARA!		OSHA-SOFT Corporation	Peter Bragdon P.O. Box 668 Amherst, NH 03031-0668 (603) 672-7230 (800) 446-3427	Generates inventory and Tier I and II reports required under SARA Title III. Monitors chemical inventories and locates hazardous chemicals in the workplace. Emergency Response version maintains inventories of all hazards and chemicals in the area for emergency response personnel.
SARA TITLE III 313 ADVISOR		E.I. Du Pont de Nemours & Company Inc. Environmental Management Services	Barley Mill Plaza (P27-2125) Wilmington, DE 19898 (800) 992-0560	Assists with completion of form R. Provides list of synonyms and copy of regulations in software. Maintains audit trail.

Table 14–3 (continued)

ACRONYM/ABBREVIATION	SYSTEM NAME	VENDOR	ADDRESS/PHONE	PURPOSE/DESCRIPTION/REQUIREMENTS
SARATRAX		IIT Research Institute, Maryland Technology Center	Dr. Quon Y. Kwan Sr. Env. Engineer 4600 Forbes Blvd Lanham, MD 20706 (800) 458-1564 (301) 459-3711	Assists with determination of facility reporting responsibilities under Sections 301-303, 304, and 311-312. Assists with notification requirements and definitions of responsibilities. Maintains lists of chemicals, quantities, locations, and properties to assist with the preparation of Tier I and Tier II reports. Generates Form R.
SENTRY		Besserman Corporation	Wes Turner 1702 East Highland Suite 120 Phoenix, AZ 85016 (602) 264-8000	Records industrial hygiene and health information. Creates reports, tracks MSDS information; MSDS information by synonym, name, mixture name, and CAS #.
SEWER MAINTENANCE SYSTEM		O'Brien & Gere Engineers, Inc.	Trish Anrig 1304 Buckley Road Syracuse, NY 13221 (315) 451-4700 (315) 451-2060	Management assistance for sewer line maintenance and recordkeeping. Database system that allows monitoring of specific operations and activities. Requires 640K.
SLUDGE MANAGER		Resource Conservation Services, Inc.	42 Main Street Yarmouth, ME 04096 (207) 846-3737	Recordkeeping and database management for treatment plants and facilities that produce useful sludge. Requires 312K memory, 5Meg hard disk, and dBase II.
SLUDGE REGULATOR		Resource Conservation Services, Inc.	42 Main Street Yarmouth, ME 04096 (207) 846-3737	Designed for state regulatory agencies. Tracks land spreading operations within the state. Produces reports, mailing lists and labels, permit expiration dates, and generator/material descriptions. Requires 312K memory and 5Meg hard disk.
SOPHIE	Selection of Procedures for Hazard Identification and Evaluation	Battelle	Columbus Division 505 King Avenue Columbus, OH 43201-2693 (614) 424-6424	Assists users with selection of methods to employ for identifying and evaluating hazards in chemical and petrochemical facilities.

Table 14–3 (continued)

ACRONYM/ABBREVIATION	SYSTEM NAME	VENDOR	ADDRESS/PHONE	PURPOSE/DESCRIPTION/REQUIREMENTS
SPCC	Spill Prevention Control and Countermeasure Data Base System	U.S. EPA	Ms. Jean H. Wright Office of Emergency and Remedial Response WHS48B 401 M Street, SW Washington, DC 20460 (202) 245-3057	Database containing compliance/ noncompliance records of oil facility discharges. Spill data include amount of material spilled, rate, response, and control measures.
SPILCOM		Globe International, Inc.	P.O. Box 1062 Buffalo, NY 14206 (716) 824-8484	Oil spill contingency planning tool intended to improve notification of federal and state agencies and improve response and reporting capabilities.
SUNHEALTH		Stewart-Todd Associates, Inc.	1016 W. 9th Ave. King of Prussia, PA 19406 (215) 962-0166	Manages occupational health records, MSDSs, chemical information, and employee records. Aids with emergency release reports.
SWIS	Solid Waste Information System	Mathtech The Technical Research and Consulting Division of Mathematica, Inc.	Barrett J. Riordan 5111 Leesburg Pike Suite 702 Falls Church, VA 22041 (703) 284-7900	Inventory and record system designed for the State of California Solid Waste Management Board.
Systems/Services Engineering		Systems/Services Engineering	P.O. Box 32008 Dayton, OH 45432 (513) 429-2709	Wastewater treatment assistance. Software includes: Data Handling System, Lab Bench File, Lab Stock Inventory, Scheduled Work System, Unscheduled Work System, Facility Stock Inventory, Tool Record System, Personnel Record System, Budget Control System, Equipment Record System, and Industrial Pretreatment File.
TECJET	Advanced Jet Dispersion Model	Technica International	David A. Jones 1400 N. Harbor Blvd Suite 800 Fullerton, CA 92635 (714) 447-9400	Jet dispersion model for PC.

Table 14–3 (continued)

ACRONYM/ABBREVIATION	SYSTEM NAME	VENDOR	ADDRESS/PHONE	PURPOSE/DESCRIPTION/REQUIREMENTS
TEM	The Environmental Manager	Environmental Information System	Sherida Mock 1101 Capital of Texas Highway South Building 8, Suite 212 Austin, TX 78746 (512) 328-5211	Tracks regulatory requirements; produces reports. Modules available on Environmental Audits, Permit Tracking, Groundwater Monitoring, Wastewater Monitoring, Air Emissions, Task Management, Waste Manifesting, Chemical Inventory, MSDS Management, Incident Reporting, and Operational Journals.
THERMOSIM Module 1: EQUIL		Gulf Publishing Company, Book Division	Melissa Beck P.O. Box 2608 Houston, TX 77252 (713) 520-4444	Database of thermodynamic properties of 200 hydrocarbons, 9 non-hydrocarbon gases, carbon, and sulfur. Requires 512K memory and 2 disk drives.
TOXIC, PUFF, SPILLS, INPUFF, AND INPUFF 2.0		Bowman Environmental Engineering	P.O. Box 29072 Dallas, TX 75229 (214) 241-1895	In ascending order of data complexity, these systems address toxic gas releases using models designed for each type of release, based on emission rate, facility characteristics and weather data.
**TOXIC ALERT		HAZOX Corporation	Daniel Fullerton P.O. Box 637 Chadds Ford, PA 19317 (215) 358-4990 (800) 558-6942	Incident management tool with some emergency planning capability. Modules for MSDS, incident documentation, inventory, and Tier I/II report generation.
TOXLINE (non-royalty based)	Toxicology Information Online	National Library of Medicine	8600 Rockville Pike Bethesda, MD 20894 (301) 496-1131	On-line bibliographic database covering the pharmacological, physiological, and toxicological effects of drugs and chemicals. Information is taken from eleven secondary sources.
TRACE II	Toxic Release Analysis of Chemical Emissions	Safer Emergency Systems, Inc.	Darlene Davis Dave Dillehay 756 Lakefield Road Westlake Village, CA 91361 (818) 707-2777	Models toxic gas and flammable vapor cloud dispersion. Intended for risk assessment and planning purposes, rather than real-time emergencies.
TRAINING MANAGER		OSHA-SOFT Corporation	P.O. Box 894 Concord, NH 03301 (603) 228-3610	Records employee training information, and allows classification and tracking of products and employees by category.

Table 14–3 (continued)

ACRONYM/ABBREVIATION	SYSTEM NAME	VENDOR	ADDRESS/PHONE	PURPOSE/DESCRIPTION/REQUIREMENTS
TREDAT		Cochrane Associates, Inc.	Jay J. Fink 236 Huntington Ave. Boston, MA 02115 (617) 247-0448	Data handling and process control software program for wastewater treatment plants. Requires Apple II.
TREMAIN		Cochrane Associates, Inc.	Jay J. Fink 236 Huntington Ave. Boston, MA 02115 (617) 247-0448	Equipment and inventory management software system for wastewater treatment plants. Requires Apple II.
TREPORT		Cochrane Associates, Inc.	Jay J. Fink 236 Huntington Ave. Boston, MA 02115 (617) 247-0444	Data handling and reporting system for wastewater treatment facilities. Assists with daily calculation of data and generation of reports.
TRI Database	Toxic Chemical Release Inventory	National Library of Medicine, Specialized Information Services	8600 Rockville Pike Bethesda, MD 20894 (301) 496-6531	Contains information on industrial location, storage, and release to air, water, and land of SARA Section 313 chemicals. Data is divided into the following categories: facility identification, substance identification, environmental release of chemical, waste treatment, and off-site waste transfer.
TSAR	Technology Selector of Alternative Remedies	Roy F. Weston, Inc.	Judith Hushon 955 L'Enfant Plaza, SW 6th Floor Washington, DC 20024 (202) 646-6800	Assists in selecting appropriate remedial technologies at waste sites. Using available quantitative and/or qualitative information the system selects potential general response actions and eliminates some specific technologies from further consideration; identifies additional data required to decide among the remaining engineering alternatives. The system can be delivered on Compaq-386 or requires PC HOST for the PC/AT.
TSDSYS	Treatment, Storage and Disposal Facilities Expert System	Roy F. Weston, Inc.	Judith Hushon 955 L'Enfant Plaza SW 6th Floor Washington, DC 20024 (202) 646-6800	Database containing information on over 400 contractors and the treatment, storage and disposal methods they offer. Treatment is broken into on-site and off-site and then by the following categories: biological, chemical, physical, and thermal treatment. Menu driven. Available through cross talk for EPA Regional offices.

Table 14–3 (continued)

ACRONYM/ABBREVIATION	SYSTEM NAME	VENDOR	ADDRESS/PHONE	PURPOSE/DESCRIPTION/REQUIREMENTS
UMT	The UNIFORM MANIFEST TRACKER	HAZOX Corporation	Daniel Fullerton P.O. Box 637 Chadds Ford, PA 19317 (800) 558-6942	Maintains information about hazardous waste generators, transporters, disposal facilities, materials shipped, and how they have been shipped. Assists with Uniform Hazardous Waste Manifest document required by RCRA. Generates records and letters. Requires 200K memory plus 1K memory for each record and a printer that can penetrate a six-part form.
VAX DEChealth		Digital	146 Main Street Maynard, MA 01754 (617) 897-5111	Employee and environmental health data records system. Maintains medical exposure data of employees.
VENTDATA		Hatch Associates Ltd.	21 St. Clair Ave. East Toronto, Ontario, Canada M4T 1L9 (416) 962-6350	Recordkeeping and analytical program for use in monitoring and maintenance of exhaust ventilation systems. Requires Apple II.
VULZONE.WK1	Vulnerability Zone Worksheet	New York State Emergency Management Office	Ed Lipps Public Security Bldg State Campus Albany, NY 12226-5000 (518) 457-9959	Calculates mileage of vulnerability zone for Extremely Hazardous Substances, giving a radial value to use on a map. Chemicals may be searched by CAS number; with each search, the system verifies the chemical name.
WASTETRAX		Engineering-Science	57 Executive Park S, NE Suite 590 Atlanta, GA 30329 (404) 325-0770	For water and wastewater treatment plants. Information management for groundwater monitoring, hazardous waste management, and air quality monitoring. Statistical capabilities.
WASTEWATER DATA MANAGEMENT SYSTEM		WDMS Computer Services	P.O. Box 27561 Tulsa, OK 74149 (918) 241-5755	Database that allows storage, retrieval, analysis, and reporting for industrial pretreatment programs. Requires 512K memory.
WATER COST		CWC-HDR Inc.	300 Admiral Way Suite 204 Edmonds, WA 98020 (206) 774-1947	Water and wastewater cost estimation software program. Contains extensive cost data.

Table 14–3 (continued)

ACRONYM/ABBREVIATION	SYSTEM NAME	VENDOR	ADDRESS/PHONE	PURPOSE/DESCRIPTION/REQUIREMENTS
WATER MASTER		Waid and Associates	8000 Centre Park Dr. Suite 270 Austin, TX 78754 (512) 835-6112	Animated training aid and simulation program for water and wastewater treatment plant operators.
WDC MANIFESTING SYSTEM		Waste Documentation and Control, Inc.	P.O. Box 7363 Beaumont, TX 77706 (409) 839-4495	Produces internal control documentation and governmentally required reports. Manifest printing from files containing information on approved transporters and disposers, waste materials, and historical data.
WHAZAN	World Bank Hazards Analysis	Technica International	David A. Jones 1440 N. Harbor Blvd. Suite 800 Fullerton, CA 92635 (714) 447-9400	Modeling of chemical dispersion and spill behavior. Database for 30 hazardous substances. 13 mathematical models that predict effects of release of flammable or toxic chemicals. Hard disk required.

References

Marsick, Daniel J., Ph.D., "Resources for Right-to-Know Compliance," presented to American Chemical Society, Division of Chemical Health and Safety, October 6, 1987.

Pollution Engineering, January 1988, "Environmental Software Review - 1988," by Gerald Rich.

Pollution Engineering, January 1987, "Environmental Software Review - 1987," by Nicholas P. Cheremisinoff, Ph.D.

Pollution Engineering, January 1986, "1986 Environmental Software Review," by Jack Brown.

Pollution Engineering, January 1985, "Environmental Software Review," by Richard Young, Editor.

Fire Command, December 1987, "Cellular Phone Access to Chemical Databases," by Keith T. Linderman.

REFERENCES

Allen, P.D., and R.B. Munger (1981): *Documentation and User's Guide to Smog-Simulation Model of Ozone Generation*. State of California Air Resources Board, Sacramento, California.

Bencala, K.E., and J.H. Seinfeld (1979): An air quality model performance assessment package. *Atmos. Environ.*, **13**:1181–1185.

Bornstein, R.D., S. Klotz, U. Pechinger, R. Salvador, R. Street, L.J. Shieh, F.L. Ludwig, and R. Miller (1985): Application of linked three-dimensional PBL and dispersion models to New York City. *Proceedings*, 15th NATO/CCMS Conference, St. Louis, Missouri, April.

Burt, E.W. (1977): *Valley Model User's Guide*. Report EPA-450/2-77-018. U.S. Environmental Protection Agency, Office of Air and Waste Management, Research Triangle Park, North Carolina (Addendum PB-274054 of December 1980).

Chang, J.S., R.A. Brost, I.S. Isaksen, S. Madronich, P. Middleton, W.R. Stockwell, and C.J. Walcek (1987): A three-dimensional Eulerian acid deposition model: Physical concepts and formulation. *J. Geophys. Res.*, **92**:14681–14700.

Davis, C.G., S.S. Bunker, and J.P. Mutschlecner (1984): Atmospheric transport models for complex terrain. *J. Climate and Appl. Meteor.*, **23**:235–238.

Dickerson, M.H. (1978): MASCON – A mass-consistent atmospheric flux model for regions with complex terrain. *J. Appl. Meteorol.*, **17**:241–253.

Dodge, M.C. (1977): Combined use of modeling techniques and smog chamber data to derive ozone-precursor relationships. *Proceedings*, International Conference on Photochemical Oxidant Pollution and Its Control, Vol. II, edited by B. Dimitriades, U.S. Environmental Protection Agency Document EPA-600/3-77-001b, pp. 881–889.

Douglas, S.G., and R.C. Kessler (1988): User's guide to the diagnostic wind model (Version 1.0). Systems Applications, Inc., San Rafael, California.

Drivas, P.J., M.W. Chan, and L.G. Wayne (1977): Validation of an improved photochemical air quality simulation model. AMS Joint Conference on Applications of Air Pollution Meteorology. Salt Lake City, Utah, November 23–December 2.

Electric Power Research Institute (1989): Acid rain research results – an environmental briefing – July 1989. EPRI Report EN.3006.7.89, Electric Power Research Institute, Palo Alto, California.

Eltgroth, M.W., and P.V. Hobbs (1979): Evolution of particles in the plumes of coal-tired power plants – II. A numerical model and comparison with field measurements. *Atmos. Environ.*, **13**:953–976.

Ermak, D.L., S.T. Chan, D.L. Morgan, and L.K. Morris (1981): A comparison of dense gas dispersion model simulations with Burro series LNG spill test results. Preprint, *J. Hazardous Materials*, Lawrence Livermore National Laboratory Document CRL-86713, Livermore, California.

Geai, P. (1987): Reconstitution tridimensionnelle d'un champ de vent dans un domaine a' topographie complexe a' partir de meusures in situ. EDF, Chatou, France, Final Report DER/HE/34-87.05.

Gipson, G.L. (1984): User's manual for OZIPM-2: Ozone isopleth plotting with optional mechanisms/Version 2. U.S. Environmental Protection Agency Document EPA-450/4-84-024, Office of Air Quality Planning and Standards, Monitoring and Data Analysis Division, Research Triangle Park, North Carolina.

Gulfreund, P.D., C.S. Liu, B.R. Nicholson, and E.M. Roberts (1983): COMPLEX I and II model performance evaluation in Nevada and New Mexico. *JAPCA*, **33**(9):864-871.

Hanna, S.R., and P.J. Drivas (1987): *Guidelines for Use of Vapor Cloud Dispersion Models*, New York: Center for Chemical Process Safety, American Society of Chemical Engineers.

Henderson-Sellers, B., (1987): Modeling of plume rise and dispersion - The University of Salford Model: USPR. *Lecture Notes in Engineering*, edited by C.A. Brebbia and S.A. Orszag. Berlin: Springer-Verlag.

King, D.S., and S.S. Bunker (1984): Application of atmospheric transport models for complex terrain. *J. Climate and Appl. Meteor.*, **23**:239.

Lange, R. (1978): ADPIC - A three-dimensional particle-in-cell model for the dispersal of atmospheric pollutants and its comparison to regional tracer studies. *J. Appl. Meteor.*, **17**:320.

Lurmann, F.W., D.A. Gooden, and H.M. Collins, Eds. (1985): User's guide to the PLMSTAR air quality simulation model. Environmental Research & Technology, Inc. Document M-2206-100, Newbury Park, California.

Martinez, J.R., R.A. Nordsieck, and M.A. Mirschberg (1973): *User's Guide to Diffusion/Kinetics (DIFKIN) Code*. General Research Corporation Final Report CR-2-273/1, prepared for U.S. Environmental Protection Agency, Research Triangle Park, North Carolina.

Nitz, K.C., and R.M. Endlich (1983): *ENAMAP-2 User's Manual*. SRI International, Menlo Park, California.

Paine, R.J., and B.A. Egan (1987): *User's Guide to the Rough Terrain Diffusion Model (RTDM) (Rev. 3.20)*. Document P-D535-585, National Technical Information Service, U.S. Department of Commerce, Springfield, Virginia.

Phillips, G.T., and R.M. Traci (1978): *A Preliminary User Guide for the NOABL Objective Analysis Code*. SAI Report SAI-78-769-LJ, U.S. Department of Energy Report RLO/2440-77-10. Systems Applications, Inc., La Jolla, California.

Pielke, R.A., R.T. McNider, M. Segal, and Y. Mahrer (1983): The use of a mesoscale numerical model for evaluations of pollutant transport and diffusion in coastal regions and over irregular terrain. *Bull. Am. Meteor. Soc.*, **64**:243-249.

Pierce, T.E., D.B. Turner, J.A. Catalano, and F.V. Hall III (1982): *PTPLU - A Single Source Gaussian Dispersion Algorithm, User's Guide*. Document EPA-600/8-82-014. U.S. Environmental Protection Agency, Environmental Sciences Research Laboratory, Research Triangle Park, North Carolina.

Roth, P.M., P.G. Georgopoulos, T.B. Smith, A.Q. Eschenroeder, J.H. Seinfeld, P.H. Guldberg, and T.C. Spangler (1988): Guidelines for air quality modeling. Draft Report prepared for the State of California Air Resources Board, Sacramento, California.

Samson, P.I., M.I. Small, and B.T. Beryland (1982): *User's Guide to the Atmospheric Contributions to Inter-Regional Deposition (ACID) Model*. University of Michigan, Ann Arbor.

Sherman, C.A. (1978): A mass-consistent model for wind fields over complex terrain. *J. Appl. Meteor.*, 17:312-319.

Seigneur, C., T.W. Tesche, P.M. Roth, M.-K. Liu (1983): On the treatment of point source emissions in urban air quality modeling. *Atmos. Environ.*, 17(9):1655-1676.

Shir, C.C., and L.J. Shieh (1974): A generalized urban air pollution model and its application to the study of SO_2 distributions in the St. Louis metropolitan area. *J. Appl. Meteor.*, 13:185-204.

Strimaitis, D.G., D.C. DiCristofaro, and T.F. Lavery (1986): The complex terrain dispersion model. EPA Document EPA-600-D-85/220, Atmospheric Sciences Research Laboratory, Research Triangle Park, North Carolina.

Sykes, R.I., W.S. Lewellen, S.F. Parker, and D.S. Henn (1989a): A hierarchy of dynamic plume models incorporating uncertainty. Vol. 2: Stack exhaust model (SEM). A.R.A.P. Division of California Research & Technology, Inc., Final Report EA-6095, Vol. 2, Princeton, New Jersey.

Sykes, R.I., W.S. Lewellen, S.F. Parker, and D.S. Henn (1989b): A hierarchy of dynamic plume models incorporating uncertainty. Volume 3: Second-order closure integrated model plume (SCIMP). A.R.A.P. Division of California Research & Technology, Inc., Final Report EA-1616-28, Vol. 3, Princeton, New Jersey.

Sykes, R.I., W.S. Lewellen, S.F. Parker, and D.S. Henn (1989c): A hierarchy of dynamic plume models incorporating uncertainty. Volume 4: Second-order closure integrated plume. A.R.A.P. Division of California Research & Technology, Inc., Final Report EA-6095, Vol. 4, Princeton, New Jersey.

Systems Applications, Inc. (1984): *Visibility and Other Air Quality Benefits of Sulfur Dioxide Emission Controls in the Eastern United States,* Volume I. Systems Applications, Inc., Draft Report SYSAPP-84/165, San Rafael, California.

Tesche, T.W., and D.E. McNalley (1989): A three-dimensional photochemical-aerosol model for episodic and long-term simulation: Formulation and initial application in the Los Angeles Basin. Presented at the annual meeting of the American Chemical Society, Miami Beach, Florida, September.

Tirabassi, T., M. Tagliazucca, and P. Zannetti (1986): KAPPA-G, a non-Gaussian plume dispersion model: Description and evaluation against tracer measurements. *JAPCA*, 36(5):592-596.

Tran, K.T., and R.C. Sklarew (1979): User guide to IMPACT: An integrated model for plumes and atmospheric chemistry in complex terrain. Form & Substance, Inc., Westlake Village, California.

Tran, K.T. (1981): User's guide for photochemical trajectory model TRACE. Applied Modeling, Inc., Report 81/003. California.

Turner, D.B., L.W. Bender, T.E. Pierce, and W.B. Peterson (1989): Air quality simulation models from EPA. *Environ. Software*, 4(2):52.

U.S. Environmental Protection Agency (1978): *Guideline on Air Quality Models.* Draft Report EPA-450/2-78-027. U.S. Environmental Protection Agency, Research Triangle Park, North Carolina.

U.S. Environmental Protection Agency (1984): *Guideline on Air Quality Models (Revised).* Draft Report EPA-450/2-78-027R. U.S. Environmental Protection Agency, Research Triangle Park, North Carolina.

U.S. Environmental Protection Agency (1987): *Supplement A to Guideline on Air Quality Models (Revised)*. Draft Report EPA-450/2-78-027R. U.S. Environmental Protection Agency, Research Triangle Park, North Carolina.

U.S. Environmental Protection Agency (1988a): *Screening Procedures for Estimating Air Quality Impact of Stationary Sources*. Document 450/4-88/010. U.S. Environmental Protection Agency, Research Triangle Park, North Carolina.

U.S. Environmental Protection Agency (1988b): *Workbook for Plume Visual Impact Screening and Analysis*. Document 450/4-88/015. U.S. Environmental Protection Agency, Research Triangle Park, North Carolina.

U.S. Environmental Protection Agency (1989): Computer Systems for Chemical Emergency Planning. Chemical Emergency Preparedness and Prevention Technical Assistance Bulletin #5. U.S. EPA Document OSWER-89-005. U.S. Environmental Protection Agency, Research Triangle Park, North Carolina.

Williams, M.D., E. Treiman, and M. Wecksung (1980): Plume blight visibility modeling with a simulated photograph technique. *JAPCA*, **30**:131-134.

Williams, M.D., L.Y. Chan, and R. Lewis (1981): Validation and sensitivity of a simulated-photograph technique for visibility modeling. *Atmos. Environ.*, **15**:2151-2170.

Yamada, T. (1978): A three-dimensional, second-order closure numerical model of mesoscale circulations in the lower atmosphere: Description of the basic model and an application to the simulation of the environmental effects of a large cooling pond. Argonne National Laboratory Report ANL/REF-78-1, Argonne, Illinois.

Yamada, T. (1985): Numerical simulation of the Night 2 data of the 1980 ASCOT experiments in the California Geysers Area. *Arch. for Meteor. , Geophys., and Biolim.*, **A34**:223-247.

Yamada, T., and S. Bunker (1988): Development of a nested grid, second moment turbulence closure model and application to the 1982 ASCOT Brush Creek data simulation. *J. Appl. Meteor.*, **27**:562-578.

Yamartino, R.J., J.S. Scire, S.R. Hanna, G.R. Carmichael, Y.S. Chang (1989): CALGRID: A mesoscale photochemical grid model. Sigma Research Corp. Report A049-1. Prepared for the California Air Resources Board, Sacramento, California.

Zannetti, P., J. Moussafir, G. Brusasca, and G. Tinarelli (1988): *MC-LAGPAR II User's Guide (Release 4.0)*. AeroVironment Report AV-R-88/519, Monrovia, California.

Author's Index*

A

B

* Index includes pages where authors are referred to as "et al." in reference citations.

C

D

E

F

G

H

I

J

K

L

M

N

O

P

R

S

T

U

V

W

Y

Z

SUBJECT INDEX